DROSOPHILA: A VERSATILE MODEL FOR MOLECULAR, PHYSIOLOGICAL AND BEHAVIORAL STUDIES

EDITED BY: Gabriella Mazzotta, Cristiano De Pitta, Paola Cusumano and Giorgio F. Gilestro

PUBLISHED IN: Frontiers in Physiology

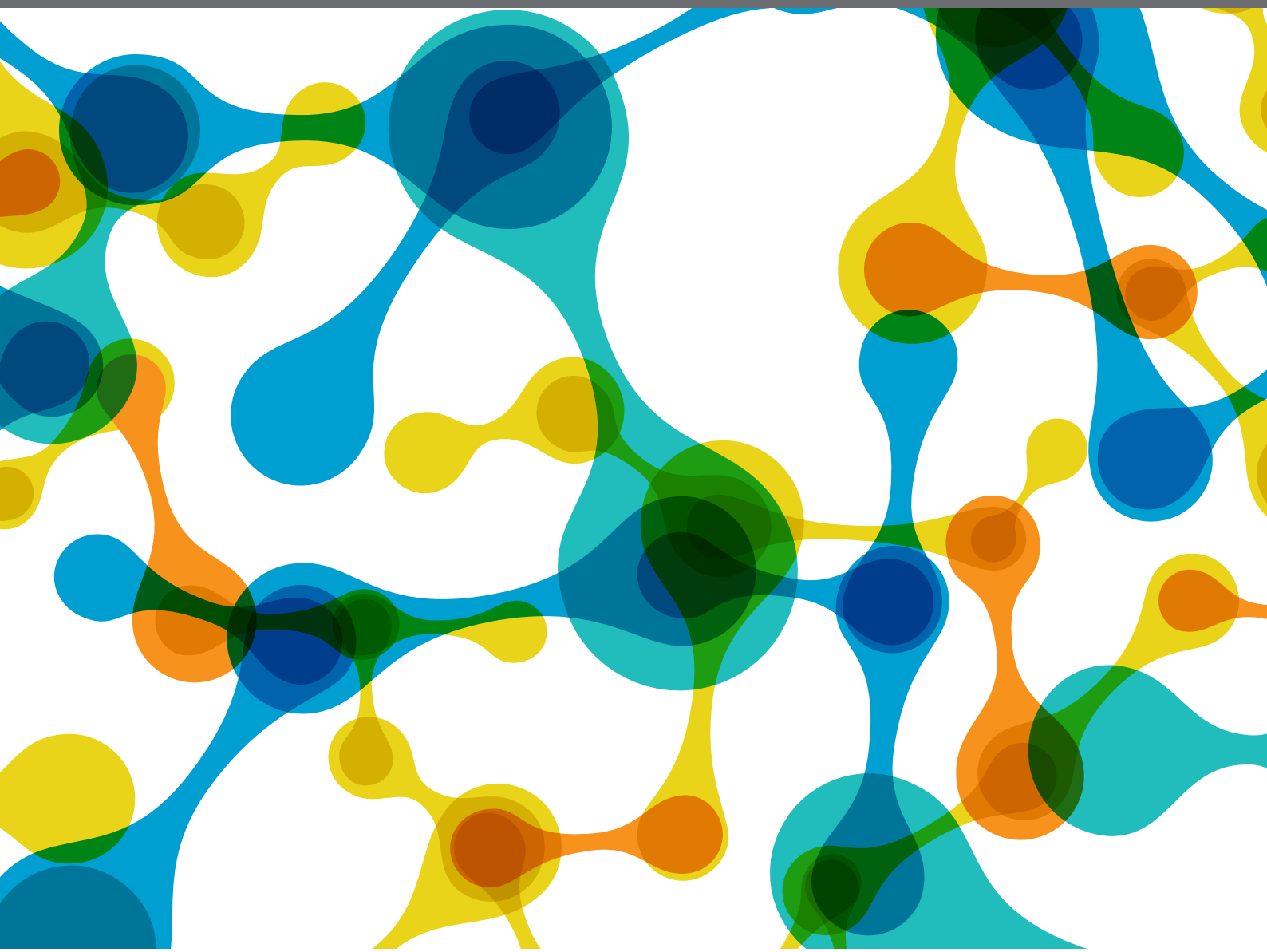

frontiers Research Topics

frontiers

ISSN 1664-8714
ISBN 978-2-88966-656-0
DOI 10.3389/978-2-88966-656-0

About Frontiers

Frontiers is more than just an open-access publisher of scholarly articles: it is a pioneering approach to the world of academia, radically improving the way scholarly research is managed. The grand vision of Frontiers is a world where all people have an equal opportunity to seek, share and generate knowledge. Frontiers provides immediate and permanent online open access to all its publications, but this alone is not enough to realize our grand goals.

Frontiers Journal Series

The Frontiers Journal Series is a multi-tier and interdisciplinary set of open-access, online journals, promising a paradigm shift from the current review, selection and dissemination processes in academic publishing. All Frontiers journals are driven by researchers for researchers; therefore, they constitute a service to the scholarly community. At the same time, the Frontiers Journal Series operates on a revolutionary invention, the tiered publishing system, initially addressing specific communities of scholars, and gradually climbing up to broader public understanding, thus serving the interests of the lay society, too.

Dedication to Quality

Each Frontiers article is a landmark of the highest quality, thanks to genuinely collaborative interactions between authors and review editors, who include some of the world's best academicians. Research must be certified by peers before entering a stream of knowledge that may eventually reach the public - and shape society; therefore, Frontiers only applies the most rigorous and unbiased reviews.
Frontiers revolutionizes research publishing by freely delivering the most outstanding research, evaluated with no bias from both the academic and social point of view. By applying the most advanced information technologies, Frontiers is catapulting scholarly publishing into a new generation.

What are Frontiers Research Topics?

Frontiers Research Topics are very popular trademarks of the Frontiers Journals Series: they are collections of at least ten articles, all centered on a particular subject. With their unique mix of varied contributions from Original Research to Review Articles, Frontiers Research Topics unify the most influential researchers, the latest key findings and historical advances in a hot research area! Find out more on how to host your own Frontiers Research Topic or contribute to one as an author by contacting the Frontiers Editorial Office: frontiersin.org/about/contact

DROSOPHILA: A VERSATILE MODEL FOR MOLECULAR, PHYSIOLOGICAL AND BEHAVIORAL STUDIES

Topic Editors:
Gabriella Mazzotta, University of Padua, Italy
Cristiano De Pitta, University of Padua, Italy
Paola Cusumano, University of Padua, Italy
Giorgio F. Gilestro, Imperial College London, United Kingdom

Citation: Mazzotta, G., De Pitta, C., Cusumano, P., Gilestro, G. F., eds. (2021). Drosophila: A Versatile Model for Molecular, Physiological and Behavioral Studies. Lausanne: Frontiers Media SA. doi: 10.3389/978-2-88966-656-0

Table of Contents

frontiers in Physiology

ORIGINAL RESEARCH
published: 29 March 2019
doi: 10.3389/fphys.2019.00345

The Exocyst Component Sec3 Controls Egg Chamber Development Through Notch During *Drosophila* Oogenesis

*Ping Wan[1], Sumei Zheng[1], Lai Chen[2], Dou Wang[3], Ting Liao[1], Xueming Yan[1] and Xiaoji Wang[1]**

[1] School of Life Science, Jiangxi Science and Technology Normal University, Nanchang, China, [2] Experimental Animal Science and Technology Center, Jiangxi University of Traditional Chinese Medicine, Nanchang, China, [3] Model Animal Research Center, Nanjing University, Nanjing, China

The exocyst complex plays multiple roles via tethering secretory or recycling vesicles to the plasma membrane. Previous studies have demonstrated that the exocyst contains eight components, which possibly have some redundant but distinct functions. It is therefore interesting to investigate the biological function of each component. Here, we found that Sec3, one component of exocyst complex, is involved in *Drosophila* egg chamber development. Loss of *sec3* results in egg chamber fusion through the abolishment of cell differentiation. In addition, loss of *sec3* increases cell numbers but decreases cell size. These defects phenocopy Notch pathway inactivation. In line with this, loss of *sec3* indeed leads to Notch protein accumulation, suggesting that the loss of Sec3 inhibits the delivery of Notch onto the plasma membrane and accumulates inactive Notch in the cytoplasm. Loss of *sec3* also leads to the ectopic expression of two Notch pathway target genes, Cut and FasciclinIII, which should normally be downregulated by Notch. Altogether, our study revealed that Sec3 governs egg chamber development through the regulation of Notch, and provides fresh insights into the regulation of oogenesis.

Keywords: Sec3, exocyst, Notch, *Drosophila*, ovary

OPEN ACCESS

Edited by:
Giorgio F. Gilestro, Imperial College London, United Kingdom

Reviewed by:
Gábor Juhász, Eötvös Loránd University, Hungary
Marko Brankatschk, Dresden University of Technology, Germany

***Correspondence:**
Xiaoji Wang
Wangxj77@hotmail.com

Specialty section:
This article was submitted to Invertebrate Physiology, a section of the journal Frontiers in Physiology

Received: *01 October 2018*
Accepted: *14 March 2019*
Published: *29 March 2019*

Citation:
Wan P, Zheng S, Chen L, Wang D, Liao T, Yan X and Wang X (2019) The Exocyst Component Sec3 Controls Egg Chamber Development Through Notch During Drosophila Oogenesis. Front. Physiol. 10:345. doi: 10.3389/fphys.2019.00345

INTRODUCTION

Notch signaling is an evolutionarily conserved pathway that controls various processes, including embryogenesis and cell differentiation (Lai, 2004; Kopan and Ilagan, 2009). Vesicle-mediated protein traffic is essential for the transduction of the Notch pathway. The newly synthesized Notch receptor and DSL (Delta/Serrate/LAG-2) ligands are transported through the endoplasmic reticulum (ER) and Golgi apparatus to reach the plasma membrane. After association with ligands, the receptors re-enter the cell via endocytosis. These endocytic vesicles from the cell membrane then fuse with early endosome. The early endosome works as a sorting center, from which the Notch can be recycled back to the plasma membrane, or to the late endosome for protein degradation (Sorkin and von Zastrow, 2009).

Increasing studies on *Drosophila*, have demonstrated that the Notch pathway is involved in multiple processes, including ovary development. The *Drosophila* ovary consists of about 16–20

ovarioles, each of which contains a series of egg chambers processed through 14 stages. Each egg chamber consists of 16 germ cells enveloped by a monolayer of follicular epithelium. The neighboring egg chamber is linked by the stock, which is a string of five to eight follicle cells. A pair of special follicle cells called polar cells differentiate during early stages at each pole of each egg chamber. Loss of polar cells induces fusion of neighboring egg chambers and results in a compound egg chamber containing two or more germline clusters. Reduction of Notch activity suppresses polar cell formation and results in fused egg chambers (Grammont and Irvine, 2001; Torres et al., 2003; Vachias et al., 2010). Moreover, *Drosophila* oogenesis is a complex but coordinated process. For example, follicle cells switch from the mitotic cycle to endocycle during mid stages. Notch signaling induces this cell-cycle switch (Sun and Deng, 2005).

Exocyst is an eight protein complex and was originally identified from mutants involved in the secretory pathway in yeast (Novick et al., 1980). Subsequent analysis of the exocyst has shown that it functions in intracellular vesicle transport and mediates the tethering of secretory or recycling vesicles to the plasma membrane. Defects in exocyst proteins result in the accumulation of secretory vesicles in cells (Novick et al., 1980; Guo et al., 1999; Zhang et al., 2005). The exocyst components, Sec3, Sec5, Sec6, Sec8, Sec10, Sec15, Exo70, and Exo84, are conserved from yeast to mammals. In yeast, the Sec3 component functions as a spatial landmark for polarized secretion, as it localizes to the exocytic site independently of other components (Finger et al., 1998; Boyd et al., 2004). The yeast Sec3 directly binds to phosphatidylinositol 4,5-bisphosphate (PIP2) and the small GTPases Rho1 and Cdc42 through its N-terminal domain, and these bindings are critical for the localization and function of Sec3 at the exocytic site in the plasma membrane (Zhang et al., 2008; Yamashita et al., 2010). The yeast Sec3 was also found to interact with the t-SNARE protein Sso2, which promotes membrane fusion between the vesicles and target membrane (Yue et al., 2017). In plants, Sec3 has also been widely investigated. Sec3 is required for root hair elongation, embryogenesis, and pollen germination (Wen et al., 2005; Zhang et al., 2013; Bloch et al., 2016). In *Drosophila*, Sec3 is involved in the polarized transport of guidance receptors during border cell migration (Wan et al., 2013). However, the function of Sec3 in animals has not been well elucidated.

In this study, we show that the loss of *sec3* phenocopies loss-of-function Notch during *Drosophila* oogenesis. Further studies show that loss of *sec3* indeed results in a Notch protein transport defect and a Notch pathway inactivation, indicating that Sec3 regulates Notch signaling during oogenesis. Altogether, our findings shed light on exocyst-mediated regulation of oogenesis through Notch.

MATERIALS AND METHODS

Fly Stocks and Husbandry

All fly stocks except for RNAi experiments were cultured at 25 ± 1°C on a standard corn-yeast-sucrose medium under constant humidity and a 12:12 h light to dark cycle. The $sec3^{GT}$ and $sec3^{PBac}$ lines were described previously (Wan et al., 2013). The line *hs-flp; ubi-GFP FRT80B* was obtained from the Bloomington *Drosophila* Stock Center (BDSC). Females of the latter line were crossed to males of $sec3^{GT}$ and $sec3^{PBac}$ lines, respectively. Progeny were heat shocked for 2 h per day at 37°C for 2 days before eclosion and 1 day after eclosion, then dissected 2–3 days after the last heat shock. Progeny with genotypes of *hs-flp;* $sec3^{GT}$ *FRT80B/ubi-GFP FRT80B* or *hs-flp;* $sec3^{PBac}$ *FRT80B/ubi-GFP FRT80B* were analyzed. The *sec3* mutant clones were marked by the absence of GFP. The *sec3* RNAi line was obtained from the Vienna *Drosophila* RNAi Center (#108085) and *c306-Gal4* from BDSC. The *c306-Gal4>sec3-RNAi* progeny were shifted to 29°C for 3–4 days before dissection.

Immunohistochemistry and Microscopy

Ovary dissection was carried out in phosphate buffered saline (PBS) and then fixed in PBS with 7% formaldehyde for 10 min. After being washed in PBS, ovaries were blocked in 10% goat serum in PBT (PBS containing 0.3% Triton X-100) for 30 min and then stained overnight at 4°C. Most primary antibodies were obtained from the Developmental Studies Hybridoma Bank (DSHB) and their dilutions were as follows: mouse anti-Orb (orb 4H8, 1:30), mouse anti-NICD (C17.9C6, 1:10), mouse anti-NECD (C458.2H, 1:100), mouse anti-FASIII (7G10, 1:100), mouse anti-Cut (2B10, 1:100), mouse anti-Delta (C594.9B, 1:100), mouse anti-Kel (Kel 1B, 1:5), mouse anti-β-Gal (40-1a, 1:25), mouse anti-CycA (A12, 1:15), rabbit anti-phosho-Histone H3 (1:1000, Cell Signaling #3377), and rabbit anti-Stau (1:1000, gift from St. Johnston D). After being washed in PBT, ovaries were incubated with secondary antibodies (Jackson ImmunoResearch) for 2 h at room temperature. Nuclei were labeled by DAPI (E607303, 1:50, Sangon Biotech) in the last half hour. Confocal images were performed on a Leica TCS SP8 confocal microscope.

Fertility Test

To check the fertility status of the *c306>sec3.RNAi* females, pair matings were set between individual *c306>sec3.RNAi* females and wild type males in a series of vials. All vials were raised in 29°C and changed to new vials every day, to retain a good oogenesis status. Egg laying/females/day of the fourth day were counted. The ratio of hatched vs. all laid eggs were then calculated after 24 h. Progeny of late stages were also observed to check the calculation. For the experimental control, wild type females were crossed with wild type males.

Quantification of Cell Number and Cell Size

Regions of mutant clones were chosen, while regions of their sister clones were chosen. Cell numbers and area were measured in ImageJ software (NIH) for each region. The mean number of cells was calculated as (nucleus number)/(clone area). The mean size of the nuclei was calculated as (nucleus area)/(nucleus number). The mean ratio is an average of ratios of each pair bar. Statistical analysis for the data set was done using paired Student's

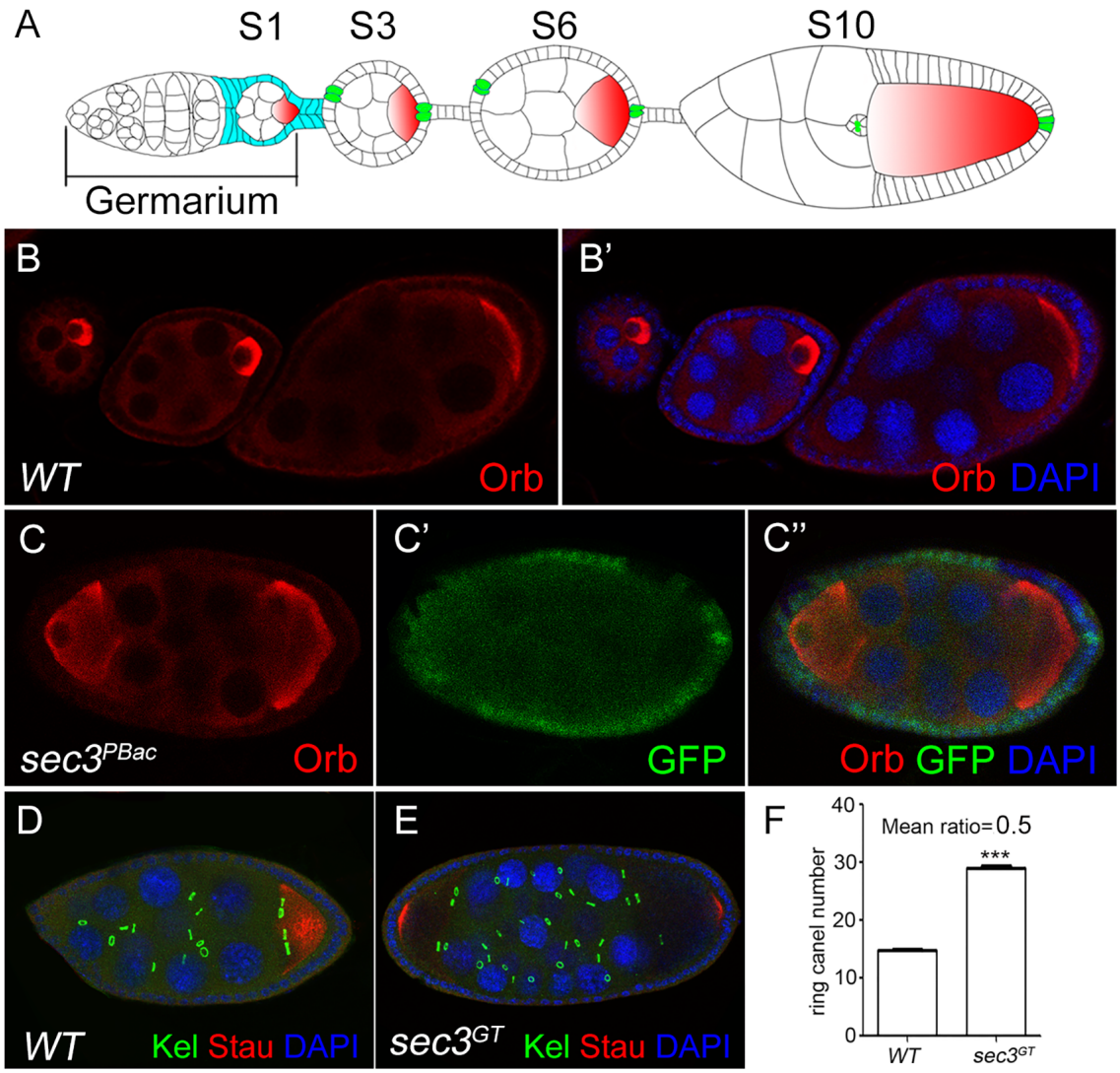

FIGURE 1 | Loss of *sec3* in follicle cells results in egg chamber fusion. **(A)** A model for *Drosophila* oogenesis showing egg chambers in different stages. Oocytes are in red and polar cells are in green from stage 3. Follicle cells cover all the germline cysts at the early stages and mainly cover the oocyte by stage 10. **(B–B')** A wild type ovariole with three egg chambers, each of which has an oocyte. **(C–C")** A compound egg chamber with $sec3^{PBac}$ clones showing two oocytes. **(D)** A wild type egg chamber showing 15 ring canals. **(E)** A compound egg chamber with two oocytes showing 30 ring canals. **(F)** Quantification of ring canal numbers in compound egg chambers and control egg chambers (29.5 ± 0.2 vs. 14.8 ± 0.1, $n = 12$, $p < 0.0001$). Images for Kel staining are overlays of the Z-section, as ring canals cannot be shown in a plane. In all the images in this report, the *sec3* mutant clones are marked by an absence of GFP, and nuclei are stained by DAPI.

t-test, using Prism 5 (GraphPad software, San Diego, CA, United States). Data comparisons were considered statistically significant if $p < 0.05$.

RESULTS

Loss of *sec3* Results in Egg Chamber Fusion

$sec3^{GT}$ and $sec3^{PBac}$ are two loss-of-function alleles of *Drosophila sec3* which were identified previously (Wan et al., 2013). *sec3* mutant follicle cell clones were generated with the Flp/FRT method and egg chambers were stained for the oocyte marker Orb. In the wild type, each egg chamber had only one Orb-positive oocyte and 15 nurse cells (**Figures 1A–B'**). In contrast, 12% ($sec3^{GT}$) or 14% ($sec3^{PBac}$) of the mutant mosaic egg chambers showed compound egg chambers, which had more than the normal complement of 15 nurse cells and an oocyte ($n = 50$) (**Figures 1C–C"** and **Supplementary Figure S1**). To confirm this, immunostaining of Kelch (Kel), a marker of ring canals, and Staufen (Stau), another marker of oocyte, was performed to count the number of germline cells in each egg chamber (**Figures 1D,E**). Ring canals are cytoplasmic bridges that intracellular materials can pass from nurse cells to oocyte. Every germline cell has one ring canal on average. Quantification results indicated that the germline cell number of these compound

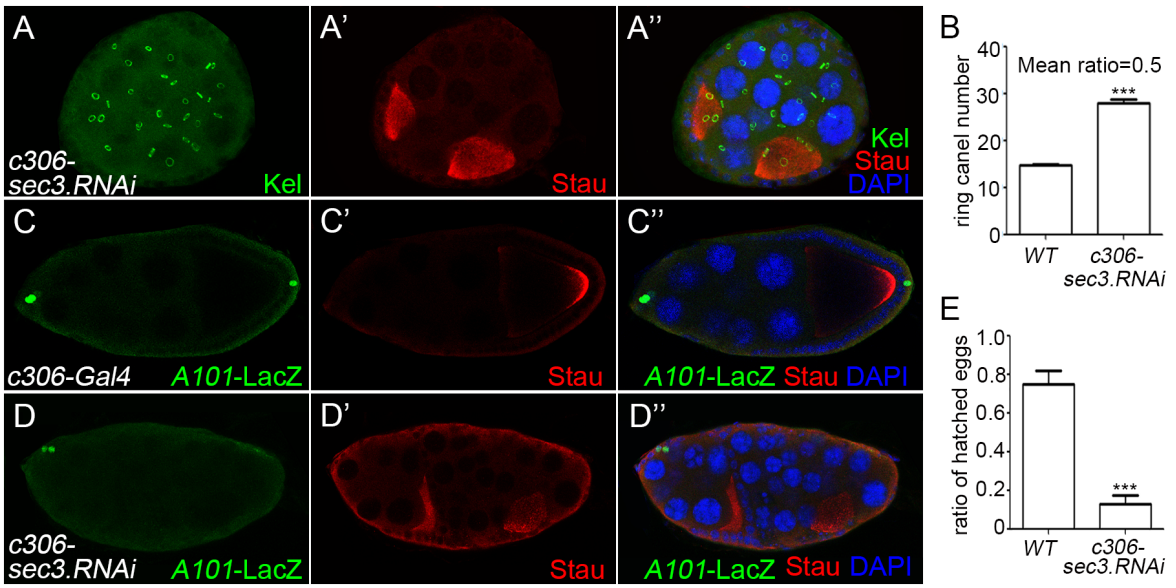

FIGURE 2 | Knocking down of *sec3* induces a fused egg chamber and suppresses polar cell differentiation. **(A–A")** In *c306>sec3-RNAi* background, a compound egg chamber with two oocytes shows 29 ring canals. Images for Kel staining are overlays of the Z-section, as ring canals cannot be shown in a plane. **(B)** Quantification of ring canal numbers in *sec3* knockdown compound egg chambers and control egg chambers (28.0 ± 0.7 vs. 14.8 ± 0.2, $n = 8$, $p < 0.0001$). **(C–C")** In *c306-Gal4* background, *A101-LacZ* shows normal expression at the two poles of egg chamber. **(D–D")** In *c306>sec3-RNAi* background, a partial fused egg chamber, which has no stock cells with only a single layer of follicle cells between the two cysts, contains only a pair of cells expressing *A101-LacZ* at only one pole of the egg chamber. Images for *A101*-LacZ staining are overlays of the Z-section, showing all the staining. **(E)** Fertility test of *c306>sec3-RNAi* females; see Methods for details. *c306>sec3-RNAi* females show a reduced ratio of hatched vs. all laid eggs (0.75 ± 0.07 vs. 0.13 ± 0.04, $n = 14$, $p < 0.0001$).

egg chambers was two copies of wild type (29.5 ± 0.2 vs. 14.8 ± 0.1, $n = 12$, $p < 0.0001$) (**Figure 1F**). Therefore, we hypothesized that loss of *sec3* led to egg chamber fusion. Some "partially" fused egg chambers undergoing the process of fusion could be observed, in which the intervening follicle cells seemed to be in the process of breaking apart (**Supplementary Figures S2A–A"**). The earliest "partially" fused egg chamber was observed at stage 3, when stock cells formed (**Supplementary Figures S2B–B"**). Most fused egg chambers were completely fused before stage 8, without an intervening wall of follicle cells between the two cysts.

Knocking Down of *sec3* Suppresses Polar Cell Differentiation

RNA interference was used to knock down *sec3* expression with the UAS/Gal4 method, using *c306-Gal4* which was expressed in most follicle cells. In *sec3* knocked down egg chambers, fused egg chambers were observed (**Figures 2A–A"**). Quantification results indicated that the germline cell number of the *sec3* knocked down compound egg chambers was two copies of the wild type (28.0 ± 0.7 vs. 14.8 ± 0.2, $n = 8$, $p < 0.0001$) (**Figure 2B**). The knock down experiment confirmed that reduced Sec3 activity induced egg chamber fusion. Signals from the polar cells are essential for stalk formation, and egg chamber fusion can be induced by suppressing polar cell differentiation (Baksa et al., 2002; McGregor et al., 2002). Polar cells in *sec3* knockdown egg chambers were examined, using an enhancer trap line *A101* (*neutralized-lacZ*), in which polar cells were marked with lacZ (Lopez-Schier and St Johnston, 2001; **Figures 2C–C"**). In *sec3* knocked down egg chambers, expression of *A101-lacZ* was reduced in fused egg chambers (**Figures 2D–D"** and **Supplementary Figure S3**). Therefore, reduced *sec3* activity resulted in the attenuation of polar cells, which contributed to the fusion of adjacent egg chambers.

A fertility test was carried out to test whether the dysfunction of the ovary was caused by the encapsulated multiple egg chambers. This was demonstrated by setting up pair matings between individual *c306> sec3.RNAi* females and wild type males. After being raised in 29°C for 4 days, egg laying/females/day and the ratio of hatched vs. all laid eggs were quantified. Most of the laid eggs from these pair matings remained unhatched and in some of the vials one to two eggs had hatched. Therefore, reduced *sec3* activity resulted in reduced fertility (**Figure 2E**).

Loss of *sec3* Shows Dysregulated Cell Cycle

During *Drosophila* oogenesis, follicle cells cease mitosis and duplicate chromosomes without cell division to generate polyploidy (endocycle) after stage 6 (Sun and Deng, 2005). The mitotic cycle/endocycle switch was then detected in *sec3* mosaic egg chambers. Follicle cells in stage 10 egg chambers were examined. Follicle cells in *sec3* mutant clones had obvious smaller nuclei, and were more densely distributed, compared with cells in the neighboring sister clone (**Figures 3A–A"**).

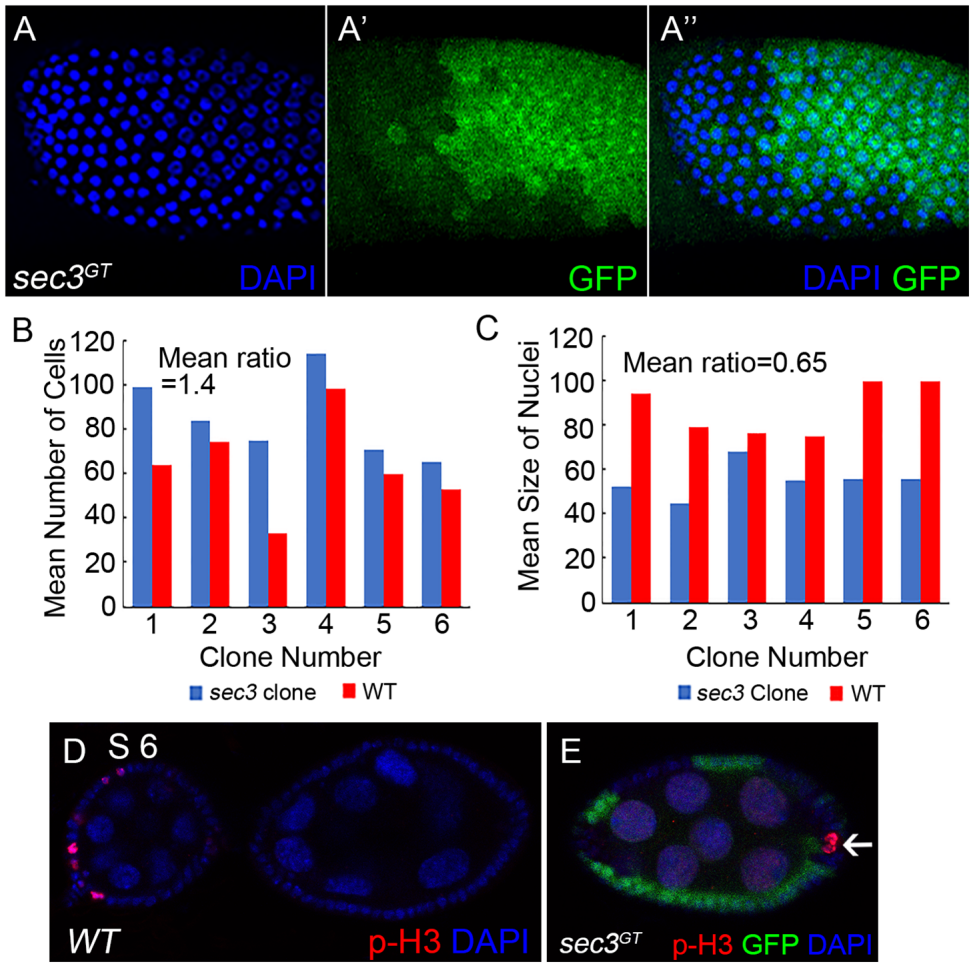

FIGURE 3 | Loss of *sec3* disrupts the mitotic cycle/endocycle switch. **(A–A")** In a stage 10 egg chamber, *sec3* mutant follicle clones show more cell numbers and smaller nuclei. Images are overlays of Z-section, as nuclei cannot be shown in a plane. **(B)** Number of nuclei in *sec3* mutant clones (blue bars) compared with that in their associated sister clones (red bars) in stage 10 egg chambers. The *x*-axis represents the clone number, and the *y*-axis represents the number of cells per clone or corresponding sister clone. Mean ratio of mutant/wt = 1.4, $n = 6$, $p = 10^{-2}$. See Methods for details. **(C)** Quantification of mean nucleus size in *sec3* mutant clones and their sister clones. Mean ratio of mutant/wt = 0.65, $n = 6$, $p = 3 \times 10^{-2}$. See Methods for details. **(D)** In wild type egg chambers, p-H3 positive follicle cells are detected only up to stage 6. Note that while mitosis of follicle cells is not synchronized, p-H3 are detected only in some cells. **(E)** In *sec3* mutant follicle cells, p-H3 staining can be detected after stage 6.

The quantification results of mean cell number supported that mutant clones had more cell numbers than their sister clones (mutant/wt = 1.4, $n = 6$, $p = 10^{-2}$) (**Figure 3B**). It suggested that *sec3* mutant cells failed to cease mitosis and processed extra rounds of cell division. The quantification results of mean nuclei size confirmed that mutant clones had smaller nuclei than their sister clones (mutant/wt = 0.65, $n = 6$, $p = 3 \times 10^{-2}$) (**Figure 3C**), which suggested that *sec3* mutant cells did not reach the endocycle.

Immunostaining results of the mitotic marker phospho-histone H3 (p-H3) also demonstrated that *sec3* mutant follicle cells continued to divide after stage 6. In wild type egg chambers, p-H3 positive follicle cells were detected only up to stage 6 during their mitotic cycle (**Figure 3D**). Note that while mitosis of follicle cells was not synchronized, p-H3 was detected only in some cells. In *sec3* mutant follicle cells p-H3 staining was observed after stage 6 (**Figure 3E** and **Supplementary Figure S4**).

Notch Protein Traffic Is Destroyed in *sec3* Mutant Follicle Cells

Both the fused eggs chamber and dysregulated cell proliferation phenocopied that of the Notch mutant clone (Deng et al., 2001; Grammont and Irvine, 2001; Vachias et al., 2010). There was therefore a need to examine whether Sec3 was involved in the traffic of Notch protein, as expected for a functional component of the exocyst complex. Without the exocyst, vesicles could not tether to the cell membrane which resulted in accumulation of vesicles and their cargo protein in the cytoplasm. The Notch receptor is a heterodimer composed of a Notch Intracellular Domain (NICD) and a Notch Extracellular Domain (NECD). In

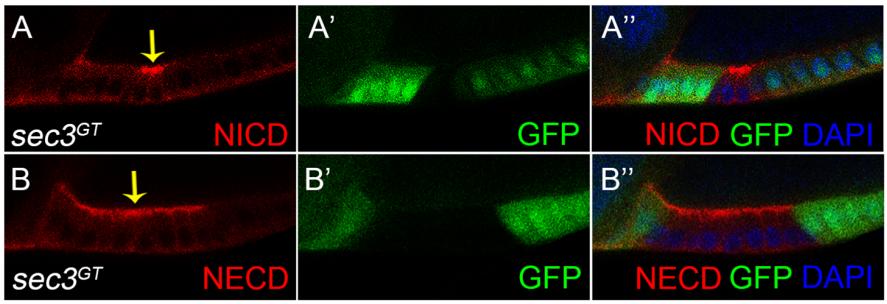

FIGURE 4 | Accumulated Notch protein in *sec3* mutant follicle cells. **(A–A")** NICD obviously accumulates in *sec3* mutant follicle cells in a stage 10 egg chamber (indicated by arrow). **(B–B")** NECD obviously accumulates in *sec3* mutant follicle cells in a stage 10 egg chamber (indicated by arrow).

mosaic egg chambers, accumulation of NICD and NECD were specifically shown in the *sec3* mutant follicle cells, compared with the neighboring wild type follicle cells (**Figure 4**). Therefore, loss of Sec3 function might inhibit the delivery of Notch onto the plasma membrane, causing an accumulation of Notch protein in the cytoplasm, suggesting that Sec3 is essential for the delivery of Notch onto he plasma membrane.

Notch Signaling Target Genes Are Falsely Expressed in *sec3* Mutant Follicle Cells

Cut, a DNA binding protein containing homeodomain, links Notch signaling and cell-cycle regulators. Cut is expressed in follicle cells during the early stages and is downregulated by the Notch signaling during the mid stages, which results in the cessation of mitosis and entry into the endocycle (Sun and Deng, 2005). We found that, in contrast to the wild type follicle cells, *sec3* mutant follicle cells showed continued expression of Cut beyond stage 6 (**Figures 5A–A"**). Consistent with Cut expression, CycA, the mitotic cyclin, continued to be expressed in mutant clones after stage 6, whereas wild type follicle cells demonstrated no CycA expression during these stages. Note that while CycA was detected in 50% of follicle cells in wild type egg chambers during stages 4–6, CycA was not uniformly expressed in mutant clones (**Figures 5B–B"**; Shcherbata et al., 2004).

Notch signaling also regulates the expressions of immature cell-fate markers in follicle cells. For example, in wild type egg chambers, FasciclinIII (FasIII) is expressed in all follicle cells during the early stages and then only expressed in two pairs of polar follicle cells at each end of the egg chamber by stage 4. This downregulation of FasIII marks the differentiation of the follicle cell. Reduced Notch activity catches follicle cells in an undifferentiated state and induces ectopic expression of FasIII at the late stages (Lopez-Schier and St Johnston, 2001). We observed strong expression of FasIII in cells mutant for *sec3* even after stage 6, suggesting that they were defective in Notch signaling (**Figures 5C–C**"). FasIII is also used as a marker of polar cells. However, mutant follicle cells failed to down regulate FasIII and should not be polar cells. Eyes absent (Eya) is normally detected in main-body follicle cells and absent from both polar cells and stalk cells during stage 1 to stage 8 (Bai and Montell, 2002). Immunostaining of Eya was performed and lack of Eya was not detected in mutant main-body follicle clones during stage 1 to stage 8 (**Supplementary Figure S5**).

DISCUSSION

This report demonstrates a role of *sec3* in regulating egg chamber development in *Drosophila* through Notch. This conclusion is based on results that show that: (1) a loss of *sec3* results in abnormal egg chamber development, which phenocopies Notch pathway inactivation; (2) notch accumulates in *sec3* clones; (3) target genes of Notch signaling are mis-expressed in *sec3* clones. The exocyst has been reported to have functions in the traffic of several membrane proteins, including the adhesion molecule, receptor, and the glucose transporter. However, in this study, the defect in the traffic of Notch protein does not seem to be a general one, as the exocyst is not required for all secretory events. For instance, the exocyst promotes recycling and tethering of E-Cadherin (E-Cad) containing vesicles in the *Drosophila* ovary or wing, but does not affect the distribution pattern and amount of another two polarity molecules, Baz/Par-3, and Dlg1 (Langevin et al., 2005; Wan et al., 2013). The exocyst is not required for synaptic vesicle release at mature synapses (Murthy et al., 2003). Fibrocystin, Polycystin-2, and Smoothened are transmembrane receptors localized in the ciliary membrane. The exocyst complex regulates the delivery of Fibrocystin and Polycystin-2 to the cilium, but not Smoothened (Monis et al., 2017). Moreover, Delta, the ligand of Notch, is not accumulated in *sec3* mutant cells (**Supplementary Figure S6**).

The positioning of the oocyte requires the upregulation of the E-cad in both the oocyte and the posterior follicle cells, which causes them to adhere to each other (Godt and Tepass, 1998; Gonzalez-Reyes and St Johnston, 1998). Although, it has been reported that E-cad accumulates in *sec3* mutant follicle cells (Wan et al., 2013), E-cad is not required for oocyte determination (Godt and Tepass, 1998; Gonzalez-Reyes and St Johnston, 1998), the change of protein levels of E-cad in follicle cells can change the position of the oocyte, but could not generate more than one oocyte in an egg chamber. Therefore, the compound egg chamber phenotype is not a consequence of abnormal E-cad intracellular traffic.

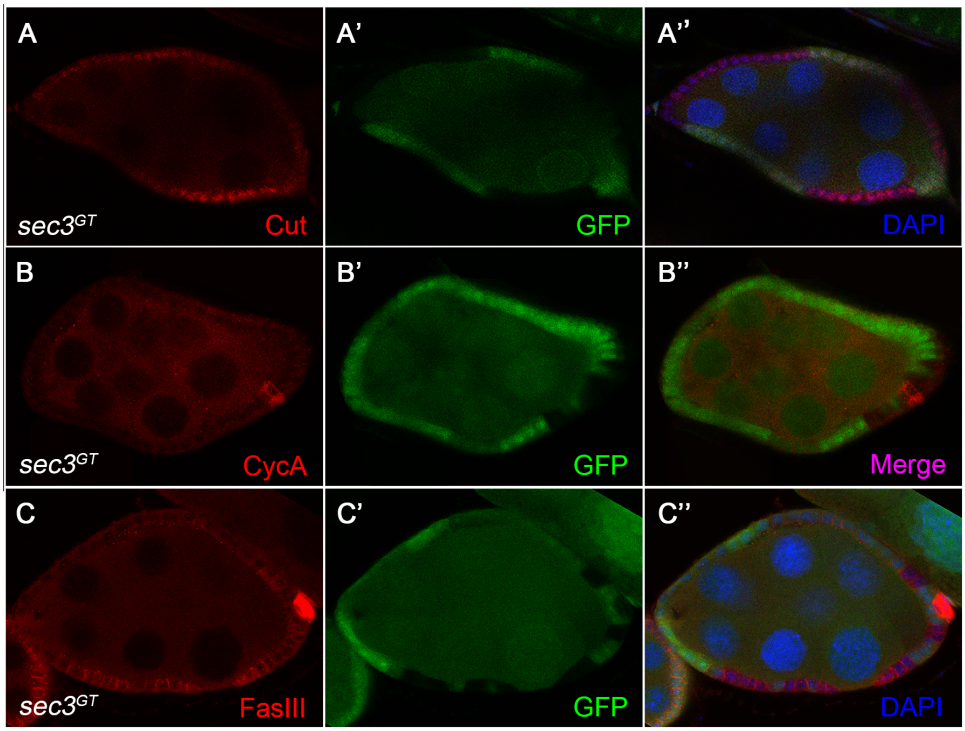

FIGURE 5 | Altered expression of Notch signaling target genes in *sec3* mutant follicle cells. **(A–A")** *sec3* mutant clones show continued expression of Cut, in contrast to the wild type follicle cells. **(B–B")** *sec3* mutant clones show continued expression of CycA, in contrast to the wild type follicle cells. Note that while CycA was detected in 50% of follicle cells in the wild type egg chambers during stages 4–6, CycA was not uniformly expressed in mutant clones. **(C–C")** *sec3* mutant clones show continued expression of FasIII, in contrast to the wild type follicle cells.

Recent studies have revealed a sophisticated regulation of the Notch receptor by vesicle trafficking. Endocytosis is important in Notch signaling as genetic interactions have been found between Notch and *shibire*, the *Drosophila* homolog of dynamin, a key regulator of endocytosis. *shibire* mutant cells may fail to internalize Notch and show Notch accumulation on the cell surface (Lu and Bilder, 2005). The Notch accumulation phenotype is also found in mutants in *avl* (*avalanche*) and *rab5*, two genes required for maturation of early endosomes (Yan et al., 2009). Active receptors can be internalized to the lysosome and degraded, which is a common mechanism of desensitization. Both NICD and NECD are detected in late endosomal compartments in *Drosophila* (Kooh et al., 1993). Rab11, a GTPase on the recycling endosomes and Sec15, another component of the exocyst complex, have functions in Delta recycling in the development of the *Drosophila* sensory organ precursor (SOP) cell lineage (Emery et al., 2005; Jafar-Nejad et al., 2005). In this study, we suppose that the accumulated Notch protein may be in recycling vesicles or in vesicles that transport from the post-Golgi to the plasma membrane. A shortcoming of this study is that we were not able to identify what kind of vesicle the Notch protein accumulated in.

Multiple intercellular signaling pathways involved in the steps of egg chamber development, and a group of mutations have shown an egg chamber fusion phenotype. In particular, reduction in *Notch* or *Delta* activity suppresses polar cell formation and results in fused egg chambers (Xu et al., 1992; Bender et al., 1993; Grammont and Irvine, 2001; Lopez-Schier and St Johnston, 2001). The polar cells signal through the JAK/STAT pathway to induce the formation of the stalk which separates adjacent cysts. Reduced JAK/STAT pathway activity results in fused egg chambers (Baksa et al., 2002; McGregor et al., 2002). The *Drosophila* gene *brainiac* (*brn*) and *egghead* (*egh*) show an identical egg chamber fusion phenotype. But they are required in the germline and not essential for differentiation of polar and stalk cells (Goode et al., 1996). The activity of the *hedgehog* (*hh*) gene stimulates the proliferation of pre-follicle somatic cells in the germarium. Reduced activity of *hh* produces compound egg chambers which result from a failure in the package of the germline cysts by somatic cells (Forbes et al., 1996). Egg chamber fusion in the *sec3* mosaic is not due to abnormal *hh* signaling, since *sec3* mutant clones can encapsulate germline cysts normally at stage 1 (**Supplementary Figure S7**). Data in this report support that the egg chamber fusion phenotype of *sec3* is due to the failure in polar cell formation for abnormal Notch activity.

In summary, this report has identified the developmental function of Sec3 and its link with Notch during *Drosophila* oogenesis. To our knowledge, this is the first report to identify a link between Sec3 and Notch. Components of the exocyst are conserved from yeast to a human, so it is conceivable that Sec3, as well as other components of the exocyst, are involved in regulating Notch in tissues of other species.

AUTHOR CONTRIBUTIONS

XW and PW designed the experiments. PW, SZ, LC, DW, and TL performed the data collection and analysis. PW and XY provided the fund. PW and XW wrote the manuscript.

FUNDING

This work was supported by the Natural Science Foundation of Jiangxi Province (20143ACB21006 and 20142BCB23028), the Science and Technology Program of the Education Department of Jiangxi Province (GJJ150802), and the National Natural Science Foundation of China (31660330 and 31460591).

ACKNOWLEDGMENTS

We thank the Bloomington *Drosophila* Stock Center, the Vienna *Drosophila* RNAi Center, and the Developmental Studies Hybridoma Bank for their *Drosophila* stocks and antibodies. We also thank St. Johnston D for the antibody reagent.

SUPPLEMENTARY MATERIAL

The Supplementary Material for this article can be found online at: https://www.frontiersin.org/articles/10.3389/fphys.2019.00345/full#supplementary-material

REFERENCES

Bai, J., and Montell, D. (2002). Eyes absent, a key repressor of polar cell fate during *Drosophila* oogenesis. *Development* 129, 5377–5388. doi: 10.1242/dev.00115

Baksa, K., Parke, T., Dobens, L. L., and Dearolf, C. R. (2002). The *Drosophila* STAT protein, stat92E, regulates follicle cell differentiation during oogenesis. *Dev. Biol.* 243, 166–175. doi: 10.1006/dbio.2001.0539

Bender, L. B., Kooh, P. J., and Muskavitch, M. A. (1993). Complex function and expression of delta during *Drosophila* oogenesis. *Genetics* 133, 967–978.

Bloch, D., Pleskot, R., Pejchar, P., Potocky, M., Trpkosova, P., Cwiklik, L., et al. (2016). Exocyst SEC3 and phosphoinositides define sites of exocytosis in pollen tube initiation and growth. *Plant Physiol.* 172, 980–1002. doi: 10.1104/pp.16.006901

Boyd, C., Hughes, T., Pypaert, M., and Novick, P. (2004). Vesicles carry most exocyst subunits to exocytic sites marked by the remaining two subunits. Sec3p and Exo70p. *J. Cell Biol.* 167, 889–901. doi: 10.1083/jcb.200408124

Deng, W. M., Althauser, C., and Ruohola-Baker, H. (2001). Notch-delta signaling induces a transition from mitotic cell cycle to endocycle in *Drosophila* follicle cells. *Development* 128, 4737–4746.

Emery, G., Hutterer, A., and Berdnik, D. (2005). Asymmetric Rab 11 endosomes regulate delta recycling and specify cell fate in the *Drosophila* nervous system. *Cell* 122, 763–773. doi: 10.1016/j.cell.2005.08.017

Finger, F. P., Hughes, T. E., and Novick, P. (1998). Sec3p is a spatial landmark for polarized secretion in budding yeast. *Cell* 92, 559–571. doi: 10.1016/S0092-8674(00)80948-4

Forbes, A. J., Lin, H., Ingham, P. W., and Spradling, A. C. (1996). hedgehog is required for the proliferation and specification of ovarian somatic cells prior to egg chamber formation in *Drosophila*. *Development* 122, 1125–1135.

Godt, D., and Tepass, U. (1998). *Drosophila* oocyte localization is mediated by differential cadherin-based adhesion. *Nature* 395, 387–391. doi: 10.1038/26493

Gonzalez-Reyes, A., and St Johnston, D. (1998). The *Drosophila* AP axis is polarised by the cadherin-mediated positioning of the oocyte. *Development* 125, 3635–3644.

Goode, S., Melnick, M., Chou, T. B., and Perrimon, N. (1996). The neurogenic genes egghead and brainiac define a novel signaling pathway essential for epithelial morphogenesis during *Drosophila* oogenesis. *Development* 122, 3863–3879.

Grammont, M., and Irvine, K. D. (2001). fringe and notch specify polar cell fate during *Drosophila* oogenesis. *Development* 128, 2243–2253.

Guo, W., Roth, D., Walch-Solimena, C., and Novick, P. (1999). The exocyst is an effector for Sec4p, targeting secretory vesicles to sites of exocytosis. *EMBO J.* 18, 1071–1080. doi: 10.1093/emboj/18.4.1071

Jafar-Nejad, H., Andrews, H. K., and Acar, M. (2005). Sec15, a component of the exocyst, promotes notch signaling during the asymmetric division of *Drosophila* sensory organ precursors. *Dev. Cell* 9, 351–363. doi: 10.1016/j.devcel.2005.06.010

Kooh, P. J., Fehon, R. G., and Muskavitch, M. A. (1993). Implications of dynamic patterns of delta and notch expression for cellular interactions during *Drosophila* development. *Development* 117, 493–507.

Kopan, R., and Ilagan, M. X. (2009). The canonical notch signaling pathway: unfolding the activation mechanism. *Cell* 137, 216–233. doi: 10.1016/j.cell.2009.03.045

Lai, E. C. (2004). Notch signaling: control of cell communication and cell fate. *Development* 131, 965–973. doi: 10.1242/dev.01074

Langevin, J., Morgan, M. J., Sibarita, J. B., Aresta, S., Murthy, M., Schwarz, T., et al. (2005). *Drosophila* exocyst components Sec5, Sec6, and Sec15 regulate DE-cadherin trafficking from recycling endosomes to the plasma membrane. *Dev. Cell* 9, 365–376. doi: 10.1016/j.devcel.2005.07.013

Lopez-Schier, H., and St Johnston, D. (2001). Delta signaling from the germ line controls the proliferation and differentiation of the somatic follicle cells during *Drosophila* oogenesis. *Genes Dev.* 15, 1393–1405. doi: 10.1101/gad.200901

Lu, H., and Bilder, D. (2005). Endocytic control of epithelial polarity and proliferation in *Drosophila*. *Nat. Cell Biol.* 7, 1232–1239. doi: 10.1038/ncb1324

McGregor, J. R., Xi, R., and Harrison, D. A. (2002). JAK signaling is somatically required for follicle cell differentiation in *Drosophila*. *Development* 129, 705–717.

Monis, W. J., Faundez, V., and Pazour, G. J. (2017). BLOC-1 is required for selective membrane protein trafficking from ensosomes to primary cilia. *J. Cell Biol.* 216, 2131–2150. doi: 10.1083/jcb.201611138

Murthy, M., Garza, D., Scheller, R. H., and Schwarz, T. L. (2003). Mutations in the exocyst component Sec5 disrupt neuronal membrane traffic, but neurotransmitter release persists. *Neuron* 37, 433–447. doi: 10.1016/S0896-6273(03)00031-X

Novick, P., Field, C., and Schekman, R. (1980). Identification of 23 complementation groups required for post-translational events in the yeast secretory pathway. *Cell* 21, 205–215. doi: 10.1016/0092-8674(80)90128-2

Shcherbata, H. R., Althauser, C., Findley, S. D., and Ruohola-Baker, H. (2004). The mitotic-to-endocycle switch in *Drosophila* follicle cells is executed by notch-dependent regulation of G1/S. G2/M and M/G1 cell-cycle transitions. *Development* 131, 3169–3181. doi: 10.1242/dev.01172

Sorkin, A., and von Zastrow, M. (2009). Endocytosis and signalling: intertwining molecular networks. *Nat. Rev. Mol. Cell Biol.* 10, 609–622. doi: 10.1038/nrm2748

Sun, J., and Deng, W. M. (2005). Notch-dependent downregulation of the homeodomain gene cut is required for the mitotic cycle/endocycle switch and cell differentiation in *Drosophila* follicle cells. *Development* 132, 4299–4308. doi: 10.1242/dev.02015

Torres, I. L., Lopez-Schier, H., and St Johnston, D. (2003). A notch/delta-dependent relay mechanism establishes anterior-posterior polarity in *Drosophila*. *Dev. Cell* 5, 547–558. doi: 10.1016/S1534-5807(03)00272-7

Vachias, C., Couderc, J. L., and Grammont, M. (2010). A two-step notch-dependant mechanism controls the selection of the polar cell pair in *Drosophila* oogenesis. *Development* 137, 2703–2711. doi: 10.1242/dev.052183

Wan, P., Wang, D., Luo, J., Chu, D., Wang, H., Zhang, L., et al. (2013). Guidance receptor promotes the asymmetric distribution of exocyst and recycling endosome during collective cell migration. *Development* 140, 4797–4806. doi: 10.1242/dev.094979

Wen, T. J., Hochholdinger, F., Sauer, M., Bruce, W., and Schnable, P. S. (2005). The roothairless1 gene of maize encodes a homolog of sec3, which is involved in polar exocytosis. *Plant Physiol.* 138, 1637–1643. doi: 10.1104/pp.105.062174

Xu, T., Caron, L. A., Fehon, R. G., and Artavanis-Tsakonas, S. (1992). The involvement of the notch locus in *Drosophila* oogenesis. *Development* 115, 913–922.

Yamashita, M., Kurokawa, K., Sato, Y., Yamagata, A., Mimura, H., Yoshikawa, A., et al. (2010). Structural basis for the Rho- and phosphoinositide-dependent localization of the exocyst subunit Sec3. *Nat. Struct. Mol. Biol.* 17, 180–186. doi: 10.1038/nsmb.1722

Yan, Y., Denef, N., and Schupbach, T. (2009). The vacuolar proton pump, V-ATPase, is required for notch signaling and endosomal trafficking in *Drosophila*. *Dev. Cell* 17, 387–402. doi: 10.1016/j.devcel.2009.07.001

Yue, P., Zhang, Y., Mei, K., Wang, S., Lesigang, J., Zhu, Y., et al. (2017). Sec3 promotes the initial binary t-SNARE complex assembly and membrane fusion. *Nat. Commun.* 8:14236. doi: 10.1038/ncomms14236

Zhang, X., Orlando, K., He, B., Xi, F., Zhang, J., Zajac, A., et al. (2008). Membrane association and functional regulation of Sec3 by phospholipids and Cdc42. *J. Cell Biol.* 180, 145–158. doi: 10.1083/jcb.200704128

Zhang, X., Wang, P., Gangar, A., Zhang, J., Brennwald, P., Terbush, D., et al. (2005). Lethal giant larvae proteins interact with the exocyst complex and are involved in polarized exocytosis. *J. Cell. Biol.* 170, 273–283. doi: 10.1083/jcb.200502055

Zhang, Y., Immink, R., Liu, C. M., Emons, A. M., and Ketelaar, T. (2013). The *Arabidopsis* exocyst subunit SEC3A is essential for embryo development and accumulates in transient puncta at the plasma membrane. *New Phytol.* 199, 74–88. doi: 10.1111/nph.12236

Conflict of Interest Statement: The authors declare that the research was conducted in the absence of any commercial or financial relationships that could be construed as a potential conflict of interest.

frontiers in Physiology

BRIEF RESEARCH REPORT
published: 04 April 2019
doi: 10.3389/fphys.2019.00383

Depletion of ATP-Citrate Lyase (ATPCL) Affects Chromosome Integrity Without Altering Histone Acetylation in *Drosophila* Mitotic Cells

*Patrizia Morciano[1†‡], Maria Laura Di Giorgio[1‡], Antonella Porrazzo[1,2], Valerio Licursi[3], Rodolfo Negri[1,4], Yikang Rong[5] and Giovanni Cenci[1,2]**

[1] Dipartimento di Biologia e Biotecnologie "Charles Darwin", Sapienza – Università di Roma, Rome, Italy, [2] Istituto Pasteur Italia - Fondazione Cenci Bolognetti, Rome, Italy, [3] Istituto di Analisi dei Sistemi ed Informatica "Antonio Ruberti", Consiglio Nazionale delle Ricerche, Rome, Italy, [4] Istituto di Biologia e Patologia Molecolari (IBPM) del CNR, Rome, Italy, [5] School of Life Sciences, State Key Laboratory of Biocontrol, Sun Yat-sen University, Guangzhou, China

OPEN ACCESS

Edited by:
Paola Cusumano,
University of Padua, Italy

Reviewed by:
Aram Megighian,
University of Padua, Italy
Angelique Christine Paulk,
Massachusetts General Hospital and Harvard Medical School,
United States

***Correspondence:**
Giovanni Cenci
giovanni.cenci@uniroma1.it

†Present address:
Patrizia Morciano,
INFN – Laboratori Nazionali del Gran Sasso, L'Aquila, Italy

‡These authors have contributed equally to this work

Specialty section:
This article was submitted to Invertebrate Physiology, a section of the journal Frontiers in Physiology

Received: 29 December 2018
Accepted: 21 March 2019
Published: 04 April 2019

Citation:
Morciano P, Di Giorgio ML, Porrazzo A, Licursi V, Negri R, Rong Y and Cenci G (2019) Depletion of ATP-Citrate Lyase (ATPCL) Affects Chromosome Integrity Without Altering Histone Acetylation in Drosophila Mitotic Cells. Front. Physiol. 10:383. doi: 10.3389/fphys.2019.00383

The Citrate Lyase (ACL) is the main cytosolic enzyme that converts the citrate exported from mitochondria by the SLC25A1 carrier in Acetyl Coenzyme A (acetyl-CoA) and oxaloacetate. Acetyl-CoA is a high-energy intermediate common to a large number of metabolic processes including protein acetylation reactions. This renders ACL a key regulator of histone acetylation levels and gene expression in diverse organisms including humans. We have found that depletion of ATPCL, the Drosophila ortholog of human ACL, reduced levels of Acetyl CoA but, unlike its human counterpart, does not affect global histone acetylation and gene expression. Nevertheless, reduced ATPCL levels caused evident, although moderate, mitotic chromosome breakage suggesting that this enzyme plays a partial role in chromosome stability. These defects did not increase upon X-ray irradiation, indicating that they are not dependent on an impairment of DNA repair. Interestingly, depletion of ATPCL drastically increased the frequency of chromosome breaks (CBs) associated to mutations in *scheggia,* which encodes the ortholog of the mitochondrial citrate carrier SLC25A1 that is also required for chromosome integrity and histone acetylation. Our results indicate that ATPCL has a dispensable role in histone acetylation and prevents massive chromosome fragmentation when citrate efflux is altered.

Keywords: citrate lyase, Drosophila chromosomes, histone acetylation, acetyl-CoA, Drosophila

INTRODUCTION

Acetyl coenzyme A (acetyl-CoA) is a high-energy intermediate common to a large number of metabolic processes, including lipogenesis and cholesterogenesis that take place in different intracellular compartments. Acetyl-CoA is also required for protein acetylation reactions, which are important in post-translation modifications of proteins such as histones.

Acetyl coenzyme A may be synthesized in mitochondria and exported to the cytosol. This transport is strictly dependent on the citrate-malate-pyruvate shuttle. For this process, mitochondrial acetyl-CoA is first condensed with oxaloacetate by citrate synthase thus producing citrate and free CoA. Citrate is then exported to the cytosol through the mitochondrial citrate

carrier SLC25A1. Here, acetyl-CoA generation is mediated by the activity of the ATP-cytrate lyase (ACL), which catalyzes the ATP-dependent cleavage of mitochondrial-derived citrate into oxaloacetate and acetyl-CoA (Chypre et al., 2012). Finally, the malate dehydrogenase 1, NAD (soluble; MDH1) converts cytosolic oxaloacetate by catalyzing the NADH-dependent synthesis of malate, which is transported back to the mitochondria through SLC25A10, an inorganic phosphate/dicarboxylate antiporter. Given its key role in the production of cytosolic acetyl-CoA, it is not surprising that ACL serves several and crucial functions in mammal metabolism (Wellen et al., 2009; Lee et al., 2014, 2015; Das et al., 2015; Covarrubias et al., 2016; Deb et al., 2017; Chen et al., 2018; White et al., 2018).

Although ACL resides mainly in the endoplasmic reticulum in mammalian cells (Chypre et al., 2012), it can be found also in the nucleus (Wellen et al., 2009). Here, as citrate can diffuse through the nuclear membrane, it produces acetyl-CoA, which is directly required to promote histone acetylation and regulate gene expression in response to growth factor stimulation and during differentiation (Wellen et al., 2009). ACL has been recently shown to be phosphorylated at S455 downstream of ataxia telangiectasia mutated (ATM) and AKT following DNA damage (Sivanand et al., 2017). This phosphorylation is necessary for BRCA1 recruitment and DNA repair by homologous recombination and identifies ACL as a molecular player in the DNA damage response.

A large amount of evidence indicate that ACL is upregulated or activated in several types of cancer (Zaidi et al., 2012b). Cancer cells rely on glucose as major carbon source for *de novo* fatty acid synthesis. Glycolysis generates citrate by tricarboxylic acid (TCA) cycle, the citrate is preferentially exported from mitochondria to cytosol and then cleaved by ACL to produce cytosolic acetyl-CoA, the building block for *de novo* lipid synthesis. Thus, by coupling energy metabolism with fatty acids synthesis, ACL plays a critical role in supporting cancer cell growth. It is not therefore unexpected that inhibition of ACL dramatically suppresses tumor cell proliferation (Zaidi et al., 2012a; Migita et al., 2013, 2014; Gao et al., 2014; Lee et al., 2015; Wang et al., 2017; Granchi, 2018).

Here we show that depletion of ATPCL, the Drosophila ortholog of human ACL, leads to a moderate frequency of chromosome breaks (CBs) indicating that this enzyme is partially required for chromosome stability in mitotic cells. Interestingly, the number of CBs is substantially enhanced when the export of citrate from mitochondria is inhibited suggesting that the ATPCL role on chromosome integrity is essential when cytosolic citrate is limited. We also show that *ATPCL* mutants exhibit decreased levels of Acetyl CoA but this reduction does not affect global histone acetylation and gene expression. This indicates that, unlike its human counterpart, the role of ATPCL in Drosophila histone acetylation could be redundant.

RESULTS

The Drosophila ATP Cytrate Lyase

We previously demonstrated that perturbation in the citrate metabolism leads to genome instability in both Drosophila and human cells as consequence of reduced Acetyl-CoA production (Morciano et al., 2009). To further understand the contribution of the acetyl-CoA metabolism to the maintenance of genome stability, we focused our characterization on the ATP Cytrate Lyase. This enzyme cleaves TCA-derived citrate in oxaloacetate OAA (that in turn is converted into malate in order to re-entry in the mitochondria) and catalyzes the formation of acetyl-CoA in the presence of ATP. In *Drosophila*, the citrate lyase-encoding gene (*CG8322*, FBgn0020236) maps on 52D9-11 chromosome 2 region and consists of 10 exons (including the 5′ and 3′ UTR sequences) that, according to the FlyBase annotation, specifies four potential transcripts (namely *ATPCL-RD, -RE, -RG*, and *-RF*) that retain all exons albeit with few differences (**Supplementary Text**). Our RT-PCR and sequencing analysis confirmed the presence of these different transcripts (**Supplementary Text**). Moreover, qPCR revealed that *ATPCL-RD* and *RF* are poorly expressed with respect to *ATPCL-RD/RE* suggesting that ATPCL-PD/PE is the most representative *ATPCL* gene product (**Figure 1B**). Despite the differences in the exons 6, all transcripts encode almost identical ATPCL proteins that overall shares 70% of identity with the human counterpart, hACL. It is therefore conceivable that ATPCL is also functionally analogous to hACL (see also below).

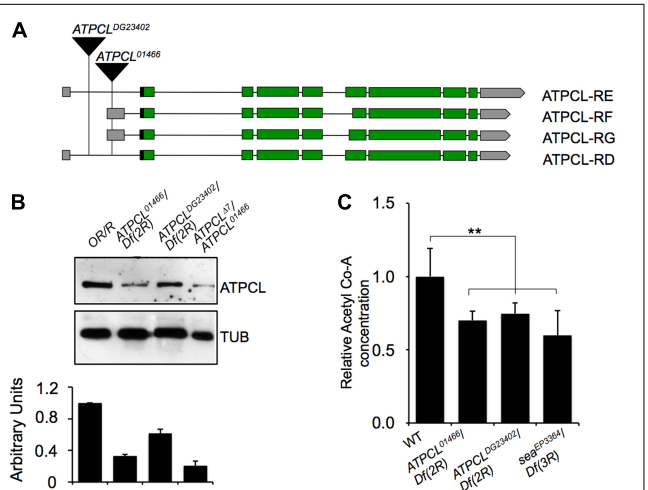

FIGURE 1 | Molecular analysis of *ATPCL* mutations. **(A)** An analysis of the published DNA sequence reveals that ATPCL-encoding gene *CG8322* specifies four potential transcripts RD, RE, RF and RG. The black triangles indicate the position of the *P{PZ}ATPCL*^{01466} and *P{wHy}ATPCL*^{DG23402} insertions in the *ATPCL* locus referred as *ATPCL*^{01466} and *ATPCL*^{DG23402}, respectively. Green boxes: encoding exons; gray boxes: UTR-containing exons; horizontal black lines: introns. **(B)** Western blot of third instar larvae brain extracts from control *(OR/R)* and *ATPCL* mutants. The anti-ATPCL antibody recognizes a ∼130 KDa band which is significantly reduced in all *ATPCL* mutant combinations. *Df (2R)* is the *Df(2R)Exel7138* deficiency that removes *ATPCL*. Tubulin is used as a loading control. The bottom figure illustrates the quantification analysis of ATPCL levels, which has been based on band intensities of three independent WBs (biological replicates). Bars indicate standard deviation. **(C)** Reduced levels of Acetyl CoA in *ATPCL* mutants. Columns indicate the percentage of Acetyl-CoA quantification (pmol/ml) in both *ATPCL*^{DG23402} and *ATPCL*^{DG23402} hemizygotes with respect to OR/R (control; $*p < 0.01$, Student *t*-test). Bars show SD.

We obtained from the Bloomington stock center two putative P-element induced *ATPCL* mutant alleles, $ATPCL^{01466}$ and $ATPCL^{DG23042}$. Our PCR analysis confirmed that $ATPCL^{01466}$ and $ATPCL^{DG23042}$ are located within the 5′ UTR of the gene at position −340 and −1167 upstream of the translation initiation site, respectively (**Figure 1A**). $ATPCL^{01466}$ homozygotes and $ATPCL^{01466}$/ *Df(2R)Exel7138* hemizygotes (*Df(2R)Exel7138* is a deficiency in the 52D1-52D12 polytene region that removes *ATPCL*) were late lethal while either $ATPCL^{DG23042}$ homozygotes and hemizygotes displayed semi-lethality. By mobilizing the $ATPCL^{DG23042}$ P-element, we generated an additional lethal *ATPCL* mutant allele (Δ7), which potentially bears partial deletions of the gene and severely affected ATPCL expression (see below). This suggests that loss of function of *ATPCL* might prevent development as it occurs also for ACL knock-out mice (Beigneux et al., 2004). Finally, the expression of a wild type *UAS ATPCL* transgene under the control of a *TubGal4* promoter in $ATPCL^{DG23042}$ or $ATPCL^{01466}$ mutant background rescued the late lethality and CBs (see section "Materials and Methods") confirming that both phenotypes are due to lesions in the *ATPCL* gene.

We have generated a guinea pig anti ATPCL polyclonal antibody that in Western blotting (WB) analysis on larval brain extracts detected a band of expected size (∼130 KDa), which decreased in *ATPCL* mutants (**Figure 1B**). $ATPCL^{01466}/ATPCL^{\Delta 7}$ *trans* heterozygotes yielded to the strongest reduction (∼80%) of expression of the ATPCL protein indicating that this mutant allele combination represents the most severe condition (**Figure 1B**). Immunofluorescence (IF) on larval neuroblasts with the same anti-ATPCL antibody revealed that ATPCL exhibits a punctuate localization pattern both in the cytoplasm and nucleus, which is absent from mutant cells (**Supplementary Figure 2**). However, as cells enter mitosis, ATPCL is excluded from the portion of nucleus containing chromatin and is retained predominantly in the cytoplasm. This pattern is clearly visible in either metaphase or ana-telophase in which ATPCL is enriched in the entire cell except the portion surrounding the dividing chromosomes (**Supplementary Figure 2**). Thus, like its human counterpart (Wellen et al., 2009), ATPCL localizes to the cytoplasm and the nucleus in interphase. Moreover, the nuclear localization changes during mitosis.

Finally, our fluorometric analysis revealed that Acetyl-CoA levels are ∼40% reduced in *ATPCL* mutants with respect to wild-type (1.30 pm/μl) indicating that, similarly to its mammalian counterpart, ATPCL is required for Acetyl-CoA synthesis (**Figure 1C**).

The ATPCL Role in Mitosis

In the citrate-dependent Acetyl CoA biosynthesis, ACL works downstream the citrate mitochondria carrier SLC25A1 (see section "Introduction"). As SLC25A1 and Scheggia (*Sea*, the SLC25A1 fly ortholog) are required for chromosome integrity in mammalian and Drosophila cells, respectively (Morciano et al., 2009), we asked if also ATPCL was involved in the same process. The analysis of DAPI-stained colchicine-treated mitotic neuroblasts from the different *ATPCL* mutant larval brains revealed that *ATPCL* mutants exhibited a moderate, although statistically significant, number of CBs (2.5–4.5%; Total Cells = 250; **Figure 2**). Moreover 2 Gy X-ray exposure did not enhance the number of CBs of *ATPCL* mutants indicating that they do not result from defective DNA repair (**Figure 2B**). However, WB and IF analyses using anti-acetylated H4 and H3 histones indicated that the overall histone acetylation in all *ATPCL* mutants was not significantly affected (**Supplementary Figure 3**). Although it cannot be ruled out the possibility that reduction of histone acetylation occurs at damaged sites, our

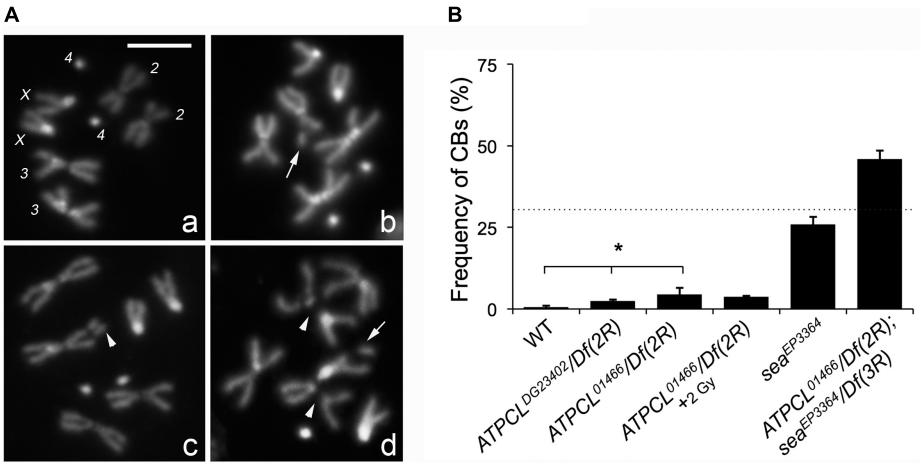

FIGURE 2 | Depletion of ATPCL yields to chromosome breaks (CBs). **(A)** DAPI-stained female metaphases from larval neuroblasts of control (Oregon R, **a**), *ATPCL* mutants **(b,c)** and *ATPCL, sea* double mutants **(d)**. Numbers in **(a)** indicate chromosomes X, 2, 3, and 4 of a normal female caryotype. White arrows and arrowheads indicated chromatid and CBs, respectively. Bar: 5 μm. **(B)** Frequency of CBs in *ATPCL* mutants. All *ATPCL* mutants exhibit a moderated (although statistically significant) frequency of CBs, which are almost absent in control cells (*$p < 0.05$, Student *t*-test). CBs frequency is not influenced by a 2 Gy X-ray irradiation. Note that the frequency of CBs in *ATPCL; sea* double mutants is higher than the sum of CB frequencies observed in either *ATPCL* or *sea* single mutants (indicated by the dotted line) suggesting a synergistic effect. ∼200 cells (4 slides) for mutant combinations and ∼500 (5 slides) for Oregon R (control) were analyzed. See text for further details. Bars refer to SD.

observations suggest that chromosome defects are not dependent on a general reduction of histone acetylation. We then verified whether *ATPCL* and *scheggia* (*sea*) could genetically interact. The cytological analysis of mitotic metaphases from late lethal *ATPCL sea* double mutants revealed that CBs frequency is synergistically increased (∼46%; Total Cells = 180) with respect to the sum of break frequencies of both *ATPCL* (4.5%) and *sea* ∼25%; (Total Cells = 200; **Figure 2B**). This indicates that ATPCL prevents genome instability when certain intracellular metabolites (i.e., citrate) are limited.

ATPCL Is Not Required for Global Gene Transcription

We next asked whether loss of ATPCL could at least influence the expression of potential ATPCL-responsive mitotic genes. Thus we extracted RNA from either wild-type or *ATPCL* mutant brains, labeled, and hybridized to CDMC 14K Drosophila arrays (Canadian Drosophila Microarray Center, Toronto, Canada). Surprisingly, only ∼5% (772) of the genes significantly changed their transcriptional profile indicating that loss of *ATPCL* only marginally affected global gene transcription. Of these, approximately 23% (182) were > 2-fold either down- or up-regulated (**Supplementary Table S1**). Gene ontology (GO) revealed a clear functional bias toward brain development and behavior gene categories indicating a potential requirement of ATPCL in the regulation of nervous system genes (**Supplementary Figure 4**). However, based on these results, we cannot discriminate whether the change in gene expression is a direct consequence of the loss of histone acetylation rather than that of secondary responses to metabolic alterations induced by loss of acetyl-CoA. Yet, as microarrays were probed with larval brain RNA we cannot exclude that the observed trends on brain development might reflect a tissue-specific function of ATPCL in gene regulation.

DISCUSSION

Here we have molecularly characterized for the first time *ATPCL* that encodes the Drosophila ortholog of human ATP citrate lyase. We have shown that, consistently with previous findings in other organisms including mammals, mutations in the *ATPCL* reduce cytosolic acetyl-CoA confirming that ACL has an evolutionarily conserved role in Acetyl-CoA biosynthesis. However, despite *Drosophila ATPCL* mutants exhibit an evident, although moderate, mitotic chromosome breakage phenotype, depletion of ATPCL, unlike human cells, has not a general impact on histone acetylation in flies suggesting that it role in histone acetylation is either partially redundant in Drosophila or compensated by alternative pathways (i.e., from acetate by acyl-CoA synthetases). However, it cannot be ruled out the possibility that ATPCL could be required for the acetylation of either nuclear or cytoplasmic factors, instead of histones, that in turn are required for chromosome integrity. Alternatively, as ATPCL plays a direct role in the homeostasis of lipids, whose modifications (i.e., peroxidation) are also required to modulate DNA repair (Tudek et al., 2017), it is possible that *ATPCL* mutants defects on chromosome integrity could arise as a consequence of protein acetylation-independent activity. Proteomic studies will be fundamental to verify these hypotheses.

We have previously demonstrated that mutations in the mitochondrial citrate carrier Sea/SLC25A1, led to frequent CBs in Drosophila mitotic cells (Morciano et al., 2009). The finding that perturbation of ATPCL, a key component of the pathway that from citrate generates Acetyl-CoA, affected mitosis only marginally was therefore unexpected. Moreover, our WB analysis revealed that, unlike Sea/SLC25A1, ATPCL is not required for the acetylation of histones, which could be required for chromosome integrity. However, this does not exclude that a decreased acetyl-CoA concentration could affect the local kinetics of HAT-dependent histone acetylation at selected genomic loci and/or damaged sites thus leading to specific changes in histone acetylation. Finally, our transcriptomic analysis that indicates that depletion of ATPCL has a modest modulatory effect on transcription, limited to few classes of genes (although with a bias toward brain development functions), further sustains the view that loss of ATPCL has a minimal effect on bulk chromatin histone acetylation.

The different effect of loss of Sea and ATPCL on Drosophila chromosome integrity is intriguing. This is not due to the molecular nature of mutant alleles of either *sea* or *ATPCL,* which are almost genetically null and exhibited a strong reduction of corresponding transcripts. It is conceivable that citrate deprivation in *sea* mutants causes much greater effects than reduction of Acetyl-CoA in *ATPCL* mutants. Indeed, citrate may play different tissue-specific metabolic roles and function as a general chelator of physiologically important cations. Thus its deprivation in the cytosol may compromise several intracellular pathways. Citrate reduction as consequence of inhibition of Sea/SLC25A1 transport activity might also inhibit *ATPCL* activity and/or expression thus exacerbating the *ATPCL* mutant phenotype. It has been recently demonstrated that in Drosophila citrate may indeed regulate a feedback mechanism that coordinates intracellular metabolism with glycolysis and TCA cycle (Li et al., 2018). It could be important to understand whether this metabolic feedback loop may also involve ATPCL. Our findings that *ATPCL* depletion in *sea* mutants yields to a synergic CBs phenotype suggest that ATPCL prevents chromosome fragmentation when citrate metabolism is impaired.

The mild phenotype associated with loss of ATPCL in Drosophila does not preclude the possibility that also the overexpression of ATPCL may impact Drosophila somatic cell proliferation. Overexpression of the human ortholog ACL supports cancer growth by fueling the glucose-dependent *de novo* lipogenesis. Whether a similar histone-acetylation independent effect takes place also in Drosophila will be an interesting issue to address in the future.

AUTHOR CONTRIBUTIONS

PM, MDG, and AP performed gene characterization and mutants analysis. VL and RN carried out the microarray analysis.

YR supervised gene characterization and discussed the data. GC supervised the experiments and wrote the manuscript.

FUNDING

This work has been supported by a grant from Italian Association for Cancer Research (AIRC, IG8589), Fondazione Cenci Bolognetti-Istituto Pasteur Roma and Pasteur Institute of Paris (PTR N. 24-17) to GC.

ACKNOWLEDGMENTS

We thank Sara Saraniero for her help in the qRNA analysis.

SUPPLEMENTARY MATERIAL

The Supplementary Material for this article can be found online at: https://www.frontiersin.org/articles/10.3389/fphys.2019.00383/full#supplementary-material

REFERENCES

Beigneux, A. P., Kosinski, C., Gavino, B., Horton, J. D., Skarnes, W. C., and Young, S. G. (2004). ATP-citrate lyase deficiency in the mouse. *J. Biol. Chem.* 279, 9557–9564. doi: 10.1074/jbc.M310512200

Chen, L. Y., Lotz, M., Terkeltaub, R., and Liu-Bryan, R. (2018). Modulation of matrix metabolism by ATP-citrate lyase in articular chondrocytes. *J. Biol. Chem.* 293, 12259–12270. doi: 10.1074/jbc.RA118.002261

Chypre, M., Zaidi, N., and Smans, K. (2012). ATP-citrate lyase: a mini-review. *Biochem. Biophys. Res. Commun.* 422, 1–4. doi: 10.1016/j.bbrc.2012.04.144

Covarrubias, A. J., Aksoylar, H. I., Yu, J., Snyder, N. W., Worth, A. J., Iyer, S. S., et al. (2016). Akt-mTORC1 signaling regulates Acly to integrate metabolic input to control of macrophage activation. *eLife* 5:e11612. doi: 10.7554/eLife.11612

Das, S., Morvan, F., Jourde, B., Meier, V., Kahle, P., Brebbia, P., et al. (2015). ATP citrate lyase improves mitochondrial function in skeletal muscle. *Cell Metab.* 21, 868–876. doi: 10.1016/j.cmet.2015.05.006

Deb, D. K., Chen, Y., Sun, J., Wang, Y., and Li, Y. C. (2017). ATP-citrate lyase is essential for high glucose-induced histone hyperacetylation and fibrogenic gene upregulation in mesangial cells. *Am. J. Physiol. Renal. Physiol.* 313, F423–F429. doi: 10.1152/ajprenal.00029.2017

Gao, Y., Islam, M. S., Tian, J., Lui, V. W., and Xiao, D. (2014). Inactivation of ATP citrate lyase by Cucurbitacin B: a bioactive compound from cucumber, inhibits prostate cancer growth. *Cancer Lett.* 349, 15–25. doi: 10.1016/j.canlet.2014.03.015

Granchi, C. (2018). ATP citrate lyase (ACLY) inhibitors: an anti-cancer strategy at the crossroads of glucose and lipid metabolism. *Eur. J. Med. Chem.* 157, 1276–1291. doi: 10.1016/j.ejmech.2018.09.001

Lee, J. H., Jang, H., Lee, S. M., Lee, J. E., Choi, J., Kim, T. W., et al. (2015). ATP-citrate lyase regulates cellular senescence via an AMPK- and p53-dependent pathway. *FEBS J.* 282, 361–371. doi: 10.1111/febs.13139

Lee, J. V., Carrer, A., Shah, S., Snyder, N. W., Wei, S., Venneti, S., et al. (2014). Akt-dependent metabolic reprogramming regulates tumor cell histone acetylation. *Cell Metab.* 20, 306–319. doi: 10.1016/j.cmet.2014.06.004

Li, H., Hurlburt, A. J., and Tennessen, J. M. (2018). A Drosophila model of combined D-2- and L-2-hydroxyglutaric aciduria reveals a mechanism linking mitochondrial citrate export with oncometabolite accumulation. *Dis. Model. Mech.* 11:dmm035337. doi: 10.1242/dmm.035337

Migita, T., Okabe, S., Ikeda, K., Igarashi, S., Sugawara, S., Tomida, A., et al. (2013). Inhibition of ATP citrate lyase induces an anticancer effect via reactive oxygen species: AMPK as a predictive biomarker for therapeutic impact. *Am. J. Pathol.* 182, 1800–1810. doi: 10.1016/j.ajpath.2013.01.048

Migita, T., Okabe, S., Ikeda, K., Igarashi, S., Sugawara, S., Tomida, A., et al. (2014). Inhibition of ATP citrate lyase induces triglyceride accumulation with altered fatty acid composition in cancer cells. *Int. J. Cancer* 135, 37–47. doi: 10.1002/ijc.28652

Morciano, P., Carrisi, C., Capobianco, L., Mannini, L., Burgio, G., Cestra, G., et al. (2009). A conserved role for the mitochondrial citrate transporter Sea/SLC25A1 in the maintenance of chromosome integrity. *Hum. Mol. Genet.* 18, 4180–4188. doi: 10.1093/hmg/ddp370

Sivanand, S., Rhoades, S., Jiang, Q., Lee, J. V., Benci, J., Zhang, J., et al. (2017). Nuclear Acetyl-CoA production by ACLY promotes homologous recombination. *Mol. Cell* 67, 252–265.e6. doi: 10.1016/j.molcel.2017.06.008

Tudek, B., Zdżalik-Bielecka, D., Tudek, A., Kosicki, K., Fabisiewicz, A., and Speina, E. (2017). Lipid peroxidation in face of DNA damage, DNA repair and other cellular processes. *Free Radic. Biol. Med.* 107, 77–89. doi: 10.1016/j.freeradbiomed.2016.11.043

Wang, D., Yin, L., Wei, J., Yang, Z., and Jiang, G. (2017). ATP citrate lyase is increased in human breast cancer, depletion of which promotes apoptosis. *Tumour Biol.* 39:1010428317698338. doi: 10.1177/1010428317698338

Wellen, K. E., Hatzivassiliou, G., Sachdeva, U. M., Bui, T. V., Cross, J. R., and Thompson, C. B. (2009). ATP-citrate lyase links cellular metabolism to histone acetylation. *Science* 324, 1076–1080. doi: 10.1126/science.1164097

White, P. J., Mcgarrah, R. W., Grimsrud, P. A., Tso, S. C., Yang, W. H., Haldeman, J. M., et al. (2018). The BCKDH kinase and phosphatase integrate BCAA and lipid metabolism via regulation of ATP-citrate lyase. *Cell Metab.* 27, 1281–1293.e7. doi: 10.1016/j.cmet.2018.04.015

Zaidi, N., Royaux, I., Swinnen, J. V., and Smans, K. (2012a). ATP citrate lyase knockdown induces growth arrest and apoptosis through different cell- and environment-dependent mechanisms. *Mol. Cancer Ther.* 11, 1925–1935. doi: 10.1158/1535-7163.MCT-12-0095

Zaidi, N., Swinnen, J. V., and Smans, K. (2012b). ATP-citrate lyase: a key player in cancer metabolism. *Cancer Res.* 72, 3709–3714. doi: 10.1158/0008-5472.CAN-11-4112

Conflict of Interest Statement: The authors declare that the research was conducted in the absence of any commercial or financial relationships that could be construed as a potential conflict of interest.

frontiers in Physiology

DATA REPORT
published: 21 May 2019
doi: 10.3389/fphys.2019.00619

Comparative Expression Profiling of Wild Type *Drosophila* Malpighian Tubules and *von Hippel-Lindau* Haploinsufficient Mutant

Marilena Ignesti[1]*, *Davide Andrenacci*[2,3], *Bettina Fischer*[4,5], *Valeria Cavaliere*[1] and *Giuseppe Gargiulo*[1]*

[1] Dipartimento di Farmacia e Biotecnologie, Alma Mater Studiorum Università di Bologna, Bologna, Italy, [2] CNR Istituto di Genetica Molecolare, Unità di Bologna, Bologna, Italy, [3] IRCCS, Istituto Ortopedico Rizzoli, Bologna, Italy, [4] Department of Genetics, University of Cambridge, Cambridge, United Kingdom, [5] Cambridge Systems Biology Centre, University of Cambridge, Cambridge, United Kingdom

Keywords: microarray analysis, *Drosophila VHL*, renal carcinoma, kidney, sensitized genetic background

OPEN ACCESS

Edited by:
Cristiano De Pitta, University of Padova, Italy

Reviewed by:
Stefano Cagnin, University of Padova, Italy
Ugo Ala, University of Turin, Italy

***Correspondence:**
Marilena Ignesti
marilena.ignesti@unibo.it
Giuseppe Gargiulo
giuseppe.gargiulo@unibo.it

Specialty section:
This article was submitted to Invertebrate Physiology, a section of the journal Frontiers in Physiology

Received: *28 December 2018*
Accepted: *02 May 2019*
Published: *21 May 2019*

Citation:
Ignesti M, Andrenacci D, Fischer B, Cavaliere V and Gargiulo G (2019) Comparative Expression Profiling of Wild Type Drosophila Malpighian Tubules and von Hippel-Lindau Haploinsufficient Mutant. Front. Physiol. 10:619. doi: 10.3389/fphys.2019.00619

INTRODUCTION

The von-Hippel Lindau (VHL) disease is a hereditary genetic disorder that predisposes to the onset of several highly vascularized benign and malignant tumors, developing with elevate frequency in the central nervous system and kidneys. The most-aggressive VHL tumor is ccRCC, the clear-cell renal cell carcinoma, affecting the kidney. VHL disease etiology can be attributed to the inheritance of a *VHL* loss-of-function allele, typically a deletion (Gnarra et al., 1994; Herman et al., 1994); this facilitates the somatic inactivation of the other allele (through amorphic mutations or gene silencing through promoter methylation), leading to the onset of the tumorous phenotype (Latif et al., 1993). This reveals the haploinsufficient behavior of the *VHL* gene.

The high vascularization of VHL tumors can be explained considering that human VHL protein is the substrate-binding subunit of an E3 ubiquitin ligase (Lonergan et al., 1998; Iwai et al., 1999; Kamura et al., 1999) involved in the poly-ubiquitination of HIF-1α transcription factor. This post-translational modification leads HIF-1α to proteosomal degradation (Maxwell et al., 1999). Loss of *VHL* function causes the stabilization of HIF-1α, triggering cellular response and adaptation to hypoxic conditions (expression of genes involved in glycolysis, angiogenesis and erythropoiesis) (Bader and Hsu, 2012). While this represents the canonical function of VHL, other HIF-1α-independent function of VHL have been identified, thanks to the contribution of model organisms (Hsu, 2012). Indeed, *VHL* gene function is conserved and also *Drosophila* has a *VHL* homolog, the *dVHL* gene (Adryan et al., 2000; Aso et al., 2000). *dVHL* is involved in the development of *Drosophila* vascular system (Adryan et al., 2000; Hsouna et al., 2010) and in morphogenesis of follicular epithelium of the egg chamber (Duchi et al., 2010). Interestingly, some *VHL* functions are mediated by Awd, an endocytic mediator whose human orthologs are NME1/2 metastasis suppressors (Rosengard et al., 1989). Awd is broadly required during *Drosophila* development since it is involved in epithelial morphogenesis (Nallamothu et al., 2008; Woolworth et al., 2009; Ignesti et al., 2014) and required for maintaining genomic stability (Romani et al., 2017). Moreover, Awd is also present into the extracellular fluids of *Drosophila* larvae (Romani et al., 2016, 2018).

In *Drosophila*, two pairs of monolayered epithelial Malpighian tubules, each composed of 100-150 cells, absolve to osmoregulation and excretion functions (Denholm and Skaer, 2009). Transcriptomic analysis of Malpighian tubules revealed that among genes that are here enriched there are homologs of human genes implicated into renal pathologies (Wang et al., 2004). This justifies the use of *Drosophila* Malpighian tubules as model system to gain insights into pathophysiology of human kidneys (Dow and Romero, 2010; Miller et al., 2013).

The $dVHL^{1.1}$ allele is a loss of function mutation of the *dVHL* locus (Duchi et al., 2010; Hsouna et al., 2010). $dVHL^{1.1}/+$ flies mimic the genetic condition of VHL patients. We carried out a genome-wide gene expression profiling of whole Malpighian tubules dissected from *Drosophila* females both heterozygous for the $dVHL^{1.1}$ mutation and with two wild type copies of the *dVHL* gene. The comparison of differentially expressed genes in the two genetic backgrounds potentially allows to identify genes that are sensible to *dVHL* functional copy number. Quality control assessments of the data were performed and results obtained from the differential expression analysis were confirmed by qRT-PCR. With this approach we aimed to provide a well-controlled dataset for a better understanding of the VHL disease. Indeed, even if further molecular and functional characterization are needed, human homologs of the differentially expressed genes, if existing, could have a role in the somatic inactivation of the wild type copy of *VHL* and/or into the very first phase of cancer onset.

MATERIALS AND METHODS

Drosophila Stocks and Genotypes

Drosophila flies were raised at 25°C on a standard cornmeal/yeast/agar culture medium. We used y^1,w^{67c23} flies as wild type stock. The $dVHL^{1.1}$ null mutation has been previously characterized (Duchi et al., 2010; Hsouna et al., 2010).

Malpighian Tubules RNA Extraction

Fifty *Drosophila* females of the appropriate genotype ($dVHL^{1.1}/+$ or wild type flies) were transferred every day into vials with fresh yeasted food for 5 days. Malpighian tubules were then dissected and 400 μl of TRIzol were added. Homogenization was performed keeping samples on ice. 10 μg of linear polyacrylamide were added before centrifuging at 16,000 g (10 min). 80 μl of chloroform were added to supernatant. Sample was vortexed for 60 s and then centrifuged at 16,000 g (15 min). The upper phase was transferred to a new RNase-free tube. 0.8 volumes of isopropanol were added. RNA was then precipitated for 1 h at −20 μC and pelleted by centrifugation at 16,000 g (30 min). Pellet was then washed with 500 μl of 70% ethanol and centrifuged at 16,000g (5 min). Ethanol was then removed and pellet re-suspended in 15 μl of DEPC water. RNA concentration and purity was assessed through NanoDrop spectrophotometer.

cDNA Generation, Amplification, and Labeling

Four biological replicates were performed. Five Hundred nana gram of RNA were amplified using the SMARTer™ PCR cDNA synthesis kit (Clontech) following manufacture's instruction. Amplified cDNA was then labeled by using the Klenow labeling of double stranded DNA protocol. The number of cycles required to obtain products in exponential phase was determined by performing a PCR using the Advantage® II PCR kit (Clontech) and following manufacture's protocol (5′ PCR Primer II used: 5′-AAGCAGTGGTATCAACGCAGAGT-3′). DNA was purified using QIAquick PCR purification columns. Nine nano gram of cDNA were labeled through incorporation of dCTP conjugated with Cy3 or Cy5 dyes using the BioPrime DNA Labeling System and following manufacture's protocol. Cy3 and Cy5 labeled sample and control pairs were combined in 1.5 ml tubes. The volume was reduced to 25–30 μl in a SpeedVac concentrator before proceeding with Sephadex G50 purification (two per sample), assembled following manufacture's instruction. Sample volumes was reduced to 2–5 μl using a SpeedVac. Finally, 2 μl of 10 mg/ml sonicated salmon sperm DNA were added with 140 μl of hybridization buffer. Samples were then boiled at 100°C (2 min), centrifuged at 16,000 × g (1 min) and then hybridized on slides.

FL003 Array Hybridization

The FlyChip in-house printed FL003 gene expression arrays on FMB PowerMatrix slides using the Genetix Qarray2 (producing 82 arrays per run), consisting of 14,444 transcript-specific 70-mer oligonucleotides were used (GEO accession GPL14121). Four biological replicates were performed including 2 dye swaps. Blocking of slides was performed (as per FMB protocol) by incubating slides for 30 min in 0.1% BSA, 0.2% SDS, 2x SSC (300 mM NaCl, 30 mM Na citrate, pH 7), followed by three washes in clean water. One hundred and thirty five microliters of samples were hybridized for 16 h at 51°C with agitation using the GeneTac Hybridisation station. Slides were then washed with pre-warmed (55°C) wash solution 1 (0.2 × SSC; 0.2% SDS) for 20 min with gentle agitation, followed by 3 washes for 1 min in warm solution 2 (0.2 × SSC), avoiding light exposure, rinsed with MilliQ water at room temperature and finally dried in a centrifuge at 96 × g (5 min).

Data Acquisition and Processing

Slides were scanned using an Axon GenePix 4000B scanner at optimal PMT gain. Manual spot-finding was operated through Dapple (Buhler et al., 2000). Raw data was imported into limma (Bioconductor R package, R version 3.1.0) and Variance stabilizing normalization (vsn) was applied (Huber et al., 2002). Significance analysis was performed using the empirical Bayes method within limma. Due to the low number of significant genes ($n = 8$ at fdr <= 0.05) thresholds were relaxed to include genes with average M value <-0.5 or >0.5 (M-value is the log2 of the ratio of sample vs. control intensities), and p-value <0.1 (187 genes).

Quantitative RT-PCR Analysis

Three biological replicates of Malpighian tubules dissected from 30 females were analyzed. Malpighian tubule total RNA was extracted in TRI Reagent (Sigma-Aldrich) and treated with TURBO DNase (Ambion). RNA was reverse transcribed using the high-capacity RNA-to-cDNA kit (Applied Biosystems) according to the manufacture's protocol. Quantitative real-time PCRs were performed in fast 48-well reaction plates (Applied Biosystems) and analyzed by StepOnePlus real-time PCR system (Applied Biosystems) according to the manufacturer's procedure. For each sample, at least two technical replicates were performed. Primers were designed using Primer 3 software (Untergasser et al., 2012). Parameters for primer design were a length of 18-27 bases, a melting temperature between 57.0-63.0°C, and a GC content from 20-80%. *dGrip75* and *CG31955* primers

were designed in different exons. Expression of target genes was normalized to the widely used reference gene *Rp49*. The qRT-PCR primers used are listed in **Table S1**. For each gene of interest, fold changes in expression levels were evaluated by using the ΔΔCt method. The mean fold change and SD were calculated. *p*-value was calculated using a one-tail *t*-test analysis on three biological replicates. Dissociation curve analysis was performed to confirm the presence of a single specific product.

DIFFERENTIALLY EXPRESSED GENES IN *dVHL*$^{1.1}$/+ MALPIGHIAN TUBULES

By using the statistical parameters reported in the material and methods section we recovered 331 hit genes whose expression significantly differ between *dVHL*$^{1.1}$/+ and wild type tubules (**Figure 1A**). One hundred and eighteen are upregulated (red dots) while 321 are downregulated (blue dots). The majority of

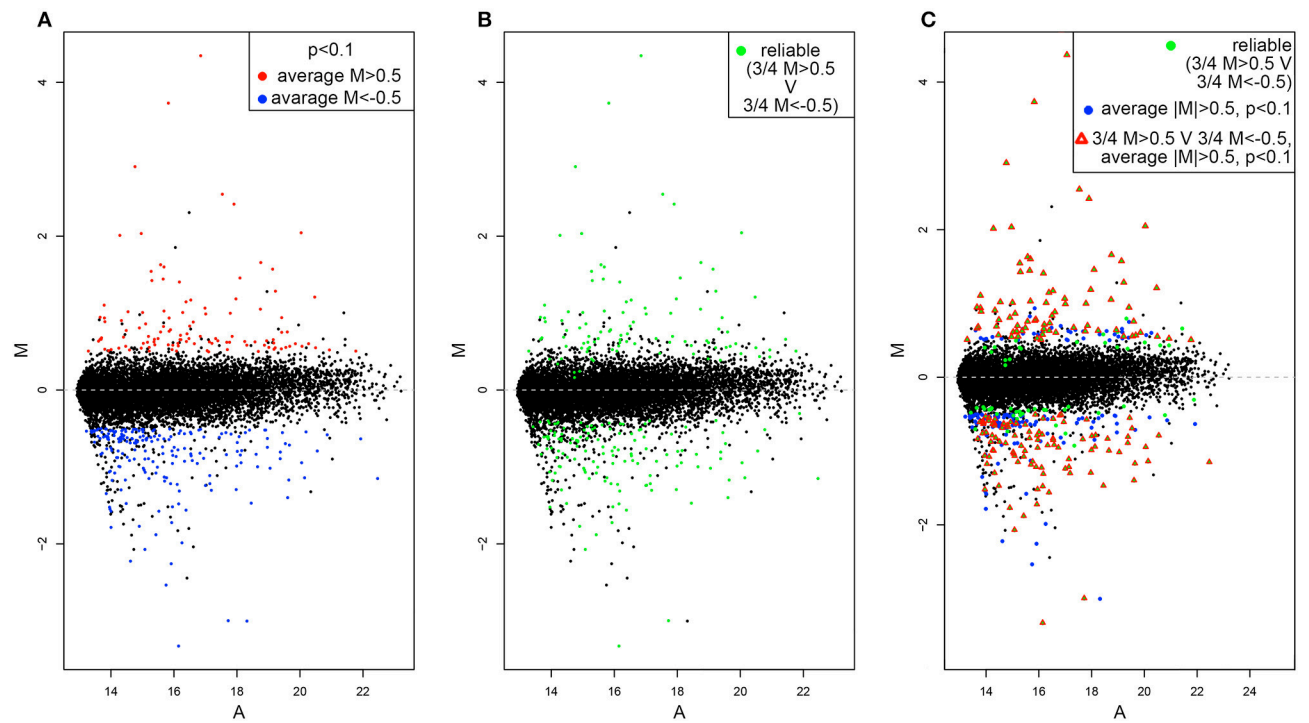

FIGURE 1 | MA-plots of differentially expressed genes in *dVHL*$^{1.1}$/+ Malpighian tubules. **(A)** Upregulated genes (average M > 0.5, $p < 0.1$) are shown in red while downregulated genes (average M<-0.5, $p < 0.1$) are shown in blue. **(B)** Genes for which the alteration in gene expression (M > 0.5 or M<-0.5) was recovered in 3 out of 4 slides are shown in green. **(C)** Genes that satisfy both the cut-off conditions in **(A,B)** are shown with red triangle.

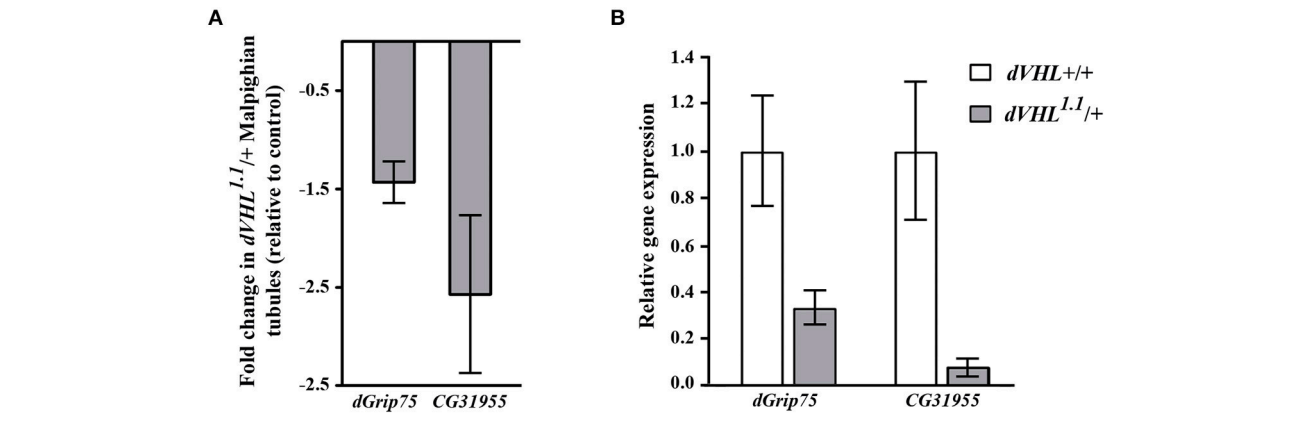

FIGURE 2 | Validation and classification of differentially expressed genes in *dVHL*$^{1.1}$/+ Malpighian tubules. **(A)** Fold change in transcription levels of *dGrip75* and *CG31955* genes in the microarray analysis. **(B)** qRT-PCR analysis of *dGrip75* and *CG31955* transcript levels in individuals of the reported genotypes. 3 biological replicates of tubules from 5-days old *dVHL*$^{1.1}$/+ and wild type females were analyzed. Graphs represent mean ± SD; $p = 0.0152$ *(dGrip75)* and $p = 0.0153$ *(CG31955)*.

genes are not significantly differentially expressed (black dots), as expected. By looking at M values of genes in each of the 4 slides we also highlighted those of them for which single absolute M values are higher than 0.5 in at least 3 slides (**Figure 1B**). This should outline genes for which the alteration in gene expression is reliable (based on alteration reproducibility). Finally, we merged the data in **Figures 1A**,**B** and found 187 genes for which the absolute value of average M is higher than 0.5, *p*-value is lower than 0.1 and in at least 3 out of 4 slides the single absolute M-values are higher than 0.5 (**Figure 1C**).

As an initial step to analyze the differentially expressed genes we performed quantitative real time PCR (qRT-PCR) experiments and we analyzed the transcript levels of two genes that we are interested on studying, *dGrip75* and *CG31955*; *rp49* was used as internal reference gene (**Figure 2B**). The qRT-PCR experiments confirmed that, in $dVHL^{1.1}$/+ Malpighian tubules, both genes are downregulated, as expected by microarray results (**Figure 2A**). *dGrip75* encodes a γ-tubulin which takes part in the assembly of the γ-tubulin ring complex (γTuRC), located at the centrosomes, at the base of a microtubule. γTuRC has a ring-shaped structure that serves as a template for a microtubule and allows the controlled polymerization of tubulin dimers (Oegema et al., 1999; Moritz et al., 2000). This protein attracted our attention since we have already demonstrated that dVHL is essential in follicle cells via stabilizing microtubules (Duchi et al., 2010). *CG31955* encodes a protein with unknown molecular function. An interesting microarray study of Andrew (Chung et al., 2011) showed that *CG31955* is downregulated in *trachealess (trh)* mutant embryos. Trh is the master regulator of trachea development, the *Drosophila* branched and tubular system which is responsible for transport of oxygen and other gases. Earlier analysis on *dVHL* highlighted its requirement in this tubular organ: heterozygous and homozygous $dVHL^{1.1}$ embryos display altered tracheal system (Hsouna et al., 2010).

We screened our candidate list with FlyMine (Lyne et al., 2007) tool for gene ontology (GO) enrichment in biological processes ($p < 0.1$, Bonferroni test) and we found enrichment in regulation of phosphoprotein phosphatase activity [GO:0043666, *p*-value=0.05] and regulation of protein serine/threonine phosphatase activity [GO:0080163, $p = 0.07$].

Transcriptome alterations in human morphologically normal cells heterozygous for a *VHL* mutation (derived from VHL patients) have also been analyzed (Peri et al., 2016). A comparison between *Drosophila* and human datasets could recover strong hits, whose molecular dissection may be performed using *Drosophila* as a model system.

The limiting-most aspect of this study is intrinsic to omics approaches: functional analyses of candidates are needed to genetically dissect gene functions and pathways, confirming their role into the VHL pathogenesis.

DATA AVAILABILITY

The datasets generated for this study can be found in the GEO data repository (http://www.ncbi.nlm.nih.gov/geo/) under the accession identification number GSE124152.

AUTHOR CONTRIBUTIONS

MI cultured flies and performed the experiments. BF assisted the microarray experiments. DA performed the qPCR analysis. MI, GG, and VC conceived the experiments and wrote the article.

FUNDING

The authors acknowledge funding from the University of Bologna (RFO 2014) to GG and VC.

ACKNOWLEDGMENTS

A special thank goes to Dr. Boris Adryan, for hosting MI in his laboratory in Cambridge (UK) and for his invaluable help in designing the experimental plan. We thank Patrizia Romani for her precious suggestion on interpreting data. MI has been awarded a PhD fellowship from University of Bologna and MIUR Fondo Giovani and a Marco Polo fellowship for the research period in Cambridge, UK.

SUPPLEMENTARY MATERIAL

The Supplementary Material for this article can be found online at: https://www.frontiersin.org/articles/10.3389/fphys.2019.00619/full#supplementary-material

REFERENCES

Adryan, B., Decker, H.J., Papas, T.S., and Hsu, T. (2000). Tracheal development and the von Hippel-Lindau tumor suppressor homolog in *Drosophila*. *Oncogene* 19, 2803–2811. doi: 10.1038/sj.onc.1203611

Aso, T., Yamazaki, K., Aigaki, T., and Kitajima, S. (2000). *Drosophila* von Hippel-Lindau tumor suppressor complex possesses E3 ubiquitin ligase activity. *Biochem. Biophys. Res. Commun*. 276, 355–361. doi: 10.1006/bbrc.2000.3451

Bader, H.L., and Hsu, T. (2012). Systemic VHL gene functions and the VHL disease. *FEBS Lett*. 586, 1562–1569. doi: 10.1016/j.febslet.2012.04.032

Buhler, J., Ideker, T., and Haynor, D. (2000). *Dapple: Improved Techniques for Finding Spots on DNA Microarrays*. UW CSE Technical Report UWTR 2000-08-05.

Chung, S., Chavez, C., and Andrew, D.J. (2011). Trachealess (Trh) regulates all tracheal genes during *Drosophila* embryogenesis. *Dev. Biol*. 360, 160–172. doi: 10.1016/j.ydbio.2011.09.014

Denholm, B., and Skaer, H. (2009). Bringing together components of the fly renal system. *Curr Opin. Genet. Dev*. 19, 526–532. doi: 10.1016/j.gde.2009.08.006

Dow, J.A., and Romero, M.F. (2010). Drosophila provides rapid modeling of renal development, function, and disease. *Am. J. Physiol. Renal. Physiol*. 299, F1237–1244. doi: 10.1152/ajprenal.00521.2010

Duchi, S., Fagnocchi, L., Cavaliere, V., Hsouna, A., Gargiulo, G., and Hsu, T. (2010). Drosophila VHL tumor-suppressor gene regulates epithelial morphogenesis by promoting microtubule and aPKC stability. *Development* 137, 1493–1503. doi: 10.1242/dev.042804

Gnarra, J.R., Tory, K., Weng, Y., Schmidt, L., Wei, M.H., Li, H., et al. (1994). Mutations of the VHL tumour suppressor gene in renal carcinoma. *Nat. Genet.* 7, 85–90. doi: 10.1038/ng0594-85

Herman, J.G., Latif, F., Weng, Y., Lerman, M.I., Zbar, B., Liu, S., et al. (1994). Silencing of the VHL tumor-suppressor gene by DNA methylation in renal carcinoma. *Proc. Natl. Acad. Sci. U.S.A.* 91, 9700–9704.

Hsouna, A., Nallamothu, G., Kose, N., Guinea, M., Dammai, V., and Hsu, T. (2010). Drosophila von Hippel-Lindau tumor suppressor gene function in epithelial tubule morphogenesis. *Mol. Cell. Biol.* 30, 3779–3794. doi: 10.1128/MCB.01578-09

Hsu, T. (2012). Complex cellular functions of the von Hippel-Lindau tumor suppressor gene: insights from model organisms. *Oncogene* 31, 2247–2257. doi: 10.1038/onc.2011.442

Huber, W., von Heydebreck, A., Sultmann, H., Poustka, A., and Vingron, M. (2002). Variance stabilization applied to microarray data calibration and to the quantification of differential expression. *Bioinformatics* 18 (Suppl. 1), S96–S104. doi: 10.1093/bioinformatics/18.suppl_1.S96

Ignesti, M., Barraco, M., Nallamothu, G., Woolworth, J.A., Duchi, S., Gargiulo, G., et al. (2014). Notch signaling during development requires the function of awd, the Drosophila homolog of human metastasis suppressor gene Nm23. *BMC Biol.* 12:12. doi: 10.1186/1741-7007-12-12

Iwai, K., Yamanaka, K., Kamura, T., Minato, N., Conaway, R.C., Conaway, J.W., et al. (1999). Identification of the von Hippel-lindau tumor-suppressor protein as part of an active E3 ubiquitin ligase complex. *Proc. Natl. Acad. Sci. U.S.A.* 96, 12436–12441.

Kamura, T., Conrad, M.N., Yan, Q., Conaway, R.C., and Conaway, J.W. (1999). The Rbx1 subunit of SCF and VHL E3 ubiquitin ligase activates Rub1 modification of cullins Cdc53 and Cul2. *Genes. Dev.* 13, 2928–2933.

Latif, F., Duh, F.M., Gnarra, J., Tory, K., Kuzmin, I., Yao, M., et al. (1993). von Hippel-Lindau syndrome: cloning and identification of the plasma membrane Ca(++)-transporting ATPase isoform 2 gene that resides in the von Hippel-Lindau gene region. *Cancer Res.* 53, 861–867.

Lonergan, K.M., Iliopoulos, O., Ohh, M., Kamura, T., Conaway, R.C., Conaway, J.W., et al. (1998). Regulation of hypoxia-inducible mRNAs by the von Hippel-Lindau tumor suppressor protein requires binding to complexes containing elongins B/C and Cul2. *Mol. Cell. Biol.* 18, 732–741.

Lyne, R., Smith, R., Rutherford, K., Wakeling, M., Varley, A., Guillier, F., et al. (2007). FlyMine: an integrated database for *Drosophila* and *Anopheles* genomics. *Genome. Biol.* 8, R129. doi: 10.1186/gb-2007-8-7-r129

Maxwell, P.H., Wiesener, M.S., Chang, G.W., Clifford, S.C., Vaux, E.C., Cockman, M.E., et al. (1999). The tumour suppressor protein VHL targets hypoxia-inducible factors for oxygen-dependent proteolysis. *Nature* 399, 271–275. doi: 10.1038/20459

Miller, J., Chi, T., Kapahi, P., Kahn, A.J., Kim, M.S., Hirata, T., et al. (2013). Drosophila melanogaster as an emerging translational model of human nephrolithiasis. *J. Urol.* 190, 1648–1656. doi: 10.1016/j.juro.2013.03.010

Moritz, M., Braunfeld, M.B., Guenebaut, V., Heuser, J., and Agard, D.A. (2000). Structure of the gamma-tubulin ring complex: a template for microtubule nucleation. *Nat. Cell Biol.* 2, 365–370. doi: 10.1038/35014058

Nallamothu, G., Woolworth, J.A., Dammai, V., and Hsu, T. (2008). Awd, the homolog of metastasis suppressor gene Nm23, regulates Drosophila epithelial cell invasion. *Mol. Cell. Biol.* 28, 1964–1973. doi: 10.1128/MCB.01743-07

Oegema, K., Wiese, C., Martin, O.C., Milligan, R.A., Iwamatsu, A., Mitchison, T.J., et al. (1999). Characterization of two related Drosophila gamma-tubulin complexes that differ in their ability to nucleate microtubules. *J. Cell Biol.* 144, 721–733.

Peri, S., Caretti, E., Tricarico, R., Devarajan, K., Cheung, M., Sementino, E., et al. (2016). Haploinsufficiency in tumor predisposition syndromes: altered genomic transcription in morphologically normal cells heterozygous for VHL or TSC mutation. *Oncotarget* 8, 17628–17642. doi: 10.18632/oncotarget.12192

Romani, P., Duchi, S., Gargiulo, G., and Cavaliere, V. (2017). Evidence for a novel function of Awd in maintenance of genomic stability. *Sci. Rep.* 7:16820. doi: 10.1038/s41598-017-17217-0

Romani, P., Ignesti, M., Gargiulo, G., Hsu, T., and Cavaliere, V. (2018). Extracellular NME proteins: a player or a bystander? *Lab Invest.* 98, 248–257. doi: 10.1038/labinvest.2017.102

Romani, P., Papi, A., Ignesti, M., Soccolini, G., Hsu, T., Gargiulo, G., et al. (2016). Dynamin controls extracellular level of Awd/Nme1 metastasis suppressor protein. *Naunyn. Schmiedebergs Arch. Pharmacol.* 389, 1171–1182. doi: 10.1007/s00210-016-1268-9

Rosengard, A.M., Krutzsch, H.C., Shearn, A., Biggs, J.R., Barker, E., Margulies, I.M., et al. (1989). Reduced Nm23/Awd protein in tumour metastasis and aberrant *Drosophila* development. *Nature* 342, 177–180. doi: 10.1038/342177a0

Untergasser, A., Cutcutache, I., Koressaar, T., Ye, J., Faircloth, B.C., Remm, M., et al. (2012). Primer3–new capabilities and interfaces. *Nucleic Acids Res.* 40:e115. doi: 10.1093/nar/gks596

Wang, J., Kean, L., Yang, J., Allan, A.K., Davies, S.A., Herzyk, P., et al. (2004). Function-informed transcriptome analysis of *Drosophila* renal tubule. *Genome. Biol.* 5:R69. doi: 10.1186/gb-2004-5-9-r69

Woolworth, J.A., Nallamothu, G., and Hsu, T. (2009). The *Drosophila* metastasis suppressor gene Nm23 homolog, awd, regulates epithelial integrity during oogenesis. *Mol. Cell. Biol.* 29, 4679–4690. doi: 10.1128/MCB.00297-09

Conflict of Interest Statement: The authors declare that the research was conducted in the absence of any commercial or financial relationships that could be construed as a potential conflict of interest.

frontiers in Physiology

ORIGINAL RESEARCH
published: 24 July 2019
doi: 10.3389/fphys.2019.00941

Locomotor Behaviour and Clock Neurons Organisation in the Agricultural Pest *Drosophila suzukii*

Celia Napier Hansen[1], *Özge Özkaya*[1], *Helen Roe*[1], *Charalambos P. Kyriacou*[1], *Lara Giongo*[2] *and Ezio Rosato*[1]*

[1] *Department of Genetics and Genome Biology, University of Leicester, Leicester, United Kingdom,* [2] *Centro Ricerca e Innovazione, Fondazione Edmund Mach, Trento, Italy*

Drosophila suzukii (Matsumara) also called Spotted Wing *Drosophila* (SWD), is an invasive pest species originally from Asia that has now spread widely across Europe and North America. The majority of drosophilids including the best known *Drosophila melanogaster* only breed on decaying fruits. On the contrary, the presence of a strong serrated ovipositor and behavioural and metabolic adaptations allow *D. suzukii* to lay eggs inside healthy, ripening fruits that are still on the plant. Here we present an analysis of the rhythmic locomotor activity behaviour of *D. suzukii* under several laboratory settings. Moreover, we identify the canonical clock neurons in this species by reporting the expression pattern of the major clock proteins in the brain. Interestingly, a fundamentally similar organisation of the clock neurons network between *D. melanogaster* and *D. suzukii* does not correspond to similar characteristics in rhythmic locomotor activity behaviour.

Keywords: circadian clock, *Drosophila*, *suzukii*, SWD, *melanogaster*, circadian rhythms, clock neurons, behaviour

OPEN ACCESS

Edited by:
Cristiano De Pitta, University of Padova, Italy

Reviewed by:
Joanna C. Chiu, University of California, Davis, United States
Matthias Schlichting, Brandeis University, United States

***Correspondence:**
Ezio Rosato
er6@leicester.ac.uk

Specialty section:
This article was submitted to Invertebrate Physiology, a section of the journal Frontiers in Physiology

Received: *02 May 2019*
Accepted: *09 July 2019*
Published: *24 July 2019*

Citation:
Hansen CN, Özkaya Ö, Roe H, Kyriacou CP, Giongo L and Rosato E (2019) Locomotor Behaviour and Clock Neurons Organisation in the Agricultural Pest Drosophila suzukii. Front. Physiol. 10:941. doi: 10.3389/fphys.2019.00941

INTRODUCTION

In the late 2000s the Asian drosophilid, *Drosophila suzukii* (Matsumura) invaded Europe and North America becoming established in just a handful of years (Asplen et al., 2015). While it is likely that the increasing world trade of goods from Asia was pivotal to the astonishing speed of the invasion, the ability to become widespread in the newly colonised territories speaks volumes about the "plasticity" of this species.

D. suzukii is native of Asia and occupies the majority of the continent, from Japan to Russia and from Korea to Pakistan (Calabria et al., 2012; Cini et al., 2012). Although the exact origins are not known, comparative genomics suggests that *D. suzukii* evolved in a region spanning across North India, Indochina, and the Chinese coasts, at a time (9 to 6 Mya) when a mountainous temperate forest was the dominant habitat in this is area (Ometto et al., 2013). *D. suzukii* is part of a species complex within the melanogaster group, hence it is phylogenetically related to the more common and best-known model species *Drosophila melanogaster* (Chiu et al., 2013). However, contrary to *D. melanogaster* and the majority of other drosophilids that only breed and feed on decaying fruits, the presence of a strong serrated ovipositor and novel behavioural and metabolic characteristics (Nguyen et al., 2016; Karageorgi et al., 2017), allow *D. suzukii* to lay eggs inside healthy, ripening fruits that are still on the plant. Damage is firstly caused by the "sting" that leaves a scar on the fruit. Then larvae begin feeding inside the fruit causing the surrounding area to collapse. Thereafter, secondary fungal or bacterial infections contribute to further fruit deterioration (i.e., rotting).

These flies have a wide range of hosts although they prefer small fruits such as cherry, strawberry, raspberry, and similar and are able to cause substantial economic losses, in particular to specialised cultivations usually important for local rural economies (Grassi et al., 2009; Goodhue et al., 2011; Cini et al., 2012). In addition, their population explosion aided by the lack of natural enemies in America and Europe constitutes an ecological threat to those regions. Wild fruits, a crucial part of any ecosystem, are under massive attack by this species; directly because of oviposition and larval feeding, and indirectly as a potential vector of plant diseases (Asplen et al., 2015). Curiously, these flies are not considered an important pest in Asia, probably due to the presence of natural predators that preclude the establishment of large populations (Asplen et al., 2015).

The spread of *D. suzukii* has generated widespread interest for its economic impact but also academic attention as a model pest species. Although phylogenetically quite close to *D. melanogaster*, *D. suzukii* has diverged profoundly due to its revolutionary ecological repositioning as a pest of soft fruits. As mentioned above, this evolutionary change was led by the development of a serrated ovipositor, but behavioural and metabolic plasticity might have provided the premise for such a morphological change to become an ecological innovation (Karageorgi et al., 2017).

To date the best documented changes are in the olfactory system. For instance, unlike other drosphilids, the smell of ripe fruits has become a strong oviposition signal for *D. suzukii* females (Karageorgi et al., 2017). Conversely, they ignore CO_2, produced during ripening, that is instead a strong repellent for *D. melanogaster* (Krause Pham and Ray, 2015). These differences are also reflected by the evolution and the regulation of olfactory genes (Hickner et al., 2016; Ramasamy et al., 2016; Crava et al., 2019). Further adaptations involve sexual and social behaviour. D *suzukii* does not produce cis-vaccenyl acetate (cVA), a male pheromone (Dekker et al., 2015). The cVA pheromone is used throughout the melanogaster group as an attractant towards females and as a complex social signal towards other males; for the latter, being a repellent or attractant depends on concentration (reviewed in Ejima, 2015). The complexity of cVA signalling is explained by two antagonist olfactory circuits with opposite behavioural valence being activated according to concentration (reviewed in Ziegler et al., 2013). *D. suzukii* flies still perceive cVA but have switched the dominance of the two circuits resulting in a constitutive behavioural repulsion (Dekker et al., 2015). What is the relevance of such a change? Many drosophilids aggregate, mate and oviposit on fermenting fruits and cVA is key to these behaviours (Laturney and Billeter, 2014). Furthermore, fermentation odours, feeding, and cVA are synergistic, acting as a potent aphrodisiac mix (Grosjean et al., 2011; Lebreton et al., 2012; Das et al., 2017). Considering that adult *D. suzukii* flies still use rotting fruits as a food source but exploit fresh fruits as preferential and "niche" mating and oviposition sites (Cloonan et al., 2018), obliterating the production of cVA (not to attract competitor species) and reverting the behavioural response to it (not to be attracted and aroused on the wrong substrate by other species) seems an obligate evolutionary path to be able to succeed in a new larval phytophagous life-style.

More generally, *D. suzukii* and *D. melanogaster* rely on a different sensory representation of the world. *D. suzukii* invests more in the visual system (larger eyes and larger optic lobes in the brain, relative to size) whereas *D. melanogaster* invests more in the olfactory system (more trichoid sensilla—they house sensory neurons detecting pheromones—in the antennae and larger antennal lobes in the brain, relative to size) (Keesey et al., 2019). Such a difference is not a consistent finding in the comparison between *D. suzukii* and the majority of other drosophilids (Keesey et al., 2019); therefore, it is not a consequence of their innovative reproductive strategy *per se*. However, it is symptomatic of the evolutionary feedback between ecological positioning and sensory modalities, which becomes more apparent when comparing species. It affects neuronal numbers and connections providing, for instance, an anatomical basis for the expected divergence in the behavioural repertoires of *D. melanogaster* and *D. suzukii* in line with their different life history strategies. Therefore, as we are interested in circadian behaviour, its evolution and its neuronal basis, we consider comparison of the well-known rhythmic behavioural characteristics of *D. melanogaster* with those of *D. suzukii* to be informative.

The circadian clock is a major player in regulating adaptation to the environment. Patterns of activity/rest, feeding, mating, oviposition and eclosion all show 24 h rhythmicity. This is explained by the existence of a self-sustained timekeeping system that aligns the physiology and the behaviour of the organism with the day/night cycle, irrespective (when within the range tolerated by the species) of random environmental fluctuations in temperature (reviewed in Özkaya and Rosato, 2012). *D. melanogaster* has been pivotal in elucidating the architecture and the logic of animal circadian clocks (Konopka and Benzer, 1971; Bargiello et al., 1984; Zehring et al., 1984). Molecularly, the core of the clock consists of a system of interlocked transcription/translation feedback loops (TTL). The transcription factors CLOCK (CLK) and CYCLE (CYC) bind as heterodimers on the promoters of the *period* (*per*) and *timeless* (*tim*) genes initiating their transcription (Allada et al., 1998; Rutila et al., 1998). Immediately after translation, their protein products, PER and TIM, become a substrate for several kinases and phosphatases, resulting in a complex series of post-translational events (Price et al., 1998; Martinek et al., 2001; Sathyanarayanan et al., 2004; Fang et al., 2007). This progressive "maturation" controls the ability of PER and TIM to dimerise, to accumulate, to enter the nucleus and finally to interact with and repress the CLK/CYC complex. The result is a *circa* 24 h rhythm in *per* and *tim* mRNA and protein abundance, which, through mechanisms still not well understood, powers rhythmic physiology and behaviour. Two additional loops interlock with the first through the common element CLK. One involves the rhythmic expression of PAR DOMAIN PROTEIN 1ε (PDP1ε) and VRILLE (VRI), the other implicates the transcription factor CLOCKWORK ORANGE (CWO) (Blau and Young, 1999; Cyran et al., 2003; Lim et al., 2007; Richier et al., 2008). However, their dynamics are less understood (reviewed in Özkaya and Rosato,

2012). Finally, CRYPTOCHROME (CRY), a blue-light sensing protein, participates in the clock by mediating circadian and visual photoresponsiveness and light-dependent neuronal firing (Emery et al., 1998; Stanewsky et al., 1998; Fogle et al., 2011, 2015; Mazzotta et al., 2018; Schlichting et al., 2018). The concerted expression of these clock genes in lateral and dorsal neurons of the brain identifies the anatomical location of the clock (reviewed in Helfrich-Förster, 2003).

Here we explore the circadian system of *D. suzukii* in the laboratory. The motivation was to investigate whether this fly could become a convenient laboratory model for studying circadian rhythmicity in an invasive pest species that is phylogenetically quite close to *D. melanogaster* but differs in its ecological specialisations and in the tuning of its sensory systems. In particular, we wanted to assess whether in *D. suzukii*, we could record robust rhythmic behaviour, describe their neuronal clock network and putatively correlate behavioural and anatomical differences they might present compared to *D. melanogaster*. We intend this work as a prerequisite for future manipulations of the circadian system in *D. suzukii* using tools such as gene editing and transgenesis, with the ultimate goal of aiding the functional characterisation of the different clock neurons in both species. Thus, we tested rhythmic locomotor activity under several laboratory conditions and we examined the cellular expression of the clock genes PER, TIM, CRY, PDP1ε and of the clock-relevant neuropeptide PDF in the brain. We report large behavioural differences and some anatomical variations between the two species; these results form the basis for future investigations.

MATERIALS AND METHODS

Fly Maintenance

Both species of flies were maintained in a light and temperature controlled room at LD 12:12, 25°C on yeast cornmeal media (water: 7,500 ml, maize meal: 504 g, glucose: 555 g, brewer's yeast: 350 g, agar: 59.5 g. Added after boiling: propionic acid: 21 ml, 20% nipagen in ethanol: 94.5 ml) in polystyrene growth vials (9 cm height x 2 cm diameter, Regina Industries, UK).

Fly Strains

Strains of *D. suzukii* (S1202, S1203, S1209, S1210, SMichele) and *D. melanogaster* (M1206, M1217) were established from wild captured flies in the summer of 2012 near Trento in the North of Italy. Several gravid females were used to found each line.

Locomotor Activity

Rearing

All flies were grown as above (Fly maintenance) irrespective of the entrainment regime they were going to be subject to when tested. Virgin females and males were collected on the day of eclosion and kept in small groups of 5–15 individuals (males only, females only or males and females, according to the experiment) into growth vials before loading into "activity tubes" (see below) and monitors. Flies were 4–7 days old when loaded. However, the population monitors were loaded on the same day of fly collection. In all but one experiment the flies were tested on the same yeast cornmeal media used for rearing. In the experiment where we compared males, virgin females and mated females, the flies (all types) were moved into an "activity tube" containing nitrogen-free medium (10% sucrose, 1.5% agar in water) on the day of loading.

Single-Fly Activity

Individual flies were loaded into a glass "activity tube" (5 mm in diameter × 80 mm in length, 1 mm in thickness) with medium at one end and a cotton plug at the other. The tubes were inserted (for a maximum of 32 channels) into an activity monitor (DAM2, Trikinetics, USA) that detects the breaking of an infrared beam (per channel) by the moving fly, sending the information to a computer for storage.

Population Rhythms

Ten males or 10 males and 10 females were placed in a growth vial after eclosion and then immediately loaded into a Drosophila Population monitor (DPM, Trikinetics, USA).

Rectangular Entrainment

All experiments using rectangular light-dark (LD) entrainment followed by constant darkness (DD) were carried out in LSM (UK) light and temperature controlled incubators equipped with three fluorescent tubes (TL-D 90 De Luxe 18W/940 SLV/10, Phillips, NL).

For every experiment 4 days in LD was followed by either 5 or 6 days in DD under constant temperature. In general we carried out experiments under LD12:12, 25°C and then DD. In one experiment we tested five entrainment conditions, followed by DD. The conditions were: L = long photoperiod (LD 16:8, 25°C), S = short photoperiod (LD 8:16, 25°C), H = hot temperature (LD 12:12, 28°C), C =cold temperature (LD 12:12, 18°C) and I = intermediate condition (LD 12:12, 25°C).

Seminatural Conditions

We used a programmable IPP500 Peltier incubator (Memmert, Germany) able to produce a precise temperature cycle that was custom modified to generate a smooth light cycle of desired spectral composition (see Green et al., 2015 for further information). We mimicked a midsummer's day in Northern Italy (where our flies had been collected) but exploring two temperature cycles, of 20–30°C (seminatural_1) or 25–35°C (seminatural_2). The day length was approximately LD 16:8 with a maximum light intensity of 350 lux and 300 lux, respectively for the two experiments. Note however that because of an error while programming the incubator *D. melanogaster* flies were exposed to a maximum of 250 lux during the first experiments while *D. suzukii* were exposed to 350 lux. In both experiments, the temperature cycle peaked 2.5 h later than the light cycle.

Statistical Analyses

The circadian period of rhythmic locomotor activity was calculated using the CLEAN package (Rosato and Kyriacou, 2006). We used GraphPad Prism7 for all other statistical calculations and graphics. Descriptive statistics are reported in Tables and Figure legends.

Immunofluorescence and Microscopy

Flies were entrained under LD 12:12, 25°C for more than 3 days. Flies were collected at ZT18 (anti-PDP1ε), at ZT11 and ZT23 (anti-PER and anti-TIM) and at ZT11 and (after 3 days in DD) at CT23 (anti-CRY). Whole flies were fixed for 2 h in 4% PFA with 0.1% Triton-X and 5% DMSO on a rotating wheel. Brains were dissected in 0.1% PBST (1xPBS with 0.1% Triton-X), permeabilized with 3 × 15 min washes in 1% PBST and blocked (either for 2 h at room temperature or 16 h at 4°C) in 0.5% PBST with added 5% goat serum. Primary antibodies were applied (in fresh blocking solution with added 0.1% Sodium Azide) for 4–6 days at 4°C. After 3 × 15 min washes in 0.5% PBST the brains were incubated with secondary antibodies (in PBST 0.5%) for 3 h. After 3 × 15 min washes in 0.5% PBST the brains were quickly rinsed in distilled water and incubated at 4°C in anti-fade solution (3% propyl gallate, 80% glycerol in PBS pH 8.5) overnight before mounting. Steps were carried out at room temperature unless specified.

Primary antibodies: anti-CRY 420753, rabbit (1:500; Dissel et al., 2014), anti-PDF C7, mouse (1:50; DSHB), anti-PER c-300, rabbit (1:50; Santa Cruz Biotech), anti-TIM UP991, rabbit (1:2000; Koh et al., 2006), anti-PDP1ε, rabbit (1:5000, Cyran et al., 2003).

Secondary antibodies: Anti-rabbit biotinylated (1:600) & streptavidin Dylight 649 (1:300) [used in conjunction with anti-CRY]; anti-mouse Cy2 (1:200); anti-rabbit Alexa 647 (1:200). All secondary antibodies were from Jackson ImmunoResearch. Images were captured with an Olympus FV100 confocal microscope.

RESULTS

Locomotor Activity Under Standard LD Conditions

We started by analysing the locomotor activity behaviour of male flies under standard laboratory conditions. Male flies are usually the preferred subject of circadian studies as they can be assayed on regular fly medium without worrying about their mating status. Instead, mated females can only be tested using medium lacking a nitrogen source to impede the development of fecundated eggs; thus avoiding interference by the progeny. In the laboratory, locomotor activity is more commonly measured testing single flies. Typically the experiments are carried out at constant temperature under 'rectangular' (i.e., on-off) 12 h light−12 h dark (LD 12:12) conditions for a few days followed by constant darkness (DD) for some more days (Rosato and Kyriacou, 2006). We collected *D. suzukii* flies from the wild in 2012 near Trento (Italy) and used several gravid females to found each strain. In parallel we collected *D. melanogaster* flies also and we founded several strains in the same way. Initially we investigated four *D. suzukii* strains (S1210, SMichele, S1203 and S1209) and we compared them to one *D. melanogaster* line (M1217). We monitored male flies for 4 days under LD 12:12, and then for 6 days under DD, at the constant temperature of 25°C. As expected, *D. melanogaster* wild type M1217 flies survived the experimental conditions well (about 10% died before the end of the experiment) and were very active. They showed a bimodal pattern of activity (a Morning and an Evening peak in correspondence to the D/L and L/D transitions) during LD, and were highly rhythmic under DD (**Figure 1A** and **Table 1**). *D. suzukii* did not perform as well under the same conditions. A considerable percentage of flies (from 30% to almost 60% according to strain, **Table 1**) did not survive until the end of the experiment, and those that did, showed a much lower level of activity than *D. melanogaster*. This can be appreciated in **Figures 1B,C** (instead **Figure 1A** is not to scale) showing, for S1210 and M1217, the average day activity profile for all rhythmic flies and representative individual activity profiles, respectively. From the figures it is also clear that S1210 flies are rather more diurnal than bimodal. To confirm this observation, we compared the distribution of activity (the number of crossing of the infrared beam for every 30 min interval—"bin"—per fly) under light (L) and dark (D) conditions between the two species. **Figure 1D** shows that for S1210 flies, "bins" with higher activity are more common during L than D, whereas the opposite is true for M1217, in agreement with the expectations for a crepuscular species. **Figure 1A** and **Figure S1** qualitatively confirm that in *D. suzukii* a "noisy" M peak, if present, is found at the end of the morning, and that a "noisy" E peak tends to eclipse after lights off. Additionally, we noticed that all *D. suzukii* strains showed a very high percentage of arrhythmic flies under DD conditions, and a large variance in period among those that were rhythmic. This contrasts with higher rhythmicity and lower period variance, which we observed for *D. melanogaster* (**Table 1**).

Temperature Compensation and Entrainment

We then decided to test two fundamental properties of the clock, temperature compensation and entrainment.

In general chemical and biochemical reactions change proportionally to temperature. Temperature compensation refers to the ability of the clock to withstand relatively large variations in temperature while only limited changes in period occur. This is an adaptive property of the clock and is subject to scrutiny by natural selection (Pittendrigh, 1993; Sawyer et al., 1997). We compared *D. melanogaster* M1217 to *D. suzukii* S1202. The latter was chosen because its behaviour is similar to S1203 and S1210 but is more prolific. To avoid the confounding influence of possible aftereffects that might arise due to exposure to different environmental conditions during development, we raised all flies under LD 12:12, 25°C. Then, we monitored virgin females (fv) and males (m) for 4 days under five entrainment conditions followed by 6 days under DD (free run). For each fly we calculated the circadian period of locomotor activity; namely, each period derives from the free run part of the experiment and represents the endogenous rhythmicity of the fly. However, to simplify the explanation, here we refer to the entrainment condition that preceded the free run when describing the period results. The five conditions were: L = long photoperiod (LD 16:8, 25°C), S = short photoperiod (LD 8:16, 25°C), H = hot temperature (LD 12:12, 28°C), C = cold temperature (LD 12:12, 18°C) and I = intermediate condition (LD 12:12, 25°C). **Figure 2A** provides

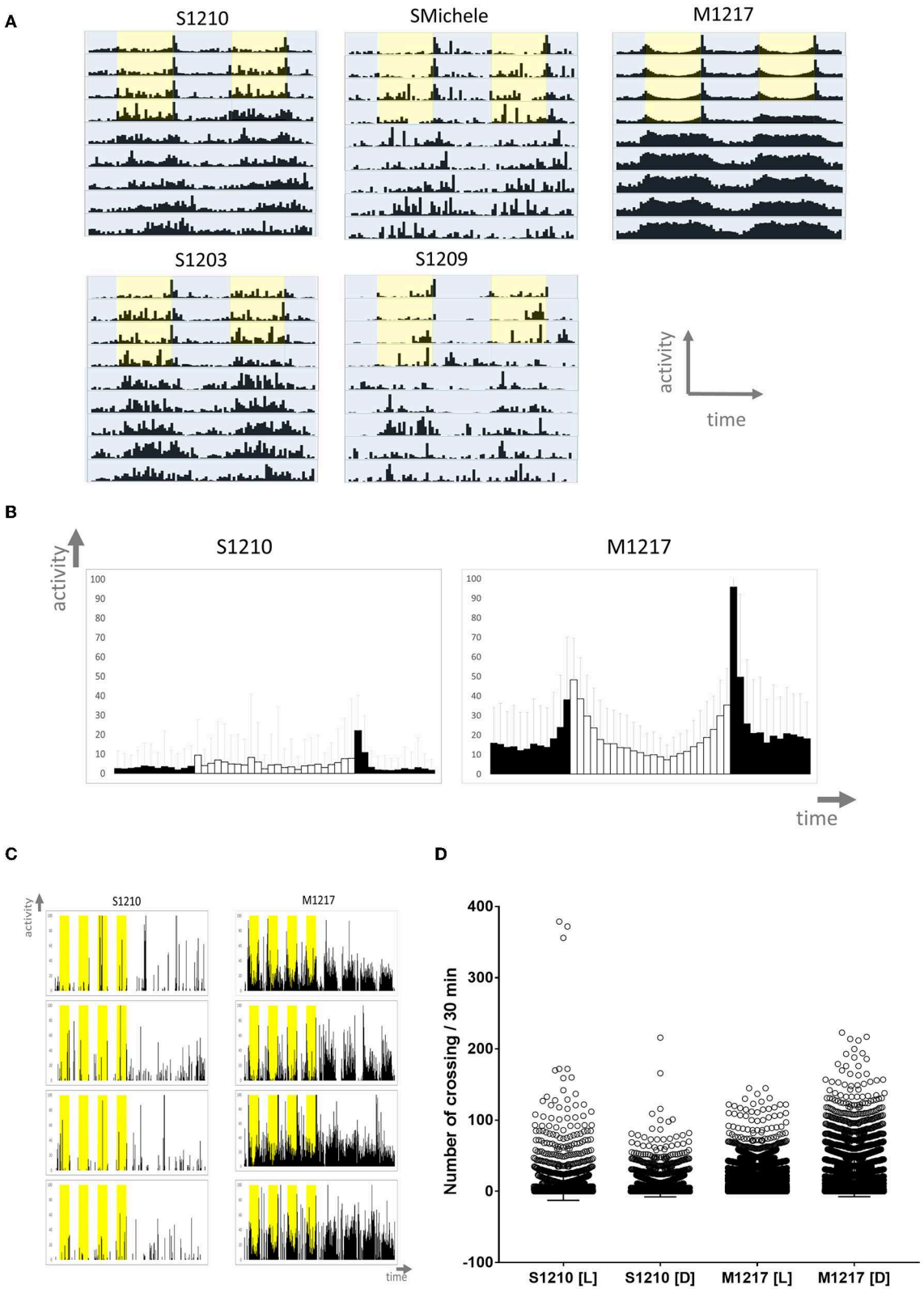

FIGURE 1 | Locomotor activity in *D. suzukii* (S) and *D. melanogaster* (M) males under standard laboratory conditions. **(A)** Average locomotor activity profiles. Activity levels (number of crossing/30 min) are shown on the Y-axis; time (96 intervals of 30 min) is on the X-axis. Data are double plotted (i.e. day1-day2, day2-day3, etc.).

(Continued)

FIGURE 1 | Flies were monitored for 4 days under LD and for 6 days under DD at 25°C. Light is shown in yellow, darkness in blue highlight. Light-dark (LD) conditions followed a rectangular pattern (On-Off) until constant darkness (DD). To aid the visual appreciation of rhythmicity, activity levels are not to scale and standard deviation is omitted. Only rhythmic flies (both SR and CR, see **Table 1**) contributed to the graphs. **(B)** Average day profile for *D suzukii* S1210 and *D. melanogaster* M1217 males. The average day was obtained by combining into one the four LD days for all rhythmic flies (SR+CR, see **Table 1)** of the same genotype. The profile for *D. melanogaster* shows clear "Morning" and "Evening" peaks separated by a "siesta." The profile for *D. suzukii* is not clearly defined. In general, it shows that the flies are most active during the light part of the day. Black columns correspond to dark and white columns to light. Error bars show standard deviation. The Y-axis shows activity levels (0–100 crossing/30 min); the X-axis shows time (48 intervals of 30 min). **(C)** Examples of activity profiles for individual flies. It is clear that *D. suzukii* are much less active than *D. melanogaster* flies and spend much of their time being inactive. During LD, *D. suzukii* are more active during the light portion of the day (yellow highlight). Conversely, *D. melanogaster* are crepuscular, being most active at the boundaries of the D to L and L to D transitions. The Y-axis shows activity levels (0–100 crossing/30 min); the X-axis shows time (384 intervals of 30 min). **(D)** Activity levels (number of crossing/30 min) for the L and D part of the day across the four LD days, have been plotted separately for rhythmic *D. suzukii* S1210 and *D. melanogaster* M1217 individual males. It is immediately evident that while in *D. suzukii* higher values are more common during light, the opposite is true for *D. melanogaster*. The four distributions are significantly different (Kruskal-Wallis, $P < 0.0001$) in all possible pairwise comparisons (Dunn's multiple comparisons test, $P < 0.0001$).

TABLE 1 | Locomotor activity statistics of five *D. suzukii* lines in comparison with one *D. melanogaster* line established from flies collected in parallel in the wild.

Species	Line	Gender	NT	D	D (%)	N	SR	SR (%)	CR	CR (%)	AR	AR (%)	τ [SR]	Sdev [SR]
Ds	S1210	m	185	75	41	110	44	40	0	0	66	60	24.52	3.12
Ds	S1209	m	64	34	53	30	6	20	2	7	22	73	23.78	1.6
Ds	SMichele	m	64	38	59	26	6	23	2	8	18	69	25.27	1.24
Ds	S1203	m	64	21	33	43	16	37	2	5	25	58	24.63	1.79
Dm	M1217	m	48	5	10	43	41	96	1	2	1	2	24.26	0.93

Ds, D.suzukii; Dm, D. melanogaster; m, males; NT, total number of flies tested; D, number of flies that died before the end of the 6th day in DD. These have been excluded from further analysis. D (%), D/NTx100; N, number of flies that survived the whole experiment; SR, flies showing a single rhythm of activity in free run; SR(%), SR/Nx100; CR, flies showing more than one (complex) activity period in free run; CR(%), CR/Nx100; AR, arrhythmic flies; AR(%), AR/Nx100; τ [SR], circadian period of locomotor activity of SR flies; Sdev [SR], standard deviation of the circadian period of SR flies.

a snapshot of the average locomotor activity profiles under all conditions; **Table 2** shows the descriptive statistics. For M1217, **Figure 2B** and **Table 2** show that the cold temperature (C, LD 12:12, 18°C) is the only condition resulting in a small but significant shortening of the circadian period for both virgin females (−0.75 h compared to H, LD 12:12, 28°C) and males (−0.68 h compared to H, LD 12:12, 28°C). Additionally, in all conditions and for both genders we observed substantially the same variance. These results are in line with previous observations for the species and confirm that *D. melanogaster* is capable of robust temperature compensation in the interval 18–28°C (Sawyer et al., 1997). The situation for S1202 was different (**Figure 2C** and **Table 2**). Both virgin females and males showed changes in circadian period across conditions but these failed to reach statistical significance. However, for both genders the cold temperature condition (LD 12:12, 18°C) showed a characteristic larger variance, which was significantly different (F test, $P < 0.0001$ for both genders) when compared to the intermediate condition (LD 12:12, 25°C) (**Figure 2C**). As a result, in the cold temperature condition (LD 12:12, 18°C) both genders showed a difference in circadian period of about 10–15 h between individuals at the extremes of the distribution. This suggests that in the laboratory, under cooler conditions, temperature compensation may be compromised in this species. This result is unexpected, not only because temperature compensation is a fundamental property of a functioning clock (Pittendrigh, 1993) but also because a temperature of 18°C should be a good match for a species that evolved in a temperate climate (Ometto et al., 2013). A caveat is that we only tested one line under these conditions and it may not be representative of the whole species.

Entrainment refers to the ability of the clock to synchronise to and "remember" external rhythmic stimuli or *Zeitgebers* (German for "time givers"). One important consequence of entrainment is the fact that circadian rhythms adopt a defined phase relationship with the external cycles, resulting in time-specific allocation of activities during the day. **Figure 2D** shows the average day for S1202 and M1217 virgin females and males. Turning our attention to *D. melanogaster* (M1217) males first, we can qualitatively appreciate that the "siesta" (the interval of reduced activity in between the M and E peaks) is more pronounced at higher temperatures ($\text{siesta}_{28°C} > \text{siesta}_{25°C} > \text{siesta}_{18°C}$) or under longer photoperiods ($\text{siesta}_{LD16:8} > \text{siesta}_{LD12:12} > \text{siesta}_{LD8:16}$). To quantify such an effect we calculated for each fly a "midday activity ratio" under all conditions. This is the ratio between the average activity during the three central hours of the light phase and the average activity across the whole LD period. **Figure 2E** shows that such a variable was significantly different across conditions (Kruskal-Wallis $P < 0.0001$) and maintained significance between many pairwise comparisons (Dunn's multiple comparison test). Likewise, *D. melanogaster* virgin females showed a more pronounced "siesta" at higher temperatures or under longer photoperiods (**Figure 2D**), which was further confirmed by comparing the "midday activity ratio" across conditions (**Figure 2E**). However, *D. melanogaster* virgin females showed less "siesta" compared to males under all conditions (**Figure 2D**), which was in agreement with an overall higher level of activity (**Figure S2**). Gender differences in locomotor activity are well documented in *D. melanogaster* (Helfrich-Förster, 2000).

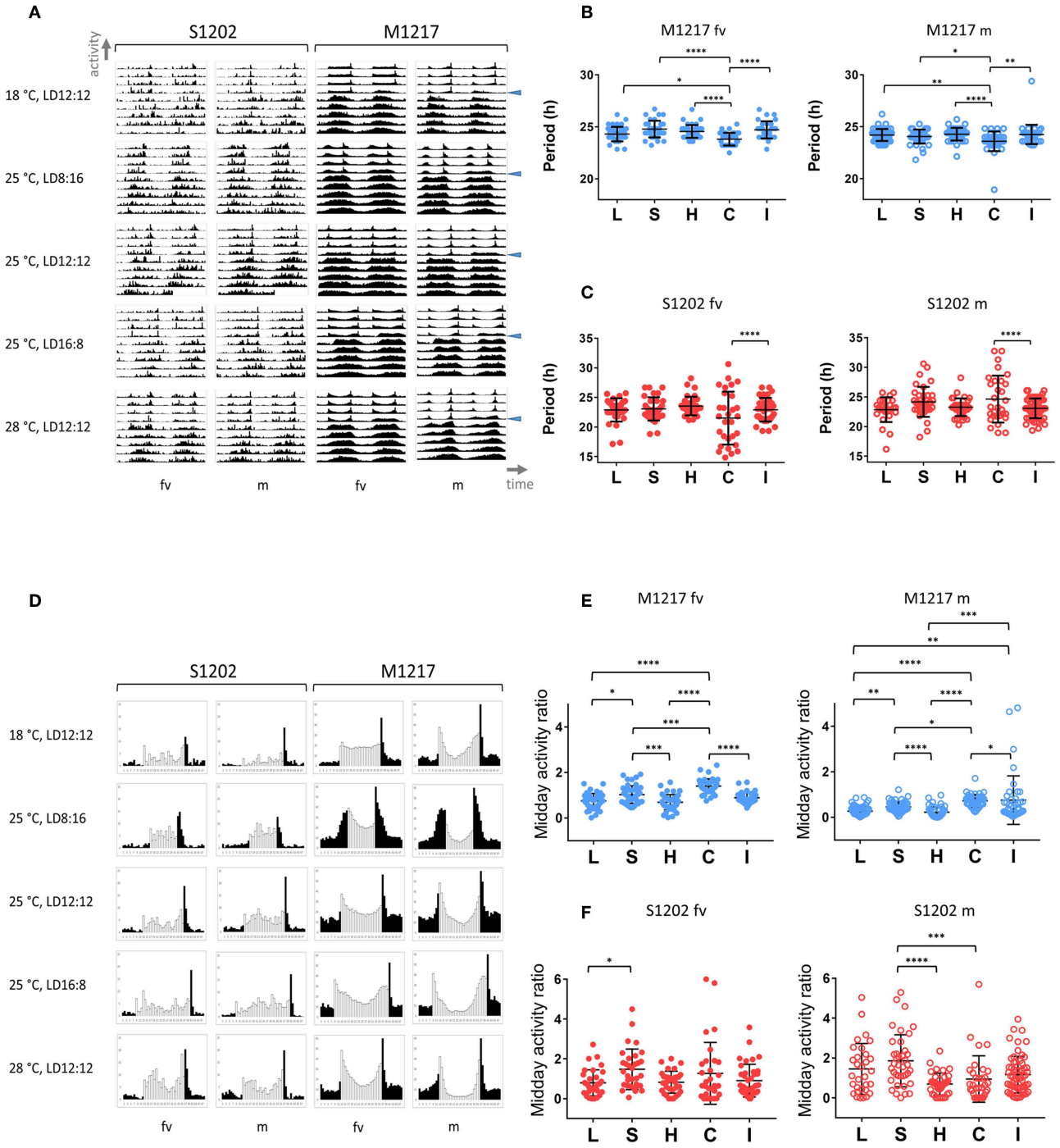

FIGURE 2 | Locomotor activity in *D. suzukii* and *D. melanogaster* virgin females (fv) and males (m) under different entrainment regimes: L, LD 16:8, 25°C (long photoperiod); S, LD 8:16, 25°C (short photoperiod); H, LD 12:12, 28°C (hot temperature); C, LD 12:12, 18°C (cold temperature); I, LD 12:12, 25°C (intermediate condition). **(A)** Average locomotor activity profiles. Activity levels (number of crossing/30 min) are shown on the Y-axis; time (96 intervals of 30 min) is on the X-axis. Data are double plotted (i.e. day1-day2, day2-day3, etc.). Flies were monitored for 4 days under LD and for 6 days under DD. The beginning of DD is shown by a blue arrow head. To aid the visual appreciation of rhythmicity, L and D are not highlighted, activity levels are not to scale and standard deviation is omitted. Only rhythmic flies (both SR and CR, see **Table 2**) contributed to the graphs. **(B)** Distribution of circadian locomotor activity periods (SR flies only, see **Table 2**) in *D. melanogaster* following different entrainment regimes. Note that we report free run periods but for ease of description the labelling refers to the preceding entrainment conditions. Virgin females are on the left, males are on the right. Periods were compared across all conditions (Kruskal-Wallis, $P < 0.0001$ for both virgin females and males). The significant difference is explained by a shorter period under C (cold temperature, LD 12:12, 18°C) compared to all other conditions (Dunn's multiple comparisons

(Continued)

FIGURE 2 | tests, $^{*}P < 0.05$; $^{**}P < 0.01$; $^{****}P < 0.0001$). However, this does not violate the principle of temperature compensation (see text). **(C)** Distribution of circadian locomotor activity periods (SR flies only, see **Table 2**) in *D. suzukii* following different entrainment regimes. Note that we report free run periods but for ease of description the labelling refers to the preceding entrainment conditions. Virgin females are on the left, males are on the right. For each group, comparing periods across all conditions did not result in a significant difference by Kruskal-Wallis test. However, for both males and virgin females there was a significant increase in the variance when locomotor activity was recorded under the cold temperature condition (F test, C vs. I, $P < 0.0001$). This suggests that under these experimental conditions *D. suzukii* might lose temperature compensation at lower temperatures. **(D)** Average day profile for *D suzukii* S1202 and *D. melanogaster* M1217 virgin females (fv) and males (m). The average day was obtained as for **Figure 1B**. Black columns correspond to dark and white columns to light. For ease of visualisation the standard deviation is not reported. The Y-axis reports activity levels: *D. suzukii* 0-25 (crossing/30 min), *D.melanogaster* 0-60 (crossing/30 min). The X-axis reports time (48 intervals of 30 min). Note that for M1217 m, LD12:12, 25°C, the figure is the same as **Figure 1B**. **(E)** Midday activity ratio (rhythmic flies only, both SR and CR, see **Table 2**) in *D. melanogaster* under different entrainment regimes. The midday activity ratio is a measure of how much a fly is active (on average) in the middle part of the light-phase (the three central hours of the light portion of the day) relative to the average activity across the whole 4 days in LD. Values closer to zero indicate a robust siesta, values higher than one indicate that the fly is more active than average in the middle of the day. Virgin females are on the left, males are on the right. Both virgin females and males showed increased midday activity at lower temperature (C) and shorter photoperiod (S), whereas more siesta occurs under higher temperature (H) and longer photoperiod (L). Significant differences are confirmed overall by Kruskal-Wallis ($P < 0.0001$ for both genders) and between conditions by the Dunn's multiple comparison test ($^{*}P < 0.05$; $^{**}P < 0.01$; $^{***}P < 0.001$; $^{****}P < 0.0001$) **(F)**. Midday activity ratio (rhythmic flies only, both SR and CR, see **Table 2**) in *D. suzukii* under different entrainment regimes. Virgin females are on the left, males are on the right. For both genders the responses were highly variable. For virgin females there was a significant difference among distributions (Kruskal-Wallis, $P < 0.05$). Although we could observe a tendency for more activity in the middle of the day at lower temperature (C, LD 12:12, 18°C) and under short photoperiod (S, LD 8:16, 25°C) compared to other conditions, only the comparison between the two extreme photoperiods (L and S) maintained significance under a multiple comparison test (Dunn's, L vs. S, $P < 0.05$). We observed a significant difference among distributions also for males (Kruskal-Wallis, $P < 0.0001$). However, the situation was less clear as we noticed a relative increase in siesta not only at the higher (H, LD 12:12, 28°C) but also at the lower (C, LD 12:12, 18°C) temperature. Both conditions were different with respect to the short photoperiod under a multiple comparison test (Dunn's; C vs. S, $P < 0.001$; H vs. S, $P < 0.0001$).

Conversely, we could not identify clear-cut differences among conditions and between genders for *D. suzukii*. Inspection of **Figure 2D** does not reveal prominent M and E peaks and "siesta" with the exception of the hot temperature condition (LD 12:12, 28°C). In addition, there were no striking gender differences. In general, males showed an increase in activity towards the end of the morning resulting in a modest M peak. Such a peak appeared earlier (LD 12:12 and LD 16:8, 25°C) or was absent (LD 8:16, 25°C) in females, except in the hot condition (LD 12:12, 28°C). However, we did not find an overall difference in activity levels between genders (**Figure S2**). Finally, we compared the "midday activity ratio" among the males and the females (**Figure 2F**). In both genders we observed an overall difference (Kruskal-Wallis, males $P < 0.0001$, virgin females $P < 0.05$). Both males and virgin females showed a general increase of the "midday activity ratio" (i.e., more activity in the middle of the day) under short photoperiod (LD 8:16, 25°C) and a reduction (less activity in the middle of the day) under the hot condition (LD 12:12, 28°C). *Post-hoc* (Dun's multiple comparison) tests revealed a significant difference between short (LD 8:16, 25°C) and long (LD 16:8, 25°C) photoperiod for virgin females ($P<0.05$). For males, two comparisons, short (LD 8:16, 25°C) vs. hot (LD 12:12, 28°C) and short (LD 8:16, 25°C) vs. cold (LD 12:12, 18°C) maintained significance ($P < 0.0001$ and $P < 0.001$, respectively). For the latter, an inspection of the average day profile (**Figure 2D**) revealed that under the cold condition (LD 12:12, 18°C) males showed a dramatic reduction in activity during the whole light portion of the LD cycle (not just the middle of the day), whereas the "startle" increase of activity at the L/D switch was still prominent. This highlights a potential difference between genders in *D. suzukii*.

The Effect of Mating on Females' Activity

In *D. melanogaster* females, mating causes an increase in activity during the light phase of the LD cycle (Isaac et al., 2010). To investigate whether mating affects *D. suzukii* also, we analysed the locomotor activity of S1202 using *D. melanogaster* M1206 as a comparison (due to a technical problem we did not obtain sufficient M1217 flies in this occasion). We tested males (m), virgin (fv) and mated females (fm) on a nitrogen-free medium at 25°C. **Figure 3A** shows the average locomotor activity profiles (not to scale) under LD 12:12 (first 4 days) and then DD (following 5 days). **Table 3** reports the descriptive statistics. First we analysed the period of rhythmic locomotor activity under DD (**Figure 3B**). In both species, differences in circadian period were not significant across the three groups (Kruskal-Wallis). However, mating resulted in reduced variance in the circadian period of females, which was significant for S1202 (F test, $P < 0.05$; **Figure 3B**). To compare activity under the light-phase of the LD cycle, we first derived the average day profiles (**Figure 3C**). Visual inspection did not reveal any obvious difference between *D. melanogaster* virgin and mated females but a possible increase in activity during the light phase for *D. suzukii* mated females compared to virgins. To quantify such a difference we calculated for each rhythmic fly the L/LD activity ratio, which measures the average relative activity under light with respect to the whole LD cycle (**Figure 3D**). For *D. melanogaster* we did not observe significant changes, but for *D. suzukii* the L/LD activity ratio was different when compared across the three conditions (Kruskal-Wallis, $P < 0.01$). *Post-hoc* analyses confirmed an increase in activity during the light phase in mated vs. virgin females (Dunn's multiple comparison test, $P < 0.01$). Possibly, small sample size and/or genetic background could explain the lack of difference across the three conditions for M1206.

Seminatural Conditions

The main difficulty in recording locomotor activity in *D. suzukii* flies lies in their inactivity. We wondered whether we could elicit higher locomotion by mimicking conditions that are closer to the natural environment. For instance, in nature both light and temperature change gradually, with temperature lagging few hours behind light. Similar conditions, dubbed

TABLE 2 | Locomotor activity statistics in *D. suzukii* (S1202) and *D. melanogaster* (M1217) males and virgin females under different entrainment conditions.

Condition	Line	Gender	NT	D	D (%)	N	SR	SR (%)	CR	CR (%)	AR	AR (%)	τ [SR]	Sdev [SR]
L	S1202	fv	86	18	21	68	32	47	1	1	35	52	22.90	1.97
S	S1202	fv	96	28	29	68	32	47	0	0	36	53	23.07	1.96
H	S1202	fv	96	44	46	52	33	63	0	0	19	37	23.55	1.58
C	S1202	fv	96	8	8	88	29	33	2	2	57	65	21.51	4.47
I	S1202	fv	125	34	27	91	35	39	3	3	53	58	22.92	2.01
L	S1202	m	90	15	17	75	27	36	4	5	44	59	22.85	2.09
S	S1202	m	96	29	30	67	37	55	3	5	27	40	24.17	2.53
H	S1202	m	96	33	34	63	36	57	0	0	27	43	23.26	1.49
C	S1202	m	96	12	13	84	30	36	3	3	51	61	24.64	3.96
I	S1202	m	127	15	12	112	60	54	3	2	49	44	23.08	1.66
L	M1217	fv	54	4	7	50	42	84	5	10	3	6	24.31	0.70
S	M1217	fv	48	3	6	45	37	82	7	16	1	2	24.79	0.80
H	M1217	fv	48	3	6	45	42	93	3	7	0	0	24.56	0.62
C	M1217	fv	48	2	4	46	39	85	1	2	6	13	23.81	0.61
I	M1217	fv	40	3	8	37	30	81	5	14	2	5	24.71	0.83
L	M1217	m	58	0	0	58	54	93	0	0	4	7	24.21	0.58
S	M1217	m	48	1	2	47	45	96	1	2	1	2	24.07	0.67
H	M1217	m	48	0	0	48	44	92	1	2	3	6	24.28	0.61
C	M1217	m	48	0	0	48	39	81	2	4	7	15	23.60	0.95
I	M1217	m*	48	5	10	43	41	96	1	2	1	2	24.26	0.93

L, long photoperiod (LD 16:8, 25°C); S, short photoperiod (LD 8:16, 25°C); H, hot temperature (LD 12:12, 28°C); C, cold temperature (LD 12:12, 18°C); I, intermediate conditions (LD 12:12, 25°C); m, males; fv, virgin females; NT, total number of flies tested; D, number of flies that died before the end of the 6th day in DD. These have been excluded from further analysis. D (%), D/NTx100; N, number of flies that survived the whole experiment; SR, flies showing a single rhythm of activity in free run; SR(%), SR/Nx100; CR, flies showing more than one (complex) activity period in free run; CR(%), CR/Nx100; AR, arrhythmic flies; AR(%), AR/Nx100; τ [SR], circadian period of locomotor activity of SR flies; Sdev [SR], standard deviation of the circadian period of SR flies. [*] These are the same as in ***Table 1****.*

seminatural, can be reproduced in the laboratory with the aid of sophisticated incubators as described by Green et al. (2015). We used the same equipment and compared S1202 and M1217 males.

In the first set of experiments S1202 males were subject to cycling light between 0–350 lux *ca*. (of spectral composition mimicking natural midsummer light in Northern Italy) and cycling temperature between 20 and 30°C (set to reach its maximum 2.5 h later than the light peak, see Green et al., 2015). The photoperiod was about LD 16:8. The M1217 *D. melanogaster* comparison was meant to be set to the same conditions but an error while programming the incubator resulted in a lower amplitude of the light cycle (0–250 lux *ca*.), the other parameters were the same. **Figure 4A** shows the average activity profile for the two species across three days, after which the mortality rate for *D. suzukii* became too high (especially during the second set of experiments). Under those conditions M1217 males substantially reduced their activity when the temperature started rising and increased their activity again in the last portion of the light-phase when the temperature began falling. The main peak of activity was in the early night followed by a short rest phase and then by a smaller bout of activity just before the lights came on corresponding to the coolest part of the day. A small increase in activity followed the beginning of light but it was quickly curbed by the rising of temperature. The complexity of this activity profile shows that in *D. melanogaster* locomotion is not regulated by a permissive/inhibitory temperature or light threshold; in fact, at the same absolute values of temperature and light flies could be mainly active or inactive depending on whether light and temperature were falling or rising. Thus, a quite sophisticated laboratory setting shows that isolated *D. melanogaster* flies are able to integrate sensory modalities and interpret their dynamic patterns to modulate locomotor activity rhythms. If we compare the profile of activity obtained under gradual changes in light and temperature and that obtained under a rectangular on-off LD 16:8 at constant 25°C (**Figure 2D**), the main difference is that under seminatural conditions the flies became primarily nocturnal as the morning and evening peaks of activity were confined to the end and the beginning of the cooling phase, respectively. Unlike the distribution, the amount of activity did not change dramatically, as shown in **Figure 4C** where we compare the amount of activity per "bin" of the average day. Conversely, under the first set of seminatural conditions, *D. suzukii* males were active almost exclusively during the light phase. Moreover, individuals were highly variable in their locomotor behaviour, as shown by the large standard deviation (**Figure 4A**). In comparison to the LD 16:8, 25°C condition (**Figure 2D**), the flies did not seem to organise their activity differently across the 24 h (a part from losing the startle response at the L to D transition) but they reduced its amount, although by a modest degree (**Figure 4C**).

In a second set of experiments both species were challenged with warmer conditions. The temperature cycled between 25 and 35°C, lagging 2.5 h behind a 0-300 lux *ca*. light cycle. In

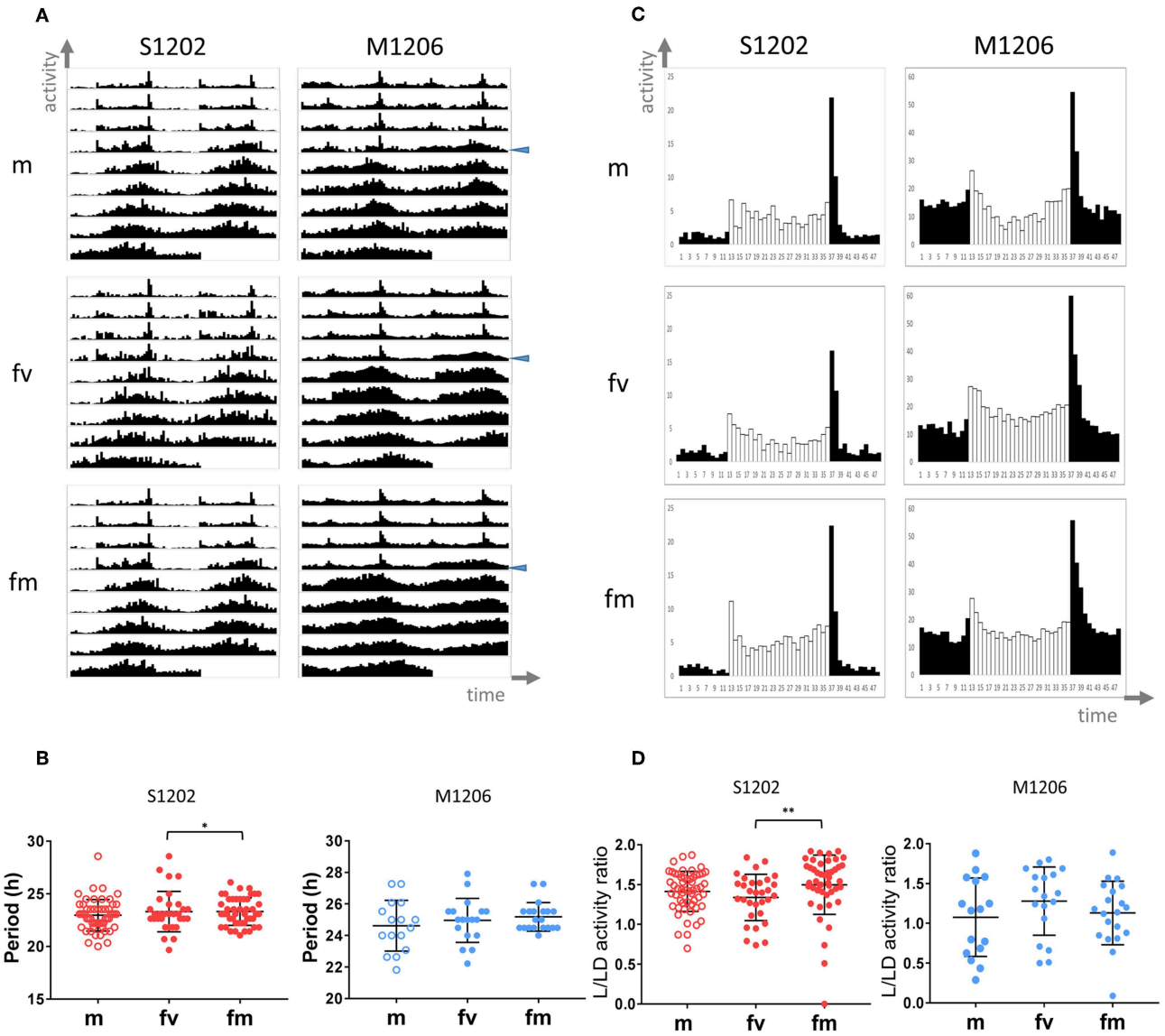

FIGURE 3 | Locomotor activity in *D. suzukii* and *D. melanogaster* males (m), virgin (fv) and mated (fm) females under standard laboratory conditions. **(A)** Average locomotor activity profiles. Activity levels (number of crossing/30 min) are shown on the Y-axis, time (96 intervals of 30 min) is on the X-axis. Data are double plotted (i.e. day1-day2, day2-day3, etc.). Flies were monitored for 4 days under LD 12:12 and for 5 days under DD at 25°C. The beginning of DD is shown by a blue arrow head. To aid the visual appreciation of rhythmicity L and D are not highlighted, activity levels are not to scale and standard deviation is omitted. Only rhythmic flies (both SR and CR, see **Table 3**) contributed to the graphs. **(B)** Circadian period of locomotor activity (SR flies only, see **Table 3**) in *D. suzukii* (left) and *D. melanogaster* (right). For each species, comparing circadian periods among males (m) virgin females (fv) and mated females (fm) did not result in a significant difference by Kruskal-Wallis test. However, both species showed reduced variance in mated *vs*. virgin females; for *D suzukii* such a difference was significant (F test, $^{*}P < 0.05$). **(C)** Average day profile for *D suzukii* S1210 and *D. melanogaster* M1206 males (m), virgin females (fv) and mated females (fm). The average day was obtained as for **Figure 1B**. Black columns correspond to dark and white columns to light. For ease of visualisation the standard deviation is not reported. The Y-axis reports activity levels: *D. suzukii* 0–25 (crossing/30 min), *D. melanogaster* 0–60 (crossing/30 min). The X-axis reports time (48 intervals of 30 min). **(D)** L/LD activity ratio (rhythmic flies only, both SR and CR, see **Table 3**) in *D. suzukii* (left) and *D. melanogaster* (right) males (m), virgin females (fv) and mated females (fm). The L/LD activity ratio is a measure of how much a fly is active (on average) during the L part of the LD cycle relative to the average activity across the whole 4 days in LD. Values closer to zero indicate a reduction of activity during L whereas values higher than one indicate more activity during L than the LD average. Both species showed large variability in the response. In *D. suzukii* the three distributions were significantly different (Kruskal-Wallis, $P < 0.01$). Dunn's multiple comparison tests confirmed an increase in activity during the light-phase in mated vs. virgin females ($^{**}P < 0.01$). In *D. melanogaster* the three distributions were not statistically different.

agreement with previous reports (Vanin et al., 2012; Green et al., 2015), *D. melanogaster* males became extremely active during the day with a large bout in the early afternoon. After a rest during the last part of the light cycle, activity started again in darkness. This time the evening and the morning peaks converged into a single rhythmic episode that terminated at the end of each cooling phase (**Figure 4B**). Overall this resulted in a large increase in activity (Kruskal-Wallis test, $P < 0.0001$.

TABLE 3 | Locomotor activity statistics in *D. suzukii* (S1202) and *D. melanogaster* (M1206) males, virgin and mated females.

Line	Gender	NT	D	D (%)	N	SR	SR (%)	CR	CR (%)	AR	AR (%)	τ [SR]	Sdev [SR]
S1202	m	128	26	20	102	54	53	1	1	47	46	22.96	1.49
S1202	fv	120	55	46	65	31	48	0	0	34	52	23.31	1.92
S1202	fm	119	45	38	74	46	62	0	0	28	38	23.31	1.31
M1206	m	32	13	41	19	16	84	0	0	3	16	24.62	1.61
M1206	fv	32	5	16	27	18	67	0	0	9	33	24.96	1.40
M1206	fm	32	7	22	25	20	80	0	0	5	20	25.19	0.91

M, males; fv, virgin females; fm, mated females; NT, total number of flies tested; D, number of flies that died before the end of the 5th day in DD. These have been excluded from further analysis. D (%), D/NTx100; N, number of flies that survived the whole experiment; SR, flies showing a single rhythm of activity in free run; SR(%), SR/Nx100; CR, flies showing more than one (complex) activity period in free run; CR(%), CR/Nx100, AR, arrhythmic flies; AR(%), AR/Nx100; τ [SR], circadian period of locomotor activity of SR flies; Sdev [SR], standard deviation of the circadian period of SR flies.

Dunn's multiple comparisons test: "seminatural_2" vs. "LD16:8, 25°C", $P = 0.0021$; "seminatural_2" vs. "seminatural_1", $P = 0.0001$. **Figure 4C**). The afternoon peak has been interpreted as a stress response that is modulated by the circadian clock and requires the thermo-sensitive channel transient receptor potential A1 (TrpA1) (Menegazzi et al., 2012; Green et al., 2015). Under this second set of seminatural conditions *D. suzukii* males became even more diurnal (**Figure 4B**). They showed a likely equivalent of the afternoon peak but no activity at other times. Thus, their total activity did not change substantially compared to rectangular LD 16:8, 25°C and to the first seminatural settings (**Figure 4C**).

Overall these experiments further confirm that in the laboratory *D. suzukii* are predominantly diurnal, in contrast to the crepuscular behaviour shown by *D. melanogaster*. Moreover, they highlight the different responses of the two species. While *D. melanogaster* flies are able to reallocate their activity to extend more into the day or the night according to the environmental conditions, *D. suzukii* seem to have just one temporal modality constantly tuned to "diurnal." In addition, they seem to be much less active especially under stress and perhaps they employ immobility (saving energy and resources) as a general strategy to overcome unfavourable conditions. Anecdotally, a startling stimulus causes different levels of arousal in the two species (see **Video 1**).

Synchronisation at the Population Level

If our hypothesis is correct and *D. suzukii* flies reduce or shut down activity in response to stress, we would expect that monitoring locomotion under more favourable conditions would result in higher activity and better rhythmicity. We carried out pilot experiments under LD 12:12, 25°C. We tested the locomotor behaviour of 10 males kept together (**Figure 5A**) or 10 males and 10 females kept together (**Figure 5B**) in a growth vial (9 cm height x 2 cm diameter, with 1.5 cm of standard fly medium at the bottom and 1.5 cm stopper at the top), employing a population monitor (DPM, Trikinetics, USA). The DPM has three rings of infrared emitters/detectors; Ring1 (R1) was located 0.5 cm above the food, Ring 2 (R2) in the middle of the tube (3 cm above the food) and Ring 3 (R3), 0.5 cm below the stopper (**Figure 5C**). **Figure 5A** shows the average activity profiles (to scale) for ten S1202 and M1217 males. *D. suzukii* males spent most of the time near the food (R1) or at the other end of the vial (R3). The flies were active mostly in the evening and showed a consistent E peak anticipating the L/D transition, although an additional, small activity bout was present towards the end of the dark period. The flies were at rest in the morning, apart from a startle response in correspondence to the D/L transition. This contrasts with the average profile of single flies under similar LD and temperature conditions, showing a more disperse pattern of activity with poorly defined M and E peaks and no activity in the dark (**Figures 1B**, **2D**). Moreover, *D. suzukii* males were much more active when monitored together than in isolation. Although a direct comparison between the two conditions is not possible, we can compare the relative activities of D. *suzukii* and *D. melanogaster* flies under the same conditions. When monitored individually S1202 males were about five times less active than M1217 males (**Figure S2**). When monitored as a group of males the combined activity (R1-R3) of S1202 flies was about 70% that of M1217 (**Figure S3** and **Table S1**). Differences in activity profile when monitoring single males or group of males were also observed for *D. melanogaster*. Under group monitoring, the morning peak was more prominent but the siesta was less defined than for single male recordings (compare **Figures 2D**, **5A**). Interestingly, most of the activity was recorded by R1 and R2, which again sets *D. melanogaster* apart from *D. suzukii*.

We then measured the locomotor activity of a group of 10 males and 10 females housed together (**Figure 5B**). For S1202 we observed an increase in morning and (especially) night activity, although the E peak was still the most prominent. We noticed that flies were mostly active near the food (R1), which we interpret as a consequence of egg-laying. Likewise, M1217 flies were much more active at night and additionally in the morning. Again, R1 recorded the majority of the activity. We saw a dramatic increment in R1 activity at the end of day 3, which we attribute to the development of wandering larvae. Our assumption is compatible with the timing of development of *D. melanogaster* and with the fact that such an increase in activity is limited to R1. The reason we did not observe a similar phenomenon for *D. suzukii* might be related to a longer developmental time for the species (Asplen et al., 2015) and to differences in larval behaviour, but we did not investigate this further.

Overall, these observations suggest that social interactions contribute to entrainment, as they refine the phase relation

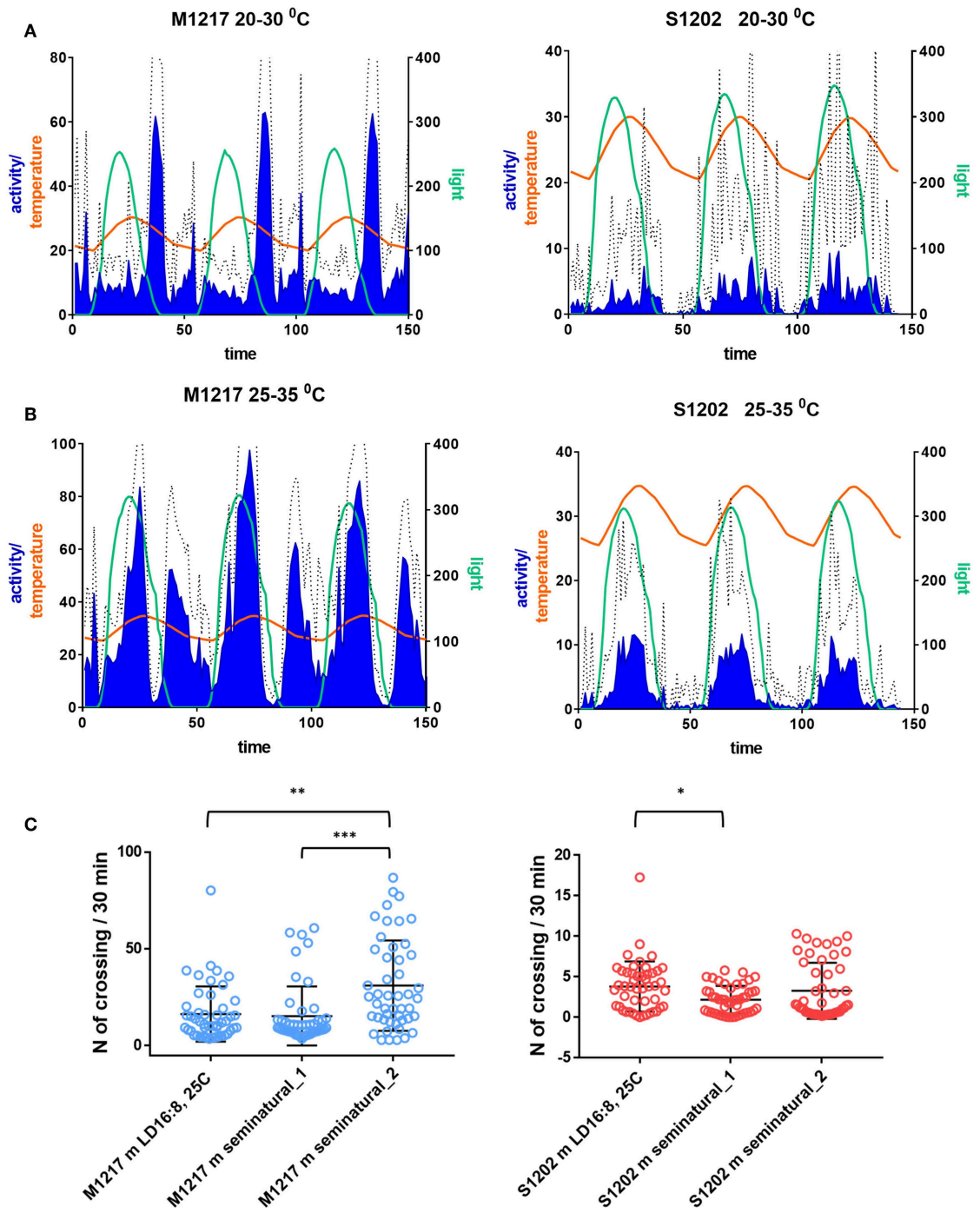

FIGURE 4 | Locomotor activity in *D. suzukii* (S1202) and *D. melanogaster* (M1217) males under seminatural conditions. Flies were exposed to cycling temperature and to cycling light of spectral composition mimicking a midsummer's day in Northern Italy. The temperature cycle peaked 2.5 h later than the light cycle. Only flies that survived in excess of 3 days were considered. **(A)** Seminatural condition 1. Left Y-axis: Activity levels (blue), *D. suzukii* 0–40 (crossing/30 min), *D. melanogaster* 0–80 (crossing/30 min). Temperature (orange), 20–30°C. Right Y-axis: Light (green), *D. suzukii* 0–350 lux, *D. melanogaster* 0–250 lux. X-axis: Time (150 intervals of 30 min). Hatched line: standard deviation of activity. S1202, $N = 66/76$. M1217, $N = 32/32$. [N = alive after 3 days/initial number]. **(B)** Seminatural condition 2. Left Y-axis: Activity levels (blue), *D. suzukii* 0–40 (crossing/30 min), *D. melanogaster* 0–100 (crossing/30 min). Temperature (orange), 25–35°C. Right Y-axis: Light (green), 0–300 lux. X-axis: Time (150 intervals of 30 min). Hatched line: standard deviation of activity. S1202, $N = 47/107$. M1217, $N = 30/30$. **(C)** Average day activity levels (number of crossing/30 min) of LD 16:8, 25°C, seminatural conditions 1 and 2. Activity levels were different in M1217 males under the three conditions (Kruskal-Wallis, $P < 0.0001$). Dunn's multiple comparisons test confirmed an increase in activity under seminatural conditions 2 (LD16:8, 25°C vs. seminatural_2, $^{**}P = 0.0021$; seminatural_1 vs. seminatural_2, $^{***}P = 0.0001$). Activity levels were different in S1202 males under the three conditions (Kruskal-Wallis, $P = 0.0317$). Dunn's multiple comparisons test confirmed a small decrease in activity of seminatural conditions 1 compared to LD16:8, 25°C ($^{*}P = 0.028$).

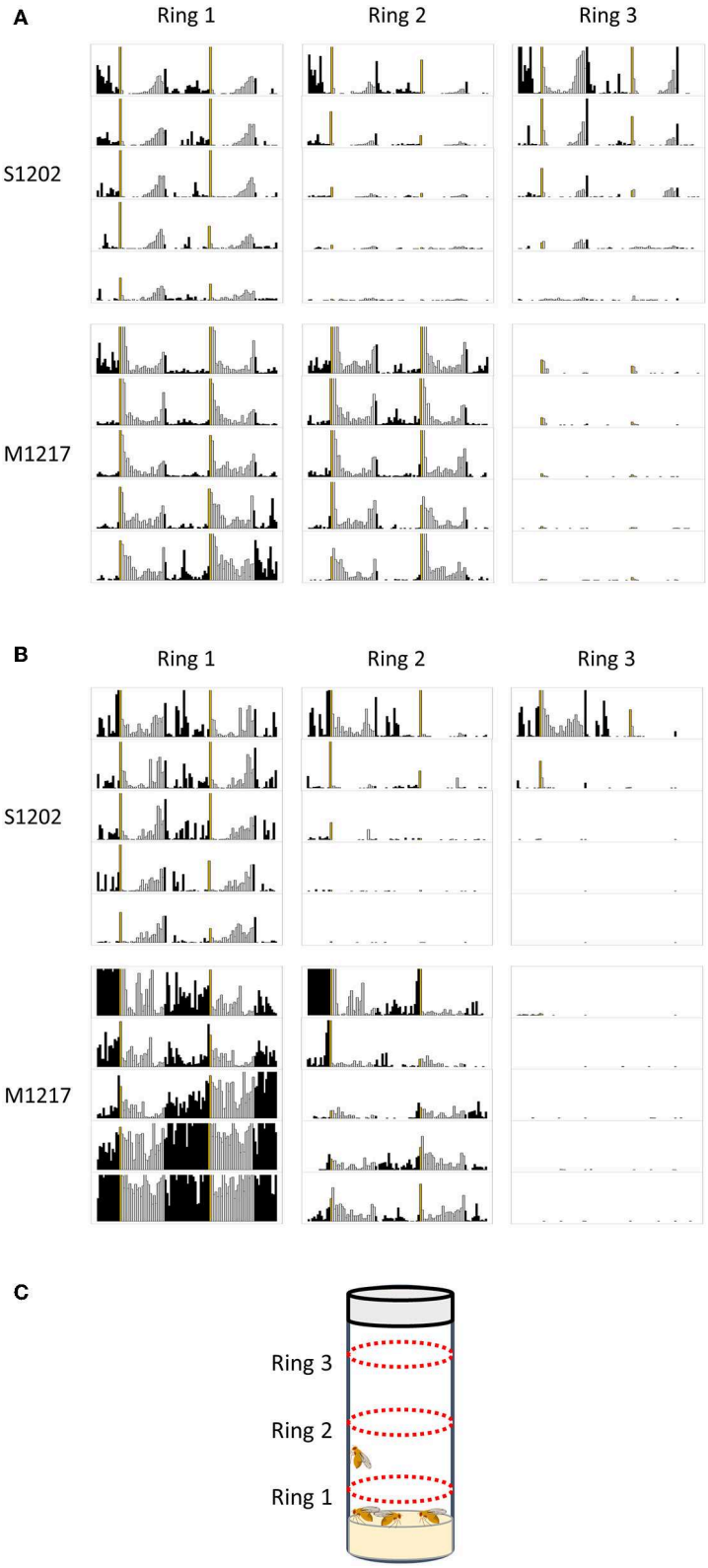

FIGURE 5 | Population rhythms in *D. suzukii* (S1202) and *D. melanogaster* (M1217). **(A)** Ten males monitored together. **(B)** Ten males and ten females monitored together. Note that for M1217 the high levels of activity detected by Ring1 after 3 days are probably caused by the development of wandering larvae (see text). **(C)**

(Continued)

FIGURE 5 | Schematic representation of the experimental set-up showing the position of the three emitters/detectors Rings. Black columns correspond to dark and white columns to light. The yellow column corresponds to lights on. The Y-axis reports activity levels: 0–300 (crossing/30 min). The X-axis reports time (96 intervals of 30 min). Data are double plotted (i.e. day1-day2, day2-day3, etc.). Flies were monitored for 5 days in a growth vial (9 cm height x 2 cm diameter, with 1.5 cm of standard fly medium at the bottom and 1.5 cm stopper at the top) loaded into a *Drosophila* population monitor (DPM, Trikinetics, USA) under LD 12:12, 25°C. The DPM has three rings of infrared emitters/detectors; Ring1 was located 0.5 cm above the food, Ring 2 in the middle of the tube (3 cm above the food) and Ring 3, 0.5 cm below the stopper.

between rhythmic locomotor activity and the LD cycle. This was already known in *D. melanogaster* (Levine et al., 2002; Fujii et al., 2007). Additionally our data suggest that for species such as *D. suzukii*, enriched social conditions might be necessary for meaningful circadian behaviour to become manifest.

The Neuronal Organisation of the Clock

The anatomical location of the clock is identified by the expression of clock genes and proteins. In *D. melanogaster* the clock consists of about 75 neurons per brain hemisphere, which are divided into lateral and dorsal neurons. The lateral neurons are then subdivided into ventral (LNv) and dorsal (LNd). The LNv consists of 4 large (l-LNv) and 4 small (s-LNv) neurons, both expressing the neuropeptide PIGMENT-DISPERSING FACTOR or PDF. Additionally, a single, PDF-null (pn-) or 5th-LNv is interspersed among the l-LNv. All LNv express CRY at high levels. More dorsal are 6 LNd. Of these, 3 express CRY at high levels whereas the others express *cry* mRNA but the protein is almost undetectable. Dorsal and posterior to the LN are the dorsal neurons, DN. These are divided into three heterogeneous groups, DN1, DN2 and DN3. In the DN1 cluster the 2 more anterior (and dorsal) neurons are called DN1a, they express high levels of CRY. More posterior, there are about 6-8 CRY-positive and 6-8 CRY-negative DN1p. Slightly ventral to the DN1 and just on top of the projections coming from the s-LNv are 2 neurons forming the DN2 group. In a more lateral and dorsal position there are about 40 neurons mainly of small size, the DN3 cluster. Finally there are 3 lateral posterior neurons (LPN) that are less characterised. DN2, DN3 (with a few exceptions) and LPN do not express CRY to visible levels (reviewed in Helfrich-Förster, 2003).

We started the anatomical investigation of the circadian neuronal network in *D. suzukii* males by testing anti-PDF immunoreactivity (all antibodies used in this study had been raised against *D. melanogaster* proteins and previously validated). In *D. melanogaster*, anti-PDF staining is a convenient cytoplasmic marker of the LNv but it is also useful to infer the identity of the other neuronal clusters by their relative positions. We detected anti-PDF staining in four l-LNv and four s-LNv. The l-LNv projected to the ipsilateral and, *via* the posterior optic commissure, to the contralateral medulla. The s-LNv projected to the ipsilateral dorsal-posterior protocerubrum. The arrangement is very similar to the one described in *D. melanogaster*, although in *D. suzukii* the two LNv groups lie much closer together (**Figure 6** and **Figure S4**).

We then applied anti-PDP1ε at ZT18 (*Zeitgeber* Time 18, with ZT0 = lights on and ZT12 = lights off), corresponding to the peak of PDP1ε expression in *D. melanogaster* (Cyran et al., 2003). We could recognise all putative clusters of clock neurons in *D. suzukii* with the exception of the LPN, which we were unable to identify unambiguously. Moreover, the numbers of neurons we observed per cluster were in agreement with those expected based on the *D. melanogaster* model. The only possible exception were the DN1a that we could not detect in half of the samples we analysed. Additionally, due to their small size and number we did not quantify the "crowded" DN3 cluster (**Figure 7**, **Table 4**).

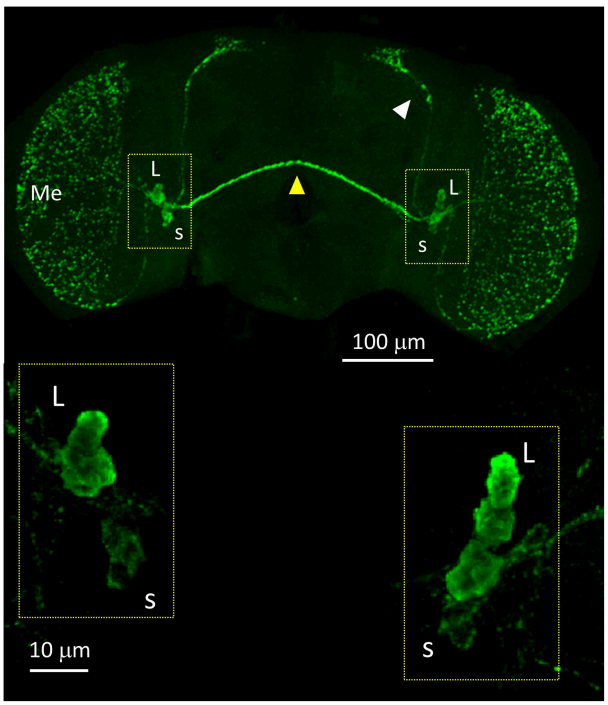

FIGURE 6 | PDF immunoreactivity. Anti-PDF staining of a whole mount brain (ZT11). White arrow head = dorsal projections of the s-LNv (s). Yellow arrow head = posterior optic commissure connecting the l-LNv (L) of both sides. Additionally, the l-LNv project to the ipsilateral medulla (Me). The bottom panels show the LNv at higher magnification. All pictures are confocal maximum projections of several z-stacks. Contrast and brightness have been optimised for each panel as a whole.

Unlike many other *Drosophila* species (Hermann et al., 2013), we discovered that the clock neurons of *D. suzukii* can be labelled by anti-PER and anti-TIM antibodies raised against *D. melanogaster* proteins. We detected both immunoreactivities at ZT23 but not at ZT11 (**Figures 8**, **9**). This is in agreement with the TTL model and increases our confidence on the specificity of the immunoreaction. We observed the expected numbers of LN; however the DN were more variable. We detected putative DN2 (often just 1 neuron) and DN1a with anti-PER but not with anti-TIM, and with both antibodies we observed just half the number of the putative DN1p revealed by anti-PDP1ε staining (**Table 4**).

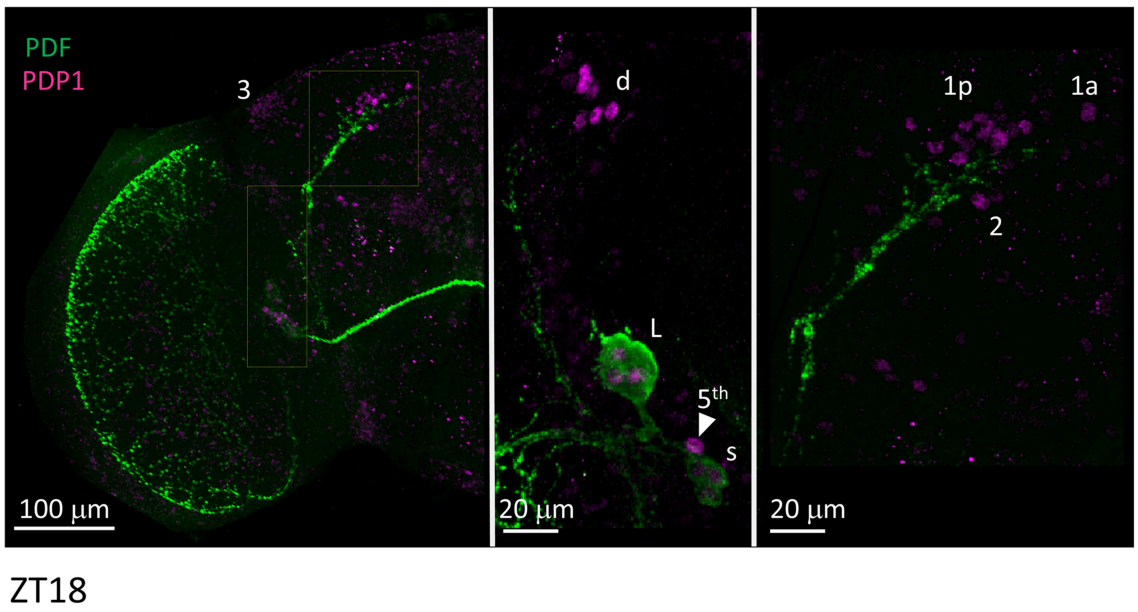

FIGURE 7 | PDP1ε immunoreactivity. Flies were collected at ZT18. PDF immunoreactivity is in green, PDP1ε immunoreactivity is in magenta. The right and the middle panels are higher magnifications of the regions highlighted on the left panel. 3 = DN3. d = LNd. L = l-LNv. Arrow head and 5th = 5th-LN. s = s-LNv. 1p = DN1p. 1a = DN1a. 2 = DN2. Each panel represents confocal maximum projections of several z-stacks. Contrast and brightness have been optimised, modifications were applied to each panel as a whole.

TABLE 4 | Identification of putative clock cells by immunolabelling.

Protein	Average number of stained cells ± Standard Deviation [Number of hemispheres]								
	ZT	s-LNv	l-LNv	5th-LNv	LNd	DN2	DN1a	DN1p	DN3
PER	23	3.8 ± 0.4 [6]	4.0 ± 0.0 [6]	1.0 ± 0.0 [6]	5.4 ± 0.9 [5]	1.3 ± 0.6 [11]	1.9 ± 0.6 [11]	7.1 ± 0.8 [11]	* [11]
PER	11	0.0 ± 0.0 [8]	0.0 ± 0.0 [8]	0.0 ± 0.0 [8]	0.0 ± 0.0 [8]	0.0 ± 0.0 [8]	0.0 ± 0.0 [8]	0.0 ± 0.0 [8]	0.0 ± 0.0 [8]
TIM	23	3.9 ± 0.4 [14]	4.1 ± 0.3 [14]	1.0 ± 0.0 [14]	5.7 ± 0.8 [13]	0.3 ± 0.5[a] [6]	0.0 ± 0.0 [6]	6.8 ± 1.0 [6]	* [6]
TIM	11	0.0 ± 0.0 [5]	0.0 ± 0.0[b] [5]	0.0 ± 0.0[c] [5]	0.0 ± 0.0[d] [5]	0.0 ± 0.0 [6]	0.0 ± 0.0 [6]	0.0 ± 0.0 [6]	0.0 ± 0.0 [6]
PDP	18	3.9 ± 0.4 [8]	4.0 ± 0.0 [8]	0.9 ± 0.4 [8]	6.0 ± 0.0 [8]	1.9 ± 0.3 [12]	1.0 ± 1.0[e] [12]	14.8 ± 1.0 [12]	* [12]
CRY	23^	3.8 ± 0.4 [5]	4.0 ± 0.0 [5]	1.0 ± 0.0 [5]	3.8 ± 0.4[f] [5]	0.0 ± 0.0 [4]	0.0 ± 0.0 [4]	6.0 ± 0.0 [4]	0.0 ± 0.0 [4]
CRY	11	0.0 ± 0.0 [5]	0.0 ± 0.0 [5]	0.0 ± 0.0 [5]	0.0 ± 0.0 [5]	0.0 ± 0.0 [5]	0.0 ± 0.0 [5]	0.0 ± 0.0 [5]	0.0 ± 0.0 [5]

**, staining observed but number of cells not quantified.*
∧, flies were kept 3 days in DD and then dissected at CT23.
a, 1 putative DN2 neuron was observed in two hemispheres only.
b, very weak and cytoplasmic staining was observed in 4 l-LNv in 2 hemispheres.
c, very weak and cytoplasmic staining was observed in 1 hemisphere.
d, very weak and cytoplasmic staining was observed in 2 LNd in 3 hemispheres.
e, 2 putative DN1a neurons were observed in 6 hemispheres only.
f, In two hemispheres 2 additional cells showing fainter staining were also observed.

Finally we examined anti-CRY immunoreactivity (**Figure 10**). CRY is degraded by light in *D. melanogaster* (Stanewsky et al., 1998). Thus, to improve detection we kept *D. suzukii* flies in DD for 3 days before dissection at CT23 (Circadian Time 23, CT0 = subjective lights on, CT12 = subjective lights off). The LN showed the most prominent immunoreactivity; we observed staining in all LNv and in 4 LNd. In the dorsal brain, 6 DN1p showed CRY-immunoreactivity but we did not observe the expected staining in the DN1a (**Table 4**). As expected we did not observe CRY staining at ZT 11 (**Figure 10**, **Table 4**).

DISCUSSION

The first overall conclusion of this work is that *D. suzukii* is a challenging species for chronobiology studies in the laboratory. The flies do not survive well the standard laboratory conditions used for measuring single-fly locomotor activity, and they move little (**Tables 1–3**). This probably contributes to the large variability in the free run (i.e., DD and constant temperature) period seen after each entrainment condition, which becomes even more pronounced at lower temperatures for both males

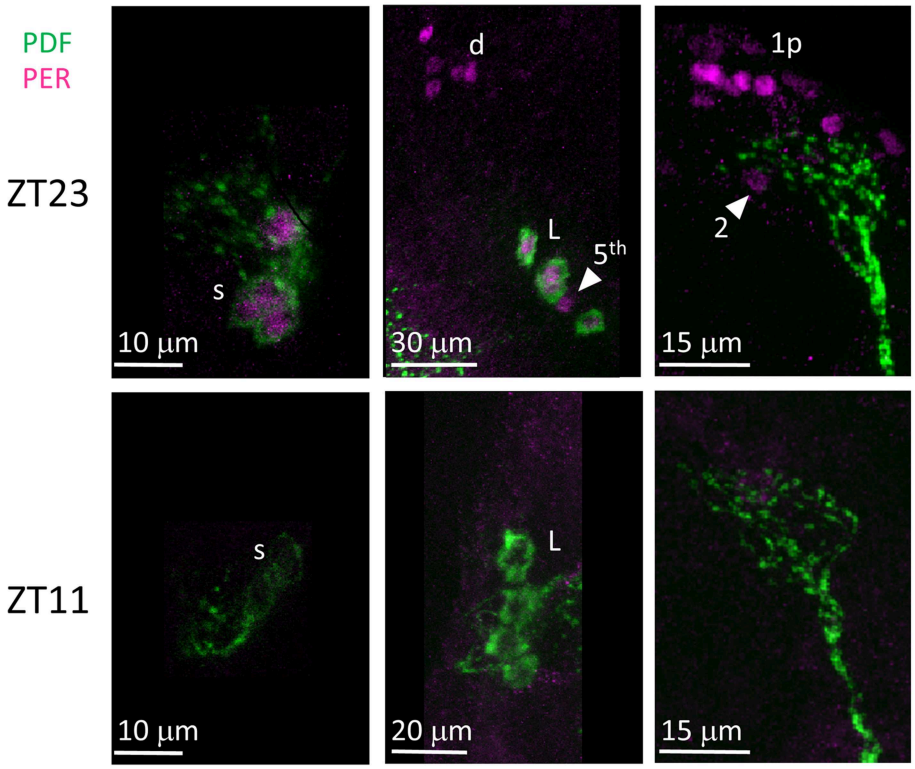

FIGURE 8 | PER immunoreactivity. Flies were collected at ZT23 (top panels) and ZT11 (bottom panels). PDF immunoreactivity is in green, PER immunoreactivity is in magenta. PER immunoreactivity was detected at ZT23 but not at ZT11. s = s-LNv. d = LNd. L = l-LNv. Arrow head and 5th = 5th-LN. 1p = DN1p. 2 = DN2. Each panel represents confocal maximum projections of several z-stacks. Contrast and brightness have been optimised, modifications were applied to each panel as a whole.

and virgin females (**Figure 2C**). At 18°C the difference in period between individuals at the extremes of the distribution can be a remarkable 10–15 h, suggesting that at least for this strain, in the laboratory and under cooler conditions, these flies appear to have very poor temperature compensation. This goes against what it is expected for a fundamental property of the clock with adaptive value (Pittendrigh, 1993; Sawyer et al., 1997). Such a result is even more surprising considering that these flies have evolved in a temperate habitat (Ometto et al., 2013) while the clock of *D. melanogaster*, of tropical origin (Mansourian et al., 2018), is well-adapted to 18°C. Our interpretation is that at 18°C the single-fly locomotor activity assay is not able to capture the true nature of the behaviour in *D. suzukii*, probably because the very low level of activity makes the determination of period imprecise. Entrainment is also different between the two species. Whereas, *D. melanogaster* are crepuscular, showing higher activity around the D/L (morning, M) and L/D (evening, E) switches, *D. suzukii* are mainly diurnal in our assay, being most active during the day (**Figure 2D**). In addition, the average day activity profiles do not show clear M and E peaks (with the exception of the hot conditions, LD 12:12, 28°C) and they are not consistently different between males and virgin females. In contrast, in *D. melanogaster* the day activity profile is a reliable predictor of gender (**Figure 2D**, **Figure S2**). We observed robust differences between virgin and mated females. Once mated, *D. suzukii* females show less variation in the circadian period of locomotor activity (**Figure 3B**) and a relative increase in day activity (**Figures 3C,D**). The latter had been observed before using group monitoring (4 flies tested together with LAM16 activity monitors, Trikinetics, USA) under both rectangular and seminatural conditions, which supports the robustness of this observation (Ferguson et al., 2015). We speculate that changes in both the entrainment profile (under LD) and the variance of the period (under DD) might underline a different coupling between clock neurons in females as a consequence of mating. Although we observed the same general trend in our *D. melanogaster* control (M1206) differences were not significant, possibly due to sample size or to genetic background (**Figures 3A–D**).

The low level of activity shown by *D. suzukii* under rectangular (on-off) light entrainment and single-fly monitoring motivated us to test alternative settings. We used custom-modified incubators producing so called seminatural conditions, such that light (of appropriate spectral composition) and temperature change gradually and in coordination simulating the natural environment (Green et al., 2015). We mimicked summer days in Northern Italy (where we collected our flies) using LD 16:8 and two temperature cycles, 20–30°C and 25–35°C. Under seminatural conditions *D. suzukii* males monitored individually

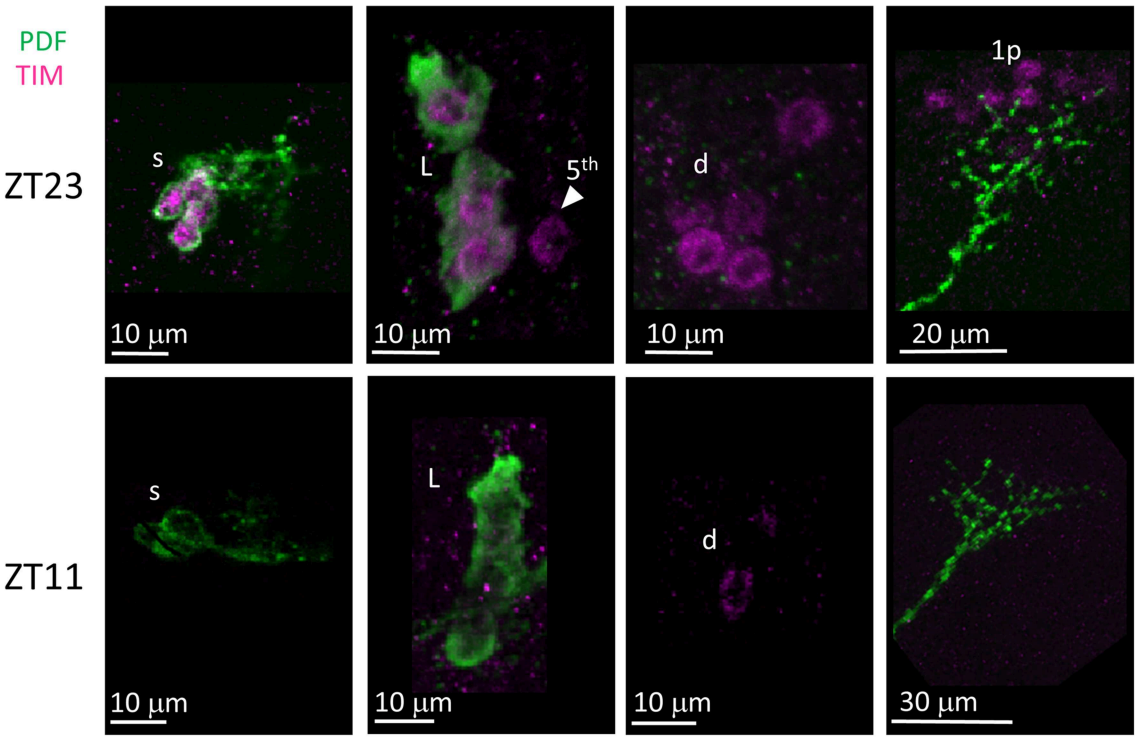

FIGURE 9 | TIM immunoreactivity. Flies were collected at ZT23 (top panels) and ZT11 (bottom panels). PDF immunoreactivity is in green, TIM immunoreactivity is in magenta. TIM immunoreactivity was detected at ZT23 but not ZT11, a part from very weak cytoplasmic staining seldom seen in LN (for instance, second panel from the right on the bottom). s = s-LNv. L = l-LNv. Arrow head and 5th = 5th-LN. d = LNd. 1p = DN1p. Each panel represents confocal maximum projections of several z-stacks. Contrast and brightness have been optimised, modifications were applied to each panel as a whole.

still moved little and just during the day (**Figures 4A,B**). The absence of evening activity was particularly pronounced under the hotter cycle (25–35°C). Furthermore, the lack of plasticity in the regulation of their locomotor behaviour was even more severe than under rectangular light entrainment (**Figure 2D**) and also compared to published observations where single-fly rhythmicity was tested under conditions mimicking summer (LD 14:10, 12.2–22.2°C) and winter (LD 11:13, 6.8–16.7°C) in Watsonville California, the site of the first *D. suzukii* detection in North America (Hamby et al., 2013). In addition, our results disagree with data from the wild (unmanaged blueberry fields in Bacon County, Georgia, US) obtained by trapping, suggesting that *D. suzukii* is mainly a crepuscular species that modulates activity in response to temperature and humidity fluctuations (Evans et al., 2017).

The *D. melanogaster* males we tested under seminatural conditions manifested the opposite behaviour, robust and persistent locomotion, further increased under the most challenging condition (**Figures 4A,B**). Under 20–30°C cycles *D. melanogaster* males were able to pace their locomotion according to the interactions between light and temperature, avoiding being active during the hottest part of the day (**Figure 4A**). However, such a process partially failed under 25–35°C cycles, giving way to a large burst of day activity called the afternoon peak, which is likely a sustained escape response (**Figure 4B**) (Vanin et al., 2012; Green et al., 2015). Extrapolating from these results we hypothesised that the two species might adopt a different strategy to overcome stressful environmental conditions, with *D. suzukii* suppressing activity and *D. melanogaster* increasing it. This is relevant because reduced locomotion can give the impression of a weak clock when in reality a low activity output might not reflect fairly its circadian regulation. To investigate this further we performed preliminary experiments where 10 males or 10 males and 10 females were tested together under LD 12:12, 25°C in a growth vial using a population monitor (DPM, Tikinetics, USA) (**Figures 5A,B**). Conceptually similar experiments but using different settings and equipment had been performed before in both *D. melanogaster* and *D. suzukii* (Levine et al., 2002; Fujii et al., 2007; Ferguson et al., 2015; Shaw et al., 2018a). One general conclusion that applies to the published work and to our own is that the presence of conspecifics influences the activity profile and thus social interactions are an important *Zeitgeber* for the circadian clock. Moreover, housing *D. melanogaster* males and females in close proximity results in increased nocturnal behaviour (Fujii et al., 2007). We have confirmed those conclusions and extended them to *D. suzukii* (**Figure 5B**). However, our most interesting observation is that when tested in a socially rich environment, *D. suzukii* flies seem much more active and synchronous than when tested in isolation

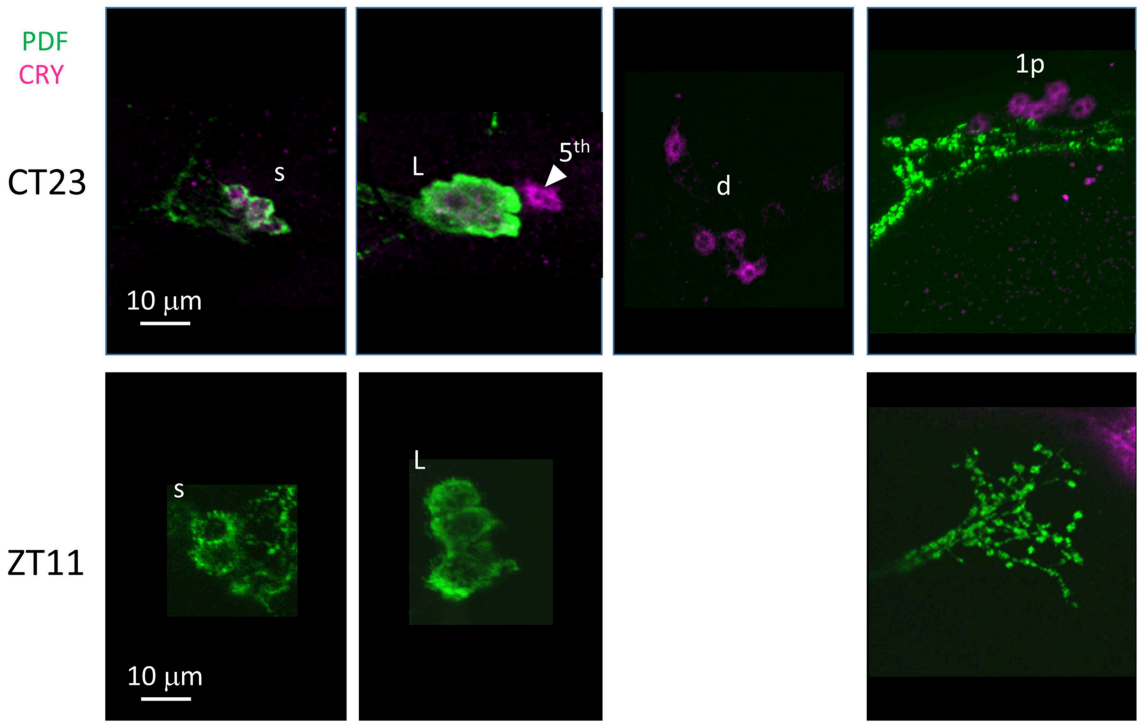

FIGURE 10 | CRY immunoreactivity. Flies were collected at CT23 after 3 days in darkness (top panels) and ZT11 (bottom panels). PDF immunoreactivity is in green, CRY immunoreactivity is in magenta. CRY immunoreactivity was detected at CT23 but not ZT11.L = l-LNv. Arrow head and 5th = 5th-LN. d = LNd. s = s-LNv. 1p = DN1p. Each panel represents confocal maximum projections of several z-stacks. Contrast and brightness have been optimised, modifications were applied to each panel as a whole.

(**Figures 5A,B**; **Figures S2, S3**). A caveat is that our results are still preliminary and limited to LD entrainment. However, they agree with an interesting study where 10 males and 10 females were monitored together on nitrogen-free medium for about 6 days in LAM25 monitors (Trikinetics, USA). The authors recreated in the laboratory temperature and light conditions found in East Malling (Kent, UK) during June (LD 18:6, 11–22°C), August (LD 16:8, 14–32°C) and October (LD 12.5:11.5, 9–18°C) 2016. The flies displayed a good level of locomotion but also they paced activity as a function of the interaction between light and temperature (Shaw et al., 2018a; **Figure 9** therein). We never observed such a plastic behaviour in *D. suzukii* flies monitored individually. Conversely, *D. melanogaster* flies were able to retain plasticity even in isolation. Therefore, our results are a warning that for some species isolation might not be permissive to the manifestation of locomotor activity rhythms as a robust and reliable experimental window to the clock, something that we take for granted. We anticipate that by testing *Drosophila* species under seminatural-socially enriched conditions we will improve the representation of the natural environment in the laboratory and gain a better understanding of the adaptive value of the clock.

Finally, we asked whether the behavioural differences we observed between the two species would correlate with differences in the organisation of the neuronal network of the clock. To identify putative clock neurons in *D. suzukii* we used well-characterised antibodies made against *D. melanogaster* clock proteins that we had tested before (see Materials and Methods for antibodies information). In *D. melanogaster* the clock neurons can be subdivided into lateral and dorsal neurons. The former consist of three clusters (s-LNv, l-LNv, and LNd) and a single neuron (5th-LNv). The LN are easily recognizable: they are quite predictable in anatomical location, in size and in relative position to each other and to anatomical landmarks. Moreover, the number of neurons in each cluster is low (1–6), they are not "tightly packed" and PDF—a clock relevant neuropeptide – is a specific marker for the two ventral groups (s-LNv and l-LNv) labelling their cytoplasm including projections. The identification of the DN is more ambiguous as they are more irregular in size and distribution, often they are very close to one another, they are numerous and we do not have a specific marker for them. We tested *D. suzukii* males for immunoreactivity against the neuropeptide PDF and the clock proteins PDP1ε, PER, TIM and CRY (**Figures 6–10**). The overall picture is that the neuronal organisation of the circadian network is quite similar in *D. suzukii* and *D. melanogaster*, but there are some differences. PDF is expressed in the LNv and we can see projections to the medulla and to the dorsal protocerebrum, reproducing the well-described pattern known for *D. melanogaster* (**Figure 6**). One difference is that in *D. suzukii* the l-LNv are much more tightly packed together and to the s-LNvs (**Figure 6** and **Figure S4**; see also **Figure 7**, middle panel). Anti-PDP1ε staining at ZT18 (the time when PDP1ε–always nuclear—is at its maximum in *D. melanogaster*;

Cyran et al., 2003) revealed that all major types of clock neurons are putatively present and in numbers comparable to *D. melanogaster*, with the proviso that we did not quantify the small and numerous DN3 neurons (more than 40 in *D. melanogaster*) and we could not unequivocally identify the LPN (**Figure 7** and **Table 4**). Anti-PER and anti-TIM staining at ZT23 and ZT11 (respectively, when they are nuclear and highly abundant or absent in *D. melanogaster*) were also consistent with an overall conservation of the clock between *D. melanogaster* and *D. suzukii* (**Figures 8**, **9**). The LN were clearly identified and the expression of the two proteins was nuclear and high or absent at the appropriate times. However, some differences in expression emerged in the DN. At ZT23 we usually observed only one (out of two) DN2 with anti-PER and none with anti-TIM staining. We were able to distinguish the two DN1a with anti-PER but not with anti-TIM. Lastly, only half the number of PDP1ε-positive DN1p showed anti-PER or anti-TIM staining (*ca.* 7 out of *ca.* 15). Double-labelling experiments will be necessary to distinguish whether the same or different DN1p show anti-PER and anti-TIM immunoreactivity and to prove co-localization with PDP1ε. The latter is particularly important as in *D. melanogaster* PDP1ε expression in not limited to clock cells and the same might occur in *D. suzukii* (Cyran et al., 2003). Curiously, at ZT11 we observed very weak anti-TIM (but not anti-PER) cytoplasmic staining in a few LN (**Figure 9**, bottom, second panel from the right and **Table 4**). In *D. melanogaster* PER and TIM start accumulating in the cytoplasm in the evening, they transition into the nucleus in the middle of the night and become fully nuclear by the end of dark phase. Then they disappear, with TIM being degraded faster than PER as TIM is directly targeted for degradation after exposure to light whereas the decline of PER is a consequence of it requiring TIM for stability (reviewed in Özkaya and Rosato, 2012). If this regulation were the same in *D. suzukii* it is unclear how the rise of TIM could lead that of PER. Time course experiments assessing the progressive accumulation and degradation of both proteins will be required to clarify this. Finally, we examined immunoreactivity to CRY (**Figure 10** and **Table 4**). Assuming the protein might be subject to light-dependent degradation as in *D. melanogaster* we maintained the flies in darkness for three days prior to their collection at CT23. The immunosignal was consistent with what was expected in comparison with the *D. melanogaster* model with the exception that we did not observe staining in DN1a cells. Again, double-labelling experiments should be carried out to test whether or not the putative 6 CRY-positive DN1p additionally express PER and/or TIM. As expected we did not observe anti-CRY immunoreactivity at ZT11.

At the beginning of our discussion we highlighted the difficulties encountered when investigating the clock of this species. However, at the end of it our overall judgement is that *D. suzukii*, although challenging, is a model worthy of future chronobiology investigations. Glimpses suggest that some elements of the circadian neuronal network might be different from *D. melanogaster* and some molecular details might have evolved. More work is required before a clear picture can be drawn, but a better understanding of the clock of *D. suzukii* is in reach using the modern tools of genetic manipulation. The most interesting aspect will be investigating how social interactions impact on the clock and on the mechanisms that regulate arousal and stress responses in this fascinating species. We speculate that the evolution of lower arousal and of stress responses that promote inactivity have been instrumental in the ecological transitioning of the species. Although *D. suzukii* can successfully lay eggs in rotting fruits, they are outcompeted by other drosophilids (Shaw et al., 2018b). Being less aroused and less active under environmental stress might allow *D. suzukii* to save eggs and energy waiting for the next short burst of fruit ripening, when fresh fruits become available to lay their eggs without competition. Perhaps, their propensity for living at a "lower gear" is the secret of their current success as an invasive pest species.

DATA AVAILABILITY

The raw data supporting the conclusions of this manuscript will be made available by the authors upon reasonable request.

AUTHOR CONTRIBUTIONS

All authors contributed to the generation of hypotheses and the interpretation of results. LG contributed materials. ER and CK contributed funding. CH, ÖÖ, and HR provided essential technical knowledge and solutions. CH and ER performed experiments and analysed data. CH and ER wrote the manuscript with input from all the authors.

FUNDING

We acknowledge funding from the BBSRC (BB/H018093/1 and BB/J005169/1), the Electromagnetic Field Biological Trust, the NC3Rs (G1100597) and the Provincia Autonoma di Trento (ADP).

ACKNOWLEDGMENTS

We thank A. Grassi for trapping the flies and M. Ajelli for help in establishing the stocks. We thank A. Seghal and J Blau for anti-TIM and anti-PDP1ε antibodies, respectively. The monoclonal anti-PDF antibody developed by J. Blau was obtained from the Developmental Studies Hybridoma Bank, created by the NICHD of the NIH and maintained at The University of Iowa, Department of Biology, Iowa City, IA 52242. We thank K. Straatman and the Leicester Advanced Imaging Facility for help with confocal microscopy.

SUPPLEMENTARY MATERIAL

The Supplementary Material for this article can be found online at: https://www.frontiersin.org/articles/10.3389/fphys.2019.00941/full#supplementary-material

Figure S1 | Average day profile for *D. suzukii* males S1210, SMichele, S1203, and S1209 under standard laboratory conditions. The average day was obtained by averaging into one the four LD days for all rhythmic flies (SR+CR, see **Table 1**) of the same genotype. Black columns correspond to dark and white columns to light. Error bars show the standard deviation. Note that the error bars reaching the

top of the graph are truncated. This reflects a compromise in the choice of the scale of the Y-axis to allow the appreciation of both the average activity profile and its variance. Activity levels (0–40 crossing/30 min) are shown on the Y-axis, time (48 intervals of 30 min) is on the X-axis. Note that the profile for S1210 is the same as in **Figure 1B** but at different scale on the Y-axis.

Figure S2 | Combined LD activity under all entrainment conditions in *D. melanogaster* (M1217) and *D. suzukii* (S1202) virgin females (fv) and males (m). To test whether virgin females and males from the two species differ in their average activity under LD we combined 31 flies (the maximum common number of rhythmic flies across conditions, genders and species) at random for each entrainment condition. In M1217, virgin females (mean LD activity = 18.21 crossing/30 min) were more active than males (mean LD activity = 16.88 crossing/30 min); the difference is statistically supported (Kolmogorov-Smirnov test, $^{***}P = 0.0003$). In S1202, virgin females (mean LD activity = 3.55 crossing/30 min) and males (mean LD activity = 3.61 crossing/30 min) showed equal activity. Note that *D. melanogaster* flies are about five times more active than *D. suzukii*.

Figure S3 | Population rhythms. Activity levels in 10 males *D. suzukii* (S1202) and 10 males *D. melanogaster* (M1217). Activity levels (number of crossing/30 min) have been plotted separately for the three detector rings (R1, R2, and R3) to give an impression of the overall activity. See also **Table S1**.

Figure S4 | Anti-PDF staining of the LNv in *D. suzukii* and *D. melanogaster*. Typically, in *D. suzukii* the l-LNv are closer to one another and to the s-LNv than in *D. melanogaster*. L = l-LNv. s = s-LNv. Each panel represents confocal maximum projections of several z-stacks. Contrast and brightness have been optimised, modifications were applied to each panel as a whole.

Table S1 | Descriptive statistics for amount of activity/bin. The locomotor activities of 10 D. suzukii males and 10 D. melanogaster males were recorded for 5 days under LD 12:12, 25°C.

Video 1 | A simple startling stimulus, banging a growth vial on the bench, is applied to *D. suzukii* and *D. melanogaster* cultures. The locomotor response of the two species is different showing high arousal and activity in *D. melanogaster* and reduced arousal and activity in *D. suzukii*.

REFERENCES

Allada, R., White, N. E., So, W. V., Hall, J. C., and Rosbash, M. A. (1998). Mutant *Drosophila* homolog of mammalian clock disrupts circadian rhythms and transcription of period and timeless. *Cell* 29, 791–804. doi: 10.1016/S0092-8674(00)81440-3

Asplen, M. K., Anfora, G., Biondi, A., Choi, D. S., Chu, D., Daane, K. M., et al. (2015). Invasion biology of spotted wing *Drosophila* (*Drosophila suzukii*): a global perspective and future priorities. *J. Pest. Sci.* 88, 469–494. doi: 10.1007/s10340-015-0681-z

Bargiello, T. A., Jackson, F. R., and Young, M. W. (1984). Restoration of circadian behavioural rhythms by gene transfer in *Drosophila*. *Nature* 312, 752–754. doi: 10.1038/312752a0

Blau, J., and Young, M. W. (1999). Cycling vrille expression is required for a functional *Drosophila* clock. *Cell* 99, 661–671. doi: 10.1016/S0092-8674(00)81554-8

Calabria, G., Máca, J., Bächli, G., Serra, L., and Pascual, M. (2012). First records of the potential pest species *Drosophila suzukii* (Diptera: Drosophilidae) in Europe. *J. App. Ent.* 136, 139–147. doi: 10.1111/j.1439-0418.2010.01583

Chiu, J. C., Jiang, X., Zhao, L., Hamm, C. A., Cridland, J. M., Saelao, P., et al. (2013). Genome of *Drosophila suzukii*, the spotted wing *Drosophila G3.* 3, 2257–2271. doi: 10.1534/g3.113.008185

Cini, A., Ioriatti, C., and Anfora, G. (2012). A review of the invasion of *Drosophila suzukii* in Europe and a draft research agenda for integrated pest management. *Bull. Insect.* 65,149–160.

Cloonan, K. R., Abraham, J., Angeli, S., Syed, Z., and Rodriguez-Saona, C. (2018). Advances in the chemical ecology of the spotted wing *Drosophila* (*Drosophila suzukii*) and its applications. *J. Chem. Ecol.* 44, 922–939. doi: 10.1007/s10886-018-1000-y

Crava, C. M., Sass,ù, F., Taita, G., Becherd, P. G., and Anfora, G. (2019). Functional transcriptome analyses of *Drosophila suzukii* antennae reveal mating-dependent olfaction plasticity in females. *Insect Biochem. Mol. Biol.* 105, 51–59. doi: 10.1016/j.ibmb.2018.12.012

Cyran, S. A., Buchsbaum, A. M., Reddy, K. L., Lin, M. C., Glossop, N. R., Hardin, P. E., et al. (2003). vrille, Pdp1, and dClock form a second feedback loop in the *Drosophila* circadian clock. *Cell* 112, 329–341. doi: 10.1016/S0092-8674(03)00074-6

Das, S., Trona, F., Khallaf, M. A., Schuh, E., Knaden, M., Hansson, B. S., et al. (2017). Electrical synapses mediate synergism between pheromone and food odors in *Drosophila melanogaster*. *Proc. Natl. Acad. Sci. U.S.A.* 114, E9962–E9971. doi: 10.1073/pnas.1712706114

Dekker, T., Revadi, S., Mansourian, S., Ramasamy, S., Lebreton, S., Becher, P., et al. (2015). Loss of *Drosophila* pheromone reverses its role in sexual communication in *Drosophila suzukii*. *Proc. Biol. Sci.* 282:20143018. doi: 10.1098/rspb.2014.3018

Dissel, S., Hansen, C. N., Özkaya, Ö., Hemsley, M., Kyriacou, C. P., and Rosato, E. (2014). The logic of circadian organization in *Drosophila*. *Curr. Biol.* 24, 2257–2266. doi: 10.1016/j.cub.2014.08.023

Ejima, A. (2015). Pleiotropic actions of the male pheromone cis-vaccenyl acetate in *Drosophila melanogaster*. *J. Comp. Physiol. A Neuroethol. Sens. Neural. Behav. Physiol.* 201, 927–932. doi: 10.1007/s00359-015-1020-

Emery, P., So, W. V., Kaneko, M., Hall, J. C., and Rosbash, M. (1998). CRY, a *Drosophila* clock and light-regulated cryptochrome, is a major contributor to circadian rhythm resetting and photosensitivity. *Cell* 95, 669–679. doi: 10.1016/s0092-8674(00)81637-2

Evans, R. K., Toews, M. D., and Sial, A. A. (2017). Diel periodicity of *Drosophila suzukii* (Diptera: Drosophilidae) under field conditions. *PLoS ONE* 12:e0171718. doi: 10.1371/journal.pone.0171718

Fang, Y., Sathyanarayanan, S., and Sehgal, A. (2007). Post-translational regulation of the *Drosophila* circadian clock requires protein phosphatase 1 (PP1). *Genes Dev.* 12, 1506–1518. doi: 10.1101/gad.1541607

Ferguson, C. T. J., O'Neill, T. L., Audsley, N., and Elwyn, R. I. (2015). The sexually dimorphic behaviour of adult *Drosophila suzukii*: elevated female locomotor activity and loss of siesta is a postmating response. *J. Exp. Biol.* 218, 3855–3861 doi: 10.1242/jeb.125468

Fogle, K. J., Baik, L. S., Houl, J. H., Tran, T. T., Roberts, L., Dahm, N. A., et al. (2015). CRYPTOCHROME-mediated phototransduction by modulation of the potassium ion channel β-subunit redox sensor. *Proc. Natl. Acad. Sci. U.S.A.* 112, 2245–2250. doi: 10.1073/pnas.1416586112

Fogle, K. J., Parson, K. G., Dahm, N. A., and Holmes, T. C. (2011). Cryptochrome is a blue-light sensor that regulates neuronal firing rate. *Science* 331, 1409–1413. doi: 10.1126/science.1199702

Fujii, S., Krishnan, P., Hardin, P., and Amrein, H. (2007). Nocturnal male sex drive in *Drosophila*. *Curr. Biol.* 17, 244–251. doi: 10.1016/j.cub.2006.11.049

Goodhue, R. E., Bolda, M., Farnsworth, D., Williams, J. C., and Zalom, F. G. (2011). Spotted wing *Drosophila* infestation of California strawberries and raspberries: economic analysis of potential revenue losses and control costs. *Pest Manag. Sci.* 67, 1396–1402. doi: 10.1002/ps.2259

Grassi, A., Palmieri, L., and Giongo, L. (2009). *Drosophila* (Sophophora) *suzukii* (Matsumura) new pest of small fruit crops in trentino (in Italian). *Terra Trent.* 10, 19–23.

Green, E. W., O'Callaghan, E. K., Hansen, C. N., Bastianello, S., Bhutani, S., Vanin, S., et al. (2015). *Drosophila* circadian rhythms in seminatural environments: summer afternoon component is not an artifact and requires TrpA1 channels. *Proc. Natl. Acad. Sci. U.S.A.* 112, 8702–8707. doi: 10.1073/pnas.1506093112

Grosjean, Y., Rytz, R., Farine, J.-P., Abuin, L., Cortot, J., Jefferis, G. S. X. E., et al. (2011). An olfactory receptor for food-derived odours promotes male courtship in *Drosophila*. *Nature* 478, 236–240. doi: 10.1038/nature10428

Hamby, K. A., Kwok, R. S., Zalom, F. G., and Chiu, J. C. (2013). Integrating circadian activity and gene expression profiles to predict chronotoxicity of *Drosophila suzukii* response to insecticides. *PLoS ONE* 8:e68472. doi: 10.1371/journal.pone.0068472.

Helfrich-Förster, C. (2000). Differential control of morning and evening components in the activity rhythm of *Drosophila melanogaster*–sex-specific differences suggest a different quality of activity. *J. Biol. Rhythms* 15, 135–154. doi: 10.1177/074873040001500208

Helfrich-Förster, C. (2003). The neuroarchitecture of the circadian clock in the brain of *Drosophila melanogaster*. *Microsc. Res. Tech*. 62, 94–102. doi: 10.1002/jemt.10357

Hermann, C., Saccon, R., Senthilan, P. R., Domnik, L., Dircksen, H., Yoshii, T., et al. (2013). The circadian clock network in the brain of different *Drosophila* species. *J. Comp. Neurol*. 521, 367–388. doi: 10.1002/cne.23178

Hickner, P. V., Rivaldi, C. L., Johnson, C. M., Siddappaji, M., Raster, G. J., and Syed, Z. (2016). The making of a pest: insights from the evolution of chemosensory receptor families in a pestiferous and invasive fly, *Drosophila suzukii*. *BMC Genom.* 17:648. doi: 10.1186/s12864-016-2983-9

Isaac, R. E., Li, C., Leedale, A. E., and Shirras, A. D. (2010). *Drosophila* male sex peptide inhibits siesta sleep and promotes locomotor activity in the post-mated female. *Proc. Biol. Sci. U.S.A*. 277, 65–70. doi: 10.1098/rspb.2009.1236.

Karageorgi, M., Bräcker, L. B., Lebreton, S., Minervino, C., Cavey, M., Siju, K. P., et al. (2017). Evolution of multiple sensory systems drives novel egg-laying behavior in the fruit pest *Drosophila suzukii*. *Curr. Biol*. 27, 847–853. doi: 10.1016/j.cub.2017.01.055

Keesey, I. W., Grabe, V., Gruber, L., Koerte, S., Obiero, G. F., Bolton, G., et al. (2019). Inverse resource allocation between vision and olfaction across the genus *Drosophila*. *Nat. Commun*. 10:1162. doi: 10.1038/s41467-019-09087-z

Koh, K., Zheng, X., and Sehgal, A. (2006). JETLAG resets the *Drosophila* circadian clock by promoting light-induced degradation of TIMELESS. *Science* 312, 1809–1812. doi: 10.1126/science.1124951

Konopka, R. J., and Benzer, S. (1971). Clock mutants of *Drosophila melanogaster*. *Proc. Natl. Acad. Sci. U.S.A*. 68, 2112–2116. doi: 10.1073/pnas.68.9.2112

Krause Pham, C., and Ray, A. (2015). Conservation of olfactory avoidance in *Drosophila* species and identification of repellents for *Drosophila suzukii*. *Sci. Rep*. 5:11527. doi: 10.1038/srep11527

Laturney, M., and Billeter, C. (2014). Neurogenetics of Female Reproductive Behaviors in *Drosophila melanogaster*. *Adv. Genet*. 85, 1–108. doi: 10.1016/B978-0-12-800271-1.00001-9

Lebreton, S., Becher, P. G., Hansson, B. S., and Witzgall, P. (2012). Attraction of *Drosophila melanogaster* males to food-related and fly odours. *J. Insect Physiol.* 58, 125–129. doi: 10.1016/j.jinsphys.2011.10.009

Levine, J. D., Funes, P., Dowse, H. B., and Hall, J. C. (2002). Resetting the circadian clock by social experience in *Drosophila melanogaster*. *Science* 298, 2010–2012. doi: 10.1126/science.1076008

Lim, C., Chung, B. Y., Pitman, J. L., McGill, J. J., Pradhan, S., Lee, J., et al. (2007). Clockwork orange encodes a transcriptional repressor important for circadian-clock amplitude in *Drosophila*. *Curr. Biol*. 17, 1082–1089. doi: 10.1016/j.cub.2007.05.039

Mansourian, S., Enjin, A., Jirle, E. V., Ramesh, V., Rehermann, G., Becher, P. G., et al. (2018). Wild African drosophila melanogaster are seasonal specialists on marula fruit. *Curr. Biol*. 28, 3960–3968.e3. doi: 10.1016/j.cub.2018.10.033

Martinek, S., Inonog, S., Manoukian, A. S., and Young, M.,W (2001). A role for the segment polarity gene shaggy/GSK-3 in the *Drosophila* circadian clock. *Cell*. 105, 769–779. doi: 10.1016/S0092-8674(01)00383-X

Mazzotta, G. M., Bellanda, M., Minervini, G., Damulewicz, M., Cusumano, P., Aufiero, S., et al. (2018). Calmodulin enhances cryptochrome binding to INAD in *Drosophila* photoreceptors. *Front. Mol. Neurosci*. 11:280. doi: 10.3389/fnmol.2018.00280

Menegazzi, P., Yoshii, T., and Helfrich-Förster, C. (2012). Laboratory versus nature: the two sides of the *Drosophila* circadian clock. *J. Biol. Rhythm*. 27, 433–442. doi: 10.1177/0748730412463181

Nguyen, P., Kim, A. Y., Jung, J. K., Donahue, K. M., and Jung, C., Choi, et al. (2016). The Biochemical adaptations of spotted wing *Drosophila* (Diptera: Drosophilidae) to fresh fruits reduced fructose concentrations and Glutathione-S transferase activities. *J. Econ. Entomol*. 109, 973–981. doi: 10.1093/jee/tow019

Ometto, L., Cestaro, A., Ramasamy, S., Grassi, A., Revadi, S., Siozios, S., et al., (2013). Linking genomics and ecology to investigate the complex evolution of an invasive *Drosophila* pest. *Genome Biol. Evol*. 5, 745–757. doi: 10.1093/gbe/evt034

Özkaya, Ö., and Rosato, E. (2012). The circadian clock of the fly: a neurogenetics journey through time. *Adv. Genet*. 77, 79–123. doi: 10.1016/b978-0-12-387687-4.00004-0

Pittendrigh, C. S. (1993). Temporal organization: reflections of a Darwinian clock-watcher. *Annu. Rev. Physiol*. 55, 16–54. doi: 10.1146/annurev.ph.55.030193.000313

Price, J. L., Blau, J., Rothenfluh, A., Abodeely, M., Kloss, B., and Young, M. W. (1998). double-time is a novel *Drosophila* clock gene that regulates PERIOD protein accumulation. *Cell* 94, 83–95. doi: 10.1016/S0092-8674(00)81224-6

Ramasamy, S., Ometto, L., Crava, C. M., Revadi, S., Kaur, R., Horner, D. S., et al. (2016). The evolution of olfactory gene families in *Drosophila* and the genomic basis of chemical-ecological adaptation in *Drosophila suzukii*. *Genome Biol. Evol*. 8, 2297–2311. doi: 10.1093/gbe/evw160

Richier, B., Michard-Vanhée, C., Lamouroux, A., Papin, C., and Rouyer, F., (2008). The clockwork orange *Drosophila* protein functions as both an activator and a repressor of clock gene expression. *J. Biol. Rhythms* 23, 103–116. doi: 10.1177/0748730407313817

Rosato, E., and Kyriacou, C. P. (2006). Analysis of locomotor activity rhythms in *Drosophila*. *Nat. Protoc*. 1, 559–568. doi: 10.1038/nprot.2006.79

Rutila, J. E., Suri, V., Le, M., So, W. V., Rosbash, M., and Hall, J. C. (1998). CYCLE is a second bHLH-PAS clock protein essential for circadian rhythmicity and transcription of *Drosophila* period and timeless. *Cell* 29, 805–814. doi: 10.1016/S0092-8674(00)81441-5

Sathyanarayanan, S., Zheng, X., Xiao, R., and Sehgal, A. (2004). Posttranslational regulation of *Drosophila* PERIOD protein by protein phosphatase 2A. *Cell* 116, 603–615. doi: 10.1016/S0092-8674(04)00128-X

Sawyer, L. A., Hennessy, J. M., Peixoto, A. A., Rosato, E., Parkinson, H., Costa, R., et al. (1997). Natural variation in a *Drosophila* clock gene and temperature compensation. *Science* 278, 2117–2120. doi: 10.1126/science.278.5346.2117

Schlichting, M., Rieger, D., Cusumano, P., Grebler, R., Costa, R., Mazzotta, G. M., et al. (2018). Cryptochrome interacts with actin and enhances eye-mediated light sensitivity of the circadian clock in *Drosophila melanogaster*. *Front. Mol. Neurosci*. 11:238. doi: 10.3389/fnmol.2018.00238

Shaw, B., Brain, P., Wijnen, H., and Fountain, M. T. (2018b). Reducing *Drosophila suzukii* emergence through inter-species competition. *Pest. Manag. Sci*. 74, 1466–1471. doi: 10.1002/ps.4836

Shaw, B., Fountain, M. T., and Wijnen, H. (2018a). Recording and reproducing the diurnal oviposition rhythms of wild populations of the soft- and stone- fruit pest *Drosophila suzukii*. *PLoS ONE*. 13:e0199406. doi: 10.1371/journal.pone.0199406

Stanewsky, R., Kaneko, M., Emery, P., Beretta, B., Wager-Smith, K., Kay, S. A., et al. (1998). The cryb mutation identifies cryptochrome as a circadian photoreceptor in *Drosophila*. *Cell* 95, 681–692. doi: 10.1016/s0092-8674(00)81638-4

Vanin, S., Bhutani, S., Montelli, S., Menegazzi, P., Green, E. W., Pegoraro, M., et al. (2012). Unexpected features of *Drosophila* circadian behavioural rhythms under natural conditions. *Nature* 484, 371–375. doi: 10.1038/nature10991

Zehring, W. A., Wheeler, D. A., Reddy, P., Konopka, R. J., Kyriacou, C. P., Rosbash, M., et al. (1984). P-element transformation with period locus DNA restores rhythmicity to mutant, arrhythmic *Drosophila melanogaster*. *Cell*. 39, 369–376. doi: 10.1016/0092-8674(84)90015-1

Ziegler, A. B., Berthelot-Grosjean, M., and Grosjean, Y. (2013). The smell of love in *Drosophila*. *Front. Physiol*. 4:72. doi: 10.3389/fphys.2013.00072

Conflict of Interest Statement: The authors declare that the research was conducted in the absence of any commercial or financial relationships that could be construed as a potential conflict of interest.

frontiers in Physiology

BRIEF RESEARCH REPORT
published: 02 August 2019
doi: 10.3389/fphys.2019.00983

Vps28 Is Involved in the Intracellular Trafficking of Awd, the *Drosophila* Homolog of NME1/2

*Elisa Mezzofanti[1], Marilena Ignesti[1], Tien Hsu[2,3], Giuseppe Gargiulo[1] and Valeria Cavaliere[1]**

[1] Dipartimento di Farmacia e Biotecnologie, Alma Mater Studiorum – Università di Bologna, Bologna, Italy, [2] Department of Biomedical Sciences and Engineering, National Central University, Zhongli, Taiwan, [3] Center for Chronic Disease Management and Research, National Central University, Zhongli, Taiwan

The *Awd* (*abnormal wing discs*) gene is the *Drosophila* homolog of human *NME1* and *NME2* metastasis suppressor genes. These genes play a key role in tumor progression. Extensive studies revealed that intracellular NME1/2 protein levels could be related to either favorable or poor prognosis depending on tissue context. More recently, extracellular activities of NME1/2 proteins have also been reported, including a tumor- promoting function. We used *Drosophila* as a genetic model to investigate the mechanism controlling intra- and extracellular levels of NME1/2. We examined the role of several components of the ESCRT (endosomal sorting complex required for transport) complex in controlling Awd trafficking. We show that the Vps28 component of the ESCRT−I complex is required for maintenance of normal intracellular level of Awd in larval adipocytes. We already showed that blocking of Shibire (Shi)/Dynamin function strongly- lowers Awd intracellular level. To further investigate this down regulative effect, we analyzed the distribution of endosomal markers in wild type and Shi-defective adipocytes. Our results suggest that Awd does not enter CD63-positive endosomes. Interestingly, we found that in fat body cells, Awd partly- colocalizes with the ESCRT accessory component ALiX, the ALG-2 (apoptosis-linked gene 2)-interacting protein X. Moreover, we show that the intracellular levels of both proteins are downregulated by blocking the function of the Dynamin encoded by the *shibire* gene.

Keywords: Awd/NME, metastasis suppressor genes, intracellular trafficking, ESCRT machinery, Vps28, ALiX, *Drosophila*, fat body

OPEN ACCESS

Edited by:
Giorgio F. Gilestro, Imperial College London, United Kingdom

Reviewed by:
Emmanuel Culetto, Université Paris-Sud, France
Sofia J. Araújo, University of Barcelona, Spain

***Correspondence:**
Valeria Cavaliere
valeria.cavaliere@unibo.it

Specialty section:
This article was submitted to Invertebrate Physiology, a section of the journal Frontiers in Physiology

Received: *18 December 2018*
Accepted: *15 July 2019*
Published: *02 August 2019*

Citation:
Mezzofanti E, Ignesti M, Hsu T, Gargiulo G and Cavaliere V (2019) Vps28 Is Involved in the Intracellular Trafficking of Awd, the Drosophila Homolog of NME1/2. Front. Physiol. 10:983. doi: 10.3389/fphys.2019.00983

INTRODUCTION

NME1 and *NME2* genes are closely related members of the *NME* gene family which consists of 10 members (Stafford et al., 2008). *NME1* was the 1st metastasis suppressor gene identified (Steeg et al., 1988) and together with *NME2* is mostly implicated in tumor progression. Several studies showed that NME1/2 intracellular content is correlated with either lowered or enhanced metastatic abilities depending on tissue context of the developing tumor (Steeg et al., 1993; Okabe-Kado et al., 1998; van Noesel and Versteeg, 2004; Tschiedel et al., 2008). Recently, a correlation between extracellular NME protein level and tumor progression has also been reported in a number of tumor types (Romani et al., 2018).

The *Drosophila Awd* gene is the fly ortholog of *NME1/2* genes (Rosengard et al., 1989). Our studies showed that Awd is an endocytic mediator that interacts with Rab5 and the *Drosophila* homolog of Dynamin1 encoded by the *shibire* (*shi*) gene (Dammai et al., 2003; Nallamothu et al., 2008; Woolworth et al., 2009; Ignesti et al., 2014). We have shown that the larval fat body, among several larval tissues, is able to secrete the Awd protein in the hemolymph (Romani et al., 2016). In addition, we found that Shi controls the balance of Awd intracellular-extracellular levels. While blocking of Shi function in adipocytes leads to downregulated Awd intracellular level, loss of Rab5 function does not. Thus, our results suggest the specific involvement of Shi in the internalization process of Awd molecules circulating in the hemolymph, and the endocytic vesicles containing Awd are sorted into the adipocytes via a Rab5-independent pathway (Romani et al., 2016).

Proteomic studies showed the presence of Awd within extracellular vesicles released in the culture medium by two different *Drosophila* cell lines (Koppen et al., 2011). Extracellular vesicles mediate cellular communication and are involved in numerous biological functions (Christ et al., 2017). These small vesicles can derive from cells of different nature and form throughout different developmental processes (van Niel et al., 2018).

The ESCRT machinery is a membrane remodeling system that acts in a variety of biological processes (Christ et al., 2017). It consists of three multi-subunit complexes ESCRT–I, –II and –III that are recruited by specific targeting molecules. Multivesicular body (MVB) formation requires the ESCRT–0 function to recruit the ESCRT machinery. The four ESCRT complexes, together with additional components, act sequentially to deliver cargoes into the intraluminal vesicles (ILVs). These ILVs could then be released as exosomes in the extracellular space upon fusion of the MVBs with plasma membrane.

The well characterized role of ESCRT in biogenesis and secretion of extracellular vesicles (Christ et al., 2017) sparked our interest in the possibility that the ESCRT machinery might be involved in Awd trafficking. Furthermore, we have recently shown that, in larval wing discs, downregulation of Awd levels coupled with blocking apoptosis causes aneuploidy (Romani et al., 2017) probably due to mitotic defects that have been described in *awd* mutant larval brains (Biggs et al., 1990). The ESCRT complex plays a key role in membrane scission at the end of cytokinesis (Christ et al., 2017) and the ALiX accessory component is required for both completion of abscission (Eikenes et al., 2015) and orientation of the mitotic spindle (Malerød et al., 2018). ALiX is also involved in the biogenesis of exosomes and in the sorting of some cargoes inside these vesicles (Baietti et al., 2012; Hurley and Odorizzi, 2012; Juan and Furthauer, 2018).

In this study, we investigate the involvement of ESCRT machinery in Awd trafficking. We use MARCM system (Lee and Luo, 1999) to generate clones of adipocytes that are null mutants in genes belonging to ESCRT–0, ESCRT–I, ESCRT–II and ESCRT–III complexes. Our analyses of the amount and distribution of intracellular Awd in mutant adipocytes highlight a role of Vps28 component of ESCRT–I complex in controlling the Awd presence inside the cell. In addition, we found that Awd colocalizes with the ALiX accessory component and that Shi function is required for normal intracellular amount of both proteins.

RESULTS

Role of ESCRT Machinery in Regulating Awd Intracellular Amount

The Awd protein is expressed over all the larval fat body that, in 3rd instar larval stage, consists of layers of tightly connected polygonal adipocytes (**Figure 1A**). Clones of larval adipocytes homozygous for null mutations of ESCRT genes were generated using the MARCM system (Lee and Luo, 1999). Then, the intracellular localization of Awd was analyzed using immunofluorescence confocal microscopy of fat bodies (see **Figure 1B** for a scheme of x-y and x-z optical sections).

We started our analysis by looking at the ESCRT–0 complex. In hrs^{D28}, $stam^{2L2896}$ double mutant adipocytes, that lack the functions of both genes (Lloyd et al., 2002; Chanut-Delalande et al., 2007), Awd level is unaltered in comparison with its level in wild type adipocytes (**Supplementary Figures S1A–C',L**).

We then investigated the role of the ESCRT–I complex. Among the four ESCRT–I subunits, we analyzed the effect of Tsg101 and Vps28 components. Absence of Tsg101 function in clones of adipocytes homozygous for the $tsg101^{2}$ loss-of-function allele (Vaccari et al., 2009) does not alter intracellular Awd distribution (**Supplementary Figures S1D–K',M**). In wild type cells, Tsg101 mediates recruitment of ESCRT–I to ESCRT–0 complex through direct interaction with Hrs (Christ et al., 2017). The absence of Tsg101 function causes the accumulation of large vesicles, positive for Hrs, which stall along the endocytic pathway. Despite accumulation of the Hrs protein, cells lacking Tsg101 function show normal intracellular profile of Awd (**Supplementary Figures S1D–K',M**), further confirming that Hrs is not involved in Awd trafficking.

We then analyzed the effect of Vps28 loss of function in MARCM clones homozygous for the $vps28^{A2}$ mutation (Vaccari et al., 2009). Surprisingly, immunofluorescence detection of Awd protein in $vps28^{A2}$ mutant clones (**Figures 1C,E,F,H,I**) shows a clear downregulation of protein level, when compared to the wild type flanking cells (**Figures 1D,G–J**). The analysis of $vps28^{A2}$ mutant adipocytes also shows that the small amount of Awd protein is detectable in its normal subcortical localization indicating that the spatial distribution of Awd is unaltered (**Figures 1H,I**).

We extended our analysis of Awd trafficking to theVps22 ESCRT–II component (Christ et al., 2017). $vps22^{ZZ13}$ homozygous adipocytes lacking the function of Vps22 (Vaccari et al., 2009) show an intracellular profile of Awd comparable to that present in the control flanking cells (**Supplementary Figures S2A–G,K**). Thus, at least this subunit of the ESCRT–II complex is not involved in modulation of the intracellular levels of Awd.

Finally, we analyzed the Vps2 component of the ESCRT–III complex (Christ et al., 2017) by taking advantage of

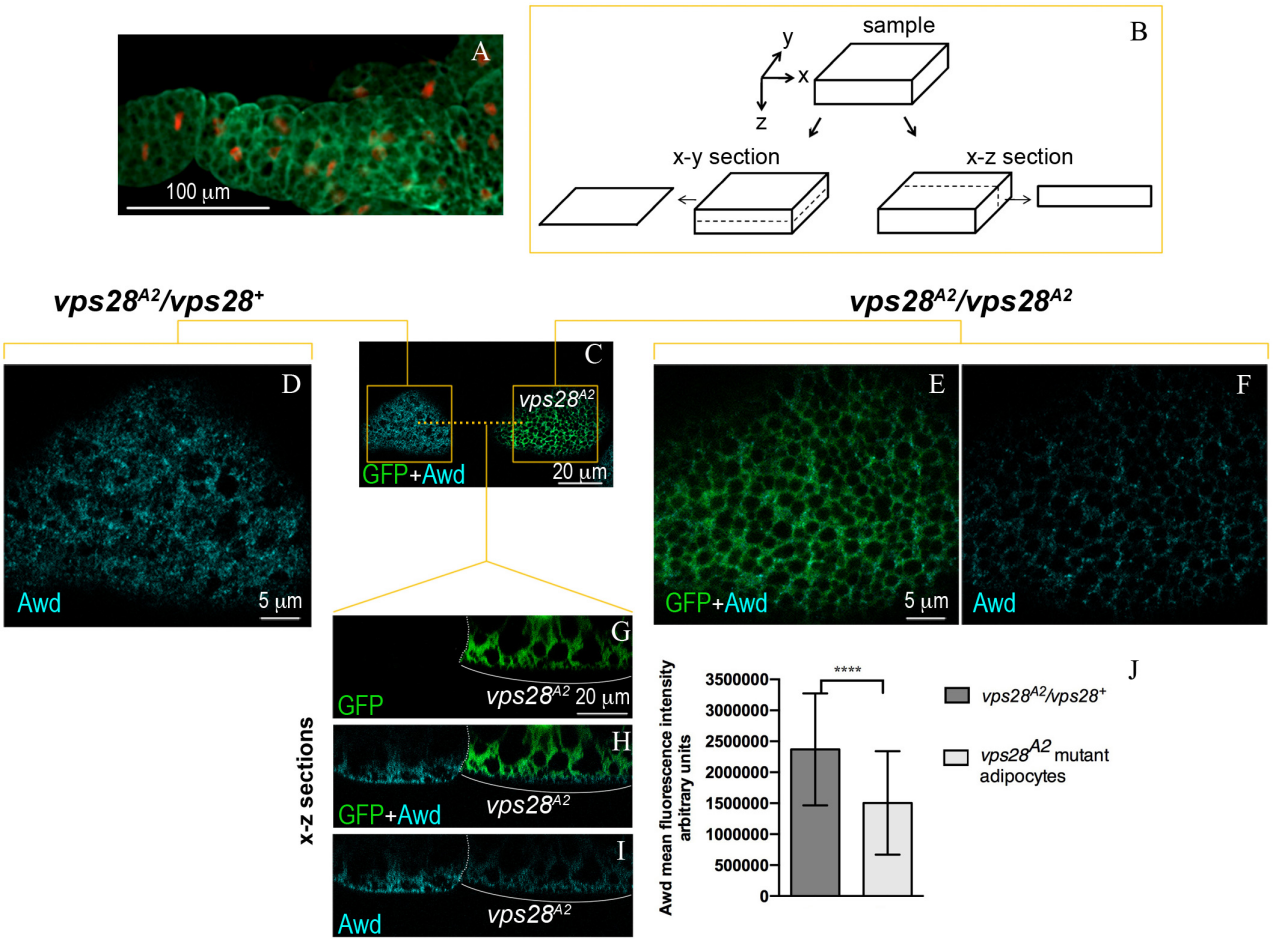

FIGURE 1 | Intracellular distribution of Awd in larval fat body. **(A)** Epifluorescence image of Awd protein expression (green) in fat body dissected from stage L3 larvae carrying the His2Av-mRFP transgene whose expression marks DNA (red). **(B)** Schematic representation of confocal optical sections of a sample in x-y and x-z planes. **(C–I)** Confocal microscopy analysis of *vps28*^{A2} MARCM clones marked by GFP expression (**C,E**,**G**,**H**, green) stained for Awd (**C,D**,**F**,**H**,**I**, cyan). **(C)** Surface section (x–y) of mosaic fat body showing a control heterozygous *vps28*^{A2}/*vps28*$^{+}$ and a mutant *vps28*^{A2}/*vps28*^{A2} adipocyte marked by GFP expression. **(D)** Magnified view of the control *vps28*^{A2}/*vps28*$^{+}$ adipocyte (left orange box in **C**). **(E,F)** Magnified view of the mutant *vps28*^{A2}/*vps28*^{A2} adipocyte (right orange box in **C**). **(G–I)** x–z sections of the adipocytes through the planes indicated by the orange dashed line in **C**. The white dotted line outlines the boundary between the control and mutant adipocyte. The white bracket indicates the mutant adipocyte. **(J)** A severe and significant decrease of Awd signal ($p = 0.000085$) is detectable in *vps28*^{A2}/*vps28*^{A2} adipocyte. Graphs represent mean ± SD amount of Awd in arbitrary units; $n = 7$; ****$p < 0.0001$ (two-tailed, paired *t*-test).

the loss-of-function allele *vps2*^{PP6} (Vaccari et al., 2009). In comparison with wild type adipocytes, *vps2*^{PP6} homozygous mutant cells show the same intracellular level and the same subcortical distribution of Awd (**Supplementary Figures S2H–J',L**). This suggests that the Vps2 component of the ESCRT–III complex is not involved in the regulation of Awd trafficking.

Analysis of the Endosomal Trafficking in Adipocytes Lacking Shi Function

We have already shown that absence of Shi function causes downregulation of Awd intracellular level in adipocytes coupled with the enhancement of the level of this protein in larval circulating hemolymph (Romani et al., 2016). Moreover, proteomic studies showed that the Awd protein is secreted within extracellular vesicles (Koppen et al., 2011). To further investigate Awd traffic inside and outside cells, we analyzed the effect of defective Shi function on endosomal compartments involved in the secretory pathway.

The exosomes are a particular type of extracellular vesicles that are released by fusion of MVBs, containing the ILVs, with the plasma membrane. The CD63 protein, belonging to the tetraspanine family, is commonly used as an exosome marker. In human cells, this protein is enriched in the ILVs and in the exosomes derived from them (Escola et al., 1998; Wubbolts et al., 2003). Beside biogenesis of exosomes, CD63 is involved in endosomal sorting and in cargo targeting to exosomes (van Niel et al., 2018).

In *Drosophila* cells, it has been shown that the CD63: GFP transgenic protein, consisting of the CD63 heterologous protein fused with GFP, can be used as a marker for MVBs (Panakova et al., 2005). We applied the Flp–Out technique

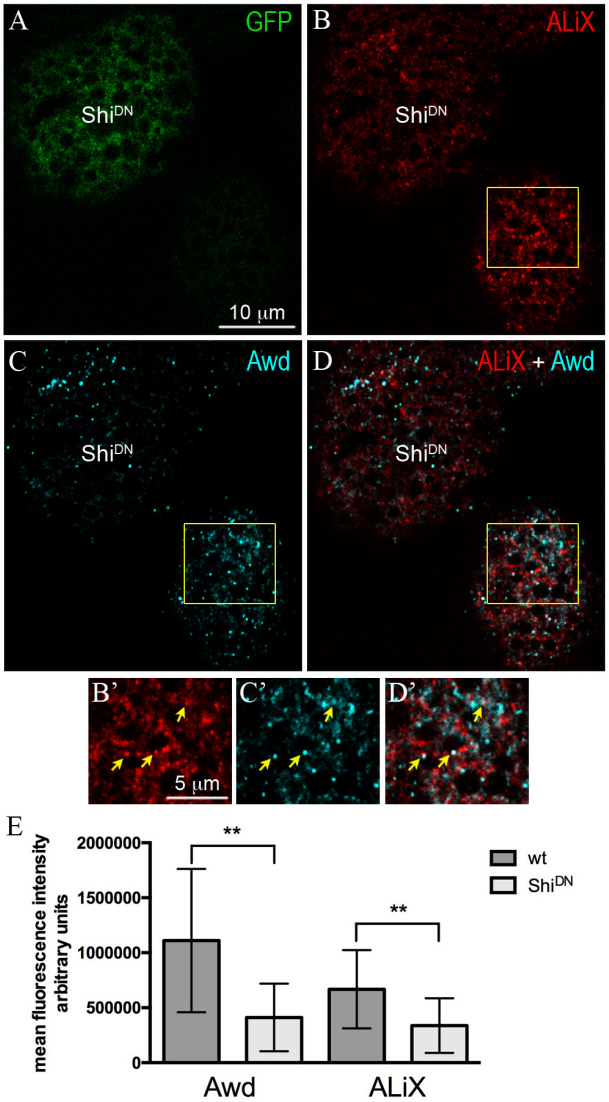

FIGURE 2 | Intracellular distribution of ALiX and Awd in adipocytes expressing Shi^{DN}. **(A)** Confocal microscopy analysis of fat body containing single-cell flip-out clone (GFP positive, green) over expressing Shi^{DN}. **(B)** Staining for ALiX (red). **(C)** Staining for Awd (cyan). **(D)** merge of **B** and **C** signals. **(B'–D')** Magnified view of the wild type adipocyte (yellow box in **B**–**D**). Yellow arrows point to colocalization of ALiX and Awd signals. **(E)** A significant decrease of Awd ($p = 0.0076$) and ALiX ($p = 0.0013$) signals is detectable in Shi^{DN} adipocytes. Graphs represent mean ± SD amount of Awd and ALiX in arbitrary units; $n = 7$; $^{**}p < 0.01$ (two-tailed, paired t-test).

(Pignoni and Zipursky, 1997) to obtain clones of adipocytes expressing CD63:GFP (**Supplementary Figures S3A,A'**). We found that the Awd protein (**Supplementary Figures S3B,B'**) does not colocalize with the CD63:GFP chimeric protein (**Supplementary Figures S3C,C'**). We then asked if blocking Shi function could cause the Awd downregulation by pushing its release through CD63:GFP positive exosomes. We took advantage of the Shi^{K44A} (Shi^{DN}) dominant negative form of Shi whose expression leads to the blocking of Shi activity (Moline et al., 1999). We induced clones of adipocytes coexpressing Shi^{DN} and CD63:GFP proteins through flp–out technique (**Supplementary Figures S3D,D'**). Shi-defective adipocytes show an increase in the number and size of vesicles positive for CD63:GFP (**Supplementary Figures S3D,D'**). In *Drosophila* wing discs CD63:GFP marks late endosomes (Panakova et al., 2005). Since Shi^{DN} adipocytes accumulate Rab7-positive late endosomes (Fang et al., 2016), it is possible that these late endosomes accumulate CD63:GFP. The analysis of Awd distribution (**Supplementary Figures S3E,E',F,F'**) shows that even within Shi-defective adipocytes there is no colocalization of Awd and CD63:GFP.

Awd Partially Colocalizes With ALiX

ALiX is an early-acting ESCRT factor that plays a key role in the assembly of ESCRT machinery. Besides its role in nucleating ESCRT–III complex, ALiX also acts in concentrating cargoes in vesicles (Schöneberg et al., 2017). To investigate the possibility that Awd transits in ALiX-positive vesicles, we analyzed Awd and ALiX distribution in adipocytes. Co-immunolocalization of Awd and ALiX was carried out in larval fat body expressing Shi^{DN} in flp–out clones (**Figure 2A**). Interestingly, confocal microscopy analysis shows that Awd (**Figures 2C,C'**) and ALiX (**Figures 2B,B'**) were partially- colocalized in wild type adipocytes (**Figures 2D,D'**) (Pearson's coefficient $R = 0{,}293 \pm 0{,}059$; $n = 5$). Furthermore, Shi-defective adipocytes show a significant lowering of the intracellular level of both ALiX and Awd, in comparison with the intracellular level of each protein detectable in the surrounding wild type cells (**Figure 2E**). Moreover, in Shi^{DN} adipocytes the colocalization level of Awd and AliX decreases as shown by the strong reduction of correlation (Pearson's coefficient $R = 0{,}027 \pm 0{,}013$; $n = 3$).

DISCUSSION

We have previously shown that Awd is secreted in the hemolymph by the fat body and the block of Shi activity causes the enhancement of Awd extracellular level coupled with a reduced intracellular level (Romani et al., 2016). Since Shi is required for lysosomal/autolysosomal acidification (Fang et al., 2016), the low level of Awd in Shi^{DN} adipocytes cannot be due to an increased protein degradation. Therefore, we propose that Shi plays a key role in maintenance of Awd intra-extracellular balance. Here we show that a subpopulation of ALiX-positive vesicles partially- colocalizes with Awd. This is of particular interest since ALiX controls the intracellular traffic of multiple proteins and is frequently present at the level of EVs secreted by cells (Juan and Furthauer, 2018). Block of Shi function results in lowered intracellular level of ALiX and Awd and their loss of colocalization may suggest that Awd/ALiX-positive vesicles could exit the cell contributing to their intracellular decrease.

Our functional analysis of ESCRT complex components shows that, among the subunits analyzed, the Vps28 is involved in Awd trafficking in larval adipocytes. Vps28 is a component of the ESCRT–I complex; however, loss-of-function of the other ESCRT–I component Tsg101 did not affect the Awd intracellular

level and distribution. This suggests that the ESCRT machinery is acting in a Non-canonical fashion. Previous works already showed that Non-canonical ESCRT mechanisms, involving few but not all subunits, act in EVs and exosomes biogenesis (Colombo et al., 2013; Juan and Furthauer, 2018). The long-range secretion of the Hedgehog (Hh) morphogen in the larval wing disc is also regulated by a subset of ESCRT components (Matusek et al., 2014). Conditioned medium of a cell line derived from the wing imaginal disc showed the presence of Vps28, ALiX and Vps32 components. Interestingly, these vesicles also contain Awd (Matusek et al., 2014).

Taken together these results suggest a possible involvement of ALiX and Vps28 in Awd secretion.

The partial colocalization of Awd and ALiX could be explained by taking into account two considerations. First, adipocytes are able to produce and secrete Awd protein (Romani et al., 2016). Proteins addressed to secretion have to traffic to several different intracellular compartments identified by specific proteins (Barlowe and Miller, 2013). Second, it is worth noting that Shi function requires Awd activity (Krishnan et al., 2001; Dammai et al., 2003). Therefore, we would not expect that all the Awd intracellular pool will localize in membrane compartments destined for secretion.

Intriguingly, alteration of both intracellular and extracellular NME1/2 levels were shown to have implication in cancer progression (Romani et al., 2018). To date, very little is known about the mechanisms regulating NME1/2 presence in the extracellular environment. The comprehension of the mechanism controlling the balance of Awd inside and outside the cell will be relevant to understand NME1/2 functions in physiological and pathological conditions.

MATERIALS AND METHODS

Fly Strains

All stocks were maintained and crossed at 25°C. For details of genotypes and mosaic techniques see the **Supplementary Data**.

Immunostaining

Fat bodies were dissected from 3rd instar larvae in Phosphate Buffered Saline (PBS) and then immediately fixed for 20 min in 4% formaldehyde in PBS at room temperature. For additional information on staining procedure see **Supplementary Data**. Fluorescent images were obtained with TCS SL Leica confocal system.

AUTHOR CONTRIBUTIONS

EM and MI performed the experiments. MI, TH, GG, and VC conceived and designed the experiments, and wrote the manuscript. All authors read and approved the final manuscript.

FUNDING

The authors acknowledge funding from the Association for International Cancer Research, AICR-WWCR grant ref. 11-0738 to VC, the University of Bologna (RFO 2018) to GG and VC, the Ministry of Science and Technology, Taiwan (106-2321-B-008-001) to TH, and the Ministry of Science and Technology, Taiwan (106-2320-B-008-007-MY3) to TH.

ACKNOWLEDGMENTS

We thank T. Vaccari, T. Aigaki, S. Eaton, and Bloomington Drosophila Stock Center for flies and reagents.

SUPPLEMENTARY MATERIAL

The Supplementary Material for this article can be found online at: https://www.frontiersin.org/articles/10.3389/fphys.2019.00983/full#supplementary-material

REFERENCES

Baietti, M. F., Zhang, Z., Mortier, E., Melchior, A., Degeest, G., Geeraerts, A., et al. (2012). Syndecan-syntenin-ALIX regulates the biogenesis of exosomes. *Nat. Cell Biol.* 14, 677–685. doi: 10.1038/ncb2502

Barlowe, C. K., and Miller, E. A. (2013). Secretory protein biogenesis and traffic in the early secretory pathway. *Genetics* 193, 383–410. doi: 10.1534/genetics.112.142810

Biggs, J., Hersperger, E., Steeg, P. S., Liotta, L. A., and Shearn, A. (1990). A *Drosophila* gene that is homologous to a mammalian gene associated with tumor metastasis codes for a nucleoside diphosphate kinase. *Cell* 63, 933–940. doi: 10.1016/0092-8674(90)90496-2

Chanut-Delalande, H., Jung, A. C., Lin, L., Baer, M. M., Bilstein, A., Cabernard, C., et al. (2007). A genetic mosaic analysis with a repressible cell marker screen to identify genes involved in tracheal cell migration during *Drosophila* air sac morphogenesis. *Genetics* 176, 2177–2187. doi: 10.1534/genetics.107.073890

Christ, L., Raiborg, C., Wenzel, E. M., Campsteijn, C., and Stenmark, H. (2017). Cellular functions and molecular mechanisms of the ESCRT membrane-scission machinery. *Trends Biochem. Sci.* 42, 42–56. doi: 10.1016/j.tibs.2016.08.016

Colombo, M., Moita, C., van Niel, G., Kowal, J., Vigneron, J., Benaroch, P., et al. (2013). Analysis of ESCRT functions in exosome biogenesis, composition and secretion highlights the heterogeneity of extracellular vesicles. *J. Cell Sci.* 126(Pt 24), 5553–5565. doi: 10.1242/jcs.128868

Dammai, V., Adryan, B., Lavenburg, K. R., and Hsu, T. (2003). *Drosophila awd*, the homolog of human *nm23*, regulates FGF receptor levels and functions synergistically with shi/dynamin during tracheal development. *Genes Dev.* 17, 2812–2824. doi: 10.1101/gad.1096903

Eikenes, A. H., Malerod, L., Christensen, A. L., Steen, C. B., Mathieu, J., Nezis, I. P., et al. (2015). ALIX and ESCRT-III coordinately control cytokinetic abscission during germline stem cell division in vivo. *PLoS Genet.* 11:e1004904. doi: 10.1371/journal.pgen.1004904

Escola, J. M., Kleijmeer, M. J., Stoorvogel, W., Griffith, J. M., Yoshie, O., and Geuze, H. J. (1998). Selective enrichment of tetraspan proteins on the internal vesicles of multivesicular endosomes and on exosomes secreted by human B-lymphocytes. *J. Biol. Chem.* 273, 20121–20127. doi: 10.1074/jbc.273.32.20121

Fang, X., Zhou, J., Liu, W., Duan, X., Gala, U., Sandoval, H., et al. (2016). Dynamin regulates autophagy by modulating lysosomal function. *J. Genet. Genomics* 43, 77–86. doi: 10.1016/j.jgg.2015.10.005

Hurley, J. H., and Odorizzi, G. (2012). Get on the exosome bus with ALIX. *Nat. Cell Biol.* 14, 654–655. doi: 10.1038/ncb2530

Ignesti, M., Barraco, M., Nallamothu, G., Woolworth, J. A., Duchi, S., Gargiulo, G., et al. (2014). Notch signaling during development requires the function of awd, the *Drosophila* homolog of human metastasis suppressor gene Nm23. *BMC Biol.* 12:12. doi: 10.1186/1741-7007-12-12

Juan, T., and Furthauer, M. (2018). Biogenesis and function of ESCRT-dependent extracellular vesicles. *Semin. Cell Dev. Biol.* 74, 66–77. doi: 10.1016/j.semcdb.2017.08.022

Koppen, T., Weckmann, A., Muller, S., Staubach, S., Bloch, W., Dohmen, R. J., et al. (2011). Proteomics analyses of microvesicles released by *Drosophila* Kc167 and S2 cells. *Proteomics* 11, 4397–4410. doi: 10.1002/pmic.201000774

Krishnan, K. S., Rikhy, R., Rao, S., Shivalkar, M., Mosko, M., Narayanan, R., et al. (2001). Nucleoside diphosphate kinase, a source of GTP, is required for dynamin-dependent synaptic vesicle recycling. *Neuron* 30, 197–210. doi: 10.1016/s0896-6273(01)00273-2

Lee, T., and Luo, L. (1999). Mosaic analysis with a repressible cell marker for studies of gene function in neuronal morphogenesis. *Neuron* 22, 451–461. doi: 10.1016/s0896-6273(00)80701-1

Lloyd, T. E., Atkinson, R., Wu, M. N., Zhou, Y., Pennetta, G., and Bellen, H. J. (2002). Hrs regulates endosome membrane invagination and tyrosine kinase receptor signaling in *Drosophila*. *Cell* 108, 261–269. doi: 10.1016/s0092-8674(02)00611-6

Malerød, L., Le Borgne, R., Lie-Jensen, A., Eikenes, A. H., Brech, A., Liestol, K., et al. (2018). Centrosomal ALIX regulates mitotic spindle orientation by modulating astral microtubule dynamics. *EMBO J.* 37:e97741. doi: 10.15252/embj.201797741

Matusek, T., Wendler, F., Poles, S., Pizette, S., D'Angelo, G., Furthauer, M., et al. (2014). The ESCRT machinery regulates the secretion and long-range activity of Hedgehog. *Nature* 516, 99–103. doi: 10.1038/nature13847

Moline, M. M., Southern, C., and Bejsovec, A. (1999). Directionality of wingless protein transport influences epidermal patterning in the *Drosophila* embryo. *Development* 126, 4375–4384.

Nallamothu, G., Woolworth, J. A., Dammai, V., and Hsu, T. (2008). *awd*, the homolog of metastasis suppressor gene *Nm23*, regulates *Drosophila* epithelial cell invasion. *Mol. Cell Biol.* 28, 1964–1973. doi: 10.1128/MCB.01743-1747

Okabe-Kado, J., Kasukabe, T., and Honma, Y. (1998). Differentiation inhibitory factor Nm23 as a prognostic factor for acute myeloid leukemia. *Leuk. Lymphoma* 32, 19–28. doi: 10.3109/10428199809059243

Panakova, D., Sprong, H., Marois, E., Thiele, C., and Eaton, S. (2005). Lipoprotein particles are required for Hedgehog and Wingless signalling. *Nature* 435, 58–65. doi: 10.1038/nature03504

Pignoni, F., and Zipursky, S. L. (1997). Induction of *Drosophila* eye development by decapentaplegic. *Development* 124, 271–278.

Romani, P., Duchi, S., Gargiulo, G., and Cavaliere, V. (2017). Evidence for a novel function of Awd in maintenance of genomic stability. *Sci. Rep.* 7:16820. doi: 10.1038/s41598-017-17217-17210

Romani, P., Ignesti, M., Gargiulo, G., Hsu, T., and Cavaliere, V. (2018). Extracellular NME proteins: a player or a bystander? *Lab. Invest.* 98, 248–257. doi: 10.1038/labinvest.2017.102

Romani, P., Papi, A., Ignesti, M., Soccolini, G., Hsu, T., Gargiulo, G., et al. (2016). Dynamin controls extracellular level of Awd/Nme1 metastasis suppressor protein. *Naunyn Schmiedebergs Arch. Pharmacol.* 389, 1171–1182. doi: 10.1007/s00210-016-1268-1269

Rosengard, A. M., Krutzsch, H. C., Shearn, A., Biggs, J. R., Barker, E., Margulies, I. M., et al. (1989). Reduced Nm23/Awd protein in tumour metastasis and aberrant *Drosophila* development. *Nature* 342, 177–180. doi: 10.1038/342177a0

Schöneberg, J., Lee, I. H., Iwasa, J. H., and Hurley, J. H. (2017). Reverse-topology membrane scission by the ESCRT proteins. *Nat. Rev. Mol. Cell Biol.* 18, 5–17. doi: 10.1038/nrm.2016.121

Stafford, L. J., Vaidya, K. S., and Welch, D. R. (2008). Metastasis suppressors genes in cancer. *Int. J. Biochem. Cell Biol.* 40, 874–891. doi: 10.1016/j.biocel.2007.12.016

Steeg, P. S., Bevilacqua, G., Kopper, L., Thorgeirsson, U. P., Talmadge, J. E., Liotta, L. A., et al. (1988). Evidence for a novel gene associated with low tumor metastatic potential. *J. Natl. Cancer Inst.* 80, 200–204. doi: 10.1093/jnci/80.3.200

Steeg, P. S., de la Rosa, A., Flatow, U., MacDonald, N. J., Benedict, M., and Leone, A. (1993). Nm23 and breast cancer metastasis. *Breast Cancer Res. Treat.* 25, 175–187. doi: 10.1007/bf00662142

Tschiedel, S., Gentilini, C., Lange, T., Wolfel, C., Wolfel, T., Lennerz, V., et al. (2008). Identification of NM23-H2 as a tumour-associated antigen in chronic myeloid leukaemia. *Leukemia* 22, 1542–1550. doi: 10.1038/leu.2008.107

Vaccari, T., Rusten, T. E., Menut, L., Nezis, I. P., Brech, A., Stenmark, H., et al. (2009). Comparative analysis of ESCRT-I. *J. Cell Sci.* 122(Pt 14), 2413–2423. doi: 10.1242/jcs.046391

van Niel, G., D'Angelo, G., and Raposo, G. (2018). Shedding light on the cell biology of extracellular vesicles. *Nat. Rev. Mol. Cell Biol.* 19, 213–228. doi: 10.1038/nrm.2017.125

van Noesel, M. M., and Versteeg, R. (2004). Pediatric neuroblastomas: genetic and epigenetic 'danse macabre'. *Gene* 325, 1–15. doi: 10.1016/j.gene.2003.09.042

Woolworth, J. A., Nallamothu, G., and Hsu, T. (2009). The *Drosophila* metastasis suppressor gene *Nm23* homolog, *awd*, regulates epithelial integrity during oogenesis. *Mol. Cell Biol.* 29, 4679–4690. doi: 10.1128/MCB.00297-299

Wubbolts, R., Leckie, R. S., Veenhuizen, P. T., Schwarzmann, G., Mobius, W., Hoernschemeyer, J., et al. (2003). Proteomic and biochemical analyses of human B cell-derived exosomes. *J. Biol. Chem.* 278, 10963–10972. doi: 10.1074/jbc.M207550200

Conflict of Interest Statement: The authors declare that the research was conducted in the absence of any commercial or financial relationships that could be construed as a potential conflict of interest.

frontiers in Physiology

MINI REVIEW
published: 07 August 2019
doi: 10.3389/fphys.2019.00987

Dissecting the Genetics of Autism Spectrum Disorders: A *Drosophila* Perspective

Paola Bellosta[1,2]* *and Alessia Soldano*[3]*

[1] Laboratory of Metabolism of Cell Growth and Neuronal Survival, Department of Cellular, Computational and Integrative Biology (CIBio), University of Trento, Trento, Italy, [2] Department of Medicine, New York University Langone Medical Center, New York, NY, United States, [3] Laboratory of Translational Genomics, Department of Cellular, Computational and Integrative Biology (CIBio), University of Trento, Trento, Italy

Autism Spectrum Disorder (ASD) is a complex group of multi-factorial developmental disorders that leads to communication and behavioral defects. Genetic alterations have been identified in around 20% of ASD patients and the use of genetic models, such as *Drosophila melanogaster*, has been of paramount importance in deciphering the significance of these alterations. In fact, many of the ASD associated genes, such as *FMR1, Neurexin, Neuroligins and SHANK* encode for proteins that have conserved functions in neurons and during synapse development, both in humans and in the fruit fly. *Drosophila* is a prominent model in neuroscience due to the conserved genetic networks that control neurodevelopmental processes and to the ease of manipulating its genetics. In the present review we will describe recent advances in the field of ASD with a particular focus on the characterization of genes where the use of *Drosophila* has been fundamental to better understand their function.

Keywords: autism (ASD), shank, FMR1, neurexin, neuroligins, mGlu receptor 5, *Drosophila*, dopamine

OPEN ACCESS

Edited by:
Gabriella Mazzotta, University of Padua, Italy

Reviewed by:
Lawrence Todd Reiter, The University of Tennessee Health Science Center, United States
Jae Park, The University of Tennessee, Knoxville, United States

***Correspondence:**
Paola Bellosta
paola.bellosta@unitn.it
Alessia Soldano
alessia.soldano@unitn.it

Specialty section:
This article was submitted to Invertebrate Physiology, a section of the journal Frontiers in Physiology

Received: *28 April 2019*
Accepted: *18 July 2019*
Published: *07 August 2019*

Citation:
Bellosta P and Soldano A (2019) Dissecting the Genetics of Autism Spectrum Disorders: A Drosophila Perspective. Front. Physiol. 10:987. doi: 10.3389/fphys.2019.00987

AUTISM

Autism Spectrum Disorder (ASD) is a complex developmental neurological disease characterized by persistent deficits in social behaviors (communication, interaction), presence of repetitive and restrictive comportments and is often associated with motor deficits and sleep abnormalities, among others. Among individuals suffering from ASD, there is a high frequency of intellectual disability and mental retardation, although the described frequency is variable due to the difficulty in assessing cognitive performance in certain groups of ASD patients (O'Brien and Pearson, 2004; Chakrabarti and Fombonne, 2005). Autism is not considered a single gene disorder because it is caused by both genetic and non-genetic risk factors that induce a complex range of different symptoms for which the precise causes are unknown (Park et al., 2016). Genetic disorders, such as Fragile X syndrome (FXS), Down syndrome, and, more recently, Asperger's and Rett syndrome, have been associated with ASD. In less than 20% of patients has a clear monogenic cause for ASD been identified and most of these studies highlighted mutations in genes involved in several aspects of synapse biology, such as synaptogenesis/synaptic plasticity/morphology/function and axon motility (De Rubeis et al., 2014; Iossifov et al., 2014; Luo et al., 2018).

ASD ASSOCIATED DEFECTS IN SYNAPTOGENESIS AND SYNAPTIC PLASTICITY

The identification of ASD susceptibility genes involved in various aspects of synapse biology, lead to the hypothesis that aberrant synaptogenesis/synaptic function might be a central process in ASD

(Peca and Feng, 2012; Zoghbi and Bear, 2012). Multiple studies in animal models converge on the concept that reproducing alterations in ASD genes leads to aberrant synaptic morphology and function (Peca and Feng, 2012; Zoghbi and Bear, 2012). Interestingly, observation of post-mortem ASD patients' tissues indicate that dendritic spines, postsynaptic sites in the mammalian brain, are present at a higher density in ASD patients and this condition is most commonly found in ASD subjects with lower levels of cognitive performance (Hutsler and Zhang, 2010). Moreover, ASD patients have an increased density of dendritic spines in layer V pyramidal neurons and reduced developmental spine pruning, a process needed to achieve correct neuronal communication (Tang et al., 2014). This is of particular interest since it has been postulated that ASD might be caused by an altered balance between excitatory and inhibitory synapses, probably due to defects in synapse elimination/formation (Ramocki and Zoghbi, 2008; Gatto and Broadie, 2010).

Drosophila as a Model to Study ASD

Drosophila is an excellent model to study ASD to understand the consequences of genetic alterations found in ASD patients and to identify the molecular mechanisms underlying the role of ASD related genes in synaptic function and plasticity (Doi et al., 2016; Tian et al., 2017). Moreover, 75% of the human disease genes have orthologs in *Drosophila* (Bier, 2005), rendering the fruit fly a highly tractable genetic model organism to understand the molecular bases of ASDs. In the past decade the panel of genetic tools that can be used to study human disease genes has expanded massively (**Table 1**; Chow and Reiter, 2017). *Drosophila* has been used for classical **unbiased screens**, using either mutagens to induce random mutations in the genome or genome-wide RNAi/CRISPR screens, to identify genes that lead to ASDs-like phenotypes. On the other hand, known ASDs genes have been perturbed to mimic the patient's condition and to study the biological consequences of these alterations.

In the present review we describe the latest studies that use *Drosophila* to clarify the function of the most representative genes associated with ASD (**Figure 1**).

TABLE 1 | Summary of the genetic tools that can be used to study the physiological role of ASD genes and to understand their contribution, alone and in combination with others, to ASD development.

Genetic tool	Application to ASDs
Binary system such as Gal4/UAS system, LexA/LexAop, Q-system	– Overexpression or silencing of ASD associated genes to mimic deletions or amplifications in patients. – Overexpression of ASD genes harboring mutations found in patients in a knockout background.
CRISPR genome engineering	– Engineering of the *Drosophila* genome to induce, when possible, genetic alterations similar to the ones observed in ASD patients. – Engineering of the *Drosophila* genome to induce the knockout or overexpression of ASD genes. – Creation of "patient specific" *Drosophila* models where the endogenous gene is replaced with the patient variant.
GeneSwitch Gal4 system (GS)	– Tissue and time specific overexpression or silencing of ASD associated genes to mimic deletions or amplifications in patients – Overexpression of ASD genes harboring mutations found in patients in a knockout background.
Clonal analysis system: MARCM, QMARCM, twin-spot MARCM.	– Overexpression or silencing of ASD genes in a subset of cells in an otherwise wt tissue to understand the contribution of the overexpressed genes to the tissue's functionality and development. The same experiment can be performed in other mutant backgrounds. – Overexpression of disease variant human ASD genes to understand the contribution of the mutations to the tissue's functionality and development.

dfmr1

Fragile X syndrome (FXS) is a neuro-developmental disease that leads to intellectual disability and is the most common form of autism of monogenic origin (Mila et al., 2018). FXS is caused by a variable expansion of a trinucleotide (CGG) repeat in the 5′ UTR of the *fragile X mental retardation-1* gene (*FMR1*), or less frequently, by point mutations in *FMR1* (Collins et al., 2010; Handt et al., 2014), that leads to loss of FMR1 protein (Pieretti et al., 1991). *FMR1* encodes for an RNA-binding protein, FMRP, that mainly inhibits translation by binding to specific sequences on mRNAs (Darnell et al., 2011; Ascano et al., 2012).

Drosophila harbors only one *FMRP* ortholog, *dfmr1,* that shares high homology with its mammalian counterpart (Wan et al., 2000). A recent study using fruit flies suggested that the **molecular function** of *dfmr1* might not only be translation repression. Ribosome-profiling of oocytes upon *dfmr1* knockdown shows that *dfmr1 RNAi* leads to both enhanced and reduced mRNA translation in proportion to protein size, with dmfr1 predominantly up-regulating bigger proteins (Greenblatt and Spradling, 2018). Interestingly, many of the down-regulated genes are orthologs of genes implicated in ASD, such as the E2 Ubiquitin-conjugating enzyme BIRC6, or the Vacuolar H + ATPase DMXL2, both of which are associated with intellectual disabilities and neurodevelopmental disorders in humans, a result that outlines the relevance of using *Drosophila* genetics to gain insights into these human pathologies.

dfmr1 plays a central role in **synaptic plasticity,** indeed loss-of-function mutants of *dfmr1* show synaptic overgrowth, increased number and enlargement of synaptic boutons, and excessive branching at the Neuromuscular Junctions (NMJ). Mutations in *dfmr1* affect synaptic transmission at histaminergic photoreceptor synapses (central) and glutamatergic NMJ synapses (peripheral) (Zhang et al., 2001).

dfmr1 controls **brain development and neural circuit assembly** (Morales et al., 2002). Loss of *dfmr1* causes axon extension defects of **Dorsal Cluster neurons (DC)** and **lateral neurons (LNvs)**, and neurite-branching abnormalities in DC neurons. Interestingly, loss and gain of function of *dfmr1* lead to similar phenotypic defects, indicating that the levels of *dfmr1* are critical for brain development (Morales et al., 2002). The role of *dfmr1* in regulating axon morphology has also been demonstrated in the **Mushroom Body neurons (MB)**, a higher hierarchy circuit involved in olfactory learning and memory (Lee et al., 1999; Akalal et al., 2006). Loss of *dfmr1* in all MB

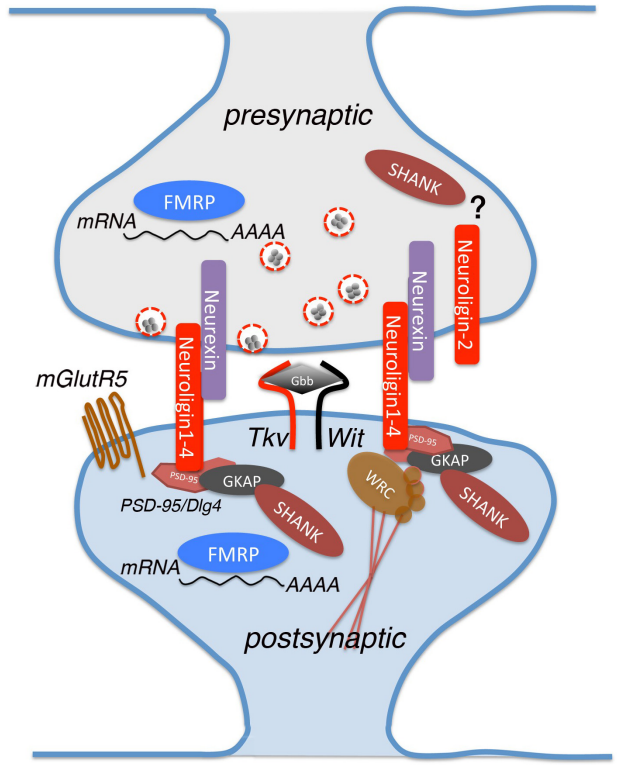

FIGURE 1 | A schematic view of a glutamatergic synapse, showing the proteins analyzed in this review and implicated in Autism Spectrum Disorder (ASD). Neurexin and neuroligin are located in pre- and post-synaptic sites where they interact with multiple partners for mediating synapse development and maturation. Neuroligins binds to PSD-95, which interacts indirectly with Shank by intracellular complexes containing also Guanylate-kinase-associated protein (GKAP). dNlg1 and 3 act mostly in pre-synaptic terminals while dNlg2 functions is both pre- and post-synaptic ends. Other proteins involved in the synaptic establishment are FMRP RNA-binding and Thickveins (Tkv), that are expressed in both synaptic sites, mGlutR5 and Wishful thinking (Wit) that are found specifically on the post-synaptic membrane. Glass Bottom Boat (Gbb) is the ligand of both Tkv and Wit, homologous to vertebrate bone morphogenic protein (BMP).

neuronal classes increases structural complexity and induces growth of additional processes from neuronal soma, supporting the overbranching and overgrowth phenotype visible in dendrites and axons (Michel et al., 2004; Pan et al., 2004; Tessier and Broadie, 2008). *dfmr1* also controls remodeling of two classes of MB body extrinsic input and output neurons, namely GABA-ergic MVP2 (MBON-γ1pedc > α/β) and projection neuron (PN). In fact, the dendritic arborizations of these neurons are enlarged in *dfmr1* null animals. MVP2 and PN neurons respond in the opposite way to this activity by remodeling their dendritic arbor and *dfmr1* is required for this function (Doll and Broadie, 2015).

Loss of *dfmr1* causes several **behavioral defects** including deficits in **memory** (Coffee et al., 2010; Gatto et al., 2014), associative **learning** defects (Choi et al., 2010; Santos et al., 2014; Doll and Broadie, 2016) and alteration of **circadian rhythm** (Sofola et al., 2008; Gatto and Broadie, 2009), which are all known to be linked to defects in LNvs morphology (Dockendorff et al., 2002; Sofola et al., 2008). Gene expression analysis at different times during the day (Circadian-time points CT) highlighted a subset of mRNAs and miRNAs that, in *dfmr1* mutant flies, were altered at a specific time point only. This pattern of gene expression alteration reflects a circadian rhythm-dependent alteration (Xu et al., 2012). *dfmr1* mutants also exhibit **sleep defects:** showing a prolonged "sleep phase", which is reduced by overexpression of *dfmr1* in the MB (Bushey et al., 2009), and a deeper sleep (night-like) phenotype at daylight (van Alphen et al., 2013). Similarly, patients with FXS suffer from sleep disorders suggesting a conserved function of *FMR1* in controlling components of the circadian rhythm.

dfmr1 modulates **grooming behavior**, recapitulating the repetitive behavior observed in ASD patients, and is therefore of great relevance for translational studies. *dfmr1* mutants groom more than control flies; this phenotype worsens with age and can be suppressed by treatment with reserpine, which blocks the *Drosophila* vesicular monoamine transporter (dVMAT) (Tauber et al., 2011).

dfmr1 mutants show also impairment in **odor-induced attraction and aversion**, due to reduced lateral interactions across the olfactory glomeruli and impairment of the lateral inhibition in the antennal lobe caused by weaker inhibition from GABAergic interneurons (Franco et al., 2017). These results are of great interest in comparative studies in humans given that alterations in GABAergic transmission and lack of inhibition might be central components of the neuropathology of FXS.

FXS patients, together with most individuals with ASD, suffer from **dysfunctions in sensory processing (SPD)**, meaning they respond to a certain behavioral stimulus differently than individuals in the average population (Sinclair et al., 2017). This dysfunction has been investigated in flies by studying the sensory processing of the *Drosophila* stress odorant (dSO) (Androschuk et al., 2018). *dfmr1* null animals have lost dSO avoidance-behavior and *dfmr1* is required in the MB and glia to mediate the dSO sensory response. This behavioral defect can be pharmacologically rescued by feeding adults with molecules that target cAMP/cGMP signaling pathways, such as the cAMP-increasing agent IBMX (3-isobutyl-1-methylxanthine), and the cAMP-dependent PKA activator and the cGMP dependent phosphodiesterase inhibitor 8-CPT (8-(4-Chlorophenylthio)adenosine 3′,5′-cyclic monophosphate), suggesting a potential use of these drugs In ASD treatments (Franco et al., 2017).

Up to now only few potentially **pathogenic mutations** have been identified in FXS patients. The most studied is an isoleucine to asparagine substitution (I304N) within the second K-homologous (KH) domain of the human FMRP, which is associated with very severe FXS (De Boulle et al., 1993). However, mutations in the highly conserved isoleucine residues I244N and I307N of the KH domain in *Drosophila* resulted in *dfmr1* null-like, MB β-lobe midline crossing phenotype, though at a lower frequencies than in *dfmr1* mutants. These KH mutants also fail to retain rhythmic locomotion activity in constant darkness, but with a milder phenotype than in *dfmr1* null animals (Banerjee et al., 2007). More recently, Okray et al. (2015) characterized in *Drosophila* a new FMR1 frameshift mutation (Guanine insertion

in *exon-15*) found in a patient with FXS. This mutation generates a novel peptide sequence with a premature stop codon, resulting in the truncation of the FMRP protein at the C-terminus and loss of the arginine-glycine-rich motif (RGG box), which is one of the FMRP RNA-binding domains. Overexpression of a mutant form of *dfmr1 (dfmr1-*$^{\Delta C+NLS}$ allele), which closely mimics the human variant, in LNvs, results in axons that fail to extend medially, leads to aberrant bifurcations of axonal bundle and to the formation of axonal "tangles."

Neurexin and Neuroligins

Neurexin (Nrx) and Neuroligins (Nlgs) are adhesion molecules that function as *trans*-synaptic binding partners involved in synaptogenesis (Knight et al., 2011). Several genetic alterations including point mutations, deletions and translocation events have been identified in *NRXN1*, *NLGN3* and *NLGN4* in ASD patients (Laumonnier et al., 2004; Kim et al., 2008; Yan et al., 2008).

In *Drosophila,* loss of *dNlgs* (*Drosophila* harbors 4 *dNlgs*) and *dNrx* results in developmental defects at the NMJ such as an altered number of boutons, aberrant **presynaptic/postsynaptic** structure, and impaired synaptic transmission (Sun et al., 2011; Chen et al., 2012; Hahn et al., 2013; Xing et al., 2014). In particular, dNlg1, 2, and 4 have a positive effect on synaptic growth at the NMJ and their loss leads to a reduction of synaptic boutons (Banovic et al., 2010; Sun et al., 2011), while loss of dNlg3 leads to the opposite phenotype (Xing et al., 2014). dNlg1 and 3 act mostly in pre-synaptic terminals while dNlg2 functions in both pre- and post-synaptic ends (Chen et al., 2012; Xing et al., 2014). dNlgs and dNrx work together to coordinate these functions.

Recent studies dissected the **molecular mechanisms** underlying these functions: Zhang and colleagues (Zhang et al., 2017) demonstrated that dNlg4 modulates BMP signaling by maintaining the protein levels of the type-I BMP receptor Thick Veins (Tkv) at the presynaptic sites. **BMP signaling** seems to be a target of several dNlgs/dNrx complexes; in fact, it has been demonstrated that Tkv levels are also reduced in dNlg1 and dNrx mutants (Banerjee et al., 2017). Interestingly, mutants of the type-II BMP receptor Wishful Thinking (Wit) show phenotypic similarities to dNlg1 and dNrx mutants (Banerjee and Riordan, 2018). dNrx, dNlg1 and Wit seem to form a complex at the NMJ, where dNrx and dNlg1 are required for both localization and stability of Wit. dNrx is found in a complex with Wit and its ligand Gbb, the ortholog of vertebrate BMP, and other downstream effectors to allow proper axonal transport and microtubule organization (Banerjee and Riordan, 2018).

dNlg1 also directly affects the actin cytoskeleton via interaction with the WAVE regulatory complex (WRC), one of the key players in **F-actin assembly** (Xing et al., 2018). In particular, dNlg1 mediates the effect of dNrx on actin at post-synaptic terminals by binding to the WRC and recruiting it to the post-synaptic membrane. dNlg1-WRC interaction mediates post-synaptic F-actin assembly, which is required for normal NMJ assembly and boutons growth, while dNrx and dNlg4 control axonal branching (Liu et al., 2017). dNrx is also expressed in the axon terminals and interstitial branches of L4 lamina neurons that project into the medulla neuropil, and is required for L4 columnar restriction. In particular, dNlg4/dNrx interaction promotes dNrx clustering on the membrane which results in dNrx/Ephrin interaction and subsequent Ephrin clustering (Neriec and Desplan, 2016).

In mammals, Neurexins and Neuroligins are also central for the establishment of functional synaptic networks (Sudhof, 2017). The findings described in *Drosophila* strongly support that dNlgs and dNrx have a primary role in synapse formation/maintenance and outline how these signaling pathways might be further assessed as pharmacological targets.

Shank

The family of SH3 and multiple ankyrin repeat domains proteins (SHANKs) is composed of three members: SHANK1, 2 and 3. These proteins are scaffolding proteins present at the post-synaptic density in glutamatergic synapses. SHANK3 deletions, duplications, and mutations have been frequently reported in patients with ASD (Durand et al., 2007; Boccuto et al., 2013; Leblond et al., 2014). *SHANK3* mutations are one of the most prevalent monogenic causes of ASD, accounting for at least 0.69% of all cases, and patients harboring SHANK3 truncating mutations display autism combined with moderate to severe intellectual disabilities. Moreover, 22q13.3 deletion syndrome, also known as Phelan–McDermid syndrome, which is characterized by ASD or ASD-traits, is caused by deletions and mutations that lead to the loss of a functional copy of *SHANK3* (Soorya et al., 2013). Recent META-analysis of SHANK family mutations in ASD identified deletions disrupting *SHANK1* and *SHANK2* genes in patients, but not duplication of either (Leblond et al., 2014). This study also suggested the existence of a gradient of severity in **cognitive impairment** depending on the SHANK gene mutated. So far, the molecular mechanisms underlying SHANK functions remain partially unclear and studies using *Drosophila* have contributed significantly in addressing this question.

Drosophila harbors only one ortholog of the SHANK family called Prosap/Shank (Liebl and Featherstone, 2008). Harris et al. (2016) described that Shank localizes to the post-synaptic membrane at the NMJ where it is involved in the regulation of synapse morphology and maturation. The levels of Shank at **synapses** are critical; *Shank* mutants exhibit a 24% reduction in synaptic boutons and an excessively high number of immature synaptic structures. On the other hand, *Shank* heterozygous animals show an intermediate phenotype, with a 15% reduction in boutons numbers but no increase in immature synaptic structures. Interestingly, post-synaptic Shank overexpression leads to phenotypes similar to those observed in *Shank* mutants, confirming that the levels of Shank are critical to achieve normal synaptic development. Shank defects have been associated with the modulation of Wnt/FNI (Frizzled Nuclear Import) pathway at the post-synaptic terminal. Shank affects the internalization of the Frizzled-2 (Fz2) receptor, most likely by organizing molecules associated with its internalization and trafficking to the nucleus (Harris et al., 2016). A more recent study from Wu et al. (2017) described Shank expression in axons and at the presynaptic terminal, but not at the post-synaptic sites of

the NMJs. Moreover, they generated new *Shank* mutant alleles that show normal morphology at the NMJ and at the post-synaptic density. The authors focused on the role of Shank in the CNS since the protein, like its mammalian counterpart, is expressed in the brain and enriched in the neuropil region. Loss of *Shank* leads to developmental defects of the synapses in the larval MB Calyx, where the protein exerts its function at both pre- and post-synaptic sites. Synapse defects are visible also in the adult MB Calyx, that presents altered microglomeruli and abnormal localization of the α7 subunit of nicotinic acetylcholine receptor (AChR Dα7) and Choline acetyltransferase (ChAT). These abnormalities result in significant impairment of the olfactory learning in *Shank* mutants.

mGluR

A genome-wide association study (GWAS) of copy-number variation (CNVs) in patients with autism that lead to defective gene family interaction networks (GFINs) (Hadley et al., 2014) identified CNVs in the metabotropic glutamate receptor (mGluR) signaling pathway in 5.8% of patients with ASD.

The involvement of mGluR in autism has been highlighted in its involvement in FXS. The "**mGluR theory**" states that loss of *FMRP* in FXS results in increased glutamatergic signaling via mGluR5, leading to uncontrolled increases in local mRNA translation (Pop et al., 2014). In fact, mGluR activation normally stimulates synthesis of proteins involved in stabilization of long-term depression (LTD) (Weiler et al., 1997). In FXR patients, this translation stimulation is not balanced by the presence of FMRP and leads to increased AMPA receptor internalization and destabilization of the synapses.

As described in the previous section, loss of *dfmr1* activity in *Drosophila* mimics classic FXS symptoms and the impact of **mGluR inhibition** on these phenotypes has been studied by several groups. McBride et al. (2005) demonstrated that **treatment with mGluR antagonists** or Lithium Chloride (LiCl), during development and adulthood, restores the naive courtship levels of the *dfmr1* mutants. Similar treatments also rescue *dfmr1* defects in immediate recall-memory and the lack of short-term memory. Moreover, the treatment with mGlur antagonists greatly reduces axon growth defects (β lobe overgrowth) observed in the MB of *dfmr1* mutants. Interestingly, the free running rest-activity rhythm defects of *dfmr1* mutant flies are not rescued by these treatments, suggesting that not all the phenotypes observed in *dfmr1* null flies are due to upregulation of mGluR signaling (McBride et al., 2005). Recently, the study of the relationship between mGluR and *dfmr1* was extended by investigating the effect of aging on *dfmr1* mutants. In particular, Choi et al. (2010) demonstrated that *dfmr1* mutants show an age-dependent loss of learning that was rescued by the administration of mGluR antagonists and LiCl. Interestingly, treatment during development rescued the learning defect but not the courtship phenotype, indicating that the rescue obtained by treatment during development alone is not permanent. In fact, when aged flies were treated during development and adulthood or during adulthood alone, the naive courtship was restored (Choi et al., 2010). The interconnection between *dfmr1* and mGluR has been demonstrated also through **genetic interaction,** where loss of *dfmr1* was shown to partially alleviate the phenotypes at the NMJ resulting from loss of *mGluR*, possibly via reduction of translational inhibition. Similarly,

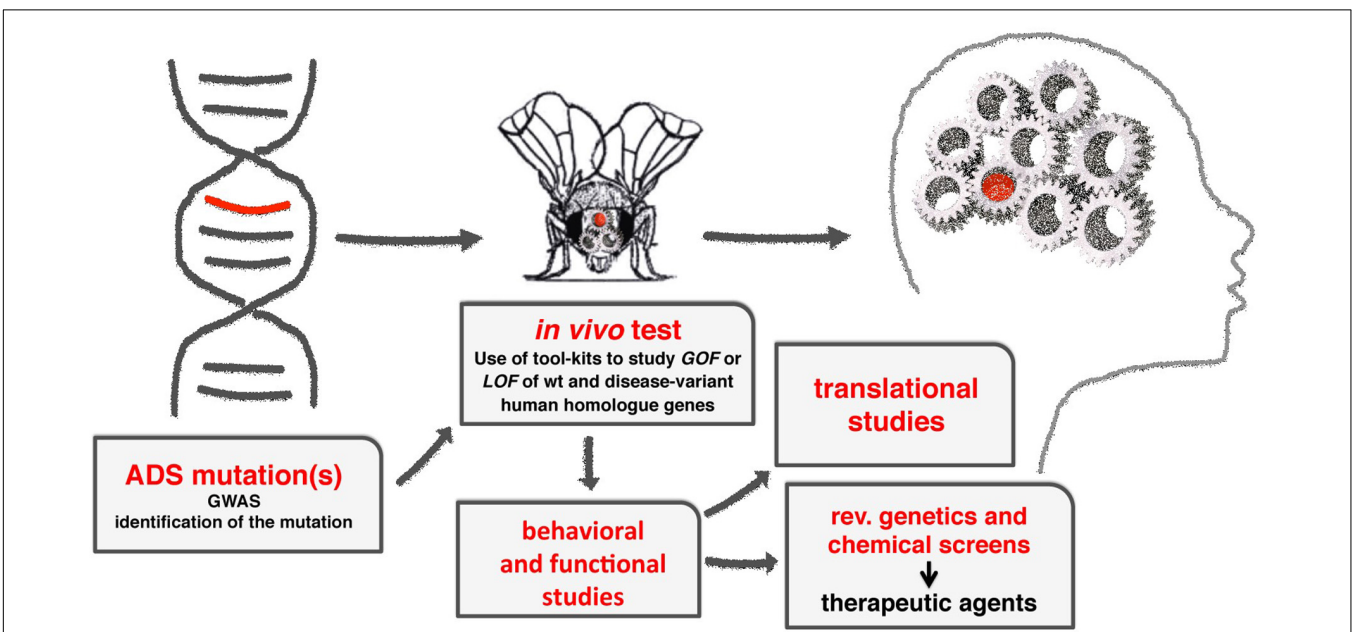

FIGURE 2 | A diagram showing the flow-through to study the molecular mechanisms of ADS using Drosophila. From the initial identification of human genes associated to ADS, to the characterization of their functions using GOF and LOF experiments, applying the milieu of genetic tools available (see **Table 1**). Using transgenic animals, functional and behavioral studies are used to provide the translational benefits necessary to identify or clarify the function of the gene in humans. Moreover, the fruit fly can be easily adapted to perform reverse genetics or chemical screens to identify novel genes or therapeutic drugs in ADSs.

loss of *mGluR* partially rescues the defects caused by loss of *dfmr1* and the consequent impairment of translation regulation (Repicky and Broadie, 2009).

Dopamine Network

The dopamine (DA) network has been widely associated with ASD, where mutations in genes of the DA signaling, such as the Dopamine transporter (DAT), Synataxin 1 (STX1), the DA-receptors, and enzymes involved in DA metabolism, have been associated with autism. Work from several groups suggested that dopamine imbalances in specific circuits of the brain could lead to ASD related behavior (Gadow et al., 2010; Nakamura et al., 2010; Paval, 2017). Moreover, increased size of DA-enriched brain regions, such as the striatum, has been associated with the severity of the disorder (Langen et al., 2014).

Several years ago, a new missense mutation in the human *DAT* gene (**hDAT-T356M**) was identified. This mutation results in reduced ability to accumulate intracellular DA, due to an increased dopamine efflux (Hamilton et al., 2013). The functional consequences of this mutation have been studied in *Drosophila* by expressing the hDAT-T356M in *DAT* null mutant flies. These animals show hyperactivity as compared to flies expressing the wt *hDAT* gene due to increased extracellular levels of DA and abnormal dopamine efflux (Hamilton et al., 2013).

Exome sequencing studies in ASD patients led to the identification of missense variants in the *hDAT* (**hDAT-R51W**) and in *STX1A* (**STX1A-R26Q**) genes. The analysis of these mutations showed defects in the reverse transport of DA that leads to behavioral abnormalities (De Rubeis et al., 2014; Iossifov et al., 2014; Cartier et al., 2015). Mechanistically, the STX1A-R26Q variant is less phosphorylated by Caseine Kinase-2 (CK2), a modification that supports the reverse transport of DA and leads to a reduction in DA efflux. Similarly, the hDAT-R51W variant shows a reduced interaction with STX1 and reduced DA efflux. The effects of these mutations have been characterized *in vivo* in *Drosophila* by assessing locomotion. In fact, Amphetamine (AMPH) feeding stimulates *Drosophila* locomotion but only in the presence of a fully functional DA network. Moreover, expression of a dominant negative form of CK2, mimicking the STX1A-R26Q variant, in DA neurons renders flies insensitive to AMPH. On the other hand, flies harboring the hDAT-R51W mutation increased their locomotion upon AMPH significantly less than wt hDAT expressing flies, confirming the reduced ability of AMPH to cause DA efflux in hDAT R/W mutants (Cartier et al., 2015).

CONCLUDING REMARKS

Drosophila melanogaster is an extremely useful model to understand the molecular mechanisms underlying the function of ASD associated genes in brain development and function (**Figure 2**).

Moreover, the fast growing body of GWAS provides detailed information on the presence of genomic alterations in patients, for which the functional consequences and their relevance in ASD are difficult to interpret (i.e., gene redundancy, complex networks etc.). The fruit fly allows for the analysis of the effects of multiple genetic modifications in different subsets of cells, allowing for the discrimination of the contributions of combinations of genetic alterations co-occurring in ASD patients.

Therefore, the combination of genomic analysis of ASD patients together with the use of an easy to manipulate *in vivo* model with a robust and comparable neuronal development, will be essential to gain insight into the pathogenesis of these disorders.

AUTHOR CONTRIBUTIONS

Both authors listed contributed to writing and reviewing the manuscript.

FUNDING

Funding from Cariplo Foundation 2014703 and EHDN 689 for PB. AS is supported by funding from the European Union's Horizon 2020 Research and Innovation programme under the Marie Skłodowska Curie grant agreement No. 752621.

ACKNOWLEDGMENTS

We thank Sheri Zola for critically reading and correcting the manuscript.

REFERENCES

Akalal, D.-B. G., Wilson, C. F., Zong, L., Tanaka, N. K., Ito, K., and Davis, R. L. (2006). Roles for *Drosophila* mushroom body neurons in olfactory learning and memory. *Learn. Mem.* 13, 659–668. doi: 10.1101/lm.221206

Androschuk, A., He, R. X., Weber, S., Rosenfelt, C., and Bolduc, F. V. (2018). Stress odorant sensory response dysfunction in *Drosophila* fragile X syndrome mutants. *Front. Mol. Neurosci.* 11:242. doi: 10.3389/fnmol.2018.00242

Ascano, M. Jr., Mukherjee, N., Bandaru, P., Miller, J. B., Nusbaum, J. D., Corcoran, D. L., et al. (2012). FMRP targets distinct mRNA sequence elements to regulate protein expression. *Nature* 492, 382–386. doi: 10.1038/nature11737

Banerjee, P., Nayar, S., Hebbar, S., Fox, C. F., Jacobs, M. C., Park, J. H., et al. (2007). Substitution of critical isoleucines in the KH domains of *Drosophila* fragile X protein results in partial loss-of-function phenotypes. *Genetics* 175, 1241–1250. doi: 10.1534/genetics.106.068908

Banerjee, S., and Riordan, M. (2018). Coordinated regulation of axonal microtubule organization and transport by *Drosophila* neurexin and BMP pathway. *Sci. Rep.* 8:17337. doi: 10.1038/s41598-018-35618-7

Banerjee, S., Venkatesan, A., and Bhat, M. A. (2017). Neurexin, neuroligin and wishful thinking coordinate synaptic cytoarchitecture and growth at neuromuscular junctions. *Mol. Cell. Neurosci.* 78, 9–24. doi: 10.1016/j.mcn.2016.11.004

Banovic, D., Khorramshahi, O., Owald, D., Wichmann, C., Riedt, T., Fouquet, W., et al. (2010). Drosophila neuroligin 1 promotes growth and postsynaptic differentiation at glutamatergic neuromuscular junctions. *Neuron* 66, 724–738. doi: 10.1016/j.neuron.2010.05.020

Bier, E. (2005). Drosophila, the golden bug, emerges as a tool for human genetics. *Nat. Rev. Genet.* 6, 9–23. doi: 10.1038/nrg1503

Boccuto, L., Lauri, M., Sarasua, S. M., Skinner, C. D., Buccella, D., Dwivedi, A., et al. (2013). Prevalence of SHANK3 variants in patients with different subtypes of autism spectrum disorders. *Eur. J. Hum. Genet.* 21, 310–316. doi: 10.1038/ejhg.2012.175

Bushey, D., Tononi, G., and Cirelli, C. (2009). The *Drosophila* fragile X mental retardation gene regulates sleep need. *J. Neurosci.* 29, 1948–1961. doi: 10.1523/JNEUROSCI.4830-08.2009

Cartier, E., Hamilton, P. J., Belovich, A. N., Shekar, A., Campbell, N. G., Saunders, C., et al. (2015). Rare autism-associated variants implicate syntaxin 1 (STX1 R26Q) phosphorylation and the dopamine transporter (hDAT R51W) in dopamine neurotransmission and behaviors. *EBioMedicine* 2, 135–146. doi: 10.1016/j.ebiom.2015.01.007

Chakrabarti, S., and Fombonne, E. (2005). Pervasive developmental disorders in preschool children: confirmation of high prevalence. *Am. J. Psychiatry* 162, 1133–1141. doi: 10.1176/appi.ajp.162.6.1133

Chen, Y. C., Lin, Y. Q., Banerjee, S., Venken, K., Li, J., Ismat, A., et al. (2012). *Drosophila* neuroligin 2 is required presynaptically and postsynaptically for proper synaptic differentiation and synaptic transmission. *J. Neurosci.* 32, 16018–16030. doi: 10.1523/JNEUROSCI.1685-12.2012

Choi, C. H., McBride, S. M., Schoenfeld, B. P., Liebelt, D. A., Ferreiro, D., Ferrick, N. J., et al. (2010). Age-dependent cognitive impairment in a *Drosophila* fragile X model and its pharmacological rescue. *Biogerontology* 11, 347–362. doi: 10.1007/s10522-009-9259-6

Chow, C. Y., and Reiter, L. T. (2017). Etiology of human genetic disease on the fly. *Trends Genet.* 33, 391–398. doi: 10.1016/j.tig.2017.03.007

Coffee, R. L., Tessier, C. R., Woodruff, E. A., and Broadie, K. (2010). Fragile X mental retardation protein has a unique, evolutionarily conserved neuronal function not shared with FXR1P or FXR2P. *Dis. Models Mech.* 3, 471–485. doi: 10.1242/dmm.004598

Collins, S. C., Bray, S. M., Suhl, J. A., Cutler, D. J., Coffee, B., Zwick, M. E., et al. (2010). Identification of novel FMR1 variants by massively parallel sequencing in developmentally delayed males. *Am. J. Med. Genet. A* 152A, 2512–2520. doi: 10.1002/ajmg.a.33626

Darnell, J. C., Van Driesche, S. J., Zhang, C., Hung, K. Y., Mele, A., Fraser, C. E., et al. (2011). FMRP stalls ribosomal translocation on mRNAs linked to synaptic function and autism. *Cell* 146, 247–261. doi: 10.1016/j.cell.2011.06.013

De Boulle, K., Verkerk, A. J., Reyniers, E., Vits, L., Hendrickx, J., Van Roy, B., et al. (1993). A point mutation in the FMR-1 gene associated with fragile X mental retardation. *Nat. Genet.* 3, 31–35. doi: 10.1038/ng0193-31

De Rubeis, S., He, X., Goldberg, A. P., Poultney, C. S., Samocha, K., Cicek, A. E., et al. (2014). Synaptic, transcriptional and chromatin genes disrupted in autism. *Nature* 515, 209–215. doi: 10.1038/nature13772

Dockendorff, T. C., Su, H. S., McBride, S. M., Yang, Z., Choi, C. H., Siwicki, K. K., et al. (2002). Drosophila lacking dfmr1 activity show defects in circadian output and fail to maintain courtship interest. *Neuron* 34, 973–984. doi: 10.1016/s0896-6273(02)00724-9

Doi, A., Takagi, M., Fujimoto, K., Kakihara, J., Hayashi, Y., Tatsumi, H., et al. (2016). Long rp' tachycardia with unusual entrainment responses: what is the mechanism? *J. Cardiovasc. Electrophysiol.* 27, 1242–1244. doi: 10.1111/jce.12987

Doll, C. A., and Broadie, K. (2015). Activity-dependent FMRP requirements in development of the neural circuitry of learning and memory. *Development* 142, 1346–1356. doi: 10.1242/dev.117127

Doll, C. A., and Broadie, K. (2016). Neuron class-specific requirements for fragile X mental retardation protein in critical period development of calcium signaling in learning and memory circuitry. *Neurobiol. Dis.* 89, 76–87. doi: 10.1016/j.nbd.2016.02.006

Durand, C. M., Betancur, C., Boeckers, T. M., Bockmann, J., Chaste, P., Fauchereau, F., et al. (2007). Mutations in the gene encoding the synaptic scaffolding protein SHANK3 are associated with autism spectrum disorders. *Nat. Genet.* 39, 25–27. doi: 10.1038/ng1933

Franco, L. M., Okray, Z., Linneweber, G. A., Hassan, B. A., and Yaksi, E. (2017). Reduced lateral inhibition impairs olfactory computations and behaviors in a drosophila model of fragile X syndrome. *Curr. Biol.* 27, 1111–1123. doi: 10.1016/j.cub.2017.02.065

Gadow, K. D., Devincent, C. J., Olvet, D. M., Pisarevskaya, V., and Hatchwell, E. (2010). Association of DRD4 polymorphism with severity of oppositional defiant disorder, separation anxiety disorder and repetitive behaviors in children with autism spectrum disorder. *Eur. J. Neurosci.* 32, 1058–1065. doi: 10.1111/j.1460-9568.2010.07382.x

Gatto, C. L., and Broadie, K. (2009). Temporal requirements of the fragile x mental retardation protein in modulating circadian clock circuit synaptic architecture. *Front. Neural Circuits* 3:8. doi: 10.3389/neuro.04.008.2009

Gatto, C. L., and Broadie, K. (2010). Genetic controls balancing excitatory and inhibitory synaptogenesis in neurodevelopmental disorder models. *Front. synaptic Neurosci.* 2:4. doi: 10.3389/fnsyn.2010.00004

Gatto, C. L., Pereira, D., and Broadie, K. (2014). GABAergic circuit dysfunction in the *Drosophila* fragile X syndrome model. *Neurobiol. Dis.* 65, 142–159. doi: 10.1016/j.nbd.2014.01.008

Greenblatt, E. J., and Spradling, A. C. (2018). Fragile X mental retardation 1 gene enhances the translation of large autism-related proteins. *Science* 361, 709–712. doi: 10.1126/science.aas9963

Hadley, D., Wu, Z. L., Kao, C., Kini, A., Mohamed-Hadley, A., Thomas, K., et al. (2014). The impact of the metabotropic glutamate receptor and other gene family interaction networks on autism. *Nat. Commun.* 5:4074. doi: 10.1038/ncomms5074

Hahn, N., Geurten, B., Gurvich, A., Piepenbrock, D., Kastner, A., Zanini, D., et al. (2013). Monogenic heritable autism gene neuroligin impacts *Drosophila* social behaviour. *Behav. Brain Res.* 252, 450–457. doi: 10.1016/j.bbr.2013.06.020

Hamilton, P. J., Campbell, N. G., Sharma, S., Erreger, K., Herborg Hansen, F., Saunders, C., et al. (2013). De novo mutation in the dopamine transporter gene associates dopamine dysfunction with autism spectrum disorder. *Mol. Psychiatry* 18, 1315–1323. doi: 10.1038/mp.2013.102

Handt, M., Epplen, A., Hoffjan, S., Mese, K., Epplen, J. T., and Dekomien, G. (2014). Point mutation frequency in the FMR1 gene as revealed by fragile X syndrome screening. *Mol. Cell. Probes* 28, 279–283. doi: 10.1016/j.mcp.2014.08.003

Harris, K. P., Akbergenova, Y., Cho, R. W., Baas-Thomas, M. S., and Littleton, J. T. (2016). Shank modulates postsynaptic wnt signaling to regulate synaptic development. *J. Neurosci.* 36, 5820–5832. doi: 10.1523/JNEUROSCI.4279-15.2016

Hutsler, J. J., and Zhang, H. (2010). Increased dendritic spine densities on cortical projection neurons in autism spectrum disorders. *Brain Res.* 1309, 83–94. doi: 10.1016/j.brainres.2009.09.120

Iossifov, I., O'Roak, B. J., Sanders, S. J., Ronemus, M., Krumm, N., Levy, D., et al. (2014). The contribution of de novo coding mutations to autism spectrum disorder. *Nature* 515, 216–221. doi: 10.1038/nature13908

Kim, H. G., Kishikawa, S., Higgins, A. W., Seong, I. S., Donovan, D. J., Shen, Y., et al. (2008). Disruption of neurexin 1 associated with autism spectrum disorder. *Am. J. Hum. Genet.* 82, 199–207. doi: 10.1016/j.ajhg.2007.09.011

Knight, D., Xie, W., and Boulianne, G. L. (2011). Neurexins and neuroligins: recent insights from invertebrates. *Mol. Neurobiol.* 44, 426–440. doi: 10.1007/s12035-011-8213-1

Langen, M., Bos, D., Noordermeer, S. D., Nederveen, H., van Engeland, H., and Durston, S. (2014). Changes in the development of striatum are involved in repetitive behavior in autism. *Biol. Psychiatry* 76, 405–411. doi: 10.1016/j.biopsych.2013.08.013

Laumonnier, F., Bonnet-Brilhault, F., Gomot, M., Blanc, R., David, A., Moizard, M. P., et al. (2004). X-linked mental retardation and autism are associated with a mutation in the NLGN4 gene, a member of the neuroligin family. *Am. J. Hum. Genet.* 74, 552–557. doi: 10.1086/382137

Leblond, C. S., Nava, C., Polge, A., Gauthier, J., Huguet, G., Lumbroso, S., et al. (2014). Meta-analysis of SHANK mutations in autism spectrum disorders: a gradient of severity in cognitive impairments. *PLoS Genet.* 10:e1004580. doi: 10.1371/journal.pgen.1004580

Lee, T., Lee, A., and Luo, L. (1999). Development of the *Drosophila* mushroom bodies: sequential generation of three distinct types of neurons from a neuroblast. *Development* 126, 4065–4076.

Liebl, F. L., and Featherstone, D. E. (2008). Identification and investigation of *Drosophila* postsynaptic density homologs. *Bioinform. Biol. Insights* 2, 369–381.

Liu, L., Tian, Y., Zhang, X. Y., Zhang, X., Li, T., Xie, W., et al. (2017). Neurexin restricts axonal branching in columns by promoting ephrin clustering. *Dev. Cell* 41, 94.e4–106.e4. doi: 10.1016/j.devcel.2017.03.004

Luo, W., Zhang, C., Jiang, Y. H., and Brouwer, C. R. (2018). Systematic reconstruction of autism biology from massive genetic mutation profiles. *Sci. Adv.* 4:e1701799. doi: 10.1126/sciadv.1701799

McBride, S. M., Choi, C. H., Wang, Y., Liebelt, D., Braunstein, E., Ferreiro, D., et al. (2005). Pharmacological rescue of synaptic plasticity, courtship behavior, and mushroom body defects in a *Drosophila* model of fragile X syndrome. *Neuron* 45, 753–764. doi: 10.1016/j.neuron.2005.01.038

Michel, C. I., Kraft, R., and Restifo, L. L. (2004). Defective neuronal development in the mushroom bodies of Drosophila fragile X mental retardation 1 mutants. *J. Neurosci.* 24, 5798–5809. doi: 10.1523/jneurosci.1102-04.2004

Mila, M., Alvarez-Mora, M. I., Madrigal, I., and Rodriguez-Revenga, L. (2018). Fragile X syndrome: an overview and update of the FMR1 gene. *Clin. Genet.* 93, 197–205. doi: 10.1111/cge.13075

Morales, J., Hiesinger, P. R., Schroeder, A. J., Kume, K., Verstreken, P., Jackson, F. R., et al. (2002). *Drosophila* fragile X protein, DFXR, regulates neuronal morphology and function in the brain. *Neuron* 34, 961–972. doi: 10.1016/s0896-6273(02)00731-6

Nakamura, K., Sekine, Y., Ouchi, Y., Tsujii, M., Yoshikawa, E., Futatsubashi, M., et al. (2010). Brain serotonin and dopamine transporter bindings in adults with high-functioning autism. *Arch. Gen. Psychiatry* 67, 59–68. doi: 10.1001/archgenpsychiatry.2009.137

Neriec, N., and Desplan, C. (2016). From the eye to the brain: development of the *Drosophila* visual system. *Curr. Top. Dev. Biol.* 116, 247–271. doi: 10.1016/bs.ctdb.2015.11.032

O'Brien, G., and Pearson, J. (2004). Autism and learning disability. *Autism* 8, 125–140. doi: 10.1177/1362361304042718

Okray, Z., de Esch, C. E., Van Esch, H., Devriendt, K., Claeys, A., Yan, J., et al. (2015). A novel fragile X syndrome mutation reveals a conserved role for the carboxy-terminus in FMRP localization and function. *EMBO Mol. Med.* 7, 423–437. doi: 10.15252/emmm.201404576

Pan, L., Zhang, Y. Q., Woodruff, E., and Broadie, K. (2004). The *Drosophila* fragile X gene negatively regulates neuronal elaboration and synaptic differentiation. *Curr. Biol.* 14, 1863–1870. doi: 10.1016/j.cub.2004.09.085

Park, H. R., Lee, J. M., Moon, H. E., Lee, D. S., Kim, B. N., Kim, J., et al. (2016). A short review on the current understanding of autism spectrum disorders. *Exp. Neurobiol.* 25, 1–13. doi: 10.5607/en.2016.25.1.1

Paval, D. (2017). A dopamine hypothesis of autism spectrum disorder. *Dev. Neurosci.* 39, 355–360. doi: 10.1159/000478725

Peca, J., and Feng, G. (2012). Cellular and synaptic network defects in autism. *Curr. Opin. Neurobiol.* 22, 866–872. doi: 10.1016/j.conb.2012.02.015

Pieretti, M., Zhang, F. P., Fu, Y. H., Warren, S. T., Oostra, B. A., Caskey, C. T., et al. (1991). Absence of expression of the FMR-1 gene in fragile X syndrome. *Cell* 66, 817–822. doi: 10.1016/0092-8674(91)90125-i

Pop, A. S., Gomez-Mancilla, B., Neri, G., Willemsen, R., and Gasparini, F. (2014). Fragile X syndrome: a preclinical review on metabotropic glutamate receptor 5 (mGluR5) antagonists and drug development. *Psychopharmacology* 231, 1217–1226. doi: 10.1007/s00213-013-3330-3

Ramocki, M. B., and Zoghbi, H. Y. (2008). Failure of neuronal homeostasis results in common neuropsychiatric phenotypes. *Nature* 455, 912–918. doi: 10.1038/nature07457

Repicky, S., and Broadie, K. (2009). Metabotropic glutamate receptor-mediated use-dependent down-regulation of synaptic excitability involves the fragile X mental retardation protein. *J. Neurophysiol.* 101, 672–687. doi: 10.1152/jn.90953.2008

Santos, A. R., Kanellopoulos, A. K., and Bagni, C. (2014). Learning and behavioral deficits associated with the absence of the fragile X mental retardation protein: what a fly and mouse model can teach us. *Learn. Mem.* 21, 543–555. doi: 10.1101/lm.035956.114

Sinclair, D., Oranje, B., Razak, K. A., Siegel, S. J., and Schmid, S. (2017). Sensory processing in autism spectrum disorders and Fragile X syndrome-From the clinic to animal models. *Neurosci. Biobehav. Rev.* 76(Pt B), 235–253. doi: 10.1016/j.neubiorev.2016.05.029

Sofola, O., Sundram, V., Ng, F., Kleyner, Y., Morales, J., Botas, J., et al. (2008). The *Drosophila* FMRP and LARK RNA-binding proteins function together to regulate eye development and circadian behavior. *J. Neurosci.* 28, 10200–10205. doi: 10.1523/JNEUROSCI.2786-08.2008

Soorya, L., Kolevzon, A., Zweifach, J., Lim, T., Dobry, Y., Schwartz, L., et al. (2013). Prospective investigation of autism and genotype-phenotype correlations in 22q13 deletion syndrome and SHANK3 deficiency. *Mol. Autism* 4:18. doi: 10.1186/2040-2392-4-18

Sudhof, T. C. (2017). Synaptic neurexin complexes: a molecular code for the logic of neural circuits. *Cell* 171, 745–769. doi: 10.1016/j.cell.2017.10.024

Sun, M., Xing, G., Yuan, L., Gan, G., Knight, D., With, S. I., et al. (2011). Neuroligin 2 is required for synapse development and function at the *Drosophila* neuromuscular junction. *J. Neurosci.* 31, 687–699. doi: 10.1523/jneurosci.3854-10.2011

Tang, G., Gudsnuk, K., Kuo, S. H., Cotrina, M. L., Rosoklija, G., Sosunov, A., et al. (2014). Loss of mTOR-dependent macroautophagy causes autistic-like synaptic pruning deficits. *Neuron* 83, 1131–1143. doi: 10.1016/j.neuron.2014.07.040

Tauber, J. M., Vanlandingham, P. A., and Zhang, B. (2011). Elevated levels of the vesicular monoamine transporter and a novel repetitive behavior in the *Drosophila* model of fragile X syndrome. *PLoS One* 6:e27100. doi: 10.1371/journal.pone.0027100

Tessier, C. R., and Broadie, K. (2008). Drosophila fragile X mental retardation protein developmentally regulates activity-dependent axon pruning. *Development* 135, 1547–1557. doi: 10.1242/dev.015867

Tian, Y., Zhang, Z. C., and Han, J. (2017). Drosophila studies on autism spectrum disorders. *Neurosci. Bull.* 33, 737–746. doi: 10.1007/s12264-017-0166-6

van Alphen, B., Yap, M. H., Kirszenblat, L., Kottler, B., and van Swinderen, B. (2013). A dynamic deep sleep stage in *Drosophila*. *J. Neurosci.* 33, 6917–6927. doi: 10.1523/JNEUROSCI.0061-13.2013

Wan, L., Dockendorff, T. C., Jongens, T. A., and Dreyfuss, G. (2000). Characterization of dFMR1, a *Drosophila melanogaster* homolog of the fragile X mental retardation protein. *Mol. Cell. Biol.* 20, 8536–8547. doi: 10.1128/mcb.20.22.8536-8547.2000

Weiler, I. J., Irwin, S. A., Klintsova, A. Y., Spencer, C. M., Brazelton, A. D., Miyashiro, K., et al. (1997). Fragile X mental retardation protein is translated near synapses in response to neurotransmitter activation. *Proc. Natl. Acad. Sci. U.S.A.* 94, 5395–5400. doi: 10.1073/pnas.94.10.5395

Wu, S., Gan, G., Zhang, Z., Sun, J., Wang, Q., Gao, Z., et al. (2017). A presynaptic function of shank protein in *Drosophila*. *J. Neurosci.* 37, 11592–11604. doi: 10.1523/JNEUROSCI.0893-17.2017

Xing, G., Gan, G., Chen, D., Sun, M., Yi, J., Lv, H., et al. (2014). *Drosophila* neuroligin3 regulates neuromuscular junction development and synaptic differentiation. *J. Biol. Chem.* 289, 31867–31877. doi: 10.1074/jbc.M114.574897

Xing, G., Li, M., Sun, Y., Rui, M., Zhuang, Y., Lv, H., et al. (2018). Neurexin-Neuroligin 1 regulates synaptic morphology and functions via the WAVE regulatory complex in *Drosophila* neuromuscular junction. *eLife* 7:e30457. doi: 10.7554/eLife.30457

Xu, S., Poidevin, M., Han, E., Bi, J., and Jin, P. (2012). Circadian rhythm-dependent alterations of gene expression in *Drosophila* brain lacking fragile X mental retardation protein. *PLoS One* 7:e37937. doi: 10.1371/journal.pone.0037937

Yan, J., Noltner, K., Feng, J., Li, W., Schroer, R., Skinner, C., et al. (2008). Neurexin 1alpha structural variants associated with autism. *Neurosci. Lett.* 438, 368–370. doi: 10.1016/j.neulet.2008.04.074

Zhang, X., Rui, M., Gan, G., Huang, C., Yi, J., Lv, H., et al. (2017). Neuroligin 4 regulates synaptic growth via the bone morphogenetic protein (BMP) signaling pathway at the *Drosophila* neuromuscular junction. *J. Biol. Chem.* 292, 17991–18005. doi: 10.1074/jbc.M117.810242

Zhang, Y. Q., Bailey, A. M., Matthies, H. J., Renden, R. B., Smith, M. A., Speese, S. D., et al. (2001). Drosophila fragile X-related gene regulates the MAP1B homolog Futsch to control synaptic structure and function. *Cell* 107, 591–603. doi: 10.1016/s0092-8674(01)00589-x

Zoghbi, H. Y., and Bear, M. F. (2012). Synaptic dysfunction in neurodevelopmental disorders associated with autism and intellectual disabilities. *Cold Spring Harb. Perspect. Biol.* 4:a009886. doi: 10.1101/cshperspect.a009886

Conflict of Interest Statement: The authors declare that the research was conducted in the absence of any commercial or financial relationships that could be construed as a potential conflict of interest.

frontiers in Physiology

REVIEW
published: 22 August 2019
doi: 10.3389/fphys.2019.01093

The True Story of *Yeti*, the "Abominable" Heterochromatic Gene of *Drosophila melanogaster*

Yuri Prozzillo[1,2], Francesca Delle Monache[2], Diego Ferreri[1,2], Stefano Cuticone[1,2], Patrizio Dimitri[1,2] and Giovanni Messina[1,2]**

[1] Pasteur Institute of Italy, Fondazione Cenci Bolognetti, Rome, Italy, [2] "Charles Darwin" Department of Biology and Biotechnology, Sapienza University of Rome, Rome, Italy

The *Drosophila Yeti* gene (CG40218) was originally identified by recessive lethal mutation and subsequently mapped to the deep pericentromeric heterochromatin of chromosome 2. Functional studies have shown that *Yeti* encodes a 241 amino acid protein called YETI belonging to the evolutionarily conserved family of Bucentaur (BCNT) proteins and exhibiting a widespread distribution in animals and plants. Later studies have demonstrated that YETI protein: (i) is able to bind both subunits of the microtubule-based motor kinesin-I; (ii) is required for proper chromosome organization in both mitosis and meiosis divisions; and more recently (iii) is a new subunit of dTip60 chromatin remodeling complex. To date, other functions of YETI counterparts in chicken (CENtromere Protein 29, CENP-29), mouse (Cranio Protein 27, CP27), zebrafish and human (CranioFacial Development Protein 1, CFDP1) have been reported in literature, but the fully understanding of the multifaceted molecular function of this protein family remains still unclear. In this review we comprehensively highlight recent work and provide a more extensive hypothesis suggesting a broader range of YETI protein functions in different cellular processes.

Keywords: ***Drosophila melanogaster*, BCNT proteins, chromatin remodeling complex, YETI, epigenetic regulation**

OPEN ACCESS

Edited by:
Cristiano De Pitta, University of Padua, Italy

Reviewed by:
René Massimiliano Marsano, University of Bari Aldo Moro, Italy
Daniel F. Eberl, The University of Iowa, United States

****Correspondence:***
Patrizio Dimitri
patrizio.dimitri@uniroma1.it
Giovanni Messina
giovanni.messina@uniroma1.it

Specialty section:
This article was submitted to Invertebrate Physiology, a section of the journal Frontiers in Physiology

Received: *29 May 2019*
Accepted: *08 August 2019*
Published: *22 August 2019*

Citation:
Prozzillo Y, Delle Monache F, Ferreri D, Cuticone S, Dimitri P and Messina G (2019) The True Story of Yeti, the "Abominable" Heterochromatic Gene of Drosophila melanogaster. Front. Physiol. 10:1093. doi: 10.3389/fphys.2019.01093

INTRODUCTION

The eukaryotic genome is packaged into a highly condensed structure known as chromatin allowing cells to organize, compact and stabilize the genome into the nucleus. The first step of this process is achieved through nucleosome assembly which DNA into an 11 nm fiber that represents an approximate 6-fold level of compaction (Luger et al., 2012). Nucleosomes are octamers consisting of H2A/H2B and H3/H4 dimers which wrap around 147 bp of DNA. To gain access to DNA for replication, transcription and repair, nucleosomes must be shifted in different positions, removed or newly loaded to the DNA.

ATP-dependent protein complexes are the "molecular machines" having the task to specifically arrange the nucleosomal state. Thus far, all ATP-dependent chromatin-remodeling complexes identified contain a catalytic subunit which is part of the SWI2/SNF2 superfamily of ATPases and utilize a Swi2/Snf2-type ATPase domain consisting of an ATP-binding domain (DExx-domain), together with a helicase domain (HELICc-domain) (Clapier et al., 2017).

Four different classes (or families) of chromatin-remodeling complexes can be identified within chromatin remodeler ATPases superfamily: SWI/SNF, ISWI, CHD, and INO80 (Clapier et al., 2017). This classification is based on the presence of additional motifs outside the ATPase region. SWI/SNF members contain a bromodomain, ISWI members contain a SANT domain, while a

TABLE 1 | SWR1 subfamily.

Organism	Yeast		Fly	Human		Synonyms	Molecular function
Complex	**NuA4**	**SWR1**	**Tip60**	**TRRAP/Tip60**	**SRCAP**		
ATPase	EAF1	SWR1	Domino	EP400	SRCAP	DOMO1, KIAA0309	Histone-tail binding/ATP-dependent helicase
Non-catalytic homolougous subunits		RVB1	Pontin	RUVBL1	RUVBL1	Pontin, ECP54, INO80H, NMP238, TIH1, Pontin52, TIP49, TIP49a	ATP-dependent helicase (unclear), scaffold
		RVB2	Reptin	RUVBL2	RUVBL2	Reptin, ECP51, INO80J, Reptin52, TIH2, TIP48, TIP49b	ATP-dependent helicase (unclear), scaffold
	ARP4	ARP4	BAP55	ACTL6A	ACTL6A	Actl6, BAF53A, INO80K	Phospho-H2A-variant-dependent DNA recruitment upon DNA damage
	ACT1	ARP6	Act87E	Actin	ACTR6	FLJ13433	Positive regulation of ATPase activity, actin related
	ESA1		Tip60	KAT5		cPLA2, PLIP, HTATIP1, ZC2HC5	HAT activity
	EAF3		MRG15	MORF4L1		HsT17725, MEAF3, MORFRG15	H3K36me2/3 binding
	EAF6		dEAF6	MEAF6		CENP-28, FLJ11730, NY-SAR-91	Unknown
	EAF7		dMRGBP	MRGBP		FLJ10914, MRG15BP	MRG15-binding, potential DNA-binding
	EPL1		E(pc)	EPC1			Protein-interaction within complex, regulation of HAT activity
	YNG2		dING3	ING3		Eaf4, FLJ20089, MEAF4, p47ING3	H3K4me3 binding
	TRA1		dTra1	TRRAP		PAF400, TR-AP	Adaptor, scaffold
	YAF9	YAF9	GAS41	YEATS4	YEATS4	NuBI-1	Transcriptional activation, nuclear matrix interaction
	SWC4	SWC4	dDMAP1	DMAP1	DMAP1	DNMAP1, DNMTAP1, EAF2, FLJ11543, KIAA1425, MEAF2	Histone-tail binding
		Bdf1	dBrd8	BRD8/TRCp120		p120, SMAP	Binding to acetylated histones, transcriptional coactivator
		VPS72	YL-1	VPS72	VPS72		H2A-variant binding
		H2AZ, H2B	H2A.V, H2B		H2AZ, H2B		Unknown
		VPS71			ZNHIT1	p18/Hamlet	Unknown
		SWC5	YETI		CFDP1	BCNT, CENP-29, CP27, p97	Unknown
Unique	EAF5, EAF1	SWC3, SWC7					Unknown

Updated subunits composition of SWR1 chromatin remodeling complexes in yeast, fly and human according to FlyBase, HUGO gene nomenclature committee, yeastgenome databases and literature (Clapier and Cairns, 2009; Hargreaves and Crabtree, 2011; Rust et al., 2018).

chromo- and a DNA-binding domain is found in CHD members. The INO80 class members do not contain any of these domains; instead, the ATPase domain is splitted into two segments (Lessard and Crabtree, 2010).

The process of chromatin remodeling generally refers to different changes in DNA–histone interaction within nucleosomes using the energy from ATP hydrolysis (Becker and Horz, 2002). They include repositioning of histone octamers in *cis* (along the same DNA template molecule) and in trans (from one DNA template molecule to another one), the loss of superhelical torsion of nucleosomal DNA, and the increase in accessibility to nucleosomal DNA for downstream processes as transcription. Interestingly, recent studies have shown that ATP-dependent chromatin remodeling may allow to change the histone composition of a nucleosome (Clapier and Cairns, 2009). Indeed, the yeast SWR1 complex, a member of the INO80 family, associates with Htz1, the homolog of mammalian histone variant H2A.Z. This complex can drive the ATP-dependent replacement of H2A–H2B with Htz1–H2B dimers (Krogan et al., 2003; Kobor et al., 2004; Mizuguchi et al., 2004; van Attikum and Gasser, 2005) by Swc1 ATPase subunit. *In vivo*, SWR1 catalyzes the incorporation of Htz1 into chromatin, which prevents the spreading of heterochromatin regions into regions of euchromatin (van Attikum and Gasser, 2005).

The human (SRCAP and P400/Tip60) and Drosophila (dTip60) orthologous chromatin remodeling complexes include proteins with high similarity to the subunits of two distinct chromatin-modifying complexes, the yeast NuA4 complex (Wang et al., 2018) harboring HAT (Histone Acetyl-transferase) activity, and the SWR1 ATP-dependent chromatin remodeling complex which catalyzes histones exchange (**Table 1**).

The dTip60 complex is made up by 14 core subunits (BAP55, dGAS41, dPontin, dReptin, Nipped-A, e(Pc), dYL1, dDMAP, Act87B, dMrg15, dMrgBP, dTRA1, dIng3, and dEaf6) and was found to be required for the replacement of acetylated phospho-H2A.V by unmodified H2A.V via Domino (Dom) ATPase (Kusch et al., 2004; March-Diaz and Reyes, 2009). In *Drosophila*, H2A.V is the only H2A variant and corresponds to mammalian H2A.X and H2A.Z (Baldi and Becker, 2013).

Similarly to H2A.X, H2A.V is phosphorylated upon DNA double strand breaks to mark the DNA lesions, stimulate DNA repair machinery, and promote an easily accessible DNA conformation (Kusch et al., 2004).

The human P400/Tip60 complex highly resembles the dTip60 complex and contains the p400 protein, which also shows high sequence similarity to SWR1, DOMINO and SRCAP (Eissenberg et al., 2005; **Table 1**). Recent studies have demonstrated that several components of the P400/Tip60 complex are amplified or overexpressed in human neuroblastoma, glioblastoma, and colorectal cancer, while loss of function is mostly lethal, leading to cell growth arrest or cell death as well as genome instability (Yamada, 2012).

The YETI protein was found to be a new subunit of Drosophila Tip60 remodeling complex (Messina et al., 2014), arousing more and more curiosity because of a growing number of biological functions that it is supposed to perform.

Here, we comprehensively review emerging findings on YETI and its orthologous proteins in other species highlighting the broad-range involvement of these proteins in many biological processes.

THE BIOLOGICAL ROLE OF YETI PROTEIN

Y*eti*, previously called CG40218, is an essential 1717-bp-long gene located in the heterochromatin of chromosome 2 of *Drosophila melanogaster* required for proper chromosome organization in both mitosis and meiosis (Hilliker, 1976; Corradini et al., 2003; Dimitri et al., 2003; Messina et al., 2014; Marsano et al., 2019). The evolutionary origin of *Yeti* gene is rather peculiar as such it has evolved from a euchromatic ancestor in drosophilids. The *Yeti* locus maps on euchromatin in two distantly related species, *D. pseudoobscura* and *D. virilis* indicating that over time (about 40 million of years, which is the estimated divergence time between *D. melanogaster* and *D. virilis*) it progressively moved closer to the heterochromatic pericentromeric regions (Moschetti et al., 2014; Caizzi et al., 2016). Interestingly, *Yeti* gene retained its original and robust organization in all analyzed species, with a short genomic region carrying a single short intron.

It is known that genes expressed at low levels harbor substantially shorter introns than those are expressed at high levels (Castillo-Davis et al., 2002). Therefore, despite of the genomic re-location, *Yeti* may have been under selective pressure maintaining a short size and ensuring high and efficient gene expression during early development (Moschetti et al., 2014).

YETI is a 241-aa-long protein belonging to BCNT protein superfamily which is characterized by a yeast-to-human highly conserved 82-amino acid domain located at the C-terminus (BCNT-C) (Takahashi et al., 1998; **Figure 1**).

The YETI protein was originally identified as a both subunits kinesin-binding protein. In addition, Immunofluorescence experiments showed both a nuclear and cytoplasmic localization of V5 -tagged YETI in Drosophila S2 cells (Wisniewski et al., 2003). However, these experiments failed to clarify whether YETI is located within the nuclei or associated with the nuclear membrane.

In the last decade, YETI protein functions have been investigated more in depth (Messina et al., 2014). In particular, YETI was found to be a chromatin-associated protein member of the dTip60 complex (**Figure 2**), whose depletion leads to larval stage lethality accompanied by profound perturbations of higher-order chromatin organization due to the failure in loading of histone H2A.V, nucleosomal histones, and chromatin marks. Moreover, the BCNT domain of YETI was found to be involved in chromatin binding through the interaction with the H2A histone variant (H2A.V), Domino-A (DOM-A) ATPase, and HP1a protein (Ryu et al., 2014; **Figure 3**).

Taken together, these results strongly suggest that YETI may be directly implicated in the exchange of the variant H2A.V onto nucleosomes impacting on the dynamic changes of chromatin, and fulfilling its role as subunit of Tip60 chromatin remodeling complex, similarly to the yeast homolog SWC5 (Morillo-Huesca et al., 2010).

Furthermore, in a genetic interaction map of cell cycle regulators, YETI (and also the DOMINO ATPase) has been defined as an additional interesting connection in the proximity of Anaphase-promoting complex/Cyclosome (APC/C) (Billmann et al., 2016), suggesting a specific role in the regulation of chromatin and transcription during mitosis (Morrison and Shen, 2009; Tanenbaum et al., 2015). Moreover, there are emerging evidence indicating that YETI is involved in synapse assembly and function (Pazos Obregon et al., 2015).

In conclusion, YETI appears to be a multifaceted chromatin protein playing a key role in different cellular pathways.

THE MOLECULAR FUNCTION OF SWC5, THE YETI ORTHOLOGOUS PROTEIN IN *S. cerevisiae*

Molecular insights of YETI orthologs come from other model organisms. For example, Swc5, the yeast ortholog protein, is a component of the SWR1 complex which catalyze the exchange of histone H2A with the H2A variant, Htz1 (Kobor et al., 2004; Mizuguchi et al., 2004). However, although Swc5 protein is not essential, *Swc5* null-mutants are defective in chromosome maintenance, and show decreased resistance to hydroxyurea (Saccharomyces Genome Database) and increased heat sensitivity (Dastidar et al., 2012).

In vitro studies report that the binding of SWR1 complex to Htz1 is not dependent on Swc5 subunit, but *Swc5* deleted mutants lack histone exchange function, indicating a key role of Swc5 during the histone replacement reaction (Wu et al., 2005). *In vivo* evidence supports this conclusion showing that the absence of Swc5 doesn't affect complex assembly while it nearly dropped down the amount of Htz1 bound to chromatin, suggesting that Swc5 is required for the binding and destabilization of the H2A/H2B dimer (Morillo-Huesca et al., 2010). More in depth, SWR1 catalyzes H2A.Z *in vitro* replacement as one H2A.Z-H2B dimer at a time, generating heterotypic nucleosomes as intermediates and homotypic H2A.Z nucleosomes as final

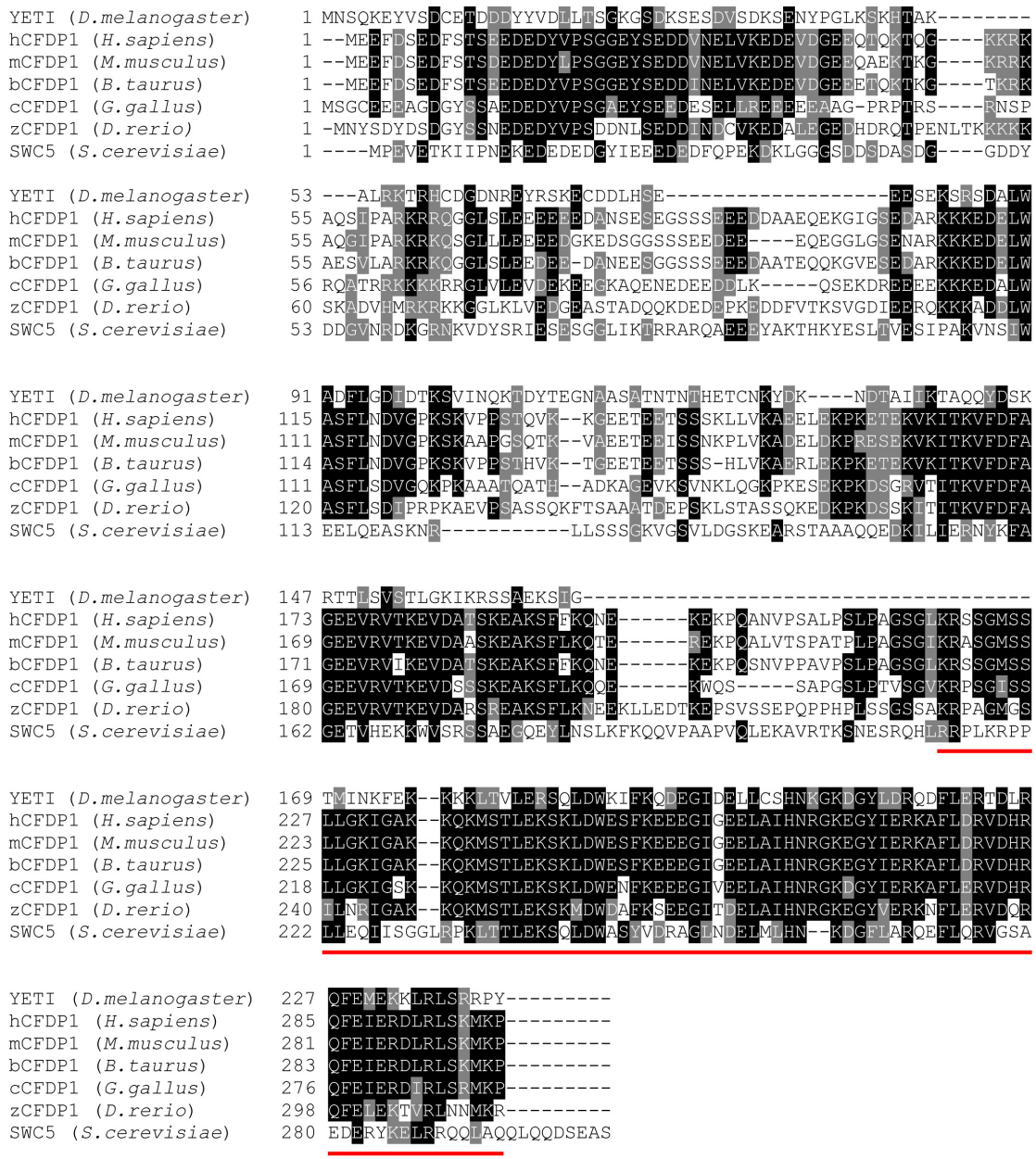

FIGURE 1 | The YETI orthologous proteins. Blast alignments of YETI and its orthologous protein sequences from human (*H. sapiens*), mouse (*M. musculus*), bovine (*B. taurus*), chicken (*G. gallus*), Zebrafish (*D. rerio*) and yeast (*S. cerevisiae*). Note the high level of conservation (about 45% similarity) in the last 80 residues of the BCNT C-terminal domain (red line).

products. The SWR1 ATPase activity is specifically stimulated by H2A-containing nucleosomes, then free H2A.Z-H2B dimer leads to hyperstimulation of ATPase activity, eviction of nucleosomal H2A-H2B, and deposition of H2A.Z-H2B onto chromatin. In this way, SWR1 complex catalyzes nucleosomal conversion from H2A/H2A to Htz1/Htz1, with the heterotypic nucleosomes H2A/Htz1 as intermediates (Luk et al., 2010). Furthermore, a truncated Swc5 lacking the BCNT domain is not able to restore the reaction, indicating that BCNT domain is required for Htz1 deposition (Sun and Luk, 2017).

CRANIOFACIAL DEVELOPMENT PROTEIN 1 (CFDP1): A "DEVELOPMENTAL FACE" OF YETI ORTHOLOGS IN MAMMALS

A 97 kDa BCNT protein (p97Bcnt) was first identified in bovine brain and found to be widely distributed in animals and plants (Nobukuni et al., 1997; Takahashi et al., 1998; Iwashita and Naoki, 2011; Messina et al., 2015).

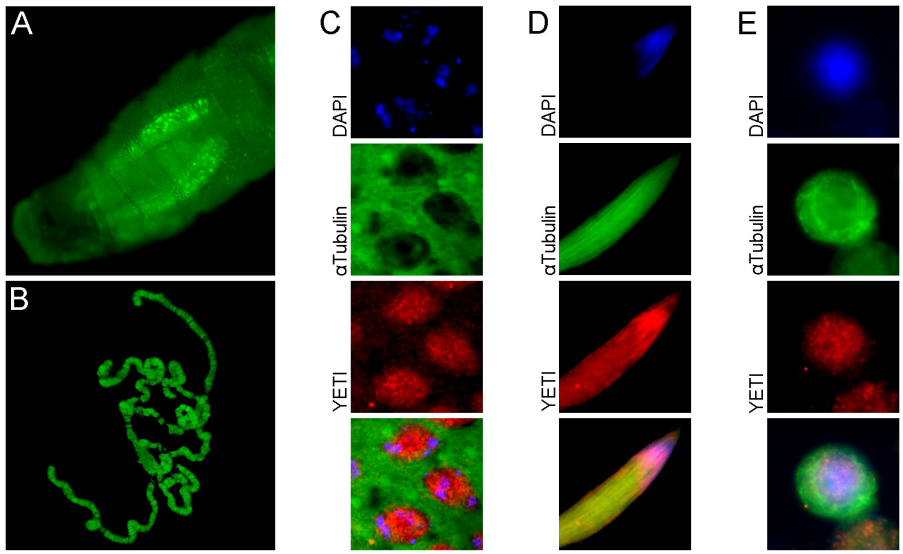

FIGURE 2 | Subcellular YETI localization. **(A)** YETI::GFP fusion protein localizes in nuclei of salivary glands and **(B)** binds to polytene chromosomes. A nuclear immunolocalization of YETI protein is accordingly found in **(C)** spermatocytes, **(D)** elongated spermatids and **(E)** Drosophila S2 cells.

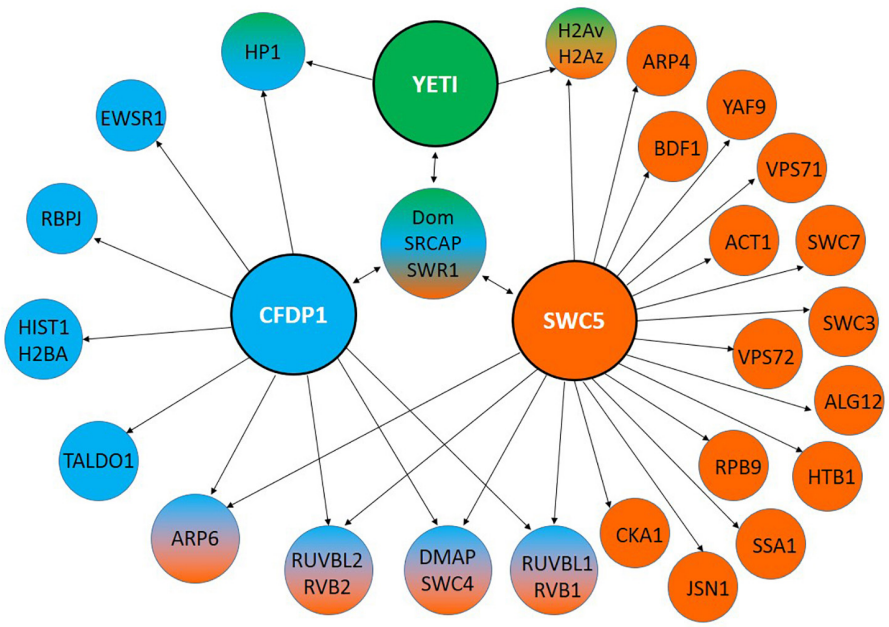

FIGURE 3 | Interaction partners of YETI and its orthologs. YETI (*D. melanogaster*), hCFDP1 (*H. sapiens*) and SWR1 (*S. cerevisiae*) interacting proteins identified by using MIST (Molecular Interaction Search Tool). They refer only to physical interactions experimentally determined.

Later on, the murine ortholog was isolated and cloned from a mouse E11 (Embrional day 11) λgt11 library using an antibody against Cem1, a tooth cementum-related protein marker of a distinct expression pattern of mouse craniofacial development (Diekwisch et al., 1999). It maps on chromosome 8 in the E1 region and is 85 kb long, with a 7 exons (888 nucleotides) open reading frame transcribing a single mRNA and encoding a 295 a.a. protein of 27 kDa weight (mCFDP1). Due to its expression pattern and protein MW, the gene was originally named *craniofacial protein 27* (*cp27)* (Diekwisch et al., 1999).

Studies on the cp27 protein (later called mCFDP1) have shown specific interaction with NF-Y nuclear factor which bind CCAAT box (Luan et al., 2010; Ito et al., 2011), and with the TFII-I transcription factors involved in craniofacial development and osteo-differentiation

(Makeyev and Bayarsaihan, 2011). Moreover, while RT-qPCR experiments revealed the presence of mCFDP1 in a pool of different genes related with transcription in osteo-differentiation (Bustos-Valenzuela et al., 2011), Northern blot analysis, combined with an *in situ* hybridization, have confirmed high level of its expression in developmental stage of mouse embryos, and in particular in neuroepithelium, cerebellum, heart, lung, liver, teeth, salivary glands, and periosteum of developing bones. These data have been also confirmed by immunohistochemical staining of developing tissues (Luan and Diekwisch, 2002).

Furthermore, cleft palate induction by persistent expression of PAX3 gene in neural crest correlates with cp27 downregulation (Wu et al., 2008).

The human BCNT ortholog maps to chromosome 16 in 16q22.2- q22.3, in proximity to several loci associated with inherited craniofacial disease genes (Diekwisch et al., 1999; Iwashita and Naoki, 2011). For this reason and for the expression pattern of the mouse ortholog it was called craniofacial development protein 1 gene (*Cfdp1*, OMIM number 608108). It is transcribed into two mRNAs differing by the alternative splicing-mediated inclusion or exclusion of exon encoding BCNT domain (Messina et al., 2017).

Independent experimental evidence suggests that the human CFDP1 (hCDFP1) protein is a subunit of the SNF2-related CBP activator protein (SRCAP) chromatin remodeling complex (Havugimana et al., 2012; Messina et al., 2017), which catalyzes the ATP-dependent replacement of canonical histone H2A with the H2A.Z variant (Monroy et al., 2001).

The first pioneer work aimed to address the mechanistic functions of hCFDP1 protein have been performed (Messina et al., 2016) by expressing human *Cfdp1* transgene in *D. melanogaster*. The results of this experiment have shown that *hCfdp1* expression lead to lethality and developmental and morphological defects, depending on the tissue-specific driver used. In particular, hCFDP1 binds to chromatin leading to abnormal polytene chromosome organization, decreased levels of H2A.V and H2A, brains and imaginal discs decreased size, developing of melanotic masses, prolonged larval stage and lethality. All these defects strongly resemble those produced by the lack of YETI (Messina et al., 2014). Thus, it is conceivable that hCFDP1 over-expression in *D. melanogaster* disrupts the physiological function of YETI resulting in a dominant-negative effect. Reciprocally, the *Drosophila* 3xFlag:YETI expressed in HeLa cells is able to go into the cell nucleus, bind to chromatin and produce a substantial decrease in the mitotic index with an important defects of cell cycle progression (Messina et al., 2016).

GST-pull down experiments have shown that both YETI and CFDP1 can undergo self-dimerization or hetero-dimerization. Thus, aberrant phenotypes could be due to the *in vivo* formation of YETI-CFDP1 non-functional hetero-dimers, together with a concomitant reduction of the amount of endogenous protein, YETI (drosophila cells) or CFDP1 (HeLa cells) (Messina et al., 2016; Messina et al., 2017).

Moreover, RNAi-mediated depletion of hCFDP1 in HeLa cells led to aberrant morphology and condensation defects of mitotic chromosomes impacting on their normal segregation during mitosis (Messina et al., 2017). These defects evoke those exhibited by *Yeti* null alleles in *Drosophila melanogaster*, suggesting a high-order chromatin organization maintenance function (Cenci et al., 2003; Messina et al., 2014).

Interestingly, the chromosome condensation defects observed in CFDP1 depleted cells resemble those found in cells lacking the MCPH1 gene encoding microcephalin, which is one of the causative genes of primary microcephaly (Yamashita et al., 2011; Messina et al., 2017).

Finally, in a human proteomic study, CFDP1 was found to interact with Ewing sarcoma related protein (EWSR1) whose mutations leads to Ewing's sarcoma, a type of cancer that forms in bone or soft tissue (Bode-Lesniewska et al., 2019; **Figure 3**).

YETI ORTHOLOGS IN NON-MAMMALIAN VERTEBRATES

Among other vertebrates, data on YETI orthologs are only available from birds and fishes. In a recent study CENP-29, the chicken BCNT member, has been reported to be associated with kinetochores and therefore was suggested to play a role in chromosome segregation (Ohta et al., 2010).

In *Danio rerio*, the BCNT family gene, previously called *rltpr* (*RGD motif, leucine-rich repeats*, *tropomodulin domain* and *proline-rich containing*) and recently renamed *zCfdp1*, was found to be developmentally expressed in the eye, Central Nervous System and in branchial arches which lead to the craniofacial structures (Thisse and Thisse, 2004).

Recently, Celauro et al. (2017) have shown that zCFDP1 is rapidly produced after Maternal-To-Zygote transition and it is highly enriched in the head structures. Moreover, depletion of zCFDP1, induced by an ATG-blocking *morpholino*, produces drastic defects in craniofacial structures and bone mineralization.

Together, these results show that, not only that zCFDP1 is an essential protein required for proper embryonal development, but more importantly, they provide the first experimental evidence that it directly implicated in the morphogenesis of craniofacial territories in vertebrates. Moreover, based on the high level of identity (about 70%) (**Figure 1**), humans and zebrafish CFDP1 proteins, may be functionally conserved. It is then plausible that CFDP1, as a subunit of the SRCAP chromatin remodeling complex, participates to the epigenetic control of chromatin regions containing developmentally regulated genes, whose activation/silencing is crucial for proper differentiation of craniofacial structures and osteogenesis in zebrafish and likely in humans (Celauro et al., 2017).

EMERGING NEW FUNCTIONS OF YETI AND ITS ORTHOLOGS

As described above, the evolutionarily conserved Tip60 chromatin remodeling complex reveal multifaceted biological roles including transcriptional regulation, DNA repair, cell cycle

progression, chromosome stability, stem cell maintenance and differentiation (Sapountzi et al., 2006; Tea and Luo, 2011).

As anticipated, depletion of YETI and CFDP1 in *D. melanogaster* and HeLa cells respectively affects mitotic index and led to chromosome segregation defects (Cenci et al., 2003; Messina et al., 2014, 2016). Moreover, the chicken YETI ortholog CENP-29 has been reported to be associated with kinetochores in chicken (Ohta et al., 2010). Finally, YETI protein has also been implicated in cell cycle control in both mitosis and meiosis (Billmann et al., 2016). According with these results, it has been reported that Myc, a well-known oncogenic player (Bellosta et al., 2005; Jonchere et al., 2017; Taylor et al., 2017), and the DOMINO ATPase interact each other and are required for normal asymmetric neuroblast (NB) division. Live-imaging analysis of *dom*-or *myc*-depleted NBs showed that spindle morphology is affected resulting in aberrant divisions (Rust et al., 2018). Similarly, Tip60 acetyl-transferase and Myc have been shown to co-regulate genes functionally involved in cell cycle and DNA replication (Zhao et al., 2018). Noteworthy, *D. melanogaster* mutants leading to symmetric division induce tumorigenesis (Albertson and Doe, 2003; Lee et al., 2006). Similarly, mutants lacking centrosomes and have severely impaired spindle asymmetry, over-proliferate and form tumors (Caous et al., 2015). Furthermore, mutations in genes encoding proteins directly or potentially implicated in chromatin biology are key players in human cancer and developmental disorders (Bickmore and van der Maarel, 2003; Fog et al., 2012; Harmacek et al., 2014).

Previous findings highlighted a role of YETI in spermatogenesis (Cenci et al., 2003). Accordingly, hCFDP1 has been found to physically interact with TALDO1 (Perl et al., 2006; Huttlin et al., 2015, 2017), an hallmark of human and murine spermatogenesis (Berkovits and Wolgemuth, 2013; Green et al., 2018), and HIST1H2BA (**Figure 3**), an intronless gene encoding a testis/sperm-specific member of the histone H2B family (Zalensky et al., 2002).

Taken together, the above-mentioned studies suggest that YETI and its orthologs, in addition to their canonical functions in chromatin remodeling, may play yet unexplored roles during both mitotic and meiotic cell division.

CONCLUSION AND FUTURE PERSPECTIVE

Most of the recent progresses in the study of the BCNT protein family originated from the functional analysis of a relatively small gene (*Yeti*) located in *D. melanogaster* constitutive heterochromatin, traditionally regarded as a transcriptionally inert or useless portion of the genome, albeit this prejudice has been debunked (Marsano et al., 2019). The fallout produced by those studies is relevant to basic research on epigenetics and to biomedical research too, as suggested by the experimental evidence showing that CFDP1 actively participates to craniofacial development in zebrafish. Craniofacial malformations are indeed developmental disorders of biomedical and clinical interest, because they represent the main cause of infant mortality and disability in humans. Therefore, it is reasonable to include the *Cfdp1* gene in the screening test for human syndromes showing alteration of craniofacial development.

AUTHOR CONTRIBUTIONS

PD and GM conceived the concept of the study and wrote the manuscript. YP and GM designed and formatted the figures and table. All authors drafted the literature search, edited and reviewed the manuscript.

FUNDING

This work was supported by Ricerche Universitarie 2017 (MIUR) (PD) and "Teresa Ariaudo" Research Program 2018–2020 from Pasteur Institute, Cenci Bolognetti Foundation (GM).

ACKNOWLEDGMENTS

We would like to acknowledge BOXSHADE (https://embnet.vital-it.ch/software/BOX_form.html) for the layout of the amino acid alignment (**Figure 1**).

REFERENCES

Albertson, R., and Doe, C. Q. (2003). Dlg, Scrib and Lgl regulate neuroblast cell size and mitotic spindle asymmetry. *Nat. Cell. Biol.* 5, 166–170. doi: 10.1038/ncb922

Baldi, S., and Becker, P. B. (2013). The variant histone H2A.V of *Drosophila*–three roles, two guises. *Chromosoma* 122, 245–258. doi: 10.1007/s00412-013-0409-x

Becker, P. B., and Horz, W. (2002). ATP-dependent nucleosome remodeling. *Annu. Rev. Biochem.* 71, 247–273. doi: 10.1146/annurev.biochem.71.110601.135400

Bellosta, P., Hulf, T., Balla Diop, S., Usseglio, F., Pradel, J., Aragnol, D., et al. (2005). Myc interacts genetically with Tip48/Reptin and Tip49/Pontin to control growth and proliferation during *Drosophila* development. *Proc. Natl. Acad. Sci. U.S.A.* 102, 11799–11804. doi: 10.1073/pnas.0408945102

Berkovits, B. D., and Wolgemuth, D. J. (2013). The role of the double bromodomain-containing BET genes during mammalian spermatogenesis. *Curr. Top. Dev. Biol.* 102, 293–326. doi: 10.1016/B978-0-12-416024-8.00011-8

Bickmore, W. A., and van der Maarel, S. M. (2003). Perturbations of chromatin structure in human genetic disease: recent advances. *Hum. Mol. Genet.* 12(Suppl. 2), R207–R213.

Billmann, M., Horn, T., Fischer, B., Sandmann, T., Huber, W., and Boutros, M. (2016). A genetic interaction map of cell cycle regulators. *Mol. Biol. Cell.* 27, 1397–1407. doi: 10.1091/mbc.E15-07-0467

Bode-Lesniewska, B., Fritz, C., Exner, G. U., Wagner, U., and Fuchs, B. (2019). EWSR1-NFATC2 and FUS-NFATC2 gene fusion-associated mesenchymal tumors: clinicopathologic correlation and literature review. *Sarcoma* 2019:9386390. doi: 10.1155/2019/9386390

Bustos-Valenzuela, J. C., Fujita, A., Halcsik, E., Granjeiro, J. M., and Sogayar, M. C. (2011). Unveiling novel genes upregulated by both rhBMP2 and rhBMP7 during early osteoblastic transdifferentiation of C2C12 cells. *BMC Res. Notes* 4:370. doi: 10.1186/1756-0500-4-370

Caizzi, R., Moschetti, R., Piacentini, L., Fanti, L., Marsano, R. M., and Dimitri, P. (2016). Comparative genomic analyses provide new insights into the evolutionary dynamics of heterochromatin in *Drosophila*. *PLoS Genet.* 12:e1006212. doi: 10.1371/journal.pgen.1006212

Caous, R., Pascal, A., Rome, P., Richard-Parpaillon, L., Karess, R., and Giet, R. (2015). Spindle assembly checkpoint inactivation fails to suppress neuroblast tumour formation in aurA mutant *Drosophila*. *Nat. Commun.* 6:8879. doi: 10.1038/ncomms9879

Castillo-Davis, C. I., Mekhedov, S. L., Hartl, D. L., Koonin, E. V., and Kondrashov, F. A. (2002). Selection for short introns in highly expressed genes. *Nat. Genet.* 31, 415–418. doi: 10.1038/ng940

Celauro, E., Carra, S., Rodriguez, A., Cotelli, F., and Dimitri, P. (2017). Functional analysis of the cfdp1 gene in zebrafish provides evidence for its crucial role in craniofacial development and osteogenesis. *Exp. Cell Res.* 361, 236–245. doi: 10.1016/j.yexcr.2017.10.022

Cenci, G., Belloni, G., and Dimitri, P. (2003). 1(2)41Aa, a heterochromatic gene of *Drosophila melanogaster*, is required for mitotic and meiotic chromosome condensation. *Genet. Res.* 81, 15–24. doi: 10.1017/s0016672302006018

Clapier, C. R., and Cairns, B. R. (2009). The biology of chromatin remodeling complexes. *Annu. Rev. Biochem.* 78, 273–304. doi: 10.1146/annurev.biochem.77.062706.153223

Clapier, C. R., Iwasa, J., Cairns, B. R., and Peterson, C. L. (2017). Mechanisms of action and regulation of ATP-dependent chromatin-remodelling complexes. *Nat. Rev. Mol. Cell Biol.* 18, 407–422. doi: 10.1038/nrm.2017.26

Corradini, N., Rossi, F., Verni, F., and Dimitri, P. (2003). FISH analysis of *Drosophila melanogaster* heterochromatin using BACs and P elements. *Chromosoma* 112, 26–37. doi: 10.1007/s00412-003-0241-9

Dastidar, R. G., Hooda, J., Shah, A., Cao, T. M., Henke, R. M., and Zhang, L. (2012). The nuclear localization of SWI/SNF proteins is subjected to oxygen regulation. *Cell Biosci.* 2:30. doi: 10.1186/2045-3701-2-30

Diekwisch, T. G., Marches, F., Williams, A., and Luan, X. (1999). Cloning, gene expression, and characterization of CP27, a novel gene in mouse embryogenesis. *Gene* 235, 19–30. doi: 10.1016/s0378-1119(99)00220-6

Dimitri, P., Corradini, N., Rossi, F., Verni, F., Cenci, G., Belloni, G., et al. (2003). Vital genes in the heterochromatin of chromosomes 2 and 3 of *Drosophila melanogaster*. *Genetica* 117, 209–215.

Eissenberg, J. C., Wong, M., and Chrivia, J. C. (2005). Human SRCAP and *Drosophila melanogaster* DOM are homologs that function in the notch signaling pathway. *Mol. Cell. Biol.* 25, 6559–6569. doi: 10.1128/mcb.25.15.6559-6569.2005

Fog, C. K., Galli, G. G., and Lund, A. H. (2012). PRDM proteins: important players in differentiation and disease. *Bioessays* 34, 50–60. doi: 10.1002/bies.201100107

Green, C. D., Ma, Q., Manske, G. L., Shami, A. N., Zheng, X., Marini, S., et al. (2018). A comprehensive roadmap of murine spermatogenesis defined by single-cell RNA-seq. *Dev. Cell* 46:e610. doi: 10.1016/j.devcel.2018.07.025

Hargreaves, D. C., and Crabtree, G. R. (2011). ATP-dependent chromatin remodeling: genetics, genomics and mechanisms. *Cell Res.* 21, 396–420. doi: 10.1038/cr.2011.32

Harmacek, L., Watkins-Chow, D. E., Chen, J., Jones, K. L., Pavan, W. J., Salbaum, J. M., et al. (2014). A unique missense allele of BAF155, a core BAF chromatin remodeling complex protein, causes neural tube closure defects in mice. *Dev. Neurobiol.* 74, 483–497. doi: 10.1002/dneu.22142

Havugimana, P. C., Hart, G. T., Nepusz, T., Yang, H., Turinsky, A. L., Li, Z., et al. (2012). A census of human soluble protein complexes. *Cell* 150, 1068–1081. doi: 10.1016/j.cell.2012.08.011

Hilliker, A. J. (1976). Genetic analysis of the centromeric heterochromatin of chromosome 2 of *Drosophila melanogaster*: deficiency mapping of EMS-induced lethal complementation groups. *Genetics* 83, 765–782.

Huttlin, E. L., Bruckner, R. J., Paulo, J. A., Cannon, J. R., Ting, L., Baltier, K., et al. (2017). Architecture of the human interactome defines protein communities and disease networks. *Nature* 545, 505–509. doi: 10.1038/nature22366

Huttlin, E. L., Ting, L., Bruckner, R. J., Gebreab, F., Gygi, M. P., Szpyt, J., et al. (2015). The BioPlex network: a systematic exploration of the human interactome. *Cell* 162, 425–440. doi: 10.1016/j.cell.2015.06.043

Ito, Y., Zhang, Y., Dangaria, S., Luan, X., and Diekwisch, T. G. (2011). NF-Y and USF1 transcription factor binding to CCAAT-box and E-box elements activates the CP27 promoter. *Gene* 473, 92–99. doi: 10.1016/j.gene.2010.11.001

Iwashita, S., and Naoki, O. (2011). *Bucentaur (Bcnt) Gene Family: Gene Duplication and Retrotransposons Insertion*. Rijeka: InTech, 383–400.

Jonchere, V., Alqadri, N., Herbert, J., Dodgson, L., Mason, D., Messina, G., et al. (2017). Transcriptional responses to hyperplastic MRL signalling in *Drosophila*. *Open Biol.* 7:160306. doi: 10.1098/rsob.160306

Kobor, M. S., Venkatasubrahmanyam, S., Meneghini, M. D., Gin, J. W., Jennings, J. L., Link, A. J., et al. (2004). A protein complex containing the conserved Swi2/Snf2-related ATPase Swr1p deposits histone variant H2A.Z into euchromatin. *PLoS Biol.* 2:E131. doi: 10.1371/journal.pbio.0020131

Krogan, N. J., Keogh, M. C., Datta, N., Sawa, C., Ryan, O. W., Ding, H., et al. (2003). A Snf2 family ATPase complex required for recruitment of the histone H2A variant Htz1. *Mol. Cell* 12, 1565–1576. doi: 10.1016/s1097-2765(03)00497-0

Kusch, T., Florens, L., Macdonald, W. H., Swanson, S. K., Glaser, R. L., Yates, J. R., et al. (2004). Acetylation by Tip60 is required for selective histone variant exchange at DNA lesions. *Science* 306, 2084–2087. doi: 10.1126/science.1103455

Lee, C. Y., Andersen, R. O., Cabernard, C., Manning, L., Tran, K. D., Lanskey, M. J., et al. (2006). *Drosophila* Aurora-A kinase inhibits neuroblast self-renewal by regulating aPKC/Numb cortical polarity and spindle orientation. *Genes Dev.* 20, 3464–3474. doi: 10.1101/gad.1489406

Lessard, J. A., and Crabtree, G. R. (2010). Chromatin regulatory mechanisms in pluripotency. *Annu. Rev. Cell Dev. Biol.* 26, 503–532. doi: 10.1146/annurev-cellbio-051809-102012

Luan, X., and Diekwisch, T. G. (2002). CP27 affects viability, proliferation, attachment and gene expression in embryonic fibroblasts. *Cell Prolif.* 35, 207–219. doi: 10.1046/j.1365-2184.2002.00238.x

Luan, X., Ito, Y., Zhang, Y., and Diekwisch, T. G. (2010). Characterization of the mouse CP27 promoter and NF-Y mediated gene regulation. *Gene* 460, 8–19. doi: 10.1016/j.gene.2010.03.014

Luger, K., Dechassa, M. L., and Tremethick, D. J. (2012). New insights into nucleosome and chromatin structure: an ordered state or a disordered affair? *Nat. Rev. Mol. Cell Biol.* 13, 436–447. doi: 10.1038/nrm3382

Luk, E., Ranjan, A., Fitzgerald, P. C., Mizuguchi, G., Huang, Y., Wei, D., et al. (2010). Stepwise histone replacement by SWR1 requires dual activation with histone H2A.Z and canonical nucleosome. *Cell* 143, 725–736. doi: 10.1016/j.cell.2010.10.019

Makeyev, A. V., and Bayarsaihan, D. (2011). Molecular basis of Williams-Beuren syndrome: TFII-I regulated targets involved in craniofacial development. *Cleft Palate Craniofac. J.* 48, 109–116. doi: 10.1597/09-093

March-Diaz, R., and Reyes, J. C. (2009). The beauty of being a variant: H2A.Z and the SWR1 complex in plants. *Mol. Plant* 2, 565–577. doi: 10.1093/mp/ssp019

Marsano, R. M., Giordano, E., Messina, G., and Dimitri, P. (2019). A new portrait of constitutive heterochromatin: lessons from *Drosophila melanogaster*. *Trends Genet.* 35, 615–631. doi: 10.1016/j.tig.2019.06.002

Messina, G., Atterrato, M. T., Fanti, L., Giordano, E., and Dimitri, P. (2016). Expression of human Cfdp1 gene in *Drosophila* reveals new insights into the function of the evolutionarily conserved BCNT protein family. *Sci. Rep.* 6:25511. doi: 10.1038/srep25511

Messina, G., Atterrato, M. T., Prozzillo, Y., Piacentini, L., Losada, A., and Dimitri, P. (2017). The human cranio facial development protein 1 (Cfdp1) gene encodes a protein required for the maintenance of higher-order chromatin organization. *Sci. Rep.* 7:45022. doi: 10.1038/srep45022

Messina, G., Celauro, E., Atterrato, M. T., Giordano, E., Iwashita, S., and Dimitri, P. (2015). The bucentaur (BCNT) protein family: a long-neglected class of essential proteins required for chromatin/chromosome organization and function. *Chromosoma* 124, 153–162. doi: 10.1007/s00412-014-0503-8

Messina, G., Damia, E., Fanti, L., Atterrato, M. T., Celauro, E., Mariotti, F. R., et al. (2014). Yeti, an essential *Drosophila melanogaster* gene, encodes a protein required for chromatin organization. *J. Cell Sci.* 127, 2577–2588. doi: 10.1242/jcs.150243

Mizuguchi, G., Shen, X., Landry, J., Wu, W. H., Sen, S., and Wu, C. (2004). ATP-driven exchange of histone H2AZ variant catalyzed by SWR1 chromatin remodeling complex. *Science* 303, 343–348. doi: 10.1126/science.1090701

Monroy, M. A., Ruhl, D. D., Xu, X., Granner, D. K., Yaciuk, P., and Chrivia, J. C. (2001). Regulation of cAMP-responsive element-binding protein-mediated transcription by the SNF2/SWI-related protein, SRCAP. *J. Biol. Chem.* 276, 40721–40726. doi: 10.1074/jbc.m103615200

Morillo-Huesca, M., Clemente-Ruiz, M., Andujar, E., and Prado, F. (2010). The SWR1 histone replacement complex causes genetic instability and genome-wide transcription misregulation in the absence of H2A.Z. *PLoS One* 5:e12143. doi: 10.1371/journal.pone.0012143

Morrison, A. J., and Shen, X. (2009). Chromatin remodelling beyond transcription: the INO80 and SWR1 complexes. *Nat. Rev. Mol. Cell Biol.* 10, 373–384. doi: 10.1038/nrm2693

Moschetti, R., Celauro, E., Cruciani, F., Caizzi, R., and Dimitri, P. (2014). On the evolution of *Yeti*, a *Drosophila melanogaster* heterochromatin gene. *PLoS One* 9:e113010. doi: 10.1371/journal.pone.0113010

Nobukuni, T., Kobayashi, M., Omori, A., Ichinose, S., Iwanaga, T., Takahashi, I., et al. (1997). An Alu-linked repetitive sequence corresponding to 280 amino acids is expressed in a novel bovine protein, but not in its human homologue. *J. Biol. Chem.* 272, 2801–2807. doi: 10.1074/jbc.272.5.2801

Ohta, S., Bukowski-Wills, J. C., Sanchez-Pulido, L., Alves Fde, L., Wood, L., Chen, Z. A., et al. (2010). The protein composition of mitotic chromosomes determined using multiclassifier combinatorial proteomics. *Cell* 142, 810–821. doi: 10.1016/j.cell.2010.07.047

Pazos Obregon, F., Papalardo, C., Castro, S., Guerberoff, G., and Cantera, R. (2015). Putative synaptic genes defined from a *Drosophila* whole body developmental transcriptome by a machine learning approach. *BMC Genomics* 16:694. doi: 10.1186/s12864-015-1888-3

Perl, A., Qian, Y., Chohan, K. R., Shirley, C. R., Amidon, W., Banerjee, S., et al. (2006). Transaldolase is essential for maintenance of the mitochondrial transmembrane potential and fertility of spermatozoa. *Proc. Natl. Acad. Sci. U.S.A.* 103, 14813–14818. doi: 10.1073/pnas.0602678103

Rust, K., Tiwari, M. D., Mishra, V. K., Grawe, F., and Wodarz, A. (2018). Myc and the Tip60 chromatin remodeling complex control neuroblast maintenance and polarity in *Drosophila*. *EMBO J.* 37:e98659. doi: 10.15252/embj.201798659

Ryu, H. W., Lee, D. H., Florens, L., Swanson, S. K., Washburn, M. P., and Kwon, S. H. (2014). Analysis of the heterochromatin protein 1 (HP1) interactome in *Drosophila*. *J. Proteom.* 102, 137–147. doi: 10.1016/j.jprot.2014.03.016

Sapountzi, V., Logan, I. R., and Robson, C. N. (2006). Cellular functions of TIP60. *Int. J. Biochem. Cell Biol.* 38, 1496–1509. doi: 10.1016/j.biocel.2006.03.003

Sun, L., and Luk, E. (2017). Dual function of Swc5 in SWR remodeling ATPase activation and histone H2A eviction. *Nucleic Acids Res.* 45, 9931–9946. doi: 10.1093/nar/gkx589

Takahashi, I., Nobukuni, T., Ohmori, H., Kobayashi, M., Tanaka, S., Ohshima, K., et al. (1998). Existence of a bovine line repetitive insert that appears in the cDNA of bovine protein BCNT in ruminant, but not in human, genomes. *Gene* 211, 387–394. doi: 10.1016/s0378-1119(98)00136-x

Tanenbaum, M. E., Stern-Ginossar, N., Weissman, J. S., and Vale, R. D. (2015). Regulation of mRNA translation during mitosis. *Elife* 4:e07957. doi: 10.7554/eLife.07957

Taylor, E., Alqadri, N., Dodgson, L., Mason, D., Lyulcheva, E., Messina, G., et al. (2017). MRL proteins cooperate with activated Ras in glia to drive distinct oncogenic outcomes. *Oncogene* 36, 4311–4322. doi: 10.1038/onc.2017.68

Tea, J. S., and Luo, L. (2011). The chromatin remodeling factor Bap55 functions through the TIP60 complex to regulate olfactory projection neuron dendrite targeting. *Neural Dev.* 6:5. doi: 10.1186/1749-8104-6-5

Thisse, B., and Thisse, C. (2004). *Fast Release Clones: A High Throughput Expression Analysis. ZFIN Direct Data Submission*. Available at: http://zfin.org

van Attikum, H., and Gasser, S. M. (2005). The histone code at DNA breaks: a guide to repair? *Nat. Rev. Mol. Cell Biol.* 6, 757–765. doi: 10.1038/nrm1737

Wang, X., Ahmad, S., Zhang, Z., Cote, J., and Cai, G. (2018). Architecture of the *Saccharomyces cerevisiae* NuA4/TIP60 complex. *Nat. Commun.* 9:1147. doi: 10.1038/s41467-018-03504-5

Wisniewski, T. P., Tanzi, C. L., and Gindhart, J. G. (2003). The *Drosophila* kinesin-I associated protein YETI binds both kinesin subunits. *Biol. Cell* 95, 595–602.

Wu, M., Li, J., Engleka, K. A., Zhou, B., Lu, M. M., Plotkin, J. B., et al. (2008). Persistent expression of Pax3 in the neural crest causes cleft palate and defective osteogenesis in mice. *J. Clin. Invest.* 118, 2076–2087. doi: 10.1172/JCI33715

Wu, W. H., Alami, S., Luk, E., Wu, C. H., Sen, S., Mizuguchi, G., et al. (2005). Swc2 is a widely conserved H2AZ-binding module essential for ATP-dependent histone exchange. *Nat. Struct. Mol. Biol.* 12, 1064–1071. doi: 10.1038/nsmb1023

Yamada, H. Y. (2012). *Human Tip60 (NuA4) Complex and Cancer*. Oklahoma, OK: University of Oklahoma Health Sciences Center (OUHSC).

Yamashita, D., Shintomi, K., Ono, T., Gavvovidis, I., Schindler, D., Neitzel, H., et al. (2011). MCPH1 regulates chromosome condensation and shaping as a composite modulator of condensin II. *J. Cell Biol.* 194, 841–854. doi: 10.1083/jcb.201106141

Zalensky, A. O., Siino, J. S., Gineitis, A. A., Zalenskaya, I. A., Tomilin, N. V., Yau, P., et al. (2002). Human testis/sperm-specific histone H2B (hTSH2B). Molecular cloning and characterization. *J. Biol. Chem.* 277, 43474–43480. doi: 10.1074/jbc.m206065200

Zhao, L. J., Loewenstein, P. M., and Green, M. (2018). Identification of a panel of MYC and Tip60 co-regulated genes functioning primarily in cell cycle and DNA replication. *Genes Cancer* 9, 101–113. doi: 10.18632/genesandcancer.175

Conflict of Interest Statement: The authors declare that the research was conducted in the absence of any commercial or financial relationships that could be construed as a potential conflict of interest.

frontiers in Physiology

BRIEF RESEARCH REPORT
published: 06 September 2019
doi: 10.3389/fphys.2019.01143

Knockdown of *APOPT1/COA8* Causes Cytochrome *c* Oxidase Deficiency, Neuromuscular Impairment, and Reduced Resistance to Oxidative Stress in *Drosophila melanogaster*

*Michele Brischigliaro[1], Samantha Corrà[1], Claudia Tregnago[2], Erika Fernandez-Vizarra[3], Massimo Zeviani[3,4], Rodolfo Costa[1] and Cristiano De Pittà[1]**

[1]Department of Biology, University of Padova, Padua, Italy, [2]Department of Women and Children's Health, University of Padova, Padua, Italy, [3]MRC Mitochondrial Biology Unit, University of Cambridge, Cambridge, United Kingdom, [4]Department of Neurosciences, University of Padova, Padua, Italy

OPEN ACCESS

Edited by:
Elzbieta M. Pyza, Jagiellonian University, Poland

Reviewed by:
Jae Park, The University of Tennessee, Knoxville, United States
Maria de la Paz Fernandez, Columbia University, United States

***Correspondence:**
Cristiano De Pittà
cristiano.depitta@unipd.it

Specialty section:
This article was submitted to Invertebrate Physiology, a section of the journal Frontiers in Physiology

Received: *18 May 2019*
Accepted: *22 August 2019*
Published: *06 September 2019*

Citation:
Brischigliaro M, Corrà S, Tregnago C, Fernandez-Vizarra E, Zeviani M, Costa R and De Pittà C (2019) Knockdown of APOPT1/COA8 Causes Cytochrome c Oxidase Deficiency, Neuromuscular Impairment, and Reduced Resistance to Oxidative Stress in Drosophila melanogaster. Front. Physiol. 10:1143. doi: 10.3389/fphys.2019.01143

Cytochrome *c* oxidase (COX) deficiency is the biochemical hallmark of several mitochondrial disorders, including subjects affected by mutations in *apoptogenic-1* (*APOPT1*), recently renamed as *COA8* (HGNC:20492). Loss-of-function mutations are responsible for a specific infantile or childhood-onset mitochondrial leukoencephalopathy with a chronic clinical course. Patients deficient in COA8 show specific COX deficiency with distinctive neuroimaging features, i.e., cavitating leukodystrophy. In human cells, COA8 is rapidly degraded by the ubiquitin-proteasome system, but oxidative stress stabilizes the protein, which is then involved in COX assembly, possibly by protecting the complex from oxidative damage. However, its precise function remains unknown. The *CG14806* gene (*dCOA8*) is the *Drosophila melanogaster* ortholog of human *COA8* encoding a highly conserved COA8 protein. We report that *dCOA8* knockdown (KD) flies show locomotor defects, and other signs of neurological impairment, reduced COX enzymatic activity, and reduced lifespan under oxidative stress conditions. Our data indicate that KD of *dCOA8* in *Drosophila* phenocopies several features of the human disease, thus being a suitable model to characterize the molecular function/s of this protein *in vivo* and the pathogenic mechanisms associated with its defects.

Keywords: *APOPT1*, *Drosophila melanogaster*, cytochrome *c* oxidase deficiency, mitochondrial disease, resistance to oxidative stress, knockdown models

INTRODUCTION

Mitochondria are subcellular organelles that play a pivotal role in the conversion of energy stored in nutrients into energy spendable in eukaryotic cells (e.g., ATP and heat). The mitochondrial respiratory chain (MRC) plays a central role in this process. MRC includes four enzymatic multiprotein complexes (named complexes I-IV) embedded in the inner mitochondrial membrane

(IMM) that catalyze electron transfer reactions that, through a redox cascade, generate a proton gradient acting as a protonmotive force (PMF) across the IMM. The PMF is then exploited by a fifth complex (complex V, mitochondrial ATP synthase) to convert adenosine diphosphate (ADP) to adenosine triphosphate (ATP), the essential energetic molecule used as a substrate for virtually all endergonic processes in living cells (Spinelli and Haigis, 2018).

Mitochondrial disorders (MD) are a group of mitochondria-related diseases caused by mutations in either nuclear DNA (nDNA) genes, encoding proteins with a role in mitochondrial function, or in mitochondrial DNA (mtDNA) protein or tRNA and rRNA encoding sequences. These diseases are among the most frequently inherited neurometabolic disorders, and are characterized by a wide diversity of clinical features making their diagnosis quite challenging. Thanks to the advances in next generation sequencing (NGS) techniques, the identification of the genetic causes of MD has considerably improved, including extremely rare genetic conditions (Carrol et al., 2014; Legati et al., 2016). For instance, loss-of-function mutations in the *COA8* gene (alias *APOPT1*, *APOP-1*, or *C14ORF153*) have been identified in seven subjects from six different families presenting a distinctive form of mitochondrial encephalopathy (Melchionda et al., 2014; Sharma et al., 2018). The *COA8* mutations include a nonsense mutation (p.Arg79*), a missense mutation (p.Phe118Ser), frameshift mutations (p.Glu121Valfs*4, p.Glu121Valfs*6), and micro-(p.Glu124del) and macro-deletions (p.Val55_Lys120del) (Melchionda et al., 2014; Sharma et al., 2018).

The clinical features include abnormalities of brain magnetic resonance imaging (cavitating leukodystrophy), and neurometabolic failure, including progressive ataxia and spastic tetraparesis (Melchionda et al., 2014; Sharma et al., 2018).

Murine *Apopt1/COA8* was firstly identified as being over-expressed in an *in vitro* model of atherosclerosis (Yasuda et al., 2006). The authors hypothesized a pro-apoptotic role for the protein, because they observed triggering of the apoptotic cascade in a mPTP (mitochondrial permeability transition pore)-dependent manner after its over-expression, causing the release of cytochrome *c* from mitochondria to the cytosol, and the subsequent activation of caspase-9 and caspase-3 (Yasuda et al., 2006; Sun et al., 2008). However, terminal deoxynucleotidyl transferase dUTP nick end labeling (TUNEL) assay failed to detect apoptosis in muscle biopsies from patients, and no difference in growth and apoptotic rate was observed in mutant *versus* control fibroblasts, even after treatment with the apoptosis-inducer staurosporine (Melchionda et al., 2014). In addition, over-expression of a GFP-tagged COA8 protein failed to induce cell death in different human cell lines (Signes et al., 2019), whereas the main biochemical hallmark of its absence was isolated mitochondrial cytochrome *c* oxidase (COX) deficiency (OMIM #220110). Deficiency of COX activity was in fact the only enzymatic abnormality detected in patients' mitochondria, and was associated in both human and mouse cells and tissues with altered COX assembly (Melchionda et al., 2014; Signes et al., 2019). *COA8* encodes a 206-amino acid protein targeted and localized within mitochondria in mammals (Yasuda et al., 2006; Sun et al., 2008; Melchionda et al., 2014; Signes et al., 2019). Recent evidence proved that it is associated with the inner membrane, with the C-terminal region facing the mitochondrial matrix (Signes et al., 2019).

Analysis of the COX structural defect associated with absence of COA8 revealed its involvement in the intermediate steps of the COX assembly pathway (Signes et al., 2019). In addition, COA8 was shown to be oppositely regulated by UPS and ROS (Melchionda et al., 2014; Signes et al., 2019). However, there is still a need to clarify the regulatory mechanisms and the role of COA8 in COX function as well as in general mitochondrial physiology.

The availability of model organisms can provide valuable insights to clarify the relationship between gene mutations and human diseases. Thus, we have investigated the behavioral and biochemical features of a *D. melanogaster* KD model of *COA8*-associated mitochondrial disease. Our findings indicate that *D. melanogaster* is a suitable model that can significantly contribute to elucidate the role of this gene in mitochondrial physiology and pathology.

MATERIALS AND METHODS

Fly Stocks and Maintenance

Flies were raised on standard cornmeal medium and maintained at 23°C, 70% relative humidity on a 12 h-light and 12 h-dark cycle. The UAS fly strain (w^{1118};P{attP,y+,w3′}VIE-260B; transformant ID 100605) used to perform post-transcriptional silencing, carrying single UAS-*CG14806*-IR autosomal insertion (line ID 100605), was obtained from VDRC (Vienna *Drosophila* Resource Center). The w^{1118} and Gal4 driver lines were obtained from the Bloomington Stock Center (y[1] w[*]; P{w[+mC] = Act5C-GAL4}17bFO1/TM6B,Tb[1] strain ID 3954; P{w[+mW.hs] = GawB}elav[C155] strain ID 458).

RNA Isolation, Reverse Transcription, and Real-Time Quantitative Reverse Transcription Polymerase Chain Reaction

Total RNA was extracted from 10 adults (whole body) or approximately 30 brains for each genotype (1:1 males-females) using TRIzol reagent (Thermo Fischer Scientific) and miRNeasy Mini Kit (Qiagen) respectively, according to the manufacturer's instructions. One microgram of total RNA was used for first strand cDNA synthesis employing 10 mM deoxynucleotides, 10 μM oligo-dT and SuperScript II (Life Technologies). Real-time quantitative reverse transcription polymerase chain reactions (qRT-PCRs) were performed in triplicate using a Bio-Rad CFX 96 Touch System (Bio-Rad) using PowerUp SYBR Green chemistry (Thermo Fisher Scientific). The $2^{-\Delta\Delta Ct}$ (RQ, relative quantification) method was used to calculate the relative expression ratio (Livak and Schmittgen, 2001). *Rp49* was used as endogenous control and the oligonucleotides employed were *Rp49*-Fw (5′-ATCGGTTACGGATCGAACAA-3′) and *Rp49*-Rv (5′-GACAA TCTCCTTGCGCTTCT-3′). The *dCOA8* oligonucleotides used were *dCOA8*-Fw (5′-CAATAAGCGCTTCTACGAGGA-3′) and *dCOA8*-Rv (5′-CCAGTTCTTGTCGAGGAACG-3′).

Analysis of Spontaneous Locomotor Activity

The amount of locomotor activity was measured by the DAMSystem3 Data Collection Software (Trikinetics). Ten 2-day-old male flies were placed into a glass tube containing food and water in the form of gel at the bottom. Glass tubes were placed into DPM population monitors (Trikinetics) vertically oriented. One day (24 h) after anesthesia, locomotor activity was recorded for 2 days (48 h) under 12:12 light/dark cycles (LD 12:12) at 23°C. At least three biological replicates per genotype were analyzed.

Climbing Test

Climbing test was performed using a modified version of the countercurrent apparatus originally designed by Seymour Benzer (Benzer, 1967). Twenty 2-day-old flies were placed into the first tube, tapped to the bottom and allowed to climb a 10-cm distance for 10 s. The flies that reached the 10-cm distance were shifted to a second tube, tapped again to the bottom and allowed to climb for further 10 s. The procedure was repeated for a total of five times. At the end, the number of flies in each tube was counted. Climbing indexes were calculated as the weighted average of flies in the different tubes, divided by five times the number of flies in the test. The test was performed 1 h after the dark–light transition and a minimum number of 60 individuals per sex and genotype were analyzed.

Lifespan Assay and Paraquat Treatment

Flies were reared at standard low density, collected after hatching and divided into males and virgin females over a 24-h window. Adults of the same sex were kept at a density of 10 per vial (for a total of 50 individuals) at 23°C. Flies were counted every day and transferred to fresh medium three times per week, with no anesthesia (Broughton et al., 2005). Lifespan was analyzed both in flies fed with standard food and with food containing 20 mM Paraquat. Standard cornmeal was cooled to 35°C before the addition of Paraquat (methyl viologen dichloride hydrate, Sigma) and then poured into plastic vials.

Isolation of Mitochondria

Mitochondria were prepared by differential centrifugation from 100 flies (1:1 males-females) as described previously (Da-Rè et al., 2014a). Briefly, samples were homogenized with a Dounce glass potter and a loose-fitting glass pestle in 10 ml of isotonic isolation buffer (225 mM mannitol, 75 mM sucrose, 5 mM HEPES, 1 mM EGTA, pH 7.4) with 1% BSA. Samples were centrifuged at 1,000 ×*g* (Eppendorf 5810R) at 4°C for 10 min. The supernatant was filtered through a fine mesh, and centrifuged at 6,000 ×*g* at 4°C for 10 min. The mitochondrial pellet was washed in 10 ml of isolation buffer and centrifuged at 6,000 ×*g* for 10 min. The wash was repeated using 10 ml of isolation buffer without BSA and centrifuged at 7,000 ×*g* for 10 min. The mitochondrial pellet was resuspended in minimal volume of isolation buffer without BSA. Protein concentration was measured by the Bradford assay (Bio-Rad protein assay).

Enzymatic Analysis

Prior to enzymatic MRC complex activity assays, isolated mitochondria were subjected to three freeze-thaw cycles in 10 mM ice-cold Tris hypotonic buffer (pH 7.6) using liquid nitrogen to disrupt the mitochondrial membranes. The activities of mitochondrial respiratory chain complexes and citrate synthase (CS) were measured by spectrophotometry as described previously (Kirby et al., 2007), with minor modifications to the protocols.

Cell Cultures

The *Drosophila* S2R+ cell line is derived from a primary culture of late stage (20–24 h old) *D. melanogaster* embryos (Schneider, 1972) and it was obtained from *Drosophila* Genomics Resource Center (DGRC). S2R+ cells grow at 25°C without CO_2 in Schneider's medium (Thermo Fisher Scientific) with 10% heat-inactivated fetal bovine serum (FBS) (Euroclone) as a loose, semi-adherent monolayer, showing a doubling time of about 48 h.

Cell Transfection and Subcellular Localization

CG14806 cDNA was cloned in pAc5-STABLE2-neo vector, fused with the EGFP reporter. S2R+ cells were transfected in 24 wells plate using Effectene Transfection Reagent (Qiagen) according to the manufacturer's instructions. After 48 h, cells were washed once with 1X PBS and incubated with 10 nM MitoTracker Red CMXRos (Thermo Fischer Scientific) and 1 μg/ml cyclosporin H (Sigma) in Schneider's Medium for 20 min (Da-Rè et al., 2014b). After three washes in PBS, cells were fixed in 4% paraformaldehyde for 20 min. After a final wash in PBS, the slides were mounted with Vectashield mounting medium (Vector Laboratories). Images were taken with a Zeiss LSM700 confocal microscope at 63× magnification.

Cell Death Analysis

Transiently transfected cells were collected and stained with Annexin V Apoptosis Detection Set PE-Cyanine7 (eBioscience-ThermoFisher Scientific) and propidium iodide (Roche Biochemicals) according to the manufacturer's protocol. Cells were analyzed using Cytomics FC500 (Beckman Coulter) as described previously (Cusumano et al., 2018).

Electron Microscopy

Thoraxes and brains from adult male flies were fixed in 2.5% glutaraldehyde overnight. Samples were rinsed in 0.1 M cacodylate buffer with 1% tannic acid and then fixed in 1:1 2% OsO_4 and 0.2 M cacodylate buffer for 1 h. Samples were rinsed, dehydrated in ethanol, and embedded in Epon. Ultrathin sections (400 Å) were examined and photographed with a FEI Tecnai G2 electron microscope.

Blue Native Gel Electrophoresis

Isolated mitochondria were resuspended in 1.5 M aminocaproic acid, 50 mM Bis-Tris/HCl pH 7.0. The samples were solubilized with 4 mg digitonin (Merck) per mg of protein. After 5 min. of incubation on ice, samples were centrifuged at 18,000 ×*g*

at 4°C for 10 min. The supernatant was collected and resuspended with Sample Buffer (750 mM aminocaproic acid, 50 mM Bis-Tris/HCl pH 7.0, 0.5 mM EDTA, and 5% Serva Blue G). Native samples were run in NativePAGE 3–12% Bis-Tris gels (Thermo Fischer Scientific) according to the manufacturer's protocol.

In Gel Activity

For the detection of the activity of mitochondrial respiratory chain complexes, gels were stained with the following solutions:

1. Complex I (NADH:ubiquinone oxidoreductase): NADH: 5 mM Tris–HCl pH 7.4, 0.14 mg/ml NADH (Roche), and 1 mg/ml nitrotetrazolium blue chloride (Sigma);
2. Complex II (succinate dehydrogenase): 5 mM Tris–HCl pH 7.4, 0.2 mM phenazine methosulfate (Sigma), 20 mM succinate, and 1 mg/ml nitrotetrazolium blue chloride;
3. Complex IV (cytochrome *c* oxidase): 50 mM potassium phosphate pH 7.4, 1 mg/ml 3′,3′-diaminobenzidine tetrahydrochloride hydrate (Sigma), 24 units/ml catalase from bovine liver (Sigma), 1 mg/ml cytochrome *c* form equine heart (Sigma), and 75 mg/ml sucrose.

RESULTS AND DISCUSSION

CG14806 Is the *Drosophila melanogaster* Ortholog of Human *COA8*

COA8 (*APOPT1*) is present in higher eukaryotes such as *Mus musculus, Rattus norvegicus, Danio rerio, Drosophila melanogaster*, and *Caenorhabditis elegans* but it is absent in lower eukaryotes such as *Saccharomyces cerevisiae.* A *COA8* ortholog is present in the *Drosophila* genome on the X chromosome (*CG14806*, hereafter named *dCOA8*). Two different transcripts of the *dCOA8* gene, both encoding the same 176-amino acid protein, are present in flies. Clustal Omega (Sievers et al., 2011) alignment of the *Drosophila* protein showed 37% of sequence similarity with the human one. Interestingly, human *dCOA8* pathological mutations involve amino acids that are conserved in *Drosophila* (**Figure 1A**).

COA8 has been shown to localize to mitochondria in both human and murine models (Yasuda et al., 2006; Melchionda et al., 2014) being associated with the inner mitochondrial membrane (IMM), with its C-terminal region facing the matrix (Signes et al., 2019). Likewise, dCOA8 has a predicted N-terminal mitochondrial targeting sequence according to the online prediction tools Target P (Emanuelsson et al., 2000) and MitoProt II (Claros and Vincens, 1996), with a probability score of 0.67 and 0.91, respectively. Notably, there is high inter-species variability in the N-terminal sequences (**Figure 1A**). Furthermore, the topology prediction tools Phobius (Käll et al., 2004) and TMpred (Hofmann and Stoffel, 1993) indicate the presence of one C-terminal transmembrane domain suggesting that dCOA8 could be associated with a mitochondrial membrane, most likely the IMM due to the presence of an MTS, while the rest of the hydrophilic domains could be localized in the mitochondrial matrix.

We transiently expressed a recombinant form of *dCOA8* fused at the C-terminus with the GFP reporter (*dCOA8-GFP*) in S2R+ cells in order to define the subcellular localization of dCOA8. Colocalization of MitoTracker staining and the GFP signal clearly indicated dCOA8 targeting to mitochondria (**Figure 1B**).

dCOA8 Deficiency Phenocopies Some Human Clinical and Biochemical Features in Flies

dCOA8 is mainly expressed in the adult brain and thoracic-abdominal ganglion, according to FlyAtlas (Leader et al., 2018). dCOA8 is likely to play an important role in the central nervous system (CNS), in line with the severe neurological manifestations described in the COA8-related disease. To corroborate this, *dCOA8* expression was modulated in a spatial and temporal way by exploiting the UAS-Gal4 system. *dCOA8* was either ubiquitously downregulated, through the act5C-Gal4 driver, or specifically downregulated in the nervous system using the elav-Gal4 driver. *dCOA8* mRNA levels dropped around 60–90% of the control levels in the ubiquitous (whole body) and pan-neuronal (brain) KD flies, respectively (**Supplementary Figure S1A**). Despite highly efficient silencing, *dCOA8* KD individuals reached the adult stage and showed similar lifespan to the controls (**Supplementary Figure S1B**). However, kinetic analysis of mitochondrial respiratory chain (MRC) complexes revealed a specific and marked reduction in COX activity in ubiquitous KD flies (**Figure 1C**). To further explore the COX deficiency and, more generally, MRC complexes activity/amount, isolated mitochondria were subjected to one dimension (1D) blue native gel electrophoresis (1D-BNGE) and the natively separated samples were analyzed by in gel activity (IGA) for complex I, complex II, and complex IV. While the activity of complexes I, II, III, and V were unaffected, the activity of complex IV was clearly reduced in mitochondria from KD flies (**Figure 1D**). Additionally, the COX-specific IGA reactivity was significantly lower in the dCOA8 KD samples, in the monomeric (IV_1), dimeric (IV_2), and super-assembled species (III_2 + IV and upper bands). Contrariwise, CI and CII activities were comparable to those of parental control mitochondria (**Figure 1E**).

In order to investigate possible phenotypic consequences of dCOA8 deficiency, we tested the amount of spontaneous locomotor activity and performed a climbing assay, since impairment of these tests would suggest neurological impairment possibly due to neurodegeneration. Both ubiquitous and pan-neuronal *dCOA8* KD flies showed behavioral alterations, with a significant decrease in both total locomotor activity (**Figure 1F**) and climbing ability (**Figure 1G**). We also analyzed mitochondrial morphology in thoracic muscles (from ubiquitous KD flies) and brains (from pan-neuronal KD flies) by transmission electron microscopy (TEM), but found no mitochondrial morphological alterations in either tissue (**Supplementary Figure S1C**).

dCOA8 Does Not Have a Direct Role in the Apoptotic Process

The possible involvement of dCOA8 in apoptosis was tested using a combination of an Annexin V Apoptosis Detection assay (detecting early apoptotic cells) and a propidium iodide staining (to quantify necrotic cells). Labeled cells were analyzed

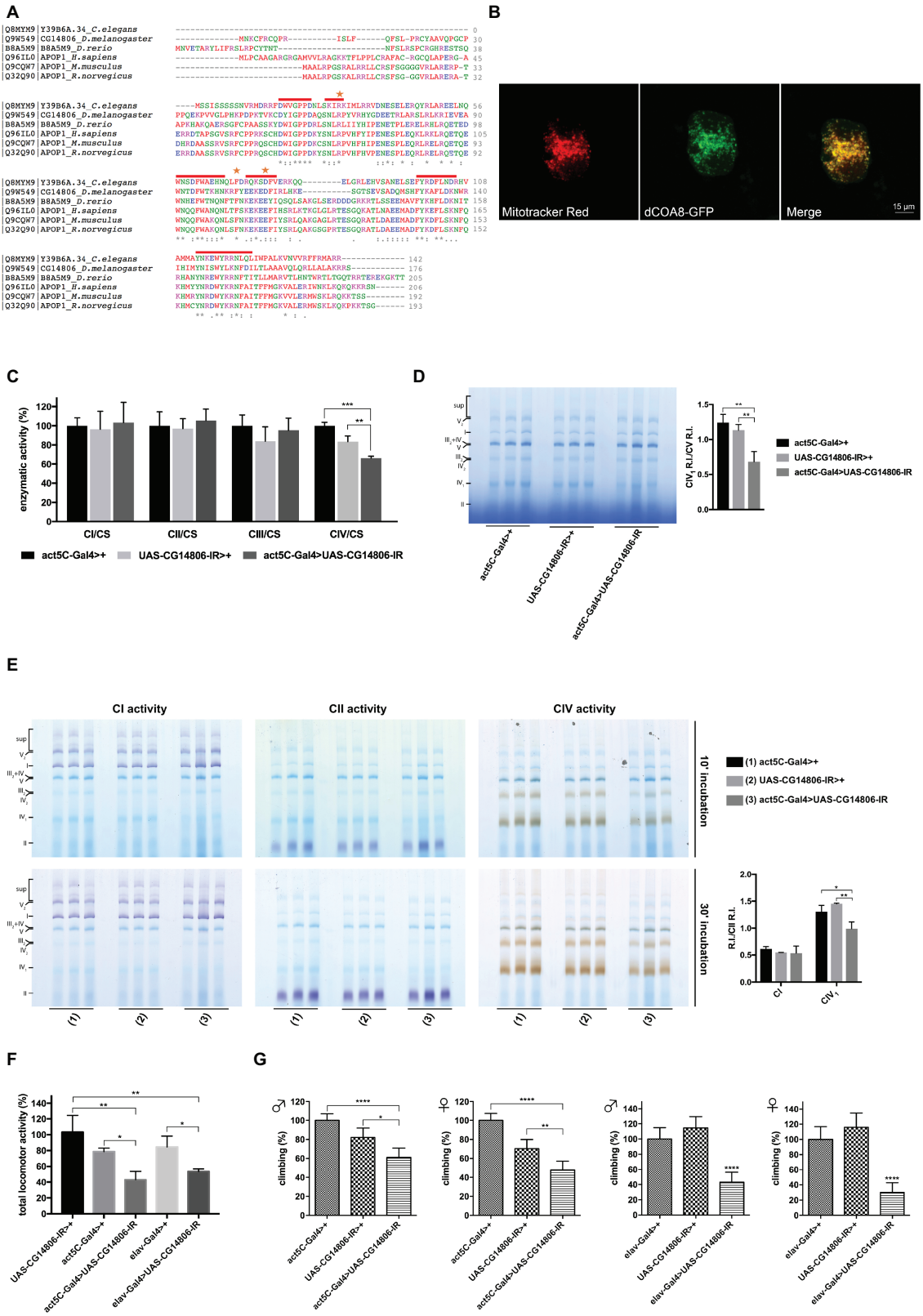

FIGURE 1 | Identification and characterization of the *D. melanogaster* ortholog of *H. sapiens* COA8 (APOPT1). **(A)** Amino acid sequence alignment of *C. elegans*, *D. melanogaster*, *D. rerio*, *H. sapiens*, *M. musculus*, and *R. norvegicus* COA8 orthologs. The shown alignment was performed using the Multiple Sequence Alignment

(Continued)

FIGURE 1 | Tool Clustal Omega and it highlights identical residues (*) and similar ones (. and:), conserved patterns and motifs (red lines) and the point mutations found in patients (orange stars). **(B)** Subcellular localization of dCOA8. *Drosophila* cells were transiently transfected with dCOA8-GFP (green), incubated with MitoTracker dye (red), and analyzed by confocal microscopy. Overlay of images (yellow) confirmed the mitochondrial localization of dCOA8. **(C)** Enzymatic activities of MRC complexes (I–IV) were measured in parental controls (act5C-Gal4>+ and UAS-CG14806-IR>+) and in ubiquitous KD flies (act5C-Gal4>UAS-CG14806-IR, dark gray column). Activities of complexes I–IV were normalized to the activity of citrate synthase (CS). For each genotype, three biological replicates of mitochondrial preparations (100 flies for each biological replicate) were analyzed. For each, enzymatic activities from at least 3 replicate reactions were performed. Data plotted are mean ± S.D. (one-way ANOVA with Sidak's multiple comparisons test $^{*}p \leq 0.05$, $^{**}p \leq 0.01$, $^{***}p \leq 0.001$). **(D)** 1D-BNGE analysis of MRC complexes and quantification of the relative intensity (RI) of CIV_1 bands normalized to the R.I. of CV band of the same sample (one-way ANOVA with Sidak's multiple comparisons test $^{**}p \leq 0.01$). Isolated mitochondria from flies of the indicated genotypes were solubilized and ran in native conditions. **(E)** In gel activity of complex I, complex II, and complex IV after short (10 min) and long (30 min) incubation times and quantification of the relative intensity (RI) of CI and CIV_1 bands normalized to the R.I. of CII band of the same sample after 10 min of reaction (one-way ANOVA with Sidak's multiple comparisons test $^{*}p \leq 0.05$, $^{**}p \leq 0.01$). Genotypes are [(1) act5C-Gal4>+, (2) UAS-CG14806-IR, (3) act5C-Gal4>UAS-CG14806-IR]. **(F)** Spontaneous locomotor activity was measured in ubiquitous (act5C-Gal4>UAS-CG14806-IR) and pan-neuronal (elav-Gal4 > UAS-CG14806-IR) *dCOA8* KD flies with respect to parental controls (UAS-CG14806-IR > +, act5C-Gal4>+, and elav-Gal4>+) for 2 days (48 h). Data plotted are mean ± S.D. (one-way ANOVA with Sidak's multiple comparisons test $^{*}p \leq 0.05$, $^{**}p \leq 0.01$). **(G)** The climbing assay was performed in ubiquitous (act5C-Gal4 > UAS-CG14806-IR) and pan-neuronal (elav-Gal4 > UAS-CG14806-IR) *dCOA8* KD flies with respect to parental controls (UAS-CG14806-IR>+, act5C-Gal4>+, and elav-Gal4>+). Charts show mean and 95% CI, $n = 60$ animals. Statistical analysis used one-way ANOVA with Dunn's multiple comparisons test ($^{*}p \leq 0.05$, $^{**}p \leq 0.01$, $^{***}p \leq 0.001$, $^{****}p \leq 0.0001$).

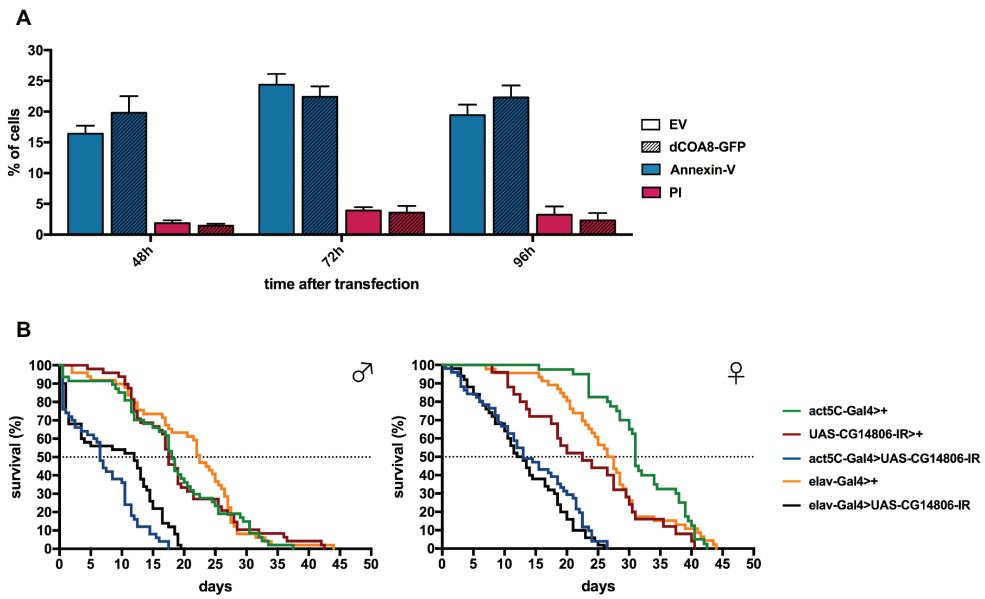

FIGURE 2 | Functional characterization of *dCOA8*. **(A)** Cell death analysis. dCOA8-GFP over-expressing and control S2R+ cells (transfected with an empty vector expressing a cytosolic GFP) were double-stained with Annexin V and propidium iodide (PI). Percentage of early apoptotic (blue bars) and necrotic (red bars) cells was measured 48, 72, and 96 h post-transfection. Data plotted are mean ± S.D. ($n = 3$ biological replicates, two-way ANOVA with Sidak's multiple comparisons test not significant). **(B)** Representative lifespan curves (Kaplan-Meier) of ubiquitous (act5C-Gal4 > UAS-CG14806-IR) and pan-neuronal (elav-Gal4 > UAS-CG14806-IR) *dCOA8* KD flies with respect to parental controls (UAS-CG14806-IR>+, act5C-Gal4>+, and elav-Gal4>+) under oxidative stress at 23°C. Flies were treated with 20 mM Paraquat in standard food. Statistical analysis was performed with log-rank (Mantel-Cox). All the comparisons between the two KD lines with respect to parental controls are statistically significant ($^{****}p \leq 0.0001$).

by cytofluorimetry in *dCOA8*-GFP over-expressing S2R+ cells at very high levels (**Supplementary Figure S1D**). No difference in the amount of apoptotic or necrotic cells was observed between dCOA8-GFP over-expressing and control cells transfected with an empty vector, carrying a cytosolic GFP (**Figure 2A**). Therefore, also in *D. melanogaster*, involvement of COA8 in apoptosis failed to be demonstrated.

dCOA8 Protects Flies From Oxidative Stress

Previous work on human cellular models showed that COA8 is rapidly degraded by the ubiquitin-proteasome system (UPS) but it is strongly stabilized after treatment with oxidants (Melchionda et al., 2014; Signes et al., 2019). Moreover, COX was especially sensitive to oxidative stress in the absence of COA8, suggesting a specific predominant role of dCOA8 to protect nascent COX under oxidative stress conditions (Signes et al., 2019).

To test the direct involvement of dCOA8 in the reactive oxygen species (ROS) response, *dCOA8* KD flies were treated with Paraquat (20 mM), which catalyzes the formation of superoxide (Farrington et al., 1973). Both ubiquitous and pan-neuronal KD flies showed significant reduction of their lifespan after Paraquat treatment, with median survival rates between 36 and 68% of the parental controls for males, and between 41 and 57% for females (**Figure 2B**). These data indicate that dCOA8 has a protective role against oxidative stress response *in vivo*, confirming in a living whole organism

that this protein is functionally related to ROS response, as previously reported in mammalian cells (Melchionda et al., 2014; Signes et al., 2019).

In conclusion, we generated and characterized *D. melanogaster* models of the human mitochondrial disorder caused by pathogenic mutations in *COA8*. This study shows that *D. melanogaster* is a suitable, user-friendly model to shed light on the molecular and physiological roles of COA8. Further investigation is needed to understand its mechanistic and homeostatic role in COX biogenesis. Ubiquitous and pan-neuronal *dCOA8* knockdown flies showed behavioral and biochemical alterations resembling the clinical features of patients and KO mice, thus demonstrating a phylogenetically essential role in MRC function of higher eukaryotes. *dCOA8* deficiency induces MRC dysfunction with marked reduction in the activity of COX. The link between the over-expression of dCOA8 and the apoptotic process originally proposed in human and mouse models (Yasuda et al., 2006; Sun et al., 2008) was also not confirmed in flies. Interestingly, reduced ability to cope with oxidative challenges was observed in *dCOA8* KD flies, demonstrating for the first time a relevant role of dCOA8 in response to oxidative stress *in vivo*. Thus, our data support the idea that COA8 plays an essential role in protecting nascent COX from oxidative damage particularly during the metallation of the COX catalytic sites. Future work is warranted to clarify this possible function of COA8 in higher eukaryotes.

DATA AVAILABILITY

The datasets generated for this study can be found in the FlyBase (CG14806).

AUTHOR CONTRIBUTIONS

CP and RC conceived and designed the research. MB and SC performed the experiments. MB, SC, and CT analyzed the data. MB, SC, CT, RC, MZ, EF-V, and CP interpreted the results of experiments. MB and CP wrote the manuscript. EF-V, RC, and MZ revised the manuscript.

FUNDING

MB was supported by a doctoral fellowship from the University of Padova (Italy) and a fellowship from "Aldo Gini" Foundation (Padova, Italy). SC was supported by a post-doctoral fellowship no. BIRD182052 from the University of Padova (Italy). CP was supported by the grant "PRAT 2014-University of Padova, no. CPDA142980." MZ was supported by Core Grant from the MRC (Grant MC_UU_00015/5), ERC Advanced Grant FP7-322424, and NRJ-Institut de France. RC was supported by the Telethon Project N. GGP11011 ("MitMed: a Multicenter Consortium for the Identification and Characterization of Nuclear Genes Responsible for Human Mitochondrial Disorders").

ACKNOWLEDGMENTS

The authors would like to acknowledge that stocks obtained from the Vienna Drosophila Resource Center (VDRC) and the Bloomington Stock Center were used in this study.

SUPPLEMENTARY MATERIAL

The Supplementary Material for this article can be found online at: https://www.frontiersin.org/articles/10.3389/fphys.2019.01143/full#supplementary-material

SUPPLEMENTARY FIGURE S1 | (A) *dCOA8* mRNA levels, expressed as relative quantity of template in the sample (RQ), in ubiquitous (act5C-Gal4>UAS-CG14806-IR) and pan-neuronal (elav-Gal4>UAS-CG14806-IR) knockdown flies with respect to parental controls (UAS-CG14806-IR>+, act5C-Gal4>+, and elav-Gal4>+). Data plotted are mean ± S.D. ($n = 3$, Student's t test $^{*}p \leq 0.05$, $^{**}p \leq 0.01$, $^{***}p \leq 0.001$, $^{****}p \leq 0.0001$). **(B)** Lifespan of ubiquitous male (left) and female (right) KD flies in standard food at 23°C. Statistical significance was assessed with log-rank (Mantel-Cox) and Gehan-Breslow-Wilcoxon tests (non-significant). **(C)** Electron microscopy analysis on thoracic muscle (upper panels) and brain (lower panels) sections. Characterization was carried out on ubiquitous (act5C-Gal4 > UAS-CG14806-IR) *dCOA8* KD flies and parental controls (UAS-CG14806-IR>+ and act5C-Gal4>+). Cross-sectional ultrastructure of thoracic muscles and brains, illustrating the distribution and morphology of mitochondria, are represented. **(D)** *dCOA8* mRNA levels, expressed as relative quantity of template in the sample (RQ), in *dCOA8* over-expressing S2R+ (dCOA8-GFP) and control cells (transfected with the empty vector, EV) 24 and 48 h post-transfection. Data plotted are mean ± S.D. ($n = 3$, Student's t test $^{*}p \leq 0.05$, $^{***}p \leq 0.001$).

REFERENCES

Benzer, S. (1967). Behavioral mutants of *Drosophila* isolated by countercurrent distribution. *Proc. Natl. Acad. Sci. USA* 58, 1112–1119. doi: 10.1073/pnas.58.3.1112

Broughton, S. J., Piper, M. D., Ikeya, T., Bass, T. M., Jacobson, J., Driege, Y., et al. (2005). Longer lifespan, altered metabolism, and stress resistance in *Drosophila* from ablation of cells making insulin-like ligands. *Proc. Natl. Acad. Sci. USA* 102, 3105–3110. doi: 10.1073/pnas.0405775102

Carrol, C. J., Brilhante, V., and Suomalainen, A. (2014). Next-generation sequencing for mitochondrial disorders. *Br. J. Pharmacol.* 171, 1837–1853. doi: 10.1111/bph.12469

Claros, M. G., and Vincens, P. (1996). Computational method to predict mitochondrially imported proteins and their targeting sequences. *Eur. J. Biochem.* 241, 779–786. doi: 10.1111/j.1432-1033.1996.00779.x

Cusumano, P., Biscontin, A., Sandrelli, F., Mazzotta, G. M., Tregnago, C., De Pittà, C., et al. (2018). Modulation of miR-210 alters phasing of circadian locomotor activity and impairs projections of PDF clock neurons in *Drosophila melanogaster*. *PLoS Genet.* 14:e1007500. doi: 10.1371/journal.pgen.1007500

Da-Rè, C., Franzolin, E., Biscontin, A., Piazzesi, A., Pacchioni, B., Gagliani, M. C., et al. (2014a). Functional characterization of *drim2*, the *Drosophila melanogaster* homolog of the yeast mitochondrial deoxynucleotide transporter. *J. Biol. Chem.* 289, 7448–7459. doi: 10.1074/jbc.M113.543926

Da-Rè, C., von Stockum, S., Biscontin, A., Millino, C., Cisotto, P., Zordan, M. A., et al. (2014b). Leigh syndrome in *Drosophila melanogaster*: morphological and biochemical characterization of Surf1 post-transcriptional silencing. *J. Biol. Chem.* 289, 29235–29246. doi: 10.1074/jbc.M114.602938

Emanuelsson, O., Nielsen, H., Brunak, S., and von Heijne, G. (2000). Predicting subcellular localization of proteins based on their N-terminal amino acid sequence. *Mol. Biol.* 300, 1005–1016. doi: 10.1006/jmbi.2000.3903

Farrington, J. A., Ebert, M., Land, E. J., and Fletcher, K. (1973). Bipyridylium quaternary salts and related compounds. V. Pulse radiolysis studies of the reaction of paraquat radical with oxygen. Implications for the mode of

action of bipyridyl herbicides. *Biochim. Biophys. Acta* 314, 372–381. doi: 10.1016/0005-2728(73)90121-7

Hofmann, K., and Stoffel, W. (1993). TMbase – a database of membrane spanning proteins segments. *Biol. Chem. Hoppe-Seyler* 374, 166.

Käll, L., Krogh, A., and Sonnhammer, E. L. (2004). A combined transmembrane topology and signal peptide prediction method. *J. Mol. Biol.* 338, 1027–1036. doi: 10.1016/j.jmb.2004.03.016

Kirby, D. M., Thorburn, D. R., Turnbull, D. M., and Taylor, R. W. (2007). Biochemical assays of respiratory chain complex activity. *Methods Cell Biol.* 80, 93–119. doi: 10.1016/S0091-679X(06)80004-X

Leader, D. P., Krause, S. A., Pandit, A., Davies, S. A., and Dow, J. A. T. (2018). FlyAtlas 2: a new version of the *Drosophila melanogaster* expression atlas with RNA-Seq, miRNA-Seq and sex-specific data. *Nucleic Acids Res.* 46, D809–D815. doi: 10.1093/nar/gkx976

Legati, A., Reyes, A., Nasca, A., Invenrizzi, F., Lamamntea, E., Tiranti, V., et al. (2016). New genes and pathomechanisms in mitochondrial disorders unraveled by NGS technologies. *Biochim. Biophys. Acta* 1857, 1326–1335. doi: 10.1016/j.bbabio.2016.02.022

Livak, K. J., and Schmittgen, T. D. (2001). Analysis of relative gene expression data using real-time quantitative PCR and the 2(ddCT) method. *Methods* 25, 402–408. doi: 10.1006/meth.2001.1262

Melchionda, L., Haack, T. B., Hardy, S., Hardy, T. E., Fernandez-Vizarra, E., Lamantea, E., et al. (2014). Mutations in APOPT1, encoding a mitochondrial protein, cause cavitating leukoencephalopathy with cytochrome c oxidase deficiency. *Am. J. Hum. Genet.* 95, 315–325. doi: 10.1016/j.ajhg.2014.08.003

Schneider, I. (1972). Cell lines derived from late embryonic stages of *Drosophila melanogaster*. *J. Embryol. Exp. Morphol.* 27, 353–365.

Sharma, S., Singh, P., Fernandez-Vizarra, E., Zeviani, M., Van der Knaap, M. S., and Saran, R. K. (2018). Cavitating leukoencephalopathy with posterior predominance caused by a deletion in the APOPT1 gene in an Indian boy. *J. Child Neurol.* 33, 428–431. doi: 10.1177/0883073818760875

Sievers, F., Wilm, A., Dineen, D. G., Gibson, T. J., Karplus, K., Li, W., et al. (2011). Fast, scalable generation of high-quality protein multiple sequence alignments using Clustal Omega. *Mol. Syst. Biol.* 7:539. doi: 10.1038/msb.2011.75

Signes, A., Cerutti, R., Dickson, A. S., Benincá, C., Hinchy, E. C., Ghezzi, D., et al. (2019). APOPT1/COA8 assists COX assembly and is oppositely regulated by UPS and ROS. *EMBO Mol. Med.* 11:e9582. doi: 10.15252/emmm.201809582

Spinelli, J. B., and Haigis, M. C. (2018). The multifaceted contributions of mitochondria to cellular metabolism. *Nat. Cell Biol.* 20, 745–754. doi: 10.1038/s41556-018-0124-1

Sun, X., Yasuda, O., Takemura, Y., Kawamoto, H., Higuchi, M., Baba, Y., et al. (2008). Akt activation prevents Apop-1-induced death of cells. *Biochem. Biophys. Res. Commun.* 377, 1097–1101. doi: 10.1016/j.bbrc.2008.10.109

Yasuda, O., Fukuo, K., Sun, X., Nishitani, M., Yotsui, T., Higuchi, M., et al. (2006). Apop-1, a novel protein inducing cyclophilin D-dependent but Bax/Bak-related channel-independent apoptosis. *J. Biol. Chem.* 281, 23899–23907. doi: 10.1074/jbc.M512610200

Conflict of Interest Statement: The authors declare that the research was conducted in the absence of any commercial or financial relationships that could be construed as a potential conflict of interest.

frontiers in Physiology

REVIEW
published: 11 September 2019
doi: 10.3389/fphys.2019.01167

Sleep in *Drosophila* and Its Context

Esteban J. Beckwith and Alice S. French*

Department of Life Sciences, Imperial College London, London, United Kingdom

A prominent idea emerging from the study of sleep is that this key behavioural state is regulated in a complex fashion by ecologically and physiologically relevant environmental factors. This concept implies that sleep, as a behaviour, is plastic and can be regulated by external agents and changes in internal state. *Drosophila melanogaster* constitutes a resourceful model system to study behaviour. In the year 2000, the utility of the fly to study sleep was realised, and has since extensively contributed to this exciting field. At the centre of this review, we will discuss studies showing that temperature, food availability/quality, and interactions with conspecifics can regulate sleep. Indeed the relationship can be reciprocal and sleep perturbation can also affect feeding and social interaction. In particular, different environmental temperatures as well as gradual changes in temperature regulate when, and how much flies sleep. Moreover, the satiation/starvation status of an individual dictates the balance between sleep and foraging. Nutritional composition of diet also has a direct impact on sleep amount and its fragmentation. Likewise, aggression between males, courtship, sexual arousal, mating, and interactions within large groups of animals has an acute and long-lasting effect on sleep amount and quality. Importantly, the genes and neuronal circuits that relay information about the external environment and internal state to sleep centres are starting to be elucidated in the fly and are the focus of this review. In conclusion, sleep, as with most behaviours, needs the full commitment of the individual, preventing participation in other vital activities. A vast array of behaviours that are modulated by external and internal factors compete with the need to sleep and thus have a significant role in regulating it.

Keywords: sleep, *Drosophila*, temperature, feeding, starvation, courtship, aggression, social interaction

OPEN ACCESS

Edited by:
Paola Cusumano,
University of Padova, Italy

Reviewed by:
Guy Bloch,
The Hebrew University of Jerusalem, Israel
Christian Wegener,
Julius Maximilian University of Würzburg, Germany

****Correspondence:***
Esteban J. Beckwith
e.beckwith@imperial.ac.uk

Specialty section:
This article was submitted to Invertebrate Physiology, a section of the journal Frontiers in Physiology

Received: *29 April 2019*
Accepted: *29 August 2019*
Published: *11 September 2019*

Citation:
Beckwith EJ and French AS (2019) Sleep in Drosophila and Its Context. Front. Physiol. 10:1167. doi: 10.3389/fphys.2019.01167

INTRODUCTION

Sleep is a behavioural state characterised by quiescence associated with a species-specific posture. This quiescence is quickly reversible to wakefulness, is accompanied by an increased arousal threshold compared to rest, and is homeostatically regulated, i.e., if removed it is compensated for. Historically, sleep has been an area of great interest and because of this, research on the subject is far reaching. Studies on many different species have contributed to this exciting field and, as a result, we are beginning to understand its function. This subject has been recently reviewed by Anafi et al. (2019). From ancient philosophy to modern technologies, no effort has been spared to study this enigmatic behaviour in numerous organisms both in the laboratory and in the wild (Rattenborg et al., 2017). The vast body of knowledge regarding sleep regulation has found a synthesis in the two-process model established by Borbély (1982). This simple and powerful paradigm describes that

two processes, the circadian clock (process C) and the sleep homeostat (process S), work together to regulate sleep along the day. The former informs the oscillation of sleep pressure along the day while the latter conveys the need for sleep based upon duration and quality of previous wakefulness. If sleep is disrupted, the S process gains weight and is able to overcome the C process, pushing sleep into a period of the day that is normally associated with wakefulness. This compensatory sleep is a hallmark of the homeostat and is often referred to as "rebound sleep." Although the Borbély (1982) model is still a standard in the field and an instrumental framework to study sleep, accumulating evidence that we review here suggests that sleep regulation goes beyond these two central processes.

Sleep is critical for fitness. In mammals, it is necessary to sustain physical and cognitive performance (Krause et al., 2017), and it actively supports the acquisition of long-term representations and synaptic homeostasis (Tononi and Cirelli, 2014; Feld and Born, 2017). It is also critical for development (Kayser and Biron, 2016) and immune function (Besedovsky et al., 2019). In insects, sleep also has an impact on fitness affecting reproductive output (Potdar et al., 2018), susceptibility to acute oxidative stress (Hill et al., 2018), and development (Kayser and Biron, 2016), and is important for learning and memory recall (Beyaert et al., 2012) and synaptic homeostasis (Gilestro et al., 2009; Bushey et al., 2011).

While there are clear fitness benefits inherent with sleep, at the same time, it can be a costly behavioural state. Being essentially offline means that animals are unable to engage in other essential activities, such as foraging or mating. This is evident in the strategies employed by different species in their attempts to balance their need for sleep and remain safe (Rattenborg et al., 1999; Voirin et al., 2014; Tisdale et al., 2018), fed (Willie et al., 2001; Keene et al., 2010), or reproductively successful (Lesku et al., 2012; Potdar et al., 2018).

After key contributions to related fields such as courtship, aggression, circadian biology, and feeding, the value of *Drosophila melanogaster* as a model organism to study sleep was realised, and in the year 2000, the humble fruit fly made its debut in the sleep field (Hendricks et al., 2000; Shaw et al., 2000). Sleep is defined in *Drosophila* from a behavioural perspective: prolonged periods of immobility are used as a proxy for sleep. In particular, under the current shared operational definition, sleep is a period of immobility longer than 5 min, after which the flies exhibit a characteristic increase in arousal threshold. The definition of a sleep state in the fruit fly was first described through the use of video-recording or ultra-sound methods (Hendricks et al., 2000; Shaw et al., 2000). Later, the favoured tool for sleep analysis in *Drosophila* became the Drosophila Activity Monitor (DAM). This tool is still the most commonly used in the *Drosophila* sleep field. Activity is measured by counting each time a fly crosses the middle of the tube in which it is confined. Thus, sleep is scored when a period of 5 min or more occurs without a midline cross. Fruit flies, under laboratory conditions, show a characteristic rest-activity pattern where they are most active in anticipation of light to dark and dark to light transitions (**Figure 1**, left panel). Therefore, sleep occurs primarily during the middle of the day or night.

As described, sleep in *Drosophila* and other insects is largely measured through behavioural metrics, notably immobility. This is in contrast to the strategy employed to measure sleep in larger animals such as mice: Electroencephalography (EEG) is often used to determine when an animal transitions into a sleep state. Indeed, there is some ambiguity in using immobility as a definition of sleep in flies, yet the genetic tractability, fast life cycle, and low cost inherent in *Drosophila* research make it an important tool to understand many aspects of this behaviour and should be considered complementary to studies in other organisms. Early findings have demonstrated that *Drosophila* shares sleep characteristics comparable to many other species not limited to: clock control, homeostatic response to sleep deprivation, increase arousal threshold during sleep, species-specific sleep posture, and response to hypnotic/stimulant drugs (Hendricks et al., 2000; Shaw et al., 2000). These similarities together with plethora of genetic tools make it an appropriate model to study sleep (Helfrich-Forster, 2018).

Here, we review recent studies contributing to the idea that external conditions like temperature, social interaction, and food quality and availability, as well as resulting changes in internal state, such as levels of sexual arousal, aggression, hunger, or mating status, regulate sleep in adult *Drosophila* flies.

TEMPERATURE IS A REGULATOR OF SLEEP

Pre-sleep behaviours of many species include nesting, huddling, and curling and is epitomised by the bedding behaviour in humans. Beyond the comfort associated with the initiation of sleep, these behaviours ensure body warming. In particular, skin warming is a sleep trigger in both humans and mice and is considered a sleep-permissive condition (Morairty et al., 1993; Raymann et al., 2008). This environmental factor induces sleep, via the median preoptic/medial preoptic hypothalamus (Harding et al., 2018; Komagata et al., 2019).

Being ectothermic, insects have a limited ability to thermo-regulate, thus, the interaction between sleep and temperature is fundamentally different to the one in mammals. However, insect development, metabolism, fecundity, as well as other physiological functions that determine fitness are, to a large extent, dictated by environmental temperature. There are two main categories of temperature sensation: the detection of an innocuous stimulus and the detection of painful temperatures (i.e., nociception). The perception of environmental temperature by adult flies relies on a family of temperature-regulated Transient Receptor Potential (TRP) channels tuned to different temperatures and are expressed in different cell types (Dillon et al., 2009). In particular, the dTRPA1 channel is critical for the detection of innocuous temperatures and instructs the distribution of wild-type flies along a thermal gradient ranging from 20 to 29°C (Hamada et al., 2008).

Temperature, as well as light, is a strong zeitgeber both in humans (Roenneberg and Merrow, 2007) and flies (Yoshii et al., 2016). As a result, fluctuations along the day constitute entrainment cues for the circadian organisation of rest-activity

cycles in *Drosophila* (Maguire and Sehgal, 2015). Moreover, changes in temperature, either permanent or sudden, modulate sleep greatly. In particular, there are three contexts in which the effects of temperature over sleep have been studied: (1) the daily oscillations, (2) the seasonal variations between high and low temperatures, and (3) the abrupt variations that take place within a day.

In a seminal work, and before the documentation of a sleep state in flies, Majercak et al. (1999) described the distribution of locomotor activity, along a day, at different temperatures. Relative to 25°C,[1] at high temperatures (29°C) flies increase their morning activity and delay their evening activity, thus becoming more active during the night. Meanwhile, at lower and stable temperatures (18°C), flies concentrate their activity during the light phase. Considering lack of activity as an index of sleep, we may take these results as the first description of sleep regulation under different, but steady, temperatures. Later works specifically measuring sleep have corroborated this schematic description: high temperature results in both an increased daytime sleep and a reduced nighttime sleep (Low et al., 2008; Ishimoto et al., 2012; Parisky et al., 2016).

Recently, complementary studies have focused on the acute response to temperature shifts (Parisky et al., 2016; Lamaze et al., 2017). In particular, changing ambient temperature from 22 to 29°C results in a reduction of sleep during the day and night. Temperatures higher that 29°C produce a clear increase in sleep latency at the beginning of the day. Lamaze et al. (2017) coined the term prolonged morning wakefulness (PMW) to describe this phenotype. Importantly, these observations support the original description. A parsimonious and encompassing interpretation would be that increases in temperature below 29°C result in increased sleep during the day and reduce sleep during the night. Higher temperatures, >29°C, result in an overall reduction in sleep, particularly at the beginning of the day, delaying it until the afternoon and the night. Considering that, given the choice, wild-type flies distribute at temperatures between 20 and 29°C (Hamada et al., 2008), a plausible explanation is that temperatures exceeding 29°C, in conjunction with the confined space associated with these types of behavioural experiments, may be triggering an escape response, manifested by a sustained reduction in sleep.

As a result of the described works, the field now has a detailed descriptive understanding of how sleep timing and amount in *Drosophila* is regulated by environmental change (**Figure 1**, left panel). This has opened the possibility to acquire a deeper mechanistic insight in the fascinating relationship between environmental factors and sleep.

Beyond variance in the extent of behavioural responses upon temperature change and some methodological differences, studies agree upon the idea that temperature dependent changes in sleep and activity during the light phase of the day are clock dependent. *period* (*per*) and *timeless* null mutants, i.e., flies with an impaired circadian clock, have an impaired behavioural response: these flies do not show an increase in daytime sleep after a temperature increase (Parisky et al., 2016). In addition, the posterior dorsal neurons 1 ($DN1_p$s) cluster, which is part of the circadian network, is critical for temperature dependent sleep regulation (Guo et al., 2016). On the contrary, sleep changes during the night seem to be less dependent on a circadian regulation (Parisky et al., 2016).

One main caveat is that most studies investigating temperature dependent changes in sleep do not consider the natural correlation between light intensity/quality and temperature. On an average day, minimum temperature typically occurs just before sunrise. Subsequently, temperature rises reaching a peak sometime after solar noon, after which the temperature starts to drop. In addition, most experimental protocols change temperature very quickly at the onset of day, while in a natural environment this change does not occur so drastically. Thus, a heat shock together with the immediate initiation of the light phase is an artificial phenomenon that is unlikely to have driven the evolution of brain circuits controlling sleep. Notably, this concern is starting to be addressed: detailed studies have

[1] Most behavioural experiments to measure sleep or activity rhythms are conducted at 25°C.

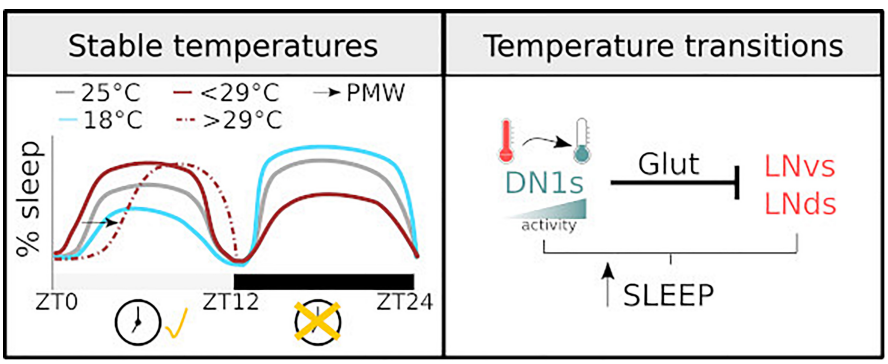

FIGURE 1 | Diagram illustrating how temperature regulates sleep. **(Left)** The sleep profile of male flies under stable temperatures. The dashed line shows PMW observed with temperature >29°C. The changes observed at different temperatures are clock-dependent during the light phase and clock-independent during the dark phase. **(Right)** the mechanisms of sleep regulation in response to temperature change. The activity of DN1 neurons increases with temperature drops, resulting in an inhibition over the lateral neurons of the circadian clock and sleep promotion.

developed a more naturalistic approach to describe behaviour and the neuronal circuits controlling sleep in response to thermal changes (Currie et al., 2009; Yadlapalli et al., 2018). It is well documented that light and temperature are the strongest entrainment cues for the fly circadian clock. Employing a sophisticated paradigm Currie et al. (2009) showed that a 4°C oscillation is sufficient for effective entrainment. Moreover, they proved that the coupling between the external zeitgebers and the internal molecular clock allows the system to ignore thermal fluctuations that can be anecdotal signals,[2] ensuring an appropriate entrainment (Currie et al., 2009). Furthermore, in a series of elegant experiments in which temperature and light were carefully administrated, Yadlapalli et al. (2018) demonstrated that $DN1_p$s neurons are constantly monitoring temperature. This cluster responds to temperature drops with an increase in activity, inducing sleep. Interestingly, using GFP reconstitution across synaptic partners (GRASP) the same group showed that $DN1_p$s contact two distinct clusters of the clock network, the small and ventral Lateral Neurons (sLNvs) and the dorsal Lateral Neurons (LNds). Upon activation, $DN1_p$s inhibits, via a glutamatergic signal, the activity of these key clusters (Guo et al., 2016). The inhibition of the $DN1_p$s by temperature increases and its impact on the sLNvs and/or the array of neurons that are downstream of this key cluster may explain, at least in part, the previously described PMW phenotype (Lamaze et al., 2017). See **Figure 1** for graphical summary.

Finally, the regulation of the midday siesta by temperature and the adaptation to seasonally cold days are one of the best-studied examples of sleep regulation beyond the two-process model paradigm. At the molecular level, this regulation relies on thermo-sensitive alternative splicing in the clock gene *per*. In particular, the more frequent excision of the eighth intron (*dmpi8*) inhibits sleep on cold days because it generates a more stable version of *per* mRNA and protein that results in an earlier evening activity peak (Majercak et al., 2004; Chen et al., 2007). This event involves the serine/arginine (SR)-rich protein B52/SRp55, and the downregulation of this splicing factor in clock neurons reduces the efficiency of *dmpi8* excision. In addition, splicing efficiency of *dmpi8* affects transcript levels of the recently described gene *daywake* (*dyw*) (Yang and Edery, 2019). Cool temperature dependent splicing increases dyw mRNA which results in midday siesta suppression. This provides us with an elegant example of how sleep remains plastic in response to environmental changes (Zhang et al., 2018).

As a conclusion, sleep is highly affected by temperature, and thermoregulatory behaviours are in place from humans to flies. A comprehensive description of the behavioural adaptation of flies to different stable temperatures as well as the responses to gradual changes is now available. A more naturalistic approach to the interaction between light, temperature, and behaviour, together with the capabilities of *Drosophila* as a model system, will be key to elucidating the molecular and cellular basis of how environmental information is conveyed to sleep centres.

[2]Temperature can change sharply in the spatial dimension when animals move from or to shadow/sunny areas, this signals need to be ignored by the system controlling the rest–activity cycles.

FEEDING AND SLEEP ARE MUTUALLY EXCLUSIVE BEHAVIOURS

Both sleep and feeding serve important functions, therefore allocation of time to each activity needs to be constantly assessed based on the animal's level of tiredness and satiety state. Moreover, animals are particularly sensitive to nutritive changes in their environment and the resulting changes in internal state can influence sleep behaviour. Conversely, sleep deprivation can lead to changes in feeding behaviour (Koban et al., 2008): in humans sleep loss can lead to altered dietary choice, hyperphagia, and weight gain (Greer et al., 2013; Markwald et al., 2013). Understanding how sleep and appetite interact is a particularly relevant area of research and timely with emergence of public health crises such as obesity, which are symptomatic of modern lifestyles also associated with insufficient sleep.

Drosophila melanogaster feeds on fruits and microorganisms, such as yeast, associated with fruit. Beyond being generalist feeders, flies are sensitive to changes in their internal nutrient status. Consequently, this species has been extensively studied and used as a model to understand diet-related behavioural changes and the underlying mechanisms.

The circadian clock controls feeding both in mammals (Panda, 2016) and in flies (Murphy et al., 2016). *Drosophila* tend to increase feeding in the morning and have a minor peak in the evening which coincides with when they are most active (Xu et al., 2008; Murphy et al., 2016). In addition, feeding can promote sleep and hunger can suppress it. It is therefore not surprising, due to the mutual exclusivity of these two behaviours, that animals have neural networks that evaluate their needs and instruct behaviour accordingly. In this section, we will discuss the effect of starvation/satiation, dietary composition, and stimulants on sleep in flies as well as the neural networks and genes involved.

Satiation Promotes Sleep

A period of quiescence following ingestion of a meal is observed in animals spanning many orders. For example, refeeding following starvation induces sleep in rats (Danguir et al., 1979), which appears to be dependent on cholecystokinin signalling (Shemyakin and Kapas, 2001). Likewise, *Caenorhabditis elegans* also shows an induction of quiescence after a high-quality meal, and this is dependent on insulin and TGF-beta (You et al., 2008). *Drosophila* also exhibit increased sleep immediately following a meal, typified by higher arousal thresholds, suggesting that sleep is deeper compared to pre-meal. Post-feeding sleep, also called postprandial sleep, positively correlates with volume ingested, and it is also dependent on dietary composition. Protein, salt, and to a lesser extent sucrose ingestion induce postprandial sleep (Murphy et al., 2016).

Induction of postprandial sleep is partly controlled by a group of Leucokinin receptor (Lkr) neurons, which arborise in the suboesophageal ganglion (SOG), in the lateral horn (LH) and in the fan-shaped body (FSB), areas of the brain known to regulate feeding, process olfactory information, and control sleep, respectively. Silencing of Lkr neurons reduces postprandial sleep specifically following protein feeding. However, Lkr silenced flies

still exhibit postprandial sleep in response to ingestion of bulky, low nutrient food indicating that other pathways exist to induce sleep when volumetric information dictates. Yurgel et al. (2019) showed that disrupting the function of AMP-activated protein kinase (AMPK) in Lk neurons inhibited sleep in fed flies. This phenotype was specifically linked to an increase in activity in Lateral horn Lk (LHLK) neurons (Yurgel et al., 2019), suggesting that these may be downstream of Lkr neurons controlling post-prandial sleep.

Another key player in balancing the need to sleep and feed is a subset of Allatostatin A-positive (AstA) neurons allocated in the postero-lateral protocerebrum (PLP). When thermogenetically activated, these neurons promote sleep, reduce locomotion, and suppress feeding. Whether they are activated upon ingestion of food is not known but AstA neurons play a role in balancing these mutually exclusive behaviours and promote sleep at the expense of feeding (Chen et al., 2016).

Starvation Suppresses Sleep

Starvation or caloric restriction is a consequence of food scarcity, which is a naturally occurring environmental stressor for many organisms. Animals encounter seasonal variations in food availability and competition for food sources, thus employ strategies to cope with and survive food deprivation. One strategy employed by animals is to increase activity, which is usually interpreted as an augmented effort to locate food. Upon short-term food deprivation, *C. elegans* exhibit increased foraging behaviour and heightened sensitivity to food-related chemosensory cues (Skora et al., 2018). Similarly, mice also exhibit more wakefulness and reduced sleep during starvation (Hua et al., 2018).

Not surprisingly, *Drosophila* also exhibit this behaviour. An early study by Connolly (1966) used a technique called "grid square" to manually count border crosses of starved and fed mixed sex groups of *Drosophila* on a perspex grid (Connolly, 1966). Using this method, the author observed that the food-deprived groups exhibited more border crosses than the fed groups and concluded that starvation induces locomotor activity. This is, to our knowledge, the first work describing an activity phenotype induced by starvation in *Drosophila*. Higher resolution and throughput techniques have since been developed allowing the reproduction of this phenotype, and a more detailed description of the behaviour.

We now know that in response to food deprivation fruit flies, as first discovered by Connolly (1966), increase their locomotor activity (both velocity and walked distance) (Lee and Park, 2004; Yang et al., 2015; Yu et al., 2016), suppress sleep (Keene et al., 2010), sensitise their gustatory and olfactory neurons to food-related cues (Root et al., 2011; Inagaki et al., 2014; Ko et al., 2015; Sonn et al., 2018), and more readily accept unpalatable foods (LeDue et al., 2016). Heightened sensory perception likely contributes to the increase in activity by fragmenting sleep and reducing arousal thresholds (Linford et al., 2012). These behavioural and physiological changes probably serve to increase the likelihood of finding and ingesting food in the vicinity but are sometimes considered counter intuitive: inactivity and sleep states are characterised by a lower metabolic rate and would be more consistent with energy conservation and longevity (Isabel et al., 2005; Stahl et al., 2017). Indeed, flies selected for starvation resistance through experimental evolution increase their sleep to conserve their energy stores (Masek et al., 2014). It is worth noting that after 48 h of starvation activity of wild-type flies does decrease (Bell et al., 1985); however, this latter behavioural alteration is likely a precursor to death and it is unlikely to be a reflection of adaptive behaviour.

Keene et al. (2010) described the starvation-induced sleep loss phenotype in detail. In a series of thorough experiments they demonstrated that food deprived flies began to exhibit sleep loss after 12 h regardless of whether starvation was initiated at the start of light period or dark period. During starvation, sleep became more fragmented and arousal thresholds were lower (Hasegawa et al., 2017). Following reintroduction of food, flies initially increased feeding and subsequently increased their sleep (Keene et al., 2010), which appears to be driven by postprandial mechanisms rather than as compensation for accrued sleep debt during starvation (Regalado et al., 2017).

Sleep suppression and food searching in starved conditions is initiated by the absence of food. Food scarcity is perceived in two main ways. Firstly, through the absence of gustatory stimuli and secondly, by internal nutrient sensing. The absence of food is communicated to brain regions that regulate sleep and locomotion via these two routes. We will now discuss the neural networks communicating external and internal nutrient deficit.

Perceived Absence of External Food Sources Suppresses Sleep

Lack of gustatory input is one indication that food is absent. Gustatory receptor neurons (GRNs) are housed in sensilla on the proboscis, tarsi, and wing margins. Different subsets are involved in detecting different foods such as sugars or amino acids and bitter or dangerous plant metabolites. GRNs project to the SOG where they synapse with projection neurons that report to higher brain centres such as the superior medial protocerebrum (SMP) (Talay et al., 2017). Considering that many sleep-related neurons arborise in the SMP (Aso et al., 2014; Donlea et al., 2018), it is likely to be an area where gustatory information is integrated into circuits governing sleep/wake behaviour.

Lack of GRN stimulation, particularly of those involved in the detection of nutritive and appetitive foods, plays a role in suppressing sleep and inducing locomotion during starvation. Two main lines of evidence support this view. First, feeding flies sweet but non-nutritive sugars such as arabinose (Yang et al., 2015), or low concentrations of D-glucose (Linford et al., 2015) which flies cannot survive on, does not trigger hyperactivity or suppress sleep (Hasegawa et al., 2017). However, flies with impaired sugar sensing do exhibit increased locomotion (Yang et al., 2015) and sleep suppression (Hasegawa et al., 2017) when fed arabinose. Second, activation of sweet GRNs using TRPA1 was also sufficient to induce sleep in starved flies (Linford et al., 2015; Hasegawa et al., 2017). Despite not playing a significant role in postprandial sleep induction in replete flies (Murphy et al., 2016), it is well evidenced that under starved conditions, sweet gustatory perception is sufficient to restore total sleep. It should be noted that gustatory receptors are also expressed

in the gut as well as the proboscis, tarsi, and wing margins; thus, these receptors could play a role in internal as well as peripheral nutrient sensing (Park and Kwon, 2011). Hasegawa et al. (2017) showed that activation of cells expressing sweet gustatory receptors GR64a, GR43a, and GR5a using TRPA1 induce sleep under starved conditions. All of these genes are expressed in the proboscis and, with the exception of GR5a, are expressed in the gut. This suggests that peripheral detection is likely to play a more significant role in this phenotype.

Interestingly, repletion, which in theory could be conveyed through stretch reception in the oesophagus or the crop, does not seem to be a cue for restoration of fed behaviour after starvation. Instead, internal nutritive assessment of food ingested appears to shift behaviour from food searching to quiescent. This is evidenced through a finding that flies fed high concentrations (3M)[3] of a tasteless but nutritional sugar called sorbitol exhibit activity levels that are equivalent to flies fed sugars that are both nutritional and sweet tasting (Yang et al., 2015). Further, it seems that flies ingesting nutritious sugars have less fragmented sleep and exhibit higher arousal thresholds compared to those that consume sweet non-nutritive ones (Hasegawa et al., 2017). These data suggest that sleep induction could be driven by taste whereas sleep depth and architecture maybe dependent on internal nutrient sensing.

Perceived Internal Nutrient Deficiency Suppresses Sleep

Recent work has elucidated how neural networks governing starvation-induced phenotypes may detect food scarcity through internal nutrient sensing. Insulin producing cells (IPCs), express *Drosophila* insulin-like peptides (DILPs) which have been implicated in starvation-induced sleep suppression: compared to a fed condition, DILP2 mRNA levels are reduced in the heads of starved flies (Cong et al., 2015). Interestingly, IPCs express Lkrs and receive input from LHLK-positive neurons. Knock-down of Lkr mRNA in IPCs eliminates starvation-induced sleep suppression. It is of particular importance that LHLK cells become active under starvation and their activity is dependent on levels of circulating glucose (Yurgel et al., 2019) as well as upregulation of the gene *translin* which is expressed in these cells (Murakami et al., 2016).

A key downstream target of DILPs is a pair of bilateral neurons in the SOG. In fed conditions, these neurons are inhibited by systemic signalling of DILPs and under starved conditions are activated by adipokinetic hormone (AKH) that results in increased walking (Lee and Park, 2004; Yu et al., 2016) and possibly suppresses sleep (Regalado et al., 2017). Thus, a model emerges, which is summarised in **Figure 2**. Under fed conditions, LHKR neurons are inhibited by circulating glucose. Under starvation, circulating glucose is reduced, and inhibition is released. This, in turn, suppresses the release of DILPS from IPCs perhaps through Lk signalling. Subsequently, DILP-dependent inhibition of circuits that promote hyperactivity (Yu et al., 2016) and may suppress sleep (Regalado et al., 2017) during starvation are alleviated. Interestingly, LHLK may also exert inhibition over Lkr neurons (distinct from IPCs) that have been implicated in the induction of postprandial sleep (Murphy et al., 2016). Murphy et al. (2016) do not address whether LHLK or other Lk-positive neurons (for example, those found in SOG) inhibit these Lkr neurons. However, it is possible that LHLK neurons have two downstream targets: the IPCs and Lkr neurons (those involved in postprandial sleep). Thus conceivably, LHLK neurons, whose activity is dependent on circulating glucose, could suppress or induce sleep depending on internally perceived satiety state via Lk signalling onto these two antagonistic circuits.

This circuitry may be the equivalent to pro-opiomelanocortin (POMC) and agouti-related protein (AgRP) neurons in the mouse hypothalamic articulate nucleus. AgRP neurons are activated in response to orexigenic hormones such as ghrelin, promote food searching behaviour, and suppress sleep under starved conditions. Conversely, POMC neurons are activated by insulin (which is a satiety signal) and promote sleep (Goldstein et al., 2018). Orexin neurons are also synonymous with feeding and sleep: they are sensitive to circulating glucose and ghrelin. Orexin neuron-ablated mice do not respond to food deprivation by increasing locomotor activity and sleep suppression (Yamanaka et al., 2003).

Dopaminergic neurons of the mushroom bodies (MBs) called DANs may also be part of the pathway(s) that evaluate and translate internal nutrient state into behavioural change in flies. MBs are involved in olfactory processing (Aso et al., 2014), learning [for review see Cognigni et al. (2018)], and sleep (Aso et al., 2014; Sitaraman et al., 2015b). Mushroom body output neurons (MBONs) are the main output of this brain region and are key regulators of sleep/wake behaviours (Sitaraman et al., 2015a). DANs can potentiate or depress MBON pre-synaptic zones and some have been shown to directly modulate activity of wake promoting MBONs, suppressing sleep upon activation (Sitaraman et al., 2015a,b). Interestingly, some DANs respond to food deprivation by increasing the size and density of their active zones. Inactivation of these same DANs impairs food seeking behaviour during starvation[4] (Landayan et al., 2018; Tsao et al., 2018). DANs thus are sensitive to nutrient scarcity, and could regulate sleep and food searching under different nutritive conditions by modulating activity of wake promoting MBONs and/or by sensitising MBONs to food odours (Tsao et al., 2018) which may fragment sleep and reduce arousal thresholds. It should be noted that a *direct* link between starvation-induced potentiation of DANs and their subsequent involvement in sleep suppression/modulation of wake promoting MBONs cannot be made, but is highly congruent.

Another study has shown that paired anterior medial (PAM) neurons, a subset of DANs, become activated upon ingestion of sucrose but not by tarsal stimulation. Interestingly,

[3]It should be noted that lower concentrations of sorbitol reduce the total amount of sleep, thus this phenotype is concentration dependent.

[4]Tsao et al. (2018) screened 34 MBON lines for impairments in food seeking behaviour under starved conditions. They then investigated the response of six corresponding DAN lines to starvation-induced potentiation, which is not exhaustive. These were either not screened by Sitaraman et al. (2015b) for sleep phenotypes or did not have a sleep phenotype. Nor is it known whether starvation-induced potentiation is a characteristic of all DANs or specific to only a subset investigated by Tsao et al. (2018).

activation by sucrose is more pronounced when flies are starved (Liu et al., 2012). Taken together it appears that DANs are modulated in response to both starvation and ingestion of high concentrations of sucrose (1 M), both of which can promote arousal and suppress sleep (Catterson et al., 2010; Murphy et al., 2016). Future work should investigate the link between starvation-induced potentiation of DANs and sleep suppression as it represents a highly promising avenue.

Genes Involved in Starvation-Induced Sleep Loss

New genes that regulate sleep during starvation are continually being discovered. Not surprisingly, a link between starvation-induced sleep suppression and metabolism is becoming evident. As discussed above, insulin is a signalling molecule involved in regulating sleep in response to food deprivation (a mechanistic summary is shown in **Figure 2**). Another major target of insulin signalling in insects is the fat body, analogous to the liver in mammals. This tissue is known to play an important role in regulating feeding and metabolism. A recent study has shown that fat body-specific knock-down of *phosphoribosylformylglycinamidine synthase* (*Ade2*), a gene that is highly conserved and involved in purine synthesis, reduces triglyceride levels and free glucose. These flies also exhibit lower levels of sleep, a finding that directly links fat body function, sugar/fat metabolism, and sleep (Yurgel et al., 2018). Partly in contention with this finding, several other studies have reported that the amount an individual sleeps is independent of body size and amount of lipid stored (Lee and Park, 2004; Meunier et al., 2007; Kent et al., 2009; Masek et al., 2014; Slocumb et al., 2015). These studies do however reach a consensus that the way in which animals mobilise energy stores and/or conserve them through modification of sleep/wake behaviour appears to translate into tolerance to starvation (measured through longevity). Epitomising this, Rover and Sitter flies possessing different alleles of the gene *foraging*, which codes for a cGMP dependent protein kinase G (PKG) (Sokolowski, 1980; Scheiner et al., 2004), differentially regulate metabolism and gene expression (Kent et al., 2009) under starvation. Compared to Rovers, Sitters have more carbohydrate stores, which they are able to mobilise under starved conditions and as a result exhibit less sleep suppression during food scarcity (Keene et al., 2010). Sitters are also more resistant to starvation measurable through increased survival on agar and an unencumbered ability to perform a learning and memory task (Donlea et al., 2012). Core differences in the way that the two variants respond to food deprivation metabolically may affect their perceived satiety level and actual nutritional requirements, which may explain the observed differences in their sleep levels.

Sonn et al. (2018) conducted the most comprehensive study looking at genes involved in starvation-induced sleep loss. Genes that are up-regulated in response to short-term starvation (6 h) are mostly involved in sensory perception, whereas genes up-regulated during chronic starvation (24 h) were concerned with metabolism or transmembrane transport of amino acids and metabolism of nucleotides. Most notably, following chronic starvation, serine levels were elevated together with three genes involved in serine biosynthesis, including *astray* (*aay*), a non-protein phosphatase part of the haloacid dehalogenase (HAD) family member that catalyses the last step in the biosynthesis of serine from carbohydrates. Flies harbouring a hypomorphic allele of *aay* failed to exhibit starvation-induced sleep suppression and had increased arousal thresholds (less waking in response to light pulse at ZT 18) (Sonn et al., 2018). Conversely, flies with a mutated *serine dehydrogenase* (*stdh*) gene, which codes a protein that breaks down serine, suppressed sleep under starved conditions to a greater extent than controls (Sonn et al., 2018). Importantly this study points to short- and long-term strategies that are in place to allow flies to cope with food deprivation. Following short-term food deprivation, sensory genes are upregulated. This may increase sensitivity of sensory neurons, making them more tuned to food-related cues. As flies become sensitised to external cues this may, in turn, optimise

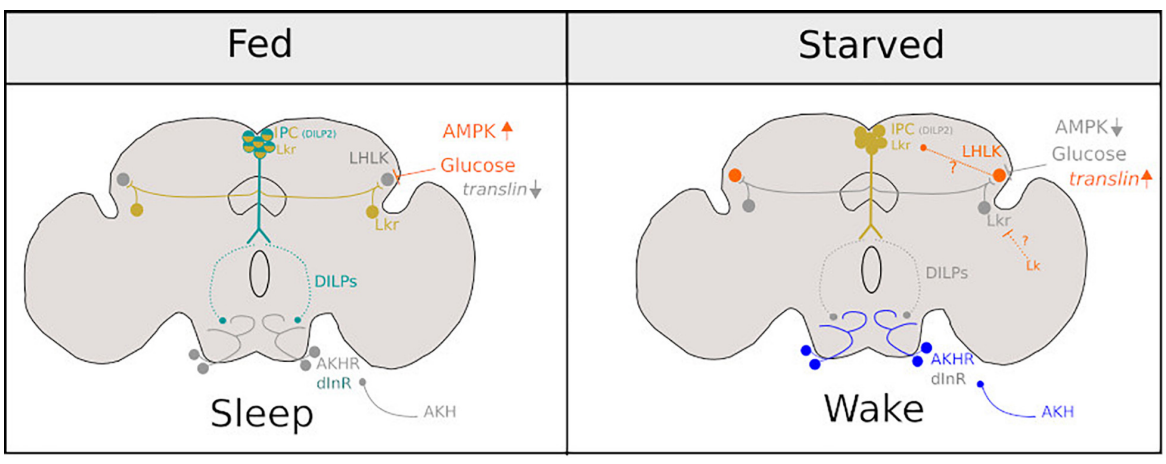

FIGURE 2 | Diagram representing the neurons involved in promoting sleep under fed conditions **(Left)** and sleep suppression under starved conditions **(Right)**. Bright colours represent neuronal activity and grey represents neuronal inactivity under fed and starved conditions in *Drosophila*. Figure is adapted from Melnattur and Shaw (2019).

food searching and may reduce arousal thresholds during sleep, ultimately increasing walking and reducing sleep.

Several genes expressed in clock cells also seem to play a permissive role rather than an instructive role in the starvation-induced sleep suppression phenotype. For example, inhibition over sleep promoting *Clk*-positive neurons is required for this phenotype (Keene et al., 2010). cyc^0, Clk^{jrk}, and Clk^{ar} mutant flies suppress sleep more than controls under starved conditions. Authors postulate that it is likely to be an antagonistic pathway overriding *clk*-expressing neuron input into sleep centres. These putative inhibitory neurons would become active during starvation. Additionally, neuropeptide F (NPF), which is expressed in l-LNvs and the FSB, among other brain regions, plays a role in exerting inhibition over sleep promotion (Hergarden et al., 2012). Loss of the NPF gene, which has been implicated in both feeding and sleep, eliminates starvation-induced sleep loss (Chung et al., 2017).

Taken together this suggests that genes regulating sleep in food deprived environments tend to encompass those involved in metabolism (Lee and Park, 2004; Meunier et al., 2007; Masek et al., 2014) and sensory acuity (Sonn et al., 2018).

Disruption to mechanisms that sense hunger state (and thus precede mobilisation of carbohydrate stores) appears to have knock-on effects on systems which prime the animals physiology and initiate food searching behaviour, both of which are required for endurance in starved conditions.

In summary, flies are equipped with mechanisms to sense internal (Murakami et al., 2016; Yurgel et al., 2019) and external (Linford et al., 2012, 2015; Yang et al., 2015; Hasegawa et al., 2017) nutrient availability to modulate sleep accordingly. Perturbation to this system ultimately results in aberrant feeding and sleep behaviour.

Dietary Composition, Caloric Restriction, and Sleep

So far, we have discussed the effect of feeding and starvation on sleep. Next, we will discuss how dietary composition, amount of food, and its quality can alter sleep amount and its structure.

Concentration of dietary sucrose has been shown to affect sleep (Catterson et al., 2010). As discussed, starved flies exhibit hyperactivity and sleep loss, which is rescued by perception of a sweet gustatory stimulus (Linford et al., 2015; Hasegawa et al., 2017) such as sucrose at concentrations as low as 0.5, 1, and 5% (Yang et al., 2015). However, drastically increasing dietary sucrose from 5 to 35% reduces sleep and induces an intense locomotor activity in male and female flies (Catterson et al., 2010). Therefore, actual ingestion of very high calorie foods may counteract the sleep promoting effects of gustatory stimuli.

Dietary protein can also alter sleep: addition of 2% yeast to a 5% sucrose diet results in an increase of walking, compared to sugar alone diet, therefore, an altered sleep architecture, characterised by shorter bouts, and a concomitant reduction on the arousal threshold in males (Catterson et al., 2010).

Nutritive value of any given diet, for example carbohydrate:protein ratio, will impact sleep. Linford et al. (2012) compared sleep in male flies being fed 2.5% yeast mixed with two different concentrations of sugar: 2.5% (low sugar diet: LSD) or 30% (high sugar diet: HSD). Total amount of sleep was unchanged by diet, but on the LSD sleep became more fragmented, typified by shorter bout lengths. Further, flies on this diet were more easily aroused by light pulses, indicating lower arousal thresholds and less consolidated sleep. A plausible interpretation of these findings is that, in low nutrient environments, flies regulate their sleep architecture to detect and exploit food sources when they become available. Interestingly, flies on the LSD had less triglyceride stores than those on HSD but this did not appear to play a significant role in fragmenting sleep. Instead, gustatory perception of low sugar concentrations fragments sleep under nutrient scarce conditions since loss of sugar gustatory receptors rescued the fragmentation phenotype in flies fed a range of LSDs (Linford et al., 2012).

High sucrose alone and yeast mixed with low concentrations of sucrose promotes wakefulness and fragments sleep (Catterson et al., 2010), but in combination, yeast and high dietary sucrose consolidate sleep (Linford et al., 2012). This indicates that the quantity and relative proportion of protein to carbohydrate may have important phenotypic implications. Considering the importance of sweet gustatory perception on promoting sleep (Linford et al., 2012, 2015; Hasegawa et al., 2017), it is plausible that taste interactions and/or internal nutrient sensing may explain this apparent paradox (Linford et al., 2015).

An important consideration here is that dietary composition can also affect the gut microbiome (Sharon et al., 2010) thus prompting the question: are food-dependent sleep behaviours, in part, explained by changes in microbiota? Microorganisms living in the gut are known to assist with the breakdown of food and provide nutrients in their own right (Wong et al., 2014; Yamada et al., 2015), thus contributing to the nutritional and metabolic state of the animal. Microbiota also appear to interact with insulin signalling which is known to regulate feeding and sleep (Shin et al., 2011). While microbiome composition has been shown to affect mating choice (Sharon et al., 2010), egg laying, and feeding (Leitao-Goncalves et al., 2017), rather surprisingly, another study found that eliminating the microbiome in fruit flies has only very modest effects on sleep and locomotion compared to controls (Selkrig et al., 2018). Considering the wealth of literature describing the interconnection between the availability and quality of food on sleep, it is surprising that loss of gut microbiota has no effect on sleep (Selkrig et al., 2018). While admittedly we cannot definitive rule out whether microbiota composition has an effect on sleep; for now we can say with a degree of confidence that food-induced changes in sleep is mostly governed by taste and nutritional quality.

Caffeine and Sleep

Plants produce secondary metabolites to protect themselves against pests that feed and/or lay eggs on their vegetal tissue. Thus, while foraging and selecting egg laying sites, fruit flies may have to contend with plant chemical defences. Caffeine is an alkaloid produced by many species, including coffee (*Coffea arabica*), tea (*Camellia sinensis*), and *yerba mate* (*Ilex paraguariensis*) making it one of the most widely consumed plant secondary metabolites by humans. Due to its psychostimulatory

and wake promoting properties, its impact on sleep has been studied in numerous model organisms (Maximino et al., 2011; Panagiotou et al., 2018) including *Drosophila*. As in humans, caffeine has been reported to be an inhibitor of sleep in fruit flies (Andretic et al., 2008; Wu et al., 2009; Nall et al., 2016). In *Drosophila*, its effects are more prominent in females and during the night compared to day. While studies tend to focus on how caffeine psychostimulatory properties impact sleep (Andretic et al., 2008; Wu et al., 2009; Nall et al., 2016), it is likely caffeine also interacts with food intake and taste (Keebaugh et al., 2017), which, as discussed, have profound effects on sleep amount and partitioning. Caffeine tastes bitter to flies and reduces feeding by inhibition of sugar sensing GRNs and through activation of bitter-sensing neurons (Jeong et al., 2013).

Because caffeine interacts with sweet gustatory receptors (Jeong et al., 2013), and may do competitively, it is possible that elimination of caffeine-induced sleep loss by increasing the sugar in the food, a finding of Keebaugh et al. (2017), could be explained by this mechanism. To our knowledge, there is no convincing evidence showing flies that cannot taste caffeine still suppress sleep when fed it. GR93a is a gustatory receptor expressed in bitter-sensing neurons and is involved in caffeine detection (Lee et al., 2009). Flies mutant for this receptor do still exhibit caffeine-induced sleep loss, however, it is clear from this study that GR93a mutants still significantly reduce their intake of caffeine laced sucrose, probably because they still taste it. Importantly, many studies have demonstrated that other gustatory receptors are also involved in caffeine detection (Marella et al., 2006; Moon et al., 2006), suggesting loss of GR93a is probably not sufficient to eliminate peripheral detection. Interestingly, other bitter tasting molecules such as papaverine and quinine, which activate bitter-sensing neurons, and also inhibit sugar sensing ones, mimic the effects of caffeine on sleep yet do not have any known psychostimulatory effects (Keebaugh et al., 2017).

Other studies have shown that the neural pathways required for caffeine-induced sleep loss are in part shared with those putatively involved in starvation-induced sleep loss, namely the dopaminergic PAM cluster of the MBs. PAM-silenced flies slept the same amount on food laced with or without caffeine. Allowing flies to feed *ad libitum* on sucrose laced with caffeine over 24 h also activated these neurons (Nall et al., 2016). As discussed earlier, PAM neurons are potentiated by food deprivation and are involved in food seeking behaviours initiated by starvation (Landayan et al., 2018; Tsao et al., 2018). In addition, Liu et al. (2012) showed that PAM neurons do not respond to caffeine ingestion but do respond to sucrose ingestion (but not tarsal stimulation) in a manner enhanced by starvation.[5] Thus, it is possible that the reduced feeding observed in flies presented with caffeine (Keebaugh et al., 2017) induces a hunger state which triggers food searching and sleep suppression. This may exacerbate the caffeine sleep phenotype. Another study has also implicated MB dopamine signalling in caffeine-induced sleep loss. Flies lacking dopamine receptor 1a (dDA1) are resistance to caffeine-induced sleep loss, a phenotype which can be rescued by expressing dDA1 in a subset of MB neurons driven by C747–GAL4 (Andretic et al., 2008).

While caffeine may influence sleep through its taste properties, there is certainly evidence to support that caffeine may also have psychostimulatory effects on sleep in flies. Firstly, some of the characteristics of caffeine-induced sleep loss and starvation are different. Caffeine affects night sleep more than day and it is more efficacious in females, whereas starvation reduces both day and night sleep in males and females. There is also evidence that the effects of caffeine and starvation are mechanistically separable (Murakami et al., 2016). It is interesting, however, that the pathways through which caffeine acts in fruit flies is not conserved in mammals (Yanik et al., 1987; Huang et al., 2005) or other vertebrates (Aho et al., 2017). The Seghal lab show that flies lacking the Adenosine receptor (dAdoR) gene, which is an important biological target of caffeine, have similar sleep levels to controls when put on caffeine laced food, but sleep bouts are slightly shorter. Instead of mediating effects through adenosine signalling, caffeine acts through cAMP/PKA pathways and antagonises PDE (Wu et al., 2009). In addition to the effects of caffeine on sleep, thus far it is unknown whether metabolites of caffeine contribute to the phenotype. Insects are equipped with cytochrome p450 enabling them to defend themselves against toxic plant secondary metabolites, such as caffeine, once ingested (Coelho et al., 2015). It is possible that caffeine is metabolised in the gut into compounds such as theobromine, paraxanthine, and theophylline, which could affect sleep via routes distinct from adenosine signalling.

In summary, animals encounter a range of nutritive landscapes and have to adapt their behaviour accordingly. Nutrient scarcity can drive food-searching behaviours, resulting in sleep loss. In addition, nutrient poor conditions can alter the architecture and depth of sleep making individuals more vigilant and easily woken. Ingestion of high calorie foods can also induce hyperactive behaviour and suppress sleep. Assessment of nutrient availability is largely achieved via peripheral detection by GRNs and through internal nutrient sensing. Both these systems can modulate sleep independently but likely work in synergy with one another. In addition to dealing with a variety of nutritive conditions, fruit flies have to contend with defence mechanisms employed by their food source to defend itself. Plant secondary metabolites can deter feeding and induce malaise or psychostimulatory effects upon ingestion, which can impact sleep. Food quality and availability therefore represents a major environmental factor that can alter the amount and structure of sleep.

SOCIAL INTERACTIONS HAVE A PROFOUND EFFECT ON SLEEP REGULATION

Depending on their ecology, lifestyle, and social organisation, animals vary in the extent of their social interactions. Although light and temperature are the main synchronisers of the sleep-wake cycles, social cues and interactions can work as modulators of the circadian entrainment (Davidson and Menaker, 2003). For

[5]It should be noted that the two studies do not use the same GAL4 drivers to label PAM clusters.

instance, blind humans who lack light entrainment can use social cues to adjust their circadian clock (Klerman et al., 1998). In addition, social jetlag can affect cognitive performance (Haraszti et al., 2014) and health (Roenneberg et al., 2012). The effect of social interactions on sleep and the circadian organisation of activity is observed across taxa and has been described in birds (Menaker and Eskin, 1966), fish (Kavaliers, 1980), and rodents (Crowley and Bovet, 1980; Tomotani et al., 2016). An outstanding work has shown that eusocial bees entrained using social cues inside of the hive can sustain long-lasting synchronisation that can overrule photic entrainment (Fuchikawa et al., 2016).

Although *D. melanogaster* does not exhibit the complexity of eusocial insect colonies, these flies do engage in a repertoire of social interactions (Ramdya et al., 2017). There is solid evidence for the presence of social networks (Schneider et al., 2012) and collective behaviour in this species (Ramdya et al., 2015). Importantly, the most studied social behaviours in the fruit fly are simplified one-to-one interactions, namely, aggression (male–male encounters) and courtship (female–male encounters) for which the fly has emerge as a powerful workhorse to understand the neurogenetics behind these behaviours. Unfortunately, whether video recording or DAMs were used, sleep had mostly been studied at the individual level, with animals in isolation. Beyond the obvious advantage of measuring sleep in unperturbed and controlled conditions, this simplified and reductionist approach means that sleep is rarely studied in different social contexts, which are known to modulate sleep. Thankfully, in the last few years, efforts were devoted to address how social interactions affect sleep and vice versa in this powerful model system (see **Figure 3** for a visual summary of this section).

Male–Male Interactions

The increase in sleep after a stressful social situation seems to be a conserved feature of sleep regulation. In humans, sleep abnormalities have been reported in patients with posttraumatic stress disorder (Kobayashi et al., 2007), and insomnia is present in 80% of patients with depression (Armitage, 2007). Likewise, in mice, both acute (Fujii et al., 2019) or chronic (Henderson et al., 2017; Olini et al., 2017) socially induced stress produces an increase in sleep after the encounter.

Upon encountering another male, *Drosophila* males display agonistic behaviour that has proven to be an extremely useful model to study aggression (Kravitz and Fernandez, 2015). The confrontation results in the establishment of a hierarchy and represents a stressful situation, that reduces the amount of sleep (Gilestro et al., 2009; Beckwith et al., 2017; Machado et al., 2017) in a way that is dependent on the dimensions of the experimental arena (Lone et al., 2016). Notably, after the interaction, males show a clear increase in sleep that can take longer to manifest if the animals are housed at lower densities.

Consequently, the increased wakefulness triggered by the encounter with a conspecific, and the corresponding homeostatic regulation of sleep after it, constitutes an ecologically meaningful context to study sleep and its regulatory factors across species (Stahl and Keene, 2017). In *Drosophila*, beyond the clear homeostatic sleep recovery, further experiments would be needed to understand if the status of individuals after the fight (winner vs. loser) has a differential impact on sleep regulation or sleep need.

At the circuitry level, R2 neurons of the ellipsoid body (EB) act as a barometer for sleep pressure (Liu et al., 2016), and the activity of these neurons increases in response to both mechanical sleep deprivation and after a male–male encounter (Beckwith et al., 2017). Additionally, the change in sleep after a male–male interaction seems to be dependent on the dopaminergic system, while the circadian clock neurons are not necessary for this behavioural change (Lone et al., 2016).

Furthermore, the relationship between sleep and aggression in flies is bidirectional: acute sleep deprivation reversibly suppresses aggressive behaviours, competition for mating, as well as male courtship (Kayser et al., 2015; Chen et al., 2017; Machado et al., 2017). While a recent study has shown that long-term sleep loss has negligible effects on longevity in males (Geissmann et al., 2019a), the discussed data show that sleep is crucial for fitness in a social context.

Decisively, at the heart of the interaction between aggression and sleep lies octopamine. This neuromodulator is a well-described promoter of aggression (Hoyer et al., 2008) and suppressor of sleep (Crocker and Sehgal, 2008; Crocker et al., 2010). As expected, stimulation with an octopamine agonist is able to rescue the reduction in aggression (Kayser et al., 2015). However, despite ample evidence implicating octopamine in the regulation of aggression and sleep, the subsets of octopaminergic neurons involved in the interaction between these two critical behaviours have not been fully described.

Female–Male Interactions

A female–male interaction is usually sexual in nature and involves courtship behaviour initiated by the male towards the female. The female will accept or reject the male's advances in a manner dependent on its mating status. Courtship behaviour has been intensively studied in many species. Through the investigation of fly behaviour and neurogenetics, a detail description of the genes and circuits involved in this behaviour is available (Greenspan and Ferveur, 2000; Yamamoto and Koganezawa, 2013). This intense two-way interaction is crucial for perpetuation of the species and, in many contexts, it is prioritised over other behaviours including sleep.

Sexually Aroused Males Suppress Sleep

A clear example of how sexual arousal and the possibility of mating can regulate sleep was described in artic birds (Lesku et al., 2012). During the mating season, these polygynous birds suppress their sleep with no obvious sleep recovery at the end of the mating season. In addition, a key study shows that mating-related stimuli also suppress sleep in mice, a behaviour that is dependent on dopaminergic neurons from the ventral tegmental area (VTA) (Eban-Rothschild et al., 2016).

Interestingly, sleep suppression by the presence of a female or by the activation of the sexual arousal circuits was also reported in *Drosophila* (Fujii et al., 2007; Beckwith et al., 2017; Chen et al., 2017; Machado et al., 2017). Moreover, the

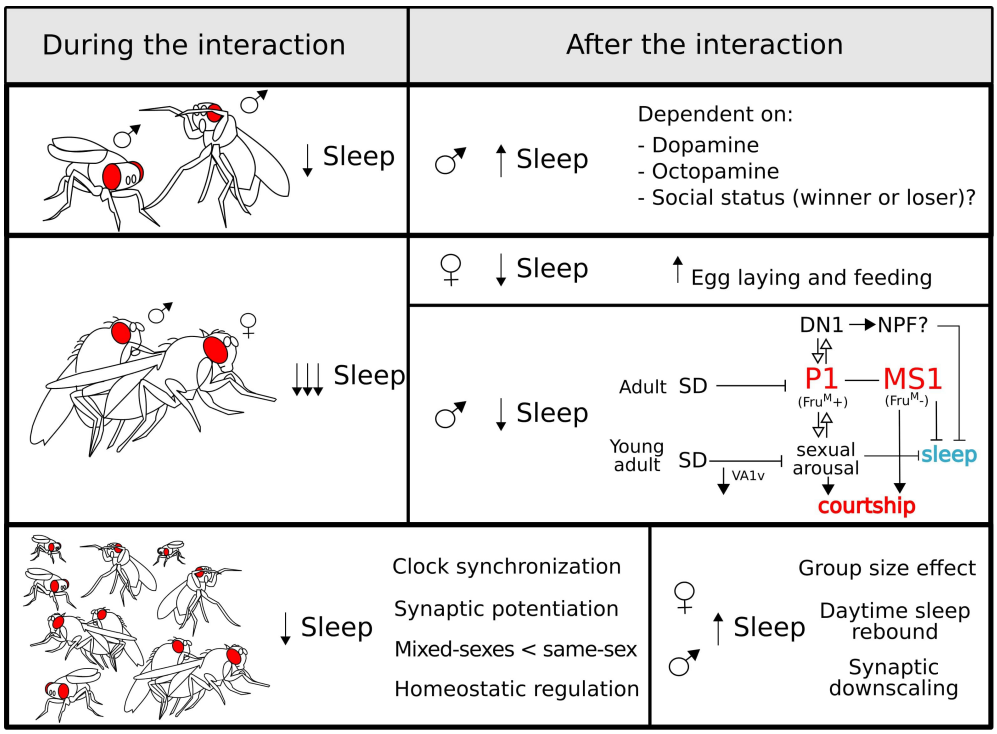

FIGURE 3 | Sleep regulation during **(left panel)** and after **(right panel)** different social interactions: sexual **(top)**, aggressive **(middle)**, and group **(bottom)**. During all the interactions, sleep is reduced which is most poignant for sexual encounters. After copulation, males undergo a negative regulation of sleep controlled by sex-drive-related neurons (see the main text for a detailed explanation). For the group interaction **(bottom panel)**, some characteristics of this type of interaction are highlighted. After a social encounter, the effects on sleep regulation vary depending on the type of interaction and the sex of the fly.

presence of short-range non-volatile pheromones 7(Z),11(Z)-non-acosadiene (7,11-ND) and 7(Z),11(Z)-heptacosadiene (7,11-HD) can even suppress sleep rebound in mechanically sleep-deprived males (Beckwith et al., 2017). Shortly after pheromone exposure, males experience a series of physiological changes mediated by pheromone-sensing neurons located in the animals' forelegs that express the *ppk23* receptor (Thistle et al., 2012; Gendron et al., 2014; Harvanek et al., 2017). These changes include the loss of triacylglyceride, an increased susceptibility to stress, faster aging and a significantly higher expression of NPF (Gendron et al., 2014). Importantly, NPF-expressing neurons are necessary and sufficient to drive this physiological switch. At the same time, these neurons represent a well-described arousal centre. NPF is a wake promoting NP and, as discussed, is a regulator of starvation-induced sleep loss (Chung et al., 2017). Thus, this NP represents a clear candidate to mediate the sleep reduction resulting from increased sex drive.

Beyond the data discussed above, the behavioural choice between engaging in courtship or sleep implies that courtship- and sleep-devoted circuits may interact to balance these competing drives. The expression of the male-specific splicing variant of the transcription factor *fruitless* (fru^M) marks the neural circuits that govern male courtship. The P1 cluster of fru^M-positive neurons in the protocerebrum integrates multisensory information and is a central hub for sex drive. P1 neurons indirectly activate the wake-promoting DH31-positive DN1 neurons (Chen et al., 2017) that are, in turn, part of the circadian network. Interestingly, this cluster is also fru^M-positive and it is able to suppress sleep through DH31 secretion (Kunst et al., 2014). The interaction between these two clusters is bidirectional, showing a mutual activation that result in a positive feedback loop that biases behaviour towards courtship (Chen et al., 2017). Moreover, basal activity of the P1 neurons are negatively modulated by sleep deprivation, and, as mentioned, sleep-deprived males have reduced courtship behaviour (Kayser et al., 2015; Machado et al., 2017). Upstream of the P1 neurons lies a newly described cluster of octopaminergic neurons named Male-Specific 1 (MS1) (Machado et al., 2017). The activation of this cluster leads to a male-specific inhibition of sleep and promotes courtship in response to sex drive. The MS1 are fru^M-negative, but there is a direct and sexually dimorphic synaptic contact with a group of fru^M-positive neurons that innervate the SOG. Interestingly, the activation of MS1 neurons induces a broad activation of fru^M-positive neurons, including the P1 cluster (Machado et al., 2017). Thus, the P1 neurons are crucial integrators of multiple sensory modalities and participate in the balance between courtship and sleep.

It is important to highlight that the interactions between networks that regulate these competing behaviours, and its hierarchical organisation, has not been fully elucidated. Regarding the link between the previously discussed networks and the reported sleep centres (Donlea, 2017), the constitutive

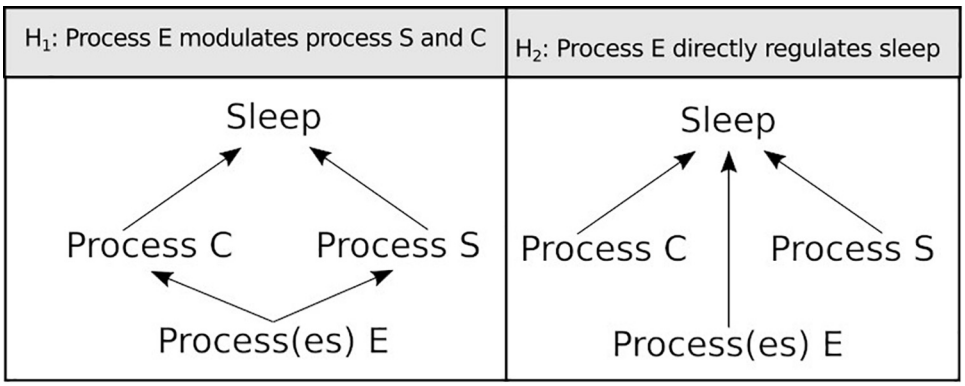

FIGURE 4 | Two alternative hypotheses on how environmental factors can be integrated into the Borbély (1982) model of sleep regulation.

activation of the sleep inducing neurons in the dorsal FSB can overcome sex-driven sleep inhibition (Machado et al., 2017). This finding reinforces the idea that the balance between sleep and courtship is bidirectional, i.e., it is not governed exclusively by sexual impulse. However, the exact interaction between the sex-drive clusters and this and/or other sleep centres like the R2 neurons of the EB is not clear. Untangling these connections will shed light on the complex balance between these two mutually exclusive behaviours.

Surprisingly, the female–male interaction and the concomitant reduction in *Drosophila* male sleep does not result in rebound sleep, a phenomena that is also observed in the artic polygynous birds study by Lesku et al. (2012). In flies, the experience of a prolonged sexual encounter, and probably the high levels of rejection that males experience due to the reluctance of females to re-mate, induces a strong reduction of sleep, which does not seem to be recovered (Beckwith et al., 2017). Further, the genetic activation of the P1 neurons or, to a lesser extent, the MS1 neurons, induces a reduction in total sleep that has a long lasting effect and does not result in a typical rebound sleep (Beckwith et al., 2017; Machado et al., 2017). A provocative idea could be that, in these conditions, sleep need is being recovered through a deeper sleep state; and these social interaction paradigms will be fundamental to address the relevance and the mechanisms underpinning such a state in flies.

These findings imply that a change in the internal state by sexual arousal can directly regulate sleep as well as modulate the homeostatic recovery of the lost sleep. Similarly, in humans, sleep quality and sleep onset are perceived to improve after achieving orgasm with a partner before bed (Lastella et al., 2019). It would be interesting to re-analyse the *Drosophila* data to address the immediate effect of mating in males and separate the effect of mating and the effect of courtship and rejection at the genetic and cellular level.

We mentioned that the interplay between sleep and courtship is bidirectional in flies, since acute sleep deprivation reduces sexual drive in a reversible manner. On a different time scale, sleep deprivation during critical periods of development has a long-lasting effect on adult behaviours like learning (Seugnet et al., 2011) and courtship (Kayser et al., 2014). In particular, the increased and deeper sleep phenotype observed in young individuals is required for the development of neural circuits necessary for courtship and mating. Consequently, sleep deprivation during the first 7 days of life specifically disrupts the development of antennal glomeruli to which *fru*M-positive neurons project. Male flies sleep deprived early in life have reduced VA1v glomerulus volume and have deficits in courtship behaviour (Kayser et al., 2014).

Mating Reduces Female Sleep

Regarding female behaviour, the effect of courtship on the regulation of sleep seems to be minimal. Two hours of exposure to a male does not result in a behavioural change in the courted but non-mated females (Geissmann et al., 2019a). However, mating triggers a series of changes in female behaviour. In addition to changes in egg laying, feeding, and courtship rejection, sleep shows a marked reduction after mating (Isaac et al., 2010; Zimmerman et al., 2012; Garbe et al., 2015, 2016; Geissmann et al., 2019a). Importantly, many of these changes, including a reduction in sleep, are reliant on the exchange of sex peptide from the male to the female during copulation (Isaac et al., 2010; Garbe et al., 2016). While it is generally agreed that copulation reduces sleep, the extent of sleep suppression varies between studies. While some reports describe a reduction of a 50% or less (Isaac et al., 2010; Zimmerman et al., 2012; Garbe et al., 2015, 2016), others reported a reduction close to the 90% (Geissmann et al., 2019a). We believe that these marked differences stem from two main reasons: method of sleep monitoring (DAMs vs. video tracking) and availability of protein-rich food. In brief, DAMs overestimate sleep and lack of protein inhibits egg laying, resulting in a gross underestimation of extent of behavioural change. Additionally, a finer description of behaviour after mating showed that sleep amount is not the only entity changed; instead, the entire behavioural profile is altered. Mated females walk less and spend a greater proportion of their time by the food performing micromovements, defined as a compendium of behaviours that includes feeding, egg laying, and grooming (Geissmann et al., 2019a).

This strong effect on sleep regulation is extremely informative and has implications for sleep research. A straightforward conclusion is that a good proportion of the sleep exhibited by virgin females can be exchanged for other physiological necessities and ecologically relevant activities. However, not all the measurable sleep disappears. Because of this, two scenarios arise: (A) sleep is exchanged for feeding and/or egg laying produces a sleep deficit in the mated female that can negatively affect its physiology or (B) virgin females show two components of sleep, one necessary and other one that can be exchanged at no cost. The fact that different reports fail to show sleep recovery after the behavioural switch would favour the second scenario. However, a component of the measurable sleep displayed by mated females confers a fitness benefit since sleep deprived mated females have reduced fecundity (Potdar et al., 2018). We believe that studying the behavioural switch after mating and the characteristics of sleep in mated females, which is likely the default state in wild fruit flies (Giardina et al., 2017), may be critical to understanding the regulation and functions of sleep.

Group Interactions

Beyond the one-to-one interactions described above, socialisation in large groups also has an effect on sleep. This regulation of sleep is not restricted to the fly and is well documented in many insect (Eban-Rothschild and Bloch, 2012). For instance, in bees, a 2-day exposure to the colony environment generates an increase in sleep compared to the sleep shown by isolated bees of the same age and cast (Eban-Rothschild and Bloch, 2015).

In nature, *D. melanogaster* flies are found around food and oviposition sites (Shorrocks, 1972) forming mixed-sex groups that show evidence of social networks and collective behaviour (Ramdya et al., 2017). Hence, studying sleep regulation by social interaction within complex groups comprised of a genetically tractable organism, in a natural environment, may lead to meaningful observations. At the same time, it represents a methodological challenge since there are many different variables, which can influence the nature of any given interaction (e.g., sex ratio, density, food, and space availability). Likewise, the sleep of one or many individual flies within a group of interacting flies needs to be assessed.

In an elegant set of experiments Levine et al. (2002) showed that chemosensory cues involved in social communication are strong regulators of the rest-activity rhythms. They evaluated the locomotor rhythms (which we take as a proxy for sleep) of individual male flies following social isolation or group housing. Flies previously housed in groups showed a stronger synchronisation of their activity rhythms, which was perturbed when they were housed in groups containing flies with a genetically ablated circadian clock. This key finding demonstrates that social cues modulate the timing of activity in a clock-dependent manner. Similar experiments have evaluated sleep levels of individual animals after long periods of social enrichment in developmentally mature adults (Ganguly-Fitzgerald et al., 2006). Socialisation in 1:1 male:female groups during 4 days showed a group-size-dependent increase in sleep that is dependent on the dopaminergic system (Ganguly-Fitzgerald et al., 2006). Interestingly, the increase in sleep resulting from socialisation is restricted to daytime sleep. This observation indicates that day and night sleep may be differentially regulated. Alternatively, increased sleep during the first part of the day could mean sleep pressure has already dissipated by night-time. Importantly, similar results were shown for groups of females housed in groups of 30 for 9 days (Zimmerman et al., 2012). Moreover, this increase in sleep after social enrichment is dependent on the flies' genetic background, specifically the presence of the Rover variant of the foraging gene (Donlea et al., 2012).

Actually, the sleep increase observed after socialisation may be necessary to downscale synapses and restore branch length, branch points, and spine number to basal levels[6] (Bushey et al., 2011). These experiments, together with a plethora of other results collected in different species, support the synaptic homeostasis hypothesis: wakeful experience results in potentiation, some of it is useful and some redundant. During sleep, synapses are downscaled returning brain activity to basal levels. This pruning process allows further potentiation during subsequent wakefulness (Tononi and Cirelli, 2006).

It is clear that social interaction during adulthood regulates sleep. Likewise, this is true for social interactions occurring during critical periods of development, both during the larval stage and the first days of adult life. In particular, high larval density causes greater sleep consolidation during adulthood, a phenotype that is clearer in females than in males (Chi et al., 2014). Similarly, young adult flies exposed to a social environment present higher levels of sleep, which is reversible if the flies are kept in isolation. This process is dependent on the core clock gene *per* (Donlea et al., 2009), but it is independent of other core clock genes like *timeless*, *cycle*, and *clock* (Ganguly-Fitzgerald et al., 2006). This may indicate that this is a clock-independent process in which *per* has a separate function.

It is important to highlight that these reports measure sleep in isolated flies following exposure to a social environment, but not during the social interaction itself. Altogether, these data allow clear conclusions relating to the regulation of sleep by social experience, which can be interpreted as a homeostatic response to sleep loss during the interaction. However, the ongoing interactions throughout a group are critical because the behaviour of individual members is not a good predictor of the group-level activity (Higgins et al., 2005). Thus, the question remains: how do flies sleep *during* the social interaction? In an attempt to evaluate the sleep of populations of flies, Liu et al. (2015) studied the overall activity of mixed and same-sex populations. Their main conclusion is that same-sex groups coordinate their sleep, showing a temporal pattern similar to that of an individual. However, population records show lower levels of sleep compared to an isolated fly, which is expected since this system would only record sleep when all the flies sleep in unison. In agreement with previously

[6] Bushey et al. (2011) studied downscaling specifically in a group of visual neurons, so it is not known whether this is universally applicable.

described data, mixed populations exhibit lower sleep than populations of female flies alone, which may be explained by the fact that males exhibit higher activity levels due to sexual arousal. Finally, sleep-deprived populations exhibit homeostatic regulation characterised by a rebound sleep. Thus, beyond the lack of an individualised assessment of sleep during housing the authors conclude that socialisation modulates sleep amount but does not obliterate the two main regulators of sleep, the clock and the homeostat.

Beyond interesting results described above, we think that a description of sleep regulation during the presence of conspecifics is still missing. We believe that recently developed tools to track individual flies within populations (Kain et al., 2013; Perez-Escudero et al., 2014; Klibaite et al., 2017; Liu et al., 2018; Scaplen et al., 2019), when used in combination with existing open source tools to analyse sleep data (Geissmann et al., 2019b), will enable us to address this particular aspect of sleep regulation. We are of the opinion that a naturalistic approach to the subject of sleep regulation will ensure clearer, more meaningful conclusions, and technical developments will be fundamental to achieving these goals.

CONCLUDING REMARKS

Sleep is critical but must remain a highly plastic behaviour to allow an organism to adapt to its ever-changing environment. Here we have discussed how three main environmental factors, temperature, food availability/quality, and social context can regulate sleep. Information about these ecological relevant contexts reaches the brain through the sensory systems, which act as an interface between the individual and its environment. In particular, an array of peripheral systems conveys information regarding ambient temperature, food availability, and presence of potential mates and aggressors/competitors. Importantly, these ecologically relevant cues are in large conveyed through chemoreception (Linford et al., 2012, 2015; Beckwith et al., 2017) and in the case of temperature, the family of temperature-regulated TRP cationic channels that transmit both innocuous and nociception information (Dillon et al., 2009). Based on the meaning conveyed by the signal itself, sensory perception is sufficient to regulate the quantity (Linford et al., 2015; Beckwith et al., 2017) and architecture of sleep (Linford et al., 2012; Hasegawa et al., 2017).

A key point is that sensory information serves to instruct behaviour in response to environmental change. For example, the absence of food-related cues or high temperature triggers food searching or escape behaviour, respectively. These behavioural modifications can also influence sleep in two main ways. Firstly, engaging more in a particular behaviour such as mating or foraging can ultimately result in less sleep simply through redistribution of a finite time budget. In addition to external cues, changes in the internal state can also drive this re-allocation of time to certain behaviours. For example, mated females engage more in egg laying, sexually aroused males relentlessly engage in courtship dismissing the need of sleep and starved flies engage in food searching as opposed to sleep. Secondly, external factors such as the presence of conspecifics of the same sex modulate the quality of wakeful experience, leading to increased need for sleep following the encounter (Bushey et al., 2011). However, following some wakeful experiences, like the mating rejection that males experiences after courting a mated female, sleep debt is not repaid *per se*, at least not in total amount of sleep. Interestingly, it is a possibility that the depth or intensity of sleep could work as a compensatory mechanism to dissipate sleep pressure. Thus, how sleep loss, as a result of different wakeful experience, determines future sleep need is not fully understood yet.

From a mechanistic perspective, external factors could differentially affect levels of oxidative stress. It is well documented, for example, that caloric restriction (Ungvari et al., 2008) and even social interaction (Ruan and Wu, 2008) can reduce accumulation of reactive oxygen species (ROS) whereas aggressive encounters may promote ROS production (Ramin et al., 2019). A recent and emerging concept in the *Drosophila* sleep field is that sleep is affected by levels of oxidative stress, and sleep deprivation can accelerate accumulation of ROS (Hill et al., 2018; Kempf et al., 2019). Then, it is plausible to hypothesise that mechanisms facilitating sleep loss or gain, both during or after environmental change, could be in part explained by the sensing of ROS levels. Thus far, this idea has been relatively unexplored but an avenue worth pursuing.

Sleep loss ultimately comes at a cost and understanding how animals weigh the cost and benefit of engaging in other behaviours instead of sleep and vice versa is a key biological quandary that begs to be investigated. A wide range of factors can influence sleep, yet these seemingly independent variables are in fact highly interactive. For instance, a manipulation such as mating can shift an animal's entire behavioural profile (Geissmann et al., 2019a). After mating, females not only spend more time egg laying and less time sleeping, their nutritional requirements change. Thus, sleep loss phenotypes observed in mated females may be exacerbated by nutrient deficiency, which is also a major regulator of sleep. Similar examples exist in which the complexity of behavioural regulation and the limitations of our methodologies can contaminate our conclusions. For instance, caffeine is thought to influence sleep through its psychostimulatory effects on the brain; however, this phenotype is likely confounded by taste-driven changes in food intake. Equally, *Drosophila* neurogenetics sometimes encompass the use of thermogenetics to manipulate neural circuits governing behaviour. As discussed, temperature has drastic effects on sleep, even in basal conditions, making data interpretation more intricate.

From a personal perspective, we believe that it is crucial to embrace the complexity and interactivity of behaviours to improve the output of our science. We encourage the community to use tools that describe behaviour more accurately, build bridges between seemingly independent fields of research and try to agree upon standards, such as rearing environmental conditions and diets, in order to make research

more coherent, facilitating the reproducibility of data and the comparison of results.

Finally, the prevailing idea is that the timing and quantity of sleep is controlled by two main processes, the circadian clock and the sleep homeostat. However, while this model has provided an important framework for understanding sleep, we now must try to understand and model how external and internal factors can perturb or interfere with sleep regulation. We see two main ways in which to incorporate environmental factors into the model of sleep regulation. One interpretation is that all the factors that affect sleep are modulators of the sleep homeostat. Under this scenario the two-process model remains intact but incorporates several layers of regulation within the S process and perhaps Process C (**Figure 4**, left panel). Alternatively, external factors composing a third process (Process E), or even several new processes (as many as factors can be identified) can be added to the model as direct regulators of sleep. This latter interpretation would have a corollary: process C informs the timing of sleep; process S encodes the need to sleep based purely on the tiredness; and Process E will antagonise or synergise with the need to sleep based on perceived weight of competing behavioural drives (e.g., need to eat or mate) (**Figure 4**, right panel). Importantly all these processes should convey the information to a centralised sleep arm that ultimately triggers the behaviour. Beyond this latter and favoured explanation, the fact that temperature, food availability, and social experience can regulate sleep suggests a high level of plasticity: sleep is context dependent and relative to many of the needs of the individual.

AUTHOR CONTRIBUTIONS

Both authors listed have made a substantial, direct and equal intellectual contribution to the work, and approved it for publication.

FUNDING

EB was supported by the People Programme (Marie Curie Actions) of European Union's Eighth Framework Programme H2020 under REA grant agreement 705930. AF was supported by the BBSRC through BB/R018839/1.

ACKNOWLEDGMENTS

We are grateful to Frédéric Marion-Poll, Nara I. Muraro, Quentin Geissmann, and Edward Harding for their invaluable input and critical review of the manuscript. We thank all former and current members of the Gilestro Laboratory, as well as the fly community at the Life Sciences Department of the Imperial College London for the innumerable discussions and the constant support. We also thank the authors who contributed to the discussed literature and we apologies in advance to the authors whose contributions may have been omitted or were not mentioned because of space constraints.

REFERENCES

Aho, V., Vainikka, M., Puttonen, H. A. J., Ikonen, H. M. K., Salminen, T., Panula, P., et al. (2017). Homeostatic response to sleep/rest deprivation by constant water flow in larval zebrafish in both dark and light conditions. *J. Sleep Res.* 26, 394–400. doi: 10.1111/jsr.12508

Anafi, R. C., Kayser, M. S., and Raizen, D. M. (2019). Exploring phylogeny to find the function of sleep. *Nat. Rev. Neurosci.* 20, 109–116. doi: 10.1038/s41583-018-0098-9

Andretic, R., Kim, Y. C., Jones, F. S., Han, K. A., and Greenspan, R. J. (2008). Drosophila D1 dopamine receptor mediates caffeine-induced arousal. *Proc. Natl. Acad. Sci. U.S.A.* 105, 20392–20397. doi: 10.1073/pnas.0806776105

Armitage, R. (2007). Sleep and circadian rhythms in mood disorders. *Acta Psychiatr. Scand. Suppl.* 104–115. doi: 10.1111/j.1600-0447.2007.00968.x

Aso, Y., Hattori, D., Yu, Y., Johnston, R. M., Iyer, N. A., Ngo, T. T., et al. (2014). The neuronal architecture of the mushroom body provides a logic for associative learning. *eLife* 3:e04577. doi: 10.7554/eLife.04577

Beckwith, E. J., Geissmann, Q., French, A. S., and Gilestro, G. F. (2017). Regulation of sleep homeostasis by sexual arousal. *eLife* 6:e27445. doi: 10.7554/eLife.27445

Bell, W. J., Tortorici, C., Roggero, R. J., Kipp, L. R., and Tobin, T. R. (1985). Sucrose-stimulated searching behavior of drosophila-melanogaster in a uniform habitat - modulation by period of deprivation. *Anim. Behav.* 33, 436–448. doi: 10.1016/s0003-3472(85)80068-3

Besedovsky, L., Lange, T., and Haack, M. (2019). The sleep-immune crosstalk in health and disease. *Physiol. Rev.* 99, 1325–1380. doi: 10.1152/physrev.00010.2018

Beyaert, L., Greggers, U., and Menzel, R. (2012). Honeybees consolidate navigation memory during sleep. *J. Exp. Biol.* 215, 3981–3988. doi: 10.1242/jeb.075499

Borbély, A. A. (1982). A two process model of sleep regulation. *Hum. Neurobiol.* 1, 195–204.

Bushey, D., Tononi, G., and Cirelli, C. (2011). Sleep and synaptic homeostasis: structural evidence in *Drosophila*. *Science* 332, 1576–1581. doi: 10.1126/science.1202839

Catterson, J. H., Knowles-Barley, S., James, K., Heck, M. M., Harmar, A. J., and Hartley, P. S. (2010). Dietary modulation of *Drosophila* sleep-wake behaviour. *PLoS One* 5:e12062. doi: 10.1371/journal.pone.0012062

Chen, D., Sitaraman, D., Chen, N., Jin, X., Han, C., Chen, J., et al. (2017). Genetic and neuronal mechanisms governing the sex-specific interaction between sleep and sexual behaviors in *Drosophila*. *Nat. Commun.* 8:154. doi: 10.1038/s41467-017-00087-5

Chen, J. T., Reiher, W., Hermann-Luibl, C., Sellami, A., Cognigni, P., Kondo, S., et al. (2016). Allatostatin a signalling in drosophila regulates feeding and sleep and is modulated by PDF. *PLoS Genet.* 12:e1006346. doi: 10.1371/journal.pgen.1006346

Chen, W. F., Low, K. H., Lim, C., and Edery, I. (2007). Thermosensitive splicing of a clock gene and seasonal adaptation. *Cold Spring Harb. Symp. Quant. Biol.* 72, 599–606. doi: 10.1101/sqb.2007.72.021

Chi, M. W., Griffith, L. C., and Vecsey, C. G. (2014). Larval population density alters adult sleep in wild-type *Drosophila melanogaster* but not in amnesiac mutant flies. *Brain Sci.* 4, 453–470. doi: 10.3390/brainsci4030453

Chung, B. Y., Ro, J., Hutter, S. A., Miller, K. M., Guduguntla, L. S., Kondo, S., et al. (2017). *Drosophila* neuropeptide F signaling independently regulates feeding and sleep-wake behavior. *Cell Rep.* 19, 2441–2450. doi: 10.1016/j.celrep.2017.05.085

Coelho, A., Fraichard, S., Le Goff, G., Faure, P., Artur, Y., Ferveur, J. F., et al. (2015). Cytochrome P450-dependent metabolism of caffeine in *Drosophila melanogaster*. *PLoS One* 10:e0117328. doi: 10.1371/journal.pone.0117328

Cognigni, P., Felsenberg, J., and Waddell, S. (2018). Do the right thing: neural network mechanisms of memory formation, expression and update in *Drosophila*. *Curr. Opin. Neurobiol.* 49, 51–58. doi: 10.1016/j.conb.2017.12.002

Cong, X., Wang, H., Liu, Z., He, C., An, C., and Zhao, Z. (2015). Regulation of sleep by insulin-like peptide system in *Drosophila melanogaster*. *Sleep* 38, 1075–1083. doi: 10.5665/sleep.4816

Connolly, K. (1966). Locomotor activity in *Drosophila*. II. Selection for active and inactive strains. *Anim. Behav.* 14, 444–449. doi: 10.1016/s0003-3472(66)80043-x

Crocker, A., and Sehgal, A. (2008). Octopamine regulates sleep in drosophila through protein kinase A-dependent mechanisms. *J. Neurosci.* 28, 9377–9385. doi: 10.1523/JNEUROSCI.3072-08a.2008

Crocker, A., Shahidullah, M., Levitan, I. B., and Sehgal, A. (2010). Identification of a neural circuit that underlies the effects of octopamine on sleep:wake behavior. *Neuron* 65, 670–681. doi: 10.1016/j.neuron.2010.01.032

Crowley, M., and Bovet, J. (1980). Social synchronization of circadian-rhythms in Deer Mice (Peromyscus-Maniculatus). *Behav. Ecol. Sociobiol.* 7, 99–105. doi: 10.1007/bf00299514

Currie, J., Goda, T., and Wijnen, H. (2009). Selective entrainment of the *Drosophila* circadian clock to daily gradients in environmental temperature. *BMC Biol.* 7:49. doi: 10.1186/1741-7007-7-49

Danguir, J., Nicolaidis, S., and Gerard, H. (1979). Relations between feeding and sleep patterns in the rat. *J. Comp. Physiol. Psychol.* 93, 820–830. doi: 10.1037/h0077616

Davidson, A. J., and Menaker, M. (2003). Birds of a feather clock together–sometimes: social synchronization of circadian rhythms. *Curr. Opin. Neurobiol.* 13, 765–769. doi: 10.1016/j.conb.2003.10.011

Dillon, M. E., Wang, G., Garrity, P. A., and Huey, R. B. (2009). Review: thermal preference in *Drosophila*. *J. Therm. Biol.* 34, 109–119. doi: 10.1016/j.jtherbio.2008.11.007

Donlea, J., Leahy, A., Thimgan, M. S., Suzuki, Y., Hughson, B. N., Sokolowski, M. B., et al. (2012). Foraging alters resilience/vulnerability to sleep disruption and starvation in *Drosophila*. *Proc. Natl. Acad. Sci. U.S.A.* 109, 2613–2618. doi: 10.1073/pnas.1112623109

Donlea, J. M. (2017). Neuronal and molecular mechanisms of sleep homeostasis. *Curr. Opin. Insect. Sci.* 24, 51–57. doi: 10.1016/j.cois.2017.09.008

Donlea, J. M., Pimentel, D., Talbot, C. B., Kempf, A., Omoto, J. J., Hartenstein, V., et al. (2018). Recurrent circuitry for balancing sleep need and sleep. *Neuron* 97, 378.e4–389.e4. doi: 10.1016/j.neuron.2017.12.016

Donlea, J. M., Ramanan, N., and Shaw, P. J. (2009). Use-dependent plasticity in clock neurons regulates sleep need in *Drosophila*. *Science* 324, 105–108. doi: 10.1126/science.1166657

Eban-Rothschild, A., and Bloch, G. (2012). Social influences on circadian rhythms and sleep in insects. *Adv. Genet.* 77, 1–32. doi: 10.1016/B978-0-12-387687-4.00001-5

Eban-Rothschild, A., and Bloch, G. (2015). The colony environment modulates sleep in honey bee workers. *J. Exp. Biol.* 218, 404–411. doi: 10.1242/jeb.110619

Eban-Rothschild, A., Rothschild, G., Giardino, W. J., Jones, J. R., and De Lecea, L. (2016). VTA dopaminergic neurons regulate ethologically relevant sleep-wake behaviors. *Nat. Neurosci.* 19, 1356–1366. doi: 10.1038/nn.4377

Feld, G. B., and Born, J. (2017). Sculpting memory during sleep: concurrent consolidation and forgetting. *Curr. Opin. Neurobiol.* 44, 20–27. doi: 10.1016/j.conb.2017.02.012

Fuchikawa, T., Eban-Rothschild, A., Nagari, M., Shemesh, Y., and Bloch, G. (2016). Potent social synchronization can override photic entrainment of circadian rhythms. *Nat. Commun.* 7:11662. doi: 10.1038/ncomms11662

Fujii, S., Kaushik, M. K., Zhou, X., Korkutata, M., and Lazarus, M. (2019). Acute social defeat stress increases sleep in mice. *Front. Neurosci.* 13:322. doi: 10.3389/fnins.2019.00322

Fujii, S., Krishnan, P., Hardin, P., and Amrein, H. (2007). Nocturnal male sex drive in *Drosophila*. *Curr. Biol.* 17, 244–251. doi: 10.1016/j.cub.2006.11.049

Ganguly-Fitzgerald, I., Donlea, J., and Shaw, P. J. (2006). Waking experience affects sleep need in *Drosophila*. *Science* 313, 1775–1781. doi: 10.1126/science.1130408

Garbe, D. S., Bollinger, W. L., Vigderman, A., Masek, P., Gertowski, J., Sehgal, A., et al. (2015). Context-specific comparison of sleep acquisition systems in *Drosophila*. *Biol. Open* 4, 1558–1568. doi: 10.1242/bio.013011

Garbe, D. S., Vigderman, A. S., Moscato, E., Dove, A. E., Vecsey, C. G., Kayser, M. S., et al. (2016). Changes in female *Drosophila* sleep following mating are mediated by SPSN-SAG neurons. *J. Biol. Rhythms* 31, 551–567. doi: 10.1177/0748730416668048

Geissmann, Q., Beckwith, E. J., and Gilestro, G. F. (2019a). Most sleep does not serve a vital function: evidence from *Drosophila melanogaster*. *Sci. Adv.* 5:eaau9253. doi: 10.1126/sciadv.aau9253

Geissmann, Q., Garcia Rodriguez, L., Beckwith, E. J., and Gilestro, G. F. (2019b). Rethomics: an R framework to analyse high-throughput behavioural data. *PLoS One* 14:e0209331. doi: 10.1371/journal.pone.0209331

Gendron, C. M., Kuo, T. H., Harvanek, Z. M., Chung, B. Y., Yew, J. Y., Dierick, H. A., et al. (2014). Drosophila life span and physiology are modulated by sexual perception and reward. *Science* 343, 544–548. doi: 10.1126/science.1243339

Giardina, T. J., Clark, A. G., and Fiumera, A. C. (2017). Estimating mating rates in wild *Drosophila melanogaster* females by decay rates of male reproductive proteins in their reproductive tracts. *Mol. Ecol. Resour.* 17, 1202–1209. doi: 10.1111/1755-0998.12661

Gilestro, G. F., Tononi, G., and Cirelli, C. (2009). Widespread changes in synaptic markers as a function of sleep and wakefulness in *Drosophila*. *Science* 324, 109–112. doi: 10.1126/science.1166673

Goldstein, N., Levine, B. J., Loy, K. A., Duke, W. L., Meyerson, O. S., Jamnik, A. A., et al. (2018). Hypothalamic neurons that regulate feeding can influence sleep/wake states based on homeostatic need. *Curr. Biol.* 28, 3736.e3–3747e.3. doi: 10.1016/j.cub.2018.09.055

Greenspan, R. J., and Ferveur, J. F. (2000). Courtship in *Drosophila*. *Annu. Rev. Genet.* 34, 205–232.

Greer, S. M., Goldstein, A. N., and Walker, M. P. (2013). The impact of sleep deprivation on food desire in the human brain. *Nat. Commun.* 4:2259. doi: 10.1038/ncomms3259

Guo, F., Yu, J., Jung, H. J., Abruzzi, K. C., Luo, W., Griffith, L. C., et al. (2016). Circadian neuron feedback controls the *Drosophila* sleep–activity profile. *Nature* 536, 292–297. doi: 10.1038/nature19097

Hamada, F. N., Rosenzweig, M., Kang, K., Pulver, S. R., Ghezzi, A., Jegla, T. J., et al. (2008). An internal thermal sensor controlling temperature preference in *Drosophila*. *Nature* 454, 217–220. doi: 10.1038/nature07001

Haraszti, R. A., Ella, K., Gyongyosi, N., Roenneberg, T., and Kaldi, K. (2014). Social jetlag negatively correlates with academic performance in undergraduates. *Chronobiol. Int.* 31, 603–612. doi: 10.3109/07420528.2013.879164

Harding, E. C., Yu, X., Miao, A., Andrews, N., Ma, Y., Ye, Z., et al. (2018). A neuronal hub binding sleep initiation and body cooling in response to a warm external stimulus. *Curr. Biol.* 28, 2263.e4–2273.e4. doi: 10.1016/j.cub.2018.05.054

Harvanek, Z. M., Lyu, Y., Gendron, C. M., Johnson, J. C., Kondo, S., Promislow, D. E. L., et al. (2017). Perceptive costs of reproduction drive ageing and physiology in male *Drosophila*. *Nat. Ecol. Evol.* 1:152. doi: 10.1038/s41559-017-0152

Hasegawa, T., Tomita, J., Hashimoto, R., Ueno, T., Kume, S., and Kume, K. (2017). Sweetness induces sleep through gustatory signalling independent of nutritional value in a starved fruit fly. *Sci. Rep.* 7:14355. doi: 10.1038/s41598-017-14608-1

Helfrich-Forster, C. (2018). Sleep in insects. *Annu. Rev. Entomol.* 63, 69–86. doi: 10.1146/annurev-ento-020117-043201

Henderson, F., Vialou, V., El Mestikawy, S., and Fabre, V. (2017). Effects of social defeat stress on sleep in mice. *Front. Behav. Neurosci.* 11:227. doi: 10.3389/fnbeh.2017.00227

Hendricks, J. C., Finn, S. M., Panckeri, K. A., Chavkin, J., Williams, J. A., Sehgal, A., et al. (2000). Rest in *Drosophila* is a sleep-like state. *Neuron* 25, 129–138. doi: 10.1016/s0896-6273(00)80877-6

Hergarden, A. C., Tayler, T. D., and Anderson, D. J. (2012). Allatostatin-A neurons inhibit feeding behavior in adult Drosophila. *Proc. Natl. Acad. Sci. U.S.A.* 109, 3967–3972. doi: 10.1073/pnas.1200778109

Higgins, L. A., Jones, K. M., and Wayne, M. L. (2005). Quantitative genetics of natural variation of behavior in *Drosophila melanogaster*: the possible role of the social environment on creating persistent patterns of group activity. *Evolution* 59, 1529–1539. doi: 10.1111/j.0014-3820.2005.tb01802.x

Hill, V. M., O'connor, R. M., Sissoko, G. B., Irobunda, I. S., Leong, S., Canman, J. C., et al. (2018). A bidirectional relationship between sleep and oxidative stress in *Drosophila*. *PLoS Biol.* 16:e2005206. doi: 10.1371/journal.pbio.2005206

Hoyer, S. C., Eckart, A., Herrel, A., Zars, T., Fischer, S. A., Hardie, S. L., et al. (2008). Octopamine in male aggression of *Drosophila*. *Curr. Biol.* 18, 159–167. doi: 10.1016/j.cub.2007.12.052

Hua, R., Wang, X., Chen, X., Wang, X., Huang, P., Li, P., et al. (2018). Calretinin neurons in the midline thalamus modulate starvation-induced arousal. *Curr. Biol.* 28, 3948.e4–3959.e4. doi: 10.1016/j.cub.2018.11.020

Huang, Z. L., Qu, W. M., Eguchi, N., Chen, J. F., Schwarzschild, M. A., Fredholm, B. B., et al. (2005). Adenosine A2(A), but not A(1), receptors mediate the arousal effect of caffeine. *Nat. Neurosci.* 8, 858–859. doi: 10.1038/nn1491

Inagaki, H. K., Panse, K. M., and Anderson, D. J. (2014). Independent, reciprocal neuromodulatory control of sweet and bitter taste sensitivity during starvation in *Drosophila*. *Neuron* 84, 806–820. doi: 10.1016/j.neuron.2014.09.032

Isaac, R. E., Li, C., Leedale, A. E., and Shirras, A. D. (2010). Drosophila male sex peptide inhibits siesta sleep and promotes locomotor activity in the post-mated female. *Proc. Biol. Sci.* 277, 65–70. doi: 10.1098/rspb.2009.1236

Isabel, G., Martin, J. R., Chidami, S., Veenstra, J. A., and Rosay, P. (2005). AKH-producing neuroendocrine cell ablation decreases trehalose and induces behavioral changes in *Drosophila*. *Am. J. Physiol. Regul. Integr. Comp. Physiol.* 288, R531–R538.

Ishimoto, H., Lark, A., and Kitamoto, T. (2012). Factors that differentially affect daytime and nighttime sleep in *Drosophila melanogaster*. *Front. Neurol.* 3:24. doi: 10.3389/fneur.2012.00024

Jeong, Y. T., Shim, J., Oh, S. R., Yoon, H. I., Kim, C. H., Moon, S. J., et al. (2013). An odorant-binding protein required for suppression of sweet taste by bitter chemicals. *Neuron* 79, 725–737. doi: 10.1016/j.neuron.2013.06.025

Kain, J., Stokes, C., Gaudry, Q., Song, X., Foley, J., Wilson, R., et al. (2013). Leg-tracking and automated behavioural classification in *Drosophila*. *Nat. Commun.* 4:1910. doi: 10.1038/ncomms2908

Kavaliers, M. (1980). Social groupings and circadian activity of the Killifish, Fundulus-Heteroclitus. *Biol. Bull.* 158, 69–76. doi: 10.2307/1540759

Kayser, M. S., and Biron, D. (2016). Sleep and development in genetically tractable model organisms. *Genetics* 203, 21–33. doi: 10.1534/genetics.116.189589

Kayser, M. S., Mainwaring, B., Yue, Z., and Sehgal, A. (2015). Sleep deprivation suppresses aggression in *Drosophila*. *eLife* 4:e07643. doi: 10.7554/eLife.07643

Kayser, M. S., Yue, Z., and Sehgal, A. (2014). A critical period of sleep for development of courtship circuitry and behavior in *Drosophila*. *Science* 344, 269–274. doi: 10.1126/science.1250553

Keebaugh, E. S., Park, J. H., Su, C., Yamada, R., and Ja, W. W. (2017). Nutrition influences caffeine-mediated sleep loss in *Drosophila*. *Sleep* 40:zsx146. doi: 10.1093/sleep/zsx146

Keene, A. C., Duboue, E. R., Mcdonald, D. M., Dus, M., Suh, G. S., Waddell, S., et al. (2010). Clock and cycle limit starvation-induced sleep loss in *Drosophila*. *Curr. Biol.* 20, 1209–1215. doi: 10.1016/j.cub.2010.05.029

Kempf, A., Song, S. M., Talbot, C. B., and Miesenbock, G. (2019). A potassium channel beta-subunit couples mitochondrial electron transport to sleep. *Nature* 568, 230–234. doi: 10.1038/s41586-019-1034-5

Kent, C. F., Daskalchuk, T., Cook, L., Sokolowski, M. B., and Greenspan, R. J. (2009). The *Drosophila* foraging gene mediates adult plasticity and gene-environment interactions in behaviour, metabolites, and gene expression in response to food deprivation. *PLoS Genet.* 5:e1000609. doi: 10.1371/journal.pgen.1000609

Klerman, E. B., Rimmer, D. W., Dijk, D. J., Kronauer, R. E., Rizzo, J. F. III, and Czeisler, C. A. (1998). Nonphotic entrainment of the human circadian pacemaker. *Am. J. Physiol.* 274, R991–R996.

Klibaite, U., Berman, G. J., Cande, J., Stern, D. L., and Shaevitz, J. W. (2017). An unsupervised method for quantifying the behavior of paired animals. *Phys. Biol.* 14:015006. doi: 10.1088/1478-3975/aa5c50

Ko, K. I., Root, C. M., Lindsay, S. A., Zaninovich, O. A., Shepherd, A. K., Wasserman, S. A., et al. (2015). Starvation promotes concerted modulation of appetitive olfactory behavior via parallel neuromodulatory circuits. *eLife* 4:e08298. doi: 10.7554/eLife.08298

Koban, M., Sita, L. V., Le, W. W., and Hoffman, G. E. (2008). Sleep deprivation of rats: the hyperphagic response is real. *Sleep* 31, 927–933.

Kobayashi, I., Boarts, J. M., and Delahanty, D. L. (2007). Polysomnographically measured sleep abnormalities in PTSD: a meta-analytic review. *Psychophysiology* 44, 660–669. doi: 10.1111/j.1469-8986.2007.00537.x

Komagata, N., Latifi, B., Rusterholz, T., Bassetti, C. L. A., Adamantidis, A., and Schmidt, M. H. (2019). Dynamic REM sleep modulation by ambient temperature and the critical role of the melanin-concentrating hormone system. *Curr. Biol.* 29, 1976.e4–1987.e4. doi: 10.1016/j.cub.2019.05.009

Krause, A. J., Simon, E. B., Mander, B. A., Greer, S. M., Saletin, J. M., Goldstein-Piekarski, A. N., et al. (2017). The sleep-deprived human brain. *Nat. Rev. Neurosci.* 18, 404–418. doi: 10.1038/nrn.2017.55

Kravitz, E. A., and Fernandez, M. P. (2015). Aggression in *Drosophila*. *Behav. Neurosci.* 129, 549–563. doi: 10.1037/bne0000089

Kunst, M., Hughes, M. E., Raccuglia, D., Felix, M., Li, M., Barnett, G., et al. (2014). Calcitonin gene-related peptide neurons mediate sleep-specific circadian output in *Drosophila*. *Curr. Biol.* 24, 2652–2664. doi: 10.1016/j.cub.2014.09.077

Lamaze, A., Ozturk-Colak, A., Fischer, R., Peschel, N., Koh, K., and Jepson, J. E. (2017). Regulation of sleep plasticity by a thermo-sensitive circuit in *Drosophila*. *Sci. Rep.* 7:40304. doi: 10.1038/srep40304

Landayan, D., Feldman, D. S., and Wolf, F. W. (2018). Satiation state-dependent dopaminergic control of foraging in *Drosophila*. *Sci. Rep.* 8:5777. doi: 10.1038/s41598-018-24217-1

Lastella, M., O'mullan, C., Paterson, J. L., and Reynolds, A. C. (2019). Sex and sleep: perceptions of sex as a sleep promoting behavior in the general adult population. *Front. Public Health* 7:33. doi: 10.3389/fpubh.2019.00033

LeDue, E. E., Mann, K., Koch, E., Chu, B., Dakin, R., and Gordon, M. D. (2016). Starvation-induced depotentiation of bitter taste in *Drosophila*. *Curr. Biol.* 26, 2854–2861. doi: 10.1016/j.cub.2016.08.028

Lee, G., and Park, J. H. (2004). Hemolymph sugar homeostasis and starvation-induced hyperactivity affected by genetic manipulations of the adipokinetic hormone-encoding gene in *Drosophila melanogaster*. *Genetics* 167, 311–323. doi: 10.1534/genetics.167.1.311

Lee, Y., Moon, S. J., and Montell, C. (2009). Multiple gustatory receptors required for the caffeine response in *Drosophila*. *Proc. Natl. Acad. Sci. U.S.A.* 106, 4495–4500. doi: 10.1073/pnas.0811744106

Leitao-Goncalves, R., Carvalho-Santos, Z., Francisco, A. P., Fioreze, G. T., Anjos, M., Baltazar, C., et al. (2017). Commensal bacteria and essential amino acids control food choice behavior and reproduction. *PLoS Biol.* 15:e2000862. doi: 10.1371/journal.pbio.2000862

Lesku, J. A., Rattenborg, N. C., Valcu, M., Vyssotski, A. L., Kuhn, S., Kuemmeth, F., et al. (2012). Adaptive sleep loss in polygynous pectoral sandpipers. *Science* 337, 1654–1658. doi: 10.1126/science.1220939

Levine, J. D., Funes, P., Dowse, H. B., and Hall, J. C. (2002). Resetting the circadian clock by social experience in *Drosophila melanogaster*. *Science* 298, 2010–2012. doi: 10.1126/science.1076008

Linford, N. J., Chan, T. P., and Pletcher, S. D. (2012). Re-patterning sleep architecture in *Drosophila* through gustatory perception and nutritional quality. *PLoS Genet.* 8:e1002668. doi: 10.1371/journal.pgen.1002668

Linford, N. J., Ro, J., Chung, B. Y., and Pletcher, S. D. (2015). Gustatory and metabolic perception of nutrient stress in *Drosophila*. *Proc. Natl. Acad. Sci. U.S.A.* 112, 2587–2592. doi: 10.1073/pnas.1401501112

Liu, C., Haynes, P. R., Donelson, N. C., Aharon, S., and Griffith, L. C. (2015). Sleep in populations of Drosophila Melanogaster. *eNeuro* 2:ENEURO.0071-15.2015. doi: 10.1523/ENEURO.0071-15.2015

Liu, C., Placais, P. Y., Yamagata, N., Pfeiffer, B. D., Aso, Y., Friedrich, A. B., et al. (2012). A subset of dopamine neurons signals reward for odour memory in *Drosophila*. *Nature* 488, 512–516. doi: 10.1038/nature11304

Liu, G., Nath, T., Linneweber, G. A., Claeys, A., Guo, Z., Li, J., et al. (2018). A simple computer vision pipeline reveals the effects of isolation on social interaction dynamics in *Drosophila*. *PLoS Comput. Biol.* 14:e1006410. doi: 10.1371/journal.pcbi.1006410

Liu, S., Liu, Q., Tabuchi, M., and Wu, M. N. (2016). Sleep drive is encoded by neural plastic changes in a dedicated circuit. *Cell* 165, 1347–1360. doi: 10.1016/j.cell.2016.04.013

Lone, S. R., Potdar, S., Srivastava, M., and Sharma, V. K. (2016). Social experience is sufficient to modulate sleep need of *Drosophila* without increasing wakefulness. *PLoS One* 11:e0150596. doi: 10.1371/journal.pone.0150596

Low, K. H., Lim, C., Ko, H. W., and Edery, I. (2008). Natural variation in the splice site strength of a clock gene and species-specific thermal adaptation. *Neuron* 60, 1054–1067. doi: 10.1016/j.neuron.2008.10.048

Machado, D. R., Afonso, D. J., Kenny, A. R., Oztu Rk-Colak, A., Moscato, E. H., Mainwaring, B., et al. (2017). Identification of octopaminergic neurons that modulate sleep suppression by male sex drive. *eLife* 6:e23130. doi: 10.7554/eLife.23130

Maguire, S. E., and Sehgal, A. (2015). Heating and cooling the *Drosophila melanogaster* clock. *Curr. Opin. Insect. Sci.* 7, 71–75. doi: 10.1016/j.cois.2014.12.007

Majercak, J., Chen, W. F., and Edery, I. (2004). Splicing of the period gene 3′-terminal intron is regulated by light, circadian clock factors, and phospholipase C. *Mol. Cell Biol.* 24, 3359–3372. doi: 10.1128/mcb.24.8.3359-3372.2004

Majercak, J., Sidote, D., Hardin, P. E., and Edery, I. (1999). How a circadian clock adapts to seasonal decreases in temperature and day length. *Neuron* 24, 219–230. doi: 10.1016/s0896-6273(00)80834-x

Marella, S., Fischler, W., Kong, P., Asgarian, S., Rueckert, E., and Scott, K. (2006). Imaging taste responses in the fly brain reveals a functional map of taste category and behavior. *Neuron* 49, 285–295. doi: 10.1016/j.neuron.2005.11.037

Markwald, R. R., Melanson, E. L., Smith, M. R., Higgins, J., Perreault, L., Eckel, R. H., et al. (2013). Impact of insufficient sleep on total daily energy expenditure, food intake, and weight gain. *Proc. Natl. Acad. Sci. U.S.A.* 110, 5695–5700. doi: 10.1073/pnas.1216951110

Masek, P., Reynolds, L. A., Bollinger, W. L., Moody, C., Mehta, A., Murakami, K., et al. (2014). Altered regulation of sleep and feeding contributes to starvation resistance in *Drosophila melanogaster*. *J. Exp. Biol.* 217, 3122–3132. doi: 10.1242/jeb.103309

Maximino, C., Lima, M. G., Olivera, K. R., Picanco-Diniz, D. L., and Herculano, A. M. (2011). Adenosine A1, but not A2, receptor blockade increases anxiety and arousal in Zebrafish. *Basic Clin. Pharmacol. Toxicol.* 109, 203–207. doi: 10.1111/j.1742-7843.2011.00710.x

Melnattur, K., and Shaw, P. (2019). Staying awake to stay alive: a circuit controlling starvation-induced waking. *PLoS Biol.* 17:e3000199. doi: 10.1371/journal.pbio.3000199

Menaker, M., and Eskin, A. (1966). Entrainment of circadian rhythms by sound in *Passer domesticus*. *Science* 154, 1579–1581. doi: 10.1126/science.154.3756.1579

Meunier, N., Belgacem, Y. H., and Martin, J. R. (2007). Regulation of feeding behaviour and locomotor activity by takeout in *Drosophila*. *J. Exp. Biol.* 210, 1424–1434. doi: 10.1242/jeb.02755

Moon, S. J., Kottgen, M., Jiao, Y., Xu, H., and Montell, C. (2006). A taste receptor required for the caffeine response in vivo. *Curr. Biol.* 16, 1812–1817. doi: 10.1016/j.cub.2006.07.024

Morairty, S. R., Szymusiak, R., Thomson, D., and Mcginty, D. J. (1993). Selective increases in non-rapid eye movement sleep following whole body heating in rats. *Brain Res.* 617, 10–16. doi: 10.1016/0006-8993(93)90606-n

Murakami, K., Yurgel, M. E., Stahl, B. A., Masek, P., Mehta, A., Heidker, R., et al. (2016). translin is required for metabolic regulation of sleep. *Curr. Biol.* 26, 972–980. doi: 10.1016/j.cub.2016.02.013

Murphy, K. R., Deshpande, S. A., Yurgel, M. E., Quinn, J. P., Weissbach, J. L., Keene, A. C., et al. (2016). Postprandial sleep mechanics in *Drosophila*. *eLife* 5:e19334. doi: 10.7554/eLife.19334

Nall, A. H., Shakhmantsir, I., Cichewicz, K., Birman, S., Hirsh, J., and Sehgal, A. (2016). Caffeine promotes wakefulness via dopamine signaling in *Drosophila*. *Sci. Rep.* 6:20938. doi: 10.1038/srep20938

Olini, N., Rothfuchs, I., Azzinnari, D., Pryce, C. R., Kurth, S., and Huber, R. (2017). Chronic social stress leads to altered sleep homeostasis in mice. *Behav. Brain Res.* 327, 167–173. doi: 10.1016/j.bbr.2017.03.022

Panagiotou, M., Meijer, M., Meijer, J. H., and Deboer, T. (2018). Effects of chronic caffeine consumption on sleep and the sleep electroencephalogram in mice. *J. Psychopharmacol.* doi: 10.1177/0269881118806300 [Epub ahead of print].

Panda, S. (2016). Circadian physiology of metabolism. *Science* 354, 1008–1015. doi: 10.1126/science.aah4967

Parisky, K. M., Agosto Rivera, J. L., Donelson, N. C., Kotecha, S., and Griffith, L. C. (2016). Reorganization of sleep by temperature in *Drosophila* requires light, the homeostat, and the circadian clock. *Curr. Biol.* 26, 882–892. doi: 10.1016/j.cub.2016.02.011

Park, J. H., and Kwon, J. Y. (2011). Heterogeneous expression of *Drosophila* gustatory receptors in enteroendocrine cells. *PLoS One* 6:e29022. doi: 10.1371/journal.pone.0029022

Perez-Escudero, A., Vicente-Page, J., Hinz, R. C., Arganda, S., and De Polavieja, G. G. (2014). idTracker: tracking individuals in a group by automatic identification of unmarked animals. *Nat. Methods* 11, 743–748. doi: 10.1038/nmeth.2994

Potdar, S., Daniel, D. K., Thomas, F. A., Lall, S., and Sheeba, V. (2018). Sleep deprivation negatively impacts reproductive output in *Drosophila melanogaster*. *J. Exp. Biol.* 221(Pt 6):jeb174771. doi: 10.1242/jeb.174771

Ramdya, P., Lichocki, P., Cruchet, S., Frisch, L., Tse, W., Floreano, D., et al. (2015). Mechanosensory interactions drive collective behaviour in *Drosophila*. *Nature* 519, 233–236. doi: 10.1038/nature14024

Ramdya, P., Schneider, J., and Levine, J. D. (2017). The neurogenetics of group behavior in *Drosophila melanogaster*. *J. Exp. Biol.* 220, 35–41. doi: 10.1242/jeb.141457

Ramin, M., Li, Y. Y., Chang, W. T., Shaw, H., and Rao, Y. (2019). The peacefulness gene promotes aggression in *Drosophila*. *Mol. Brain* 12:1. doi: 10.1186/s13041-018-0417-0

Rattenborg, N. C., De La Iglesia, H. O., Kempenaers, B., Lesku, J. A., Meerlo, P., and Scriba, M. F. (2017). Sleep research goes wild: new methods and approaches to investigate the ecology, evolution and functions of sleep. *Philos. Trans. R. Soc. Lond. B Biol. Sci.* 372:20160251. doi: 10.1098/rstb.2016.0251

Rattenborg, N. C., Lima, S. L., and Amlaner, C. J. (1999). Half-awake to the risk of predation. *Nature* 397, 397–398. doi: 10.1038/17037

Raymann, R. J., Swaab, D. F., and Van Someren, E. J. (2008). Skin deep: enhanced sleep depth by cutaneous temperature manipulation. *Brain* 131, 500–513. doi: 10.1093/brain/awm315

Regalado, J. M., Cortez, M. B., Grubbs, J., Link, J. A., Van Der Linden, A., and Zhang, Y. (2017). Increased food intake after starvation enhances sleep in *Drosophila melanogaster*. *J. Genet. Genomics* 44, 319–326. doi: 10.1016/j.jgg.2017.05.006

Roenneberg, T., Allebrandt, K. V., Merrow, M., and Vetter, C. (2012). Social jetlag and obesity. *Curr. Biol.* 22, 939–943. doi: 10.1016/j.cub.2012.03.038

Roenneberg, T., and Merrow, M. (2007). Entrainment of the human circadian clock. *Cold Spring Harb. Symp. Quant. Biol.* 72, 293–299. doi: 10.1101/sqb.2007.72.043

Root, C. M., Ko, K. I., Jafari, A., and Wang, J. W. (2011). Presynaptic facilitation by neuropeptide signaling mediates odor-driven food search. *Cell* 145, 133–144. doi: 10.1016/j.cell.2011.02.008

Ruan, H. Y., and Wu, C. F. (2008). Social interaction-mediated lifespan extension of *Drosophila* Cu/Zn superoxide dismutase mutants. *Proc. Natl. Acad. Sci. U.S.A.* 105, 7506–7510. doi: 10.1073/pnas.0711127105

Scaplen, K. M., Mei, N. J., Bounds, H. A., Song, S. L., Azanchi, R., and Kaun, K. R. (2019). Automated real-time quantification of group locomotor activity in *Drosophila melanogaster*. *Sci. Rep.* 9:4427. doi: 10.1038/s41598-019-40952-5

Scheiner, R., Sokolowski, M. B., and Erber, J. (2004). Activity of cGMP-dependent protein kinase (PKG) affects sucrose responsiveness and habituation in *Drosophila melanogaster*. *Learn. Mem.* 11, 303–311. doi: 10.1101/lm.71604

Schneider, J., Atallah, J., and Levine, J. D. (2012). One, two, and many–a perspective on what groups of *Drosophila melanogaster* can tell us about social dynamics. *Adv. Genet.* 77, 59–78. doi: 10.1016/B978-0-12-387687-4.00003-9

Selkrig, J., Mohammad, F., Ng, S. H., Chua, J. Y., Tumkaya, T., Ho, J., et al. (2018). The *Drosophila* microbiome has a limited influence on sleep, activity, and courtship behaviors. *Sci. Rep.* 8:10646. doi: 10.1038/s41598-018-28764-5

Seugnet, L., Suzuki, Y., Donlea, J. M., Gottschalk, L., and Shaw, P. J. (2011). Sleep deprivation during early-adult development results in long-lasting learning deficits in adult *Drosophila*. *Sleep* 34, 137–146. doi: 10.1093/sleep/34.2.137

Sharon, G., Segal, D., Ringo, J. M., Hefetz, A., Zilber-Rosenberg, I., and Rosenberg, E. (2010). Commensal bacteria play a role in mating preference of *Drosophila melanogaster*. *Proc. Natl. Acad. Sci. U.S.A.* 107, 20051–20056. doi: 10.1073/pnas.1009906107

Shaw, P. J., Cirelli, C., Greenspan, R. J., and Tononi, G. (2000). Correlates of sleep and waking in *Drosophila melanogaster*. *Science* 287, 1834–1837. doi: 10.1126/science.287.5459.1834

Shemyakin, A., and Kapas, L. (2001). L-364,718, a cholecystokinin-A receptor antagonist, suppresses feeding-induced sleep in rats. *Am. J. Physiol. Regul. Integr. Comp. Physiol.* 280, R1420–R1426.

Shin, S. C., Kim, S. H., You, H., Kim, B., Kim, A. C., Lee, K. A., et al. (2011). *Drosophila* microbiome modulates host developmental and metabolic homeostasis via insulin signaling. *Science* 334, 670–674. doi: 10.1126/science.1212782

Shorrocks, B. (1972). *Drosophila*. London: Ginn.

Sitaraman, D., Aso, Y., Jin, X., Chen, N., Felix, M., Rubin, G. M., et al. (2015a). Propagation of homeostatic sleep signals by segregated synaptic microcircuits

of the *Drosophila* mushroom body. *Curr. Biol.* 25, 2915–2927. doi: 10.1016/j.cub.2015.09.017

Sitaraman, D., Aso, Y., Rubin, G. M., and Nitabach, M. N. (2015b). Control of sleep by dopaminergic inputs to the *Drosophila* mushroom body. *Front. Neural Circuits* 9:73. doi: 10.3389/fncir.2015.00073

Skora, S., Mende, F., and Zimmer, M. (2018). Energy scarcity promotes a brain-wide sleep state modulated by insulin signaling in *C. elegans*. *Cell Rep.* 22, 953–966. doi: 10.1016/j.celrep.2017.12.091

Slocumb, M. E., Regalado, J. M., Yoshizawa, M., Neely, G. G., Masek, P., Gibbs, A. G., et al. (2015). Enhanced sleep is an evolutionarily adaptive response to starvation stress in *Drosophila*. *PLoS One* 10:e0131275. doi: 10.1371/journal.pone.0131275

Sokolowski, M. B. (1980). Foraging strategies of *Drosophila melanogaster*: a chromosomal analysis. *Behav. Genet.* 10, 291–302. doi: 10.1007/bf01067774

Sonn, J. Y., Lee, J., Sung, M. K., Ri, H., Choi, J. K., Lim, C., et al. (2018). Serine metabolism in the brain regulates starvation-induced sleep suppression in *Drosophila melanogaster*. *Proc. Natl. Acad. Sci. U.S.A.* 115, 7129–7134. doi: 10.1073/pnas.1719033115

Stahl, B. A., and Keene, A. C. (2017). To rebound or not to rebound. *eLife* 6:e31646. doi: 10.7554/eLife.31646

Stahl, B. A., Slocumb, M. E., Chaitin, H., Diangelo, J. R., and Keene, A. C. (2017). Sleep-dependent modulation of metabolic rate in *Drosophila*. *Sleep* 40:zsx084. doi: 10.1093/sleep/zsx084

Talay, M., Richman, E. B., Snell, N. J., Hartmann, G. G., Fisher, J. D., Sorkac, A., et al. (2017). Transsynaptic mapping of second-order taste neurons in flies by trans-Tango. *Neuron* 96, 783.e4–795.e4. doi: 10.1016/j.neuron.2017.10.011

Thistle, R., Cameron, P., Ghorayshi, A., Dennison, L., and Scott, K. (2012). Contact chemoreceptors mediate male-male repulsion and male-female attraction during *Drosophila* courtship. *Cell* 149, 1140–1151. doi: 10.1016/j.cell.2012.03.045

Tisdale, R. K., Lesku, J. A., Beckers, G. J. L., Vyssotski, A. L., and Rattenborg, N. C. (2018). The low-down on sleeping down low: pigeons shift to lighter forms of sleep when sleeping near the ground. *J. Exp. Biol.* 221:182634. doi: 10.1242/jeb.182634

Tomotani, B. M., Amaya, J. P., Oda, G. A., and Valentinuzzi, V. S. (2016). Social modulation of the daily activity rhythm in a solitary subterranean rodent, the tuco-tuco (Ctenomys sp). *Sleep Sci.* 9, 280–284. doi: 10.1016/j.slsci.2016.06.001

Tononi, G., and Cirelli, C. (2006). Sleep function and synaptic homeostasis. *Sleep Med. Rev.* 10, 49–62. doi: 10.1016/j.smrv.2005.05.002

Tononi, G., and Cirelli, C. (2014). Sleep and the price of plasticity: from synaptic and cellular homeostasis to memory consolidation and integration. *Neuron* 81, 12–34. doi: 10.1016/j.neuron.2013.12.025

Tsao, C. H., Chen, C. C., Lin, C. H., Yang, H. Y., and Lin, S. (2018). *Drosophila* mushroom bodies integrate hunger and satiety signals to control innate food-seeking behavior. *eLife* 7:e35264. doi: 10.7554/eLife.35264

Ungvari, Z., Parrado-Fernandez, C., Csiszar, A., and De Cabo, R. (2008). Mechanisms underlying caloric restriction and lifespan regulation - implications for vascular aging. *Circ. Res.* 102, 519–528. doi: 10.1161/CIRCRESAHA.107.168369

Voirin, B., Scriba, M. F., Martinez-Gonzalez, D., Vyssotski, A. L., Wikelski, M., and Rattenborg, N. C. (2014). Ecology and neurophysiology of sleep in two wild sloth species. *Sleep* 37, 753–761. doi: 10.5665/sleep.3584

Willie, J. T., Chemelli, R. M., Sinton, C. M., and Yanagisawa, M. (2001). To eat or to sleep? Orexin in the regulation of feeding and wakefulness. *Annu. Rev. Neurosci.* 24, 429–458. doi: 10.1146/annurev.neuro.24.1.429

Wong, A. C., Dobson, A. J., and Douglas, A. E. (2014). Gut microbiota dictates the metabolic response of *Drosophila* to diet. *J. Exp. Biol.* 217, 1894–1901. doi: 10.1242/jeb.101725

Wu, M. N., Ho, K., Crocker, A., Yue, Z., Koh, K., and Sehgal, A. (2009). The effects of caffeine on sleep in *Drosophila* require PKA activity, but not the adenosine receptor. *J. Neurosci.* 29, 11029–11037. doi: 10.1523/JNEUROSCI.1653-09.2009

Xu, K., Zheng, X., and Sehgal, A. (2008). Regulation of feeding and metabolism by neuronal and peripheral clocks in *Drosophila*. *Cell Metab.* 8, 289–300. doi: 10.1016/j.cmet.2008.09.006

Yadlapalli, S., Jiang, C., Bahle, A., Reddy, P., Meyhofer, E., and Shafer, O. T. (2018). Circadian clock neurons constantly monitor environmental temperature to set sleep timing. *Nature* 555, 98–102. doi: 10.1038/nature25740

Yamada, R., Deshpande, S. A., Bruce, K. D., Mak, E. M., and Ja, W. W. (2015). Microbes promote amino acid harvest to rescue undernutrition in *Drosophila*. *Cell Rep.* 10, 865–872. doi: 10.1016/j.celrep.2015.01.018

Yamamoto, D., and Koganezawa, M. (2013). Genes and circuits of courtship behaviour in *Drosophila* males. *Nat. Rev. Neurosci.* 14, 681–692. doi: 10.1038/nrn3567

Yamanaka, A., Beuckmann, C. T., Willie, J. T., Hara, J., Tsujino, N., Mieda, M., et al. (2003). Hypothalamic orexin neurons regulate arousal according to energy balance in mice. *Neuron* 38, 701–713. doi: 10.1016/s0896-6273(03)00331-3

Yang, Y., and Edery, I. (2019). Daywake, an anti-siesta gene linked to a splicing-based thermostat from an adjoining clock gene. *Curr. Biol.* 29, 1728.e4–1734e.4. doi: 10.1016/j.cub.2019.04.039

Yang, Z., Yu, Y., Zhang, V., Tian, Y., Qi, W., and Wang, L. (2015). Octopamine mediates starvation-induced hyperactivity in adult *Drosophila*. *Proc. Natl. Acad. Sci. U.S.A.* 112, 5219–5224. doi: 10.1073/pnas.1417838112

Yanik, G., Glaum, S., and Radulovacki, M. (1987). The dose-response effects of caffeine on sleep in rats. *Brain Res.* 403, 177–180. doi: 10.1016/0006-8993(87)90141-7

Yoshii, T., Hermann-Luibl, C., and Helfrich-Forster, C. (2016). Circadian light-input pathways in *Drosophila*. *Commun. Integr. Biol.* 9:e1102805. doi: 10.1080/19420889.2015.1102805

You, Y. J., Kim, J., Raizen, D. M., and Avery, L. (2008). Insulin, cGMP, and TGF-beta signals regulate food intake and quiescence in C. *elegans*: a model for satiety. *Cell Metab.* 7, 249–257. doi: 10.1016/j.cmet.2008.01.005

Yu, Y., Huang, R., Ye, J., Zhang, V., Wu, C., Cheng, G., et al. (2016). Regulation of starvation-induced hyperactivity by insulin and glucagon signaling in adult *Drosophila*. *eLife* 5:e15693. doi: 10.7554/eLife.15693

Yurgel, M. E., Kakad, P., Zandawala, M., Nassel, D. R., Godenschwege, T. A., and Keene, A. C. (2019). A single pair of leucokinin neurons are modulated by feeding state and regulate sleep-metabolism interactions. *PLoS Biol.* 17:e2006409. doi: 10.1371/journal.pbio.2006409

Yurgel, M. E., Shah, K. D., Brown, E. B., Burns, C., Bennick, R. A., Diangelo, J. R., et al. (2018). Ade2 functions in the *Drosophila* fat body to promote sleep. *G3* 8, 3385–3395. doi: 10.1534/g3.118.200554

Zhang, Z., Cao, W., and Edery, I. (2018). The SR protein B52/SRp55 regulates splicing of the period thermosensitive intron and mid-day siesta in *Drosophila*. *Sci. Rep.* 8:1872. doi: 10.1038/s41598-017-18167-3

Zimmerman, J. E., Chan, M. T., Jackson, N., Maislin, G., and Pack, A. I. (2012). Genetic background has a major impact on differences in sleep resulting from environmental influences in *Drosophila*. *Sleep* 35, 545–557. doi: 10.5665/sleep.1744

Conflict of Interest Statement: The authors declare that the research was conducted in the absence of any commercial or financial relationships that could be construed as a potential conflict of interest.

frontiers in Physiology

ORIGINAL RESEARCH
published: 01 November 2019
doi: 10.3389/fphys.2019.01374

The Circadian Clock Improves Fitness in the Fruit Fly, *Drosophila melanogaster*

Melanie Horn[1], Oliver Mitesser[2], Thomas Hovestadt[2], Taishi Yoshii[3], Dirk Rieger[1] and Charlotte Helfrich-Förster[1]**

[1] Neurobiology and Genetics, Theodor-Boveri Institute, Biocenter, Julius-Maximilians University Würzburg, Würzburg, Germany, [2] Theoretical Evolutionary Ecology Group, Biocenter, Department of Animal Ecology and Tropical Biology, Julius-Maximilians University Würzburg, Würzburg, Germany, [3] Graduate School of Natural Science and Technology, Okayama University, Okayama, Japan

OPEN ACCESS

Edited by:
Cristiano De Pitta,
University of Padova, Italy

Reviewed by:
André Klarsfeld,
ESPCI ParisTech, France
Sheeba Vasu,
Jawaharlal Nehru Centre for Advanced Scientific Research, India

***Correspondence:**
Dirk Rieger
dirk.rieger@biozentrum.uni-wuerzburg.de
Charlotte Helfrich-Förster
charlotte.foerster@biozentrum.uni-wuerzburg.de

Specialty section:
This article was submitted to Invertebrate Physiology, a section of the journal Frontiers in Physiology

Received: 30 March 2019
Accepted: 17 October 2019
Published: 01 November 2019

Citation:
Horn M, Mitesser O, Hovestadt T, Yoshii T, Rieger D and Helfrich-Förster C (2019) The Circadian Clock Improves Fitness in the Fruit Fly, Drosophila melanogaster. Front. Physiol. 10:1374. doi: 10.3389/fphys.2019.01374

It is assumed that a properly timed circadian clock enhances fitness, but only few studies have truly demonstrated this in animals. We raised each of the three classical *Drosophila period* mutants for >50 generations in the laboratory in competition with wildtype flies. The populations were either kept under a conventional 24-h day or under cycles that matched the mutant's natural cycle, i.e., a 19-h day in the case of per^S mutants and a 29-h day for per^l mutants. The arrhythmic per^0 mutants were grown together with wildtype flies under constant light that renders wildtype flies similar arrhythmic as the mutants. In addition, the mutants had to compete with wildtype flies for two summers in two consecutive years under outdoor conditions. We found that wildtype flies quickly outcompeted the mutant flies under the 24-h laboratory day and under outdoor conditions, but per^l mutants persisted and even outnumbered the wildtype flies under the 29-h day in the laboratory. In contrast, per^S and per^0 mutants did not win against wildtype flies under the 19-h day and constant light, respectively. Our results demonstrate that wildtype flies have a clear fitness advantage in terms of fertility and offspring survival over the *period* mutants and – as revealed for per^l mutants – this advantage appears maximal when the endogenous period resonates with the period of the environment. However, the experiments indicate that per^l and per^S persist at low frequencies in the population even under the 24-h day. This may be a consequence of a certain mating preference of wildtype and heterozygous females for mutant males and time differences in activity patterns between wildtype and mutants.

Keywords: competition, *period* mutants, resonance theory, mating preference, fertility

INTRODUCTION

One of the main tasks of a circadian clock is to time animal daily activity and sleep to the right time of the day. The activity-sleep patterns of clock mutants without a circadian clock or with a clock running too fast or too slow are usually different from wild-type animals as has been demonstrated for rodents (Ralph and Menaker, 1988; van der Horst et al., 1999; Pendergast et al., 2010), fruit flies (Konopka and Benzer, 1971; Hamblen-Coyle et al., 1992; Hamblen et al., 1998) and humans (Toh et al., 2001; Patke et al., 2017). While animals without functional clock appear to merely respond

to the daily light-dark changes, animals with too fast clocks have early activity-sleep phases and animals with too slow clocks have late activity phases, respectively (Hamblen-Coyle et al., 1992; Wheeler et al., 1993).

The adaptive value of circadian clocks for fitness has been demonstrated by diverse strategies that have been nicely reviewed by Vaze and Sharma (2013), Abhilash and Sharma (2016), and Nikhil and Sharma (2017). One of many possible strategies is to investigate whether a trait confers higher adaptive advantage in the context of species competition. For example, Ouyang et al. (1998) and Dodd et al. (2005) showed that organisms with an endogenous period (τ) close to the period of the Zeitgeber (T) have a greater competitive advantage over those with a deviant τ. Ouyang et al. (1998) have grown a wildtype cyanobacteria strain in competition with mutants possessing too fast, too slow or no clock at all for about 50 generations. In this competition assay, the mutants lost against the wildtype strains when grown under a 24-h day. However, when grown under environmental period lengths ("T-cycles") that matched the endogenous circadian period of the mutants, the mutants outcompeted the wildtype strain, respectively. The result shows that cyanobacteria have a significant competitive advantage under T-cycles that resonate with their endogenous free-running period, because under such conditions they achieve an optimal phase relationship between the light-dark (LD) cycle and the endogenous clock - also known as the resonance hypothesis (Pittendrigh and Minis, 1972; Ouyang et al., 1998; Johnson et al., 2008). Dodd et al. (2005) performed a similar experiment in the plant, *Arabidopsis thaliana*, during one vegetative growth season. Mutant and wildtype plants were grown in competitions together under different T-cycles and – similar to cyanobacteria – the plants whose endogenous periods matched with the external T-cycle had more photosynthesis and growth and enhanced survival.

In mammals, researchers tried to demonstrate the importance of the circadian clock for fitness under natural conditions, under which the animals are exposed to harsh weather conditions, competition for food and the risk of predation. DeCoursey and colleagues compared the survival of chipmunks with surgical ablated circadian clock in the suprachiasmatic nucleus of the hypothalamus with that of sham-operated siblings for 18 months under natural conditions in a high-density population of free-living eastern chipmunks at a 4-ha forest site in the Allegheny Mountains (United States) (DeCoursey and Krulas, 1998; DeCoursey et al., 2000). They found that a significantly higher proportion of clock-ablated animals than sham-operated individual were killed by weasel predation, most probably because the clock ablated animals showed nocturnal restlessness and left their burrows more frequently at night when predator risk is highest for these diurnal animals. DeCoursey (2014) replicated these experiments with further rodent species, nocturnal flying squirrels, diurnal Antelope squirrels and diurnal Golden-mantled ground squirrels. In all species the circadian clock significantly reduced the time being awake during the daily sleep times (for Golden-mantled ground squirrel also during hibernation), and by this way helped to save energy and to avoid predation.

Nevertheless, other studies did not reveal any benefits of possessing a circadian clock. For example, clock mutant ($per2^{Brdm1}$) mice that were kept for 2 years in 400 m^2 outdoor pens within a remote woodland in Western Russia showed survival rates that were equal to wild-type mice (Daan et al., 2011). Although the circadian organization and entrainment of $per2^{Brdm1}$ mutants is compromised in the laboratory (Albrecht et al., 2001; Mendoza et al., 2010), their activity pattern did not differ from that of wild-type mice in nature (Daan et al., 2011). This result questions the importance for a functional clock under natural conditions. Vanin et al. (2012) came to similar conclusions with regard to fruit flies that were kept over the summer under semi-natural conditions: clock-less per^0 mutants exhibited similar bimodal activity patterns with prominent morning and evening activity bouts as did wild-type flies, and there was only a marginal difference in the timing of evening activity between wild-type flies and per^s and per^l mutants. Similar results were obtained in the laboratory when either realistic temperature and light cycles were simulated (Vanin et al., 2012) or when only realistic light cycles were simulated (Schlichting et al., 2015). This suggests that more naturally cycling environmental stimuli than the standard ones in the laboratory allow even mutant flies to behave normally. Schlichting et al. (2015) found that the eyes play an essential role in this process. Eyeless per^0 mutants lacked the normal bimodal organization of activity, suggesting that functional eyes can largely compensate for the loss of the circadian clock by directly modulating the activity of the flies, which is also known as masking effect. Although in fruit flies no survival tests were performed under outdoor conditions and in mice these lasted only for 2 years and might be too short to draw strong conclusions, the natural-like activity patterns of arrhythmic mice and flies under natural conditions due to masking may explain, why none or only a minor impact on the mutants' fitness was found.

In the laboratory, when fruit flies live under comfortable, constant temperatures, are provided with super-abundant food, and lack any competition with flies of other genotypes as well as any predation risk, a properly running circadian clock may not be essential for survival, although the activity patterns of wildtype flies and clock mutants are quite different under these conditions (**Figure 1**). Klarsfeld and Rouyer (1998) and Vaccaro et al. (2016) observed only tiny differences in lifespan between per^0, per^T (another short-period mutant) and per^l and wildtype flies. Wildtype flies lived marginally longer than the mutants under a 24-h day, while under a 16-h day, that mimics the period of per^T mutants, the latter did not live longer than wild-type flies and even no longer than per^l mutants (Klarsfeld and Rouyer, 1998). The results suggest that the influence of the clock on lifespan is rather small and does not follow the resonance hypothesis.

Nevertheless, most of the mentioned studies have certain limitations (see Abhilash and Sharma, 2016). Some focused on a single readout of fitness (e.g., lifespan) and did not regard others (e.g., fecundity) that may have compensatory effects on overall fitness (see Sheeba et al., 2000 for an example). Other studies used mutants that are inbred in the lab for many years and might have undergone random genetic drift producing spurious correlations

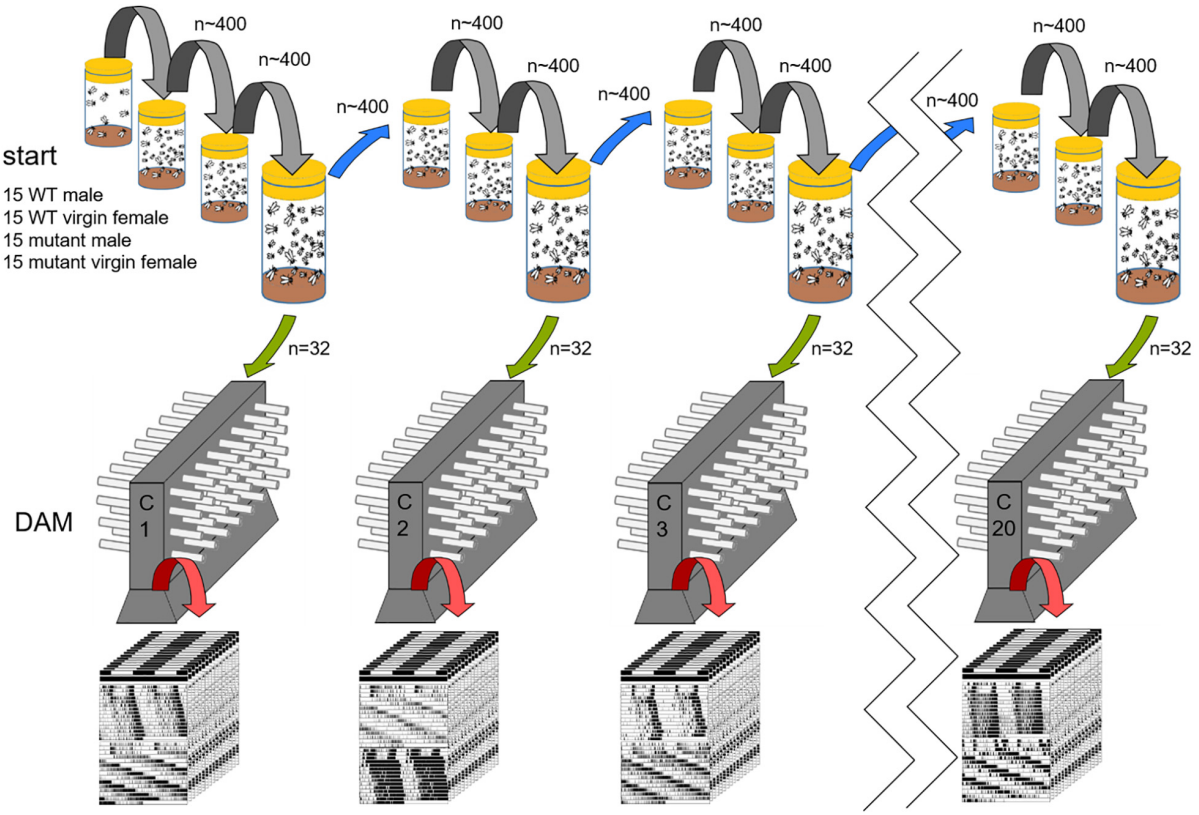

FIGURE 1 | Experimental procedure. At the start of the experiment, 15 male and virgin female flies each of wildtype (WT) and one *period* mutant were placed in a large food vial (60 flies in total). The mutant flies were either per^s, per^l or per^0. All wild type/mutant competitions were started with 10 vials (=populations) each. Here, the procedure is only shown for one population. Every 14 days (gray and blue transfer arrows), all hatched animals (~ 400 flies) were transferred into fresh food vials. After every third transfer, a census was taken. For this, the vials were kept for another 2 to 3 days so that more flies could hatch. From these, 32 males were randomly chosen (green arrow) and their activity was recorded in a *Drosophila* Activity Monitor (DAM), [Census 1 (C1), Census 2 (C2), etc.]. After 4–7 days of entrainment under light dark cycles (LD12:12) the animals were recorded in constant darkness (DD) for another 2 to 3 weeks. Afterward the genotype of the flies was determined and the period of the rhythmic flies calculated (see section "Materials and Methods").

between different fitness traits. Thus, it is premature to conclude from these studies that the circadian clock plays only a minor role in fitness, even under such "comfortable" lab conditions.

Here we report a long-term study, in which we raised the original *period* mutants, per^0, per^s, and per^l (Konopka and Benzer, 1971), in competition with wildtype flies for more than 2 years (>50 generations) and under different T-cycles, while regularly determining the proportion of mutant flies in the population. Such a long-term study was, so far, only performed on the already mentioned cyanobacteria that have a very short generation time (Ouyang et al., 1998), but not in any animal. Although fruit flies have a significant longer generation time than cyanobacteria (~14 days in comparison to ~10 h), it appeared feasible to us to perform this experiment with fruit flies. In addition, we performed a short-term competition study (over three generations in two consecutive years) under outdoor conditions to test the impact of the circadian clock on fitness under more natural-like climatic and light conditions. Both, the long-term and short-term competition study, showed that a properly running circadian clock significantly improves the fitness of fruit flies under competition. Furthermore, the long-term competition study did partly obey the resonance hypothesis. Most interestingly, in spite of losing against wild-type flies under a 24-h day, the per^s and per^l mutants stably remained at low percentages in the fly population. To understand this, we additionally performed fertility, survival and mating preference tests.

MATERIALS AND METHODS

Fly Strains and Rearing

Wildtype CantonS flies (WT_{CS}) and the *period* mutants (per^s, per^l, and per^{01}) from Konopka and Benzer (1971) were used for the experiments. In the following the per^{01} mutants will just be named per^0. We obtained the flies from the Kyriacou group, who state in their paper that the flies are congenic and cantonized (Vanin et al., 2012). We could not obtain further information about the number of performed crosses with CantonS flies, but the flies have been co-isogenised for 12 generations in 1992 as is described in detail in Greenacre et al. (1993). Flies were reared on cornmeal/agar medium consisting of 0.8% agar, 2.2%

sugar-beet syrup, 8.0% malt extract, 1.8% yeast, 1.0% soy flour, 8.0% corn flour, and 0.3% hydroxybenzoic acid at 25°C and 60% relative humidity under a light-dark (LD) cycle of 12:12 h (h). We started the first competition experiments under T = 24 h in 2013 (running until 2015) and the second ones, depending on the mutant either under long and short T-cycles or in LL in 2014 (running until 2016).

Long-Term Competition Assay in the Laboratory

Ten food vials (diameter 48 mm, height 104 mm, filled with 28.5 ml food), each containing 15 virgin female and 15 male flies each of wild-type (CS) and *period* mutant flies were used to start the competition experiments (in sum, 60 flies per vial). The mutant flies were either per^s, per^l or per^0 (**Table 1**). All vials were kept in a climate chamber at 25°C ± 0.2°C with 60% ± 2% of relative humidity. The light condition was either a T-cycle of 24 h (LD 12:12), a T-cycle of 29 h (LD 14.5:14.5) or of 19 h (LD 9.5:9.5) or constant light (LL) depending on the *period* mutant flies used for the subset of the experiment (**Table 1**). Light intensity was always 100 lux. LL conditions were only used for competing wildtype flies and per^0 mutants, because wildtype flies become arrhythmic under LL. Thus, the wildtype activity pattern is no longer distinguishable from that of the arrhythmic per^0 mutants and any selective advantages of possessing a circadian clock should disappear.

At 25°C, the generation time of fruit flies is ∼10 days and we did not observe any evident differences in developmental timing in the mutants. Therefore, we transferred all flies from the vials to new vials with fresh food every 14 days. At this time, ∼400 flies of the new generation had eclosed. The parental flies had died before the flies were flipped (when the larvae grow, the food becomes soft and fluid and the adults submerge in it being finally eaten by the larvae). Every third generation, the old vials were kept for another 2 to 3 days for more flies to hatch to carry out a census on mutant allele frequency (**Figure 1**). At these censuses, 32 males from each vial of these later hatching flies where used for locomotor activity recording to determine the genotype of each fly. Since the *period* gene is on the X-chromosome of which males carry only one copy, the genotype of each male becomes evident in its free-running period (short, long, ∼24 h or arrhythmic). Based on these tests, the genotype distribution among all flies in the experimental vials was determined (see below). In sum, 320 males (stemming from 10 vials) were used for determination of male genotype distribution at every census. This procedure was repeated over 60 generations for the 24 h T-cycle experiment and over 54 generations for the short- and long T-cycles. **Figure 1** illustrates the procedure. Most importantly, the population size in the single vials stayed approximately constant throughout the entire experiments as far as we could judge by eye; this observation suggests the existence of a carry capacity and thus of competition among flies, respectively, larvae.

TABLE 1 | Experimental settings of long-term competition experiments.

	Condition 1	Condition 2
WT_{CS} × per^l	LD 12:12	LD 14.5:14.5
WT_{CS} × per^s	LD 12:12	LD 9.5:9.5
WT_{CS} × per^0	LD 12:12	LL

In each case condition 1 mimics the standard 24 h cycle whereas condition 2 that (approximately) resonating the endogenous rhythm of the mutant involved in the experiment.

Outdoor Competition Assay

The outdoor experiments were performed in 2013 and 2014 outside the Biocenter and at the bee-station of the University of Würzburg – sheltered from rain and direct sunlight – where the flies could sense all changes in light, temperature and relative humidity (**Figure 2**). The outline of the competitions assay was in principle similar to that described above. However, due to low and variable temperatures, the flies took far more time to develop and to generate the next generation. Therefore, only three generations could be raised during each summer period (June to September/early October). The third generation was investigated for the genotype distribution of WT_{CS} and *period* mutant flies as described above. We compared these data with the third generation data (=census 1) from the long-term indoor experiments, using a general linear model with a "quasibinomial" error structure due to overdispersion of data. As suggested by Crawley (2013) we used *F*-tests for model comparison (procedure "anova" in R) – separately for each mutant – between the full model and a model version with the effect of "year" removed (the 2 years of outdoor experiments and 1 year of indoor experiment). Even though these constitute three independent experiments we apply *post hoc* Bonferroni adjustment for multiple testing.

Locomotor Activity Recording and Analysis

Locomotor activity was recorded in *Drosophila* Activity Monitors (DAM; Trikinetics system, Waltham, MA, United States) at 25°C and 100 lux as described previously (Schlichting and Helfrich-Förster, 2015). Light was provided by white LEDs (Lumitronix, LED Technik, Hechingen, Germany). We recorded the activity of male wildtype, per^s, per^l and per^0 flies (1) before the competition experiments, (2) at the censuses during the competition experiments and (3) in parallel to the competition

FIGURE 2 | Location of the vials during the outdoor experiment in the summer months. **(A)** and **(B)** show the location at the Biocenter, 1st floor, **(C)** the sheltered location at the Bee station of the University of Würzburg.

experiments, in flies of each genotype that were kept without competition under the same conditions. The flies were recorded for 4–7 days under LD 12:12 cycles (light intensity 100 lux) and consecutively for 2–3 weeks under constant darkness (DD). In addition, we recorded male wildtype flies and per^0 mutants under constant light of 100 lux to confirm that the great majority of flies in both strains are arrhythmic under such conditions. Furthermore, we recorded the activity of male wildtype flies and per^s and per^l mutants under the different T-cycles (T = 19 h and T = 29 h) in order to see how the phasing of their activity bouts changed under these conditions.

The raw activity data was exported as text files by the DAM-System Software, displayed as actograms using a Fiji[1] plugin – ActogramJ (v0.9, (Schmid et al., 2011) and saved as pdf files. Average activity profiles during the LD-cycles were calculated for each genotype as described in Schlichting and Helfrich-Förster (2015). From the average activity profile the fly's overall activity (=number of beam crosses) during the first 3 h of the day [Zeitgeber Time (ZT) 0 to 3] was determined for each individual fly. Data were tested for normal distribution and investigated for genotype influences by a One-Way ANOVA followed by a *post hoc* test with Bonferroni adaptation. To determine rhythmicity and the endogenous free-running period of every single fly in DD, the raw data were analyzed by χ^2-periodogram analysis in ActogramJ. At $p > 0.05$ the flies were assumed to be arrhythmic. From the periodogram analyses, the proportion of wildtype and mutant flies was determined for each competition pair in the competition assay, and the frequency to which the mutant flies persisted in the population was plotted for every census in a diagram.

Diverse Assays to Determine Fitness Components of the Clock Mutants

Overall fitness depends on several components, e.g., fertility, mating success, survival during development, number of offspring, etc. In order to reveal the fitness of the clock mutant in comparison to wildtype flies in more detail, we determined several fitness components. All tests were done under LD12:12 with 100 lux during the light period and a constant temperature of 25°C.

Sperm Counts

Pairs of flies of the same genotype were placed in mating chambers and allowed to mate. After successful copulation, the female reproductive organs – consisting of the uterus, seminal receptacle and the spermatheca were dissected in PBS, transferred to a glass slide and stained with DAPI (1 μg/ml in PBS). The preparations were scanned with a Leica confocal laser scanning microscope (DM5500; stack width 2 μm). The sperms heads in the seminal receptacle, the uterus and the spermathecal were counted with ImageJ (Fiji) via defining ROIs and automated counting as described in Garbaczewska et al. (2013). Mating and sperm counts were taken for 8 wildtype flies, per^0 and per^l mutants, respectively, and 7 per^s mutants. Sperm count data were first tested for conforming with normality assumption using the Shapiro test and for homogeneity of variance using the Bartlett test; both tests provided no evidence of significant violations of these assumptions. As we were interested in the comparison between the wildtype *CS* and the three mutants only, we then carried out *post hoc* tests with Dunnett correction (utilizing the "emmean" package, Lenth, 2019, in R) only contrasting each mutant to the CS wildtype.

Survival From Egg to Adults

To test whether survival rates during development are different between wildtype and mutant flies, females of each genotype were allowed to lay eggs on apple agar plates for 6 h. From these, 100 eggs, were transferred into 10 food vials, respectively, and the pupae and adult flies emerging from these eggs were determined. The egg-pupae-adult survival data were analyzed using a generalized model with a "quasibinomial" error family for the egg to pupae survival due to overdispersed data and the standard "binomial" family for the survival from pupae to adults. Significance testing was thus based on the F-ratio test for the former but on the likelihood-ratio test with Chi^2 statistics for the latter type of analysis (Crawley, 2013). For the egg to pupae survival all experiments started with exactly 100 eggs per vial that had been laid by a group of females within few hours. For each genotype we had 10 such vials (=1000 eggs in total for each genotype). The number of pupae produced provided, in turn, the initial sample for then testing the survival from the pupal to the adult stage. Again, we were primarily interested in comparing the different mutant to the wildtype and thus performed pairwise testing of mutant homozygotes versus the mutant wildtype females. A similar approach (Dunnett's correction) as for the sperm count data was used for *post hoc* testing, contrasting only the mutants with the wild type.

Female Mating Success and Preferences

Individual single female flies – heterozygous or homozygous for either WT_{CS} or *period* mutant – and two male flies (a WT_{CS} and a mutant) were placed in mating chambers (**Figure 3**). The males were allowed to court for 2 h. If females did not mate within this time interval, the flies were discarded and new flies were tested. Overall, 280 experiments were conducted with heterozygous and 140 experiments with homozygous females of each type. If one male managed to copulate successfully with the female, its genotype was noted and it was left undisturbed until copulation ended (usually this lasted ∼25 min). To distinguish between the two males with different genotypes, one of the two males was marked by a white spot on the thorax between the wings. The experiments were conducted at ZT 0–2 during the flies' morning activity.

The overall mating success was determined and analyzed using a general linear model with "quasibinomial" error structure, including the genotypes of the mutant males (per^s, per^l or per^0), of the females (WT/WT, WT/mutant, and mutant/mutant). Model comparison was carried out by backward elimination using F-ratio tests as described before.

The analysis of mating preferences was complicated because one of the two males presented to the females had to be marked to distinguish the mutant from the wildtype male (mutants do

[1]https://fiji.sc/

FIGURE 3 | Mating wheel with seven mating chambers. Each chamber is filled with one female and two male flies, respectively, for testing female mating preferences. One of the two males is marked by a white spot on its thorax (arrow) to distinguish the genotypes.

not carry external markers). In a given setting it is thus not clear whether a female took her choice based on the genotype of the male or the presence/absence of the marker. Experiments were thus replicated in two versions, in one the wildtype males carried the mark in the others the mutant male. In our analysis we thus need to separate the effect of being a mutant (a_m) from that of being marked (a_x) on the underlying "base attractiveness" (A) of males (note that we assume additive effects only). Consequently, the two setting provide the following ratios for each female type tested (for clarity we drop index i indicating the different female genotypes in the following):

$$\alpha = \frac{A + a_m}{A + a_x} \quad \text{or} \quad \rho_\alpha = \frac{A + a_m}{2A + a_x + a_m}, \tag{1}$$

with p_α the probability of choosing an unmarked mutant over a marked wild-type male and

$$\frac{1}{\beta} = \frac{A + a_m + a_x}{A} \quad \text{or} \quad \rho_\beta = \frac{A + a_m + a_x}{2A + a_x + a_m}, \tag{2}$$

with p_β the probability of choosing a marked mutant over an unmarked wild-type male. These are two equations with three unknown variables. However, we are only interested in the relative attractiveness of mutant vs. wild-type males, i.e.,

$$\frac{A + a_m}{A} = v_m, \tag{3}$$

or alternatively the probability ρ_m that a female of genotype i will choose a mutant male over the wild-type, i.e.,

$$\rho_m = \frac{A + a_m}{A + A + a_m} = \left(\frac{A}{A + a_m} + 1\right)^{-1} = \left(1 + \frac{1}{v_m}\right)^{-1} = \frac{v_m}{1 + v_m}. \tag{4}$$

Simple algebraic manipulations yields the following equation

$$v_m = \alpha\left(1 + \frac{1 - \beta\alpha}{\beta\,(1 + \alpha)}\right) \tag{5}$$

that allows calculating the desired values for p_m (see Eq. 4).

Calculation of confidence intervals for p_m is complicated by this fact, however, and not liable to standard methods. We thus implement a Monte-Carlo approach to estimate confidence intervals for values of p_m by exactly replicating the numerical calculations of Eqs 4 and 5 but drawing random values for the number of mutant males selected by females from a binomial distribution with probabilities for p_α and p_β as empirically estimated from the experiments (cf. Eqs 1 and 2) and sample sizes exactly as those in the experiments. This random drawing of p^r_α and p^r_β and calculation of p^r_m is replicated 100,000 times for each of the female genotypes x male genotype combinations. The 2.5 and 97.5% quantiles of the distribution of these p^r_m values are then used to specify the 95% confidence limits of p_m. We are primarily interested in the presence of a non-random mating preference, i.e., whether the preference is significantly different from $p_m = 0.5$. A significant mating preference is thus indicated if the 95% CI-Interval does not include the value of 0.5.

Offspring per Female Fly

The mated females from the mating preference tests were used to determine the number of offspring per female fly. Each female was allowed to lay eggs for 3 days into one food vial. Then the female was removed and the emerged offspring was counted after 14 days at 25°C. Due to the discrete nature of the offspring count-data, they were analyzed using a generalized linear model with a "quasipoisson" error structure and a *post hoc* testing with Bonferroni correction. Again, statistical significance testing and model simplification was based on model comparison using the F-ratio test.

Statistics

All statistics were performed with R, version 3.4.4 (R Core Team, 2018).

RESULTS

Activity Profiles of Wildtype and Mutant Flies Under 12:12 LD Cycles, Constant Darkness, Constant Light and 19 h/29 h T-Cycles

Our first aim was to compare the activity patterns of wildtype flies and the *period* mutants under LD 12:12 and constant darkness (DD) with the reported data and to check whether per^0 and wildtype flies behave similarly arrhythmic under constant light (LL). **Figure 4A** shows typical actograms and activity profiles for wildtype flies, per^s, per^l, and per^0 mutants under LD and DD, while **Figure 5** depicts typical actograms of wildtype flies and per^0 mutants under LD and LL. Under LL, the great majority of wildtype and per^0 flies were arrhythmic (details see legend of **Figure 5**). Under DD conditions, only per^0

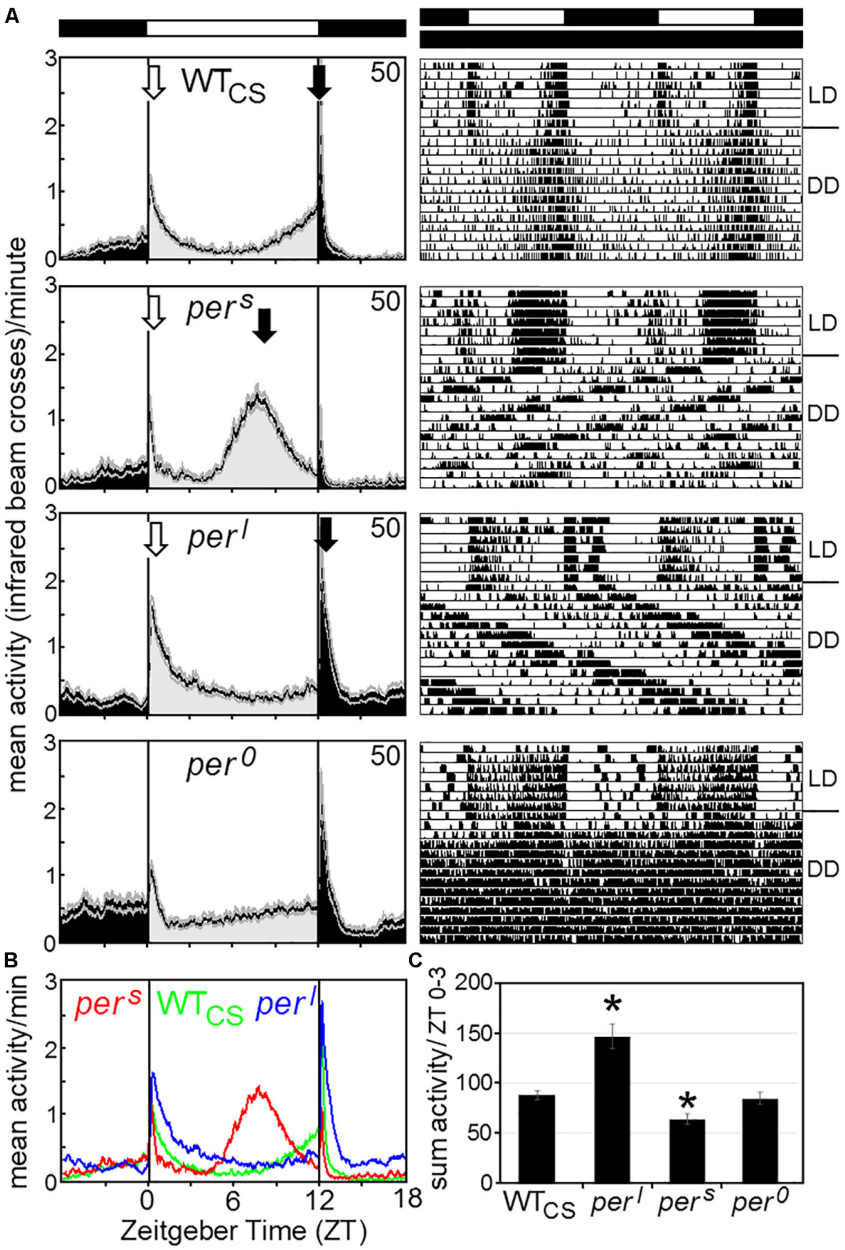

FIGURE 4 | Average activity profiles and typical actograms of individual wildtype (WT_{CS}) and *period* mutant (per^s, per^l and per^0) flies under LD and constant darkness (DD). **(A)**: Under LD cycles, WT_{CS} flies show a bimodal activity pattern with morning (open arrow) and evening (closed arrow) activity bouts. In per^s mutants the evening activity bout is advanced into the early afternoon while it is delayed into the night in per^l mutants. The morning activity bout appears to be reduced in per^s mutants, while it is pronounced and long-lasting in per^l mutants [see also **(B,C)**]. per^0 mutants are active during the day and night and strongly respond to lights-on and lights-off, but lack evident morning and evening activity bouts. Under DD, the actograms (right diagrams) show that the WT_{CS} fly free-runs with an endogenous period of ∼24 h, while the per^s mutant free-runs with a short period, the per^l mutant with a long period and the per^0 mutant becomes arrhythmic. **(B)**: Overlay of the average activity profiles of per^s, WT_{CS} and per^l flies, showing the different phases of the evening activity bout and the different activity levels during morning activity. **(C)**: Sum of activity (beam crosses) during the first 3 h (ZT0-3) after lights-on for all fly strains. Significant differences to WT_{CS} flies are indicated by asterisks.

mutants exhibited arrhythmic activity patterns, all other fly strains were clearly rhythmic, whereby wildtype flies free-ran with a period close to 24 h, per^s with short period and per^l with long period (**Figure 4**; detailed period calculation see in section "Changes in free-running period over the course of the indoor competition experiment"). As reported previously (Hamblen-Coyle et al., 1992), wildtype flies exhibited two activity bouts around lights-on and lights-off (also called morning and evening peaks). Morning and evening activity anticipated lights-on and lights-off, respectively, and were separated by a siesta. per^s mutants showed a much earlier and shorter siesta and their evening activity occurred already in the early afternoon. The

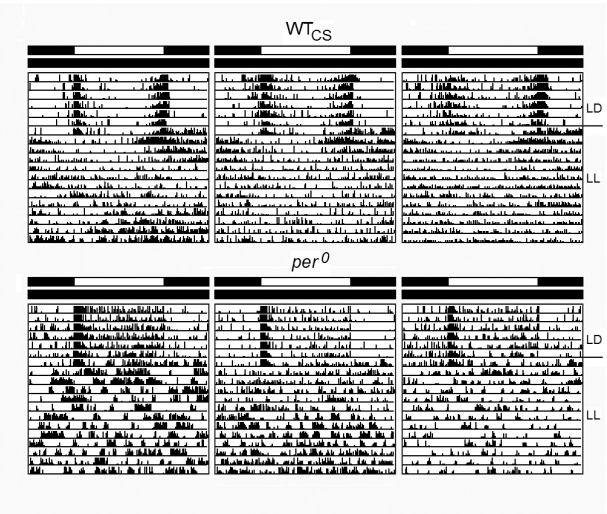

FIGURE 5 | Typical actograms of wildtype flies (WT_{CS}) and per^0 mutants under LD and constant light (LL). For both strains three individual actograms are selected that revealed the strongest rhythmicity under LL. Of 32 recorded wildtype flies 6 revealed weak rhythms with a mean period of 26.0 ± 0.6 h (SEM). The other flies were arrhythmic. In per^0 mutants, periodogram analysis found weak rhythms in 5 of 32 flies. These had a mean period of 25.0 ± 1.4 h (SEM). All other flies were arrhythmic.

morning activity might take place already before lights-on, but it seemed largely suppressed by darkness. In contrast, per^l mutants, exhibited a large morning activity that extended until midday. The following siesta was very late and stretched until lights-off. Evening activity started after lights-off and appeared largely suppressed by darkness, as was the case for the morning activity of per^s mutants. The calculation of the activity amounts during the first 3 h of the day, revealed significant differences between wildtype flies and per^s and per^l mutants (**Figure 4C**): per^l mutants were much more active than wildtype flies, while per^s mutants were less active. per^0 mutants lacked the siesta and showed no evident morning and evening activity bouts, but instead merely responded to lights-on and lights-off.

Under long and short T-cycles, the activity profiles of wildtype flies and per^s and per^l mutants changed drastically (**Figures 6A,B**). Under short T-cycles (19 h), wildtype flies did not at all anticipate lights-on but showed instead a long-lasting pronounced morning activity resembling very much the morning activity of per^l mutants under 24-h cycles (**Figure 4A**). Evening activity of wildtype flies shifted completely into the night, even more than that of per^l mutants under 24-h cycles. Under long T-cycles (29 h), wildtype flies showed early morning and evening activity, again resembling the activity profiles of per^s mutants under 24 h cycles with the exception that the nocturnal morning activity of wildtype flies was clearly visible, while it appeared suppressed in per^s mutants. The mutants' activity profile under 19 and 29 h cycles, respectively, came close to the activity profile of wildtype flies under 24-h cycles. Overall, this experiment revealed that, under the T-cycles that matched the endogenous period of the mutants, the mutants had an almost "wildtype-like" phase-relationship of morning and evening activity to lights-on and lights-off, while wildtype flies behaved "mutant-like". Consequently, the mutants should have a selective advantage over the wildtype flies under T-cycles, at least if fitness depends solely on the phasing of their activity bouts.

Indoor Competition Experiments

Figure 7 depicts the sampled frequency at which the *period* mutant flies persisted in the fly population over time when grown in competition to WT_{CS} flies. We directly compared the outcome of the experiment under the 24-h cycle with the outcome under the 29-h T-cycle for the per^l mutants, with the outcome under the 19-h T-cycle for the per^s mutants and with the outcome under LL for the per^0 mutants, respectively. Under the 24-h day, the frequency of the mutants quickly declined in most of the food vials for all three *period* mutants (**Figure 7** left). While per^0 mutants declined to low proportions in all food vials (both, 24-h cycle and LL) and presumably completely disappeared from several vials (what we cannot say with certainty, as we only genotyped a fraction of the male population on each census), the per^l mutants persisted in at least 4 vials (in one of them to 80% and in another one to 40%) under 24-h cycle and in all ten vials under the 29-h cycle. per^s mutants persisted in at least 3 vials under both T-cycles. On average, per^l and per^s mutants remained to a certain low percentage in the population (per^l ∼20%, per^s ∼5%; Thick line in **Figure 7** left).

To test whether these results could also be explained by genetic drift, we created 95% confidence intervals for the "true" frequency of mutant males in the population and (hatched gray lines in **Figure 7**) and just for samples of 32 males (hatched black lines) under the assumption of pure genetic drift. Because only males were genotyped, the *period* mutants are linked to the sex chromosome, data sets represent time-series, and a census was only taken every 3rd generation, a direct (analytical) calculation of confidence intervals is not possible in this case. Instead, we simulated the competition experiments exactly replicating the protocol of population initialization, generation transfer, and random sampling of 32 males every 3rd generation as applied in the experiments but under the (neutral) assumption of identical fitness of wildtype and mutant genotypes and the assumption of random mating and random sex determination. To account for sampling effects at any of these steps, discrete values for the number of females and males as well as the different genotypes by drawing random values from a binomial (two sexes, two possible male genotypes) or multinomial (three female genotypes) distribution, were assumed. These simulations were replicated 100,000 times and the lower and upper 2.5% quantiles were then used to define the 95% confidence intervals for both, the frequency of the mutant allele in the whole population and for the frequency in just a sample of 32 males. The calculated confidence intervals are shown in **Figure 7**. The results for the per^0 and the per^s mutants can clearly not be explained by genetic drift alone but indicate strong selection against the mutants in both, the 24-h cycles and the LL, respectively, the 19-h cycle. For per^l, however, the results under the 29-h cycle are consistent with genetic drift and also under the 24-h cycle some of the populations show fluctuations in the mutant's frequency

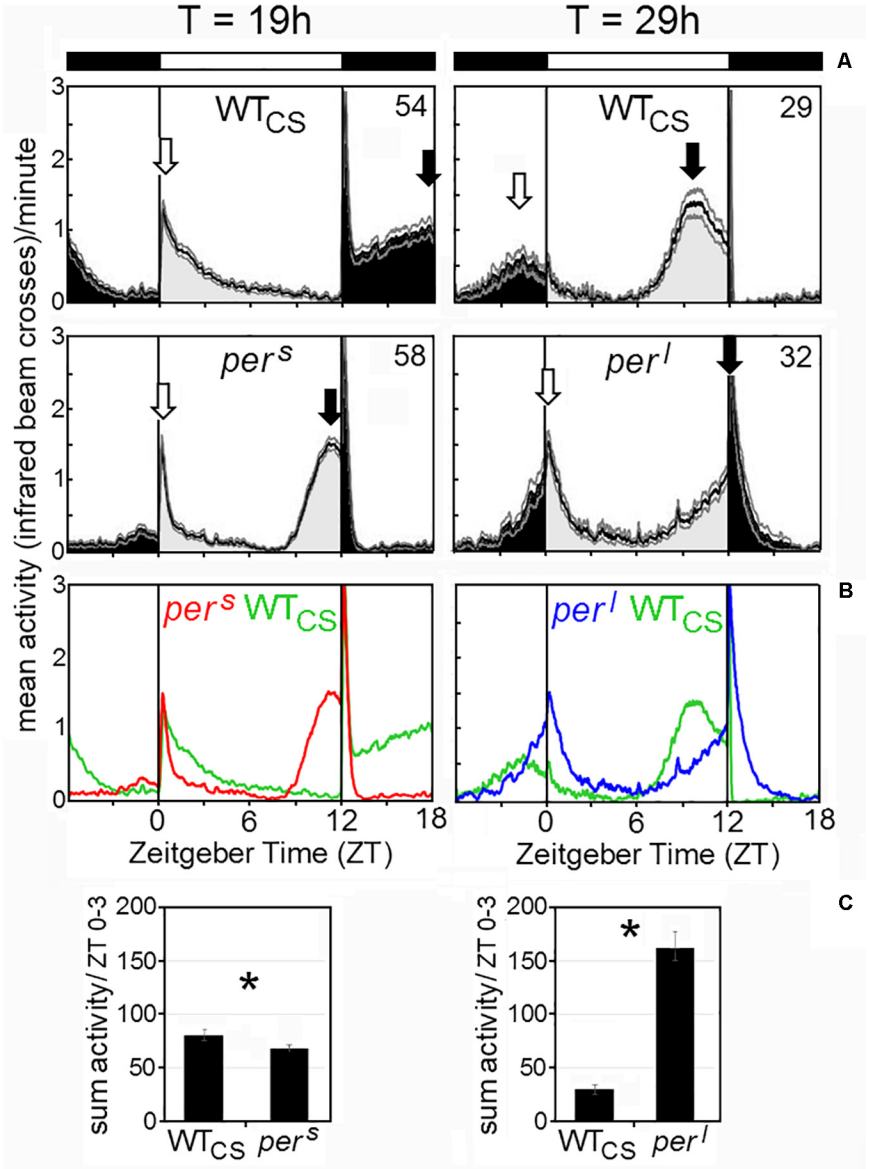

FIGURE 6 | Average activity profiles of wildtype (WT_{CS}) and *period* mutant (per^s, per^l) flies under T-cycles of 19 and 29 h. **(A)**: The flies show a bimodal activity pattern with morning (open arrow) and evening (closed arrow) activity bouts. In wildtype flies, morning and evening activity are delayed under 19 h T-cycles, while they are advanced under 29 h T-cycles. In per^s and per^l mutants the timing of morning and evening activity under 19 h T-cycles and 29 h T-cycles, respectively, resembles the timing in wildtype flies under 24 h cycles (compare **Figure 1**). **(B)**: Overlay of the average activity profiles of per^s, WT_{CS} and per^l flies, showing the different phases of the evening activity bout and the different activity levels during morning activity. **(C)**: Sum of activity (beam crosses) during the first 3 h (ZT0-3) after lights-on for all fly strains. Significant differences to WT_{CS} flies are indicated by asterisks.

consistent with genetic drift (but see below for deviations from the genetic drift hypothesis).

If the decrease of the *period* mutants in the fly population depends only on the presence and speed of circadian clock, per^l mutants are expected to improve performance against wildtype flies under the 29-h T-cycle and per^s mutants under the 19-h T-cycle, while per^0 mutants should be equally fit as wildtype flies under LL conditions. However, only per^l mutants performed better under the 29-h T-cycle than under the 24-h cycle, while per^s and per^0 mutants performed equally poor under the 19-h T-cycle and LL as they did under the 24-h cycle, respectively (**Figure 7** right). Under the 29-h T-cycle, per^l mutants persisted in all 10 vials to varying percentages, on average to ∼50%. In two vials, the mutants outcompeted the wildtype flies, meaning that in the end they represented presumably 100% of the population. This cannot be due to genetic drift. The final frequency of per^l mutants in the other vials are within the confidence intervals of genetic drift and might theoretically be caused by it (see above). However, the strong decline of the mutant frequency at the beginning of the experiment (lasting until census 6) that is followed by a clear

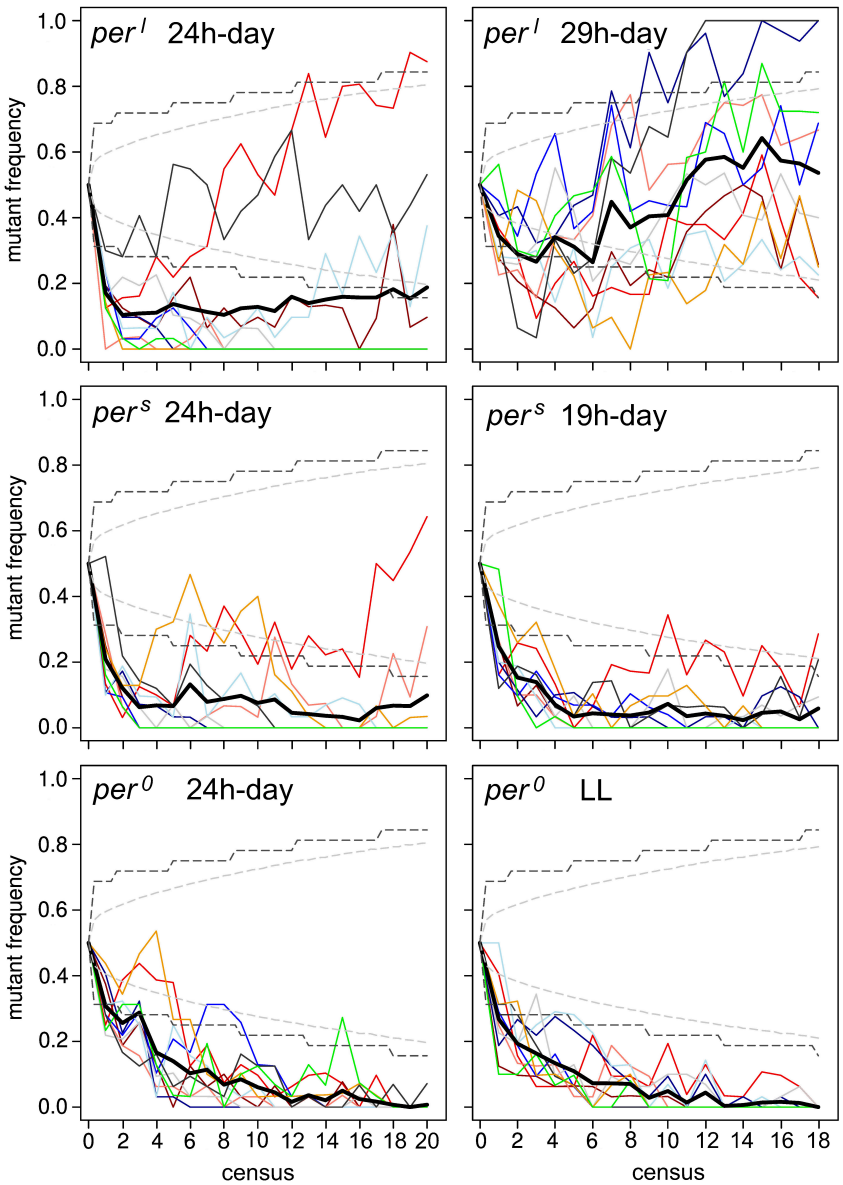

FIGURE 7 | Results of the competition assay experiment in 24-h, 29-h and 19-h days (for per^l and per^s mutants, respectively) and 24-h and constant light (LL) for per^0 and WT_{CS}. For each assay 10 food vials with the *period* mutants competing with wildtype flies were established. The mutant frequency per generation was determined separately in each vial (thin colored lines) and averaged over all vials (thick black line). Hatched gray lines show simulated 95% confidence limits for the frequency in the whole population in scenarios assuming pure genetic drift (identical fitness of wild-type and mutant) and hatched black lines the corresponding 95% confidence limits for samples of 32 males as taken in the experiments (see text for more details on the creation of these intervals; for details see section "Materials and Methods"). Except for the assay in which per^l mutants competed with wildtype flies under the 29 h-day (top right), on average the wildtype flies dominated the *period* mutant flies in all experiments. Nevertheless, in some vials the per^l and per^s mutants performed better than the wildtype flies even in the 24 h-day, so that the mutants persisted in the overall population.

increase in frequency are hard to reconcile with genetic drift. In particular, the comparison between the shape of the "frequency curves" at $T = 24$ h and $T = 29$ h shows that per^l mutants perform clearly better under the 29-h day, which supports the resonance hypothesis. Nevertheless, the poor performance of the per^s and per^0 mutants under both T-cycles clearly shows that additional factors contribute to the fitness of the mutants. These factors can be related or completely independent of the circadian clock.

Outdoor Competition Experiments

In the outdoor experiments, the generation time of the flies was ∼1 month and we could breed through only three generations in each summer. In both summers, 2013 and 2014, the wildtype flies clearly outnumbered the mutants in the third generation (**Figure 8**). Roughly speaking, the mean proportion of the mutant fell from 0.5 to about 0.25 in all the experiments significantly deviating from the initial 1:1 ratio ($p < 0.001$) indicating selection

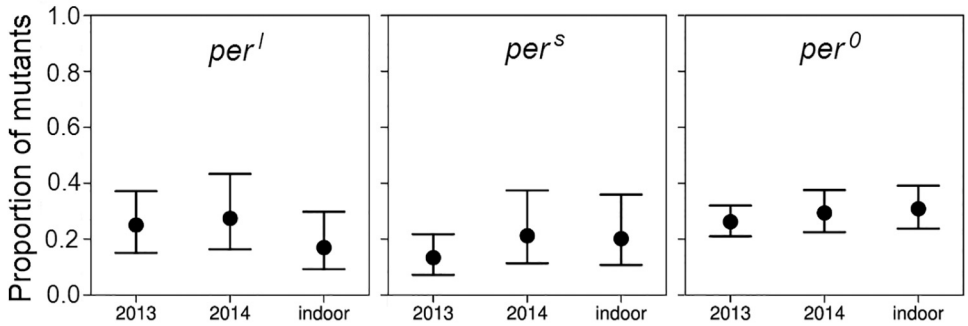

FIGURE 8 | Proportion and binomial 95% CI-intervals of mutant males after three generations of competition with wildtype flies under outdoor and indoor conditions. Data stem from the experiments carried out under external (natural) light conditions in 2013 and 2014 and from the third generation census of the long-term competition experiments under the 24-h day in the laboratory (see **Figure 7**).

against the mutant alleles. There was no significant difference in the percentage of remaining mutants between the 2 years under outdoor conditions and also not between the outdoor and indoor conditions (d.f. 2, 23, deviance reduction = 10.25, $F = 3.065$, $p > 0.05$ following *post hoc* Bonferroni correction). The fact that the decline in the mutant abundance was about similar in the out- and indoor experiments suggests that the different conditions, in particular also the differences in the light regime, between indoor and outdoor conditions do not have a relevant impact on the mutants' success. However, different selective response may also not have been possible due to limited genetic variance in the inbred initial populations.

Changes in Free-Running Period Over the Course of the Indoor Competition Experiment

In the original paper (Konopka and Benzer, 1971), per^s mutants were reported to free-run with a period of ∼19 h and per^l mutants with a period of ∼ 28 h under constant darkness. We determined the free-running period and the activity patterns under LD12:12 for 60 wildtype and mutant flies, respectively, before they underwent the competition experiment. We found a mean period of 24.3 ± 0.04 h for wildtype flies, a period of 19.0 ± 0.03 h for per^s mutants and a period of 27.6 ± 0.06 h for per^l mutants. Thus, while the free-running period of per^s mutants matched the one previously reported, the free-running period of our per^l mutants was about 0.4 h shorter than originally reported and only 3.3 h longer than that of wildtype flies. To see whether the periods remained the same during the competition experiments, we determined them in the flies that were recorded every census throughout the competition experiment. The results are plotted in **Figure 9**. To our surprise, we found that per^l mutants lengthened their period continuously, at the beginning very fast (at census 4 they reached already 29 h) and later slower. At the end they reached a period of 31.1 ± 0.87 h (± SD) in the $T = 24$ h experiment and a period of 30.5 ± 0.71 h (± SD) in the $T = 29$ h experiment. This period lengthening was similar in all vials (**Figure 9B**), indicating that it was not due to founder effects or genetic drift. The other fly strains (wildtype flies and per^s mutants) kept their period rather constant throughout the different experiments (**Figure 9**). The same was true for the wildtype flies and per^s mutants that were kept alone, but maintained and recorded in parallel to the competing flies (data not shown). Again, the situation was a bit different for the per^l mutants (pale blue line in **Figure 9**). per^l mutants kept alone, without competition with the wildtype flies did also lengthen their period over time but this lengthening was far less than for the flies kept in competition with wildtype flies: per^l mutants reached a maximal period of 28.7 ± 0.57 h (±SD) in the first experiment ($T = 24$ h) and of 28.6 ± 0.62 h (±SD) in the second experiment ($T = 29$ h). This shows that a period lengthening of ∼2 h was caused by growing per^l flies together with wildtype flies.

Experiments Done to Reveal Putative Reasons for the Different Fitness of the Mutants

Differences in Sperm Number

To test whether a reduced fertility of the males contributes to the poor performance of the *period* mutants as was shown in a previous study (Beaver et al., 2002), we counted the number of sperms that were transferred during a successful mating for the different genotypes (**Figure 10A**). We found no evidence for a significant difference in sperm numbers between the different genotypes (ANOVA, $F = 1.438$, df 3,27, $p > 0.05$). Wildtype males transferred on average 1257 sperms whereas males of per^S mutants transferred 949 sperms, about a quarter less than wildtype males. However, a female can only store about 500 sperms (Miller and Pitnick, 2002; Manier et al., 2010) and produces less than 200 offspring (see **Figure 10E**), so that all males supplied enough sperm to make it unlikely that the fertility of females is limited by sperm availability.

Differences in Survival During Development

The poor performance of the *period* mutants in the competition experiment may also be due to a lower survival of larvae during development. To test this, we counted the number of pupae and adults that emerged from 1000 eggs for each genotype. We revealed a loss of individuals during larval development in all

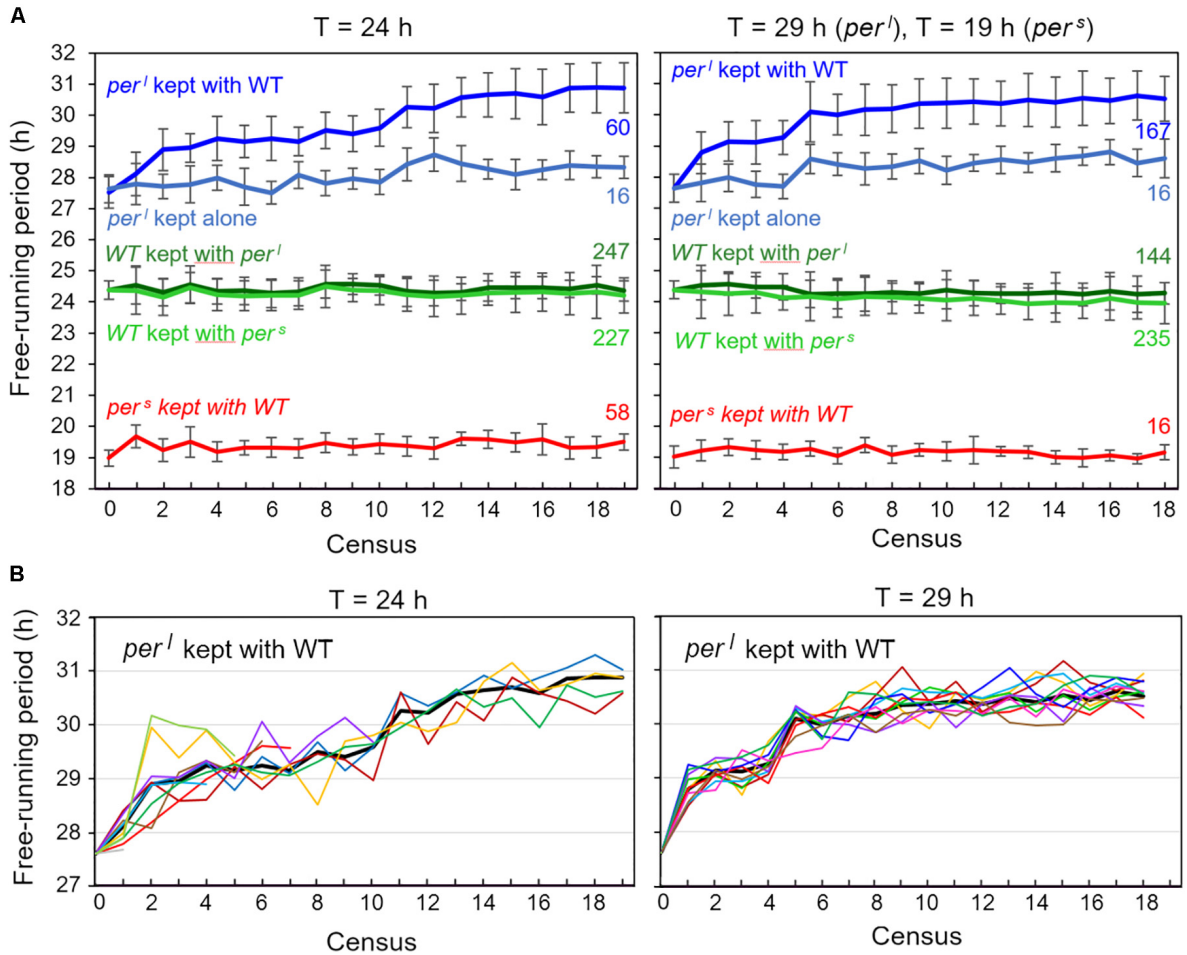

FIGURE 9 | Free-running periods of the flies recorded during the two competition experiments [at Zeitgeber cycles (T) of 24 h (left) and T = 29 h or T = 19 h (right)]. Every census, 32 flies of each of the 10 vials with the competing genotypes (per^l/WT, per^s/WT) were recorded in DD (= 4 × 320 flies per census, see **Figure 2**) and the flies' free-running periods determined and plotted (mean of all flies from all 10 vials ± SD) **(A)**. The experiment started with equal numbers (∼160 at census 1) for each genotype and ended with a lower number of mutants, except for per^l mutants kept under T = 29 h (right diagram). The numbers at the right margin give the number of individuals for each genotype at the last census (19 under T = 24 h and 18 under T = 19 /29 h). In case of per^s the flies included in the determination of period stem only from few vials (3 under T = 24 h, and 1 under T = 19 h). In case of per^l, the number of vials was larger (4 under T = 24 h, and 10 under T = 29 h). Wildtype flies were present in all 10 vials, except for the competition experiment with per^l mutants under T = 29 h. Here the calculated periods at census 18 stem from flies in 8 vials. Note that the sum of mutants and WT flies is always lower than 320, because some flies died during the recording. The pale blue curve give the mean period of per^l mutants that were kept separately (not in competition with wildtype flies under the same environmental conditions as the experimental animals) and that were recorded in parallel to the other flies (16 flies per census). While the per^l mutants grown in competition with WT flies lengthened their period by ∼3 h, the ones kept separately did so only by <1 h **(B)**. Period lengthening of per^l mutants over the course of the competition studies in the single fly vials at T = 24 h and T = 29 h. The mean free-running periods of the flies for each of the 10 vials are shown as colored lines. The thick black line shows the average period of all flies that is also depicted in **A**. At T = 24 h, per^l mutants persisted only in 4 vials until the end of the experiment. Therefore, six colored lines ended before census 19. This is different at T = 29 h, where per^l mutants persisted in all 10 fly vials (compare **Figure 7**).

genotypes that was clearly more dramatic in the *period* mutants as compared to the wildtype flies (**Figure 10B**). The statistical comparison (general linear model with quasibinomial error structure and Dunnett's correction for *post hoc* testing) revealed that the egg to pupal survival rate (s_e) was significantly higher for wildtype females ($s_e^{WT} = 0.863$) compared to any of the three homozygous mutant females: per^l ($s_e^{perL} = 0.466$, d.f. 1, 18, dev. reduction = −371.39, F = 110.62, $p_{adj} < 0.001$), per^s ($s_e^{perS} = 0.472$, *d.f.* 1, 18, dev. reduction = −361.62, F = 165.2 $p_{adj} < 0.001$) and per^0 ($s_e^{per0} = 0.768$, *d.f.* 1, 18, dev. reduction = −30.272, F = 13.774, $p_{adj} < 0.01$). Survival of per^0 mutants was also significantly larger than that of the other two mutants ($p_{adj} < 0.001$).

Survival from the pupal stage to adult (s_p) was very high in all genotypes with no significant difference (GLM with binomial error structure and Dunnett's *post hoc* correction) between wildtype flies, per^l and per^s mutants ($s_p^{WT} = 0.971$, $s_p^{perL} = 0.968$, $s_p^{perS} = 0.971$, χ^2 test likelihood ratio test, $p_{adj} > 0.9$ for both comparisons). However, survivorship of per^0 pupae to adult was even higher than that of wildtype pupae

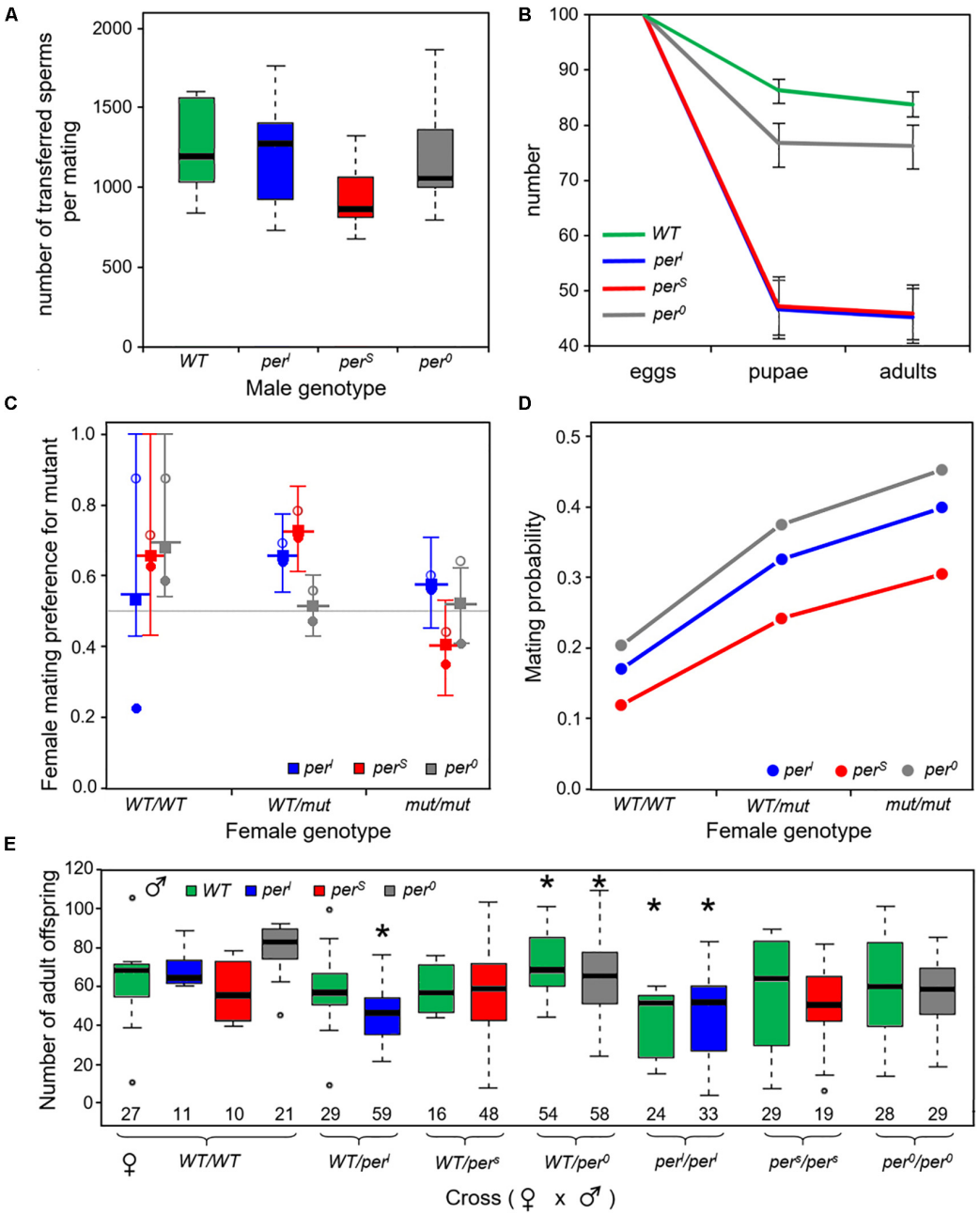

FIGURE 10 | Number of transferred sperms, flies developing from 100 eggs, mating preferences of female flies and offspring of a female fly **(A)**. Mean number of transferred sperm lies between around 950 and 1250 sperms (n = 7 or 8 per genotype) and was not significantly different between the different fly strains **(B)**. Number of developing pupae and adults from 100 eggs of homozygous wildtype and *period* mutant flies, respectively, showing that the mutants had significant lower developmental survival rates than the wildtype flies. Error bars provide binomial 95% confidence intervals. Separate statistical analysis and significance testing was carried out from egg to pupae and then from pupae to adults (details see text) **(C)**. Estimated female mating preferences (probability to favor a mutant male over a wildtype male). The different genotypes are color coded. Open circles reflect choice in experiments where wildtype males were marked, dots in experiments were the mutant male was marked (see section"Materials and Methods"). The square shows the preference for mutant males estimated from the empirical data according to Eqs 1–5 from the main text. The longer horizontal line provides the median value and the error bars span the 95% confidence limits based on the Monte-Carlo simulations (100,000 replicates; see section "Materials and Methods"). Heterozygous WT/per^{l} and WT/per^{s} females preferred the mutant male, respectively. Similarly, wildtype females had a slight preference for per^{s} and per^{0} males (for details see text) **(D)**. Overall probability of successful mating in the mating preference tests dependent of female genotype [color code as in **(C)**]. Logistic regression indicates a significant effect of both, the female's genotype and the mutant male under investigation. Mutant females had a higher probability to mate than wildtype females and per^{0} and per^{l} males were more successful in mating than per^{s} males (for details, see text) **(E)**. Number of adult offspring from the mated females shown in **(C)**. The data showed a large variability, but nevertheless revealed that per^{l} females had a lower and WT/per^{0} a higher number of offspring (asterisks). Details see text. The number of females contributing to this analysis is indicated at the bottom of each box plot.

($s_p^{per0} = 0.992$, d.f. 1, 18, dev. reduction = 10.588, $p_{adj} < 0.05$; Dunnett's *post hoc* correction).

The results provide clear evidence for a significant effect of the clock mutants on a possible fitness component and can explain the poor performance of per^s mutants in the competition assay under the 24 h-day. However, they cannot explain why per^l mutants performed much better during the competition than the other two mutants. They can also not explain, why per^0 mutants, which had the best survival among the three mutants, lost very fast and completely in the competition experiments.

Differences in Female Mating Preferences and Overall Mating Success

To investigate whether the persistence of per^s and especially per^l mutants in the population is due to the preferential selection of mutant males as mating partners by female flies (=rare male advantage), we determined the mating preference of females. It is known that the *period* gene affects not only daily and circadian behavior, but also the frequency of the male courtship song, which in turn strongly affects the mating willingness of females (Kyriacou et al., 1990b, 2017). Females usually prefer males that sing in the frequency of their own genotype, meaning that per^s females prefer per^s males, per^l females per^l males and wild-type females wild-type males (Greenacre et al., 1993). The mating preference of females that were heterozygous for one of the *period* mutations was, however, not tested before. Since we expect most females in our populations to be homozygous or heterozygous wildtypes, their mating preferences could clearly influence the persistence of certain mutations in the population. Therefore, we let each of 280 heterozygous females and 140 homozygous females choose between two males, a wildtype and a mutant one. We tested twice the number of heterozygous females as we wanted to account for possible effects of whether the mutant allele was inherited from the female's mother or father; however, we could not find any difference and thus pooled the data for further analyses. Based on the creation of the Monte-Carlo confidence intervals (see Methods) we found that heterozygous WT/per^s and WT/per^l females significantly favored per^s and per^l males over wildtype males, respectively (**Figure 10C**, $p < 0.05$). In our assay, even homozygous wildtype females showed a tendency to prefer mutant males, but this was only significant for per^0 males (**Figure 6C**, $p < 0.05$). In conclusion, the female mating preference might be a possible reason for the persistence of the mutants in the population as it would allow the mutant alleles to persist at low frequency if negative effects of the mutant gene primarily show up in homozygous individuals.

The mating preference experiments also provided information on the fraction of females that mated successfully during the 2 monitored hours (**Figure 10D**). Mating success ranged between 10% and 45% and was very consistently influenced by the genotype: homozygous wildtype females mated with lower probability than heterozygous females and in particular homozygous mutant females (d.f. = 2, dev. reduction = 56.605, $F = 16.18$, $p < 0.001$). In addition, mating success also depended on the male genotype (d.f. = 1, dev. reduction = 22.571, $F = 6.45$, $p < 0.05$), with the highest success when a per^0 or per^l mutant male was among the potential mating partners. Since overall mating success depends not only on the female choice but also on the male's courting activity there are several possible explanations for these results. Either the mutant females were less choosy than wildtype females, possibly because of their generally reduced fitness, or, for unknown reasons, they were more attractive for males. In addition, we assume that male activity affects mating success. Mating success in trios including a per^l male was generally higher than in trios including a per^s male, which fits to the high morning activity of per^l males as compared to that of per^s males (**Figure 4C**). However, per^0 males had the highest mating success, which cannot be explained by male activity alone.

In summary, the higher mating success of mutant flies together with the preference of heterozygous females for mutant males may explain why per^l and per^s mutants persisted at low frequency in the population when grown in competition with wildtype flies. However, both observations can again not explain why per^0 mutants apparently disappeared completely. Without investigating in more detail the behavioral mechanisms underlying female choice and male courtship activity we cannot be sure about underlying reasons explaining these results. One possibility is that females generally prefer to mate with "different" males providing a selective benefit for the rare males, but mating behavior and female choice may also fundamentally differ between original (highly inbred) populations.

Differences in the Number of Offspring per Female

After having successfully mated in the female mating preference test, the females were used to evaluate the net number of their offspring (=net fertility, **Figure 10E**). The data showed a large over-dispersion (variation) requiring a "quasipoisson" error structure in the general linear model used for the statistical analysis (see materials and methods). Typically, such over-dispersion indicates that some important explanatory variables such as temperature, light, food supply (quality and amount) were not included into the statistical model. All these factors have been tightly controlled, but nevertheless, we observed that sometimes the food dried to a different degree slowing down the development of the larvae. This might explain the large between vial variance observed in the data.

In spite of the large variance, the statistical analysis revealed an effect of the mutant allele via the female genotype for per^l and per^0 but no effect of the mating partner's genotype (per^l d.f. 2, 104, dev. reduction = 93.926, $F = 6.83$, $p < 0.01$; per^0: d.f. 2, 159, dev. reduction = 63.716, $F = 4.8032$ $p < 0.01$). *Posthoc* testing with Bonferroni correction showed that both the WT/per^l and the per^l/per^l females were significantly less fertile than homozygous wildtype flies ($p_{adj} < 0.05$), while WT/per^0 females had a higher fertility than homozygous per^0/per^0 females ($p_{adj} < 0.05$). The other pairwise comparisons revealed no significant differences. For per^s mutants we could not find any evidence for an effect of the mutant on fertility. For per^l mutants these results are in line with the developmental survival analysis (**Figure 10B**), in which the number of flies developing from 100 eggs was tested. In both experiments, per^l mutants showed significantly lower fitness parameters. For per^s and per^0 mutants this was different.

Although significantly less flies developed from 1000 eggs in comparison to wildtype flies (**Figure 10B**), a single female mutant fly had the same number of offspring or in case of WT/per^0 heterozygotes even more offspring (**Figure 10E**). Possibly, the female mutants had laid more eggs. It is also possible that the genotype of the larvae affected survival. Since we have not genotyped the offspring in our fertility test, we do not know whether a different mortality risk of the larval genotype has contributed to the number of offspring.

In summary, we conclude that multiple factors contribute to the fitness of the *period* mutant flies. There was little effect of the genotype on sperm number, but the per^l mutants had clearly less offspring when kept without competition. On the other hand, per^s and per^l mutants were preferred as mating partners by heterozygous females and the mating success was larger with mutant females, which might explain why the mutant alleles remained in the population. We could not identify any reason explaining why per^0 mutants disappeared rather quickly in the population when grown under competition, as the performance of the per^0 mutants was better than that of the other two mutants in all tested fitness components. We acknowledge that there are many more factors that may contribute to genotype distribution in the competition assays that we have not investigated here. For example, competition could have affected developmental time differently in the genotypes, or the genotypes could have responded differently to larval crowding.

DISCUSSION

We show here - for the first time for an animal - that the circadian clock confers a significant competitive fitness advantage under laboratory and semi-natural outdoor conditions. In the case of per^l mutants, we also show that, this selective advantage depends on the resonance between the endogenous period of the animals and the period of the Zeitgeber cycle. Thus, for per^l mutants grown in competition with wild-type flies the resonance hypothesis is partly confirmed: proper timing (=optimal phase of the rhythm in relation to the environmental cycle) appears of significant advantage for the reproductive success of flies that compete with others.

In contrast, per^s mutants did not outcompete wild-type flies when grown under 19-h days, although the 19 h cycle matches their endogenous period. Furthermore, per^0 mutants are not equally fit as wild-type flies under LL conditions despite the fact that LL makes wild-type flies equally arrhythmic as per^0 so that they should lose all timing-advantages over the mutants. These results clearly indicate that other factors besides timing contribute to the competitive fitness benefit of wild-type flies.

It is known that the *period* gene has pleiotropic effects on fly behavior, development and fecundity. Besides affecting the frequency of the male courtship song (Kyriacou et al., 1990b, 2017), it affects developmental timing (Kyriacou et al., 1990a), sleep length (Shaw et al., 2002), the activity of neurons involved in fast escape responses (Megighian et al., 2001), the fecundity of male and female fruit flies (Beaver et al., 2002, 2003) and the duration of the copulation (Beaver and Giebultowicz, 2004). All this may negatively affect the fitness of the mutants under the 24-h day, but it is not clear why per^l mutants had the best and per^0 the worst performance in the long-term competition experiments despite the fact that per^0 performed better on any of the direct fitness estimators investigated than the two other *period* mutants. Putative reasons will be discussed in the following paragraphs. It is important to note here that all experiments addressing fitness parameters in the *period* mutants, including the ones performed here, have been undertaken under a 24-h day. Therefore, in the strict sense, our discussion applies only to the 24-h day and not to the T-cycle experiments.

Per^l Mutants Appear to Have a Higher Fitness Than the Other Period Mutants

In the 24-h day, per^l mutants remained at ∼20% in the fly population and in one food vial they even dominated over the wildtype flies (**Figure 7**). The main reason for their relative higher competitive fitness, may lie in their longer endogenous period that enabled them to have a long and pronounced morning activity (**Figure 4**). Since courting and mating occurs mainly in the morning (Sakai and Ishida, 2001a,b), per^l males might be more successful in mating with females simply because they are rather active in the morning hours. It might be irrelevant for their competitive fitness when they afterward extend the siesta until the evening and start eating only in the night. Indeed, we found that per^l mutants had a relatively high mating success in the female mating preference assay (**Figure 10D**). Another positive factor for their fitness may be the mating preference of virgin WT_{CS}/per^l heterozygotes for per^l males (**Figure 10C**). These positive effects may have dominated over the lower survival rate of per^l larvae (**Figure 10B**) and the reduced number of adult offspring of per^l females (**Figure 10E**); note also that we only have egg-to-adult survival data only for homozygous individuals so that we do not know how strong the survival effect of *period* alleles is in heterozygous individuals. Earlier studies even reported a slower development of per^l mutants (Kyriacou et al., 1990a). In our study, we did not observe evident differences in developmental timing, but we cannot exclude that minor differences exist, especially not under competition. In any case, such differences had obviously no negative effects on the competitive fitness of per^l mutants.

Per^s Mutants Are Clearly Less Fit Than Wild-Type Flies in the 24-h and 19-h Day, but Nevertheless Persist in the Population

per^s mutants persist in the population at ∼10%, independently of the external Zeitgeber period. Putative reasons for their persistence may be the strong preference of WT/per^s heterozygote females and even of homozygote wildtype females for per^s males. In particular, when the mutant allele becomes rare and thus hardly occurs in homozygous females, the mutant male benefit may compensate for the female fitness disadvantages thus resulting in a stable coexistence of wild-type and mutant alleles.

Perhaps more difficult to explain is the very low overall fitness of per^s mutants in comparison to wildtype flies. per^s males

transfer slightly less number of sperm (**Figure 10A**), but as explained earlier this is unlikely to affect the reproductive fitness of the females. The low number of surviving per^s larvae is for sure reducing the fitness of per^s mutants and in contrast to per^l mutants this is not compensated by a higher mating success of per^s males (**Figure 10D**). Nevertheless, the per^s genotype had no negative effect on the number of adult offspring (**Figure 10E**), suggesting that per^s female may compensate the high larval mortality by laying more eggs. Once again, the most likely reason for the low fitness of per^s mutants may lie in the activity pattern of per^s males (**Figure 4A**). In contrast to per^l mutants and wildtype flies, per^s mutants are rather inactive during the morning. Before lights-on, their activity appears suppressed by darkness and after lights-on they show only a very brief morning activity before they enter the siesta. Consequently, the mating activity of male flies may be rather low and this fits with their rather low mating success (**Figure 10D**). Most interestingly, this may also explain why per^s mutants do not perform better under the 19-h day, because even then the morning activity of male mutants was lower than that of wildtype males (**Figure 6**). Nevertheless, still other factors that are independent of timing may contribute to the low fitness of per^s mutants.

Per^0 Mutants Lose Completely Against Wild-Type Flies Under Both Tested Conditions

per^0 mutants appear to have no fitness advantage against wild-type flies. The initial decline in the first generations was in fact somewhat slower than that for the other two mutants (cf. **Figure 7**) but did not stabilize at low proportion as seems to be the case for other two mutants. They even lose quickly against wildtype flies under LL conditions, under which the wildtype flies are similarly arrhythmic and can therefore take no advantage of their circadian clock. These findings are hard to explain in light of the experiments performed in this study. In contrast to previous observations (Greenacre et al., 1993; Beaver et al., 2002), we found no reduction of transferred sperm in per^0 mutants (**Figure 10A**). Furthermore, the survival of per^0 from egg to pupa was much better than that of per^l and per^s mutants (**Figure 10B**) and homozygote wildtype flies showed a mating preference for per^0 males (**Figure 10C**). The mating success of per^0 males was also very good (**Figure 10D**) and heterozygous WT/per^0 mutants showed even a tendency to have more adult offspring than wildtype flies (**Figure 10E**). Consequently, there must exist other factors that reduce the fitness of per^0 mutants and that possible only contribute when the flies have to compete with wildtype flies. per^0 mutants are reported to sleep less (Shaw et al., 2002), to have deficits in certain aspects of learning and memory (Chouhan et al., 2015), to show a lower neuronal activity in neurons that control fast escape responses (Megighian et al., 2001), and to be more sensitive to oxidative stress (Krishnan et al., 2008). Constant light (especially short-wavelength light) also generates stress, and this might be one reason why per^0 flies have disadvantages against wildtype flies under such conditions. Altogether, this might explain the observed reduced reproductive fitness of per^0 mutants when raised in competition to wildtype flies. To sort this out in more detail, additional experiments are needed, which also decipher the effects of population density on the mutant's fitness under competition conditions.

Period Lengthening of per^l Mutants and Putative Effects of the Genetic Background

One of the most surprising result of our study was the dramatic period lengthening of the per^l mutants over the course of the competition experiment. At the beginning, the mutants had slightly shorter periods than reported in previous studies (Konopka and Benzer, 1971), but already at census 2 (generation 6) they reached periods of ∼29 h, and then asymptotically approached periods of 31 h in both experiments (under the 24 h and the 29 h day; **Figure 9**). A selection for long periods by the 29 h cycle cannot be the cause of this period lengthening, because it occurred also under the 24 h cycle. Most interestingly, the 31 h period precisely coincides with the period that Ewer et al. (1990) measured in per^l mutants at 25°C. Possibly, during the long inbreeding, our per^l mutants have accumulated genetic modifiers that shortened their period so that it stayed closer to 24 h. This would imply that wildtype and mutant flies had not the identical genetic background and were probably not outcrossed with each other at the beginning of the experiment as we had presumed. During the gradual exchange of the genetic background between wildtype and per^l mutants in the competition experiment, the genetic modifiers may have got lost and the original period of per^l mutants has reappeared. This interpretation is supported by the fact that per^l kept in isolation do not show a comparable lengthening of their period. In wildtype flies and per^s mutants, we could not see any evident changes in period during the competition experiment. However, this does not mean that these flies had an identical genetic background. Future studies with the now perfectly "cantonized" *period* mutants are necessary to clarify this.

Conclusion

We have shown that possessing an endogenous clock that runs with a period close to 24 h has a clear fitness advantage when flies have to compete with others for food and mating partners. The right timing of activity, especially in the morning when courting and mating occurs, may be crucial for the survival in the population. In addition, we have shown that multiple other factors contribute to the performance of the mutants. Especially the per^s and per^0 mutants are clearly less fit as compared to wildtype flies. This confirms previous observations that the *period* gene has pleiotrophic effects on physiology, metabolism and behavior, independent of its effect on timing. Furthermore, we have clear evidences that the genetic background contributes, too. At least per^l mutants appeared to have accumulated background mutations that modulated the effects of the per^l mutation on the circadian period in such a way that it remained closer to 24 h than in the original stocks maintained at 24 h cycles. After now having outcrossed the flies for >50 generations, we have

certainly eliminated such background differences. Thus, we are in the perfect situation to test the impact of the *period* gene on fitness in more detail in future experiments.

DATA AVAILABILITY STATEMENT

The raw data supporting the conclusion of this manuscript will be made available by the authors, without undue reservation, to any qualified researcher.

AUTHOR CONTRIBUTIONS

MH performed the experiments. OM and TH analyzed the data statistically, made predictions, and contributed to planning of the experiments. TY, DR, and CH-F conceived the study and planned the experiments. DR supervised the experiments. CH-F wrote the manuscript with contributions by DR and TH.

FUNDING

This study was supported by the German Research Foundation (DFG), Collaborative Research Center SFB 1047 "Insect timing," project C5 and C6. This publication was funded by the German Research Foundation (DFG) and the University of Würzburg in the funding programme Open Access Publishing.

ACKNOWLEDGMENTS

We thank Barbara Mühlbauer for excellent technical support and Pia Römer for help with the mating preference tests.

REFERENCES

Abhilash, L., and Sharma, V. K. (2016). On the relevance of using laboratory selection to study the adaptive value of circadian clocks. *Physiol. Entomol.* 41, 293–306. doi: 10.1111/phen.12158

Albrecht, U., Zheng, B., Larkin, D., Sun, Z. S., and Lee, C. C. (2001). MPer1 and mper2 are essential for normal resetting of the circadian clock. *J. Biol. Rhythms* 16, 100–104. doi: 10.1177/074873001129001791

Beaver, L. M., and Giebultowicz, J. M. (2004). Regulation of copulation duration by period and timeless in *Drosophila melanogaster*. *Curr. Biol.* 14, 1492–1497. doi: 10.1016/j.cub.2004.08.022

Beaver, L. M., Gvakharia, B. O., Vollintine, T. S., Hege, D. M., Stanewsky, R., and Giebultowicz, J. M. (2002). Loss of circadian clock function decreases reproductive fitness in males of *Drosophila melanogaster*. *Proc. Natl. Acad. Sci. U.S.A.* 99, 2134–2139. doi: 10.1073/pnas.032426699

Beaver, L. M., Rush, B. L., Gvakharia, B. O., and Giebultowicz, J. M. (2003). Noncircadian regulation and function of clock genes period and timeless in oogenesis of *Drosophila melanogaster*. *J. Biol. Rhythms* 18, 463–472. doi: 10.1177/0748730403259108

Chouhan, N. S., Wolf, R., Helfrich-Förster, C., and Heisenberg, M. (2015). Flies remember the time of day. *Curr. Biol.* 25, 1619–1624. doi: 10.1016/j.cub.2015.04.032

Crawley, M. J. (2013). *The R Book*, 2nd Edn. Chichester: Wiley.

Daan, S., Spoelstra, K., Albrecht, U., Schmutz, I., Daan, M., Daan, B., et al. (2011). Lab mice in the field: unorthodox daily activity and effects of a dysfunctional circadian clock allele. *J. Biol. Rhythms* 26, 118–129. doi: 10.1177/0748730410397645

DeCoursey, P. J. (2014). Survival value of suprachiasmatic nuclei (SCN) in four wild sciurid rodents. *Behav. Neurosci.* 128, 240–249. doi: 10.1037/a0036696

DeCoursey, P. J., and Krulas, J. R. (1998). Behavior of SCN-lesioned chipmunks in natural habitat: a pilot study. *J. Biol. Rhythms* 13, 229–244. doi: 10.1177/074873098129000075

DeCoursey, P. J., Walker, J. K., and Smith, S. A. (2000). A circadian pacemaker in free-living chipmunks: essential for survival? *J. Comp. Physiol. A* 186, 169–180. doi: 10.1007/s003590050017

Dodd, A. N., Salathia, N., Hall, A., Kévei, E., Tóth, R., Nagy, F., et al. (2005). Plant circadian clocks increase photosynthesis, growth, survival, and competitive advantage. *Science* 309, 630–633. doi: 10.1126/science.1115581

Ewer, J., Hamblen-Coyle, M., Rosbash, M., and Hall, J. C. (1990). Requirement for period gene expression in the adult and not during development for locomotor activity rhythms of imaginal *Drosophila melanogaster*. *J. Neurogenet.* 7, 31–73. doi: 10.3109/01677069009084151

Garbaczewska, M., Billeter, J.-C., and Levine, J. D. (2013). *Drosophila melanogaster* males increase the number of sperm in their ejaculate when perceiving rival males. *J. Insect Physiol.* 59, 306–310. doi: 10.1016/j.jinsphys.2012.08.016

Greenacre, M. L., Ritchie, M. G., Byrne, B. C., and Kyriacou, C. P. (1993). Female song preference and the period gene in *Drosophila*. *Behav. Genet.* 23, 85–90. doi: 10.1007/bf01067557

Hamblen, M. J., White, N. E., Emery, P. T., Kaiser, K., and Hall, J. C. (1998). Molecular and behavioral analysis of four period mutants in *Drosophila melanogaster* encompassing extreme short, novel long, and unorthodox arrhythmic types. *Genetics* 149, 165–178.

Hamblen-Coyle, M. J., Wheeler, D. A., Rutila, J. E., Rosbash, M., and Hall, J. C. (1992). Behavior of period-altered circadian rhythm mutants of *Drosophila* in light: dark cycles (Diptera: Drosophilidae). *J. Insect Behav.* 5, 417–446. doi: 10.1007/BF01058189

Johnson, C. H., Mori, T., and Xu, Y. (2008). A cyanobacterial circadian clockwork. *Curr. Biol.* 18, R816–R825. doi: 10.1016/j.cub.2008.07.012

Klarsfeld, A., and Rouyer, F. (1998). Effects of circadian mutations and LD periodicity on the life span of *Drosophila melanogaster*. *J. Biol. Rhythms* 13, 471–478. doi: 10.1177/074873098129000309

Konopka, R. J., and Benzer, S. (1971). Clock mutants of *Drosophila melanogaster*. *Proc. Natl. Acad. Sci. U.S.A.* 68, 2112–2116. doi: 10.1073/pnas.68.9.2112

Krishnan, N., Davis, A. J., and Giebultowicz, J. M. (2008). Circadian regulation of response to oxidative stress in *Drosophila melanogaster*. *Biochem. Biophys. Res. Commun.* 374, 299–303. doi: 10.1016/j.bbrc.2008.07.011

Kyriacou, C. P., Green, E. W., Piffer, A., and Dowse, H. B. (2017). Failure to reproduce period-dependent song cycles in *Drosophila* is due to poor automated pulse-detection and low-intensity courtship. *Proc. Natl. Acad. Sci. U.S.A.* 114, 1970–1975. doi: 10.1073/pnas.1615198114

Kyriacou, C. P., Oldroyd, M., Wood, J., Sharp, M., and Hill, M. (1990a). Clock mutations alter developmental timing in *Drosophila*. *Heredity* 64(Pt 3), 395–401. doi: 10.1038/hdy.1990.50

Kyriacou, C. P., van den Berg, M. J., and Hall, J. C. (1990b). *Drosophila* courtship song cycles in normal and period mutant males revisited. *Behav. Genet.* 20, 617–644. doi: 10.1007/bf01065875

Lenth, R. (2019). *Emmeans: Estimated Marginal Means, aka Least-Squares Means. R Package Version 1.4*. Available at: https://CRAN.R-project.org/package=emmeans

Manier, M. K., Belote, J. M., Berben, K. S., Novikov, D., Stuart, W. T., and Pitnick, S. (2010). Resolving mechanisms of competitive fertilization success in *Drosophila melanogaster*. *Science* 328, 354–357. doi: 10.1126/science.1187096

Megighian, A., Zordan, M., and Costa, R. (2001). Giant neuron pathway neurophysiological activity in per(0) mutants of *Drosophila melanogaster*. *J. Neurogenet.* 15, 221–231. doi: 10.3109/01677060109167378

Mendoza, J., Albrecht, U., and Challet, E. (2010). Behavioural food anticipation in clock genes deficient mice: confirming old phenotypes, describing new phenotypes. *Genes Brain Behav.* 9, 467–477. doi: 10.1111/j.1601-183X.2010.00576.x

Miller, G. T., and Pitnick, S. (2002). Sperm-female coevolution in *Drosophila*. *Science* 298, 1230–1233. doi: 10.1126/science.1076968

Nikhil, K., and Sharma, V. K. (2017). "On the origin and implications of circadian time-keeping: an evolutionary perspective," in *Biological Timekeeping: Clocks, Rhythms and Behaviour*, ed. V. Kumar, (Berlin: Springer), 81–129. doi: 10.1007/978-81-322-3688-7_5

Ouyang, Y., Andersson, C. R., Kondo, T., Golden, S. S., and Johnson, C. H. (1998). Resonating circadian clocks enhance fitness in cyanobacteria. *Proc. Natl. Acad. Sci. U.S.A.* 95, 8660–8664. doi: 10.1073/pnas.95.15.8660

Patke, A., Murphy, P. J., Onat, O. E., Krieger, A. C., Özçelik, T., Campbell, S. S., et al. (2017). Mutation of the human circadian clock gene CRY1 in familial delayed sleep phase disorder. *Cell* 169, 203.e13–215.e13. doi: 10.1016/j.cell.2017.03.027

Pendergast, J. S., Friday, R. C., and Yamazaki, S. (2010). Photic entrainment of period mutant mice is predicted from their phase response curves. *J. Neurosci.* 30, 12179–12184. doi: 10.1523/JNEUROSCI.2607-10.2010

Pittendrigh, C. S., and Minis, D. H. (1972). Circadian systems: longevity as a function of circadian resonance in *Drosophila melanogaster*. *Proc. Natl. Acad. Sci. U.S.A.* 69, 1537–1539. doi: 10.1073/pnas.69.6.1537

R Core Team (2018). *R: A Language and Environment for Statistical Computing*. Vienna: R Foundation for Statistical Computing. Available at: https://www.R-project.org/

Ralph, M. R., and Menaker, M. (1988). A mutation of the circadian system in golden hamsters. *Science* 241, 1225–1227. doi: 10.1126/science.3413487

Sakai, T., and Ishida, N. (2001a). Circadian rhythms of female mating activity governed by clock genes in *Drosophila*. *Proc. Natl. Acad. Sci. U.S.A.* 98, 9221–9225. doi: 10.1073/pnas.151443298

Sakai, T., and Ishida, N. (2001b). Time, love and species. *Neuro. Endocrinol. Lett.* 22, 222–228.

Schlichting, M., and Helfrich-Förster, C. (2015). Photic entrainment in *Drosophila* assessed by locomotor activity recordings. *Meth. Enzymol.* 552, 105–123. doi: 10.1016/bs.mie.2014.10.017

Schlichting, M., Menegazzi, P., and Helfrich-Förster, C. (2015). Normal vision can compensate for the loss of the circadian clock. *Proc. Biol. Sci. U.S.A.* 282:20151846. doi: 10.1098/rspb.2015.1846

Schmid, B., Helfrich-Förster, C., and Yoshii, T. (2011). A new imagej plug-in "actogramj" for chronobiological analyses. *J. Biol. Rhythms* 26, 464–467. doi: 10.1177/0748730411414264

Shaw, P. J., Tononi, G., Greenspan, R. J., and Robinson, D. F. (2002). Stress response genes protect against lethal effects of sleep deprivation in *Drosophila*. *Nature* 417, 287–291. doi: 10.1038/417287a

Sheeba, V., Sharma, V. K., Shubha, K., Chandrashekaran, M. K., and Joshi, A. (2000). The effect of different light regimes on adult life span in *Drosophila melanogaster* is partly mediated through reproductive output. *J. Biol. Rhythms* 15, 380–392. doi: 10.1177/074873000129001477

Toh, K. L., Jones, C. R., He, Y., Eide, E. J., Hinz, W. A., Virshup, D. M., et al. (2001). An hPer2 phosphorylation site mutation in familial advanced sleep phase syndrome. *Science* 291, 1040–1043. doi: 10.1126/science.1057499

Vaccaro, A., Birman, S., and Klarsfeld, A. (2016). Chronic jet lag impairs startled-induced locomotion in *Drosophila*. *Exp. Gerontol.* 85, 24–27. doi: 10.1016/j.exger.2016.09.012

van der Horst, G. T., Muijtjens, M., Kobayashi, K., Takano, R., Kanno, S., Takao, M., et al. (1999). Mammalian cry1 and cry2 are essential for maintenance of circadian rhythms. *Nature* 398, 627–630. doi: 10.1038/19323

Vanin, S., Bhutani, S., Montelli, S., Menegazzi, P., Green, E. W., Pegoraro, M., et al. (2012). Unexpected features of *Drosophila* circadian behavioural rhythms under natural conditions. *Nature* 484, 371–375. doi: 10.1038/nature10991

Vaze, K. M., and Sharma, V. K. (2013). On the adaptive significance of circadian clocks for their owners. *Chronobiol. Int.* 30, 413–433. doi: 10.3109/07420528.2012.754457

Wheeler, D. A., Hamblen-Coyle, M. J., Dushay, M. S., and Hall, J. C. (1993). Behavior in light-dark cycles of *Drosophila* mutants that are arrhythmic, blind, or both. *J. Biol. Rhythms* 8, 67–94. doi: 10.1177/074873049300800106

Conflict of Interest: The authors declare that the research was conducted in the absence of any commercial or financial relationships that could be construed as a potential conflict of interest.

frontiers in Physiology

ORIGINAL RESEARCH
published: 03 December 2019
doi: 10.3389/fphys.2019.01442

New *Drosophila* Circadian Clock Mutants Affecting Temperature Compensation Induced by Targeted Mutagenesis of *Timeless*

Samarjeet Singh[1,2], Astrid Giesecke[3], Milena Damulewicz[1,4], Silvie Fexova[1], Gabriella M. Mazzotta[1,5], Ralf Stanewsky[3] and David Dolezel[1,2]**

[1] Institute of Entomology, Biology Centre of Academy of Sciences of the Czech Republic, České Budějovice, Czechia, [2] Faculty of Science, University of South Bohemia in České Budějovice, České Budějovice, Czechia, [3] Institute of Neuro- and Behavioral Biology, Westfälische Wilhelms University, Münster, Germany, [4] Department of Cell Biology and Imaging, Institute of Zoology and Biomedical Research, Jagiellonian University, Kraków, Poland, [5] Department of Biology, University of Padua, Padua, Italy

OPEN ACCESS

Edited by:
Robert Huber,
Bowling Green State University,
United States

Reviewed by:
William Ja,
The Scripps Research Institute,
United States
Timothy D. Wiggin,
Brandeis University, United States

***Correspondence:**
Ralf Stanewsky
stanewsky@wwu.de
David Dolezel
david.dolezel@entu.cas.cz;
dolezel@entu.cas.cz

Specialty section:
This article was submitted to Invertebrate Physiology, a section of the journal Frontiers in Physiology

Received: 30 April 2019
Accepted: 07 November 2019
Published: 03 December 2019

Citation:
Singh S, Giesecke A, Damulewicz M, Fexova S, Mazzotta GM, Stanewsky R and Dolezel D (2019) New Drosophila Circadian Clock Mutants Affecting Temperature Compensation Induced by Targeted Mutagenesis of Timeless. Front. Physiol. 10:1442. doi: 10.3389/fphys.2019.01442

Drosophila melanogaster has served as an excellent genetic model to decipher the molecular basis of the circadian clock. Two key proteins, PERIOD (PER) and TIMELESS (TIM), are particularly well explored and a number of various arrhythmic, slow, and fast clock mutants have been identified in classical genetic screens. Interestingly, the free running period (tau, τ) is influenced by temperature in some of these mutants, whereas τ is temperature-independent in other mutant lines as in wild-type flies. This, so-called "temperature compensation" ability is compromised in the mutant *timeless* allele *"ritsu"* (tim^{rit}), and, as we show here, also in the tim^{blind} allele, mapping to the same region of TIM. To test if this region of TIM is indeed important for temperature compensation, we generated a collection of new mutants and mapped functional protein domains involved in the regulation of τ and in general clock function. We developed a protocol for targeted mutagenesis of specific gene regions utilizing the CRISPR/Cas9 technology, followed by behavioral screening. In this pilot study, we identified 20 new *timeless* mutant alleles with various impairments of temperature compensation. Molecular characterization revealed that the mutations included short in-frame insertions, deletions, or substitutions of a few amino acids resulting from the non-homologous end joining repair process. Our protocol is a fast and cost-efficient systematic approach for functional analysis of protein-coding genes and promoter analysis *in vivo*. Interestingly, several mutations with a strong temperature compensation defect map to one specific region of TIM. Although the exact mechanism of how these mutations affect TIM function is as yet unknown, our *in silico* analysis suggests they affect a putative nuclear export signal (NES) and phosphorylation sites of TIM. Immunostaining for PER was performed on two TIM mutants that display longer τ at 25°C and complete arrhythmicity at 28°C. Consistently with the behavioral phenotype, PER immunoreactivity was reduced in circadian clock neurons of flies exposed to elevated temperatures.

Keywords: circadian clock, reverse genetics, screening, candidate genes, temperature compensation, CRISPR-CAS9, *Drosophila melanogaster*

INTRODUCTION

Circadian clocks orchestrate the physiology, metabolism, and behavior of living organisms to be optimally aligned to the periodic day and night changes in the environment. For that reason, circadian clocks "keep ticking" even under constant conditions with a free running period (*tau*, τ) close to 24 h. A crucial functional feature of circadian clocks is their ability to run with a comparable speed at a wide range of physiological temperatures, a phenomenon termed "temperature compensation." From a mechanistic point of view, these biological oscillators are a series of interconnected biochemical reactions, which involve transcriptional and translational feedback loops. The exceptional genetic tools available in the fruit fly, *Drosophila melanogaster*, have enabled the identification and detailed analysis of the functional components of the circadian system and their interactions. Many excellent and detailed reviews are available on this topic (Hardin, 2011; Ozkaya and Rosato, 2012; Tataroglu and Emery, 2015; Tomioka and Matsumoto, 2015).

At the core of the fruit fly's circadian clock, the transcription factors CLOCK (CLK) and CYCLE (CYC) drive the expression of genes with E-box motif(s) in the promoter region, including *period* (*per*) and *timeless* (*tim*). PER and TIM proteins slowly accumulate, dimerize in the cytoplasm, and later start to translocate to the cell nucleus, where they inhibit CLK–CYC mediated transcription (Darlington et al., 1998; Glossop et al., 1999). As a result of this negative feedback loop, *per* and *tim* mRNA is repressed, which consequently results in depletion of PER and TIM proteins, allowing the whole cycle to start again with a new round of CLK-CYC mediated transcription. Several kinases and phosphatases tightly regulate the stability of PER and TIM, fine-tuning the pace of the oscillator to roughly 24 h (Price et al., 1998; Martinek et al., 2001; Sathyanarayanan et al., 2004; Agrawal and Hardin, 2016). Additional interconnected transcription/translational feedback loops that contribute to the circadian system were described in *Drosophila* as well as other insects. The PER/TIM feedback loop model was established and further refined through a combination of immunocytochemistry (ICC) (Siwicki et al., 1988), time-course expression profiling (Hardin et al., 1990, 1992), protein biochemical approaches addressing phosphorylation (Edery et al., 1994; Chiu et al., 2011), glycosylation (Li et al., 2019), protein coexpression in *Drosophila* Schneider cell culture (Saez and Young, 1996; Nawathean and Rosbash, 2004; Meyer et al., 2006), and yeast two-hybrid experiments (Rutila et al., 1996). But the key starting point in the *per* and *tim* research was the identification of mutants in extensive genetic screens using either chemical mutagens (Konopka and Benzer, 1971; Konopka et al., 1994; Rothenfluh et al., 2000a), or P-element mobilization (Sehgal et al., 1994). Additionally, spontaneous clock mutations were recovered from wild populations (Matsumoto et al., 1999), or laboratory stocks (Hamblen et al., 1998). Importantly, not only null mutations were obtained, but also mutants with altered protein sequences resulting in faster or slower τ in both *per* (Konopka and Benzer, 1971; Konopka et al., 1994; Hamblen et al., 1998) and *tim* (Matsumoto et al., 1999; Rothenfluh et al., 2000a,b; Wülbeck et al., 2005) genes.

The protein–protein interaction between PER and TIM is a complex and dynamic event (Meyer et al., 2006), including PER homodimerization (Landskron et al., 2009), multiple sequential phosphorylations (Martinek et al., 2001; Ko et al., 2010; Chiu et al., 2011), dephosphorylations (Sathyanarayanan et al., 2004; Fang et al., 2007), and possibly additional posttranslational modifications (Li et al., 2019). A key feature of the negative feedback loop in *Drosophila* is the ∼ 6 h delay that exists between the cytoplasmic accumulation and nuclear translocation of PER and TIM. Both PER and TIM proteins contain a nuclear localization signal (NLS) and cytoplasmic localization domain (CLD) (Saez and Young, 1996). Transgenic flies with mutated TIM NLS have a slower τ, and even though PER and TIM reach high cytoplasmic levels, their nuclear translocation is substantially reduced (Saez et al., 2011). Nuclear entry of PER and TIM requires Importin α1 (IMPα1), which specifically interacts with TIM (Jang et al., 2015). TIM–IMPα1 interaction is abolished by TIM^{PL} (proline 115 to leucine substitution) or TIM^{TA} (threonine 113 to alanine) mutations. Consistently, tim^{PL} and tim^{TA} flies are arrhythmic and TIM^{PL} remains cytoplasmic in circadian clock neurons (Hara et al., 2011). Additionally, TIM is actively exported from the nucleus by CRM1 and this export is affected by interaction with PER (Ashmore et al., 2003). Another mutation with slower τ and abnormal response to light pulses, tim^{blind}, encodes a protein with impaired nuclear accumulation. One of the amino acid substitutions in TIM^{blind} is located within a putative nuclear export signal (NES) (Wülbeck et al., 2005). Collectively, these observations demonstrate the crucial importance of precise regulation of subcellular TIM localization.

Along with light, a primary cue for entrainment, *Drosophila* circadian clocks can be entrained by regular alternations of warmer and colder temperatures (Glaser and Stanewsky, 2005; Sehadova et al., 2009). Also, the distribution of daily activity differs between warm and cold days, which is regulated by temperature-dependent splicing of a *per* intron located within the 3′ untranslated region of mRNA in *D. melanogaster* (Majercak et al., 1999; Zhang et al., 2018). However, at constant conditions, the period length of the circadian clock remains unchanged over a wide range of physiological temperatures. Temperature compensation is a general feature of circadian clocks (Pittendrigh, 1954; Hastings and Sweeney, 1957) conserved from cyanobacteria to mammals (Izumo et al., 2003; Nakajima et al., 2005). In essence, any (bio)chemical reaction runs faster with rising temperature (Arrhenius, 1889), therefore, temperature compensation mechanism should involve multiple reactions, which are differently influenced by temperature, opposing each other (Ruoff, 1992). For example, in the red bread mold, *Neurospora crassa*, temperature-dependent alternative splicing of *frequency* results in long and short FREQUENCY protein isoforms, which have opposing effect on clock speed (Diernfellner et al., 2007). In mammals, distinct phosphorylation of PER2 is important for a temperature-compensated circadian clock (Zhou et al., 2015). Moreover, recently it was shown that the overall activity of the important PER2 kinase CK1δ is temperature-compensated, contributing to

temperature-independent τ in the mammals (Shinohara et al., 2017). Interestingly, the τ of some period-altering *Drosophila* mutations remains constant over a wide range of temperatures (the circadian clock is well temperature-compensated), whereas others have temperature-dependent phenotypes. In the case of per^L, higher temperature further slows down τ from 27.8 h at 17°C to 30.5 h at 25°C (Konopka et al., 1989). A similar and even more profound trend was identified in tim^{rit} where τ is 25.5 h at 24°C and rises to 35 h at 30°C (Matsumoto et al., 1999). An opposite temperature compensation abnormality was reported for $per^{SLIH\ (Some\ Like\ It\ Hot)}$, a spontaneous mutation frequently found in various laboratory stocks (Hamblen et al., 1998). Interestingly, the tim^{SL} (*Suppressor of* per^{Long}) mutation eliminates the temperature compensation defect of per^L, whereas tim^{SL} has no circadian phenotype on its own (Rutila et al., 1996).

Given the length of PER (1218aa) and TIM (1421aa) proteins, however, even the existing remarkable collection of mutants has not been sufficient to uncover all the regions important for the circadian clock machinery and particularly for temperature compensation. Here we discovered that the previously isolated tim^{blind} allele is defective in temperature compensation similar to the neighboring tim^{ritsu} allele. To further explore the role of this and other regions of TIM in temperature compensation and clock function, we performed a targeted CRISPR/CAS9 screen, challenging eight different TIM protein regions and isolated ∼20 new mutants with a functional circadian clock, but altered τ. Our data revealed that manipulation of one region of TIM in particular, consistently produces temperature compensation defects. In addition, we developed a screening protocol that is an efficient alternative to classical mutagenesis approaches (Price, 2005) or rescue experiments with modified transgenes (Baylies et al., 1992; Landskron et al., 2009).

MATERIALS AND METHODS

Fly Strains and *per*, *cry*, *tim* Combinations

Mutant and wild-type alleles of *per* (per^{wt}, per^S, per^T, per^{SLIH}, per^L) (Konopka and Benzer, 1971; Hamblen et al., 1998), *tim* (tim^{wt}, tim^{blind}, tim^{S1}, tim^{L1}, tim^{rit}, tim^{UL}) (Matsumoto et al., 1999; Rothenfluh et al., 2000a,b, Wülbeck et al., 2005), and *cry* ($cry^{01,02,03}$, cry^b, cry^m, and cry^{wt}) (Stanewsky et al., 1998; Busza et al., 2004; Dolezelova et al., 2007) genes were combined by genetics crosses using balancer chromosomes and if necessary, the presence of a particular allele was confirmed by sequencing.

Locomotor Activity Measurement and Analysis

Constant Temperature

Two- to four-days-old males were CO_2 anesthetized and transferred to 70 mm tubes containing 5% sucrose in agar and loaded into the DAM2 TriKinetics system (Waltham, MA, United States), entrained to light:dark (LD, 12:12) conditions for 5 days and released to constant darkness (DD) for additional 10–14 days. The last 3 days were omitted from the analyses but were used to determine fly survival. To determine τ during the first 10 days in DD, chi-square periodogram analysis was performed using ActogramJ (Schmid et al., 2011) and double-plotted actograms were eye inspected in parallel. The same temperature (17, 20, 25, 28°C) was used during the LD entrainment and DD conditions, with the exception of the temperature step-up protocol (see below). For the tim^{blind}, tim^{A1128V}, and tim^{L1131M} mutations generated by site-directed mutagenesis and homologous recombination, flies were exposed to LD for 3 days, followed by 5–7 days in DD at constant temperatures of 18, 25, or 29°C. Period length and their significance (RS values) were determined using autocorrelation and Chi-square periodogram analysis functions of the fly tool box implemented in MATLAB (MathWorks) (Levine et al., 2002). Period values with associated RS values ≥ 1.5 were considered rhythmic (Levine et al., 2002).

Temperature Step-Up Protocol

To be able to measure τ in individual flies at different temperatures, 2- to 4-days-old males were CO_2 anesthetized, loaded into DAM2 TriKinetics system, and entrained in LD (12:12) regime at 20°C for 4 days and then released to DD for 7 days at 20°C (MIR 154 incubators, Panasonic). On eighth day, the temperature was raised to 28°C during 24 h (1°C every 3 h) and locomotor activity was recorded for additional 7 days at 28°C. Step-up protocol was used during the screen to facilitate identification of even subtle temperature-dependent change in τ and to enhance throughput during screening.

Interspecific Comparison of TIM Proteins

Protein sequences of TIM representing dipteran flies *Chymomyza costata* (Kobelkova et al., 2010; Poupardin et al., 2015) and *Musca domestica* (Bazalova and Dolezel, 2017), lepidopteran moth *Ephestia kuehniella* (Kobelkova et al., 2015), heteropteran bug *Pyrrhocoris apterus* used frequently in research of photoperiodic clock (Pivarciova et al., 2016; Urbanova et al., 2016; Kotwica-Rolinska et al., 2017), and basal insect species German cockroach *Blatella germanica* (Bazalova et al., 2016) and firebrat *Thermobia domestica* (Kamae and Tomioka, 2012) were aligned in Geneious 11 using Clustal W algorithm.

Nuclear Export Signal (NES) Prediction

The putative NESs were identified using motif search in Geneious software according to following consensus patterns after Fung et al. (2015) and Ashmore et al. (2003), respectively, where X corresponds to any amino acid, L = leucine, V = valine, I = isoleucine, F = phenylalanine, M = methionine, and square brackets indicate alternatives:

NES-1a (Fung et al.) [LVIFM]XXX[LVIFM]XX[LVIFM]X[LVIFM]
NES-1b (Fung et al.) [LVIFM]XX[LVIFM]XX[LVIFM]X[LVIFM]
NES-1c (Fung et al.) [LVIFM]XXX[LVIFM]XXX[LVIFM]X[LVIFM]
NES-1d (Fung et al.) [LVIFM]XX[LVIFM]XXX[LVIFM]X[LVIFM]

NES-2 (Fung et al.) [LVIFM]X[LVIFM]XX[LVIFM]X[LVIFM]
NES-3 (Fung et al.) [LVIFM]XX[LVIFM]XXX[LVIFM]XX[LVIFM]
NES-1a-R (Fung et al.) [LVIFM]X[LVIFM]XX[LVIFM]XXX[LVIFM]
NES-1b-R (Fung et al.) [LVIFM]X[LVIFM]XX[LVIFM]XX[LVIFM]
NES-1c-R (Fung et al.) [LVIFM]X[LVIFM]XXX[LVIFM]XXX[LVIFM]
NES-1d-R (Fung et al.) [LVIFM]X[LVIFM]XXX[LVIFM]XX[LVIFM]
NES (Ashmore et al.) $Lx_{(1-3)}Lx_{(1-3)}Lx$[LVIM].

Prediction of Phosphorylation Sites

The putative phosphorylation sites were predicted *in silico* using NetPhos 3.1 server at http://www.cbs.dtu.dk/services/NetPhos/ and scores higher than 0.5 were plotted in alignments.

Gene Editing Inducing Non-homologous-End-Joining (NHEJ)—gRNA Design

Target sites were identified using CRISPR target finder[1] and gRNA design was validated according to parameters mentioned in Ren et al. (2014). To start transcription from U6 promoter 5′ guanine is required; therefore, target sites that lack this feature were extended by single guanine in the 5′ direction (see **Table 1** for gRNA sequences and their position on *tim*/TIM). To construct a gRNA expression vector with U6 promoter upstream of *tim*-specific gRNA, two complementary 24-bp oligonucleotides (custom synthesized, Generi Biotech Ltd.) were annealed to obtain a double-strand DNA with 4-bp overhangs compatible to BbsI-linearized pBFv-U6.2 vector (Kondo and Ueda, 2013) obtained from fly stocks of National Institute of Genetics, Japan (NIG-FLY). Plasmid and inserts were ligated with T4 DNA ligase overnight at 4°C and transformed to DH5α competent cells. Presence of the insert was confirmed by PCR and positive clones were sequenced.

Gene Editing Inducing Homology Directed Repair (HDR)—gRNA Design

Target gRNA sites were selected so that Cas9 mediated cleavage was directed to a target locus of 100 bp upstream and downstream of the tim^{blind} mutation. To avoid off target cleavage optimal target sites were identified using CRISPR target finder (see footnote 1). Two gRNA targets were chosen that are close to the target locus. Complementary target site oligos also contained a 5′ guanine for transcription from the U6 promoter and a 3 bp overhang compatible to BbsI sites. Oligos were annealed using standard primer annealing reactions and cloned into BbsI linearized pCFD3 plasmid (Port et al., 2014) via T4 DNA ligation.

[1]https://flycrispr.org/target-finder/

Gene Editing Inducing HDR—Donor Plasmid Construction

Donor plasmids that contain the desired *tim* point mutations and all elements necessary for homologous recombination were constructed in three subsequent cloning steps. In each round of cloning the 1.5 kb 5′ homology arm and the 1.5 kb 3′ homology arm were individually PCR amplified using outside primers *tim*BMHRF and *tim*BMHRR2 in combination with respective internal primers. Outside primers *tim*BMHRF and *tim*BMHRR2 contain a 15 bp overhang for In-Fusion cloning that is homolog to linearized vector ends. Inside primers have 5′ 15–20 bp extensions that are complementary to each other in addition to one defined mutation for each round of cloning. In the initial round of cloning, Pam site mutations were introduced to avoid unwanted Cas9 cleavage within the donor plasmid. The two fragments (5′ homology arm and 3′ homology arm) were amplified from *y w* flies and assembled into plasmid pBS-KS-attB1-2-PT-SA-SD-0-2xTY1-V5 (Addgene) that was linearized with XbaI and HindIII using In-Fusion cloning. In a second round of cloning, the homology arms were amplified again using the pBS donor plasmid from the previous round as a template. Outside primers were as described above while the inside primers introduced a silent SalI site that can be used to screen for transformants. In-fusion cloning was used to assemble the fragments as described above. The resulting plasmid was then used in a final round of PCR to introduce the individual tim^{blind} mutations A1128V, L1131M and for remaking the original tim^{blind} double mutation (see **Table 2** for a detailed list of all primers).

Transgenesis for NHEJ Mutagenesis

gRNA-encoding plasmids were purified with Qiagen miniprep kit and DNA was eluted in H_2O. Plasmids were diluted to concentration 100 ng/μl and injected into freshly laid embryos of y^2 cho^2 v^1 *P{nos-phiC31\int.NLS}X; attP2 (III)* stock (NIG-FLY#: TBX-0003) with embryonically expressed phiC31 integrase from transgene located on the X chromosome, attP landing site on the third chromosome, and *chocolate* and *vermillion* (cho^2 v^1) mutations on the X chromosome. G0 flies were crossed to y^2 cho^2 v^1; *Pr Dr/TM6C, Sb Tb* (NIG-FLY#: TBX-0010) and F1 offspring were selected for eye color rescue (v^+ transgene in the cho^2 v^1 background turns the eye color from light orange to dark brown). Strains with gRNA-encoding transgene were balanced with TM6C, *Sb Tb* and kept as stock.

Transgenesis for HDR Experiments

Donor plasmids containing the desired mutation along with gRNA plasmids were verified by sequence analysis and scaled up for injections using Qiagen plasmid midiprep; 6 μg of each plasmid was precipitated and eluted in injection buffer. gRNA construct and donor plasmids were mixed prior to injection and the mix was injected into freshly laid embryos of *nos*-Cas9 flies (Port et al., 2014). Surviving adults were backcrossed in batch crosses to *y w*, *Bl/CyO*, + flies to balance second chromosome modifications

TABLE 1 | List of gRNA used in this study.

Region in TIM	gRNA name	gRNA sequence[PAM] (5′→3′)	Protein sequence corresponding to gRNA
upstream of UL (two gRNAs)	UL rev	ACAGAGAGGCTTCGAACCAG[AGG]	268-SLWFEASLS-276
	UL fw	TAATACCTCGCCCCCCAAAC[AAG]	284-SNTSPPKQ-291
$NES^{776-785}$	fw 781-789	CCTACTCATTCTGGACAGTT[CGG]	781-LLLILDSSA-789
$NES^{1015-1023}$	fw 1017-1025	CCTGCTGGACCTGATCATTA[AGG]	1017-ILLDLIIKE-1025
$NES^{1093-1104}$	rev 1090-1098	GGAGCAGGAGAACAAAAGGC[TGG]	1090-YQPFVLLLH-1098
ritsu and blind (two gRNAs)	rev ritsu	GTCTCCGGTGTCCAGTAGTC[CGG]	1116-PDYWTPET-1123
	fw blind	GTACGGACTCGCCAAAAAGC[TGG]	1124-MYGLAKKLG-1132
$NES^{1166-1174}$	rev 1171-1179	TATCGCCGAGATCCACGTCC[AGG]	1171-SLDVDLGDT-1179
Unspliced^{1387} (EKEKEL^{Kstop})	fw unspliced 1387	AAAGTGAGTGCGATTGAGCC[TGG]	Mostly intronic sequence

First column indicates protein region of interest. The name of gRNA specifies its directionality (fw—forward, rev—revers) and position corresponding to protein sequence. Square brackets after each gRNA indicate protospacer adjacent motif (PAM) sequence. Gray background highlights situation when construct contains two gRNAs. Superscript indicates protein sequence resulting from retained intron.

TABLE 2 | Primers used for HDR experiments.

Primer name	Sequence	Used for
timBMHRF	GATGGTCGACTCTAGACGGAGAGTTTGTCAATGACTGC	Outside primer for amplifying 5′ homology region
timBMHRR2	GATGGTCGACAAGCTTCTTGAGACGTAGACGGAGTCGG	Outside primer for amplifying 3′ homology region
TimBMPAMmutF1a	GGAGACAATGTATGGACTCGCCAAAAAGCTGGGAC	Introduces Pam site mutation for gRNA target 1
TimBMPAMmutR1a	AGTCCATACATTGTCTCCGGTGTCCAGTAGT	Introduces Pam site mutation for gRNA target 1
timSalIF	CGTGAGTTAAAGTCGACCACAGAAAAAAACAACCCATTTG	Introduces SalI site
timSalIR	GGTCGACTTTAACTCACGTTTGTCCAGC	Introduces SalI site
timA1128VF	CAATGTATGGACTCGTCAAAAAGCTGGGACCGCT	Introduces A1128V mutation
timA1128VR	GACGAGTCCATACATTGTCTCCGGTGTCCA	Introduces A1128V mutation
timL1131MF	GACTCGTCAAAAAGATGGGACCGCTGGACAAACG	Introduces L1131M mutation for double tim^{blind} mutant
timL1131MR	CATCTTTTTGACGAGTCCATACATTGTCTCCGG	Introduces L1131M mutation for double tim^{blind} mutant
timL1131MFa	GACTCGCCAAAAAGATGGGACCGCTGGACAAACG	Introduces L1131M mutation
timL1131MRa	CATCTTTTTGGCGAGTCCATACATTGTCTCCGG	Introduces L1131M mutation
TimBMPAMmutF2a	GACTACTGGACACCAGAAACAATGTATGGACTCGCCA	Introduces Pam site mutation for gRNA target 2
TimBMPAMmutF2b	GACTACTGGACACCAGAAACAATGTATGGACTCGTCA	Introduces Pam site mutation for gRNA target 2
TimBMPAMmutR2a	TTCTGGTGTCCAGTAGTCCGGAATTCTGGCG	Introduces Pam site mutation for gRNA target 2
ScreenTimF1	CTCCCACTTCCGCAACAACAGAGTCTG	Molecular screen of transformants
ScreenTimR2	GCTGCTTACCGAGCTGAGCGAGTTGCG	Molecular screen of transformants
timgRNAT1F	GTCGTGGACACCGGAGACAATGTA	gRNAtarget 1
timgRNAT1R	AAACTACATTGTCTCCGGTGTCCAC	gRNAtarget 1
timgRNAT2F	GTCGCGAGTCCGTACATTGTCTC	gRNAtarget 2
timgRNAT2R	AAACGAGACAATGTACGGACTCGC	gRNAtarget 2

with CyO. Individual male and female flies from this cross were crossed again to *y w*, *Bl/CyO*, +. After egg deposition for 3–5 days, adult transformant flies were used for molecular screening.

Because initial attempts to introduce the A1128V mutation did not result in any positive transformants, a slightly different approach was used. The original tim^{blind} EMS stock was crossed to nosCas9 flies and embryos of this cross were injected with donor plasmids containing the A1128V mutation and the wild-type residue at position 1131 to back mutate the M at this position to L.

Genetic Crosses Inducing NHEJ

The CAS9 editing procedure utilized fly strains and tools established by Kondo and Ueda (2013). Flies expressing Cas9 specifically in germ cells (nos-Cas9) from third chromosome insertion (NIG-FLY#: CAS-0003; y^2 cho^2 v^1; *P{nos-Cas9*, *y+*, *v+}3A/TM6C*, *Sb Tb*) were crossed with individual U6gRNA-encoded transgenic strains (also located on the third chromosome). Resulting offspring thus expressed both gRNA and CAS9 on third chromosome, which potentially targeted *tim* gene located on the second chromosome and induce insertions and deletions as a result of non-homologous-end-joining (NHEJ) mechanism. The resulting offspring were crossed to y^2 cho^2 v^1; *Sco/CyO* (NIG-FLY#: TBX-0007) to balance modified second chromosome by *CyO*. Males and females with second chromosome balancer were individually crossed again to y^2 cho^2 v^1; *Sco/CyO* flies to establish lines with identically modified second chromosomes (see **Supplementary Figure S1** for the crossing scheme).

Behavioral Screening in NHEJ Experiments

To identify mutants, locomotor activity of eight males per line (homozygous for the second chromosome) was recorded in temperature step-up protocol and any alternations in locomotor activity pattern (arrhythmicity, change in τ) were identified from the double-plotted actograms. In parallel, reference strains with either functional (w^{1118} or Canton S) or altered temperature compensation (tim^{rit}) were recorded as a negative and positive control. Phenotypes of putative mutant lines were further confirmed on a large sample in temperature step-up protocol and also independently at low (17°C), ambient (25°C), and high (28°C) constant temperatures.

Molecular Screening in HDR Experiments

A total of 95 flies for each mutation were screened using PCR and restriction digests. In detail, a ∼800 bp target locus containing the expected mutations along with the introduced SalI restriction site was amplified by PCR using genomic DNA from individual flies; 1 μl of SalI was then added to half of the PCR and incubated for 2 h at 37°C. Resulting products were analyzed on agarose gels. The remaining PCR product of samples that showed digested products of the correct size was then used for sequencing to verify the presence of the desired mutations.

Sequencing of Mutated Region

To characterize the molecular nature of the CRISPR/Cas9-induced mutations, target loci were first amplified by PCR using genomic DNA extracted from individual flies. One fly was crushed in 50 μl of Squishing buffer (10 mM Tris-HCl pH8; 1 mM EDTA; 25 mM NaCl; 200 g/ml Proteinase K), followed by incubation at 37°C for 30 min and later Proteinase K inactivation at 95°C for 3 min. Using 1 μl of the crude DNA extract as a template, a DNA sequence surrounding the target site was amplified by PCR for 35 cycles in a 10 μl reaction with 2X PPP Master Mix (Top-Bio, Prague, Czech Republic). The PCR products were analyzed by agarose gel electrophoresis and Sanger sequencing. Primers used for PCR and DNA sequencing are listed in **Table 3** and the actual number of obtained mutants is in **Table 4**.

Immunocytochemistry

Seven-days-old males kept in LD regime and constant temperature of 17, 20, or 28°C were collected at specific time points (every 4 h) during the day; red light was used for collection in the dark time points. Flies were fixed in 4% paraformaldehyde in phosphate buffer saline (PBS; pH 7.4) for 1.5 h, washed in PBS twice, and brains were dissected. Next, tissues were fixed again for 45 min in 4% PFA and washed five times in PBS with an addition of 0.2% Triton X-100 (PBT). After that, brains were incubated in 5% normal goat serum (NGS) with an addition of 0.5% bovine serum albumin (BSA) for 30 min first at room temperature, and then incubated with primary anti-PER antibodies (rabbit, 1:5000, Stanewsky et al., 1997) for 3 days and with anti-PDF (mouse, 1:500, Hybridoma Bank) for 1 day at 4°C. Afterward, brains were washed six times in PBT/BSA and blocked in 5% NGS for 45 min. After that, goat anti-rabbit (conjugated with Cy3, 1:500, Jackson Immuno Research) and goat anti-mouse (conjugated with Alexa 488, 1:1000, Molecular Probes) secondary antibodies were applied overnight in 4°C. Finally, brains were washed twice in BSA, six times in PBT, and twice in PBS. Then, brains were mounted in Vectashield medium (Vector) and examined under a Zeiss Meta 510 laser scanning microscope. The identical laser settings were used for all images.

Quantitative Comparison of Immunofluorescence Values

Collected images were analyzed using ImageJ software (NIH, Bethesda). PDF-immune-positive cells were marked (green channel) and PER fluorescence intensity (red channel) was measured in the selected area and outside of the PDF-expressing cells (background). Fluorescence intensity is represented by the mean gray value (the sum of the values of all pixels in the area divided by the number of pixels within the selection). The final value was obtained by subtracting the background value from the staining in the selected area. At least 10 brains per each time point were checked. Experiments were repeated three times.

Compensation for Different Staining Affinity After Antibody Re-use

Brains from every genotype were isolated at ZT0 at 17, 25, and 28°C in parallel. After immunostaining, mean gray value was measured. The mean was used to calculate the ratio between the intensity staining in different temperatures for every genotype separately. Then the ratio between means at ZT0 at different temperatures from previous experiments was calculated, which allowed identifying the factor used for data compensation. This allowed us to avoid differences in staining intensity caused by changes in antibodies affinity after re-use.

Statistical Analysis

The differences between τ were tested for statistical significance by one-way ANOVA with Tukey–Kramer's *post hoc* test using Graphpad7 (Prism) software. ICC staining intensities were compared by one-way ANOVA between genotypes for each timepoint, temperature, and cell type.

RESULTS

Genetic Interaction Between *tim*, *cry*, and *per*

We combined existing *cry* alleles ($cry^{01,02,03}$, cry^{b}, cry^{m}, and cry^{wt}) with available alleles of *per* (per^{wt}, per^{S}, per^{T}, per^{SLIH}, per^{L}) and *tim* (tim^{wt}, tim^{blind}, tim^{S1}, tim^{L1}, tim^{rit}, tim^{UL}). Locomotor activity was recorded in 65 genetic combinations at low (18°C), standard (25°C), and high (28°C) temperatures. In general, the observed free running periods were consistent with published data including previously reported temperature compensation defects of per^{L} (Konopka et al., 1989), tim^{rit} (Matsumoto et al., 1999), and per^{SLIH} (Hamblen et al., 1998). Similarly, combination of per^{L} with *cry* mutants ($cry^{01,02,03}$, cry^{b}, cry^{m}) resulted in flies

TABLE 3 | Primers used for amplification and subsequent sequencing of mutants.

Targeted region	Note	Orientation	Primer sequence	Amplicon size (bp)
Upstream of UL	Used for sequencing	Forward	ACTCCTGTATCTGATGACC	334
		Reverse	GATACTCCTGACCCTTGC	
	Used for detection of the in/del only	Forward	TACAAGGATCAGCATGTG	185
		Reverse	GCCATTGCTGCCATTGT	
$NES^{776-785}$		Forward	GCGAAATGTCCGATCTGAGG	188
		Reverse	CCCTACTGTGTTATGTGCTC	
$NES^{1015-1023}$		Forward	CCTCAGATGATGTTCAGGTG	156
		Reverse	GCAGCACTCAATGAGGATCC	
$NES^{1093-1104}$		Forward	CCGGAAGGCGATCACATCAT	217
		Reverse	GTCCGTACATTGTCTCCGGT	
ritsu and blind	Used for detection of the in/del only	Forward	GCAGTGGAACAACGAGCAAT	225
		Reverse	TGTGGAATGACAAATGGGT	
	Used for detection of the in/del only	forward	CTCCACAAGCTGGGCATT	132
		Reverse	CTTTAACTCACGTTTGTCCAGC	
	Used for sequencing	Forward	GATCACATCATGGAGCCGGTG	565
		Reverse	TGAGCGAGTTGCGGGGTC	
$NES^{1166-1174}$		Forward	CCTCAAGTTCGACGCCAGTG	238
		Reverse	GTTGCAGTGCTTCGTCTTGG	
$Unspliced^{1387}$		Forward	GGCTGGAAATGGATGTGGAC	280
		Reverse	CTGTCAAACTGAGAGGTGAC	

with temperature compensation defects comparable to per^L alone (Fexová, 2010, M.Sc. thesis, and **Supplementary Table S1**), in agreement with the retraction note for Kaushik et al. (2007) (PLoS Biol 2016, 14:e1002403).

tim^{blind} Is a Temperature Compensation Mutant

tim^{blind} was identified in a chemical mutagenesis screen for mutations altering *period* gene expression and contains two conservative amino acid substitutions, alanine to valine (V) at position 1128 and leucine (L) to methionine (M) at position 1131 (Wülbeck et al., 2005). While tim^{blind} flies exhibit a long (26 h) free running period length of locomotor activity (measured at 25°C), the period length of eclosion rhythms (measured at 20°C) is normal (24.5 h) (Wülbeck et al., 2005). We therefore tested the possibility that tim^{blind} mutants are defective in temperature compensation. Indeed, tim^{blind} showed a normal τ of locomotor activity rhythms at 17°C (23.7 h), and gradually longer τ at higher temperatures (24.0 h at 20°C; 25.7 h at 25°C; 26.8 at 28°C; $P < 0.001$, **Figures 1B,D** and **Table 5**), confirming that this *tim* allele affects temperature compensation. In agreement with Wülbeck et al. (2005), the mutant is fully recessive (**Figures 1C,D**). One of the two tim^{blind} amino-acid substitutions (L1131M) maps to one of the six potential NESs originally predicted for TIM (Ashmore et al., 2003), indicating that this mutation is responsible for the tim^{blind} phenotypes (Wülbeck et al., 2005). To test this hypothesis, we introduced the individual substitutions as well as the double-mutant into the endogenous *tim* gene, using site-directed mutagenesis combined with CRISPR/Cas9 mediated homologous recombination (Port et al., 2014; see section "Materials and Methods"). Locomotor behavior of the resulting mutants (tim^{A1128V}, tim^{L1131M}, $tim^{blind-2.1}$) was analyzed in DD at 18, 25, and 29°C to determine rhythmicity and potential defects in temperature compensation. Surprisingly, none of the single mutants recapitulated the phenotypes of the original tim^{blind} double-mutant. The tim^{A1128V} mutation led to high percentage of arrhythmicity, ranging from 57% at 18°C to 77% at 29°C (**Figure 1E** and **Table 5**). Although the remaining rhythmic flies had variable periods at all three temperatures, overall they still indicate a potential period lengthening with increasing temperatures (**Figures 1E,H** and **Table 5**). The severe impact of the tim^{A1128V} mutation on rhythmicity is surprising, given the conservative nature of this amino acid replacement. In contrast, the predicted NES mutation tim^{L1131M} basically had no effect on rhythmicity and period length at any temperature. Between 84% (18°C) and 63% (29°C) of the mutant flies were rhythmic with period values slightly below 24 h at all temperatures (**Figures 1F,H** and **Table 5**). On the other hand, the re-engineered tim^{blind} double-mutant ($tim^{blind-2.1}$) showed temperature-dependent period lengthening and robust rhythmicity at all temperatures, closely matching the phenotypes of the tim^{blind} EMS allele (**Figures 1G,H** and **Table 5**, Wülbeck et al., 2005). At 25°C, the period length of $tim^{blind-2.1}$ is about 1 h shorter compared to tim^{blind} (**Figures 1B,G** and **Table 5**, Wülbeck et al., 2005), while at 29°C $tim^{blind-2.1}$ it is about 1 h longer compared to tim^{blind} at 28°C. Because the experiments with the original tim^{blind} allele and $tim^{blind-2.1}$ were performed in different laboratories (České Budějovice and Münster, respectively), small differences in the experimental set-up (e.g., temperature), or period length determinations could explain these discrepancies. Importantly, both the synthetic and original tim^{blind} alleles show a pronounced defect in

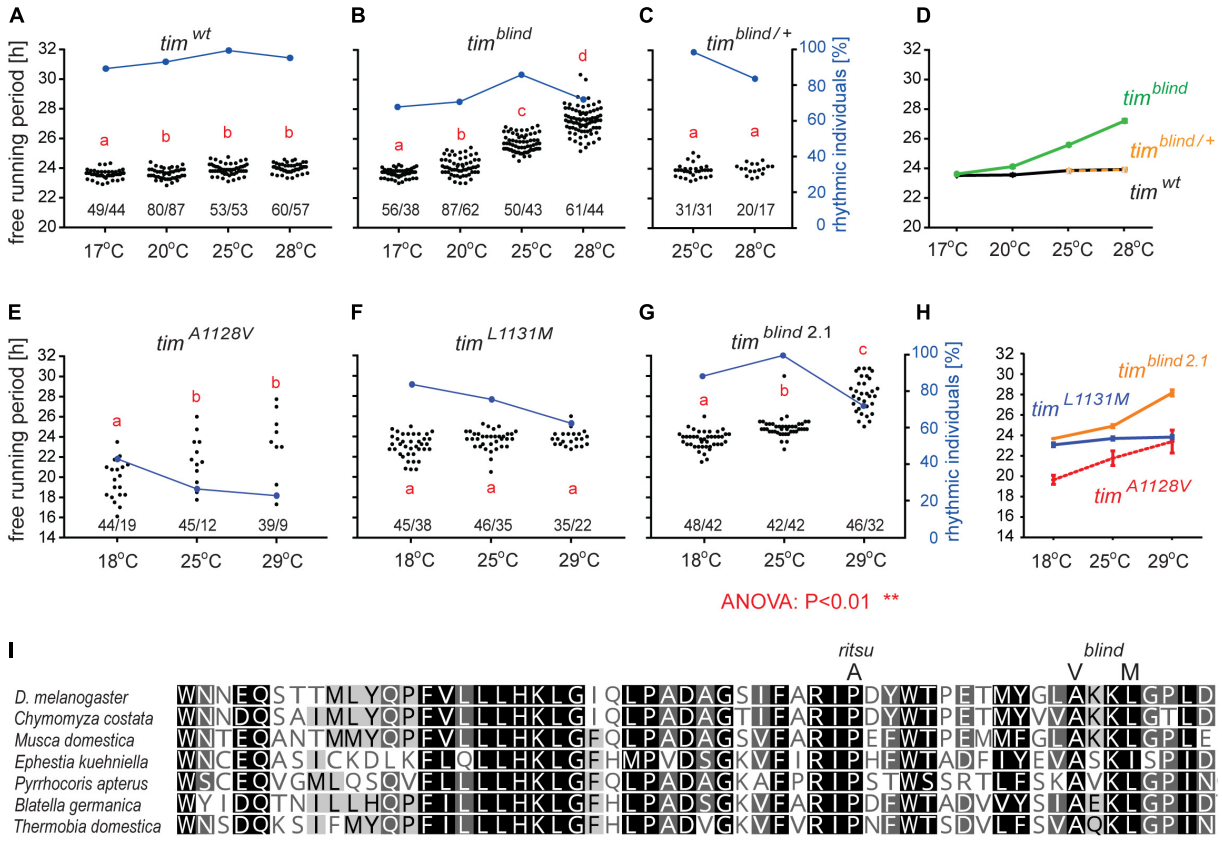

FIGURE 1 | *timeless*^{blind} is a circadian clock mutant with defect in temperature compensation [each dot in panels **A–C** and **E–G** represents the free running period (*tau*, τ) of individual male flies recorded during 10 days in DD at the specified temperature]. Blue dots connected with a line indicate the percentage of rhythmic individuals (scale is on the right *y*-axis) at a particular temperature). **(A)** τ of control Canton S wild-type (wt) flies, **(B)** *tim*^{blind} homozygous, and **(C)** *tim*$^{blind/+}$ heterozygous *D. melanogaster* males in constant darkness (DD) and constant temperature (17, 20, 25, and 28°C). **(D)** Comparison of τ (shown as mean ± SEM) for all three genotypes indicates the temperature-dependent τ lengthening in *tim*^{blind} and confirms that the mutant is fully recessive. **(E)** *tim*^{A1128V}, a mutant with only the first *tim*^{blind} position mutated, is mostly arrhythmic with a potential temperature compensation defect in rhythmic individuals, **(F)** *tim*^{L1131M}, a mutant with only the second *tim*^{blind} position mutated, exhibits normal and fully temperature-compensated τ. **(G)** The synthetic *tim*$^{blind2.1}$ allele shows temperature compensation defects and solid rhythmicity. **(H)** Comparison of τ (shown as mean ± SEM) for re-engineered single and double-mutant versions of *tim*^{blind}. **(I)** Alignment of various insect TIM proteins near TIM^{rit} and TIM^{blind} mutations (specific substitution in *rit* and *blind* is shown above the alignment). Insects are ordered according to their phylogenetic relationship from the most diverged at the top to the most ancestral at the bottom, with the following insect groups: Diptera (*Drosophila*, *Chymomyza* and *Musca*), Lepidoptera (*Ephestia*), Heteroptera (*Pyrrhocoris*), Blattodea (*Blatella*), and Ametabola (*Thermobia*). A, V, and M refer to the single letter aminoacid code.

temperature compensation, and we show here that both amino acid substitutions are required to elicit this phenotype.

Interestingly, in both *tim* temperature compensation alleles, *tim*^{rit} and *tim*^{blind}, the mutations are located in the same region of the TIM protein, separated by only 11–14 amino acids (**Figure 1I**). TIM^{rit} was isolated from a natural fruitfly population and harbors a proline (P) to alanine (A) amino acid substitution at position 1093 (Matsumoto et al., 1999) which corresponds to position 1116 in the L-TIM protein, where additional 23 amino acids are added at the N-terminus (Tauber et al., 2007). Protein alignment indicates that these TIM regions are highly conserved across even distantly related insect species, including hemimetabolan *P. apterus*, *B. germanica*, and ametabolan *T. domestica* (**Figure 1I**).

The most common NES motif that is recognized by CRM1 is best described by the consensus sequence L-X(2,3)-[LIVFM]-X(2,3)-L-X-[LI], where X(2,3) represents any two or three amino acids that separate the four key hydrophobic residues. Although a large amount of proteins contain this consensus sequence, only a small percentage of NESs are actually functional. On the other hand, only 36% of experimentally identified functional NESs match this consensus (Kosugi et al., 2008). Thus, predicting functional NES motives is still challenging and a reliable approach has not yet been described. Therefore, we used different approaches to analyze potential NES motives in TIM.

First, we assess the evolutionary conservation of NES in TIM by identifying and comparing NES motifs in the above-mentioned "primitive" insect species and included two additional dipteran (*C. costata* and *M. domestica*) and one lepidopteran (*E. kuehniella*) representatives. We searched for strict NES motifs using the consensus after Ashmore et al. (2003). Six NES motifs were found in the entire *Drosophila* TIM, and two of them located near the TIM^{blind} and TIM^{rit} mutations. The NES 1031-1139, which overlaps with TIM^{blind}, is further conserved in all Diptera

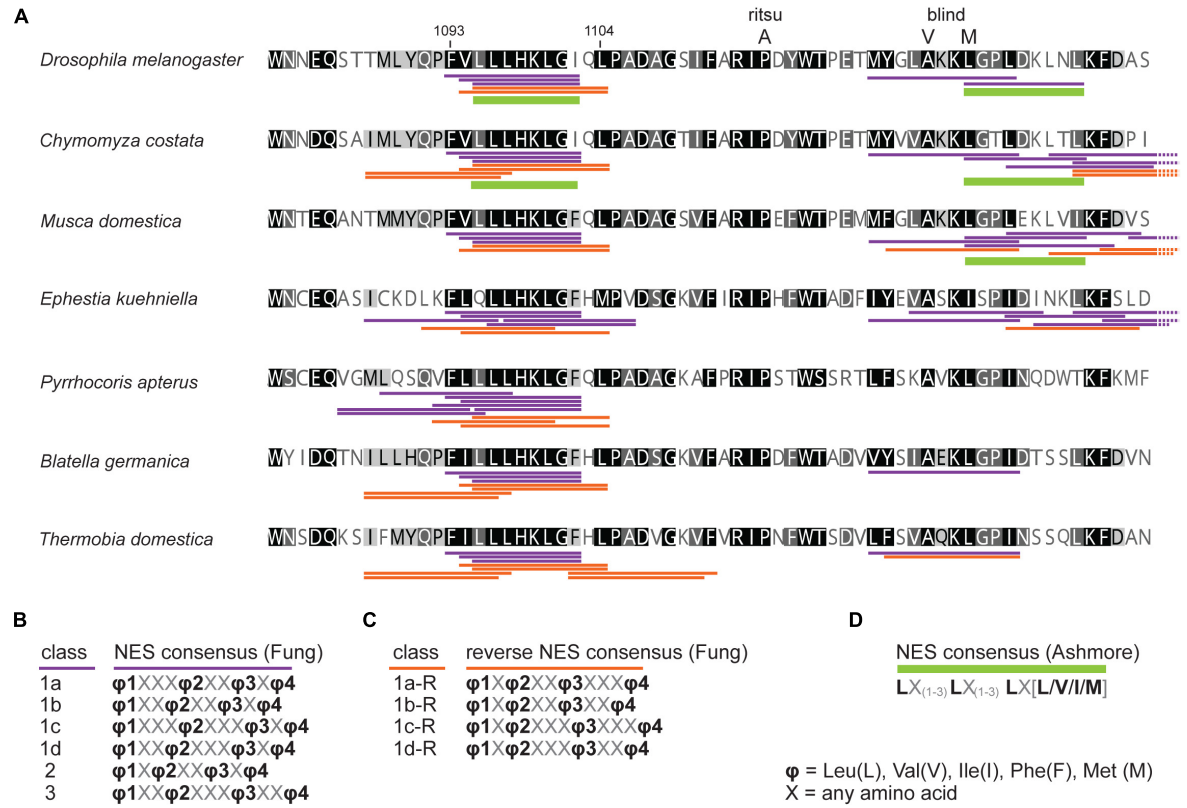

FIGURE 2 | *In silico* prediction of nuclear export signals (NESs) in TIM^{rit} vicinity. **(A)** Protein alignment (ancestral species are at the bottom) with underlined NES motifs. Purple and orange colors code for forward and reverse NES classes, respectively, and green bar indicates strict NES prediction after Ashmore et al. (2003). **(B–D)** The consensus sequences of NES classes. Numbers above the alignment correspond to amino acid residues in L-TIM (*D. melanogaster*).

(**Figure 2**). The second NES, located upstream of TIM^{rit} (residues 1095-1012), is apart from *D. melanogaster* only found in the drosophilid fly *C. costata*. To identify additional putative NES in the TIM^{blind} and TIM^{rit} regions, we applied less strict motifs as described in Fung et al. (2015). Multiple NES motifs were found in *D. melanogaster* near the TIM^{blind} and TIM^{rit} mutations, all of them at least partially overlapping with the two strict "Ashmore's" NES (**Figure 2A**). Using the less rigid "Fung" consensus, NES motifs were even found in species for which the strict consensus did not reveal any NES. Importantly, these less strict NES motifs are still present in homologous sequences (**Figure 2**).

We hypothesized that the fact that both *tim* temperature compensation mutants, *tim^{rit}* and *tim^{blind}*, are spaced close to each other is not merely accidental, as all the other known *tim* mutations that are dispersed throughout the *tim* gene region have not been reported to have a temperature-dependent phenotype. To test this assumption, we decided to conduct a targeted mutagenesis screen for temperature compensation mutations in *tim*.

Step-Up Protocol for Detection of Temperature Compensation Mutants

To unambiguously determine and compare τ at different temperatures in individual flies, we developed and optimized a protocol for assaying locomotor activity in flies exposed to two different temperatures. Fruit flies can survive for more than 2 weeks in the glass tubes (5 mm diameter, 70 mm length, and at least 1 cm of agar with 5% sucrose) used in DAM2 monitors, so we decided to record their activity at low temperature for 7 days followed by further 7 days at high temperature providing enough data for each condition in a single fly (**Figures 3A,B,D**). The transition from the low to the high temperatures was experimentally optimized to an 8°C increase spread over 24 h (this gradual temperature rise was programmed in MIR 154, Panasonic, as eight successive steps, each 2 h long with 1°C increase) (**Figures 3A,B,D**). We verified that the τ values measured in this step-up protocol are comparable to values obtained at constant temperatures (**Figures 3E–G**). Representative actograms in **Figure 3C** illustrate that even the relatively subtle τ change of *tim^{blind}* can be easily spotted by eye and so that this approach is suitable for efficient screening of large datasets for altered circadian phenotypes.

CRISPR/CAS9 Targeted Mutagenesis of *tim*

Seven regions of TIM were selected for targeted mutagenesis based on phylogenetic conservation analyses and/or their position with respect to known temperature compensation

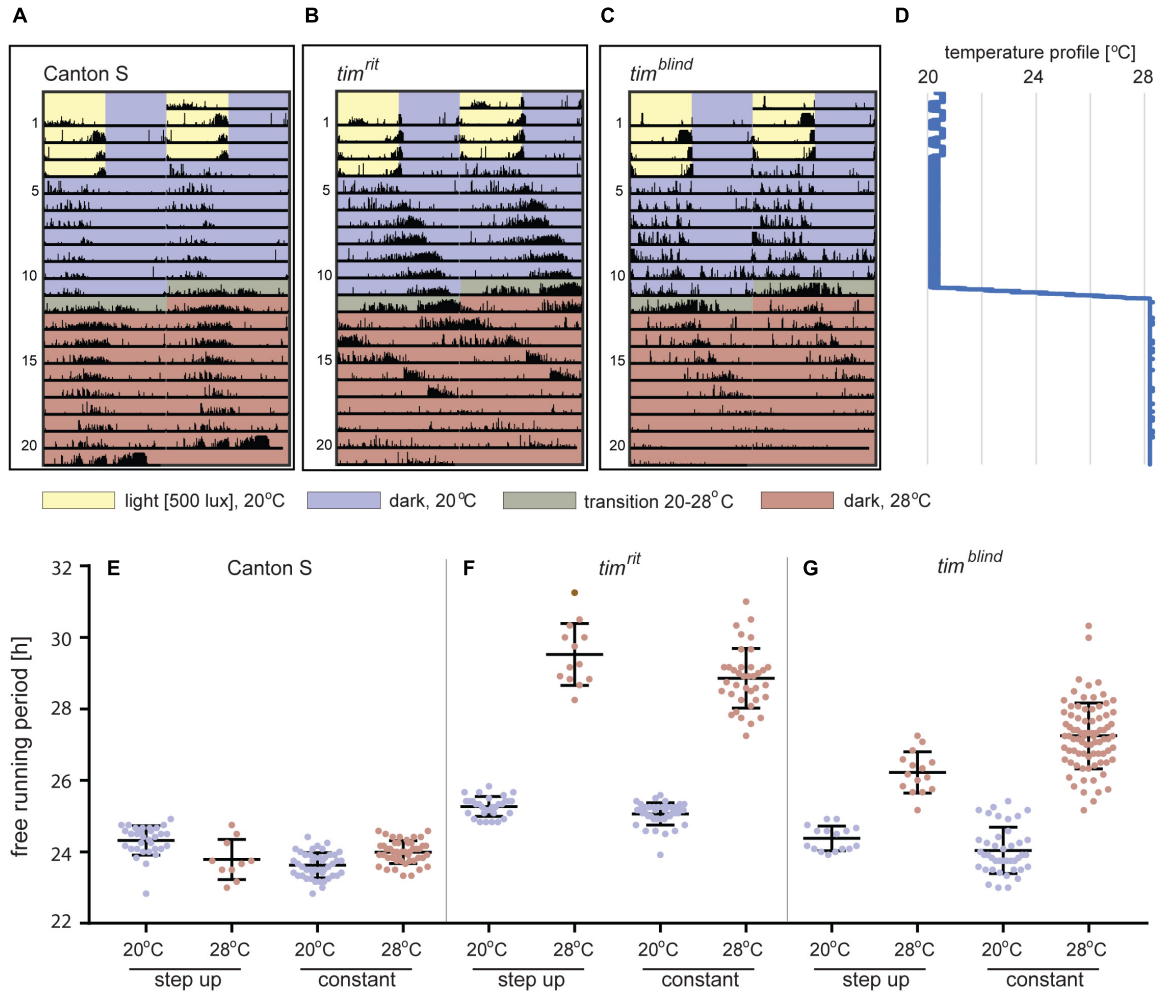

FIGURE 3 | Locomotor activity of *D. melanogaster* at different temperatures. **(A–C)** Typical double-plotted actograms obtained during the step-up protocol consisting of 4-day LD entrainment at 20°C followed by 7 days of DD at 20°C. Then, temperature was raised to 28°C during 16 h (1°C every 2 h) and kept constant for the rest of the experiment. **(D)** Temperature profile recorded during the step-up protocol (note small thermoperiodic oscillations typical for LD conditions). **(E–G)** Comparison of the free running periods (τ) measured at low and high portions of the step-up protocol, respectively, with data obtained from flies entrained and recorded at one constant temperature. Each dot corresponds to FRP of individual male fly, and colors correspond to the temperature-coding used in actogram backgrounds. Not all males survived entire step-up experiment (note lower *n* at 28°C). Bars show the mean ± SD.

mutations (**Figure 4**): (a) a conserved sequence motif located in the first quarter of the protein near the UL mutation, (b) $TIM^{unspliced}$ comprising the last intron which is alternatively retained at low temperatures (Boothroyd et al., 2007; Montelli et al., 2015), (c) the area where TIM^{rit} and TIM^{blind} mutations are located, (d) $NES^{1093-1104}$, a conserved region 12-23 aa upstream of TIM^{rit}, (e) $NES^{1015-1023}$ motif 93-98 aa upstream of TIM^{rit}, (f) $NES^{1166-1174}$ motif 56-62 aa downstream of TIM^{rit}, and (g) $NES^{776-785}$ located approximately in the middle of TIM (see **Table 1** for gRNA sequences, cleavage sites and corresponding sequences and **Figure 4** for position of selected regions on TIM).

Corresponding gRNA expressing plasmids were cloned, verified, and stably transformed into the attP2 landing site on the third chromosome following an established protocol (Kondo and Ueda, 2013). The targeted cleavage of genomic DNA within the *tim* gene region was induced in the embryonic stage by combining the nosCAS9 and U6gRNA-expressing transgenes to create in/dels resulting from NHEJ mechanism. The targeted chromosomes were balanced and subsequently brought into homozygosity (see **Supplementary Figure S1** for genotypes and genetic crosses and **Supplementary Figure S2** for τ of used *Drosophila* lines and lines suitable for similar experiments). In total, 618 lines covering seven *tim* regions were established and screened for altered circadian rhythmicity using our step-up protocol (**Table 4**).

Both arrhythmic mutants and mutant lines displaying altered rhythmicity were identified in the screen. In total, we isolated 113 arrhythmic lines of which a subset was molecularly characterized. In all cases, this uncovered out-of-frame in/del mutations resulting in premature stop codons. In contrast, τ-altering mutations always contained in-frame modifications. Deletions were approximately 15 times more frequent than insertions, the

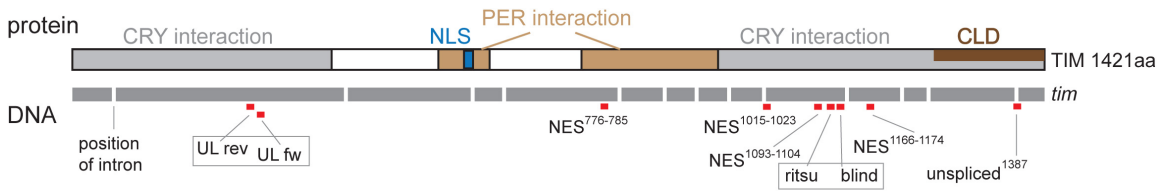

FIGURE 4 | Schematic depiction of TIM protein with highlighted functional domains and interacting regions: nuclear localization signal (NLS), PERIOD interacting domain (PER interaction), CRYPTOCHROME interacting domain (CRY interaction), and cytoplasmic localization domain (CLD). Below, schematic depiction of DNA is shown with exons in gray (length of the bar corresponds to exon length) separated by introns (the length is not shown). Red boxes indicate position of gRNA; the number in gRNA corresponds to amino acid residues in the TIM protein. Gray frame indicates when two gRNAs were used simultaneously in one construct (UL rev + UL fw; ritsu + blind).

length of deletions ranged from 1 to 71 bp, insertions were 2 to 8 bp long, and one-third of in/dels were combined with a substitution (see **Supplementary Figure S3** for DNA sequences of isolated mutants); 35 behaviorally normal flies were also sequenced and no modifications were observed.

FUNCTIONAL CHARACTERIZATION OF NOVEL MUTANT LINES

The step-up protocol was efficient for quick identification of putative mutants with either arrhythmic behavior or with a change in τ including even small temperature-dependent lengthening. However, for precise phenotype assessment, follow-up experimental replicates were performed allowing us to determine the accurate percentage of rhythmicity associated with each mutation, the exact τ at four tested temperatures, and the phenotypes in heterozygous conditions (heteroallelic combinations with wild-type *tim* and tim^{01}).

Region Upstream of TIM^{UL}

Three lines with altered τ were recovered for the region 13 aa upstream from TIM^{UL} and we analyzed each of them in more detail (**Table 4**). Interestingly, all three included modification of tryptophan 270 (**Figure 5E**). The $tim^{\Delta W270}$ deletion prolonged τ by ∼1.8 h and the single aa substitution tim^{W270Y} resulted in 0.6–1 h shortening of the free-running period. The effect was temperature independent in both cases and both lines were robustly rhythmic (>80% of rhythmic males at any temperature tested) (**Figures 5A,A',B,B',D**). In contrast, substitution of the tryptophan with three tyrosines ($tim^{W270YYY}$) produced temperature-dependent lengthening of τ and severe arrhythmicity in homozygotes (see blue dots connected by line; scale on right *y*-axis); however, a comparable drop in rhythmicity was not observed in heteroallelic combinations with tim^{01} (**Figures 5C,C',D,D'**). For statistical comparison of τ in homozygotes, heteroallelic combinations with tim^{01}, and wild-type flies, see **Supplementary Figure S4**.

Furthermore, according to NetPhos 3.1 predictions, these mutations may impact the phosphorylation of the nearby serines in position 268 and 274, and although this needs to be experimentally tested, it presents an intriguing possible explanation of the functional significance of this region (**Figure 5E**). In the wild-type protein (TIM^{wt}), serine 268 is not likely to be phosphorylated (score 0.47, below the threshold 0.5), whereas the W270 deletion raises the prediction score to 0.78 and substitution by three tyrosines ($tim^{W270YYY}$) to 0.55. Similarly, serine at position 274 has a phosphorylation prediction score of 0.56, just above the threshold, but this is substantially increased by the presence of either $tim^{\Delta W270}$, tim^{W270Y}, or $tim^{W270YYY}$ (to 0.94, 0.82, or 0.92, respectively).

Regions in Vicinity of TIM^{rit} and TIM^{blind} Mutations

An interspecific comparison of insect TIM proteins identified a conserved region near and especially upstream of the TIM^{blind} and TIM^{rit} mutations. This includes a putative NES overlapping with TIM^{blind} and a second putative NES, FVLLLHKLGIQL (residues 1093-1104), located 12-23 aa upstream of TIM^{rit}. Both NESs were also predicted by the strict ("Ashmore") and the less strict ("Fung") consensus searches (**Figure 2**). Again, we probed the functional significance of this region by inducing NHEJ-mediated mutagenesis followed by locomotor activity screening. Four different mutants with abnormal τ were recovered for $NES^{1093-1104}$ consisting of 2 to 11 aa long deletions (**Figure 7D**). In all four cases, τ gradually increased with rising temperature and was significantly longer compared to controls at 25°C and even more so at 28°C. For statistical comparison of τ in homozygotes, heteroallelic combinations with tim^{01}, and wild-type flies, see **Supplementary Figure S5**. Furthermore, the percentage of rhythmicity was severely reduced in three of these mutants at 28°C with $tim^{\Delta 1092-97:PFVLLL;K1099L}$ being completely arrhythmic both as homozygotes and in heteroallelic combination with tim^{01} (**Figures 6A–D,A'–D'**). This strongly contrasts with the relatively robust rhythmicity (>75%) observed in all four mutants at 25°C. Detailed sequence analysis revealed various degrees of $NES^{1093-1104}$ motif disruption in all four mutants (**Figure 8A**). Five overlapping NES classes ("Fung") and one strict motif ("Ashmore's") can be found within the region 1093-1104 in wild-type TIM and all of them are completely lost in $tim^{\Delta LYQPFVLLLHK1089-99}$, while $tim^{\Delta 1092-97:PFVLLL;K1099L}$ has one putative "Fung's" NES class remaining, while in $tim^{\Delta FV1093-94}$ and $tim^{\Delta PFVLL1092-96}$, two $NES^{1093-1104}$ according to "Fung" classes and one strict motif remain. Although all four $NES^{1093-1104}$ mutants are

TABLE 4 | Summary of screened lines and identified mutants.

TIM region/targeted motif	gRNA	Lines analyzed (*n*)	Arrhythmic strains (*n*)	Altered τ (*n*)	Unique strains with altered τ (*n*)	Mutation frequency (%)
Upstream of UL SLWFEASLS SNTSPPKQ	UL rev	122	26+1	5	3	26.22
	UL fw	122	2+1	0	0	2.45
$NES^{776-785}$ LLLILDSSA	fw 781-789	72	8	0	0	11.11
$NES^{1015-1023}$ ILLDLIIKE	fw 1017-1025	67	9	1	1	14.92
$NES^{1093-1104}$ YQPFVLLLH	rev 1090-1098	79	27	7	6	43.03
ritsu PDYWTPET blind MYGLAKKLG	rev ritsu	130	30+1	26+3	7+1	43.84
	fw-blind	130	1	3	1	3.08
$NES^{1166-1174}$ SLDVDLGDT	rev 1171-1179	73	8	2	2	13.70
$TIM^{unspliced}$ EKEKEL^{Kstop}	fw cold	75	0	0	0	0
total:	9 gRNAs	618	112	41	20	24.75

Gray background refers to situation when two gRNAs were used simultaneously (double gRNA construct). Red color highlights mutants resulting from cleavage directed by both gRNAs. Mutation frequency refers to mutants with altered circadian phenotypes, whereas actual frequency of mutations at DNA level was not determined. Superscript indicates protein sequence resulting from retained intron.

phenotypically very similar, the degree of NES modification is quite different. The common feature of all mutants is the absence of the 1c-R class NES consensus (**Figure 8A**).

Another mutant completely removing the $NES^{1124-1139}$, $tim^{1118AR\Delta 12}$, overlaps with the TIM^{blind} mutations. However, this mutant also contains a substitution of tyrosine 1118 (a residue which is predicted to be phosphorylated) with alanine and arginine. Moreover, another predicted phosphorylation target, Y1125, is also missing in $tim^{1118AR\Delta 12}$ making it hard to interpret the relative importance of any of these sites for the observed phenotype (**Figure 8**). Similarly to the $NES^{1093-1104}$ mutants, $tim^{1118AR\Delta 12}$ produces a longer τ at 25°C and severe (nearly complete) arrhythmicity at 28°C (**Figures 6E,E'**). We further addressed the role of the two TIM^{blind} residues and corresponding NES in the two re-engineered mutants. All predicted NES motifs near TIM^{blind} remained intact in TIM^{A1128V}, yet this mutation produces mostly arrhythmic individuals and the few rhythmic flies show a potential temperature compensation defect (**Figure 1E**). In contrast, TIM^{L1128M} which affects the strict ("Ashmore") NES motif is robustly rhythmic and perfectly temperature-compensated (**Figure 1F**). Notably, both the TIM^{blind} and TIM^{A1128V} mutations enhance the phosphorylation prediction score of Y1125 (**Figure 8A**). However, it is unknown, if Y1125 is phosphorylated *in vivo*.

Several τ-altering mutants mapping close to the TIM^{rit} mutation were recovered (**Figure 7D**). The most severe phenotype was seen in $tim^{\Delta FARIPD1112-1117}$ (**Figures 6H,H', 7B,B'**) with overall low rhythmicity across temperatures and complete arrhythmicity at 28°C. Free running period is ∼30 h at 25°C for homozygotes, the longest τ of all mutants recovered in this region. However, τ was significantly shorter (∼27 h) in heteroallelic combinations with tim^{01} at 25°C (**Supplementary Figure S5**). A slightly less severe impact on rhythmicity was found in $tim^{\Delta PDYWT1116-20}$, which is rhythmic at all temperatures, although rhythmicity at 28°C drops below 20% in homozygotes, whereas two-third of heteroallelic combinations with tim^{01} remain rhythmic (**Figures 6G,G'**). The flies also display loss of temperature compensation as their free-running period gets longer at high temperatures. For comparison, the proline 1116 to alanine substitution in tim^{rit} produces gradually longer τ at 25 and 28°C with rhythmicity above 80% at all temperatures tested (**Figures 6I,J,L**). The smallest, yet significant extension of τ was observed in $tim^{\Delta Y1118}$ (**Figure 6F**), a mutant lacking tyrosine 1118, which is likely phosphorylated (score 0.68, **Figure 8A**). Phosphorylation score of Y1118 is reduced in TIM^{rit} to 0.52 and this residue is deleted, together with the surrounding four amino acids, in $tim^{\Delta PDYWT1116-20}$. The mutant with the strongest phenotype, $tim^{\Delta FARIPD1112-1117}$, has a lower predicted phosphorylation score for Y1118, identical with the score calculated in TIM^{rit}. In addition, deletion of residues 1112-1117 (FARIPD) also changes the phosphorylation score of the upstream S1110 from a non-significant level to 0.91.

Systematic targeting of the TIM^{rit} and TIM^{blind} region and the conserved region 12-23 aa upstream of TIM^{rit} encompassing a putative $NES^{1093-1104}$ motifs (FVLLLHKLGIQL) resulted in mutants showing various degrees of arrhythmicity and temperature-dependent τ increase. To elucidate whether the above-mentioned region including TIM^{rit}, TIM^{blind}, and $NES^{1093-1104}$ is uniquely important for temperature compensation of the circadian clock, comparable mutagenesis was performed in regions with NES motifs located ∼50 aa downstream ($NES^{1166-1174}$) and ∼50 aa upstream ($NES^{1015-1023}$). The mutagenesis was successful in both regions, which is demonstrated by our ability to isolate 9 and 8 fully arrhythmic mutant lines, respectively (**Table 3**). In contrast, only three rhythmic mutants with altered rhythmicity or changed τ were found and although one of them, $tim^{\Delta DVDLG1173-77}$, produces significant lengthening of τ with rising temperature, the change is minimal, about 1 h (**Figures 6I,J,K,K',L, 7C,C',E–G**). The deletion in $tim^{\Delta DVDLG1173-77}$ destroys the putative $NES^{1166-1174}$ motif and slightly changes the phosphorylation score of S1071 (from 0.49 to 0.58) and T1079 (from 0.56 to 0.50) (**Figure 8C**). A partially overlapping deletion, $tim^{\Delta LD1172-73}$, does not remove the $NES^{1166-1174}$, but the phosphorylation scores are similarly affected for both S1071 (from 0.49 to 0.60)

TABLE 5 | Summary of circadian phenotypes in new mutants and reference lines.

		17°C				20°C				25°C				28°C			
TIM region	**Genotype**	**(*n*)**	**Rhythm %**	**FRP (h)**	**SEM**	**(*n*)**	**Rhythm %**	**FRP (h)**	**SEM**	**(*n*)**	**Rhythm %**	**FRP (h)**	**SEM**	**(*n*)**	**Rhythm %**	**FRP (h)**	**SEM**
	wt-CS (Canton S)	56	89.80	23.59	0.05	88	93.75	23.62	0.04	66	100.00	23.91	0.05	72	95.00	23.99	0.04
	CS/*tim*^{01}	30	96.67	32.66	0.06	26	96.15	23.78	0.05	25	100.00	23.95	0.06	28	92.86	23.57	0.05
Upstream of UL	*tim*$^{\Delta W270}$	48	80.43	25.25	0.05	56	93.75	25.41	0.06	48	92.50	25.74	0.10	48	86.67	25.55	0.07
	tim$^{\Delta W270}$/+	32	93.55	24.62	0.07	32	100.00	24.22	0.05	32	100.00	24.45	0.04	32	76.67	24.74	0.08
	tim$^{\Delta W270}$/*tim*^{01}	32	100.00	25.31	0.05	32	100.00	25.69	0.06	32	96.43	25.86	0.07	32	96.67	26.32	0.09
	tim^{W270Y}	32	90.32	23.04	0.06	48	97.87	22.97	0.05	40	92.50	22.95	0.05	47	97.87	23.13	0.05
	tim$^{\Delta W270Y}$/+	32	93.75	22.89	0.06	32	93.33	22.73	0.05	32	100.00	23.34	0.06	32	79.31	22.93	0.08
	tim$^{\Delta W270Y}$/*tim*^{01}	32	100.00	22.91	0.04	32	96.15	23.21	0.05	32	96.77	23.30	0.08	64	96.36	23.33	0.07
	tim^{W270YYY}	56	21.82	24.48	0.14	48	53.49	24.81	0.07	56	19.61	25.14	0.28	48	11.90	26.95	0.43
	tim$^{\Delta W270YYY}$/+	32	93.10	24.19	0.08	32	100.00	24.03	0.05	32	96.67	24.03	0.09	32	93.33	24.52	0.16
	tim$^{\Delta W270YYY}$/*tim*^{01}	32	93.33	24.55	0.05	32	100.00	24.73	0.06	32	100.00	25.61	0.07	32	82.76	26.61	0.17
NES$^{1017-1025}$	*tim* $^{\Delta I1022}$	48	87.23	23.04	0.06	48	97.73	23.34	0.04	16	100.00	23.23	0.05	32	80.65	23.27	0.10
	tim $^{\Delta I1022}$/+	32	96.55	23.39	0.06	64	95.16	23.42	0.03	48	93.62	23.29	0.07	32	93.55	23.01	0.08
	tim $^{\Delta I1022}$/*tim*^{01}	32	93.75	23.74	0.04	32	93.75	23.70	0.04	32	100.00	23.42	0.07	32	93.33	23.11	0.07
NES$^{1093-1104}$	*tim*$^{\Delta LYQPFVLLLHK1089-99}$	40	47.37	24.56	0.07	48	43.48	24.77	0.18	48	81.82	28.09	0.14	48	12.77	30.75	0.71
	tim$^{\Delta LYQPFVLLLHK1089-99}$/+	48	90.48	23.27	0.05	32	96.67	23.54	0.06	48	93.75	24.01	0.06	32	90.00	23.88	0.05
	tim$^{\Delta LYQPFVLLLHK1089-99}$/*tim*^{01}	32	84.38	23.82	0.10	32	82.76	24.19	0.10	40	94.87	26.38	0.17	32	31.25	30.61	0.38
	tim$^{\Delta PFVLL1092-96}$	56	50.94	25.13	0.10	48	64.58	24.61	0.08	56	86.79	26.29	0.06	48	45.83	30.72	0.16
	tim$^{\Delta PFVLL1092-96}$/+	32	84.38	23.45	0.05	32	93.33	23.31	0.05	32	96.88	23.66	0.04	32	100.00	24.74	0.14
	tim$^{\Delta PFVLL1092-96}$/*tim*^{01}	49	89.58	23.71	0.07	32	96.43	23.82	0.08	48	97.62	25.48	0.08	36	72.73	28.92	0.29
	tim$^{\Delta PFVLLL1092-97;K1099L}$	80	72.15	24.74	0.05	48	76.60	25.08	0.06	66	83.93	28.37	0.08	80	0.00		
	tim$^{\Delta PFVLLL1092-97;K1099L}$/+	32	81.25	23.64	0.02	32	81.48	24.10	0.09	48	95.24	24.59	0.06	32	92.59	24.56	0.06
	tim$^{\Delta PFVLLL1092-97;K1099L}$/*tim*^{01}	32	89.29	24.08	0.13	32	78.13	24.68	0.14	64	76.67	27.10	0.16	32	0.00		
	tim$^{\Delta FV1093-94}$	32	81.25	23.61	0.08	48	95.74	24.06	0.05	48	82.93	27.66	0.13	48	12.77	31.54	0.05
	tim$^{\Delta FV1093-94}$/+	32	87.50	23.22	0.05	32	100.00	23.49	0.05	32	96.67	23.82	0.07	32	96.67	24.86	0.22
	tim$^{\Delta FV1093-94}$/*tim*^{01}	32	77.42	23.62	0.09	32	96.67	23.89	0.06	32	87.50	25.96	0.13	40	55.88	27.35	0.67
ritsu	*tim*^{rit}	48	89.74	24.82	0.28	80	97.67	25.06	0.31	32	93.33	26.08	0.33	64	84.75	28.86	0.82
	tim^{rit}/+	28	100.00	24.11	0.06	15	100.00	24.03	0.03	16	100.00	24.28	0.06	14	100.00	24.35	0.03
	tim^{rit}/*tim*^{01}	28	100.00	23.53	0.12	29	100.00	24.41	0.04	30	100.00	25.51	0.05	32	100.00	27.57	0.18
	tim$^{\Delta FARIPD1112-17}$	48	14.58	24.55	0.22	48	42.55	25.13	0.08	48	52.08	30.16	0.14	56	0.00		
	tim$^{\Delta FARIPD1112-17}$/+	32	48.39	23.42	0.09	32	90.32	23.57	0.06	32	100.00	23.62	0.06	32	100.00	24.41	0.09
	tim$^{\Delta FARIPD1112-17}$/*tim*^{01}	32	65.52	22.89	0.12	32	86.21	24.06	0.09	48	87.50	27.04	0.21	32	0.00		
	tim$^{\Delta PDYWT1116-20}$	48	71.74	24.44	0.08	48	70.21	24.73	0.10	32	79.31	27.42	0.17	80	16.00	30.28	0.36
	tim$^{\Delta PDYWT1116-20}$/+	62	93.33	23.42	0.06	32	96.88	23.38	0.06	48	100.00	23.93	0.04	36	97.06	24.55	0.08
	tim$^{\Delta PDYWT1116-20}$/*tim*^{01}	32	87.50	23.30	0.08	32	96.88	24.05	0.07	32	80.65	26.23	0.23	40	66.67	30.09	0.23
	tim $^{\Delta Y1118}$	49	60.87	23.95	0.08	48	93.48	23.99	0.04	40	94.44	24.65	0.05	48	71.11	25.55	0.08
	tim $^{\Delta Y1118}$/+	32	90.63	23.51	0.06	32	100.00	23.61	0.06	32	90.32	24.10	0.09	32	96.30	24.29	0.08

(Continued)

TABLE 5 | Continued

		17°C				20°C				25°C				28°C			
TIM region	**Genotype**	**(*n*)**	**Rhythm %**	**FRP (h)**	**SEM**	**(*n*)**	**Rhythm %**	**FRP (h)**	**SEM**	**(*n*)**	**Rhythm %**	**FRP (h)**	**SEM**	**(*n*)**	**Rhythm %**	**FRP (h)**	**SEM**
	tim $^{\Delta Y1118/}$ *tim*^{01}	32	96.77	23.61	0.05	32	100.00	24.12	0.04	32	100.00	24.48	0.08	48	100.00	25.20	0.10
NES$^{1166-1174}$	*tim*$^{\Delta LD1172-73}$	48	50.00	23.43	0.04	48	65.22	23.67	0.05	16	40.00	23.57	0.10	48	50.00	23.18	0.06
	tim$^{\Delta LD1172-73}$/+	32	83.33	23.46	0.07	32	100.00	23.50	0.06	32	100.00	23.29	0.07	32	91.67	23.14	0.12
	tim$^{\Delta LD1172-73}$/*tim*^{01}	40	93.94	23.80	0.05	32	100.00	23.67	0.06	40	90.63	23.93	0.08	32	93.75	23.16	0.07
	tim$^{\Delta DVDLG1173-77}$	40	71.79	23.24	0.06	56	80.77	23.67	0.05	10	80.00	23.60	0.10	32	48.15	24.26	0.18
	tim$^{\Delta DVDLG1173-77}$/+	32	90.32	23.62	0.05	32	100.00	23.68	0.04	32	96.77	23.93	0.05	32	100	23.58	0.07
	tim$^{\Delta DVDLG1173-77}$/*tim*^{01}	32	96.77	23.58	0.05	32	100.00	24.33	0.05	32	96.88	24.20	0.06	64	94.643	24.75	0.11
blind	*tim*$^{1118AR; \Delta 12aa}$	112	64.52	24.95	0.09	48	70.73	25.24	0.18	64	68.33	27.92	0.15	88	3.70	29.42	1.00
	tim$^{1118AR; \Delta 12aa}$/+	32	66.67	23.68	0.10	32	83.87	23.81	0.09	80	100.00	24.58	0.04	48	97.83	24.72	0.08
	tim$^{1118AR; \Delta 12aa}$/*tim*^{01}	32	73.08	24.21	0.15	32	73.68	25.20	0.15	40	66.67	28.10	0.20	32	0.00		
	tim^{blind}	83	72.29	23.71	0.05	104	70.77	24.04	0.08	56	86.00	25.65	0.08	80	72.13	26.80	0.27
	tim^{blind}/+	30	100.00	23.85	0.09	11	100.00	23.63	0.09	32	100.00	23.89	0.08	23	85.00	23.99	0.09
	tim^{blind}/*tim*^{01}	30	83.33	23.18	0.08	30	100.00	23.93	0.03	30	100.00	25.00	0.05	30	96.67	26.19	0.13
		18°C								25°C				29°C			
blind	*tim*^{A1128V}	44	43.18	21.67	1.02	–	–	–	–	45	26.67	22.54	0.97	39	23.07	24.70	0.92
	tim$^{blind\ 2.1}$	48	87.50	23.74	0.91	–	–	–	–	42	100.00	24.88	0.13	46	69.57	27.61	0.16
	tim^{L1131M}	45	84.44	23.22	0.19	–	–	–	–	46	76.09	23.70	0.16	35	62.86	23.82	0.17

Rhythm % indicates percentage of rhythmic males.

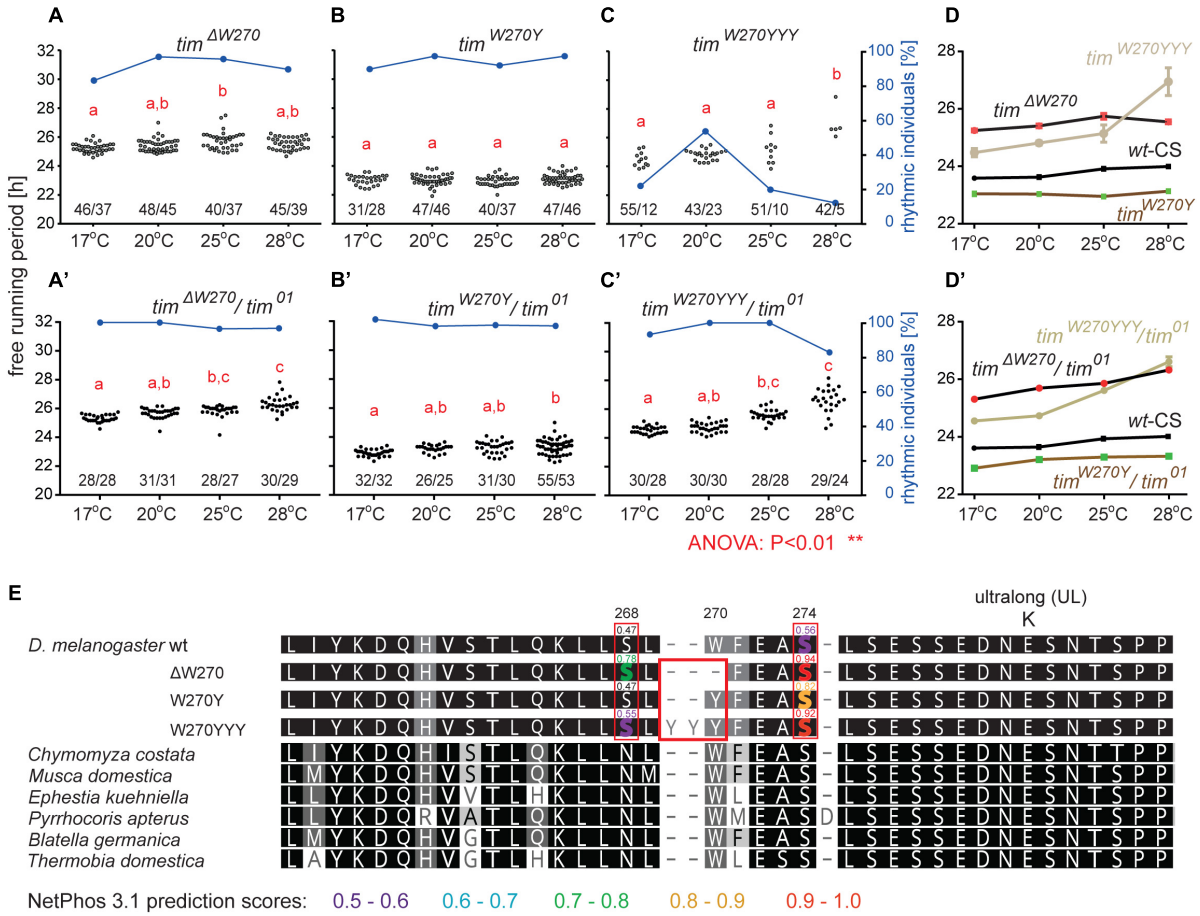

FIGURE 5 | Mutants isolated upstream of tim^{UL}. **(A–C)** Each dot represents τ of individual fly as was recorded during 10 days in DD and specified temperature. Lowercase red letters above dots indicate a significant difference between "a" and "b" and "c" and "d" (one-way ANOVA with Tukey–Kramer's *post hoc* test, $P < 0.01$). Numbers below dots correspond to number of measured/rhythmic flies at particular temperature. Blue dots connected with line correspond to percentage of rhythmic individuals (scale on right *y*-axis) at particular temperature. Panels **A–C** contain phenotypes of homozygous flies, whereas **A'–C'** are dedicated to heteroallelic combinations with tim^{01}. Comparison of τ (shown as mean ± SEM) for all three mutants and wild-type (Canton strain) flies (wt-CS) for **(D)** homozygotes and **(D')** heteroallelic combinations with tim^{01}. **(E)** Alignment of mutant protein sequences with TIM from representative insects (see the text and legend of **Figure 1** for more details on insect taxons). Mutation in position 270 (red box) possibly affects phosphorylation of serine residues in positions 268 and 274 (highlighted by red boxes). Only residues which phosphorylation is possibly affected by mutation are highlighted in the alignment of mutants and wt TIM proteins and prediction scores are indicated above the amino acid. The colors correspond to score prediction from NetPhos 3.1 (color coding is shown below the alignment).

and T1079 (from 0.56 to 0.53). This mutant is characterized by a minimal shortening of τ at 28°C (0.8 h shorter than wt, **Supplementary Figure S5J**). Finally, the $tim^{\Delta I1022}$ mutant produces a 0.3–0.75 h shorter τ than wt flies at all temperatures (**Figures 7C,C'** and **Supplementary Figure S5I**). This single amino acid deletion removes the $NES^{1015-1023}$ motif (**Figure 8B**).

Immunocytochemistry

In order to elucidate the impact of the newly isolated *tim* mutations on the temporal clock protein expression pattern in the circadian clock neurons, we performed ICC on whole mount fly brains. Since no TIM antibody was available, we used PER immunostainings as a proxy to visualize the progression of the PER-TIM negative feedback loop. Two mutants covering the *rit* ($tim^{\Delta 1092-97:PFVLLL;K1099L}$) and *blind* ($tim^{1118AR\Delta 12}$) region were selected. Both mutants show relatively robust rhythmicity at 17–25°C, but are completely arrhythmic at 28°C (**Figures 6C,E**). In both, wt and mutants, the PER level was cycling during the day at every temperature, but in mutants, the amplitude of the oscillation was reduced (**Figure 9** and **Supplementary Figure S6**). At 17°C, PER intensity was almost comparable in small ventrolateral (s-LNv) neurons between wt, $tim^{\Delta 1092-97:PFVLLL;K1099L}$, and $tim^{1118AR\Delta 12}$, with a peak at ZT0 and a trough around ZT12. A similar trend was observed in the large ventrolateral (l-LNv) neurons, with the difference that the relative staining intensity was about half the intensity detected in s-LNv (**Figure 9D**). At 25°C, a clear difference in the intensity of the PER signal was observed between wt and the two *tim* mutants in both s-LNv and l-LNv in all ZTs with the exception of ZT12 (**Figures 9B,E** and **Supplementary Figures S6B,C**). At 28°C, the highest level of PER was detected in wt, lower levels in $tim^{\Delta 1092-97:PFVLLL;K1099L}$

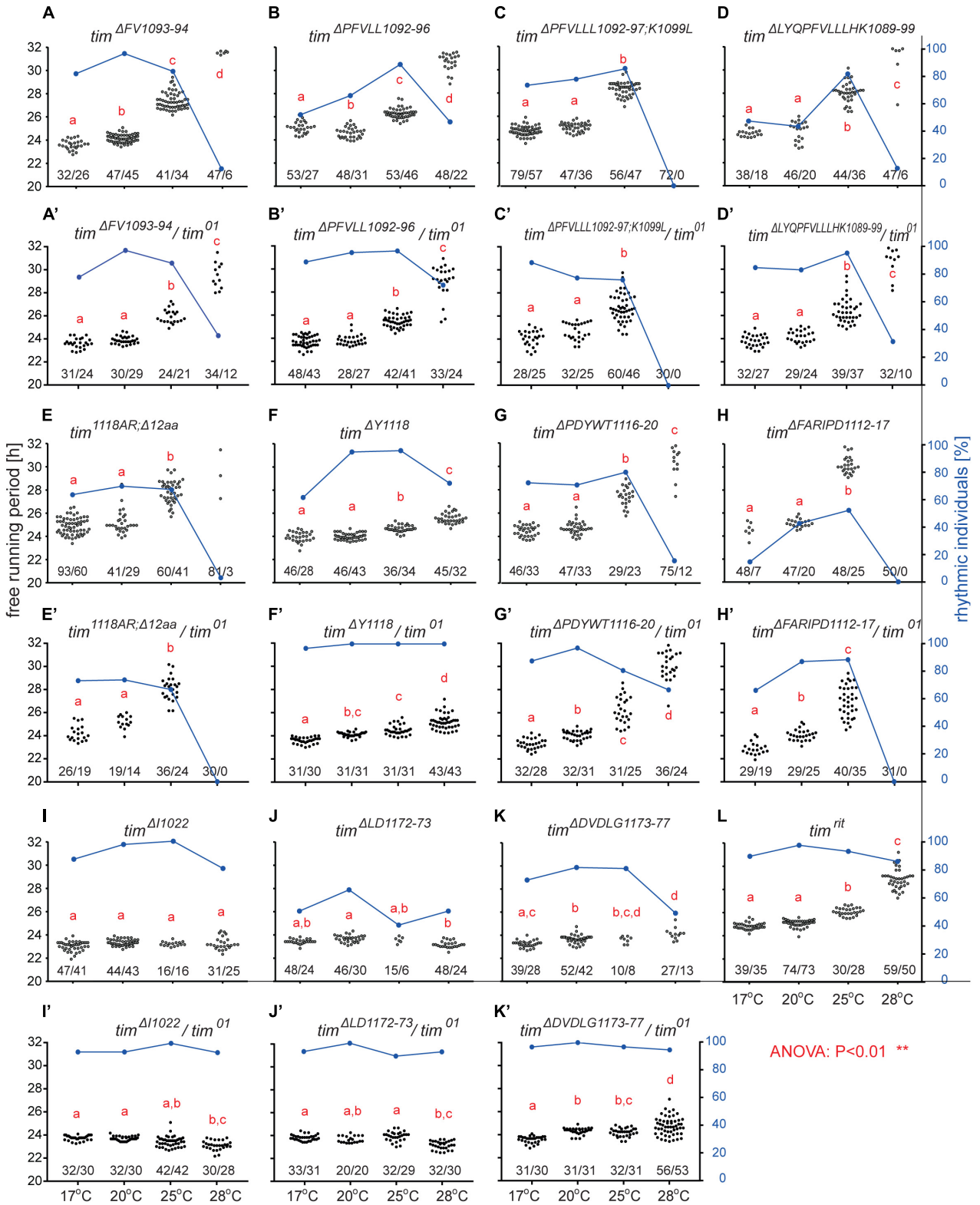

FIGURE 6 | Mutants isolated in vicinity of *tim*^{rit} and *tim*^{blind}. **(A–L)** Each dot represents τ of individual fly as was recorded during 10 days in DD and specified temperature. Lowercase red letters above dots indicate a significant difference between "a" and "b" and "c" and "d" (one-way ANOVA with Tukey–Kramer's *post hoc* test, $P < 0.01$). Numbers below dots correspond to number of measured/rhythmic flies at particular temperature. Blue dots connected with line correspond to percentage of rhythmic individuals (right *y*-axis) at particular temperature.

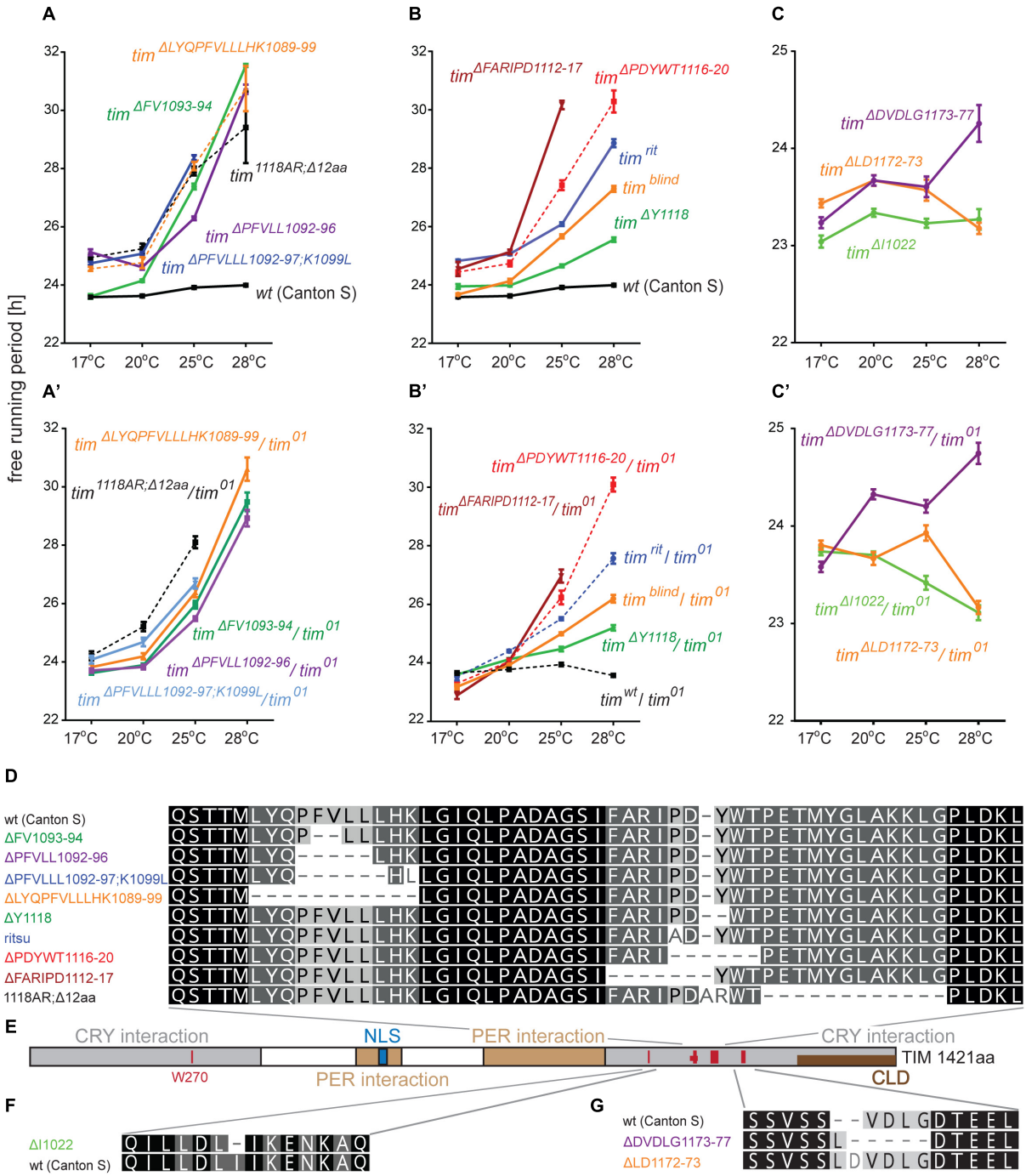

FIGURE 7 | Summary of phenotypes for homozygous **(A–C)** and heteroallelic combinations with tim^{01} **(A'–C')** mutants isolated in vicinity of tim^{rit} and tim^{blind}. Name of each mutation is color-coded to ease orientation in the sequence alignments **(D,F,G)**. **(E)** Schematic depiction of TIM protein with position of mutated regions (red bars), nuclear localization signal (NLS), PERIOD interacting domain (PER interaction), CRYPTOCHROME interacting domain (CRY interaction), and cytoplasmic localization domain (CLD). Dashes (–) correspond to gaps in the alignment (which result from insertions or deletions). For statistical comparison between mutants and heteroallelic combinations, see **Supplementary Figure S5**.

and the lowest level was detected in $tim^{1118AR\Delta12}$ at ZT0, ZT4, and ZT20 (**Figures 9C,F**, **Supplementary Figure S7**). The pattern of immunostaining intensity at 17 and 25°C is thus consistent with the locomotor activity phenotypes observed in the mutants. However, both mutants are virtually arrhythmic at 28°C, yet the expression levels of PER were clearly different between them at the beginning of the day and at the end of the night.

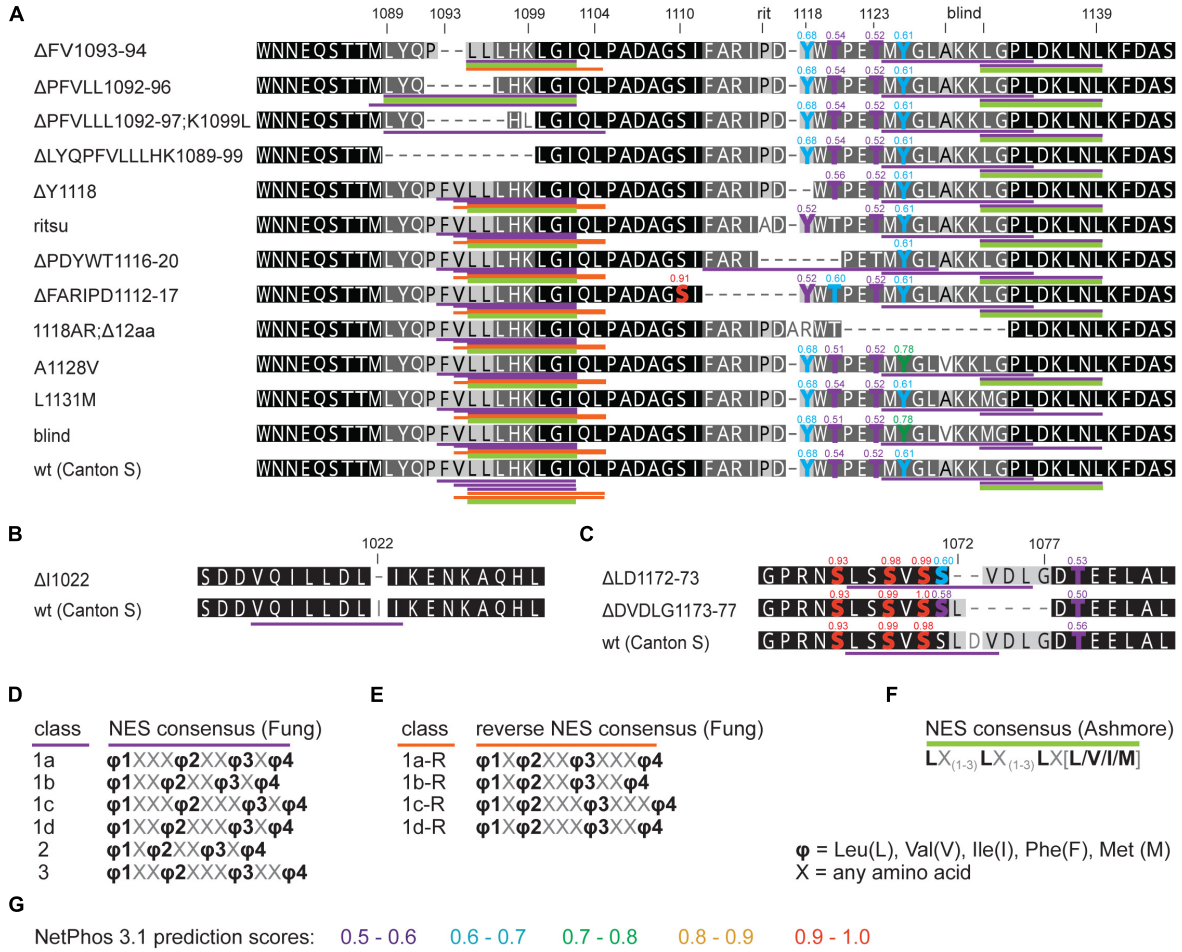

FIGURE 8 | *in silico* prediction of nuclear export signals (NESs) and phosphorylation in *tim* mutants. Protein alignments of **(A)** *ritsu*, *blind*, and NES 1093-1104 regions, **(B)** NES 1015-1023, and **(C)** NES 1166-1174 with underlined NES motifs. Purple, orange, and green colors code for NES classes according to consensus shown in **D–F**. Residues which phosphorylation is possibly affected by mutation are highlighted in the alignment and scores are indicated above the amino acid. **(G)** The colors correspond to prediction from NetPhos 3.1.

The experimental set-up allowed us to perform semi-quantitative comparisons between temperatures within each genotype. In s-LNv neurons of wt flies, the lowest signal intensities were observed at 17°C, whereas expression levels were more or less comparable at 25 and 28°C. In l-LNv neurons, signal intensities increased with temperature: the lowest expression was observed at 17°C, intermediate levels at 28°C, and the maximal expression at 25°C. In both mutants, expression levels varied much less across temperatures due to lower levels detected at 25 and 28°C.

DISCUSSION

Targeted Screen for Temperature Compensation Mutants

Circadian clock research is a remarkably successful field of experimental biology and the molecular mechanisms that build up circadian oscillators are well understood, especially in *Drosophila*. Despite these huge successes, there are a number of distressingly large gaps in our understanding of biological timekeeping. One of the key features of circadian clocks is their ability to keep a largely unchanged pace regardless of temperature, a phenomenon termed temperature compensation. To specifically generate new mutants with temperature compensation defects, we utilize the efficacy of the CRISPR/CAS9 technology as a tool for targeted mutagenesis. Simple genetic crosses are used to establish homozygous mutants and their τ is determined in a temperature step-up protocol to specifically identify mutants even if they only exhibit very subtle impairments in temperature compensation.

Although the position where the CAS9 protein cleaves chromosomal DNA is defined by the gRNA sequence, the actual mutations resulting from subsequent NHEJ are variable and virtually unpredictable in/dels. As a consequence, various degrees of gradual amino acid deletions (see **Figures 5E**, **7D**) and phenotypic changes (see **Figures 7A–C**) were obtained. More than one-quarter of created lines were circadian mutants, but

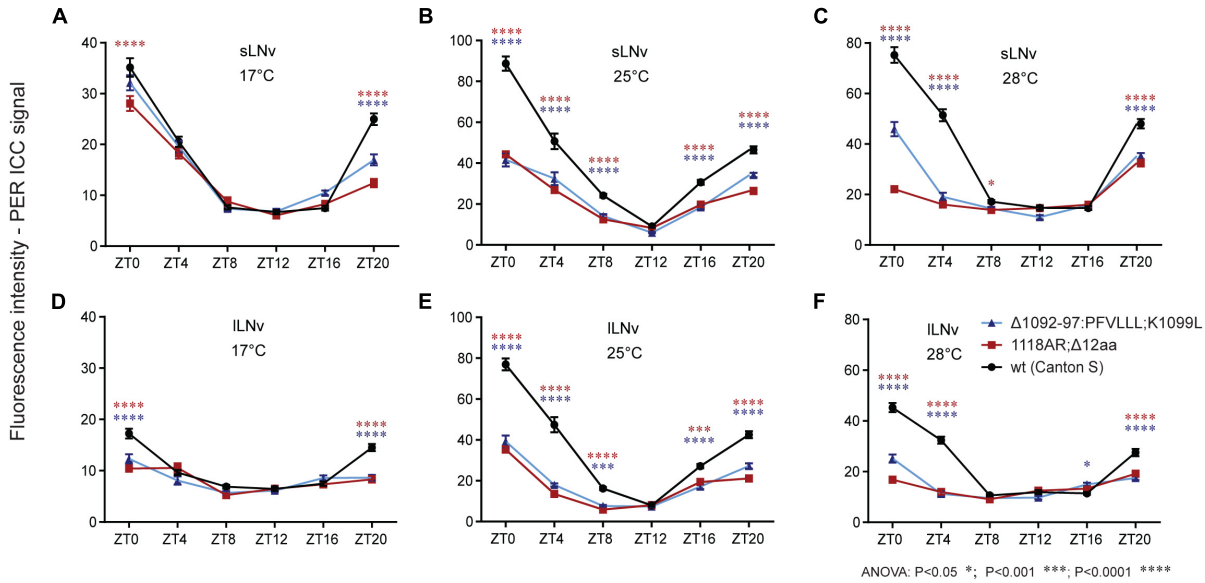

FIGURE 9 | Immuno-localization of PER in small and large ventrolateral neurons (s-LNv, l-LNv). Relative quantifications show role of **(A–F)** temperature on PER immunoreactivity within genotype. Only statistical difference between wt and mutants is shown for each ZT. For differences, see **Supplementary Figure S6**. s-LNv and l-LNv were plotted separately.

only 3% of screened lines were unique mutants with altered τ. Obviously, a higher percentage of mutants was probably induced, but if the phenotypic change was below our recognition, these lines were discarded. Yet, the success rate is remarkably higher than in EMS screens and importantly, identification of mutation is straightforward, fast, and cheap, compared to time demanding mapping after classical mutagenesis. The obvious limitation is that the screen presented here is strictly hypothesis-driven (Curtiz and Wallis, 1942) and mutations are created only in candidate regions of already established circadian clock genes. Therefore, this approach is suitable to saturate genes with targeted mutations and to assess the function of specific regions including coding sequence or cis-regulatory motifs in promoters.

Timeless in Temperature Compensation of the Circadian Clock

This study exploited TIM in selected insect representatives. Despite the long history from the common insect ancestor (>400 million years ago), some regions of TIM are well conserved across insect species, pointing to their possible functional significance. Therefore, we experimentally tested the role of eight conserved motifs by targeted mutagenesis and isolated circadian clock mutants in seven of them. Three remarkably conserved regions located closely together, TIM$^{\mathrm{rit}}$, TIM^{blind}, and NES$^{1093-1104}$, were functionally identified as particularly critical for temperature compensation. The importance of nuclear export for proper function of TIM is well established (Ashmore et al., 2003) and *tim*^{blind} overlaps with NES$^{1131-1139}$ (Wülbeck et al., 2005). It is surprising that the two amino-acid replacements encoded by *tim*^{blind} lead to a strong temperature compensation phenotype, because both the alanine to valine substitution at position 1128 and the leucine to methionine change at position 1131 are conservative replacements. Even more surprising is the strong impact on clock function observed in the single mutant *tim*^{A1128V}. The few rhythmic *tim*^{A1128V} individuals are associated with variable periods but do exhibit potential period lengthening with increasing temperatures (**Figures 1E,H** and **Table 5**). It is therefore possible that in the *tim*^{blind} double-mutant, the L1131M substitution, which shows no phenotype on its own, somehow suppresses the A1128V substitution, resulting in restauration of rhythmicity but maintenance of the temperature compensation phenotype. It would be very interesting to see, whether TIM$^{\mathrm{blind}}$ residues play a similar role in *P. apterus* TIM, where neither "Ashmore's" nor "Fung's" NESs are predicted (**Figure 2A**). This type of experiment might be possible in future, as genome editing slowly becomes accessible even in non-model insects including *P. apterus* (Kotwica-Rolinska et al., 2019).

The NES$^{1093-1104}$ region described here consists of three forward and two reverses NES consensuses. However, comparably strong temperature compensation defects were observed in all mutants targeting NES$^{1093-1104}$, although different numbers of NES consensuses were depleted. Either 1c-R NES is the only essential export signal, or residues 1089-1099 have some additional role for TIM structure. Notably, all three mutants in the *tim*^{rit} region mapping just 8–14 amino acids downstream from NES$^{1093-1104}$ show a temperature compensation defect, although none of these mutations directly affects NES$^{1093-1104}$. Additionally, neither mutation in NES$^{1015-1023}$ nor in NES$^{1166-1174}$ had an impact on temperature compensation. Currently, it is therefore unclear if nuclear export is indeed important for temperature compensation, or if other alterations (e.g., changes in phosphorylation), or a combination of both, contribute to the temperature compensation phenotypes

observed in several of the mutants described in this study. Analysis of the detailed subcellular localization of the mutated TIM proteins will hopefully point to the possible mechanism contributing to temperature compensation.

Our comparison often revealed a shorter τ in heteroallelic combinations of various mutants with tim^{01}, a combination with only one partially functional *tim* copy, when compared to homozygous mutants (**Supplementary Figure S5**). This contrasts with the dose-independent role of wild-type TIM reported previously at 25°C (Rothenfluh et al., 2000a,b; Ashmore et al., 2003) and our results obtained for TIM^{wt} at all four tested temperatures (**Supplementary Figure S5A**). Notably, a ∼1 h shorter τ was also observed for tim^{rit}/tim^{01} heterozygotes exposed to different temperatures (Matsumoto et al., 1999) supporting the possibility that in specific temperature conditions, the amount of a mutated TIM protein might be important for τ .

Our ICC data indicate that the PER immunostaining signal is strongly affected by *tim* mutations and that the low PER signal is more profound at high temperatures. Although the ICC data were obtained during LD, whereas circadian phenotypes were recorded in DD, PER immunostaining intensities are consistent with the behavioral defects of particular mutants. It is not clear if the stability of mutant TIM is primarily affected at 28°C, or if the interaction between PER and TIM is somehow influenced by the mutations. Therefore, PER immunostaining only serves as a proxy for the status of the PER-TIM negative feedback loop. In this regard, it is worth noting that PER and TIM do not co-localize perfectly in various neurons during the circadian cycle (Shafer et al., 2002; Wülbeck et al., 2005). Moreover, TIM also interacts with CRY in a light-dependent manner (Ceriani et al., 1999) and thus the here newly induced mutations may also affect this interaction. However, the possible change in CRY-TIM interaction should not impact free running period in DD, as CRY-depleted flies have a normal τ (Stanewsky et al., 1998; Dolezelova et al., 2007). The light resetting capacity of the new *tim* mutants is currently unknown, but given the light entrainment phenotype of tim^{blind} connected with the partial resistance of TIM^{blind} to light-induced degradation, it is possible that at least some of the new alleles are affected (Wülbeck et al., 2005).

The subcellular localization of TIM is connected with its phosphorylation. Long τ *tim* mutants are characterized by hypophosphorylated TIM constrained in the cytoplasm as it is known that interaction with the nuclear transport machinery is dependent on the phosphorylation state of TIM (Jang et al., 2015). Likewise, TIM^{BLIND} is hypophosporylated at all times during the circadian cycle and accumulates in the cytoplasm of photoreceptor cells and LNv clock neurons, with only minor effects on PER phosphorylation and subcellular localization (Wülbeck et al., 2005). Indeed, several of our mutants between positions 1112 and 1120 affect phosphorylation predictions without altering the NES sequence. For example, deletion of tyrosine 1118 produces mild and gradual lengthening of τ at 25 and 28°C. Interestingly, a more pronounced τ extension is observed in tim^{rit} mutants even though its 1116 proline to alanine substitution only reduces the phosphorylation prediction score for tyrosine 1118. The $tim^{\Delta PDYWT1116-20}$ mutation results in an even longer τ combined with substantially reduced rhythmicity at 28°C. The most severe phenotype with complete arrhythmicity at 28°C, generally low rhythmicity, and remarkable τ extension at 25°C is observed in $tim^{\Delta FARIPD1112-17}$ mutants. Interestingly, deletion of FARIPD changes the phosphorylation prediction score for serine 1110 (from a non-significant score to 0.91) in addition to mild changes in scores for tyrosine 1118 and threonine 1120. Although further functional experiments are needed to determine the actual impact of the novel mutations on TIM localization and phosphorylation, the collection of mutants presented here points to a new region of TIM important for temperature compensation.

DATA AVAILABILITY STATEMENT

All datasets generated and analyzed for this study are included in the article/**Supplementary Material**.

AUTHOR CONTRIBUTIONS

SS and DD designed the study. SS performed majority of NHEJ experiments, analyzed, and interpreted the results. SF combined *per*, *tim*, and *cry* alleles and assessed their phenotypes. RS and SF independently observed the temperature compensation phenotype associated with tim^{blind}. AG performed HDR reengineering of tim^{blind} mutants and their behavioral analysis. MD performed immunohistochemical experiments. GM contributed gRNA design and participated in early steps of the screen. DD supervised the study and together with SF wrote the manuscript with input from all co-authors.

FUNDING

This work was supported by the National Science Foundation of the Czech Republic (GACR project 17-01003S). DD and SS were supported by the European Research Council (ERC) under the European Union's Horizon 2020 Program Grant Agreement 726049. RS and AG were supported by the Deutsche Forschungsgemeinschaft grant STA 421/7-1.

ACKNOWLEDGMENTS

We thank Roman Neužil and Mechthild Rosing for technical support, Jeffrey C. Hall for the PER antibody, Kenji Tomioka for tim^{rit} strain, and Joanna Kotwica-Rolinska for advice on CRISPR/CAS9 experiments. We appreciate critical reading of the manuscript and suggestions from Vlastík Smýkal, Nirav Thakkar, and Joanna Kotwica-Rolinska.

SUPPLEMENTARY MATERIAL

The Supplementary Material for this article can be found online at: https://www.frontiersin.org/articles/10.3389/fphys.2019.01442/full#supplementary-material

REFERENCES

Agrawal, P., and Hardin, P. E. (2016). An RNAi screen to identify protein phosphatases that function within the Drosophila circadian clock. *G3-Genes Genomes Genet.* 6, 4227–4238. doi: 10.1534/g3.116.035345

Arrhenius, S. (1889). Über die reaktionsgeschwindigkeit bei der inversion von Rohrzucker durch Saeuren. *Zeitschrit fuer physikalische Chemie* 4, 226–248.

Ashmore, L. J., Sathyanarayanan, S., Silvestre, D. W., Emerson, M. M., Schotland, P., and Sehgal, A. (2003). Novel insights into the regulation of the timeless protein. *J. Neurosci.* 23, 7810–7819. doi: 10.1523/jneurosci.23-21-07810.2003

Baylies, M. K., Vosshall, L. B., Sehgal, A., and Young, M. W. (1992). New short period mutations of the Drosophila clock gene per. *Neuron* 9, 575–581. doi: 10.1016/0896-6273(92)90194-i

Bazalova, O., and Dolezel, D. (2017). Daily activity of the housefly, musca domestica, is influenced by temperature independent of 3′ UTR period gene splicing. *G3-Genes Genomes Genet.* 7, 2637–2649. doi: 10.1534/g3.117.042374

Bazalova, O., Kvicalova, M., Valkova, T., Slaby, P., Bartos, P., Netusil, R., et al. (2016). Cryptochrome 2 mediates directional magnetoreception in cockroaches. *Proc. Natl. Acad. Sci. U.S.A.* 113, 1660–1665. doi: 10.1073/pnas.1518622113

Boothroyd, C. E., Wijnen, H., Naef, F., Saez, L., and Young, M. W. (2007). Integration of light and temperature in the regulation of circadian gene expression in Drosophila. *PLoS Genet.* 3:e54. doi: 10.1371/journal.pgen.0030054

Busza, A., Emery-Le, M., Rosbash, M., and Emery, P. (2004). Roles of the two Drosophila CRYPTOCHROME structural domains in circadian photoreception. *Science* 304, 1503–1506. doi: 10.1126/science.1096973

Ceriani, M. F., Darlington, T. K., Staknis, D., Mas, P., Petti, A. A., Weitz, C. J., et al. (1999). Light-dependent sequestration of TIMELESS by CRYPTOCHROME. *Science* 285, 553–556. doi: 10.1126/science.285.5427.553

Chiu, J. C., Ko, H. W., and Edery, I. (2011). NEMO/NLK Phosphorylates PERIOD to initiate a time delay phosphorylation circuit that sets circadian clock speed. *Cell* 145, 357–370. doi: 10.1016/j.cell.2011.04.002

Curtiz, M., and Wallis, B. H. (1942). *Round Up the Usual Suspects. Casablanca Warner Bros*. Burbank, CA: First National Pictures.

Darlington, T. K., Wager-Smith, K., Ceriani, M. F., Staknis, D., Gekakis, N., Steeves, T. D. L., et al. (1998). Closing the circadian loop: CLOCK-induced transcription of its own inhibitors per and tim. *Science* 280, 1599–1603. doi: 10.1126/science.280.5369.1599

Diernfellner, A., Colot, H. V., Dintsis, O., Loros, J. J., Dunlap, J. C., and Brunner, M. (2007). Long and short isoforms of *Neurospora* clock protein FRQ support temperature-compensated circadian rhythms. *FEBS Lett.* 581, 5759–5764. doi: 10.1016/j.febslet.2007.11.043

Dolezelova, E., Dolezel, D., and Hall, J. C. (2007). Rhythm defects caused by newly engineered null mutations in Drosophila's cryptochrome gene. *Genetics* 177, 329–345. doi: 10.1534/genetics.107.076513

Edery, I., Zwiebel, L. J., Dembinska, M. E., and Rosbash, M. (1994). Temporal phosphorylation of the Drosophila period protein. *Proc. Natl. Acad. Sci. U.S.A.* 91, 2260–2264. doi: 10.1073/pnas.91.6.2260

Fang, Y., Sathyanarayanan, S., and Sehgal, A. (2007). Post-translational regulation of the Drosophila circadian clock requires protein phosphatase 1 (PP1). *Genes Dev.* 21, 1506–1518. doi: 10.1101/gad.1541607

Fexová, S. (2010). *Circadian Clock of Two Insect Model Species - Drosophila Melanogaster and Tribolium Castaneum*. MSc thesis, University of South Bohemia, České Budějovice.

Fung, H. Y., Fu, S. C., Brautigam, C. A., and Chook, Y. M. (2015). Structural determinants of nuclear export signal orientation in binding to exportin CRM1. *eLife* 4:10034. doi: 10.7554/eLife.10034

Glaser, F. T., and Stanewsky, R. (2005). Temperature synchronization of the Drosophila circadian clock. *Curr. Biol.* 15, 1352–1363. doi: 10.1016/j.cub.2005.06.056

Glossop, N. R., Lyons, L. C., and Hardin, P. E. (1999). Interlocked feedback loops within the Drosophila circadian oscillator. *Science* 286, 766–768. doi: 10.1126/science.286.5440.766

Hamblen, M. J., White, N. E., Emery, P., Kaiser, K., and Hall, J. C. (1998). Molecular and behavioral analysis of four period mutants in Drosophila melanogaster encompassing extreme short, novel long, and unorthodox arrhythmic types. *Genetics* 149, 165–178.

Hara, T., Koh, K., Combs, D. J., and Sehgal, A. (2011). Post-translational regulation and nuclear entry of TIMELESS and PERIOD are affected in new timeless mutant. *J. Neurosci.* 31, 9982–9990. doi: 10.1523/JNEUROSCI.0993-11.2011

Hardin, P. E. (2011). Molecular genetic analysis of circadian timekeeping in Drosophila. *Genet. Circadian Rhythms* 74, 141–173. doi: 10.1016/B978-0-12-387690-4.00005-2

Hardin, P. E., Hall, J. C., and Rosbash, M. (1990). Feedback of the Drosophila period gene product on circadian cycling of its messenger RNA levels. *Nature* 343, 536–540. doi: 10.1038/343536a0

Hardin, P. E., Hall, J. C., and Rosbash, M. (1992). Circadian oscillations in period gene messenger-RNA levels are transcriptionally regulated. *Proc. Natl. Acad. Sci. U.S.A.* 89, 11711–11715. doi: 10.1073/pnas.89.24.11711

Hastings, J. W., and Sweeney, B. M. (1957). On the mechanism of temperature independence in a biological clock. *Proc. Natl. Acad. Sci. U.S.A.* 43, 804–811. doi: 10.1073/pnas.43.9.804

Izumo, M., Johnson, C. H., and Yamazaki, S. (2003). Circadian gene expression in mammalian fibroblasts revealed by real-time luminescence reporting: temperature compensation and damping. *Proc. Natl. Acad. Sci. U.S.A.* 100, 16089–16094. doi: 10.1073/pnas.2536313100

Jang, A. R., Moravcevic, K., Saez, L., Young, M. W., and Sehgal, A. (2015). Drosophila TIM binds importin alpha1, and acts as an adapter to transport PER to the nucleus. *PLoS Genet.* 11:e1004974. doi: 10.1371/journal.pgen.1004974

Kamae, Y., and Tomioka, K. (2012). timeless is an essential component of the circadian clock in a primitive insect, the firebrat Thermobia domestica. *J. Biol. Rhythms* 27, 126–134. doi: 10.1177/0748730411435997

Kaushik, R., Nawathean, P., Busza, A., Murad, A., Emery, P., and Rosbash, M. (2007). PER-TIM interactions with the photoreceptor cryptochrome mediate circadian temperature responses in Drosophila. *PLoS Biol.* 5:e0050146. doi: 10.1371/journal.pbio.0050146

Ko, H. W., Kim, E. Y., Chiu, J., Vanselow, J. T., Kramer, A., and Edery, I. (2010). A hierarchical phosphorylation cascade that regulates the timing of PERIOD nuclear entry reveals novel roles for proline-directed kinases and GSK-3 beta/SGG in circadian clocks. *J. Neurosci.* 30, 12664–12675. doi: 10.1523/Jneurosci.1586-10.2010

Kobelkova, A., Bajgar, A., and Dolezel, D. (2010). Functional molecular analysis of a circadian clock Gene timeless promoter from the drosophilid fly *Chymomyza costata*. *J. Biol. Rhythm* 25, 399–409. doi: 10.1177/0748730410385283

Kobelkova, A., Zavodska, R., Sauman, I., Bazalova, O., and Dolezel, D. (2015). Expression of clock genes period and timeless in the central nervous system of the Mediterranean flour moth, *Ephestia kuehniella*. *J. Biol. Rhythms* 30, 104–116. doi: 10.1177/0748730414568430

Kondo, S., and Ueda, R. (2013). Highly improved gene targeting by germline-specific Cas9 expression in Drosophila. *Genetics* 195, 715–721. doi: 10.1534/genetics.113.156737

Konopka, R. J., and Benzer, S. (1971). Clock mutants of Drosophila melanogaster. *Proc. Natl. Acad. Sci. U.S.A.* 68, 2112–2116. doi: 10.1073/pnas.68.9.2112

Konopka, R. J., Hamblencoyle, M. J., Jamison, C. F., and Hall, J. C. (1994). An ultrashort clock mutation at the period locus of Drosophila melanogaster that reveals some new features of the flys circadian system. *J. Biol. Rhythm* 9, 189–216. doi: 10.1177/074873049400900303

Konopka, R. J., Pittendrigh, C., and Orr, D. (1989). Reciprocal behaviour associated with altered homeostasis and photosensitivity of Drosophila clock mutants. *J. Neurogenet.* 6, 1–10. doi: 10.3109/01677068909107096

Kosugi, S., Hasebe, M., Tomita, M., and Yanagawa, H. (2008). Nuclear export signal consensus sequences defined using a localization-based yeast selection system. *Traffic* 9, 2053–2062. doi: 10.1111/j.1600-0854.2008.00825.x

Kotwica-Rolinska, J., Chodakova, L., Chvalova, D., Kristofova, L., Fenclova, I., Provaznik, J., et al. (2019). CRISPR/Cas9 genome editing introduction and optimization in the non-model insect *Pyrrhocoris apterus*. *Front. Physiol.* 10:891. doi: 10.3389/fphys.2019.00891

Kotwica-Rolinska, J., Pivarciova, L., Vaneckova, H., and Dolezel, D. (2017). The role of circadian clock genes in the photoperiodic timer of the linden bug, *Pyrrhocoris apterus*, during the nymphal stage. *Physiol. Entomol.* 42, 266–273. doi: 10.1111/phen.12197

Landskron, J., Chen, K. F., Wolf, E., and Stanewsky, R. (2009). A role for the PERIOD:PERIOD homodimer in the Drosophila circadian clock. *PLoS Biol.* 7:e1000003. doi: 10.1371/journal.pbio.1000003

Levine, J. D., Funes, P., Dowse, H. B., and Hall, J. C. (2002). Signal analysis of behavioral and molecular cycles. *BMC Neurosci.* 3:1. doi: 10.1186/1471-2202-3-1

Li, Y. H., Liu, X., Vanselow, J. T., Zheng, H., Schlosser, A., and Chiu, J. C. (2019). O-GlcNAcylation of PERIOD regulates its interaction with CLOCK and timing of circadian transcriptional repression. *PLoS Genet.* 15:e1007953. doi: 10.1371/journal.pgen.1007953

Majercak, J., Sidote, D., Hardin, P. E., and Edery, I. (1999). How a circadian clock adapts to seasonal decreases in temperature and day length. *Neuron* 24, 219–230. doi: 10.1016/s0896-6273(00)80834-x

Martinek, S., Inonog, S., Manoukian, A. S., and Young, M. W. (2001). A role for the segment polarity gene shaggy/GSK-3 in the Drosophila circadian clock. *Cell* 105, 769–779. doi: 10.1016/S0092-8674(01)00383-X

Matsumoto, A., Tomioka, K., Chiba, Y., and Tanimura, T. (1999). timrit lengthens circadian period in a temperature-dependent manner through suppression of PERIOD protein cycling and nuclear localization. *Mol. Cell. Biol.* 19, 4343–4354. doi: 10.1128/mcb.19.6.4343

Meyer, P., Saez, L., and Young, M. W. (2006). PER-TIM interactions in living Drosophila cells: an interval timer for the circadian clock. *Science* 311, 226–229. doi: 10.1126/science.1118126

Montelli, S., Mazzotta, G., Vanin, S., Caccin, L., Corra, S., De Pitta, C., et al. (2015). period and timeless mRNA splicing profiles under natural conditions in Drosophila melanogaster. *J. Biol. Rhythms* 30, 217–227. doi: 10.1177/0748730415583575

Nakajima, M., Imai, K., Ito, H., Nishiwaki, T., Murayama, Y., Iwasaki, H., et al. (2005). Reconstitution of circadian oscillation of cyanobacterial KaiC phosphorylation in vitro. *Science* 308, 414–415. doi: 10.1126/science.1108451

Nawathean, P., and Rosbash, M. (2004). The doubletime and CKII kinases collaborate to potentiate Drosophila PER transcriptional repressor activity. *Mol. Cell.* 13, 213–223. doi: 10.1016/S1097-2765(03)00503-3

Ozkaya, O., and Rosato, E. (2012). The circadian clock of the fly: a neurogenetics journey through time. *Adv. Genet.* 77, 79–123. doi: 10.1016/B978-0-12-387687-4.00004-0

Pittendrigh, C. S. (1954). On temperature independence in the clock system controlling emergence time in Drosophila. *Proc. Natl. Acad. Sci. U.S.A.* 40, 1018–1029. doi: 10.1073/pnas.40.10.1018

Pivarciova, L., Vaneckova, H., Provaznik, J., Wu, B. C., Pivarci, M., Peckova, O., et al. (2016). Unexpected geographic variability of the free running period in the linden bug, *Pyrrhocoris apterus*. *J. Biol. Rhythms* 31, 568–576. doi: 10.1177/0748730416671213

Port, F., Chen, H. M., Lee, T., and Bullock, S. L. (2014). Optimized CRISPR/Cas tools for efficient germline and somatic genome engineering in Drosophila. *Proc. Natl. Acad. Sci. U.S.A.* 111, E2967–E2976. doi: 10.1073/pnas.1405500111

Poupardin, R., Schottner, K., Korbelova, J., Provaznik, J., Dolezel, D., Pavlinic, D., et al. (2015). Early transcriptional events linked to induction of diapause revealed by RNAseq in larvae of drosophilid fly, *Chymomyza costata*. *BMC Genomics* 16:720. doi: 10.1186/s12864-015-1907-4

Price, J. L. (2005). Genetic screens for clock mutants in Drosophila. *Method Enzymol.* 393, 35–60. doi: 10.1016/S0076-6879(05)93003-6

Price, J. L., Blau, J., Rothenfluh, A., Abodeely, M., Kloss, B., and Young, M. W. (1998). Double-time is a novel Drosophila clock gene that regulates PERIOD protein accumulation. *Cell* 94, 83–95. doi: 10.1016/s0092-8674(00)81224-6

Ren, X., Yang, Z., Xu, J., Sun, J., Mao, D., Hu, Y., et al. (2014). Enhanced specificity and efficiency of the CRISPR/Cas9 system with optimized sgRNA parameters in Drosophila. *Cell Rep.* 9, 1151–1162. doi: 10.1016/j.celrep.2014.09.044

Rothenfluh, A., Abodeely, M., Price, J. L., and Young, M. W. (2000a). Isolation and analysis of six timeless alleles that cause short- or long-period circadian rhythms in Drosophila. *Genetics* 156, 665–675.

Rothenfluh, A., Young, M. W., and Saez, L. (2000b). A TIMELESS-independent function for PERIOD proteins in the Drosophila clock. *Neuron* 26, 505–514. doi: 10.1016/S0896-6273(00)81182-4

Ruoff, P. (1992). Introducing temperature compensation in any reaction kinetic oscillator model. *J. Interdiscipl. Cycle* 23, 92–99.

Rutila, J. E., Zeng, H., Le, M., Curtin, K. D., Hall, J. C., and Rosbash, M. (1996). The timSL mutant of the Drosophila rhythm gene timeless manifests allele-specific interactions with period gene mutants. *Neuron* 17, 921–929. doi: 10.1016/s0896-6273(00)80223-8

Saez, L., Derasmo, M., Meyer, P., Stieglitz, J., and Young, M. W. (2011). A key temporal delay in the circadian cycle of Drosophila is mediated by a nuclear localization signal in the timeless protein. *Genetics* 188, 591–U166. doi: 10.1534/genetics.111.127225

Saez, L., and Young, M. W. (1996). Regulation of nuclear entry of the Drosophila clock proteins period and timeless. *Neuron* 17, 911–920. doi: 10.1016/S0896-6273(00)80222-6

Sathyanarayanan, S., Zheng, X., Xiao, R., and Sehgal, A. (2004). Posttranslational regulation of Drosophila PERIOD protein by protein phosphatase 2A. *Cell* 116, 603–615. doi: 10.1016/s0092-8674(04)00128-x

Schmid, B., Helfrich-Forster, C., and Yoshii, T. (2011). A new ImageJ plug-in "ActogramJ" for chronobiological analyses. *J. Biol. Rhythms* 26, 464–467. doi: 10.1177/0748730411414264

Sehadova, H., Glaser, F. T., Gentile, C., Simoni, A., Giesecke, A., Albert, J. T., et al. (2009). Temperature entrainment of Drosophila's circadian clock involves the gene nocte and signaling from peripheral sensory tissues to the brain. *Neuron* 64, 251–266. doi: 10.1016/j.neuron.2009.08.026

Sehgal, A., Price, J. L., Man, B., and Young, M. W. (1994). Loss of circadian behavioral rhythms and per RNA oscillations in the Drosophila mutant timeless. *Science* 263, 1603–1606. doi: 10.1126/science.8128246

Shafer, O. T., Rosbash, M., and Truman, J. W. (2002). Sequential nuclear accumulation of the clock proteins period and timeless in the pacemaker neurons of Drosophila melanogaster. *J. Neurosci.* 22, 5946–5954.

Shinohara, Y., Koyama, Y. M., Ukai-Tadenuma, M., Hirokawa, T., Kikuchi, M., Yamada, R. G., et al. (2017). Temperature-sensitive substrate and product binding underlie temperature-compensated phosphorylation in the clock. *Mol. Cell.* 67, 783–798. doi: 10.1016/j.molcel.2017.08.009

Siwicki, K. K., Eastman, C., Petersen, G., Rosbash, M., and Hall, J. C. (1988). Antibodies to the period gene product of Drosophila reveal diverse tissue distribution and rhythmic changes in the visual system. *Neuron* 1, 141–150. doi: 10.1016/0896-6273(88)90198-5

Stanewsky, R., Frisch, B., Brandes, C., HamblenCoyle, M. J., Rosbash, M., and Hall, J. C. (1997). Temporal and spatial expression patterns of transgenes containing increasing amounts of the Drosophila clock gene period and a lacZ reporter: mapping elements of the PER protein involved in circadian cycling. *J. Neurosci.* 17, 676–696.

Stanewsky, R., Kaneko, M., Emery, P., Beretta, B., Wager-Smith, K., Kay, S. A., et al. (1998). The cry(b) mutation identifies cryptochrome as a circadian photoreceptor in Drosophila. *Cell* 95, 681–692. doi: 10.1016/S0092-8674(00)81638-4

Tataroglu, O., and Emery, P. (2015). The molecular ticks of the Drosophila circadian clock. *Curr. Opin. Insect. Sci.* 7, 51–57. doi: 10.1016/j.cois.2015.01.002

Tauber, E., Zordan, M., Sandrelli, F., Pegoraro, M., Osterwalder, N., Breda, C., et al. (2007). Natural selection favors a newly derived timeless allele in Drosophila melanogaster. *Science* 316, 1895–1898. doi: 10.1126/science.1138412

Tomioka, K., and Matsumoto, A. (2015). Circadian molecular clockworks in non-model insects. *Curr. Opin. Insect. Sci.* 7, 58–64. doi: 10.1016/j.cois.2014.12.006

Urbanova, V., Bazalova, O., Vaneckova, H., and Dolezel, D. (2016). Photoperiod regulates growth of male accessory glands through juvenile hormone signaling in the linden bug, *Pyrrhocoris apterus*. *Insect Biochem. Mol. Biol.* 70, 184–190. doi: 10.1016/j.ibmb.2016.01.003

Wülbeck, C., Szabo, G., Shafer, O. T., Helfrich-Forster, C., and Stanewsky, R. (2005). The novel Drosophila tim(blind) mutation affects behavioral rhythms but not periodic eclosion. *Genetics* 169, 751–766. doi: 10.1534/genetics.104.036244

Zhang, Z., Cao, W., and Edery, I. (2018). The SR protein B52/SRp55 regulates splicing of the period thermosensitive intron and mid-day siesta in Drosophila. *Sci. Rep.* 8:1872. doi: 10.1038/s41598-017-18167-3

Zhou, M., Kim, J. K., Eng, G. W., Forger, D. B., and Virshup, D. M. (2015). A Period2 phosphoswitch regulates and temperature compensates circadian period. *Mol. Cell.* 60, 77–88. doi: 10.1016/j.molcel.2015.08.022

Conflict of Interest: The authors declare that the research was conducted in the absence of any commercial or financial relationships that could be construed as a potential conflict of interest.

frontiers in Physiology

ORIGINAL RESEARCH
published: 20 December 2019
doi: 10.3389/fphys.2019.01544

Microtubules Stabilization by Mutant Spastin Affects ER Morphology and Ca^{2+} Handling

Nicola Vajente[1], *Rosa Norante*[1], *Nelly Redolfi*[1], *Andrea Daga*[2], *Paola Pizzo*[1,3] *and Diana Pendin*[1,3]*

[1] Department of Biomedical Sciences, University of Padua, Padua, Italy, [2] Laboratory of Molecular Biology, Scientific Institute IRCCS E. Medea, Lecco, Italy, [3] Neuroscience Institute—Italian National Research Council (CNR), Padua, Italy

The endoplasmic reticulum (ER) extends as a network of interconnected tubules and sheet-like structures in eukaryotic cells. ER tubules dynamically change their morphology and position within the cells in response to physiological stimuli and these network rearrangements depend on the microtubule (MT) cytoskeleton. Store-operated calcium entry (SOCE) relies on the repositioning of ER tubules to form specific ER-plasma membrane junctions. Indeed, the tips of polymerizing MTs are supposed to provide the anchor for ER tubules to move toward the plasma membrane, however the precise role of the cytoskeleton during SOCE has not been conclusively clarified. Here we exploit an *in vivo* approach involving the manipulation of MT dynamics in *Drosophila melanogaster* by neuronal expression of a dominant-negative variant of the MT-severing protein spastin to induce MT hyper-stabilization. We show that MT stabilization alters ER morphology, favoring an enrichment in ER sheets at the expense of tubules. Stabilizing MTs has a negative impact on the process of SOCE and results in a reduced ER Ca^{2+} content, affecting the flight ability of the flies. Restoring proper MT organization by administering the MT-destabilizing drug vinblastine, chronically or acutely, rescues ER morphology, SOCE and flight ability, indicating that MT dynamics impairment is responsible for all the phenotypes observed.

Keywords: spastin, drosophila, microtubules, endoplasmic reticulum, calcium, SOCE, calcium imaging

OPEN ACCESS

Edited by:
Giorgio F. Gilestro, Imperial College London, United Kingdom

Reviewed by:
Fabian M. Feiguin, International Centre for Genetic Engineering and Biotechnology, Italy
Emi Nagoshi, Université de Genève, Switzerland

***Correspondence:**
Diana Pendin
diana.pendin@unipd.it

Specialty section:
This article was submitted to Invertebrate Physiology, a section of the journal Frontiers in Physiology

Received: *04 June 2019*
Accepted: *05 December 2019*
Published: *20 December 2019*

Citation:
Vajente N, Norante R, Redolfi N, Daga A, Pizzo P and Pendin D (2019) Microtubules Stabilization by Mutant Spastin Affects ER Morphology and Ca^{2+} Handling. Front. Physiol. 10:1544. doi: 10.3389/fphys.2019.01544

INTRODUCTION

The endoplasmic reticulum (ER) coordinates a variety of cellular processes, such as synthesis, modification, quality control and transport of proteins, as well as lipid metabolism and Ca^{2+} homeostasis. It extends as a single membrane-bound entity composed of interconnecting sheets and tubules spreading all over the cell. Although the ER can form a reticular network independently of cytoskeletal structures (Dreier and Rapoport, 2000), in mammalian cells its distribution and sheet/tubule balance are influenced by microtubules (MTs) (Terasaki et al., 1986; Dabora and Sheetz, 1988; Lee and Chen, 1988; Waterman-Storer and Salmon, 1998; Lu et al., 2009; Joensuu et al., 2014).

MTs are composed of tubulin polymers and constitute essential components of the cytoskeleton. In neurons, they are critical in order to support long-range motor-driven cargo transport within neuronal processes and play fundamental roles in polarity, axon differentiation and growth (Conde and Cáceres, 2009; Kapitein and Hoogenraad, 2015). Although a part of the neuronal MTs is

considered stable, a fraction retains high levels of dynamics, as demonstrated by their frequent and continuous growth and shortening (Desai and Mitchison, 1997; Nogales, 2001; Burbank and Mitchison, 2006). This dynamic instability is central to MT biological functions, allowing their rapid reorganization at need (Kirschner and Mitchison, 1986). The organization of MTs in neurons is tightly regulated by assembly-promoting factors, stabilizing and destabilizing factors and severing proteins. Dysfunctional MTs, due to mutations in genes that encode tubulin or MT-associated proteins, have been linked to a range of neuronal diseases, such as motor neuropathies, Hereditary Spastic Paraplegias (HSPs), Charcot–Marie–Tooth disease.

Two major types of MT-dependent ER movement have been described: sliding, the motor-based transfer along stable, pre-existing MTs; and movement mediated by the tip attachment complex (TAC), by which a plus end-attached ER tubule extends together with a MT growing end (Waterman-Storer and Salmon, 1998; Friedman et al., 2010). TAC has been proposed to have a role in one of the major functions of ER, i.e., intracellular Ca^{2+} handling. Indeed, the ER lumen contains a 10,000-fold higher Ca^{2+} concentration than that of the bulk cytosol, working as the primary intracellular Ca^{2+} store, releasing Ca^{2+} in the cytosol upon different cellular stimulations (Zampese and Pizzo, 2012; Pendin et al., 2017). The main source of Ca^{2+} for ER refilling is the extracellular space, and the plasma membrane (PM) is contacted by ER tubules in a process called store-operated Ca^{2+} entry (SOCE) (Várnai et al., 2009), which serves to generate a sustained cytosolic Ca^{2+} elevation and refill the depleted ER Ca^{2+} store.

The molecular players involved in SOCE include the pore-forming subunit of the Ca^{2+}-release activated Ca^{2+} channel encoded by the *Orai* gene (Feske et al., 2006; Prakriya et al., 2006; Vig et al., 2006a,b; Yeromin et al., 2006; Zhang et al., 2006) and the ER-resident protein STIM (stromal interaction molecule) (Liou et al., 2005; Zhang et al., 2005), that serves as a luminal Ca^{2+} sensor (Grigoriev et al., 2008; Friedman et al., 2010; Soboloff et al., 2012). It has been demonstrated that after Ca^{2+} store depletion, STIM oligomerizes and redistributes to predetermined foci in the peripheral ER (Luik et al., 2008). STIM binds the MT plus-end binding protein EB1, which facilitates TAC-dependent STIM translocation toward the PM (Liou et al., 2007; Honnappa et al., 2009; Chen et al., 2013, 2019; Tsai et al., 2014). At the ER–PM junctions, STIM interacts with Orai channels to promote influx of extracellular Ca^{2+} into the ER (Liou et al., 2007; Grigoriev et al., 2008; Galán et al., 2011). In this STIM redistribution process, the physical movement of ER is required for ER tubules to reach out to the PM and form new ER-PM junctions (Wu et al., 2006; Carrasco and Meyer, 2011). The precise role of TAC-based ER movement in this reorganization, however, is controversial and variable among cell types (Redondo et al., 2006; Smyth et al., 2007; Grigoriev et al., 2008; Galán et al., 2011). One model proposes that TAC-mediated ER movement is required prior to SOCE activation to appropriately locate STIM on ER membrane, while ER Ca^{2+} depletion causes MT-independent STIM translocation to the PM (Smyth et al., 2007). Although the molecular details of this process are unclear, local cytoskeleton reorganization is supposed to play a major role (Gurel et al., 2014).

Spastin is an ATPase with MT-severing activity (Hazan et al., 1999; Errico et al., 2002; Roll-Mecak and McNally, 2010; Sharp and Ross, 2012; Sandate et al., 2019). Mutations in the *spastin* gene cause over 50% of cases of pure autosomal dominant HSPs, a group of neurodegenerative disorders characterized by lower-limb spasticity and weakness (Fink, 2013); primarily due to degeneration of the descending axons of cortico-spinal neurons. Fly models for spastin-dependent HSP have been created both by inactivating protein function (Sherwood et al., 2004; Trotta et al., 2004) or by expressing a pathogenic mutant version of fly spastin (Orso et al., 2005). Despite the extensive progress in the comprehension of spastin functions, the specific mechanisms by which its mutants lead to HSPs remain unclear. Spastin has been implicated in axonal transport (Errico et al., 2002; Yu et al., 2008; Kasher et al., 2009; Fassier et al., 2013), neuromuscular junctions (NMJ) morphology and function (Sherwood et al., 2004; Trotta et al., 2004) and axon guidance (Wood et al., 2006; Butler et al., 2010), suggesting that its role in maintaining neuronal heath is likely related to its MT severing activity.

Here we show that MT alteration due to the expression of spastin carrying the pathogenic mutation K467R reduces SOCE and decreases ER Ca^{2+} content in Drosophila neurons. ER morphology appears altered, as an increase in ER sheets is observed at the expense of tubules. Importantly, both morphological and functional ER defects are rescued when flies are exposed to the MT-destabilizing drug vinblastine, indicating that rescue of MT structure is sufficient to restore ER normal shape and function.

MATERIALS AND METHODS

Drosophila Stocks and Crosses

The UAS-Dspastin-K467R and UAS-BiP-sf-GFP-ER fly lines used in this study were described previously (Orso et al., 2005; Summerville et al., 2016). The Gal4 strains used were: Elav-Gal4 (pan neuronal expression); D42-Gal4 (motor neurons restricted), obtained from Bloomington Drosophila Stock Center. To increase protein expression, all experimental crosses were performed at 28°C. Control genotypes included promoter-Gal4/+ individuals. Fly food was prepared using NUTRI-fly-IF mixture (Genesee Scientific), according to the manufacturer instructions. For chronic vinblastine treatment, NUTRI-fly-IF was additioned with 50 nM vinblastine.

Electron Microscopy

Larval brains were fixed in 4% paraformaldehyde and 2% glutaraldehyde and embedded as previously described (Orso et al., 2009). Electron microscopy images were acquired from thin sections under a FEI Tecnai-12 electron microscope at the DeBio imaging Electron Microscopy Facility (University of Padova).

Confocal Images of Larval Brains

Brains and ventral ganglia from third instar larvae expressing BiP-sf-GFP-ER alone or together with spastin^{K467R} were dissected in M1 medium (see below) containing 1 mM Ca^{2+}, then

motor neuron cell bodies were imaged on a Leica TCS SP5 II confocal microscope equipped with a HCX PL APO lambda blue 63x/1.40-0.60 Oil objective, using a 488 nm laser.

For the quantification of ER distribution along nerves, BiP-sf-GFP-ER fluorescence was measured in regions located near the ganglion, along the axon, and at the end of the larval body. Mean fluorescence was calculated using ImageJ software.

Protein Extraction and Western Blotting

Proteins were extracted from 15 flies expressing BiP-sf-GFP-ER alone or together with spastin^{K467R} under the control of the motoneuron promoter D42-Gal4. GRS Full Sample Purification Kit (GRiSP, Lda.) was used according to the manufacturer's instructions. The protein pellet was solubilized in 80 μL of RIPA Buffer (50 mM Tris, 150 mM NaCl, 1% Nonidet P-40, 0.5% deoxycolic acid, 0.1% SDS, pH 7.5), supplemented with proteases and phosphatases inhibitors mixtures (Roche, 04693132001 and 04906837001) and 3 M urea. Insoluble particles were spun down at 10,000 g for 5 min. Proteins were separated by SDS-PAGE, transferred into nitrocellulose membranes (GE Healthcare, 10600001) and probed using the following antibodies: anti-GFP (Cell Signaling, 2956S), 1:1000; anti-ACT (beta-actin) (Sigma Aldrich, A2228), 1:2500. The intensity of the bands was analyzed using ImageJ software.

Preparation of Larval Neurons

Larval neurons were dissociated as previously reported (Chakraborty and Hasan, 2018). Briefly, third instar larvae were collected in a Petri dish, rinsed once with double-distilled water, twice with 70% ethanol, then with M3 complete medium (Shields and Sang M3 Insect Medium, supplemented with 10% heat-inactivated FBS, 50 U/mL penicillin, 50 μg/mL streptomycin). Brains were dissected with sterilized forceps under a light microscope. Brains were washed twice with M3 complete medium, then transferred to an enzymatic solution (0.75 μg/μL collagenase A and 0.4 μg/μL dispase II in M3 complete medium) and incubated for 20 min at room temperature in agitation. During incubation, brains were mechanically dissociated by gentle pipetting. Cell lysates were centrifuged at 600 × g for 5 min in a table top centrifuge and washed twice with dissecting solution to remove any residual enzymes. The cell pellet was resuspended with 100 μL of M3 complete medium for each brain; 100 μL were plated for each coverslip, approximately corresponding to one brain. Coverslips were previously autoclaved and coated with a drop of 0.1 mg/mL of poly-L-lysine for 30 min at 37°C.

Climbing Assay

Climbing assay was performed as previously described (Agrawal and Hasan, 2015) using a 2.5 cm diameter glass cylinder. A group of 20 seven-days-old flies of the indicated genotype were dropped in the cylinder and a gentle taps were given to convey the flies to the bottom of the cylinder. The number of flies that crossed a mark drawn 10 cm above the bottom of the tube in a 60 s time window was counted manually. Each batch of flies was tested three times. The number of climbing flies for each batch was calculated as the mean of the climbing flies in the three repetitions. The total number of climbing flies for each genotype was calculated as the sum of the means. An independent proportion analysis was used to determine statistical differences between populations.

Flight Assay

The flight assay was adapted from a previously published protocol (Banerjee, 2004) using a 1 m long, Plexiglas cylinder (diameter 5 cm) connected with an ethanol filled chamber at the bottom. Groups of 20 flies of a selected genotype were dropped into the cylinder through the top entry. A fly was determined to be capable of flight if it manages to reach the cylinder wall. Flies that could not perform this task fell directly to the ethanol filled chamber. Flight assays were performed on day 7 post eclosion. Data represent the percentage of flies capable of flight, at least 100 flies per condition were tested. Independent proportion analysis was used to determine the differences between groups.

Cytosolic Ca^{2+} Imaging

Neuronal cells were incubated with fura-2/AM (1 μM), pluronic F-127 (0.02%), and sulfinpyrazone (200 μM) for 20 min at room temperature (RT) in a M1 buffer (see below) and then in a fresh solution without the Ca^{2+} indicator for 20 min at RT. Fura-2–loaded cells were visualized with a 20x ultraviolet-permeable objective (CFI Sfluor 20x N.A. 0.75, Nikon) on an inverted microscope (Nikon Ti-E). Fluorescence illumination was achieved by 50–75W Lamp (USHIO UXLS50A) and alternating excitation wavelengths (340/380 nm) were obtained by a monochromator (Optoscan CAIRN-Research) controlled by NIS-ELEMENTS AR (Nikon) software. A neutral density filter, ND4 (Nikon, USA) and a FF-409-DiO3 Dichroic (Semrock) were used in the excitation pathway. The emitted fluorescence was collected using a 510/84 nm (Semrock) filter. Images were acquired every 1 s, with 100 ms exposure time at each wavelength, by a Zyla-CMOS 4.2-P (Andor, Oxford Instruments) controlled by the same software. During the experiment, cells plated on coverslips were mounted into an open-topped chamber and maintained in an extracellular-like medium containing the following:

(1) M1 (Na^+-based) medium: 30 mM HEPES, 150 mM NaCl, 5 mM KCl, 1 mM MgCl2, 35 mM sucrose, 5 glucose, pH 7.2 with NaOH at RT;

(2) K^+-based medium: 30 mM HEPES, 145 mM K-D-gluconate, 10 mM NaCl, 1 mM $MgCl_2$, 35 mM sucrose, 5 mM glucose pH 7.2 with KOH at RT.

For store Ca^{2+} content evaluation, cells were firstly perfused with M1 containing 1 mM $CaCl_2$; after addition of 500 μM EGTA, cells were stimulated by addition of ionomycin (10 μM) or cyclopiazonic acid (CPA, 50 μM). In the second case, for residual Ca^{2+} evaluation, cells were further stimulated with addition of ionomycin (10 μM). For SOCE activation experiments, cells were pre-treated with the irreversible SERCA inhibitor thapsigargin (100 nM) for 10 min in a Ca^{2+}-free, EGTA (500 μM)-containing M1; cells were then perfused with the same medium without the SERCA inhibitor and challenged with $CaCl_2$ (2 or 5 mM). Where indicated, M1 (Na^+-based) medium was substituted with K^+-based medium.

For acute vinblastine treatment, the drug (1 μM) was added in each solution and step of the experimental protocol, from fura-2/AM cell loading to cell stimulations. Neurons dissociated from larvae exposed to chronic vinblastine treatment, were similarly treated.

Ca^{2+} Imaging Experiments Analysis

Off-line analysis of Ca^{2+} imaging experiments was performed using the NIS-Elements software. F_{340} and F_{380} images were subtracted of background signals and proper regions of interest (ROIs) were selected on each imaged cell. The ratio of the emitted fluorescence intensities ($R = F_{340}/F_{380}$) was calculated for each ROI, normalized to the value measured before stimulus addition, or at the Ca^{2+}-free status, and averaged offline. Data were analyzed using Microsoft Excel and Graphpad Prism 8 to calculate areas under the curves (AUC).

Statistical Analyses

Fura-2 traces represent average values of 100 to 1,000 cells collected in 3–10 independent experiments. Average values are expressed as mean ± standard error of the mean (n = number of cells, unless otherwise specified). Statistical analyses were

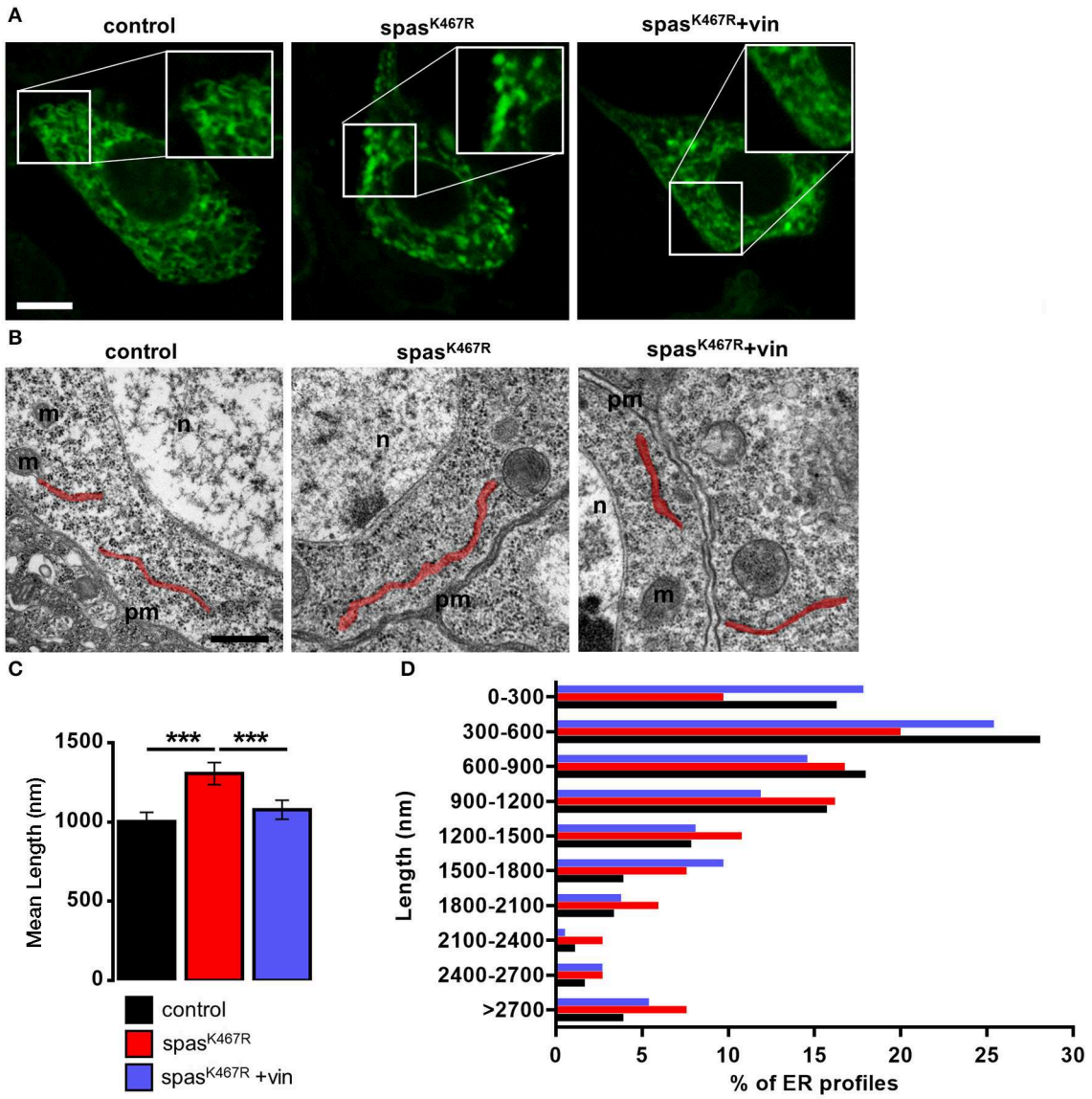

FIGURE 1 | (A) Ventral ganglion motor neurons cell bodies of larvae of the indicated genotypes co-expressing BiP-sf-GFP-ER were imaged at the confocal microscope. Where indicated, spastin^{K467R} flies were raised in vinblastine-containing food (50 nM). Scale bar, 5 μm. **(B)** TEM images of ventral ganglion neuronal cell bodies of larvae expressing spastin^{K467R} and relative control; ER profiles are highlighted in red. pm, plasma membrane; n, nucleus; m, mitochondria. Scale bar, 500 nm. **(C)** Quantification of the mean length of ER profiles in TEM images for the indicated genotypes. Mean ± SEM, $n \geq 50$ profiles. ***$p < 0.001$. **(D)** Distribution of ER profile length in TEM images. The percentage of measured profiles for each 300 nm-class is reported for the indicated genotypes.

performed using unpaired Student's t-test. Analyses of differences between fly populations were made using chi-square independent proportion analysis. Both tests were applied with a confidence interval of 95% ($^{*}p < 0.05$, $^{**}p < 0.01$, $^{***}p < 0.001$).

Materials

Shields and Sang M3 Insect Medium, Dispase II, vinblastine, thapsigargin, EGTA and $CaCl_2$ were purchased from Sigma-Aldrich. CPA, and ionomycin were purchased from Abcam, Collagenase A was purchased from Roche. Fura-2/AM was purchased from Thermo Fisher. All other materials were analytical or of the highest available grade.

RESULTS

Neuronal Expression of Spastin^{K467R} Influences ER Morphology

To alter MT stability, we used a transgenic line for the expression of Drosophila spastin carrying the mutation K467R under the control of UAS promoter (UAS-Dspastin-K467R). The amino acid substitution, located in the AAA ATPase domain, corresponds to the pathogenic mutation K388R in the human spastin protein, known to produce a dominant-negative effect (Orso et al., 2005). Indeed, when spastin^{K467R} is expressed in a wild-type background, hyper-stabilization of MTs has been observed, similar to that produced by downregulation of spastin (Orso et al., 2005). We expressed spastin^{K467R} in the fly nervous system, using the pan-neuronal driver elav-Gal4. The birth rate of flies expressing spastin^{K467R} was partially reduced, compared to control flies (**Supplementary Figure 1A**). Moreover, we confirmed that these flies show a shorter lifespan and locomotor dysfunction (**Supplementary Figures 1B,C**), as previously reported (Orso et al., 2005).

Because MTs are known to regulate ER distribution and sheet/tubule balance (Terasaki et al., 1986; Lu et al., 2009), we examined ER morphology in fly neurons expressing spastin^{K467R}. To visualize ER structure, we co-expressed the ER luminal marker BiP–sfGFP–HDEL (Summerville et al., 2016) under the control of the motoneuron-specific promoter D42-Gal4. In control motor neuron cell bodies, the ER appears mostly as a network of interconnected tubules (**Figure 1A**). In motor neurons expressing spastin^{K467R}, ER morphology was markedly changed and extended fluorescent areas, likely representing ER sheets, were often present (**Figure 1A**, **Supplementary Videos 1–3**). Axons are believed to contain mainly tubular, smooth ER that tracks to axon termini (Tsukita and Ishikawa, 1976; Terasaki and Reese, 1994; Krijnse-Locker et al., 1995; Terasaki, 2018). Moving along the longest motor neurons from the cell body to the axon termini, the density of ER only slightly decreases in control larvae (**Supplementary Figures 2A,B**). In contrast, in larvae expressing spastin^{K467R}, distal axons appear almost devoid of ER (**Supplementary Figures 2A,B**). This phenotype, although consistent with an impairment of axonal transport of ER tubules, could be also the result of a decrease in ER tubules amount. Noteworthy, western blotting analysis of BiP–sfGFP–HDEL amount in individuals expressing spastin^{K467R} or in controls indicated that the morphological alterations observed in cell bodies and axons does not affect total ER mass (**Supplementary Figures 2C,D**). To investigate in more depth the morphological change observed, we performed transmission electron microscopy (TEM) analysis of larval brains. The length of ER profiles measured in TEM thin sections, corresponding to a cut through sheet-like structures, reflects the organization of the ER (Puhka et al., 2012): a shift to longer profiles corresponds to an increase in sheets vs tubules ratio. The analysis of TEM thin sections revealed an increase in the length of ER profiles in spastin^{K467R}-expressing neurons, compared to controls (**Figures 1B,C**). In particular, the relative abundance of profiles of the shortest classes (0–300 nm and 300–600 nm) is decreased in spastin^{K467R} expressing neurons, while an increase in profiles longer than 2 μm is evident (**Figure 1D**). This is consistent with an increase in ER sheets compared to tubules.

Altogether, these results suggest that the expression of a dominant-negative spastin mutant leads preferentially to the formation of ER sheets to the detriment of tubules.

Neuronal Expression of Spastin^{K467R} Affects ER Ca^{2+} Handling

We reasoned that such morphological changes would have an impact on definite ER functions that depend very much on the presence of tubular ER. Specifically, TAC-mediated movement of ER tubules is believed to be directly involved in SOCE activation, the process necessary to refill depleted ER Ca^{2+} stores. In order to investigate the impact of spastin^{K467R} expression on ER Ca^{2+} dynamics, and specifically on SOCE, neurons were isolated from larval brains expressing spastin^{K467R} under the control of a pan-neuronal promoter (elav-Gal4/UAS-spastin^{K467R}), or from controls (elav-Gal4/+) (**Supplementary Figure 3**), loaded with the Ca^{2+} indicator fura-2 and examined by fluorescence microscopy. A typical protocol to elicit SOCE was applied to neurons: store depletion was induced by adding the SERCA inhibitor thapsigargin in a Ca^{2+}-free medium; SOCE was then monitored upon $CaCl_2$ addition (Ca^{2+}, 2 mM). A large cytosolic Ca^{2+} concentration ($[Ca^{2+}]_c$) increase, followed by a sustained plateau, due to Ca^{2+} influx across the PM, was observed in control neurons (**Figure 2A**). The effect of spastin mutation on the Ca^{2+} influx activated by store depletion was quantified by calculating the area under the curve corresponding to the first 2 min of Ca^{2+} influx. A marked decrease in SOCE was observed in neurons from larvae expressing spastin^{K467R}, compared to controls (37% reduction, $p < 0.001$; $n = 350$ control cells; $n = 300$ spastin^{K467R} cells; **Figure 2B**).

It is known that differences in PM potential alter the driving force for Ca^{2+} entry, thus potentially affecting the extent of SOCE (Penner et al., 1993). To nullify possible differences in membrane potential between the two genotypes, SOCE was measured as described above but in a medium where NaCl was iso-osmotically substituted by potassium-D-gluconate (K^+-based medium, see Methods for details), causing the collapse of the membrane potential. A higher concentration of $CaCl_2$ (5 mM) was applied, after emptying stores, to obtain an appreciable Ca^{2+} influx even under a reduced electrical gradient. Under such

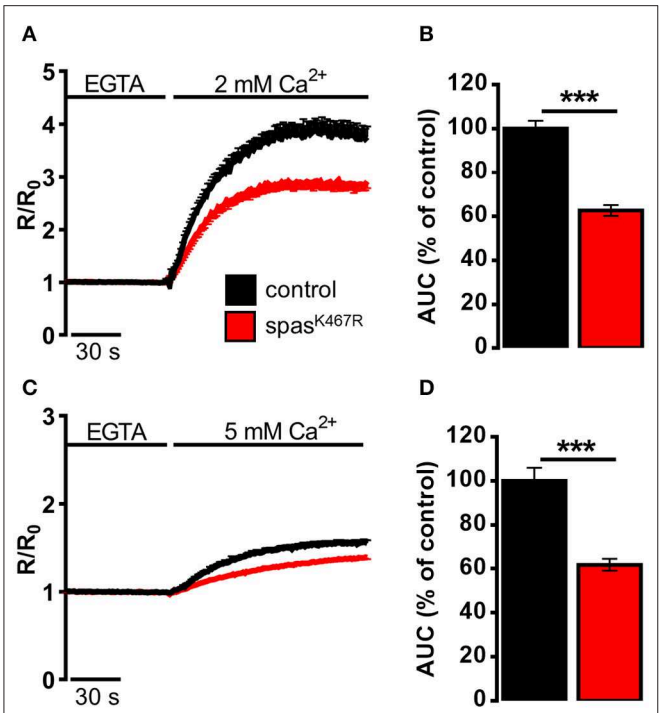

FIGURE 2 | Ca^{2+} dynamics induced by **(A,B)** SOCE activation, **(C,D)** SOCE activation in K^+-based medium (see Materials and Methods) in neurons dissociated from larval brains expressing spastin^{K467R}, and relative controls, as detected by fura-2. **(A,C)** Cells were pre-treated with thapsigargin in a Ca^{2+}-free medium for 8 min, to empty intracellular stores, and then **(A)** 2 mM or **(C)** 5 mM $CaCl_2$ was added. In all panels, average traces are represented as R/R_0 values of $n > 100$ cells. **(B,D)** Histograms report the average area under curve (AUC) values of the traces recorded. Data are presented as mean ± SEM of $n > 100$ cells. ***$p < 0.001$.

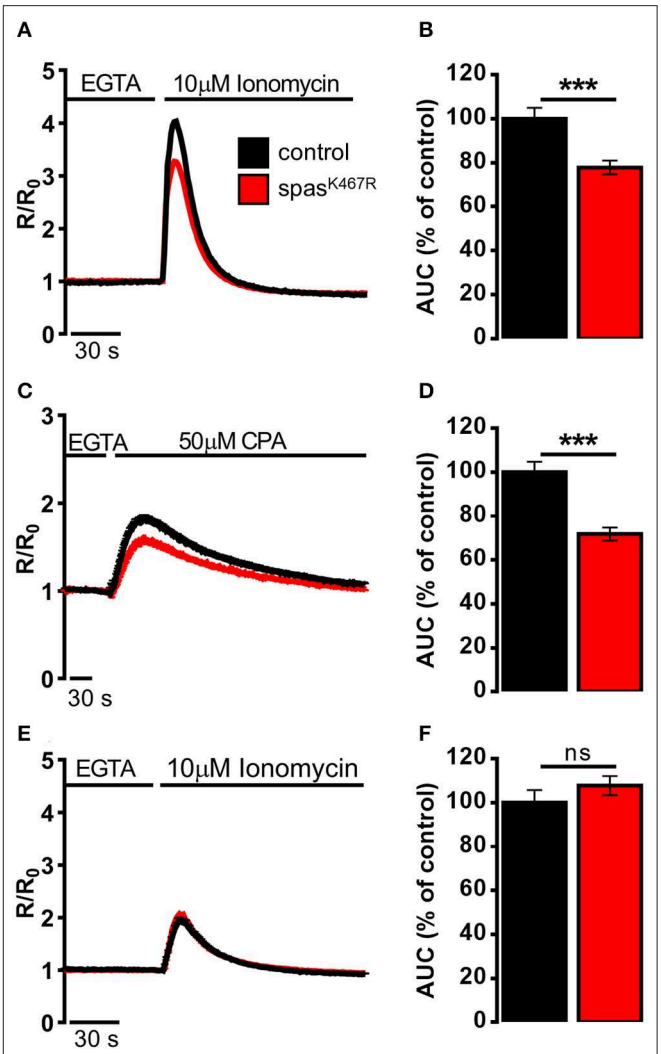

FIGURE 3 | Ca^{2+} dynamics induced by **(A,B)** ionomycin, **(C,D)** CPA, **(E,F)** ionomycin after CPA-induced ER depletion in neurons dissociated from larval brains expressing spastin^{K467R}, and relative controls, detected by fura-2. **(A,C,E)** Cells were stimulated with **(A,E)** 10 μM ionomycin or **(C)** 50 μM CPA in the presence of extracellular Ca^{2+} chelator EGTA. In all panels, average traces are represented as R/R_0 values of $n > 100$ cells. **(B,D,F)** Histograms report the average area under curve (AUC) values of the traces recorded. Data are presented as mean ± SEM of $n > 100$ cells. ***$p < 0.001$.

depolarizing conditions, the effect of spastin^{K467R} expression on SOCE was similar to that found in the standard Na^+-containing medium (38% reduction, $p < 0.001$; $n = 300$ control cells; $n = 280$ spastin^{K467R} cells; **Figures 2C,D**). When basal SOCE was measured in the same cells, by simply adding back Ca^{2+} to cells bathed in a Ca^{2+}-free medium, no difference was found between the two genotypes, neither in standard medium nor in K^+-based medium (**Supplementary Figures 4A–D**).

The decrease in Ca^{2+} entry upon store depletion could cause a partial depletion of intracellular Ca^{2+} stores in spastin^{K467R} expressing neurons. To investigate this possibility, the Ca^{2+} ionophore ionomycin was applied to neurons bathed in a Ca^{2+}-free medium containing the Ca^{2+} chelator EGTA. In this situation, the rise observed in $[Ca^{2+}]_c$ is due to the discharge of the majority of intracellular Ca^{2+} store pools (**Figure 3A**). The increase in $[Ca^{2+}]_c$ elicited by ionomycin was significantly reduced in spastin^{K467R} expressing neurons, relative to controls, as indicated by the area under the curve obtained upon ionomycin addition (22% reduction, $p < 0.001$; $n = 90$ control cells; $n = 100$ spastin^{K467R} cells; **Figure 3B**). A subsequent addition of monensin, in order to discharge any residual Ca^{2+} present in the acidic pool (Fasolato et al., 1991), did not result in an appreciable $[Ca^{2+}]_c$ increase in either genotypes (data not shown), indicating the relative low abundance of this type of Ca^{2+} stores in these cells. This result indicates that Ca^{2+} content of intracellular stores is diminished in cells expressing the spastin^{K467R} mutation. To determine whether the observed reduction was due to a specific partial depletion of the ER Ca^{2+} store, dissociated neurons were treated with the SERCA inhibitor CPA, thus inducing the passive release of Ca^{2+} from the organelle, resulting in a transient increase in $[Ca^{2+}]_c$ (**Figure 3C**). The amplitude of the increase in $[Ca^{2+}]_c$ reflects the Ca^{2+} content derived only from the ER and the cis/medial-Golgi, the main intracellular Ca^{2+} stores equipped

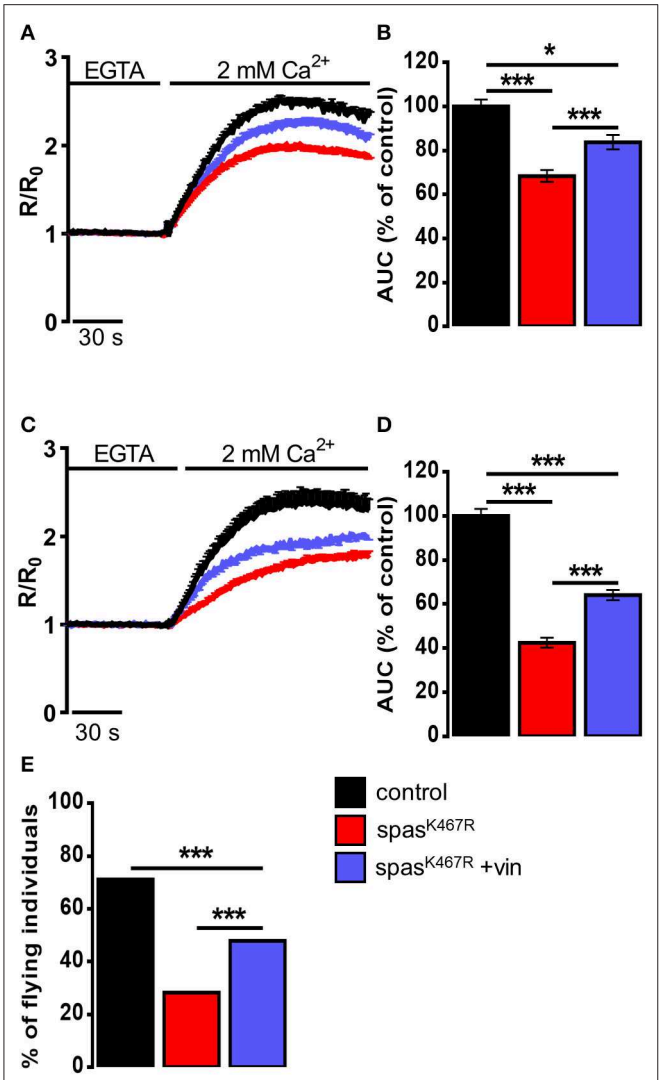

FIGURE 4 | (A–D) Ca^{2+} dynamics induced by SOCE activation in neurons dissociated from larval brains expressing spastin^{K467R}, and relative control, as detected by fura-2. Were indicated, vinblastine was applied: **(A,B)** during development, larvae were chronically treated with 50 nM vinblastine or **(C,D)** after dissociation, neurons were acutely treated with 1 μM vinblastine. Cells were pre-treated with thapsigargin for 8 min to empty intracellular stores, then 2 mM $CaCl_2$ was added. Traces are presented as average R/R_0 values of $n >$ 100 cells. **(B,D)** Histograms reporting the average area under curve (AUC) values of the corresponding traces. Data are presented as mean ± SEM of $n >$ 100 cells. $^*p < 0.05$; $^{***}p < 0.001$. **(E)** Flight ability, assayed by the cylinder drop test, of animals expressing spastin^{K467R} and relative control. Where indicated, animals were chronically exposed to vinblastine (50 nM). Data are presented as the percentage of flying individuals. Mean of $n >$ 100 cells. $^{***}p < 0.001$.

with SERCA pumps (Lissandron et al., 2010; Wong et al., 2013). The increase in $[Ca^{2+}]_c$ elicited by CPA was significantly reduced in spastin^{K467R}-expressing neurons, relative to controls (**Figure 3C**). The extent of such reduction, estimated calculating the area under the curve above resting $[Ca^{2+}]_c$ values, was 28% ($p < 0.001$; $n = 220$ control cells; $n = 160$ spastin^{K467R} cells; **Figure 3D**). Thus, ER Ca^{2+} content is diminished in cells expressing the spastin^{K467R} mutation. After CPA application, the discharge of residual Ca^{2+} pools, by ionomycin addition, did not show any differences between control and spastin^{K467R}-expressing neurons (**Figures 3E,F**), indicating that the $[Ca^{2+}]_{ER}$ is primarily affected by spastin mutation. Of note, basal $[Ca^{2+}]_c$ content is not affected (**Supplementary Figure 4E**). Altogether, these data indicate that expression of spastin^{K467R} causes an impairment of the ER Ca^{2+} replenishment mechanism of SOCE. This likely results in a reduction of the steady-state $[Ca^{2+}]_{ER}$.

Vinblastine Treatment Rescues ER Morphology and Ca^{2+} Handling Defects Induced by Spastin^{K467R} Expression

In order to assess whether MT cytoskeleton impairment was directly responsible for ER morphology and Ca^{2+} handling defects observed in spastin^{K467R}-expressing flies, and to exclude other possible effects of mutant spastin expression, we exploited a pharmacological approach. It has been shown that administration of low concentrations of the MT-targeting drug vinblastine rescued the excessive stabilization of MTs in spastin^{K467R}-expressing flies (Orso et al., 2005). We thus administered vinblastine to control and spastin^{K467R} flies by adding the drug to the food at a concentration of 50 nM (Orso et al., 2005). When we examined the fluorescence of the ER marker BiP–sfGFP–HDEL (Summerville et al., 2016), we found that exposure to the MT-targeting drug resulted in recovery of ER morphology in flies expressing spastin^{K467R} (**Figure 1A**). The rescue is confirmed also by the quantification of ER profiles length in TEM thin sections (**Figures 1B,C**). Moreover, in neurons dissociated from brains of the same larvae, we evaluated SOCE, as described above. We found that the reduction in the Ca^{2+} entry following stores depletion, observed in neurons derived from larvae expressing spastin^{K467R}, was partially recovered by vinblastine treatment (**Figures 4A,B**), indicating that the drug-induced destabilization of hyper-stabilized MTs rescues the spastin^{K467R}-induced SOCE defects.

It has been shown that loss of MT polymers in response to vinblastine occurs very rapidly, starting in as little as 30 min (Harkcom et al., 2014). In order to further demonstrate that the rescue of MT cytoskeleton is directly responsible for the recovery of SOCE impairment observed in spastin^{K467R}-expressing flies, we acutely applied vinblastine (1 μM) on neurons dissociated from spastin^{K467R} larvae raised in the absence of drug in the food. Application of vinblastine for 40 min before SOCE activation and visualization was able to induce a partial rescue in the extent of Ca^{2+} entry, compared to untreated spastin^{K467R}-expressing neurons (**Figures 4C,D**). This result indicates that reestablishment of proper MT organization is sufficient to rescue the process of Ca^{2+} entry upon stores depletion, affected by the spastin mutant.

Pan-neural downregulation of *dStim* or *dOrai* leads to a significant reduction of SOCE and ER $[Ca^{2+}]$ in primary neuronal cultures (Venkiteswaran and Hasan, 2009). Reduced SOCE has been shown to affect fly neuronal functions, in particular a significant loss of flight has been observed. In order

to assess whether the defect in SOCE observed upon spastin^{K467R} expression was also associated with an impairment in flight, we performed the "cylinder drop" test assay, which revealed a defect in the flight ability of spastin^{K467R}-expressing flies (42% reduction of spastin^{K467R} compared to control, $p < 0.001$; $n =$ 100 control cells; $n = 100$ spastin^{K467R} cells; **Figure 4E**). This defect was partially rescued when flies were raised in vinblastine-containing food (**Figure 4E**).

DISCUSSION

Ca^{2+} signals regulate fundamental aspects of neuronal function and physiology and contribute in determining the morphology of neural circuits (Berridge, 1998; Borodinsky and Spitzer, 2007). Traditionally, most of these signals were attributed to the entry of Ca^{2+} from the extracellular *milieu* through voltage-operated channels or ionotropic receptors. However, the "Ca^{2+} toolkit" components related to Ca^{2+} release from intracellular stores are also present in neurons. Increasing evidence suggests that also neurons rely on SOCE and its dysregulation may participate in the pathogenesis of diverse neurodegenerative diseases, such as Alzheimer's, Parkinson's, Charcot-Marie-Tooth (Secondo et al., 2018).

The aim of this study was to determine the influence of neuronal MT cytoskeleton architecture on the process of SOCE, the opening of PM Ca^{2+} channels that follows the release of Ca^{2+} from intracellular stores. The molecular mechanism of cytoskeleton regulation over the relocation of STIM to ER-PM junctions during SOCE is not fully understood. It appears clear that coordinated interplay between different molecules is necessary to mediate the transient formation of ER-PM junctions (Grigoriev et al., 2008; Sharma et al., 2013; Maléth et al., 2014; Woo et al., 2016), but whether the integrity of cytoskeleton is needed for proper SOCE activation is not clear. Opposing data are present in literature, suggesting both inhibition (Oka et al., 2005; Smyth et al., 2007) or potentiation (Galán et al., 2011) of SOCE in the presence of MT-depolymerizing agents (Russa et al., 2009; Martin-Romero et al., 2017). To sort this out, we performed an *in vivo* approach in *Drosophila melanogaster* exploiting an endogenous means to manipulate MT dynamic instability. We expressed in Drosophila a variant of the MT-severing protein spastin carrying an amino acid substitution known to function as a dominant-negative, thus inducing MT hyper-stabilization. Our results clearly indicate that the process of Ca^{2+} entry upon ER Ca^{2+} depletion is negatively affected by MT stabilization. This impairment results in a reduced ER Ca^{2+} content without, however, affecting cytosolic basal Ca^{2+} levels.

The phenotypes we observed upon neuronal expression of spastin^{K467R} recapitulate those observed upon dStim or dOrai reduction in flies. Pan-neural downregulation of *dStim* or *dOrai* leads to a significant decrease in SOCE and ER [Ca^{2+}] in primary larval neurons (Venkiteswaran and Hasan, 2009). Reduced SOCE has been shown to affect fly neuronal functions, in particular a significant loss of flight has been observed, accompanied by the loss of rhythmic flight patterns (Venkiteswaran and Hasan, 2009), indicating that, in neurons, the replenishment of intracellular Ca^{2+} stores is required for Drosophila flight. We observed a similar defect in flight ability, tested in the cylinder drop assay, in flies expressing spastin^{K467R}. This phenotype is specific, since dSERCA mutant flies, where stored Ca^{2+} is decreased but SOCE is increased, do not display flight defects (Banerjee et al., 2006; Venkiteswaran and Hasan, 2009).

We found that spastin^{K467R}-induced MT stabilization causes a change in ER morphology, shifting ER sheets/tubules balance toward the formation of sheets. Interestingly, an accumulation of ER sheets has also been reported in mammalian cells upon treatment with MT-depolymerizing (Terasaki et al., 1986; Joensuu et al., 2014) as well as -stabilizing agents (Joensuu and Jokitalo, 2015), suggesting that ER morphology is similarly affected upon MT cytoskeleton disruption or hyper-stabilization.

It is widely assumed that the structural heterogeneity of the ER contributes to its functional compartmentalization. Despite the fact that a clear-cut attribution of function to either sheets or tubules has yet to be defined, tubules appear to perform some specific functions. The involvement of TAC-mediated movement on MT tips suggests that the regulated process of SOCE is allocated specifically to ER tubules. The data we obtained allow us to speculate that MT disorganization and SOCE impairment are causally linked by the alteration of ER morphology observed upon spastin^{K467R} expression in flies: MT hyperstabilization shifts the ER sheets/tubules balance in favor of ER sheets; this in turn affects SOCE, a specific ER function that relies on the physical movement of ER tubules toward the PM. However, MT dynamics itself is critical to generate pushing and pulling forces during polymerization and depolymerization, respectively (Inoué and Salmon, 1995) providing the force required for membrane movement that can result in membrane translocation from one point to another within the cell. For this reason, we cannot exclude that MT impairment *per se* is responsible for the observed reduction of SOCE.

Beneficial effects from treatments with vinblastine have been reported in flies expressing spastin^{K467R} (Orso et al., 2005). By recovering MT organization, vinblastine rescues NMJs morphology and function, together with fly viability and climbing defects (Orso et al., 2005). We demonstrate that vinblastine treatment is able to rescue also ER morphology, Ca^{2+} handling defects and flight ability, indicating that MT impairment is the earliest responsible for all the phenotypes observed. Notably, acute vinblastine treatment (40 min application on dissociated neurons) is sufficient to rescue SOCE and ER Ca^{2+} content. Within this time-window, transcriptional activation is unlikely to occur, suggesting that the level of Ca^{2+} handling proteins, and in particular of the SOCE machinery, is expected to be unaltered and the defects observed are directly ascribable to a MT dynamics impairment.

Tubulin represents about 4% of total cellular proteins in many cultured cells, however it reaches 25% in the brain (Zhai and Borisy, 1994). In axons and dendrites, MTs serve as the major railways for organelles and other cargoes and dysfunctional MT scaffolding has been primarily associated with impaired transport. Neuronal functionalities, including learning and memory, are associated with the normal functioning

of dendritic spines that could be compromised if organelles and proteins do not reach their proper location. In addition to this evident relationship between MT organization and neuronal function, our present work supports the idea that other fundamental cellular mechanism, namely ER shape and function, are affected by MT disorganization caused by mutant spastin expression. This is critically important considering that increasing evidence suggests the presence of a causative link between derangement of ER morphology/function and the pathogenesis of HSPs.

DATA AVAILABILITY STATEMENT

The datasets generated for this study are available on request to the corresponding author.

AUTHOR CONTRIBUTIONS

DP conceived the work. NV and RN performed the experiments. NV and NR analyzed the results. PP and AD contributed to the interpretation of the results. DP wrote the manuscript. DP and PP secured funding. All the authors revised the manuscript.

FUNDING

This work was supported by the Ministry of Education, University and Research (MIUR) (PRIN 2017 to PP; fellowship to NV); University of Padua (SID 2019 to PP; BIRD 2017 to DP for fellowships to RN and NR; UNIPD funds for research equipment-2015); Fondazione Cassa di Risparmio di Padova e Rovigo (CARIPARO Foundation, Starting Grant 2015 to DP and PP); Fondazione Telethon (Grant 2019 GGP19304 to DP).

ACKNOWLEDGMENTS

We thank Tullio Pozzan and Cristina Fasolato for helpful advice and discussion and Riccardo Osello for help with fly work. Stocks obtained from the Bloomington Drosophila Stock Center (NIH P40OD018537) were used in this study.

SUPPLEMENTARY MATERIAL

The Supplementary Material for this article can be found online at: https://www.frontiersin.org/articles/10.3389/fphys.2019.01544/full#supplementary-material

REFERENCES

Agrawal, T., and Hasan, G. (2015). Maturation of a central brain flight circuit in Drosophila requires Fz2/Ca2+ signaling. *Elife* 4:e07046. doi: 10.7554/eLife.07046.035

Banerjee, S. (2004). Loss of flight and associated neuronal rhythmicity in inositol 1,4,5-trisphosphate receptor mutants of Drosophila. *J. Neurosci.* 24, 7869–7878. doi: 10.1523/JNEUROSCI.0656-04.2004

Banerjee, S., Joshi, R., Venkiteswaran, G., Agrawal, N., Srikanth, S., Alam, F., et al. (2006). Compensation of inositol 1,4,5-trisphosphate receptor function by altering sarco-endoplasmic reticulum calcium atpase activity in the Drosophila flight circuit. *J. Neurosci.* 26, 8278–8288. doi: 10.1523/JNEUROSCI.1231-06.2006

Berridge, M. J. (1998). Neuronal calcium signaling. *Neuron*. 21, 13–26. doi: 10.1016/S0896-6273(00)80510-3

Borodinsky, L. N., and Spitzer, N. C. (2007). Activity-dependent neurotransmitter-receptor matching at the neuromuscular junction. *Proc. Natl. Acad. Sci. U.S.A.* 104, 335–340. doi: 10.1073/pnas.0607450104

Burbank, K. S., and Mitchison, T. J. (2006). Microtubule dynamic instability. *Curr. Biol.* 16, 1375–1478. doi: 10.1016/j.cub.2006.06.044

Butler, R., Wood, J. D., Landers, J. A., and Cunliffe, V. T. (2010). Genetic and chemical modulation of spastin-dependent axon outgrowth in zebrafish embryos indicates a role for impaired microtubule dynamics in hereditary spastic paraplegia. *Dis. Model. Mech.* 3, 743–751. doi: 10.1242/dmm.004002

Carrasco, S., and Meyer, T. (2011). STIM proteins and the endoplasmic reticulum-plasma membrane junctions. *Annu. Rev. Biochem.* 80, 973–1000. doi: 10.1146/annurev-biochem-061609-165311

Chakraborty, S., and Hasan, G. (2018). Store-operated Ca2+ entry in Drosophila primary neuronal cultures. *Methods Mol. Biol.* 1843, 125–136. doi: 10.1007/978-1-4939-8704-7_11

Chen, Y. F., Chen, L. H., and Shen, M. R. (2019). The distinct role of STIM1 and STIM2 in the regulation of store-operated Ca 2+ entry and cellular function. *J. Cell. Physiol.* 234, 8727–8739. doi: 10.1002/jcp.27532

Chen, Y. T., Chen, Y. F., Chiu, W. T., Liu, K. Y., Liu, Y. L., Chang, J. Y., et al. (2013). Microtubule-associated histone deacetylase 6 supports the calcium store sensor STIM1 in mediating malignant cell behaviors. *Cancer Res.* 73, 4500-4509. doi: 10.1158/0008-5472.CAN-12-4127

Conde, C., and Cáceres, A. (2009). Microtubule assembly, organization and dynamics in axons and dendrites. *Nat. Rev. Neurosci.* 10, 319–332. doi: 10.1038/nrn2631

Dabora, S. L., and Sheetz, M. F. (1988). The microtubule-dependent formation of a tubulovesicular network with characteristics of the ER from cultured cell extracts. *Cell.* 54, 27–35. doi: 10.1016/0092-8674(88)90176-6

Desai, A., and Mitchison, T. J. (1997). Microtubule polymerization dynamics. *Annu. Rev. Cell Dev. Biol.* 13, 83–117. doi: 10.1146/annurev.cellbio.13.1.83

Dreier, L., and Rapoport, T. A. (2000). *In vitro* formation of the endoplasmic reticulum occurs independently of microtubules by a controlled fusion reaction. *J. Cell Biol.* 148, 883–898. doi: 10.1083/jcb.148.5.883

Errico, A., Ballabio, A., and Rugarli, E. I. (2002). Spastin, the protein mutated in autosomal dominant hereditary spastic paraplegia, is involved in microtubule dynamics. *Hum. Mol. Genet.* 11, 153–163. doi: 10.1093/hmg/11.2.153

Fasolato, C., Zottini, M., Clementi, E., Zacchetti, D., Meldolesi, J., and Pozzan, T. (1991). Intracellular Ca2+ pools in PC12 cells: three intracellular pools are distinguished by their turnover and mechanisms of Ca2+ accumulation, storage, *and release. J. Biol. Chem.* 266, 20159–20167.

Fassier, C., Tarrade, A., Peris, L., Courageot, S., Mailly, P., Dalard, C., et al. (2013). Microtubule-targeting drugs rescue axonal swellings in cortical neurons from spastin knockout mice. *Dis. Model. Mech.* 6, 72–83. doi: 10.1242/dmm.008946

Feske, S., Gwack, Y., Prakriya, M., Srikanth, S., Puppel, S. H., Tanasa, B., et al. (2006). A mutation in orai1 causes immune deficiency by abrogating CRAC channel function. *Nature*. 441, 179–185. doi: 10.1038/nature04702

Fink, J. K. (2013). Hereditary spastic paraplegia: clinico-pathologic features and emerging molecular mechanisms. *Acta Neuropathol.* 126, 307–328. doi: 10.1007/s00401-013-1115-8

Friedman, J. R., Webster, B. M., Mastronarde, D. N., Verhey, K. J., and Voeltz, G. K. (2010). ER sliding dynamics and ER-mitochondrial contacts occur on acetylated microtubules. *J. Cell Biol.* 190, 363–375. doi: 10.1083/jcb.200911024

Galán, C., Dionisio, N., Smani, T., Salido, G. M., and Rosado, J. A. (2011). The cytoskeleton plays a modulatory role in the association between STIM1 and the Ca2+ channel subunits Orai1 and TRPC1. *Biochem. Pharmacol.* 82, 400–410. doi: 10.1016/j.bcp.2011.05.017

Grigoriev, I., Gouveia, S. M., van der Vaart, B., Demmers, J., Smyth, J. T., Honnappa, S., et al. (2008). STIM1 is a MT-plus-end-tracking protein involved in remodeling of the ER. *Curr. Biol.* 18, 177–182. doi: 10.1016/j.cub.2007.12.050

Gurel, P. S., Hatch, A. L., and Higgs, H. N. (2014). Connecting the cytoskeleton to the endoplasmic reticulum and Golgi. *Curr. Biol.* 24, R660–R672. doi: 10.1016/j.cub.2014.05.033

Harkcom, W. T., Ghosh, A. K., Sung, M. S., Matov, A., Brown, K. D., Giannakakou, P., et al. (2014). NAD+ and SIRT3 control microtubule dynamics and reduce susceptibility to antimicrotubule agents. *Proc. Natl. Acad. Sci. U.S.A.* 111, E2443–E2452. doi: 10.1073/pnas.1404269111

Hazan, J., Fonknechten, N., Mavel, D., Paternotte, C., Samson, D., Artiguenave, F., et al. (1999). Spastin, a new AAA protein, is altered in the most frequent form of autosomal dominant spastic paraplegia. *Nat. Genet.* 23, 296–303. doi: 10.1038/15472

Honnappa, S., Gouveia, S. M., Weisbrich, A., Damberger, F. F., Bhavesh, N. S., Jawhari, H., et al. (2009). An EB1-binding motif acts as a microtubule tip localization signal. *Cell.* 138, 366–376. doi: 10.1016/j.cell.2009.04.065

Inoué, S., and Salmon, E. D. (1995). Force generation by microtubule assembly/disassembly in mitosis and related movements. *Mol. Biol. Cell* 6, 1619–1640. doi: 10.1091/mbc.6.12.1619

Joensuu, M., Belevich, I., Rämö, O., Nevzorov, I., Vihinen, H., Puhka, M., et al. (2014). ER sheet persistence is coupled to myosin 1c-regulated dynamic actin filament arrays. *Mol. Biol. Cell.* 25, 1111–1126. doi: 10.1091/mbc.e13-12-0712

Joensuu, M., and Jokitalo, E. (2015). ER sheet-tubule balance is regulated by an array of actin filaments and microtubules. *Exp. Cell Res.* 337, 170–178. doi: 10.1016/j.yexcr.2015.04.009

Kapitein, L. C., and Hoogenraad, C. C. (2015). Building the neuronal microtubule cytoskeleton. *Neuron* 87, 492–506. doi: 10.1016/j.neuron.2015.05.046

Kasher, P. R., De Vos, K. J., Wharton, S. B., Manser, C., Bennett, E. J., Bingley, M., et al. (2009). Direct evidence for axonal transport defects in a novel mouse model of mutant spastin-induced hereditary spastic paraplegia (HSP) and human HSP patients. *J. Neurochem.* 110, 34–44. doi: 10.1111/j.1471-4159.2009.06104.x

Kirschner, M., and Mitchison, T. (1986). Beyond self-assembly: from microtubules to morphogenesis. *Cell.* 45, 329–342. doi: 10.1016/0092-8674(86)90318-1

Krijnse-Locker, J., Parton, R. G., Fuller, S. D., Griffiths, G., and Dotti, C. G. (1995). The organization of the endoplasmic reticulum and the intermediate compartment in cultured rat hippocampal neurons. *Mol. Biol. Cell.* 6, 1315–1332. doi: 10.1091/mbc.6.10.1315

Lee, C., and Chen, L. B. (1988). Dynamic behavior of endoplasmic reticulum in living cells. *Cell.* 54, 37–46. doi: 10.1016/0092-8674(88)90177-8

Liou, J., Fivaz, M., Inoue, T., and Meyer, T. (2007). Live-cell imaging reveals sequential oligomerization and local plasma membrane targeting of stromal interaction molecule 1 after Ca2+ store depletion. *Proc. Natl. Acad. Sci. U.S.A.* 104, 9301–9306. doi: 10.1073/pnas.0702866104

Liou, J., Kim, M. L., Won, D. H., Jones, J. T., Myers, J. W., Ferrell, J. E., et al. (2005). STIM is a Ca2+ sensor essential for Ca2+-store- depletion-triggered Ca2+ influx. *Curr. Biol.* 15, 1235–1241. doi: 10.1016/j.cub.2005.05.055

Lissandron, V., Podini, P., Pizzo, P., and Pozzan, T. (2010). Unique characteristics of Ca2+ homeostasis of the trans-Golgi compartment. *Proc. Natl. Acad. Sci. U.S.A.* 107, 9198–9203. doi: 10.1073/pnas.1004702107

Lu, L., Ladinsky, M. S., and Kirchhausen, T. (2009). Cisternal organization of the endoplasmic reticulum during mitosis. *Mol. Biol. Cell.* 20, 3471–3480. doi: 10.1091/mbc.e09-04-0327

Luik, R. M., Wang, B., Prakriya, M., Wu, M. M., and Lewis, R. S. (2008). Oligomerization of STIM1 couples ER calcium depletion to CRAC channel activation. *Nature* 454, 538–542. doi: 10.1038/nature07065

Maléth, J., Choi, S., Muallem, S., and Ahuja, M. (2014). Translocation between PI(4,5)P 2 -poor and PI(4,5)P 2 -rich microdomains during store depletion determines STIM1 conformation and Orai1 gating. *Nat. Commun.* 5:5843. doi: 10.1038/ncomms6843

Martin-Romero, F. J., Lopez-Guerrero, A. M., Pascual-Caro, C., and Pozo-Guisado, E. (2017). "The interplay between cytoskeleton and calcium dynamics," in *Cytoskeleton - Structure, Dynamics, Function and Disease,* ed J. C. Jimenez-Lopez (London: IntechOpen). doi: 10.5772/66862

Nogales, E. (2001). Structural insights into microtubule function. *Annu. Rev. Biochem.* 69, 277–302. doi: 10.1146/annurev.biochem.69.1.277

Oka, T., Hori, M., and Ozaki, H. (2005). Microtubule disruption suppresses allergic response through the inhibition of calcium influx in the mast cell degranulation pathway. *J. Immunol.* 174, 4584–459. doi: 10.4049/jimmunol.174.8.4584

Orso, G., Martinuzzi, A., Rossetto, M. G., Sartori, E., Feany, M., and Daga, A. (2005). Disease-related phenotypes in a Drosophila model of hereditary spastic paraplegia are ameliorated by treatment with vinblastine. *J. Clin. Invest.* 115, 3026–3034. doi: 10.1172/JCI24694

Orso, G., Pendin, D., Liu, S., Tosetto, J., Moss, T. J., Faust, J. E., et al. (2009). Homotypic fusion of ER membranes requires the dynamin-like GTPase atlastin. *Nature* 460, 978–983. doi: 10.1038/nature08280

Pendin, D., Greotti, E., Lefkimmiatis, K., and Pozzan, T. (2017). Exploring cells with targeted biosensors. *J. Gen. Physiol.* 149, 1–36. doi: 10.1085/jgp.201611654

Penner, R., Fasolato, C., and Hoth, M. (1993). Calcium influx and its control by calcium release. *Curr. Opin. Neurobiol.* 3, 368–374. doi: 10.1016/0959-4388(93)90130-Q

Prakriya, M., Feske, S., Gwack, Y., Srikanth, S., Rao, A., and Hogan, P. G. (2006). Orai1 is an essential pore subunit of the CRAC channel. *Nature.* 443, 230-233. doi: 10.1038/nature05122

Puhka, M., Joensuu, M., Vihinen, H., Belevich, I., and Jokitalo, E. (2012). Progressive sheet-to-tubule transformation is a general mechanism for endoplasmic reticulum partitioning in dividing mammalian cells. *Mol. Biol. Cell.* 23, 2424–2432. doi: 10.1091/mbc.e10-12-0950

Redondo, P. C., Harper, M. T., Rosado, J. A., and Sage, S. O. (2006). A role for cofilin in the activation of store-operated calcium entry by *de novo* conformational coupling in human platelets. *Blood* 107, 973–979. doi: 10.1182/blood-2005-05-2015

Roll-Mecak, A., and McNally, F. J. (2010). Microtubule-severing enzymes. *Curr. Opin. Cell Biol.* 22, 96–103. doi: 10.1016/j.ceb.2009.11.001

Russa, A. D., Ishikita, N., Masu, K., Akutsu, H., Saino, T., and Satoh, Y. (2009). Microtubule remodeling mediates the inhibition of store-operated calcium entry (SOCE) during mitosis in COS-7 cells. *Arch. Histol. Cytol.* 71, 249–263. doi: 10.1679/aohc.71.249

Sandate, C. R., Szyk, A., Zehr, E. A., Lander, G. C., and Roll-Mecak, A. (2019). An allosteric network in spastin couples multiple activities required for microtubule severing. *Nat. Struct. Mol. Biol.* 26, 671–678. doi: 10.1038/s41594-019-0257-3

Secondo, A., Bagetta, G., and Amantea, D. (2018). On the role of store-operated calcium entry in acute and chronic neurodegenerative diseases. *Front. Mol. Neurosci.* 11:87. doi: 10.3389/fnmol.2018.00087

Sharma, S., Quintana, A., Findlay, G. M., Mettlen, M., Baust, B., Jain, M., et al. (2013). An siRNA screen for NFAT activation identifies septins as coordinators of store-operated Ca2+ entry. *Nature* 499, 238–242. doi: 10.1038/nature12229

Sharp, D. J., and Ross, J. L. (2012). Microtubule-severing enzymes at the cutting edge. *J. Cell Sci.* 125(Pt. 11), 2561–2569. doi: 10.1242/jcs.101139

Sherwood, N. T., Sun, Q., Xue, M., Zhang, B., and Zinn, K. (2004). Drosophila spastin regulates synaptic microtubule networks and is required for normal motor function. *PLoS Biol.* 2:e429. doi: 10.1371/journal.pbio.0020429

Smyth, J. T., DeHaven, W. I., Bird, G. S., and Putney, J. W. (2007). Role of the microtubule cytoskeleton in the function of the store-operated Ca2+ channel activator STIM1. *J. Cell Sci.* 120(Pt. 21), 3762–3771. doi: 10.1242/jcs.015735

Soboloff, J., Rothberg, B. S., Madesh, M., and Gill, D. L. (2012). *STIM* proteins: dynamic calcium signal transducers. *Nat. Rev. Mol. Cell Biol.* 13, 549–565. doi: 10.1038/nrm3414

Summerville, J. B., Faust, J. F., Fan, E., Pendin, D., Daga, A., Formella, J., et al. (2016). The effects of ER morphology on synaptic structure and function in Drosophila melanogaster. *J. Cell Sci.* 129, 1635–1648. doi: 10.1242/jcs.184929

Terasaki, M. (2018). Axonal endoplasmic reticulum is very narrow. *J. Cell Sci.* 131:210450. doi: 10.1242/jcs.210450

Terasaki, M., Chen, L. B., and Fujiwara, K. (1986). Microtubules and the endoplasmic reticulum are highly interdependent structures. *J. Cell Biol.* 103, 1557–1568. doi: 10.1083/jcb.103.4.1557

Terasaki, M., and Reese, T. S. (1994). Interactions among *endoplasmic reticulum*, microtubules, and retrograde movements of the cell surface. *Cell Motil. Cytoskeleton.* 29, 291–300. doi: 10.1002/cm.970290402

Trotta, N., Orso, G., Rossetto, M. G., Daga, A., and Broadie, K. (2004). The hereditary spastic paraplegia gene, spastin, regulates microtubule stability to modulate synaptic structure and function. *Curr. Biol.* 14, 1135–1147. doi: 10.1016/j.cub.2004.06.058

Tsai, F. C., Seki, A., Yang, H. W., Hayer, A., Carrasco, S., Malmersjö, S., et al. (2014). A polarized Ca2+, diacylglycerol and STIM1 signalling system regulates directed cell migration. *Nat. Cell Biol.* 16, 133–144. doi: 10.1038/ncb2906

Tsukita, S., and Ishikawa, H. (1976). Three-dimensional distributionof smooth endoplasmic reticulum in myelinated axons. *J. Electron Microsc*. 25, 141–149.

Várnai, P., Hunyady, L., and Balla, T. (2009). STIM and orai: the long-awaited constituents of store-operated calcium entry. *Trends Pharmacol. Sci.* 30, 118–128. doi: 10.1016/j.tips.2008.11.005

Venkiteswaran, G., and Hasan, G. (2009). Intracellular Ca2+ signaling and store-operated Ca2+ entry are required in Drosophila neurons for flight. *Proc. Natl. Acad. Sci. U.S.A.* 106, 10326–10331. doi: 10.1073/pnas.0902982106

Vig, M., Beck, A., Billingsley, J. M., Lis, A., Parvez, S., Peinelt, C., et al. (2006a). CRACM1 multimers form the ion-selective pore of the CRAC channel. *Curr. Biol.* 16, 2073–2079. doi: 10.1016/j.cub.2006.08.085

Vig, M., Peinelt, C., Beck, A., Koomoa, D. L., Rabah, D., Koblan-Huberson, M., et al. (2006b). CRACM1 is a plasma membrane protein essential for store-operated Ca 2+ entry. *Science* 312, 1220–1223. doi: 10.1126/science.1127883

Waterman-Storer, C. M., and Salmon, E. D. (1998). Endoplasmic reticulum membrane tubules are distributed by microtubules in living cells using three distinct mechanisms. *Curr. Biol.* 8, 798–807. doi: 10.1016/S0960-9822(98)70321-5

Wong, A. K. C., Capitanio, P., Lissandron, V., Bortolozzi, M., Pozzan, T., and Pizzo, P. (2013). Heterogeneity of Ca2+ handling among and within Golgi compartments. *J. Mol. Cell Biol.* 5, 266–276. doi: 10.1093/jmcb/mjt024

Woo, J. S., Srikanth, S., Nishi, M., Ping, P., Takeshima, H., and Gwack, Y. (2016). Junctophilin-4, a component of the endoplasmic reticulum–plasma membrane junctions, regulates Ca 2+ dynamics in T cells . *Proc. Natl. Acad. Sci. U.S.A.* 113, 2762–2767. doi: 10.1073/pnas.1524229113

Wood, J. D., Landers, J. A., Bingley, M., McDermott, C. J., Thomas-McArthur, V., Gleadall, L. J., et al. (2006). The microtubule-severing protein Spastin is essential for axon outgrowth in the zebrafish embryo. *Hum. Mol. Genet.* 15, 2763–2771. doi: 10.1093/hmg/ddl212

Wu, M. M., Buchanan, J., Luik, R. M., and Lewis, R. S. (2006). Ca 2+ store depletion causes STIM1 to accumulate in ER regions closely associated with the plasma membrane. *J. Cell Biol.* 174, 803–813. doi: 10.1083/jcb.200604014

Yeromin, A. V., Zhang, S. L., Jiang, W., Yu, Y., Safrina, O., and Cahalan, M. D. (2006). Molecular identification of the CRAC channel by altered ion selectivity in a mutant of Orai. *Nature* 443, 226–229. doi: 10.1038/nature05108

Yu, W., Qiang, L., Solowska, J. M., Karabay, A., Korulu, S., and Baas, P. W. (2008). The microtubule-severing proteins spastin and katanin participate differently in the formation of axonal branches. *Mol. Biol. Cell.* 19, 1485–1498. doi: 10.1091/mbc.e07-09-0878

Zampese, E., and Pizzo, P. (2012). Intracellular organelles in the *saga of Ca 2+* homeostasis: different molecules for different purposes? *Cell. Mol. Life Sci.* 69, 1077–1104. doi: 10.1007/s00018-011-0845-9

Zhai, Y., and Borisy, G. G. (1994). Quantitative determination of the proportion of microtubule polymer present during the mitosis-interphase transition. *J. Cell Sci.* 107(Pt. 4), 881–890.

Zhang, S. L., Yeromin, A. V., Zhang, X. H.-F., Yu, Y., Safrina, O., Penna, A., et al. (2006). Genome-wide RNAi screen of Ca2+ influx identifies genes that regulate Ca2+ release-activated Ca2+ channel activity. *Proc. Natl. Acad. Sci. U.S.A.* 103, 9357–9362. doi: 10.1073/pnas.0603161103

Zhang, S. L., Yu, Y., Roos, J., Kozak, J. A., Deerinck, T. J., Ellisman, M. H., et al. (2005). STIM1 is a Ca2+ sensor that activates CRAC channels and migrates from the Ca2+ store to the plasma membrane. *Nature* 437, 902–905. doi: 10.1038/nature04147

Conflict of Interest: The authors declare that the research was conducted in the absence of any commercial or financial relationships that could be construed as a potential conflict of interest.

frontiers in Physiology

REVIEW
published: 25 February 2020
doi: 10.3389/fphys.2020.00161

Activity-Dependent Synaptic Plasticity in *Drosophila melanogaster*

*Yiming Bai and Takashi Suzuki**

School of Life Sciences and Technology, Tokyo Institute of Technology, Yokohama, Japan

The *Drosophila* nervous system is a valuable model to examine the mechanisms of activity-dependent synaptic modification (plasticity) owing to its relatively simple organization and the availability of powerful genetic tools. The larval neuromuscular junction (NMJ) in particular is an accessible model for the study of synaptic development and plasticity. In addition to the NMJ, huge strides have also been made on understanding activity-dependent synaptic plasticity in the *Drosophila* olfactory and visual systems. In this review, we focus mainly on the underlying processes of activity-dependent synaptic plasticity at both pre-synaptic and post-synaptic terminals, and summarize current knowledge on activity-dependent synaptic plasticity in different parts of the *Drosophila melanogaster* nervous system (larval NMJ, olfactory system, larval visual system, and adult visual system). We also examine links between synaptic development and activity-dependent synaptic plasticity, and the relationships between morphological and physiological plasticity. We provide a point of view from which we discern that the underlying mechanism of activity-dependent plasticity may be common throughout the nervous systems in *Drosophila melanogaster*.

Keywords: synaptic plasticity, activity-dependent neuroplasticity, *Drosophila melanogaster*, neuroplasticity, nervous system

OPEN ACCESS

Edited by:
Giorgio F. Gilestro, Imperial College London, United Kingdom

Reviewed by:
Simon G. Sprecher, Université de Fribourg, Switzerland
Bruno Van Swinderen, The University of Queensland, Australia

***Correspondence:**
Takashi Suzuki
suzukit@gmail.com

Specialty section:
This article was submitted to Invertebrate Physiology, a section of the journal Frontiers in Physiology

Received: *25 April 2019*
Accepted: *12 February 2020*
Published: *25 February 2020*

Citation:
Bai Y and Suzuki T (2020) Activity-Dependent Synaptic Plasticity in Drosophila melanogaster. Front. Physiol. 11:161. doi: 10.3389/fphys.2020.00161

INTRODUCTION

Activity-dependent synaptic plasticity is a crucial component of activity-dependent neuroplasticity. Modern research has demonstrated that most of the neuroplasticity that occurs in our daily lives is synaptic. Synaptic plasticity is believed to be the most important neurological mechanism for learning and memory (Neves et al., 2008). Synaptic plasticity refers to the ability of synapses to increase or decrease their potential activity in response to environmental stimulation. It involves calcium influx (Zucker, 1999; Zhao et al., 2011), cell–cell communication (Dalva et al., 2007; Carrillo et al., 2010; Kochlamazashvili et al., 2010), reorganization of synaptic components (Packard et al., 2002; Packard et al., 2003; Okamoto et al., 2004; Sugie et al., 2015), localization of receptors (Raymond et al., 1993; Packard et al., 2002, 2003; Song and Huganir, 2002), regulation of pre-synaptic neurotransmission (Ho et al., 2011), autophagy (Liang, 2019), and many other biological processes. In brief, activity-dependent synaptic plasticity modulates how pre-synaptic neurons respond to activity-invoked physiological changes, and how post-synaptic neurons respond to changed neurotransmission from pre-synaptic neurons.

Drosophila is a powerful model organism that has been used to decipher numerous biological mechanisms over the past century (Stephenson and Metcalfe, 2013). Indeed, many important findings in higher organisms such as rats, mice, and humans are based on discoveries in *Drosophila*. The abundance of mutant lines and potent genetic tools, easy and rapid breeding, the applicability

of these small organisms to imaging technologies and large-scale behavioral analysis, and conserved neurobiological mechanisms render *Drosophila* an ideal model for neuroscience research, including the study of synaptic function at the molecular, functional, and behavioral levels. Numerous studies have been performed on synaptic plasticity at the *Drosophila* neuromuscular junction (NMJ), and many molecules, proteins, and pathways implicated in NMJ plasticity have been subsequently shown to mediate similar functions at other synapses in *Drosophila* as well as in higher organisms. Findings on synaptic development at the *Drosophila* NMJ in the 1990s have inspired subsequent studies on synaptic refinement/plasticity in other systems, such as on the mechanisms involved in olfactory habituation and learning and memory. Some crucial pathways discovered in studies of synaptic development have also been found in the adult nervous system, which implies that similar mechanisms underlie synaptic development and plasticity.

Synaptic plasticity can be classified into two general types: (i) morphological (structural) plasticity involving branching, volume change, bouton formation, and alteration of synaptic contacts, and (ii) physiological (functional) plasticity involving regulation of neurotransmission, reorganization of synaptic components and receptors, and other processes regulating the strength of information flow between synapses. While a multitude of studies have suggested that morphological and physiological plasticity share many common mechanisms (Das et al., 2011; Yuan et al., 2011), some recent studies indicate that morphological and physiological plasticity may not be dependent on each other in the olfactory system, which renders the relationship complicated (Kidd and Lieber, 2016).

In this review, we describe activity-dependent synaptic plasticity in different parts of the *Drosophila* nervous system (larval NMJ, olfactory system, larval visual system, and adult visual system). We also discuss issues regarding the link between synaptic development and activity-dependent synaptic plasticity, the relationship between morphological and physiological plasticity, and potential common mechanisms underlying activity-dependent plasticity throughout the *Drosophila* nervous system.

PRE-SYNAPTIC PLASTICITY AT THE LARVAL NEUROMUSCULAR JUNCTION

The relatively simple structure of the *Drosophila* nervous system and the availability of powerful genetic tools have facilitated the elucidation of various molecular components ubiquitously involved in synaptic modification, such as transcription factors, receptors, kinases and various effectors, and neuromodulators. The larval NMJ has been well-studied since 1990, and shown to be a highly representative model of synaptic development and plasticity. In the *Drosophila* NMJ, the sizes of pre-synaptic boutons, the number of active zones (AZs) in each bouton, and the complexity of the subsynaptic reticulum, a post-synaptic structure, increase during development (Lahey et al., 1994; Budnik, 1996). Refinement of neuronal connections during development, such as branching and regulation of synaptic components and receptors, resembles the process of neuroplasticity during critical periods after eclosion in adult flies (Golovin et al., 2019). Synaptic development is thus suggested to share signaling pathways and other mechanisms with neuronal plasticity, and discoveries made in studies of activity-dependent synaptic refinement during NMJ development have provided the foundation for subsequent studies on synaptic remodeling in various regions of the *Drosophila* nervous system (Sears and Broadie, 2017). Among those findings, the functions of the cAMP pathway and Wnt signaling pathway are particularly important.

The Role of cAMP Pathway in Activity-Dependent Plasticity at the NMJ

Drosophila is a convenient model to explore the functions of genes, proteins, and biological processes because there are abundant mutant lines for nearly all genes (Jenett et al., 2012; Yamamoto et al., 2014). For elucidation of neuronal plasticity in *Drosophila*, it is common to study existing mutants or isolate new mutants with altered brain development or function. Keshishian and colleagues found that loss of electrical activity in pre-synaptic motor neurons in mutants with disrupted Na^+ channel activity and in wild types treated with various toxins to prevent synaptic activity altered NMJ connectivity, which demonstrated that the development plasticity observed at the NMJ is activity-dependent. Loss of pre-synaptic activity increased inappropriate innervation of motor neurons onto muscle fibers (Jarecki and Keshishian, 1995). Alternatively, mutants in which neurons are hyperexcitable, such as *Shaker* (*Sh*) and *ether a go-go* (*eag*) (Burg and Wu, 1989), were examined at the NMJ, and it was found that during the pre-synaptic apparatus expansion stage, increased activity caused increased neurotransmitter release (Budnik et al., 1990).

Fasciclin II (Fas II), a major cell adhesion molecule in pre-synaptic and post-synaptic membranes at the NMJ (Lin and Goodman, 1994; Zito et al., 1997), is necessary for the stabilization and growth of synapses and has an essential function in long-term synaptic structural plasticity, especially in the pre-synaptic apparatus (Schuster et al., 1996). The pre-synaptic sprouting phenotype of *Fas II* mutants resembles that of *eag Shaker* double mutants and *dunce* (cAMP phosphodiesterase II) mutants (Byers et al., 1981). *eag Shaker* and *dunce* increase neuronal activity and cyclic AMP (cAMP) concentration, respectively, and Fas II functions downstream (Schuster et al., 1996). However, *Fas II* mutation alone does not affect synaptic function and strength. Rather, the cAMP response element-binding protein (CREB) works cooperatively with Fas II to increase synaptic strength. Both the activation of CREB and downregulation of Fas II are cAMP-dependent and lead to increased pre-synaptic transmitter release (**Figure 1A**). cAMP pathway activation is induced by pre-synaptic calcium accumulation, which activates the calcium/calmodulin-dependent adenylate cyclase rutabaga (Livingstone et al., 1984; Levin et al., 1992).

Calcium/calmodulin-dependent protein kinase II (CaMKII) also contributes to activity-dependent plasticity through a separate pathway (Davis et al., 1996; Carrillo et al., 2010). Clustering of Discs large (DLG), which controls synaptic

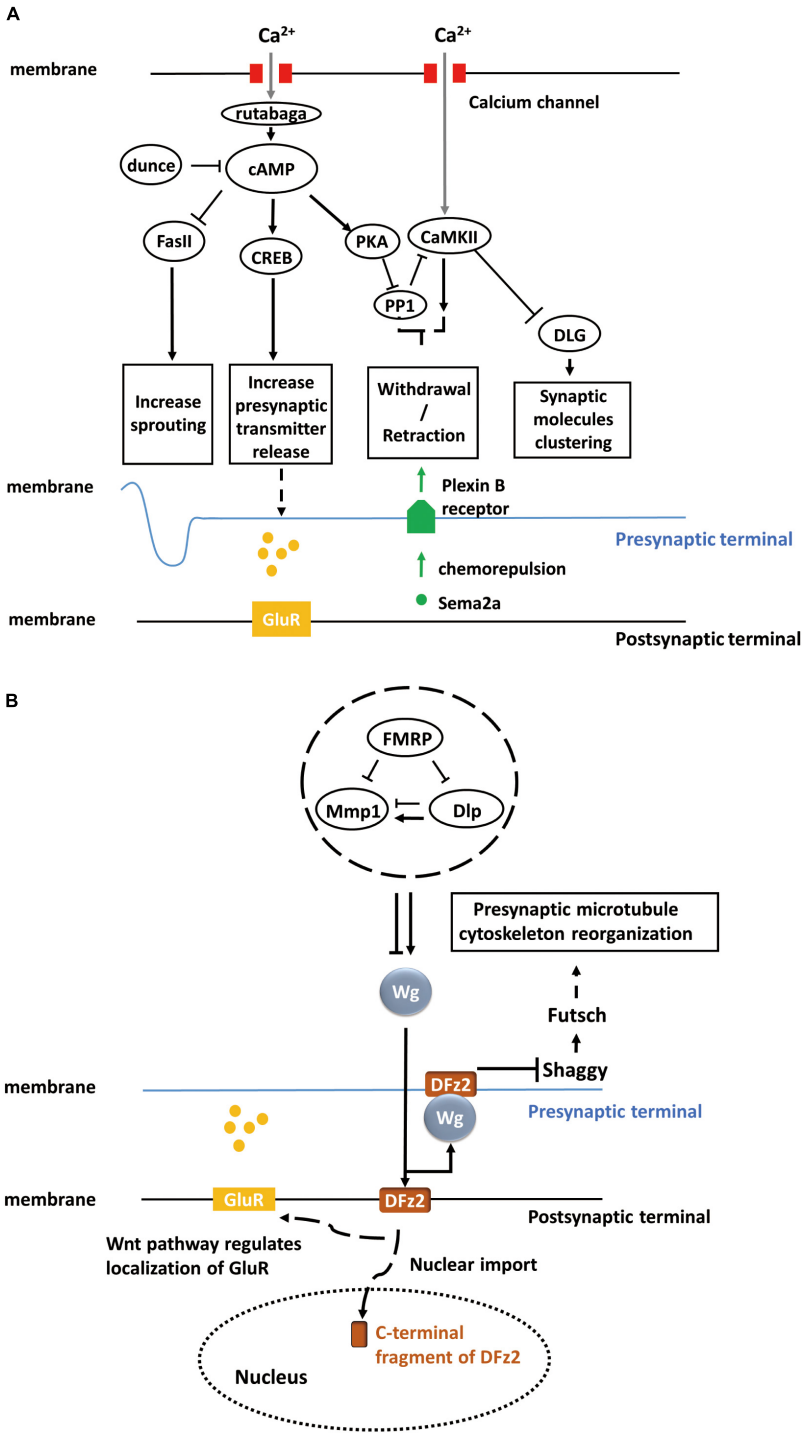

FIGURE 1 | Activity-dependent synaptic plasticity at the *Drosophila* larval NMJ. **(A)** Calcium accumulation, along with neuronal activity, regulates the calcium/calmodulin-dependent adenylate cyclase, rutabaga. Dunce and rutabaga regulate the level of cAMP. Cell adhesion molecule Fas II and cAMP response element-binding proteins (CREB) are downstream of the cAMP pathway and responsible for increasing sprouting and pre-synaptic transmitter release. PKA and PP1 are also regulated by increased cAMP levels, and they, in turn, regulate CaMKII. The PKA-PP1-CaMKII interaction controls the withdrawal/retraction process through Plexin B receptor and Semaphorin-2a (Sema2a) chemorepulsion. The synaptic localization of Discs large (DLG) regulated by CaMKII controls the clustering of synaptic molecules, such as Fas II or Shaker. **(B)** The secretion of Wg proteins is enhanced in a calcium-dependent manner. The activation of a bidirectional Wg signaling pathway causes the nuclear import of the C-terminal fragment of Dfrizzled-2 (DFz2, receptor of Wg) at the post-synaptic terminal of NMJ and the rearrangement of pre-synaptic terminal structures involving the Shaggy/GSK-3β kinase, which controls the organization of the cytoskeleton and number of boutons through Futsch at the pre-synaptic terminal of NMJ. Moreover, activated Wnt pathway at the post-synaptic terminal also regulates the localization of glutamate receptors (GluRs) around synaptic boutons.

molecules such as Fas II, is regulated by CaMKII (Lahey et al., 1994; Zito et al., 1997; Koh et al., 1999) (**Figure 1A**). Moreover, rutabaga, cAMP-dependent protein kinase (PKA), and protein phosphatase 1 (PP1) act collaboratively with CaMKII to regulate chemorepulsion mediated by the muscle-secreted trans-synaptic chemorepellant Semaphorin-2a (Sema2a) during activity-dependent synaptic refinement, a process that serves to reduce aberrant neuromuscular connections (**Figure 1A**) (Vonhoff and Keshishian, 2017a,b).

To summarize, activity-dependent plasticity at the NMJ pre-synaptic structure of the NMJ requires mainly a calcium accumulation-induced, cAMP-dependent, second-messenger pathway, which involves crucial components, such as calcium/calmodulin-dependent adenylate cyclases (rutabaga), cell adhesion molecules (Fas II), and cAMP response element-binding proteins (CREB) (**Figure 1A**).

The Role of Wingless in Activity-Dependent Plasticity at the NMJ

Wingless (Wg), a member of the Wnt family, is an important secreted protein involved in the development of *Drosophila* embryos. Wg is not only responsible for body segmentation (Pfeiffer et al., 2000) but also for the appropriate formation and arrangement of synapses. NMJ studies have shown that Wg is first secreted from pre-synaptic motor neuron terminals and endocytosed by post-synaptic muscles, where it triggers the Wnt signaling pathway in post-synaptic cells. The mutant *shibire* (*shi*) with deficient post-synaptic endocytosis exhibited post-synaptic Wg accumulation (Packard et al., 2002). Since Wg is necessary for embryonic development, late-stage larval mutants cannot be analyzed in these mutants. Therefore, a temperature-sensitive *wg* mutant was used to suppress Wg functions during the third instar stage. It was found that *wg* deficiency disrupted the distribution and localization of receptors, such as glutamate receptors (GluR), on the surface of post-synaptic terminals (**Figure 1B**). Further, *wg* deficiency can induce loss of both pre-synaptic and post-synaptic components. In summary, these studies indicate that Wg is an essential anterograde signal for the proper maturation of synapses at the NMJ.

Over the past decade, several studies have demonstrated that the bidirectional Wnt/Wg signaling pathway participates in activity-dependent synaptic structural and functional plasticity at the NMJ. Not only chronic but also acute activity alterations, along with development, shape the synapse structures (Packard et al., 2003). Rapid changes in synaptic structure dependent on acute activity alterations require the Wg signaling pathway. For example, the actin regulator Cortactin, present in both pre-synaptic and post-synaptic terminals of the NMJ, is a pre-synaptic regulator of rapid activity-dependent plasticity. Cortactin levels in stimulated pre-synaptic terminals which is necessary for activity-dependent plasticity requires the Wg pathway (Alicea et al., 2017). Acute activity of pre-synaptic neurons can enhance calcium-dependent Wg secretion and ensuing Wg signaling activity leads to (i) nuclear import of the C-terminal fragment of the Wg receptor Dfrizzled-2 (DFz2) in the post-synaptic terminals of NMJs and (ii) rearrangement of pre-synaptic terminal structures involving the Shaggy/GSK-3β kinase, which controls the organization of the cytoskeleton and the number of boutons at NMJs (Ataman et al., 2008) (**Figure 1B**). In the illustrated study, GFP was used to tag pre-synaptic and post-synaptic components such as GluRs (Heckscher et al., 2007) and Bruchpilot (Brp) (Wagh et al., 2006), and live-imaging technology was utilized to examine dynamic changes in these components under changes in activity. Moreover, Wg was shown to inhibit Shaggy and regulate cytoskeletal reorganization through the microtubule-associated protein Futsch (Miech et al., 2008). In conclusion, Wg, Shaggy, and Futsch form Wnt/Wg signaling pathway and regulate the cytoskeleton reorganization (**Figure 1B**).

Fragile X mental retardation protein (FMRP), an RNA-binding translational repressor (Darnell et al., 2001), has recently been demonstrated to regulate the Wnt/Wg signaling pathway. Extracellular matrix metalloproteinase (MMP) and the heparan sulfate proteoglycan (HSPG) Dally-like protein (Dlp), a Wg co-receptor (Khare and Baumgartner, 2000; Kirkpatrick et al., 2004), work together to regulate rapid activity-dependent synaptic bouton formation (Dear et al., 2017). Dlp can upregulate or downregulate the Wg pathway depending on the relative abundance of Wg pathway components. FMRP-MMP-Dlp play an essential role in activity-dependent synaptogenesis via Wnt/Wg trans-synaptic signaling pathway (Dear et al., 2017; Sears and Broadie, 2017) (**Figure 1B**).

To summarize, Wingless is responsible not only for synaptic maturation but also for activity-dependent synaptic structural and functional plasticity at the NMJ. Wnt/Wg signaling pathway composed of Wingless, Shaggy, and Futsch regulates the rearrangement of pre-synaptic terminal structures in an activity-dependent manner. The distribution and localization of receptors in the post-synaptic terminals are also regulated by Wg. FMRP, MMP, and Dlp cooperate to modulate the level of Wg and act as upstream regulators of Wnt/Wg signaling.

SYNAPTIC PLASTICITY IN THE OLFACTORY SYSTEM

The *Drosophila* olfactory system has long been regarded as an accessible model for studying the development and plasticity of a primary sensory system owing to its well-described anatomical structure. The olfactory system is particularly attractive for studies on structural and functional plasticity related to behavior as it is the locus of a reliable odorant habituation behavior. Olfactory sensory neurons (OSNs) distributed in the antenna and maxillary palps receive odor information through odorant receptors (Miazzi et al., 2016) and then project axons to glomeruli in the antennal lobe (AL), where they form synapses with projection neurons (PNs) or local interneurons (LNs). The PNs of the inner antennocerebral tract (iACT) send axons to the mushroom body (MB) synapse with Kenyon cells in the calyx, and finally terminate in the lateral horn (LH). Alternatively, PNs of the medial antennocerebral tract (mACT) project directly to the LH from glomeruli (Keene and Waddell, 2007; Golovin and Broadie, 2016).

Numerous studies have been conducted on activity-dependent AL plasticity during critical periods after eclosion, including studies on glomerulus volume changes (Sachse et al., 2007) and short-term or long-term habituation (Das et al., 2011). Findings from activity-dependent plasticity studies in AL have benefited from previous studies on other *Drosophila* nervous systems, particularly the NMJ, since activity-dependent AL plasticity involves many similar signaling pathways. However, studies of the olfactory system have also revealed novel plasticity mechanisms. Activity-dependent AL plasticity involves the cAMP pathway (Das et al., 2011), translational regulation (McCann et al., 2011; Sudhakaran et al., 2014), central *N*-Methyl-D-aspartate (NMDA) glutamatergic signaling pathway (Das et al., 2011), and the Notch pathway (Kidd and Lieber, 2016). While the Wnt signaling pathway does not appear to be involved in AL plasticity during the critical period, Shaggy contributes to glomerulus remodeling through other pathways (Acebes et al., 2011; Golovin et al., 2019).

A major form of morphological plasticity in AL is the increased volume of the V glomerulus in the antennal lobe induced by early long-term exposure to CO_2 after eclosion (Sachse et al., 2007). This increase is reversible after returning the flies to ambient conditions, indicating a highly flexible synaptoplastic mechanism. Based on experiments with *Drosophila* expressing the genetically encoded calcium indicator GCaMP in the V glomerulus, this plasticity was shown to be activity-dependent. Prolonged exposure to CO_2 also increased the activity of LNs in the V glomerulus, especially inhibitory LNs, which in turn enhanced the inhibitory effects of gamma-aminobutyric acid (GABA) released from LNs onto PNs (Wilson and Laurent, 2005; Liu and Wilson, 2013). As a result, the output of PNs to the LH should be reduced, a notion validated by Sachse et al. (2007) in a study expressing GCaMP in PNs from the V glomeruli. These authors also found that there is a critical period after eclosion for this olfactory plasticity (Sachse et al., 2007; Golovin et al., 2019).

It was also shown that long-term exposure to CO_2 can selectively reduce the subsequent behavioral responses to CO_2, termed habituation (Sachse et al., 2007). Olfactory habituation, including short-term habituation (STH) and long-term habituation (LTH), requires rutabaga-encoded adenylate cyclase, which is induced by calcium accumulation and G protein-coupled receptor (GPCR) activation (Das et al., 2011). The upregulation of rutabaga in LTH induces cAMP signaling in inhibitory GABAergic LNs, resulting in reduced PN activity. Moreover, NMDA receptors in post-synaptic PNs (Schoppa et al., 1998) are responsible for the odorant selectivity of olfactory habituation. Both STH and LTH were blocked when GABA and glutamate release from LN1 neurons was impeded through RNAi-based knockdown of the GABA synthesis enzyme glutamic acid decarboxylase (GAD1) (Ng et al., 2002) and the vesicular glutamate transporter DVGLUT (Daniels et al., 2008). Thus, co-release of GABA and glutamate from LN1 neurons is essential for olfactory habituation.

Activation of the cAMP downstream transcription factor CREB2 in LNs is required for LTH, but not for STH, indicating that LTH requires additional components compared with STH. Ataxin-2 (Atx2), an RNA regulation-related protein, works with miRNA components such as Me31B and Argonaute 1 (Ago1) in PNs to regulate olfactory LTH (McCann et al., 2011). The Atx2-involved miRNA pathway represses mRNA translation via the Ago1-RNA-induced silencing complex (Ago1-RISC). Interestingly, Ago1-RISC in olfactory PNs requires FMRP, which also contributes to Wnt/Wg signaling during activity-dependent NMJ plasticity. FMRP, together with Atx2 and Ago1, functions to repress CaMKII expression (Sudhakaran et al., 2014) in both pre-synaptic inhibitory LNs and post-synaptic PNs, and this suppression is required for olfactory LTH, although the underlying mechanism remains obscure. Recent studies show that CaMKII is responsible for spontaneous release, which implies that reduced spontaneous transmitter release contributes to LTH maintenance (Kuklin et al., 2017).

While morphological structural plasticity and physiological habituation in the olfactory system occur almost simultaneously and share some fundamental underlying mechanisms such as dependence on rutabaga, DVGLUT, and NMDA receptors, they still have differences. For instance, $GABA_A$ receptors appear unnecessary for the volume change in the glomerulus after long-term exposure to odors. Instead, $GABA_A$ receptors may be necessary for physiological rather than structural plasticity (Das et al., 2011). Moreover, the non-canonical Notch signaling pathway is implicated in glomerulus structural plasticity (volume changes) while physiological plasticity requires only the canonical Notch signaling pathway (Kidd and Lieber, 2016).

POST-SYNAPTIC PLASTICITY IN LARVAL VISUAL SYSTEM BRANCHING

In the *Drosophila* larval visual system, Bolwig's organ (BO) functions as the light sensing organ. BO sends information to ventral lateral neurons or LN(v)s through Bolwig's nerve (BN), which terminates in a region rich in LN(v) dendrites (Malpel et al., 2002; Farca-Luna and Sprecher, 2013). Using the green fluorescent protein reconstitution across synaptic partners (GRASP) technique, it was shown that LN(v)s are post-synaptic to BN (Feinberg et al., 2008; Yuan et al., 2011). Upon light stimulation, LN(v)s are activated by BN, and BO maintains LN(v) dendrites. Light exposure hinders the growth or branching of LN(v) dendrites during larval visual system development, and this plasticity requires pre-synaptic BO input instead of post-synaptic LN(v) light sensing function. Excitation of the BO or LN(v)s can decrease the dendrite length of LN(v)s. In addition, expression of certain pre-synaptic terminal components, such as the calcium channel Cacophony (Kawasaki et al., 2004), are downregulated in the presence of light stimulation, resulting in loss of synaptic connection between BN and LN(v)s.

The cAMP phosphodiesterase II dunce also participates in the plasticity of post-synaptic LN(v) branching. In the *Drosophila dunce* mutant, larval LN(v)s do not exhibit significant differences in length under changing light conditions. Further, experiments in which post-synaptic LN(v)s express the catalytic subunit of protein kinase A (PKAmc) or a dominant-negative form of CREB (CREBdn) to up- or down-regulate cAMP levels demonstrated

that cAMP levels are essential for modifying the structure and function of LN(v)s (Yuan et al., 2011). Moreover, babos-1, a cell surface protein containing the extracellular immunoglobulin domain, also participates in regulation of plasticity, but it remains unknown how it controls dendrite length.

To summarize, structural and functional plasticity at post-synaptic LN(v)s requires both LN(v) activity and light-induced pre-synaptic BN activity. The cAMP signaling pathway and cell surface proteins such as babos-1 in post-synaptic LN(v)s also play essential roles in this modification for light adaption.

PRE-SYNAPTIC PLASTICITY IN THE *Drosophila* ADULT VISUAL SYSTEM

The visual system of *Drosophila* is composed of the retina and optic lobe. The optic lobe is composed of the lamina, medulla, lobula, and lobula plate. There are around 750 small eyes called ommatidia in the retina, and each ommatidium has eight photoreceptor neurons (R1 to R8). Photoreceptor neurons R1-R6 innervate the lamina layer, whereas R7 and R8 innervate the medulla layer. Photoreceptor neurons mainly release histamine to post-synaptic neurons. Previous studies showed that activity-dependent remodeling of central synapses occurs with natural stimuli, and this also applies to the *Drosophila* adult visual system. AZ components in photoreceptor neurons were found to be reorganized depending on activity, and the Wnt pathway is involved in this process.

Activity-Dependent Reorganization of AZ Components in Photoreceptor Neurons

It was found that some AZ components, including Bruchpilot (Brp), DLiprin-α, and the conserved RIM-binding protein DRBP, which are crucial for arranging synaptic vesicles and calcium channels, can be redistributed after long-term exposure to light in R8 photoreceptor neurons (Sugie et al., 2015). Endogenous Brp in R8 photoreceptor neurons was labeled via synaptic tagging by the recombination (STaR) method (Chen et al., 2014). When flies were kept in constant light (LL) for 1–3 days after eclosion, the expression of Brp in each R8 photoreceptor was significantly reduced compared to flies kept under normal 12-12-h light-dark (LD) conditions. The same result was observed when fluorescently tagged Brp-short-mcherry was used to label Brp. Electron microscopy (EM) revealed that the number of T-bars in the AZ also decreased after LL compared to LD and as a result eliminated transmitter release from R8. The authors also tagged other AZ components, such as DLiprin-α, DRBP, Dsyd-1, and Cacophony (Cac), using GFP and found that DLiprin-α and DRBP were reorganized after LL, whereas Dsyd-1 and Cac remained unaffected.

To examine whether the changes in AZ are activity-dependent, they used temperature-sensitive shibire [UAS-shi(ts)] (Kitamoto, 2001) to restrict the activity of R8 photoreceptor neurons and found that the reorganization of Brp after LL was suppressed. Moreover, post-synaptic histamine receptor mutants also suppressed the loss of Brp after LL. These results indicate that both pre-synaptic photoreceptor and post-synaptic second-order neuron activity via histamine receptor modulate Brp localization.

Pathways Involved in Activity-Dependent Reorganization of AZ Components in Photoreceptor Neurons

The divergent canonical Wnt pathway is involved in this activity-dependent reorganization of AZ components after continuous light exposure. Canonical Wnt pathway-related proteins, such as Arrow (Arr), a Wnt co-receptor with Frizzled-2 (He et al., 2004), Dsh, a cytosolic phosphoprotein (Clevers, 2006), and Shaggy all contribute to the maintenance AZ component localization. Since Shaggy phosphorylates Fustch, which is involved in microtubule stabilization, and Shaggy is negatively regulated by the Wnt pathway (Miech et al., 2008), Wnt signaling may regulate reorganization of AZ components through microtubule destabilization. Indeed, further experiments on AZ component localization after directly disturbing microtubule stabilization revealed that the delocalization of AZ components can be ascribed to microtubule destabilization (Sugie et al., 2015).

When faced with environmental changes or stressors, cells will activate the unfolded protein response (UPR) (Ron and Walter, 2007) in the ER as a protective mechanism, a process that involves adenylylation of the core UPR regulator BiP (Bertolotti et al., 2000). After flies were treated with constant light for 72 h, photoreceptors with mutations in UPR-related proteins, such as BiP, severely lost synaptic function and this loss was reversible once these mutant flies were returned to a normal 12-12-h LD cycle (Moehlman et al., 2018). This finding

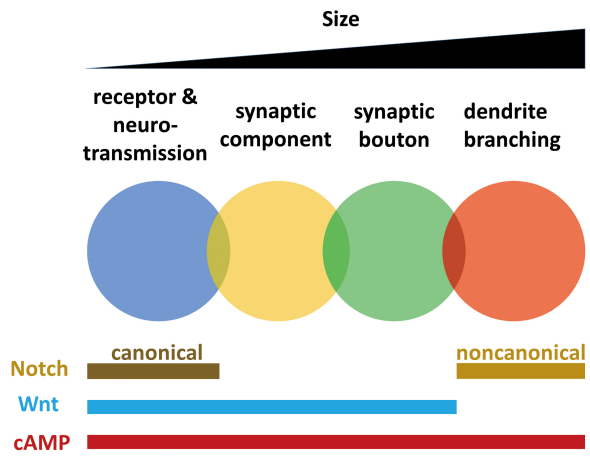

FIGURE 2 | Mechanisms of synaptic plasticity working at different scales from neurotransmission to branching are overlapped and interwoven. Synaptic plasticity occurs in different scales, including receptors and neurotransmission, synaptic components, synaptic boutons and dendrites. Localization of receptors and regulation of neurotransmission, synaptic component reorganization, bouton formation and dendrite branching all require cAMP pathway. Dendrite branching does not need Wnt pathway, while plasticity at other smaller scales require Wingless. Neurotransmission requires canonical Notch pathway, while dendrite branching requires non-canonical Notch pathway.

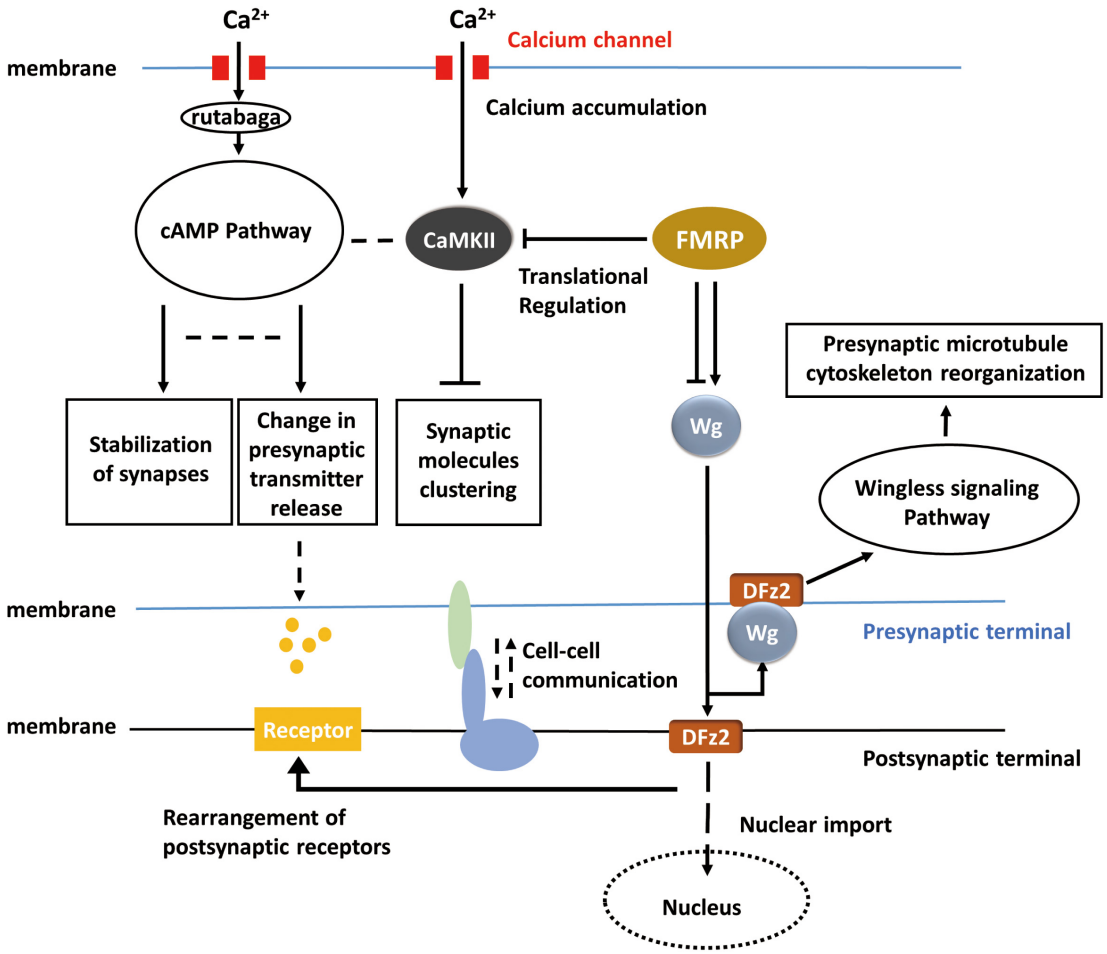

FIGURE 3 | Hypothetical universal model for activity-dependent plasticity. Calcium accumulation invokes the cAMP pathway and CaMKII pathway. Translational regulation (RNA-induced silencing complex, RISC) modulates CaMKII and the Wnt/Wg pathway. Wg pathway is responsible for pre-synaptic microtubule destabilization and rearrangement of post-synaptic receptors, whereas cAMP pathway is responsible for the change in neurotransmitter release. CaMKII, cAMP, and Wg pathway reorganized pre-synaptic components together. The bidirectional regulation of synaptic plasticity also requires cell–cell talk/communication.

demonstrates that cellular homeostasis and adenylylation may be involved in the activity-dependent plasticity of photoreceptor pre-synaptic functions.

To summarize, continuous light exposure in adult *Drosophila* leads to activation of pre-synaptic photoreceptors and hyperpolarization of post-synaptic neurons. The Wnt/Wg pathway in photoreceptors induces microtubule destabilization, which causes the delocalization of AZ components and finally the loss of synaptic connections between photoreceptors and second-order neurons. Homeostatic protective mechanisms also act to prevent degeneration of photoreceptors during continuous light exposure.

CONCLUSION AND FUTURE DIRECTIONS

Huge strides have been made on understanding activity-dependent synaptic plasticity at the *Drosophila* NMJ and in the olfactory system. This progress has benefited from the well-studied anatomic structure of the *Drosophila* nervous system. The anatomical information provides details about neuronal connections that have allowed researchers to identify where connections are changed or lost under specific conditions or in organisms with specific mutations. Even though the *Drosophila* adult visual system has well-described anatomical structures and connectome, the mechanisms underlying activity-dependent plasticity are still largely unclear. Nonetheless, the *Drosophila* adult visual system warrants further study since it possesses complex layered structures that resemble those of mammals.

Early studies on synaptic maturation at the NMJ have laid the cornerstone for subsequent research on other regions of the *Drosophila* nervous system. Molecular and functional pathways described at NMJ, such as cAMP and Wingless, participate in many activity-dependent synaptoplastic process in other regions, such as *Drosophila* sensory systems. The similarity between the development of neuronal connections and synaptic plasticity suggests that synaptic plasticity may be

a recapitulation of synaptic development, so knowledge gained on synaptic development should guide studies on activity-dependent plasticity.

Studies on the olfactory system show that while activity-dependent morphological and physiological plasticity share some components such as rutabaga, NMDA receptors and DVGLUT in olfactory system, there may be no direct connection between them since they require different Notch pathways. Two types of plasticity, morphological and physiological, or structural and functional, often occur simultaneously, but in some cases these events appear independent. Thus, caution is advised when extrapolating conclusions drawn from studies on morphological plasticity to physiological plasticity and vice versa.

Localization of receptors and regulation of neurotransmission, synaptic component reorganization, bouton formation, and dendrite branching all require the cAMP pathway. Dendrite branching does not require the Wnt pathway (Golovin et al., 2019), but synaptic plasticity at other smaller scales requires Wingless. Neurotransmission and dendrite branching require different Notch pathways. These findings indicate that mechanisms of synaptic plasticity working at different scales from neurotransmission to branching are not isolated but are overlapped and interwoven (**Figure 2**).

Nonetheless, there are mechanisms common to activity-dependent plasticity among regions. Crucial pathways at the NMJ include (i) the calcium accumulation-induced cAMP-dependent second-messenger signaling pathway, which involves rutabaga and CREB, (ii) cell adhesion molecules such as Fas II, and (iii) the Wnt/Wg signaling pathway. Olfactory habituation (Sato et al., 2018) and post-synaptic plasticity in the larval visual system also involve the cAMP pathway. The Wnt signaling pathway also functions in adult visual system plasticity by regulating microtubule stabilization. FMRP is crucial for modulating the Wnt pathway at the NMJ and also cooperates with Ago1-RISC to suppress CaMKII expression for long-term olfactory habituation. NMJ plasticity, olfactory habituation, post-synaptic plasticity in the larval visual system, and pre-synaptic plasticity in the adult visual system all require reorganization of synaptic components and regulation of neurotransmitter release.

It is intriguing that many of the underlying mechanisms for activity-dependent plasticity may be common throughout the nervous systems in *Drosophila*. A big picture of activity-dependent synaptic plasticity can be drawn, and the apparently lost pieces according to the general view can in return provide some promising directions for the study in activity-dependent synaptic plasticity. For instance, in the adult visual system, the cAMP pathway, RISC, cell adhesion molecules, and similar cell surface proteins may also be required but related studies are absent so far. In the big picture (**Figure 3**), when activity occurs, calcium influx activates cAMP pathway and in result reorganizes pre-synaptic components and regulates the release of neurotransmitters. Calcium accumulation also affects clustering of synaptic molecules via CaMKII. FMRP regulates the translation of CaMKII and involves in Wingless signaling pathway which controls reorganization of pre-synaptic microtubule cytoskeleton. However, the molecules upstream of the Wnt or FMRP pathways remain unidentified, and the link between neuronal activity and Wg signaling requires further studies. At the post-synaptic terminal, neurotransmitter receptors can be correspondingly rearranged according to pre-synaptic activity, and this process may be dependent on Wingless signaling pathway. It remains unclear whether cAMP pathway is also involved in the rearrangement of post-synaptic receptors or not. Furthermore, will the activity of post-synaptic sides affect the synaptic component organization or neurotransmitter releasing in the pre-synaptic sides? Some sorts of cell–cell communications may exist between pre-synaptic and post-synaptic terminals, which possibly coordinate the morphological and physiological changes on both sides, but related studies are missing in *Drosophila*. It is believed that activity-dependent synaptic plasticity requires the participation of both pre-synaptic and post-synaptic sides. However, the mechanisms of 'feedback' from post-synaptic side are not well-studied in *Drosophila*. Conclusions, techniques, and experiences from previous studies may inspire the exploration of activity-dependent synaptic plasticity in *Drosophila melanogaster* and complete the entire picture.

AUTHOR CONTRIBUTIONS

YB designed, wrote, and revised the manuscript and prepared the figures. TS designed, revised, and approved the manuscript and figures.

FUNDING

YB was supported by Japanese Government (Monbukagakusho: MEXT) Scholarship. This work was supported by Grant-in-Aid for Scientific Research on Innovation Areas from MEXT (Dynamic regulation of Brain Function by Scrap & Build System: 16H06457) and Takeda Science Foundation (Visionary Research Areas) (TS).

REFERENCES

Acebes, A., Martin-Pena, A., Chevalier, V., and Ferrus, A. (2011). Synapse loss in olfactory local interneurons modifies perception. *J. Neurosci.* 31, 2734–2745. doi: 10.1523/JNEUROSCI.5046-10.2011

Alicea, D., Perez, M., Maldonado, C., Dominicci-Cotto, C., and Marie, B. (2017). Cortactin is a regulator of activity-dependent synaptic plasticity controlled by wingless. *J. Neurosci.* 37, 2203–2215. doi: 10.1523/JNEUROSCI.1375-16.2017

Ataman, B., Ashley, J., Gorczyca, M., Ramachandran, P., Fouquet, W., Sigrist, S. J., et al. (2008). Rapid activity-dependent modifications in synaptic structure and function require bidirectional Wnt signaling. *Neuron* 57, 705–718. doi: 10.1016/j.neuron.2008.01.026

Bertolotti, A., Zhang, Y., Hendershot, L. M., Harding, H. P., and Ron, D. (2000). Dynamic interaction of BiP and ER stress transducers in the unfolded-protein response. *Nat. Cell Biol.* 2, 326–332. doi: 10.1038/35014014

Budnik, V. (1996). Synapse maturation and structural plasticity at *Drosophila* neuromuscular junctions. *Curr. Opin. Neurobiol* 6, 858–867. doi: 10.1016/S0959-4388(96)80038-80039

Budnik, V., Zhong, Y., and Wu, C. F. (1990). Morphological plasticity of motor axons in *Drosophila* mutants with altered excitability. *J. Neurosci.* 10, 3754–3768. doi: 10.1523/jneurosci.10-11-03754.1990

Burg, M. G., and Wu, C. F. (1989). Central projections of peripheral mechanosensory cells with increased excitability in *Drosophila* mosaics. *Dev. Biol.* 131, 505–514. doi: 10.1016/s0012-1606(89)80021-1

Byers, D., Davis, R. L., and Kiger, J. A. (1981). Defect in cyclic-amp phosphodiesterase due to the dunce mutation of learning in *Drosophila*-Melanogaster. *Nature* 289, 79–81. doi: 10.1038/289079a0

Carrillo, R. A., Olsen, D. P., Yoon, K. S., and Keshishian, H. (2010). Presynaptic activity and CaMKII modulate retrograde semaphorin signaling and synaptic refinement. *Neuron* 68, 32–44. doi: 10.1016/j.neuron.2010.09.005

Chen, Y., Akin, O., Nern, A., Tsui, C. Y., Pecot, M. Y., and Zipursky, S. L. (2014). Cell-type-specific labeling of synapses in vivo through synaptic tagging with recombination. *Neuron* 81, 280–293. doi: 10.1016/j.neuron.2013.12.021

Clevers, H. (2006). Wnt/beta-catenin signaling in development and disease. *Cell* 127, 469–480. doi: 10.1016/j.cell.2006.10.018

Dalva, M. B., McClelland, A. C., and Kayser, M. S. (2007). Cell adhesion molecules: signalling functions at the synapse. *Nat. Rev. Neurosci.* 8, 206–220. doi: 10.1038/nrn2075

Daniels, R. W., Gelfand, M. V., Collins, C. A., and DiAntonio, A. (2008). Visualizing glutamatergic cell bodies and synapses in *Drosophila* larval and adult CNS. *J. Comp. Neurol.* 508, 131–152. doi: 10.1002/cne.21670

Darnell, J. C., Jensen, K. B., Jin, P., Brown, V., Warren, S. T., and Darnell, R. B. (2001). Fragile X mental retardation protein targets G quartet mRNAs important for neuronal function. *Cell* 107, 489–499. doi: 10.1016/s0092-8674(01)00566-9

Das, S., Sadanandappa, M. K., Dervan, A., Larkin, A., Lee, J. A., Sudhakaran, I. P., et al. (2011). Plasticity of local GABAergic interneurons drives olfactory habituation. *Proc. Natl. Acad. Sci. U.S.A.* 108, E646–E654. doi: 10.1073/pnas.1106411108

Davis, G. W., Schuster, C. M., and Goodman, C. S. (1996). Genetic dissection of structural and functional components of synaptic plasticity. III. CREB is necessary for presynaptic functional plasticity. *Neuron* 17, 669–679. doi: 10.1016/s0896-6273(00)80199-3

Dear, M. L., Shilts, J., and Broadie, K. (2017). Neuronal activity drives FMRP- and HSPG-dependent matrix metalloproteinase function required for rapid synaptogenesis. *Sci. Signal.* 143, 75–87. doi: 10.1126/scisignal.aan3181

Farca-Luna, A. J., and Sprecher, S. G. (2013). Plasticity in the *Drosophila* larval visual system. *Front. Cell Neurosci.* 7:105. doi: 10.3389/fncel.2013.00105

Feinberg, E. H., Vanhoven, M. K., Bendesky, A., Wang, G., Fetter, R. D., Shen, K., et al. (2008). GFP reconstitution across synaptic partners (GRASP) defines cell contacts and synapses in living nervous systems. *Neuron* 57, 353–363. doi: 10.1016/j.neuron.2007.11.030

Golovin, R. M., and Broadie, K. (2016). Developmental experience-dependent plasticity in the first synapse of the *Drosophila* olfactory circuit. *J. Neurophysiol.* 116, 2730–2738. doi: 10.1152/jn.00616.2016

Golovin, R. M., Vest, J., Vita, D. J., and Broadie, K. (2019). Activity-dependent remodeling of *Drosophila* olfactory sensory neuron brain innervation during an early-life critical period. *J. Neurosci.* 39, 2995–3012. doi: 10.1523/JNEUROSCI.2223-18.2019

He, X., Semenov, M., Tamai, K., and Zeng, X. (2004). LDL receptor-related proteins 5 and 6 in Wnt/beta-catenin signaling: arrows point the way. *Development* 131, 1663–1677. doi: 10.1242/dev.01117

Heckscher, E. S., Fetter, R. D., Marek, K. W., Albin, S. D., and Davis, G. W. (2007). NF-κB, IκB, and IRAK control glutamate receptor density at the *Drosophila* NMJ. *Neuron* 55, 859–873. doi: 10.1016/j.neuron.2007.08.005

Ho, V. M., Lee, J. A., and Martin, K. C. (2011). The cell biology of synaptic plasticity. *Science* 334, 623–628. doi: 10.1126/science.1209236

Jarecki, J., and Keshishian, H. (1995). Role of neural activity during synaptogenesis in *Drosophilas*. *J. Neurosci.* 15, 8177–8190. doi: 10.1523/jneurosci.15-12-08177.1995

Jenett, A., Rubin, G. M., Ngo, T. T., Shepherd, D., Murphy, C., Dionne, H., et al. (2012). A GAL4-driver line resource for *Drosophila* neurobiology. *Cell Rep.* 2, 991–1001. doi: 10.1016/j.celrep.2012.09.011

Kawasaki, F., Zou, B., Xu, X., and Ordway, R. W. (2004). Active zone localization of presynaptic calcium channels encoded by the cacophony locus of *Drosophila*. *J. Neurosci.* 24, 282–285. doi: 10.1523/JNEUROSCI.3553-03.2004

Keene, A. C., and Waddell, S. (2007). *Drosophila* olfactory memory: single genes to complex neural circuits. *Nat. Rev. Neurosci.* 8, 341–354. doi: 10.1038/nrn2098

Khare, N., and Baumgartner, S. (2000). Dally-like protein, a new *Drosophila* glypican with expression overlapping with wingless. *Mech. Dev.* 99, 199–202. doi: 10.1016/s0925-4773(00)00502-5

Kidd, S., and Lieber, T. (2016). Mechanism of notch pathway activation and its role in the regulation of olfactory plasticity in *Drosophila* melanogaster. *PLoS One* 11:e0151279. doi: 10.1371/journal.pone.0151279

Kirkpatrick, C. A., Dimitroff, B. D., Rawson, J. M., and Selleck, S. B. (2004). Spatial regulation of Wingless morphogen distribution and signaling by Dally-like protein. *Dev Cell* 7, 513–523. doi: 10.1016/j.devcel.2004.08.004

Kitamoto, T. (2001). Conditional modification of behavior in *Drosophila* by targeted expression of a temperature-sensitive shibire allele in defined neurons. *J. Neurobiol.* 47, 81–92. doi: 10.1002/neu.1018

Kochlamazashvili, G., Senkov, O., Grebenyuk, S., Robinson, C., Xiao, M. F., Stummeyer, K., et al. (2010). Neural cell adhesion molecule-associated polysialic acid regulates synaptic plasticity and learning by restraining the signaling through GluN2B-containing NMDA receptors. *J. Neurosci.* 30, 4171–4183. doi: 10.1523/JNEUROSCI.5806-09.2010

Koh, Y. H., Popova, E., Thomas, U., Griffith, L. C., and Budnik, V. (1999). Regulation of DLG localization at synapses by CaMKII-dependent phosphorylation. *Cell* 98, 353–363. doi: 10.1016/S0092-8674(00)81964-81969

Kuklin, E. A., Alkins, S., Bakthavachalu, B., Genco, M. C., Sudhakaran, I., Raghavan, K. V., et al. (2017). The Long 3'UTR mRNA of camkii is essential for translation-dependent plasticity of spontaneous release in *Drosophila* melanogaster. *J. Neurosci.* 37, 10554–10566. doi: 10.1523/JNEUROSCI.1313-17.2017

Lahey, T., Gorczyca, M., Jia, X. X., and Budnik, V. (1994). The *Drosophila* tumor-suppressor gene dlg is required for normal synaptic bouton structure. *Neuron* 13, 823–835. doi: 10.1016/0896-6273(94)90249-90246

Levin, L. R., Han, P. L., Hwang, P. M., Feinstein, P. G., Davis, R. L., and Reed, R. R. (1992). The *Drosophila* learning and memory gene rutabaga encodes a Ca2+/Calmodulin-responsive adenylyl cyclase. *Cell* 68, 479–489. doi: 10.1016/0092-8674(92)90185-f

Liang, Y. (2019). Emerging concepts and functions of autophagy as a regulator of synaptic components and plasticity. *Cells* 8:34. doi: 10.3390/cells8010034

Lin, D. M., and Goodman, C. S. (1994). Ectopic and increased expression of Fasciclin II alters motoneuron growth cone guidance. *Neuron* 13, 507–523. doi: 10.1016/0896-6273(94)90022-1

Liu, W. W., and Wilson, R. I. (2013). Glutamate is an inhibitory neurotransmitter in the *Drosophila* olfactory system. *Proc. Natl. Acad. Sci. U.S.A.* 110, 10294–10299. doi: 10.1073/pnas.1220560110

Livingstone, M. S., Sziber, P. P., and Quinn, W. G. (1984). Loss of calcium/calmodulin responsiveness in adenylate cyclase of rutabaga, a *Drosophila* learning mutant. *Cell* 37, 205–215. doi: 10.1016/0092-8674(84)90316-7

Malpel, S., Klarsfeld, A., and Rouyer, F. (2002). Larval optic nerve and adult extra-retinal photoreceptors sequentially associate with clock neurons during *Drosophila* brain development. *Development* 129, 1443–1453.

McCann, C., Holohan, E. E., Das, S., Dervan, A., Larkin, A., Lee, J. A., et al. (2011). The Ataxin-2 protein is required for microRNA function and synapse-specific long-term olfactory habituation. *Proc. Natl. Acad. Sci. U.S.A.* 108, E655–E662. doi: 10.1073/pnas.1107198108

Miazzi, F., Hansson, B. S., and Wicher, D. (2016). Odor-induced cAMP production in *Drosophila* melanogaster olfactory sensory neurons. *J. Exp. Biol.* 219(Pt 12), 1798–1803. doi: 10.1242/jeb.137901

Miech, C., Pauer, H. U., He, X., and Schwarz, T. L. (2008). Presynaptic local signaling by a canonical wingless pathway regulates development of the *Drosophila* neuromuscular junction. *J. Neurosci.* 28, 10875–10884. doi: 10.1523/JNEUROSCI.0164-08.2008

Moehlman, A. T., Casey, A. K., Servage, K., Orth, K., and Kramer, H. (2018). Adaptation to constant light requires Fic-mediated AMPylation of BiP to protect against reversible photoreceptor degeneration. *Elife* 7:e38752

Neves, G., Cooke, S. F., and Bliss, T. V. (2008). Synaptic plasticity, memory and the hippocampus: a neural network approach to causality. *Nat. Rev. Neurosci.* 9, 65–75. doi: 10.1038/nrn2303

Ng, M., Roorda, R. D., Lima, S. Q., Zemelman, B. V., Morcillo, P., and Miesenbock, G. (2002). Transmission of olfactory information between three populations of neurons in the antennal lobe of the fly. *Neuron* 36, 463–474. doi: 10.1016/S0896-6273(02)00975-973

Okamoto, K., Nagai, T., Miyawaki, A., and Hayashi, Y. (2004). Rapid and persistent modulation of actin dynamics regulates postsynaptic reorganization underlying bidirectional plasticity. *Nat. Neurosci.* 7, 1104–1112. doi: 10.1038/nn1311

Packard, M., Koo, E. S., Gorczyca, M., Sharpe, J., Cumberledge, S., and Budnik, V. (2002). The *Drosophila* Wnt, wingless, provides an essential signal for pre- and postsynaptic differentiation. *Cell* 111, 319–330. doi: 10.1016/s0092-8674(02)01047-4

Packard, M., Mathew, D., and Budnik, V. (2003). Wnts and TGF beta in synaptogenesis: old friends signalling at new places. *Nat. Rev. Neurosci.* 4, 113–120. doi: 10.1038/nrn1036

Pfeiffer, S., Alexandre, C., Calleja, M., and Vincent, J. P. (2000). The progeny of wingless-expressing cells deliver the signal at a distance in *Drosophila* embryos. *Curr. Biol.* 10, 321–324. doi: 10.1016/S0960-9822(00)00381-X

Raymond, L. A., Blackstone, C. D., and Huganir, R. L. (1993). Phosphorylation of amino acid neurotransmitter receptors in synaptic plasticity. *Trends Neurosci.* 16, 147–153. doi: 10.1016/0166-2236(93)90123-90124

Ron, D., and Walter, P. (2007). Signal integration in the endoplasmic reticulum unfolded protein response. *Nat. Rev. Mol. Cell Biol.* 8, 519–529. doi: 10.1038/nrm2199

Sachse, S., Rueckert, E., Keller, A., Okada, R., Tanaka, N. K., Ito, K., et al. (2007). Activity-dependent plasticity in an olfactory circuit. *Neuron* 56, 838–850. doi: 10.1016/j.neuron.2007.10.035

Sato, S., Ueno, K., Saitoe, M., and Sakai, T. (2018). Synaptic depression induced by postsynaptic cAMP production in the *Drosophila* mushroom body calyx. *J. Physiol.* 596, 2447–2461. doi: 10.1113/JP275799

Schoppa, N. E., Kinzie, J. M., Sahara, Y., Segerson, T. P., and Westbrook, G. L. (1998). Dendrodendritic inhibition in the olfactory bulb is driven by NMDA receptors. *J. Neurosci.* 18, 6790–6802. doi: 10.1523/jneurosci.18-17-06790.1998

Schuster, C. M., Davis, G. W., Fetter, R. D., and Goodman, C. S. (1996). Genetic dissection of structural and functional components of synaptic plasticity. I. Fasciclin II controls synaptic stabilization and growth. *Neuron* 17, 641–654. doi: 10.1016/s0896-6273(00)80197-x

Sears, J. C., and Broadie, K. (2017). Fragile X mental retardation protein regulates activity-dependent membrane trafficking and trans-synaptic signaling mediating synaptic remodeling. *Front. Mol. Neurosci.* 10:440. doi: 10.3389/fnmol.2017.00440

Song, I., and Huganir, R. L. (2002). Regulation of AMPA receptors during synaptic plasticity. *Trends Neurosci.* 25, 578–588. doi: 10.1016/s0166-2236(02)02270-1

Stephenson, R., and Metcalfe, N. H. (2013). *Drosophila* melanogaster: a fly through its history and current use. *J. R. Coll. Physicians Edinb.* 43, 70–75. doi: 10.4997/JRCPE.2013.116

Sudhakaran, I. P., Hillebrand, J., Dervan, A., Das, S., Holohan, E. E., Hulsmeier, J., et al. (2014). FMRP and Ataxin-2 function together in long-term olfactory habituation and neuronal translational control. *Proc. Natl. Acad. Sci. U.S.A.* 111, E99–E108. doi: 10.1073/pnas.1309543111

Sugie, A., Hakeda-Suzuki, S., Suzuki, E., Silies, M., Shimozono, M., Mohl, C., et al. (2015). Molecular remodeling of the presynaptic active zone of *Drosophila* Photoreceptors via activity-dependent feedback. *Neuron* 86, 711–725. doi: 10.1016/j.neuron.2015.03.046

Vonhoff, F., and Keshishian, H. (2017a). Activity-dependent synaptic refinement: new insights from *Drosophila*. *Front. Syst. Neurosci.* 11:23. doi: 10.3389/fnsys.2017.00023

Vonhoff, F., and Keshishian, H. (2017b). Cyclic nucleotide signaling is required during synaptic refinement at the *Drosophila* neuromuscular junction. *Dev. Neurobiol.* 77, 39–60. doi: 10.1002/dneu.22407

Wagh, D. A., Rasse, T. M., Asan, E., Hofbauer, A., Schwenkert, I., Durrbeck, H., et al. (2006). Bruchpilot, a protein with homology to ELKS/CAST, is required for structural integrity and function of synaptic active zones in *Drosophila*. *Neuron* 49, 833–844. doi: 10.1016/j.neuron.2006.02.008

Wilson, R. I., and Laurent, G. (2005). Role of GABAergic inhibition in shaping odor-evoked spatiotemporal patterns in the *Drosophila* antennal lobe. *J. Neurosci.* 25, 9069–9079. doi: 10.1523/JNEUROSCI.2070-05.2005

Yamamoto, S., Jaiswal, M., Charng, W. L., Gambin, T., Karaca, E., Mirzaa, G., et al. (2014). A *drosophila* genetic resource of mutants to study mechanisms underlying human genetic diseases. *Cell* 159, 200–214. doi: 10.1016/j.cell.2014.09.002

Yuan, Q., Xiang, Y., Yan, Z., Han, C., Jan, L. Y., and Jan, Y. N. (2011). Light-induced structural and functional plasticity in *Drosophila* larval visual system. *Science* 333, 1458–1462. doi: 10.1126/science.1207121

Zhao, C., Dreosti, E., and Lagnado, L. (2011). Homeostatic synaptic plasticity through changes in presynaptic calcium influx. *J. Neurosci.* 31, 7492–7496. doi: 10.1523/JNEUROSCI.6636-10.2011

Zito, K., Fetter, R. D., Goodman, C. S., and Isacoff, E. Y. (1997). Synaptic clustering of Fasciclin II and shaker: essential targeting sequences and role of Dlg. *Neuron* 19, 1007–1016. doi: 10.1016/S0896-6273(00)80393-80391

Zucker, R. S. (1999). Calcium- and activity-dependent synaptic plasticity. *Curr. Opin. Neurobiol.* 9, 305–313. doi: 10.1016/s0959-4388(99)80045-2

Conflict of Interest: The authors declare that the research was conducted in the absence of any commercial or financial relationships that could be construed as a potential conflict of interest.

frontiers in Physiology

REVIEW
published: 05 March 2020
doi: 10.3389/fphys.2020.00099

One Actor, Multiple Roles: The Performances of Cryptochrome in *Drosophila*

Milena Damulewicz[1] *and Gabriella M. Mazzotta*[2]*

[1] Department of Cell Biology and Imaging, Jagiellonian University, Kraków, Poland, [2] Department of Biology, University of Padua, Padua, Italy

Cryptochromes (CRYs) are flavoproteins that are sensitive to blue light, first identified in *Arabidopsis* and then in *Drosophila* and mice. They are evolutionarily conserved and play fundamental roles in the circadian clock of living organisms, enabling them to adapt to the daily 24-h cycles. The role of CRYs in circadian clocks differs among different species: in plants, they have a blue light-sensing activity whereas in mammals they act as light-independent transcriptional repressors within the circadian clock. These two different functions are accomplished by two principal types of CRYs, the light-sensitive plant/insect type 1 CRY and the mammalian type 2 CRY acting as a negative autoregulator in the molecular circadian clockwork. *Drosophila melanogaster* possesses just one CRY, belonging to type 1 CRYs. Nevertheless, this single CRY appears to have different functions, specific to different organs, tissues, and even subset of cells in which it is expressed. In this review, we will dissect the multiple roles of this single CRY in *Drosophila*, focusing on the regulatory mechanisms that make its pleiotropy possible.

Keywords: cryptochrome, *Drosophila*, circadian clock, phototransduction, circadian plasticity, light-independent activity

OPEN ACCESS

Edited by:
Shigehiro Namiki,
The University of Tokyo, Japan

Reviewed by:
Nuri Ozturk,
Gebze Technical University, Turkey
Makio None Takeda,
Kobe University, Japan

***Correspondence:**
Gabriella M. Mazzotta
gabriella.mazzotta@unipd.it

Specialty section:
This article was submitted to Invertebrate Physiology, a section of the journal Frontiers in Physiology

Received: *15 November 2019*
Accepted: *27 January 2020*
Published: *05 March 2020*

Citation:
Damulewicz M and Mazzotta GM (2020) One Actor, Multiple Roles: The Performances of Cryptochrome in Drosophila. Front. Physiol. 11:99. doi: 10.3389/fphys.2020.00099

INTRODUCTION

Cryptochromes are highly conserved proteins belonging to the flavoprotein superfamily, identified in species from all three domains of life (Chaves et al., 2011). They are structurally related to photolyases (Müller and Carell, 2009), evolutionarily conserved flavoproteins that catalyze light-dependent DNA repair (Todo, 1999; Sancar, 2003). Cryptochromes and photolyases bind the same cofactors: the flavin adenine dinucleotide (FAD) and a secondary cofactor such as methenyltetrahydrofolate (MTHF), deazariboflavin, or others (Sancar, 2003). Cryptochromes have essentially lost their DNA repair activity and have acquired a very divergent C-terminal domain, intrinsically unstructured (Hemsley et al., 2007) and critical for light signaling (Chaves et al., 2011). A class of cryptochromes, CRY-DASH (*Drosophila*, *Arabidopsis*, *Synechocystis*, and *Homo*), with structural and photochemical properties more similar to photolyases and residual single-stranded DNA repair activity, has been described in bacteria, plants, and animals (Selby and Sancar, 2006; Pokorny et al., 2008).

Cryptochromes are involved in the regulation of circadian clocks, but they also display several signaling functions, ranging from growth and development in plants (Yang et al., 2017) to putative magnetoreception in animals (Ritz et al., 2000). From a circadian perspective, animal cryptochromes can be essentially divided into two classes of proteins: light-responsive

type 1 (from invertebrates), involved in clock entrainment, and light-insensitive type 2 (mainly found in vertebrates but also in some insects), acting as transcriptional repressors in the central clock mechanism (Chaves et al., 2011). In recent years, new types of CRY/PHR (cryptochromes/photolyases) have also been described, providing evidences for the large functional diversity of this group of proteins (for a comprehensive description and phylogenetic classification, refer to Ozturk, 2017).

STRUCTURE AND PHOTOACTIVATION

Drosophila CRY, defined as type 1 cryptochrome (Yuan et al., 2007; Öztürk et al., 2008), is a photoactive pigment whose action spectrum peaks in the UV-A range (350–400 nm) with a plateau in the near blue (430–450 nm) (VanVickle-Chavez and Van Gelder, 2007). The 542-amino-acid (aa) protein harbors two different domains (**Table 1**): an N-terminal photolyase homology region (PHR) and a C-terminus tail (CTT), unique in its sequence, responsible for mediating phototransduction (Busza et al., 2004; Dissel et al., 2004; Hemsley et al., 2007; **Figure 1**). The CTT forms a helix structure that binds alongside the main body of the PHR domain establishing contacts with the FAD binding pocket, mimicking the damaged DNA photolyase–DNA interaction (Zoltowski et al., 2011; Czarna et al., 2013; Levy et al., 2013; Masiero et al., 2014; Lin et al., 2018). Upon illumination with blue light (440 nm), the CRY FAD cofactor is reduced to the anionic semiquinone (ASQ) state by a fast electron transfer involving four conserved tryptophan residues (W420, W397, W342, and W394). FAD photoreduction induces conformational changes in the Trp tetrad, which result in the displacement of the CTT from the PHR domain and consequent protein activation (Zoltowski et al., 2011; Czarna et al., 2013; Levy et al., 2013; Vaidya et al., 2013; Masiero et al., 2014; Lin et al., 2018). However, the Trp-tetrad-dependent photoreduction and circadian photic resetting were suggested to be independent of each other (Ozturk et al., 2014).

Very recently, a role for the Trp triad (W420, W397, and W342) in circadian photoentrainment of locomotor activity rhythm was tested *in vivo*, by analyzing the behavioral response to moderately and very low light. While W420Y and W397Y CRY flies were predominately arrhythmic (similar to wild type), transgenic flies expressing W342Y CRY showed high levels of rhythmicity and long periods, similar to cry^0 flies (Dolezelova et al., 2007; Baik et al., 2019).

Molecular dynamics (MD) simulations have suggested that the CTT detachment is also a result of changes in the hydrogen bonding network due to protonation of a conserved His residue (His378), located between the CTT and the flavin cofactor (Ganguly et al., 2016). H378 stabilizes the CTT in the resting-state conformation in the dark; light induces a series of conformational changes from nanoseconds to milliseconds that lead to the formation of the final signaling state, which depends on pH and requires uptake of a proton (Berntsson et al., 2019). MD simulations have also suggested for the FAD cofactor roles other than photoreduction and CRY activation: the FAD presence would confer to the receptor a more fluctuation-prone behavior, thus decreasing the amount of necessary light input energy for CRY activation (Masiero et al., 2014). Recent studies performed on a longer timescale have revealed that following photoactivation, FAD is released from the FAD-binding pocket, providing evidence that CRY undergoes an inactivation reaction rather than a photocycle (Kutta et al., 2018), in agreement with the reported irreversible nature of the light-induced conformational changes (Ozturk et al., 2009; Kattnig et al., 2018; Lin et al., 2018). The active form of CRY is then able to bind the circadian components TIMELESS (Ceriani et al., 1999) and PERIOD (Rosato et al., 2001).

The CTT of CRY has been extensively studied, and a combination of *in silico* analyses and experimental validation has revealed the presence of an intrinsically disordered region containing several interaction motifs that turn this tail into a hot spot for molecular interactions (Hemsley et al., 2007; Mazzotta et al., 2013; Masiero et al., 2014). It can be divided into two subregions: one (493–520 aa) required for the interaction with PER and TIM (Hemsley et al., 2007) and the other (521–542 aa) specifically involved in the light activation of the CRY protein (Rosato et al., 2001; Busza et al., 2004; Dissel et al., 2004). The absence of part of the CTT (aa 521–540_CRYΔ or aa 524–542_CRY^M) results in constitutive activation of the protein (Rosato et al., 2001; Busza et al., 2004). In this state, CRY may bind TIM and PER in the absence of light (Rosato et al., 2001); in flies overexpressing CRYΔ in the pacemaker neurons, the accumulation of clock proteins is reduced, and their subcellular distribution altered. At a behavioral level, these flies display long periods of locomotor activity rhythms in constant darkness (Dissel et al., 2004). This is reminiscent of the similarly long period shown by wild-type flies exposed to constant light of low intensity (Konopka et al., 1989; Dissel et al., 2004) (see **Table 2**). The first subregion of CRY CTT (aa 515–521) harbors the interaction motifs DM1 (DILIMOT database, Neduva and Russell, 2005) and EM1 (ELM database (Gould et al., 2009) and contains a proline-directed kinase phosphorylation site (Hemsley et al., 2007). In the second subregion, four putative ELM interaction motifs have been identified (EM2–EM5) (Hemsley et al., 2007). EM2 (526–529) is a TRAF2 ligand motif and part of a putative phosphorylation site, EM3 (523–529) contains putative phosphorylation sites for casein kinase 2 (CK2) and cAMP-dependent protein kinase A (PKA), EM4 (528–531) and EM5 (538–541) are PDZ binding motifs (Hemsley et al., 2007).

An alternative model proposed for the light activation of CRY involves the binding of CTT by still unknown factor(s), acting as repressor(s) in the dark and released upon light exposure (Rosato et al., 2001; Hemsley et al., 2007). Residue Glu530 (E530) might be involved in the binding of a repressor in the darkness, which would block the Ser526 (S526) residue in the TRAF2 ligand motif, thus inhibiting further bindings. After light exposure, the repressor would be released, and modulator proteins might bind to TRAF2 (Hemsley et al., 2007; **Figure 2**).

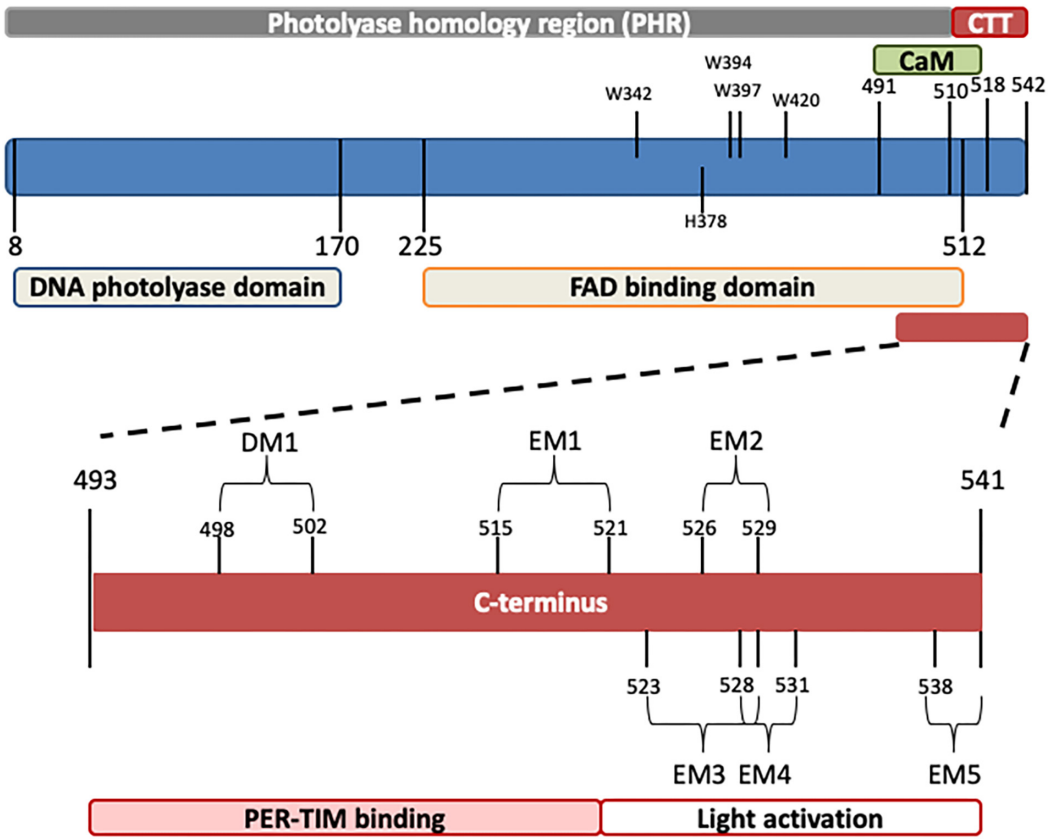

FIGURE 1 | Schematic representation of *Drosophila* CRY. The photolyase-like and FAD binding domains (below) as well as the calmodulin binding motif (CaM) and the C-terminus tail (CTT) (above) are indicated. In the C-terminus, relevant domains are also depicted. Numbers indicate position (amino acids). For details, see **Table 1**.

CRY AND CIRCADIAN CLOCK RESETTING

Drosophila CRY acts as photoreceptor involved in the light synchronization of the molecular circadian clock machinery (Stanewsky et al., 1998; Helfrich-Förster et al., 2001) based, as in virtually all eukaryotes, on interlocked feedback loops. In the *Drosophila* main negative feedback loop, PERIOD (PER) and TIMELESS (TIM) proteins act as negative elements, inhibiting the transcription of their own genes. Their expression is activated by CLOCK (CLK) and CYCLE (CYC): in the evening, they dimerize, enter the nucleus and bind to the E-box, thus inducing the expression of *per*, *tim*, and other clock-controlled genes (*ccg*). PER and TIM proteins accumulate in the cytoplasm, and late at night, they dimerize and translocate to the nucleus, where they bind to CLK/CYC and inhibit their activity, repressing the transcription of *ccg* [for a review, refer to Özkaya and Rosato (2012) and **Figure 3**]. The second feedback loop is based on rhythmic *vrille* (*vri*) and *Pdp1*ε (PAR-domain protein 1) expression (McDonald and Rosbash, 2001; Ueda et al., 2002). Both genes are transcribed with the same phase, but while VRI protein expression quickly follows that of its mRNA, PDP1ε starts to accumulate 3–6 h later (Cyran et al., 2003). VRI forms homodimers that bind to the V/P box located in the promoters of morning genes (i.e. *clk* and *cry*), blocking their transcription (Cyran et al., 2003; Glossop et al., 2003). After 3–6 h, PDP1ε starts to compete with VRI for the V/P box binding position, and because of a higher affinity, it releases the inhibitor and activates the expression of controlled genes in the late night (Cyran et al., 2003). This mechanism ensures the circadian expression of CRY, with mRNA peaking at the end of the day and maximum levels of protein level during the night (Emery et al., 1998). This rhythm of RNA expression is maintained in constant darkness conditions (DD), although with decreased amplitude, while CRY protein levels in DD increase continuously during the subjective day and night (Emery et al., 1998). In constant-light conditions, CRY is overactivated, which causes the amplitude of TIM and PER cycling to be reduced and TIM phosphorylation status to be attenuated (Marrus et al., 1996). As a consequence, flies are arrhythmic or exhibit longer period of locomotor activity rhythm, depending on the intensity of light (Konopka et al., 1989).

The *Drosophila* pacemaker operates within a circuitry consisting of a network of 150 clock neurons divided into nine groups: four groups of dorsal neurons ($DN1_a$, $DN1_p$, DN2, and DN3) and five groups of lateral neurons, further divided into lateral posterior neurons (LPNs), ventral lateral neurons (LN_vs),

TABLE 1 | Functional domains and relevant residues in the CRY protein.

	Position (amino acids)	Motifs	Function
N-terminus	1–492		
DNA photolyase domains	8–170		Light detection
FAD binding domain	225–512		
TRP tetrad	W342, W394, W397, W420		Fast electron transfer Conformational change
H378	H378		Stabilization of CTT in the resting state conformation in the dark
C-terminus	493–541		
DM1	498–502	Interaction motif	
CaM binding motif	491–518		Ca^{2+}-dependent Calmodulin binding
C-terminus tail (CTT)	510–542		
EM1	515–521	Proline-directed kinase phosphorylation site	PER and TIM binding
EM2	526–529	TRAF2 ligand motif and part of a putative phosphorylation site	Light-dependent activation
EM3	523–529	Casein kinase 2 and cAMP-dependent protein kinase A (PKA) phosphorylation site	Light-dependent activation Phosphorylation of S526 induces the modulator replacement by TIM/PER
EM4	528–531	PDZ binding motif	Light-dependent activation E530-repressor binding
EM5	538–541	PDZ binding motif	Light-dependent activation

and dorsal lateral neurons (LN_ds). The ventral lateral neurons are classified, based on their relative size, into small and large (s-LN_vs and l-LN_vs, respectively), and fifth s-LN_v (Miyasako et al., 2007; Hermann-Luibl and Helfrich-Förster, 2015). s-LN_v and l-LN_v express a pigment-dispersing factor (PDF), a neuropeptide involved in intercellular communication between clock neurons (Shafer et al., 2008; Yoshii et al., 2009).

Cryptochrome is expressed in a subset of clock neurons (all four s-LN_vs, all four l-LN_vs, the fifth s-LN_v, three of the six LN_ds, and some of the DN1s), enabling them to directly perceive photic information (Shafer et al., 2006; Benito et al., 2008; Yoshii et al., 2008; Damulewicz and Pyza, 2011; Fogle et al., 2011). Upon light exposure, CRY binds to TIM, promoting its degradation (Ceriani et al., 1999; Koh et al., 2006b; Peschel et al., 2009). As the presence and binding of TIM are essential for PER stability, the light-induced degradation of TIM releases the PER–TIM mediated transcriptional repression, hence synchronizing the circadian clock to light–dark cycles (Ishida et al., 1999; Helfrich-Förster, 2005). CRY is also rapidly degraded in the presence of light through the proteasome (Lin et al., 2001; Sathyanarayanan et al., 2008): the light-dependent CRY–TIM complex is bound by JETLAG (JET), which promotes TIM ubiquitination and degradation. In the absence of TIM, CRY binds JET (Peschel et al., 2009) or Ramshackle (BRWD3) (Ozturk et al., 2013) or both. JET is a component of a Skp1-Cullin/F-Box (SCF) E3 ubiquitin ligase complex and functions as a substrate receptor for CRL1 E3 ligase (Koh et al., 2006b), while BRWD3 is a substrate receptor for CRL4 E3 ligase (Ozturk et al., 2013). JET and BRWD3 initiate CRY ubiquitination and degradation in the proteasome (**Figure 3**). The light dependence of this binding, which is enhanced in the absence of TIM, leads to a rapid decrease in CRY levels during the day, just after TIM degradation. This way, CRY resets the molecular clock and entrains the oscillator to light conditions.

Besides its relevance for circadian photo-synchronization, the CRY–TIM interaction has also important functional implications in the clock adaptation to seasonal environments. Indeed, natural variants of TIM known to trigger seasonal responses as a function of photoperiod show, at a molecular level, differential affinity for CRY (Boothroyd et al., 2007; Sandrelli et al., 2007; Tauber et al., 2007; Montelli et al., 2015).

Interestingly, CRY interacts also with PER, detecting PER as a possible pacemaker target of the cryptochrome: in a yeast two-hybrid assay, this interaction is light dependent, while in S2 cells, the physical association between CRY and PER is independent of light (Rosato et al., 2001).

From the first described CRY mutant, cry^b, a missense mutation in the FAD binding site (Stanewsky et al., 1998), several *cry* mutations have been shown to affect circadian light response (for a detailed description, refer to **Table 2**). Conversely, CRY overexpression increases flies' sensitivity to low-intensity light (Emery et al., 1998).

The *Drosophila* circadian clock can be readily synchronized by temperature cycles with an amplitude of 2–3°C (Glaser and Stanewsky, 2005; Yoshii et al., 2005; Goda et al., 2014; Currie et al., 2009), and different subsets of clock neurons are specifically involved in mediating clock synchronization at high or low temperatures (Zhang Y. et al., 2010; Gentile et al., 2013). Interestingly, among the various subsets of clock neurons, those more easily synchronized by temperature are the ones that do not express CRY (Yoshii et al., 2010; Gentile et al., 2013; Yadlapalli et al., 2018), and consistent with this finding, removal of CRY from clock neurons increases flies' ability to synchronize to temperature cycles (Gentile et al., 2013). Thus, in clock neurons, CRY plays an important role in counteracting the effects of temperature cycles on the molecular circadian clock, thus contributing to the integration of different zeitgebers.

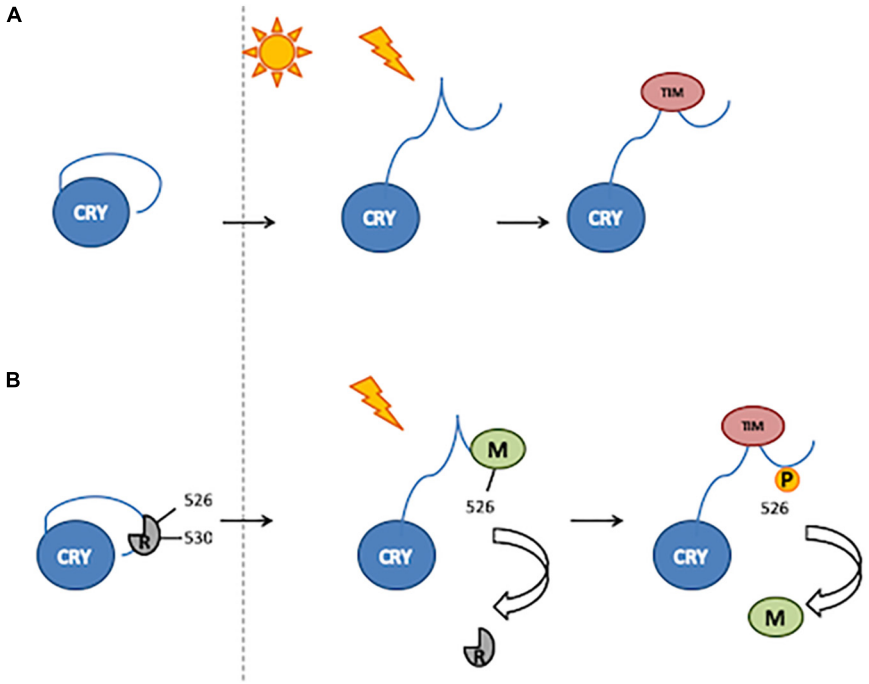

FIGURE 2 | Two mechanisms of CRY activation. **(A)** Light induces a conformational change resulting in the release of CTT, thus enabling TIM binding. **(B)** In the darkness, a putative repressor (R) binds to the 530 residue and blocks the 526 position. After light exposure, the repressor is released and a modulator (M) binds to the 526 position. Phosphorylation of the 526 residue is involved in modulator release and thus TIM binding.

CRY AND CIRCADIAN PACEMAKING

Cryptochrome also acts as a circadian transcriptional repressor necessary for the daily cycling of peripheral circadian clocks. Indeed, the endogenous rhythms of olfactory responses are severely reduced or abolished in *cry*^{b} mutants, as well as molecular oscillations of *per* and *tim* during and after entrainment to light–dark cycles (Krishnan et al., 2001). The same *cry*^{b} mutation dramatically affects the pattern of PER and TIM oscillation in Malpighian tubules (MTs), where both proteins display very low levels during most of the DD cycle (Ivanchenko et al., 2001). By contrast, the same mutation does not affect circadian oscillator functions in central circadian pacemaker neurons (Ivanchenko et al., 2001; Stanewsky et al., 1998). Moreover, the expression level of genes activated by CLK/CYC is reduced in *cry*^{b} mutant eyes (Collins et al., 2006; Damulewicz and Pyza, 2011); on the other hand, CRY and PER co-expression in the compound eyes represses CLK/CYC activity (Collins et al., 2006). This role of CRY as a clock component seems limited to peripheral oscillators.

Besides this role as a circadian repressor, an involvement of CRY in the posttranscriptional control of the circadian clock can also be hypothesized. Indeed, we have recently shown that CRY interacts with BELLE (Cusumano et al., 2019), a DEAD-box RNA helicase essential for viability and fertility (Johnstone et al., 2005), and plays important functions in RNA metabolism, from splicing and translational regulation to miRNA and siRNA pathways (Worringer et al., 2009; Pek and Kai, 2011; Ihry et al., 2012). We have observed an involvement of BELLE in circadian rhythmicity and in the piRNA-mediated regulation of transposable elements, suggesting that this specific posttranscriptional mechanism could be in place to ensure proper rhythmicity (Cusumano et al., 2019).

CRY AND MAGNETORECEPTION

In several organisms, circadian rhythms are influenced by little changes in the intensity of the Earth's magnetic field. In particular, a low-frequency electromagnetic field shows a pronounced 24-h oscillation (König, 1959), and therefore, it could act as a geophysical synchronizer for the circadian clock (Yoshii et al., 2009). Insects detect the geomagnetic field using photochemical reactions: photon absorption by pigment molecules induces the transfer of an electron from a donor to an acceptor molecule, generating a donor–acceptor couple, each molecule containing one unpaired electron, called radical pair in singlet state (antiparallel spin orientation). The two unpaired electrons are at a proper distance to undergo transition to the triplet state (parallel orientation), and the geomagnetic field can influence the interconversion between single and triplet states of the radical pair (Ritz et al., 2000).

In *Drosophila*, CRY is a good candidate for sensing small changes in the magnetic field. In fact, in CRY, radical pairs are formed between the FAD cofactor and proximate tryptophan and/or tyrosine residues within a conserved Trp triad (W342, W397, and W420) (Zoltowski et al., 2011;

TABLE 2 | *Cry* mutants.

Mutant	Defect	Molecular	Behavioral	References
cry^{b}	Missense mutation (D412N) in the conserved FAD binding domain	No cycling of mRNA; very low protein levels No cycling of *per/tim* in peripheral clocks Light-independent interaction with TIM No light-dependent degradation	No phase shift in response to light pulses Free-running circadian rhythms in constant light	Stanewsky et al., 1998; Emery et al., 2000; Krishnan et al., 2001; Levine et al., 2002; Busza et al., 2004; Yoshii et al., 2004; Rieger et al., 2006
cry^{M}	Deletion of C-terminus (amino acids 524–542)	Low protein levels No light-dependent degradation. Light-independent interaction with TIM	Free-running circadian rhythms in constant light	Busza et al., 2004
cry^{0}	Knockout	Reduced *per* oscillation in wings and antennae under LD conditions	Two separate circadian components in constant light	Dolezelova et al., 2007
$cry\Delta$	Deletion in C-terminus (amino acids 521–540)	Low protein levels No light-dependent degradation Reduced PER/TIM levels, cycling amplitude, and phosphorylation status Impaired nuclear localization of TIM/PER in LN_vs Light-independent interaction with PER/TIM	Longer free-running period Entrainment defects	Rosato et al., 2001; Dissel et al., 2004
cry^{out}	Deletion of N-terminal (amino acids 1–96)		Free running in LD Entrainment to temperature cycles	Yoshii et al., 2008, 2010

Czarna et al., 2013; Levy et al., 2013). The photon is absorbed by the pigment molecule, and then one electron is transferred from the triad following electron excitation of the FAD and consequent protonation and deprotonation (Dodson et al., 2013). Radical formation activates CRY, which changes its conformation. A reverse reaction (reoxidation) restores the fully oxidized (inactive) form of CRY in the dark. This process can also generate magnetically sensitive radical pairs (superoxide and peroxide radicals and flavin radicals) (Dodson et al., 2013). There is also evidence that CRY is co-expressed and, in the presence of light and the magnetic field, forms a stable complex with CG8198 [Lethal (1) G0136], thereafter named MagR (Qin et al., 2016), an iron–sulfur cluster assembly protein involved in iron metabolism and required for proper circadian rhythmicity (Mandilaras and Missirlis, 2012).

Drosophila behavior is influenced by the magnetic field. Indeed, in a binary-choice behavioral assay for magneto-sensitivity, flies exhibit a naïve avoidance of the magnetic field under full-spectrum light but did not respond when UV-A/blue light (<420 nm) was blocked (Gegear et al., 2008). This response was also lost in *cry* mutants, clearly indicating that CRY is directly involved in the light-dependent magnetic sensing in *Drosophila* (Gegear et al., 2008). The electromagnetic field influences the period length of the locomotor activity, as a result of enhanced CRY signaling. Indeed, electromagnetic field application caused lengthening of the circadian period of locomotor activity, and this effect was greater when the flies were exposed to constant blue light, reasonably as a result of an enhanced CRY function upon blue-light activation (Yoshii et al., 2009). Furthermore, *cry* mutants showed no magnetic field sensitivity for period changes, whereas flies overexpressing CRY were magnetically oversensitive (Ritz et al., 2010). Further analyses of low-frequency electromagnetic field-induced changes on circadian period and activity levels have shown that the terminal tryptophan of the Trp triad (W342) is not necessary for field responses, but a mechanism different from radical pairs involving the Trp triad might be used by CRY to sense the electromagnetic field (Fedele et al., 2014a). Indeed, superoxide radicals and ascorbic acid could form a radical pair with the FAD (Müller and Ahmad, 2011; Lee et al., 2014). However, deletion of the CRY C-terminus weakens the period changes in response to the magnetic field, while the N-terminus increases hyperactivity (Fedele et al., 2014a).

Climbing activity (negative geotaxis) is disrupted by a static electromagnetic field (Fedele et al., 2014b). This effect is observed after blue-light exposure but is not present in red light, indicating the involvement of light-activated CRY (Fedele et al., 2014b). Mutation of the terminal Trp in the triad (W342) in CRY does not affect magnetoreception (Gegear et al., 2010; Fedele et al., 2014b), but C-terminus deletion disrupts the fly's response to the electromagnetic field (Fedele et al., 2014b). *cry* mutants show decreased climbing ability, which can be rescued by overexpressing CRY in LN_d clock neurons (Rakshit and Giebultowicz, 2013), antennae, and eyes (R8 photoreceptors of pale ommatidia, R8 yellow ommatidia, H-B eyelet, or R7 cell) (Fedele et al., 2014b).

Cryptochrome is involved also in the modulation of other responses of *Drosophila* to the magnetic field. The courtship activity of wild-type males is significantly increased when they were exposed to a ≥20-Gauss static magnetic field (Wu et al., 2016), but not in *cry*-deficient mutants (cry^{b} and cry^{M}) and in flies with CRY RNAi-mediated knockdown in *cry*-expressing

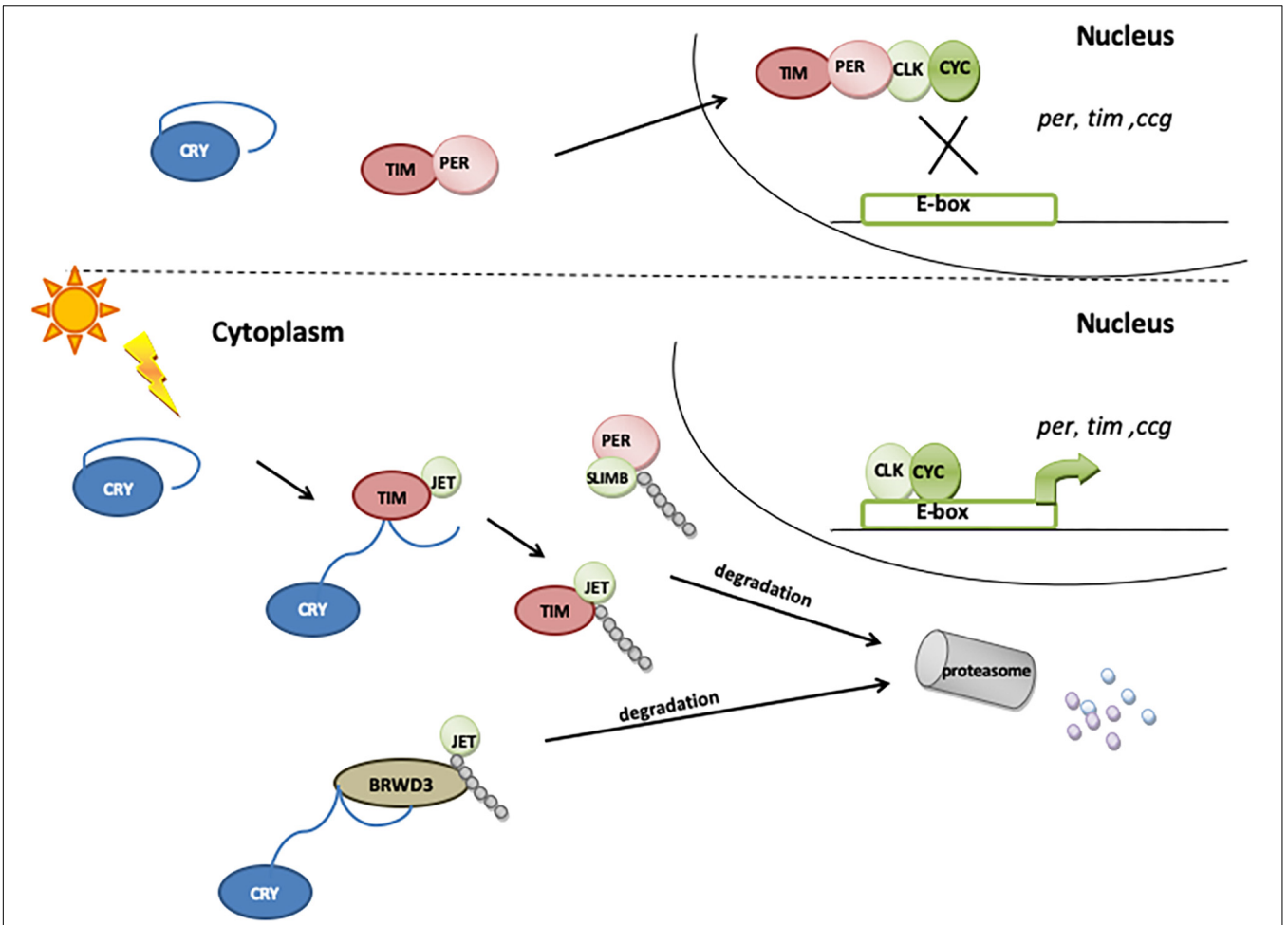

FIGURE 3 | The role of CRY in molecular clock resetting. In the presence of light, CRY binds TIM and promotes its degradation via proteasome by a mechanism that involves the F-box protein JETLAG (JET). When exposed to light, CRY also becomes a substrate for JET and for Ramshackle (BRWD3), which initiates its ubiquitination and degradation in proteasome.

neurons (Wu et al., 2016). Nevertheless, the phenotype is rescued when CRY is genetically expressed under the control of *cry*-Gal4 (Wu et al., 2016).

The magnetic field influences also the seizure response in *Drosophila*, specifically the recovery time of larvae from an electric shock (Marley et al., 2014). Indeed, a stronger seizure phenotype is observed after blue light or magnetic field exposition, and the lack of this effect in either cry^0 mutants or in orange light (590 nm) clearly indicates it to be CRY dependent (Marley et al., 2014). Moreover, this strong seizure phenotype is associated with increased synaptic excitation in the locomotor circuitry, as it may be blocked by antiepileptic drugs (Marley and Baines, 2011; Lin et al., 2012). Indeed, the CRY- and light-dependent magnetic field modulates the action potential firing of individual neurons, by increasing input resistance and depolarization of the membrane potential of "anterior Corner Cell" (aCC) and "Raw Prawn 2" (RP2) motoneurons (Giachello et al., 2016).

The ability of cryptochromes to form radical pairs upon photoexcitation makes them excellent candidate proteins for light-dependent magnetoreception also in other organisms.

The vertebrate-like Cry2 is involved in the response to magnetic field of two species of cockroaches, the American cockroach, *Periplaneta americana* (which most likely contains only Cry2), and *Blattella germanica*, which has both CRY types (Bazalova et al., 2016). Cry2 is expressed in laminal glia cells underneath the retina and is necessary for sensing the directional component of the magnetic field (Bazalova et al., 2016).

The night-migratory European robins (*Erithacus rubecula*) possess four different cryptochromes, but only Cry4 is predicted to be the magnetoreceptive protein (Günther et al., 2018). Cry4 is expressed in every cell type within the retina, at significantly higher levels during the migratory season compared to the non-migratory season. Moreover, the modeled structure revealed a high similarity with *Drosophila* CRY, also in the position of residues important for FAD binding (Kutta et al., 2017; Günther et al., 2018).

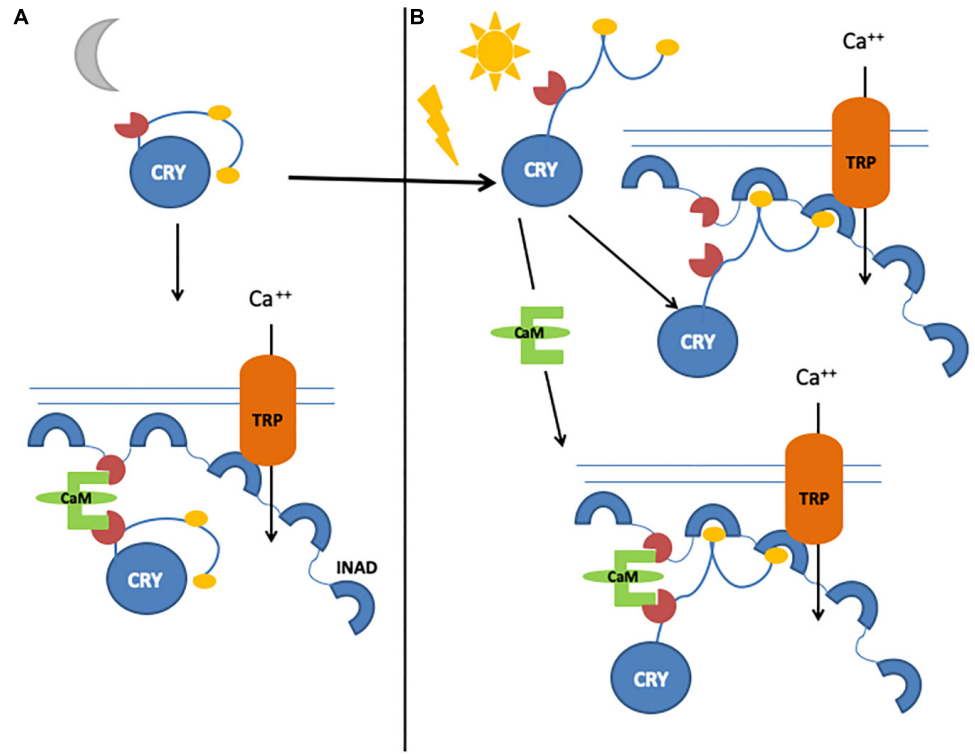

FIGURE 4 | Graphical representation of CRY/calmodulin interaction mechanisms. **(A)** Light-independent, CaM-dependent pathway. Inactive CRY binds to CaM, which allows the formation of a ternary complex with INAD. **(B)** In the presence of light, CRY can bind INAD directly. In the presence of both light and calmodulin, CRY–INAD binding is strengthened, thus consolidating the initial light-induced response.

CRY IN THE VISUAL SYSTEM

In addition to the pacemaker neurons, CRY is also present in non-clock cells in the anterior brain, in the glia cells located between the central brain and the optic lobe, as well as in the terminals of photoreceptor cells R7 and R8 (Yoshii et al., 2008; Damulewicz and Pyza, 2011). In photoreceptor cells, it is mainly involved in the functioning and localization of the phototransduction cascade proteins (Mazzotta et al., 2013; Schlichting et al., 2018). The visual cascade proteins are located in the rhabdomeres, densely packed microvilli formed by evaginations of the photoreceptors' plasma membrane. These are arranged in a multiprotein complex called Signalplex, organized by the inactivation-no-afterpotential D (INAD), a PDZ [postsynaptic density protein (PSD95), *Drosophila* disc large tumor suppressor (Dlg1), and zonula occludens-1 protein (zo-1)] domains-containing protein [reviewed by Hardie and Juusola (2015)].

In the photoreceptor cells, CRY binds to INAD, which, in turn, enables the interaction with other phototransduction components (Mazzotta et al., 2013). INAD binds the neither-inactivation-nor-afterpotential C (NINAC) myosin III, involved in the shuttling of signaling proteins (Gqα and arrestin 2) from the cell bodies to the rhabdomeres [reviewed by Montell (2012)] and in the inactivation of metarhodopsin by speeding up the binding of arrestin (Liu et al., 2008). INAD/NINAC interaction allows binding of the complex to F-actin filaments (Montell, 2007), which contributes to maintaining the rhabdomere structure (Arikawa et al., 1990; Porter et al., 1992). Especially in the dark, INAD binds to TRP channels and keeps them in the rhabdomeres, ready for activation, while after light adaptation, TRP channels translocate into the cell body (Montell, 2007).

An important component of the Signalplex is calmodulin (CaM), which binds to INAD (Chevesich et al., 1997; Tsunoda et al., 1997; Xu et al., 1998), NINAC, TRP, and TRPL channels (Phillips et al., 1992; Warr and Kelly, 1996), and the rhodopsin phosphatase Retinal degeneration C (RdgC), inducing photoresponse termination (Lee and Montell, 2001). We have identified and characterized a functional CaM binding motif in the CRY CTT and demonstrated that CaM bridges CRY and INAD, forming a ternary complex *in vivo* (Mazzotta et al., 2018). We therefore hypothesized that the light-dependent CRY function in the photoreceptors may consist of fast and slow responses: a rapid light response, mediated by CRY conformational changes, would stimulate the direct interaction with INAD, and a novel, slower mechanism regulated by CaM would enhance its functional response (Mazzotta et al., 2018; **Figure 4**).

Cryptochrome interaction with the visual signaling cascade at the membrane of photoreceptor cells appears to enhance photosensitivity, especially during the night, perhaps by strengthening the interaction between INAD, NINAC, and

F-actin and thus increasing the activation of TRP channels (Mazzotta et al., 2013). CRY in photoreceptor cells ultimately modulates circadian visual sensitivity: indeed, while wild-type flies show maximal sensitivity (measured by electroretinogram, ERG) in the first part of the night (Chen et al., 1992), in *cry* mutants, such sensitivity does not depend on the time of day (Mazzotta et al., 2013). Similar results are observed for optomotor turning response (Barth et al., 2010; Mazzotta et al., 2013), and rescue experiments show that this effect is specific for CRY expressed only in photoreceptors (Mazzotta et al., 2013). Moreover, flies expressing constitutively active CRY (CRYΔ) show optomotor turning response at very low levels, as a result of an impairment in either detecting movements or processing information (Damulewicz et al., 2017). Indeed, we have observed an involvement of CRY in the light-dependent degradation of the presynaptic scaffolding protein Bruchpilot (BRP), its direct partner in the photoreceptor terminals within the lamina (Damulewicz et al., 2017). The daily pattern of BRP in tetrad synapses in the distal lamina (Meinertzhagen and O'Neil, 1991; Górska-Andrzejak et al., 2013) is altered in cry^0 mutants, with higher levels during the day; by contrast, in CRYΔ-overexpressing flies, the daily pattern of BRP is maintained, albeit with extremely low levels of protein (Damulewicz et al., 2017).

We have shown that in the rhabdomeres, CRY interacts also with F-actin, probably reinforcing the binding of the phototransduction cascade signaling components to the rhabdomere cytoskeleton (Schlichting et al., 2018). CRY/F-actin interaction is enhanced by light, but it exists also during darkness, keeping the Signalplex close to the membrane and ready for activation during the night (Schlichting et al., 2018). Furthermore, the strong affinity of CRY for F-actin could also prevent its degradation through the proteasome: indeed, in the rhabdomeres, CRY is not degraded by light, while in the somata of photoreceptors cells, its levels strongly decrease after light exposure (Schlichting et al., 2018). CRY in the photoreceptor cells is involved in the ability of flies to entrain their locomotor behavior to red-light cycles, a role that is largely independent of its photoreceptive function, since red light is not able to induce CRY-mediated photoresetting of the clock (Schlichting et al., 2018).

CRY AND NEURONAL ACTIVITY: UV-LIGHT RESPONSE AND AROUSAL

Drosophila l-LN_vs show higher daytime light-driven spontaneous action potential firing rate: this electrophysiological response is attenuated either in the cry^b hypomorphic mutant or in flies with disrupted opsin-based phototransduction (Sheeba et al., 2008; Fogle et al., 2015) and completely abolished in cry^0 flies (Fogle et al., 2011) but is functionally rescued by targeted expression of CRY in the l-LN_vs (Fogle et al., 2015). Indeed, these neurons undergo a CRY-dependent rapid membrane depolarization and augmented spontaneous action potential firing rate upon illumination with blue light (Fogle et al., 2011). CRY is involved in membrane depolarization by a redox-based mechanism mediated by potassium channel heteromultimeric complexes consisting of redox sensor potassium channel beta-subunit (Kvβ) HYPERKINETIC (Hk) and other channels such as Shaker, Ether-a-go-go, and Ether-a-go-go-related gene (Fogle et al., 2015; Hong et al., 2018). Interestingly, the expression of CRY in innately light-insensitive neurons renders them light responsive (Fogle et al., 2011). Furthermore, it is worth noticing that such CRY-mediated light response, involving a flavin redox-based mechanism and relying on potassium channel conductance, is independent of the circadian interaction of CRY with TIM (Fogle et al., 2011). Also, in non-neural tissues, like salivary glands, which lack a peripheral clock, CRY maintains high membrane input resistance in an Hk, Shaker, and Ether-a-go-go-dependent but light-independent manner (Agrawal et al., 2017). Very interestingly, it was recently reported that light-evoked CRY membrane electrical depolarization involves W420, located in proximity to CRY FAD and important for CRY-mediated depolarization in responses to not only UV and blue but also red light, at relatively low light intensity (Baik et al., 2019).

The electric activity of l-LN_vs triggers two circadian behaviors in *Drosophila*: UV light avoidance/attraction and sleep/arousal (Baik et al., 2017, 2018).

Like several insects, *Drosophila* shows a rhythmic short-wavelength (UV) light avoidance, a physiological and behavioral response to sunlight which is essential for survival. This peak of UV avoidance coincides with siesta in adult flies and with peak UV light intensity in the environment (Baik et al., 2017). CRY mediates the l-LN_vs electrophysiological response to UV light: indeed, it is significantly attenuated in cry^0 and hk^0 mutant flies and rescued by LN_v-targeted expression of CRY (Baik et al., 2017, 2018).

In l-LN_vs, CRY is also involved in the dopamine signaling pathway responsible for acute arousal upon sensory stimulation. Indeed, the clock mutant Clk^{Jrk} flies, which exhibit nocturnal behavior and a clock-independent reduction in total sleep time (Kim et al., 2002; Lu et al., 2008), also display high levels of CRY, which drive nighttime activity (Kumar et al., 2012). This nocturnal behavior of Clk^{Jrk} mutants largely depends on increased dopamine, since it is suppressed by blocking dopamine signaling, either pharmacologically or genetically (Kumar et al., 2012). High levels of dopamine act as a trigger to activate CRY, which promotes nocturnal activity. This role of CRY is limited to the night since light induces either CRY degradation (Lin et al., 2001) or the inhibition of dopamine signaling (Shang et al., 2011).

CRY AND THE REGULATION OF METABOLIC PROCESSES

Wild-type flies show a rhythmic feeding behavior, which is under circadian and homeostatic control and depends on light exposure and food availability (Xu et al., 2008). Under LD cycles, flies show a feeding peak at ZT 0–2; this rhythm is maintained in DD, but a late-evening feeding bout is observed at CT20-4 (Seay and Thummel, 2011). Although endogenous, the rhythm is regulated by light, and CRY has been identified as the light-signaling factor

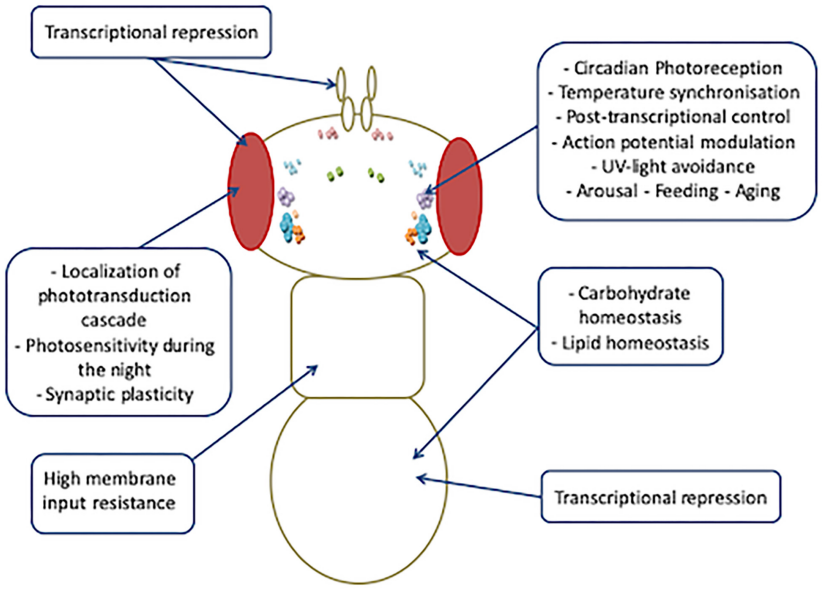

FIGURE 5 | Overview of tissue-specific activities of CRY.

involved in suppression of the evening feed activity observed in DD (Xu et al., 2008). Indeed, in LD, *cry* mutants exhibit the early morning feeding activity displayed by wild-type flies, but in addition, they also show the late-evening feeding activity, similar to that of wild-type flies in DD (Xu et al., 2008). However, this role of light-activated CRY is not dependent on light-induced TIM degradation, since *tim* mutants in LD do not show the evening feeding activity (Xu et al., 2008).

Cryptochrome function is also important for metabolic processes and carbohydrate homeostasis. Indeed, in LD-entrained wild-type flies, trehalose, the predominant circulating form of sugar in flies, is at its lowest values at the beginning of the day and increases to up 80% 4 h after feeding. Most of this sugar is confined as stored energy, and glycogen levels reach maximum values at the end of the day, accordingly (Seay and Thummel, 2011). The oscillation in glycogen concentrations is a clock-dependent process as, although dampened, it persists in constant conditions, while a clear rhythm is absent in *tim* mutants in both LD and DD (Seay and Thummel, 2011). The phase of glycogen accumulation is significantly anticipated in cry^{01} flies entrained in LD, indicating the involvement of light-activated CRY in setting the phase of this oscillation, and this observation is further supported by the dampened oscillation of glycogen accumulation observed in DD, when CRY is not activated by light (Seay and Thummel, 2011). This metabolic alteration observed in cry^{01} flies, which still possess a functioning clock, indicates that the role of CRY in setting the phase of accumulation and utilization of glycogen is not related to the canonical clock function.

In mammals, CRY1 is also involved in the regulation of gluconeogenesis by CREB/cAMP signaling through rhythmic repression of glucocorticoid receptor and decreasing the level of nuclear FoxO1 (Hatori and Panda, 2010; Zhang E.E. et al., 2010; Lamia et al., 2011; Jang et al., 2016). Moreover, CRY1 interacts with the autophagosome marker light chain 3 (LC3), responsible for its time-dependent autophagic degradation (Toledo et al., 2018). (LC3)-interacting region (LIR) motifs are found in the CRY1 sequence, and their role has been confirmed by the observation that mice in which autophagy is genetically blocked exhibit accumulation of CRY1 and disruption of the circadian clock in the liver (Toledo et al., 2018). Moreover, autophagic degradation of CRY1 is important in maintaining blood glucose levels by driving gluconeogenesis (Toledo et al., 2018). As in mammals (Turek et al., 2005; Green et al., 2008), the circadian clock is involved in fat storage and mobilization also in *Drosophila*. Indeed, a significantly reduced triacylglycerol concentration is observed in tim^{0} compared to wild-type LD-entrained flies (Seay and Thummel, 2011), and an altered *Clk* function in the PDF neurons results in increased fat body triglycerides (DiAngelo et al., 2011). On the other hand, a significant reduction in triacylglycerol levels is observed in both *cry* mutants reared in LD and in wild-type flies after 2 days of DD compared to LD, indicating that also light input seems to be necessary for lipid homeostasis (Seay and Thummel, 2011). In mammals, *Cry1* mutation does not significantly affect triglycerides and fatty acid blood levels (Griebel et al., 2014), while *Cry1/2*-deficient mice exhibit increased insulin secretion and lipid storage in the adipose tissue under a high-fat diet (Barclay et al., 2013).

CRY AND AGING

Aging is a process affecting most physiological processes. The circadian clock plays an important role in the aging processes: indeed, its disruption leads to accelerated aging in animals

(Davidson et al., 2006; Kondratov et al., 2006; Antoch et al., 2008; Yu and Weaver, 2011), and older individuals show decreased amplitude of clock gene oscillation and changes in rhythmicity, that is, sleep/wake cycles and hormonal fluctuations (Valentinuzzi et al., 1997; Huang et al., 2002; Hofman and Swaab, 2006; Kondratova and Kondratov, 2012). Similar effects are observed in *Drosophila*, where clock mutants exhibit increased oxidative stress levels and neurodegeneration (Krishnan et al., 2009, 2012) and changes in sleep patterns and clock gene expression amplitude are observed in older flies (Koh et al., 2006a; Luo et al., 2012; Rakshit et al., 2012; Umezaki et al., 2012; Solovev et al., 2019). It has been reported that CRY is reduced at both mRNA and protein levels in the heads of older flies and that its overexpression in the nervous system or in all clock-expressing cells is able to increase the amplitude of clock gene expression levels and survival under hypoxia (Rakshit and Giebultowicz, 2013; Solovev et al., 2019). cry^0 flies exhibit an accelerated functional decline, in terms of decreased climbing activity, accumulation of oxidatively damaged proteins and reduced health span (Rakshit and Giebultowicz, 2013; Solovev et al., 2019). CRY overexpression in the entire nervous system and in both central and peripheral oscillators maintains the rhythmicity of locomotor activity, increases climbing performance, and decreases recovery time after short-term hypoxia in older flies (Rakshit and Giebultowicz, 2013; Solovev et al., 2019). Nevertheless, the overexpression of CRY limited to clock neurons is not sufficient to slow down the aging processes or to reverse age-associated phenotypes (Rakshit and Giebultowicz, 2013).

CONCLUSION

Increasing evidence indicates that the spectrum of biological functions of *Drosophila* CRY is wider than that exerted in circadian clocks (**Figure 5**).

More intriguingly, all such photoreceptor-independent roles of CRY seem to be cell or tissue specific, and different regulating mechanisms might account for the high versatility of its functioning. At least four different tissue-specific regulation mechanisms could make CRY pleiotropy possible: (1) In the clock neurons, the blue light-dependent FAD photoreduction induces conformational changes in the Trp tetrad, which results in the displacement of the CTT from the photolyase homology domain and in consequent protein activation (Zoltowski et al., 2011; Czarna et al., 2013; Levy et al., 2013; Vaidya et al., 2013; Masiero et al., 2014; Lin et al., 2018). (2) In the l-LN_vs, light-evoked CRY membrane electrical depolarization involves W420, which is located closest to CRY FAD and is important for CRY-mediated depolarization in response not only to UV and blue light but also to red light, at a relatively low intensity (Baik et al., 2019). (3) Also in the l-LN_vs, the CRY-mediated nocturnal activity of *Clk* mutant flies largely depends on dopamine signaling that increases CRY levels and switches these cells, which normally promote arousal in response to light, to nocturnal behavior (Kumar et al., 2012). (4) In the photoreceptor cells, CRY interacts with CaM in a Ca^{2+}-dependent and light-independent manner. We have hypothesized this interaction to be functional to a Ca^{2+}–CaM-dependent activation that would enhance the light-dependent CRY response (Mazzotta et al., 2018). It is possible that this mechanism might not be restricted to the photoreceptor cells, and further studies are needed to investigate whether a Ca^{2+}–CaM-dependent mechanism might account for the activation/regulation of CRY activity in roles other than photoreception.

The versatility of CRY functioning in *Drosophila* shows several similarities with vertebrate CRYs that, besides being negative autoregulators of the circadian clock, also act as second messengers between the core clock and other cellular processes, such as maintenance of cellular and genomic integrity, and metabolism (Van Der Horst et al., 1999; Shearman et al., 2000; Hirayama et al., 2003; Kiyohara et al., 2006; Sato et al., 2006; McCarthy et al., 2009; Kang et al., 2010; Lamia et al., 2011; Narasimamurthy et al., 2012; Kang and Leem, 2014; Papp et al., 2015).

However, the nature of the transduction signaling involving CRYs remains largely unknown. Further studies, aimed at identifying the signal transduction underlying light-independent CRY functions, will help to improve the understanding of the biology of circadian rhythm regulation.

AUTHOR CONTRIBUTIONS

MD and GM wrote the manuscript.

FUNDING

This work was funded by grants from the Polish National Science Centre (Narodowe Centrum Nauki, NCN_Grant UMO-2014/15/D/NZ3/05207) and Polish National Agency for Academic Exchange to MD.

REFERENCES

Agrawal, P., Houl, J. H., Gunawardhana, K. L., Liu, T., Zhou, J., and Zoran, M. J. (2017). *Drosophila* CRY entrains clocks in body tissues to light and maintains passive membrane properties in a non-clock body tissue independent of light. *Curr. Biol.* 27, 2431.e3–2441.e3. doi: 10.1016/j.cub.2017.06.064

Antoch, M. P., Gorbacheva, V. Y., Vykhovanets, O., Toshkov, I. A., Kondratov, R. V., and Kondratova, A. A. (2008). Disruption of the circadian clock due to the clock mutation has discrete effects on aging and carcinogenesis. *Cell Cycle* 7, 1197–1204. doi: 10.4161/cc.7.9.5886

Arikawa, K., Hicks, J. L., and Williams, D. S. (1990). Identification of actin filaments in the rhabdomeral microvilli of *Drosophila* photoreceptors. *J. Cell Biol.* 110, 1993–1998. doi: 10.1083/jcb.110.6.1993

Baik, L. S., Fogle, K. J., Roberts, L., Galschiodt, A. M., Chevez, J. A., and Recinos, Y. (2017). CRYPTOCHROME mediates behavioral executive choice in response to UV light. *Proc. Natl. Acad. Sci. U.S.A.* 114, 776–781. doi: 10.1073/pnas.1607989114

Baik, L. S., Recinos, Y., Chevez, J. A., Au, D. D., and Holmes, T. C. (2019). Multiple phototransduction inputs integrate to mediate UV light–evoked avoidance/attraction behavior in *Drosophila*. *J. Biol. Rhythms* 34, 391–400. doi: 10.1177/0748730419847339

Baik, L. S., Recinos, Y., Chevez, J. A., and Holmes, T. C. (2018). Circadian modulation of light-evoked avoidance/attraction behavior in *Drosophila*. *PLoS One* 13:e0201927. doi: 10.1371/journal.pone.0201927

Barclay, J. L., Shostak, A., Leliavski, A., Tsang, A. H., Jöhren, O., and Müller-Fielitz, H. (2013). High-fat diet-induced hyperinsulinemia and tissue-specific insulin resistance in Cry-deficient mice. *Am. J. Physiol. Endocrinol. Metab.* 304, E1053–E1063. doi: 10.1152/ajpendo.00512.2012

Barth, M., Schultze, M., Schuster, C. M., and Strauss, R. (2010). Circadian plasticity in photoreceptor cells controls visual coding efficiency in *Drosophila melanogaster*. *PLoS One* 5:e9217. doi: 10.1371/journal.pone.0009217

Bazalova, O., Kvicalova, M., Valkova, T., Slaby, P., Bartos, P., Netusil, R., et al. (2016). Cryptochrome 2 mediates directional magnetoreception in cockroaches. *Proc. Natl. Acad. Sci. U.S.A.* 113:201518622. doi: 10.1073/pnas.1518622113

Benito, J., Houl, J. H., Roman, G. W., and Hardin, P. E. (2008). The blue-light photoreceptor CRYPTOCHROME is expressed in a subset of circadian oscillator neurons in the *Drosophila* CNS. *J. Biol. Rhythms* 23, 296–307. doi: 10.1177/0748730408318588

Berntsson, O., Rodriguez, R., Henry, L., Panman, M. R., Hughes, A. J., and Einholz, C. (2019). Photoactivation of Drosophila melanogaster cryptochrome through sequential conformational transitions. *Sci. Adv.* 5:eaaw1531. doi: 10.1126/sciadv.aaw1531

Boothroyd, C. E., Wijnen, H., Naef, F., Saez, L., and Young, M. W. (2007). Integration of light and temperature in the regulation of circadian gene expression in *Drosophila*. *PLoS Genet.* 3:e54. doi: 10.1371/journal.pgen.0030054

Busza, A., Emery-Le, M., Rosbash, M., and Emery, P. (2004). Roles of the two *Drosophila* CRYPTOCHROME structural domains in circadian photoreception. *Science* 304, 1503–1506. doi: 10.1126/science.1096973

Ceriani, M. F., Darlington, T. K., Staknis, D., Más, P., Petti, A. A., Weitz, C. J., et al. (1999). Light-dependent sequestration of TIMELESS by CRYPTOCHROME. *Science* 285, 553–556. doi: 10.1126/science.285.5427.553

Chaves, I., Pokorny, R., Byrdin, M., Hoang, N., Ritz, T., and Brettel, K. (2011). The cryptochromes: blue light photoreceptors in plants and animals. *Annu. Rev. Plant Biol.* 62, 335–364. doi: 10.1146/annurev-arplant-042110-103759

Chen, D. M., Christianson, J. S., Sapp, R. J., and Stark, W. S. (1992). Visual receptor cycle in normal and period mutant *Drosophila*: microspectrophotometry, electrophysiology, and ultrastructural morphometry. *Vis. Neurosci.* 9, 125–135. doi: 10.1017/S0952523800009585

Chevesich, J., Kreuz, A. J., and Montell, C. (1997). Requirement for the PDZ domain protein, INAD, for localization of the TRP store-operated channel to a signaling complex. *Neuron* 18, 95–105. doi: 10.1016/s0896-6273(01)80049-0

Collins, B., Mazzoni, E. O., Stanewsky, R., and Blau, J. (2006). *Drosophila* CRYPTOCHROME is a circadian transcriptional repressor. *Curr. Biol.* 16, 441–449. doi: 10.1016/j.cub.2006.01.034

Currie, J., Goda, T., and Wijnen, H. (2009). Selective entrainment of the *Drosophila* circadian clock to daily gradients in environmental temperature. *BMC Biol.* 7:49. doi: 10.1186/1741-7007-7-49

Cusumano, P., Damulewicz, M., Carbognin, E., Caccin, L., Puricella, A., and Specchia, V. (2019). The RNA helicase BELLE Is involved in circadian rhythmicity and in transposons regulation in drosophila melanogaster. *Front. Physiol.* 10:133. doi: 10.3389/fphys.2019.00133

Cyran, S. A., Buchsbaum, A. M., Reddy, K. L., Lin, M. C., Glossop, N. R. J., Hardin, P. E., et al. (2003). vrille, Pdp1, and dClock form a second feedback loop in the *Drosophila* circadian clock. *Cell* 112, 329–341. doi: 10.1016/s0092-8674(03)00074-6

Czarna, A., Berndt, A., Singh, H. R., Grudziecki, A., Ladurner, A. G., and Timinszky, G. (2013). Structures of drosophila cryptochrome and mouse cryptochrome1 provide insight into circadian function. *Cell* 153, 1394–1405. doi: 10.1016/j.cell.2013.05.011

Damulewicz, M., Mazzotta, G. M., Sartori, E., Rosato, E., Costa, R., and Pyza, E. M. (2017). Cryptochrome is a regulator of synaptic plasticity in the visual system of *Drosophila melanogaster*. *Front. Mol. Neurosci.* 10:165. doi: 10.3389/fnmol.2017.00165

Damulewicz, M., and Pyza, E. (2011). The clock input to the first optic neuropil of *Drosophila melanogaster* expressing neuronal circadian plasticity. *PLoS One* 6:e21258. doi: 10.1371/journal.pone.0021258

Davidson, A. J., Sellix, M. T., Daniel, J., Yamazaki, S., Menaker, M., and Block, G. D. (2006). Chronic jet-lag increases mortality in aged mice. *Curr. Biol.* 16, R914–R916. doi: 10.1016/j.cub.2006.09.058

DiAngelo, J. R., Erion, R., Crocker, A., and Sehgal, A. (2011). The central clock neurons regulate lipid storage in *Drosophila*. *PLoS One* 6:e19921. doi: 10.1371/journal.pone.0019921

Dissel, S., Codd, V., Fedic, R., Garner, K. J., Costa, R., Kyriacou, C. P., et al. (2004). A constitutively active cryptochrome in *Drosophila melanogaster*. *Nat. Neurosci.* 7, 834–840. doi: 10.1038/nn1285

Dodson, C. A., Hore, P. J., and Wallace, M. I. (2013). A radical sense of direction: signalling and mechanism in cryptochrome magnetoreception. *Trends Biochem. Sci.* 38, 435–446. doi: 10.1016/j.tibs.2013.07.002

Dolezelova, E., Dolezel, D., and Hall, J. C. (2007). Rhythm defects caused by newly engineered null mutations in *Drosophila*'s cryptochrome gene. *Genetics* 177, 329–345. doi: 10.1534/genetics.107.076513

Emery, P., So, W. V., Kaneko, M., Hall, J. C., and Rosbash, M. (1998). CRY, a *Drosophila* clock and light-regulated cryptochrome, is a major contributor to circadian rhythm resetting and photosensitivity. *Cell* 95, 669–679. doi: 10.1016/s0092-8674(00)81637-2

Emery, P., Stanewsky, R., Hall, J. C., and Rosbash, M. (2000). A unique circadian-rhythm photoreceptor. *Nature* 404, 456–457. doi: 10.1038/35006558

Fedele, G., Edwards, M. D., Bhutani, S., Hares, J. M., Murbach, M., Green, E. W., et al. (2014a). Genetic analysis of circadian responses to low frequency electromagnetic fields in *Drosophila melanogaster*. *PLoS Genet.* 10:e1004804. doi: 10.1371/journal.pgen.1004804

Fedele, G., Green, E. W., Rosato, E., and Kyriacou, C. P. (2014b). An electromagnetic field disrupts negative geotaxis in *Drosophila* via a CRY-dependent pathway. *Nat. Commun.* 5:4391. doi: 10.1038/ncomms5391

Fogle, K. J., Baik, L. S., Houl, J. H., Tran, T. T., Roberts, L., and Dahm, N. A. (2015). CRYPTOCHROME-mediated phototransduction by modulation of the potassium ion channel β-subunit redox sensor. *Proc. Natl. Acad. Sci. U.S.A.* 112, 2245–2250. doi: 10.1073/pnas.1416586112

Fogle, K. J., Parson, K. G., Dahm, N. A., Holmes, T. C., Sheeba, V., Parisky, K. M., et al. (2011). CRYPTOCHROME is a blue-light sensor that regulates neuronal firing rate. *Science* 331, 1409–1413. doi: 10.1126/science.1199702

Ganguly, A., Manahan, C. C., Top, D., Yee, E. F., Lin, C., and Young, M. W. (2016). Changes in active site histidine hydrogen bonding trigger cryptochrome activation. *Proc. Natl. Acad. Sci. U.S.A.* 113, 10073–10078. doi: 10.1073/pnas.1606610113

Gegear, R. J., Casselman, A., Waddell, S., and Reppert, S. M. (2008). Cryptochrome mediates light-dependent magnetosensitivity in *Drosophila*. *Nature* 454, 1014–1018. doi: 10.1038/nature07183

Gegear, R. J., Foley, L. E., Casselman, A., and Reppert, S. M. (2010). Animal cryptochromes mediate magnetoreception by an unconventional photochemical mechanism. *Nature* 463, 804–807. doi: 10.1038/nature08719

Gentile, C., Sehadova, H., Simoni, A., Chen, C., and Stanewsky, R. (2013). Cryptochrome antagonizes synchronization of *Drosophila*'s circadian clock to temperature cycles. *Curr. Biol.* 23, 185–195. doi: 10.1016/j.cub.2012.12.023

Giachello, C. N. G., Scrutton, N. S., Jones, A. R., and Baines, R. A. (2016). Magnetic fields modulate blue-light-dependent regulation of neuronal firing by cryptochrome. *J. Neurosci.* 36, 10742–10749. doi: 10.1523/JNEUROSCI.2140-16.2016

Glaser, F. T., and Stanewsky, R. (2005). Temperature synchronization of the *Drosophila* circadian clock. *Curr. Biol.* 15, 1352–1363. doi: 10.1016/j.cub.2005.06.056

Glossop, N. R. J., Houl, J. H., Zheng, H., Ng, F. S., Dudek, S. M., and Hardin, P. E. (2003). vrille feeds back to control circadian transcription of Clock in the *Drosophila* circadian oscillator. *Neuron* 37, 249–261. doi: 10.1016/s0896-6273(03)00002-3

Goda, T., Sharp, B., and Wijnen, H. (2014). Temperature-dependent resetting of the molecular circadian oscillator in *Drosophila*. *Proc. Biol. Sci.* 281:20141714. doi: 10.1098/rspb.2014.1714

Górska-Andrzejak, J., Makuch, R., Stefan, J., Görlich, A., Semik, D., and Pyza, E. (2013). Circadian expression of the presynaptic active zone protein bruchpilot in the lamina of *Drosophila melanogaster*. *Dev. Neurobiol.* 73, 14–26. doi: 10.1002/dneu.22032

Gould, C. M., Diella, F., Via, A., Puntervoll, P., Gemünd, C., and Chabanis-Davidson, S. (2009). ELM: the status of the 2010 eukaryotic linear motif resource. *Nucleic Acids Res.* 38, D167–D180. doi: 10.1093/nar/gkp1016

Green, C. B., Takahashi, J. S., and Bass, J. (2008). The meter of metabolism. *Cell* 134, 728–742. doi: 10.1016/j.cell.2008.08.022

Griebel, G., Ravinet-Trillou, C., Beeské, S., Avenet, P., and Pichat, P. (2014). Mice deficient in cryptochrome 1 (Cry1-/-) exhibit resistance to obesity induced by a high-fat diet. *Front. Endocrinol.* 5:49. doi: 10.3389/fendo.2014.00049

Günther, A., Einwich, A., Sjulstok, E., Feederle, R., Bolte, P., and Koch, K. W. (2018). Double-cone localization and seasonal expression pattern suggest a role in magnetoreception for European robin cryptochrome 4. *Curr. Biol.* 28, 211.e4–223.e4. doi: 10.1016/j.cub.2017.12.003

Hardie, R. C., and Juusola, M. (2015). Phototransduction in *Drosophila*. *Curr. Opin. Neurobiol.* 34, 37–45. doi: 10.1016/j.conb.2015.01.008

Hatori, M., and Panda, S. (2010). CRY links the circadian clock and CREB-mediated gluconeogenesis. *Cell Res.* 20, 1285–1288. doi: 10.1038/cr.2010.152

Helfrich-Förster, C. (2005). Neurobiology of the fruit fly's circadian clock. *Genes Brain Behav.* 4, 65–76. doi: 10.1111/j.1601-183X.2004.00092.x

Helfrich-Förster, C., Winter, C., Hofbauer, A., Hall, J. C., and Stanewsky, R. (2001). The circadian clock of fruit flies is blind after elimination of all known photoreceptors. *Neuron* 30, 249–261. doi: 10.1016/S0896-6273(01)00277-X

Hemsley, M. J., Mazzotta, G. M., Mason, M., Dissel, S., Toppo, S., Pagano, M. A., et al. (2007). Linear motifs in the C-terminus of *D. melanogaster* cryptochrome. *Biochem. Biophys. Res. Commun.* 355, 531–537.doi: 10.1016/j.bbrc.2007.01.189

Hermann-Luibl, C., and Helfrich-Förster, C. (2015). Clock network in *Drosophila*. *Curr. Opin. Insect Sci.* 7, 65–70. doi: 10.1016/j.cois.2014.11.003

Hirayama, J., Nakamura, H., Ishikawa, T., Kobayashi, Y., and Todo, T. (2003). Functional and structural analyses of cryptochrome. Vertebrate CRY regions responsible for interaction with the CLOCK:BMAL1 heterodimer and its nuclear localization. *J. Biol. Chem.* 278, 35620–35628. doi: 10.1074/jbc.M305028200

Hofman, M. A., and Swaab, D. F. (2006). Living by the clock: the circadian pacemaker in older people. *Ageing Res. Rev.* 5, 33–51. doi: 10.1016/j.arr.2005.07.001

Hong, G., Pachter, R., and Ritz, T. (2018). Coupling *Drosophila melanogaster* cryptochrome light activation and oxidation of the Kvβ subunit hyperkinetic NADPH cofactor. *J. Phys. Chem. B* 122, 6503–6510. doi: 10.1021/acs.jpcb.8b03493

Huang, Y. L., Liu, R. Y., Wang, Q. S., Van Someren, E. J. W., Xu, H., and Zhou, J. N. (2002). Age-associated difference in circadian sleep-wake and rest-activity rhythms. *Physiol. Behav.* 76, 597–603. doi: 10.1016/s0031-9384(02)00733-3

Ihry, R. J., Sapiro, A. L., and Bashirullah, A. (2012). Translational control by the DEAD box RNA helicase belle regulates ecdysone-triggered transcriptional cascades. *PLoS Genet.* 8:e1003085. doi: 10.1371/journal.pgen.1003085

Ishida, N., Kaneko, M., and Allada, R. (1999). Biological clocks. *Proc. Natl. Acad. Sci. U.S.A.* 96, 8819–8820. doi: 10.1073/pnas.96.16.8819

Ivanchenko, M., Stanewsky, R., and Giebultowicz, J. M. (2001). Circadian photoreception in Drosophila: functions of cryptochrome in peripheral and central clocks. *J. Biol. Rhythms* 16, 205–215. doi: 10.1177/074873040101600303

Jang, H., Lee, G. Y., Selby, C. P., Lee, G., Jeon, Y. G., and Lee, J. H. (2016). SREBP1c-CRY1 signalling represses hepatic glucose production by promoting FOXO1 degradation during refeeding. *Nat. Commun.* 7:12180. doi: 10.1038/ncomms12180

Johnstone, O., Deuring, R., Bock, R., Linder, P., Fuller, M. T., and Lasko, P. (2005). Belle is a *Drosophila* DEAD-box protein required for viability and in the germ line. *Dev. Biol.* 277, 92–101. doi: 10.1016/j.ydbio.2004.09.009

Kang, T. H., and Leem, S. H. (2014). Modulation of ATR-mediated DNA damage checkpoint response by cryptochrome 1. *Nucleic Acids Res.* 42, 4427–4434. doi: 10.1093/nar/gku094

Kang, T. H., Lindsey-Boltz, L. A., Reardon, J. T., and Sancar, A. (2010). Circadian control of XPA and excision repair of cisplatin-DNA damage by cryptochrome and HERC2 ubiquitin ligase. *Proc. Natl. Acad. Sci. U.S.A.* 107, 4890–4895. doi: 10.1073/pnas.0915085107

Kattnig, D. R., Nielsen, C., and Solov'Yov, I. A. (2018). Molecular dynamics simulations disclose early stages of the photo-Activation of cryptochrome 4. *New J. Phys.* 20:083018. doi: 10.1088/1367-2630/aad70f

Kim, E. Y., Bae, K., Ng, F. S., Glossop, N. R. J., Hardin, P. E., and Edery, I. (2002). *Drosophila* clock protein is under posttranscriptional control and influences light-induced activity. *Neuron* 34, 69–81. doi: 10.1016/s0896-6273(02)00639-6

Kiyohara, Y. B., Tagao, S., Tamanini, F., Morita, A., Sugisawa, Y., and Yasuda, M. (2006). The BMAL1 C terminus regulates the circadian transcription feedback loop. *Proc. Natl. Acad. Sci. U.S.A.* 103, 10074–10079. doi: 10.1073/pnas.0601416103

Koh, K., Evans, J. M., Hendricks, J. C., and Sehgal, A. (2006a). A *Drosophila* model for age-associated changes in sleep: wake cycles. *Proc. Natl. Acad. Sci. U.S.A.* 103, 13843–13847. doi: 10.1073/pnas.0605903103

Koh, K., Zheng, X., and Sehgal, A. (2006b). JETLAG resets the *Drosophila* circadian clock by promoting light-induced degradation of TIMELESS. *Science* 312, 1809–1812. doi: 10.1126/science.1124951

Kondratov, R. V., Kondratova, A. A., Gorbacheva, V. Y., Vykhovanets, O. V., and Antoch, M. P. (2006). Early aging and age-related pathologies in mice deficient in BMAL1, the core component of the circadian clock. *Genes Dev.* 20, 1868–1873. doi: 10.1101/gad.1432206

Kondratova, A. A., and Kondratov, R. V. (2012). The circadian clock and pathology of the ageing brain. *Nat. Rev. Neurosci.* 13, 325–335. doi: 10.1038/nrn3208

König, H. (1959). Atmospherics niedriger frequenzen. *Z. angew. Physik.* 11:264.

Konopka, R. J., Pittendrigh, C., and Orr, D. (1989). Reciprocal behaviour associated with altered homeostasis and photosensitivity of *Drosophila* clock mutants. *J. Neurogenet.* 6, 1–10. doi: 10.1080/01677060701695391

Krishnan, B., Levine, J. D., Lynch, M. K., Dowse, H. B., Funes, P., Hall, J. C., et al. (2001). A new role for cryptochrome in a *Drosophila* circadian oscillator. *Nature* 411, 313–317. doi: 10.1038/35077094

Krishnan, N., Kretzschmar, D., Rakshit, K., Chow, E., and Giebultowicz, J. M. (2009). The circadian clock gene period extends healthspan in aging *Drosophila melanogaster*. *Aging (Albany N. Y.)* 1, 937–948. doi: 10.18632/aging.100103

Krishnan, N., Rakshit, K., Chow, E. S., Wentzell, J. S., Kretzschmar, D., and Giebultowicz, J. M. (2012). Loss of circadian clock accelerates aging in neurodegeneration-prone mutants. *Neurobiol. Dis.* 45, 1129–1135. doi: 10.1016/j.nbd.2011.12.034

Kumar, S., Chen, D., and Sehgal, A. (2012). Dopamine acts through cryptochrome to promote acute arousal in *Drosophila*. *Genes Dev.* 26, 1224–1234. doi: 10.1101/gad.186338.111

Kutta, R. J., Archipowa, N., Johannissen, L. O., Jones, A. R., and Scrutton, N. S. (2017). Vertebrate cryptochromes are vestigial flavoproteins. *Sci. Rep.* 7:44906. doi: 10.1038/srep44906

Kutta, R. J., Archipowa, N., and Scrutton, N. S. (2018). The sacrificial inactivation of the blue-light photosensor cryptochrome from: *Drosophila melanogaster*. *Phys. Chem. Chem. Phys.* 20, 28767–28776. doi: 10.1039/c8cp04671a

Lamia, K. A., Papp, S. J., Yu, R. T., Barish, G. D., Uhlenhaut, N. H., and Jonker, J. W. (2011). Cryptochromes mediate rhythmic repression of the glucocorticoid receptor. *Nature* 480, 552–556. doi: 10.1038/nature10700

Lee, A. A., Lau, J. C. S., Hogben, H. J., Biskup, T., Kattnig, D. R., and Hore, P. J. (2014). Alternative radical pairs for cryptochrome-based magnetoreception. *J. R. Soc. Interface* 11:20131063. doi: 10.1098/rsif.2013.1063

Lee, S. J., and Montell, C. (2001). Regulation of the rhodopsin protein phosphatase, RDGC, through interaction with calmodulin. *Neuron* 32, 1097–1106. doi: 10.1016/s0896-6273(01)00538-4

Levine, J. D., Funes, P., Dowse, H. B., and Hall, J. C. (2002). Advanced analysis of a *cryptochrome* mutation's effects on the robustness and phase of molecular cycles in isolated peripheral tissues of *Drosophila*. *BMC Neurosci.* 3:5. doi: 10.1186/1471-2202-3-5

Levy, C., Zoltowski, B. D., Jones, A. R., Vaidya, A. T., Top, D., and Widom, J. (2013). Updated structure of *Drosophila* cryptochrome. *Nature* 495, E3–E4. doi: 10.1038/nature11995

Lin, C., Top, D., Manahan, C. C., Young, M. W., and Crane, B. R. (2018). Circadian clock activity of cryptochrome relies on tryptophan-mediated photoreduction. *Proc. Natl. Acad. Sci. U.S.A.* 115, 3822–3827. doi: 10.1073/pnas.1719376115

Lin, F.-J., Song, W., Meyer-Bernstein, E., Naidoo, N., and Sehgal, A. (2001). Photic signaling by cryptochrome in the *Drosophila* circadian system. *Mol. Cell. Biol.* 21, 7287–7294. doi: 10.1128/mcb.21.21.7287-7294.2001

Lin, W.-H., Gunay, C., Marley, R., Prinz, A. A., and Baines, R. A. (2012). Activity-dependent alternative splicing increases persistent sodium current and promotes seizure. *J. Neurosci.* 32, 7267–7277. doi: 10.1523/JNEUROSCI.6042-11.2012

Liu, C. H., Satoh, A. K., Postma, M., Huang, J., Ready, D. F., and Hardie, R. C. (2008). Ca2+-dependent metarhodopsin inactivation mediated by calmodulin and NINAC myosin III. *Neuron* 59, 778–789. doi: 10.1016/j.neuron.2008.07.007

Lu, B., Liu, W., Guo, F., and Guo, A. (2008). Circadian modulation of light-induced locomotion responses in *Drosophila melanogaster*. *Genes Brain Behav.* 7, 730–739. doi: 10.1111/j.1601-183X.2008.00411.x

Luo, W., Chen, W. F., Yue, Z., Chen, D., Sowcik, M., and Sehgal, A. (2012). Old flies have a robust central oscillator but weaker behavioral rhythms that can be improved by genetic and environmental manipulations. *Aging Cell* 11, 428–438. doi: 10.1111/j.1474-9726.2012.00800.x

Mandilaras, K., and Missirlis, F. (2012). Genes for iron metabolism influence circadian rhythms in *Drosophila melanogaster*. *Metallomics* 4, 928–936. doi: 10.1039/c2mt20065a

Marley, R., and Baines, R. A. (2011). Increased persistent Na+ current contributes to seizure in the slamdance bang-sensitive *Drosophila* mutant. *J. Neurophysiol.* 106, 18–29. doi: 10.1152/jn.00808.2010

Marley, R., Giachello, C. N. G., Scrutton, N. S., Baines, R. A., and Jones, A. R. (2014). Cryptochrome-dependent magnetic field effect on seizure response in *Drosophila larvae*. *Sci. Rep.* 4:5799. doi: 10.1038/srep05799

Marrus, S. B., Zeng, H., and Rosbash, M. (1996). Effect of constant light and circadian entrainment of perS flies: evidence for light-mediated delay of the negative feedback loop in *Drosophila*. *EMBO J.* 15, 6877–6886. doi: 10.1002/j.1460-2075.1996.tb01080.x

Masiero, A., Aufiero, S., Minervini, G., Moro, S., Costa, R., and Tosatto, S. C. E. (2014). Evaluation of the steric impact of flavin adenine dinucleotide in *Drosophila melanogaster* cryptochrome function. *Biochem. Biophys. Res. Commun.* 450, 1606–1611. doi: 10.1016/j.bbrc.2014.07.038

Mazzotta, G., Rossi, A., Leonardi, E., Mason, M., Bertolucci, C., Caccin, L., et al. (2013). Fly cryptochrome and the visual system. *Proc. Natl. Acad. Sci. U.S.A.* 110, 6163–6168. doi: 10.1073/pnas.1212317110

Mazzotta, G. M., Bellanda, M., Minervini, G., Damulewicz, M., Cusumano, P., and Aufiero, S. (2018). Calmodulin enhances cryptochrome binding to INAD in *Drosophila* photoreceptors. *Front. Mol. Neurosci.* 11:280. doi: 10.3389/fnmol.2018.00280

McCarthy, E. V., Baggs, J. E., Geskes, J. M., Hogenesch, J. B., and Green, C. B. (2009). Generation of a novel allelic series of cryptochrome mutants via mutagenesis reveals residues involved in protein-protein interaction and CRY2-specific repression. *Mol. Cell. Biol.* 29, 5465–5476. doi: 10.1128/MCB.00641-09

McDonald, M. J., and Rosbash, M. (2001). Microarray analysis and organization of circadian gene expression in *Drosophila*. *Cell* 107, 567–578. doi: 10.1016/s0092-8674(01)00545-1

Meinertzhagen, I. A., and O'Neil, S. D. (1991). Synaptic organization of columnar elements in the lamina of the wild type in *Drosophila melanogaster*. *J. Comp. Neurol.* 305, 232–263. doi: 10.1002/cne.903050206

Miyasako, Y., Umezaki, Y., and Tomioka, K. (2007). Separate sets of cerebral clock neurons are responsible for light and temperature entrainment of *Drosophila* circadian locomotor rhythms. *J. Biol. Rhythms* 22, 115–126. doi: 10.1177/0748730407299344

Montell, C. (2007). Dynamic regulation of the INAD signaling scaffold becomes crystal clear. *Cell* 131, 19–21. doi: 10.1016/j.cell.2007.09.022

Montell, C. (2012). *Drosophila* visual transduction. *Trends Neurosci.* 35, 356–363. doi: 10.1016/j.tins.2012.03.004

Montelli, S., Mazzotta, G., Vanin, S., Caccin, L., Corrà, S., De Pittà, C., et al. (2015). period and timeless mRNA splicing profiles under natural conditions in *Drosophila melanogaster*. *J. Biol. Rhythms* 30, 217–227. doi: 10.1177/0748730415583575

Müller, M., and Carell, T. (2009). Structural biology of DNA photolyases and cryptochromes. *Curr. Opin. Struct. Biol.* 19, 277–285. doi: 10.1016/j.sbi.2009.05.003

Müller, P., and Ahmad, M. (2011). Light-activated cryptochrome reacts with molecular oxygen to form a flavin-superoxide radical pair consistent with magnetoreception. *J. Biol. Chem.* 286, 21033–21040. doi: 10.1074/jbc.M111.228940

Narasimamurthy, R., Hatori, M., Nayak, S. K., Liu, F., Panda, S., and Verma, I. M. (2012). Circadian clock protein cryptochrome regulates the expression of proinflammatory cytokines. *Proc. Natl. Acad. Sci. U.S.A.* 109, 12662–12667. doi: 10.1073/pnas.1209965109

Neduva, V., and Russell, R. B. (2005). Linear motifs: evolutionary interaction switches. *FEBS Lett.* 579, 3342–3345. doi: 10.1016/j.febslet.2005.04.005

Özkaya, Ö, and Rosato, E. (2012). The circadian clock of the fly: a neurogenetics journey through time. *Adv. Genet.* 77, 79–123. doi: 10.1016/B978-0-12-387687-4.00004-0

Ozturk, N. (2017). Phylogenetic and functional classification of the photolyase/cryptochrome family. *Photochem. Photobiol.* 93, 104–111. doi: 10.1111/php.12676

Ozturk, N., Selby, C. P., Song, S. H., Ye, R., Tan, C., and Kao, Y. T. (2009). Comparative photochemistry of animal type 1 and type 4 cryptochromes. *Biochemistry* 48, 8585–8593. doi: 10.1021/bi901043s

Ozturk, N., Selby, C. P., Zhong, D., and Sancar, A. (2014). Mechanism of photosignaling by drosophila cryptochrome ROLE of the REDOX status of the flavin chromophore. *J. Biol. Chem.* 289, 4634–4642. doi: 10.1074/jbc.M113.542498

Öztürk, N., Song, S. H., Selby, C. P., and Sancar, A. (2008). Animal type 1 cryptochromes: analysis of the redox state of the flavin cofactor by site-directed mutagenesis. *J. Biol. Chem.* 283, 3256–3263. doi: 10.1074/jbc.M708612200

Ozturk, N., VanVickle-Chavez, S. J., Akileswaran, L., Van Gelder, R. N., and Sancar, A. (2013). Ramshackle (Brwd3) promotes light-induced ubiquitylation of *Drosophila* cryptochrome by DDB1-CUL4-ROC1 E3 ligase complex. *Proc. Natl. Acad. Sci.* 110, 4980–4985. doi: 10.1073/pnas.1303234110

Papp, S. J., Huber, A. L., Jordan, S. D., Kriebs, A., Nguyen, M., and Moresco, J. J. (2015). DNA damage shifts circadian clock time via hausp-dependent cry1 stabilization. *eLife* 4:e04883. doi: 10.7554/eLife.04883.001

Pek, J. W., and Kai, T. (2011). DEAD-box RNA helicase Belle/DDX3 and the RNA interference pathway promote mitotic chromosome segregation. *Proc. Natl. Acad. Sci. U.S.A.* 108, 12007–12012. doi: 10.1073/pnas.1106245108

Peschel, N., Chen, K. F., Szabo, G., and Stanewsky, R. (2009). Light-dependent interactions between the *Drosophila* circadian clock factors cryptochrome, jetlag, and timeless. *Curr. Biol.* 19, 241–247. doi: 10.1016/j.cub.2008.12.042

Phillips, A. M., Bull, A., and Kelly, L. E. (1992). Identification of a *Drosophila* gene encoding a calmodulin-binding protein with homology to the trp phototransduction gene. *Neuron* 8, 631–642. doi: 10.1016/0896-6273(92)90085-R

Pokorny, R., Klar, T., Hennecke, U., Carell, T., Batschauer, A., and Essen, L. O. (2008). Recognition and repair of UV lesions in loop structures of duplex DNA by DASH-type cryptochrome. *Proc. Natl. Acad. Sci. U.S.A.* 105, 21023–21027. doi: 10.1073/pnas.0805830106

Porter, J. A., Hicks, J. L., Williams, D. S., and Montell, C. (1992). Differential localizations of and requirements for the two *Drosophila* ninaC kinase/myosins in photoreceptor cells. *J. Cell Biol.* 116, 683–693. doi: 10.1083/jcb.116.3.683

Qin, S., Yin, H., Yang, C., Dou, Y., Liu, Z., Zhang, P., et al. (2016). A magnetic protein biocompass. *Nat. Mater.* 15, 217–226. doi: 10.1038/nmat4484

Rakshit, K., and Giebultowicz, J. M. (2013). Cryptochrome restores dampened circadian rhythms and promotes healthspan in aging *Drosophila*. *Aging Cell* 12, 752–762. doi: 10.1111/acel.12100

Rakshit, K., Krishnan, N., Guzik, E. M., Pyza, E., Giebultowicz, J. M., Jadwiga, M., et al. (2012). Effects of aging on the molecular circadian oscillations in *Drosophila*. *Chronobiol. Int.* 29, 5–14. doi: 10.3109/07420528.2011.635237. Effects

Rieger, D., Shafer, O. T., Tomioka, K., and Helfrich-Förster, C. (2006). Functional analysis of circadian pacemaker neurons in *Drosophila melanogaster*. *J. Neurosci.* 26, 2531–2543. doi: 10.1523/JNEUROSCI.1234-05.2006

Ritz, T., Adem, S., and Schulten, K. (2000). A model for photoreceptor-based magnetoreception in birds. *Biophys. J.* 78, 707–718. doi: 10.1016/S0006-3495(00)76629-X

Ritz, T., Yoshii, T., Helfrich-Foerster, C., and Ahmad, M. (2010). Cryptochrome: a photoreceptor with the properties of a magnetoreceptor? *Commun. Integr. Biol.* 3, 70–74. doi: 10.4161/cib.3.1.10300

Rosato, E., Codd, V., Mazzotta, G., Piccin, A., Zordan, M., Costa, R., et al. (2001). Light-dependent interaction between *Drosophila* CRY and the clock protein PER mediated by the carboxy terminus of CRY. *Curr. Biol.* 11, 909–917. doi: 10.1016/s0960-9822(01)00259-7

Sancar, A. (2003). Structure and function of DNA photolyase and cryptochrome blue-light photoreceptors. *Chem. Rev.* 103, 2203–2237. doi: 10.1021/cr0204348

Sandrelli, F., Tauber, E., Pegoraro, M., Mazzotta, G., Cisotto, P., and Landskron, J. (2007). A molecular basis for natural selection at the timeless locus in *Drosophila melanogaster*. *Science* 316, 1898–900. doi: 10.1126/science.1138426

Sathyanarayanan, S., Zheng, X., Kumar, S., Chen, C. H., Chen, D., Hay, B., et al. (2008). Identification of novel genes involved in light-dependent CRY degradation through a genome-wide RNAi screen. *Genes Dev.* 22, 1522–1533. doi: 10.1101/gad.1652308

Sato, T. K., Yamada, R. G., Ukai, H., Baggs, J. E., Miraglia, L. J., and Kobayashi, T. J. (2006). Feedback repression is required for mammalian circadian clock function. *Nat. Genet.* 38, 312–319. doi: 10.1038/ng1745

Schlichting, M., Rieger, D., Cusumano, P., Grebler, R., Costa, R., and Mazzotta, G. M. (2018). Cryptochrome interacts with actin and enhances eye-mediated light sensitivity of the circadian clock in *Drosophila melanogaster*. *Front. Mol. Neurosci.* 11:238. doi: 10.3389/fnmol.2018.00238

Seay, D. J., and Thummel, C. S. (2011). The circadian clock, light, and cryptochrome regulate feeding and metabolism in *Drosophila*. *J. Biol. Rhythms* 26, 497–506. doi: 10.1177/0748730411420080

Selby, C. P., and Sancar, A. (2006). A cryptochrome/photolyase class of enzymes with single-stranded DNA-specific photolyase activity. *Proc. Natl. Acad. Sci. U.S.A.* 103, 17696–17700. doi: 10.1073/pnas.0607993103

Shafer, O. T., Helfrich-Förster, C., Renn, S. C. P., and Taghert, P. H. (2006). Reevaluation of *Drosophila melanogaster*'s neuronal circadian pacemakers reveals new neuronal classes. *J. Comp. Neurol.* 498, 180–193. doi: 10.1002/cne.21021

Shafer, O. T., Kim, D. J., Dunbar-Yaffe, R., Nikolaev, V. O., Lohse, M. J., and Taghert, P. H. (2008). Widespread receptivity to neuropeptide pdf throughout the neuronal circadian clock network of *Drosophila* revealed by real-time cyclic AMP imaging. *Neuron* 58, 223–237. doi: 10.1016/j.neuron.2008.02.018

Shang, Y., Haynes, P., Pírez, N., Harrington, K. I, Guo, F., and Pollack, J. (2011). Imaging analysis of clock neurons reveals light buffers the wake-promoting effect of dopamine. *Nat. Neurosci.* 14, 889–895. doi: 10.1038/nn.2860

Shearman, L. P., Sriram, S., Weaver, D. R., Maywood, E. S., Chaves, I., and Zheng, B. (2000). Interacting molecular loops in the mammalian circadian clock. *Science* 288, 1013–1019. doi: 10.1126/science.288.5468.1013

Sheeba, V., Gu, H., Sharma, V. K., O'Dowd, D. K., and Holmes, T. C. (2008). Circadian- and light-dependent regulation of resting membrane potential and spontaneous action potential firing of *Drosophila* circadian pacemaker neurons. *J. Neurophys.* 99, 976–988. doi: 10.1152/jn.00930.2007

Solovev, I., Dobrovolskaya, E., Shaposhnikov, M., Sheptyakov, M., and Moskalev, A. (2019). Neuron-specific overexpression of core clock genes improves stress-resistance and extends lifespan of *Drosophila melanogaster*. *Exp. Gerontol.* 117, 61–71. doi: 10.1016/j.exger.2018.11.005

Stanewsky, R., Kaneko, M., Emery, P., Beretta, B., Wager-Smith, K., and Kay, S. A. (1998). The cryb mutation identifies cryptochrome as a circadian photoreceptor in *Drosophila*. *Cell* 95, 681–692. doi: 10.1016/s0092-8674(00)81638-4

Tauber, E., Zordan, M., Sandrelli, F., Pegoraro, M., Osterwalder, N., and Breda, C. (2007). Natural selection favors a newly derived timeless allele in *Drosophila melanogaster*. *Science* 316, 1895–1898. doi: 10.1126/science.1138412

Todo, T. (1999). Functional diversity of the DNA photolyase/blue light receptor family. *Mutat. Res. DNA Repair* 434, 89–97. doi: 10.1016/s0921-8777(99)00013-0

Toledo, M., Batista-Gonzalez, A., Merheb, E., Aoun, M. L., Tarabra, E., and Feng, D. (2018). Autophagy regulates the liver clock and glucose metabolism by degrading CRY1. *Cell Metab.* 28, 268.e4–281.e4. doi: 10.1016/j.cmet.2018.05.023

Tsunoda, S., Sierralta, J., Sun, Y., Bodner, R., Suzuki, E., Becker, A., et al. (1997). A multivalent PDZ-domain protein assembles signalling complexes in a G-protein-coupled cascade. *Nature* 388, 243–249. doi: 10.1038/40805

Turek, F. W., Joshu, C., Kohsaka, A., Lin, E., Ivanova, G., and McDearmon, E. (2005). Obesity and metabolic syndrome in circadian clock mutant nice. *Science* 308, 1043–1045. doi: 10.1126/science.1108750

Ueda, H. R., Matsumoto, A., Kawamura, M., Iino, M., Tanimura, T., and Hashimoto, S. (2002). Genome-wide transcriptional orchestration of circadian rhythms in *Drosophila*. *J. Biol. Chem.* 277, 14048–14052. doi: 10.1074/jbc.C100765200

Umezaki, Y., Yoshii, T., Kawaguchi, T., Helfrich-Förster, C., and Tomioka, K. (2012). Pigment-dispersing factor is involved in age-dependent rhythm changes in *Drosophila melanogaster*. *J. Biol. Rhythms* 27, 423–432. doi: 10.1177/0748730412462206

Vaidya, A. T., Top, D., Manahan, C. C., Tokuda, J. M., Zhang, S., and Pollack, L. (2013). Flavin reduction activates *Drosophila* cryptochrome. *Proc. Natl. Acad. Sci. U.S.A.* 110, 20455–20460. doi: 10.1073/pnas.1313336110

Valentinuzzi, V. S., Scarbrough, K., Takahashi, J. S., and Turek, F. W. (1997). Effects of aging on the circadian rhythm of wheel-running activity in C57BL/6 mice. *Am. J. Physiol. Regul. Integr. Comp. Physiol.* 273, R1957–R1964. doi: 10.1152/ajpregu.1997.273.6.r1957

Van Der Horst, G. T. J., Muijtjens, M., Kobayashi, K., Takano, R., Kanno, I., and Takao, M. (1999). Mammalian Cry1 and Cry2 are essential for maintenance of circadian rhythms. *Nature* 398, 627–630. doi: 10.1038/19323

VanVickle-Chavez, S. J., and Van Gelder, R. N. (2007). Action spectrum of *Drosophila* cryptochrome. *J. Biol. Chem.* 282, 10561–10566. doi: 10.1074/jbc.M609314200

Warr, C. G., and Kelly, L. E. (1996). Identification and characterization of two distinct calmodulin-binding sites in the Trpl ion-channel protein of *Drosophila melanogaster*. *Biochem. J.* 314, 497–503. doi: 10.1042/bj3140497

Worringer, K. A., Chu, F., and Panning, B. (2009). The zinc finger protein Zn72D and DEAD box helicase Belle interact and control maleless mRNA and protein levels. *BMC Mol. Biol.* 10:33. doi: 10.1186/1471-2199-10-33

Wu, C. L., Fu, T. F., Chiang, M. H., Chang, Y. W., Her, J. L., and Wu, T. (2016). Magnetoreception regulates male courtship activity in *Drosophila*. *PLoS One* 11:e0155942. doi: 10.1371/journal.pone.0155942

Xu, K., Zheng, X., and Sehgal, A. (2008). Regulation of feeding and metabolism by neuronal and peripheral clocks in *Drosophila*. *Cell Metab.* 8, 289–300. doi: 10.1016/j.cmet.2008.09.006

Xu, X. Z. S., Choudhury, A., Li, X., and Montell, C. (1998). Coordination of an array of signaling proteins through homo- and heteromeric interactions between PDZ domains and target proteins. *J. Cell Biol.* 142, 545–555. doi: 10.1083/jcb.142.2.545

Yadlapalli, S., Jiang, C., Bahle, A., Reddy, P., Meyhofer, E., and Shafer, O. T. (2018). Circadian clock neurons constantly monitor environmental temperature to set sleep timing. *Nature* 555, 98–102. doi: 10.1038/nature25740

Yang, Z., Liu, B., Su, J., Liao, J., Lin, C., and Oka, Y. (2017). Cryptochromes orchestrate transcription regulation of diverse blue light responses in plants. *Photochem. Photobiol.* 93, 112–127.

Yoshii, T., Ahmad, M., and Helfrich-Förster, C. (2009). Cryptochrome mediates light-dependent magnetosensitivity of *Drosophila*'s circadian clock. *PLoS Biol.* 7:e1000086. doi: 10.1371/journal.pbio.1000086

Yoshii, T., Funada, Y., Ibuki-Ishibashi, T., Matsumoto, A., Tanimura, T., and Tomioka, K. (2004). *Drosophila cry*^{b} mutation reveals two circadian clocks that drive locomotor rhythm and have different responsiveness to light. *J. Insect Physiol.* 50, 479–488. doi: 10.1016/j.jinsphys.2004.02.011

Yoshii, T., Hermann, C., and Helfrich-Förster, C. (2010). Cryptochrome-positive and -negative clock neurons in *Drosophila* entrain differentially to light and temperature. *J. Biol. Rhythms* 25, 387–398. doi: 10.1177/0748730410381962

Yoshii, T., Heshiki, Y., Ibuki-Ishibashi, T., Matsumoto, A., Tanimura, T., and Tomioka, K. (2005). Temperature cycles drive *Drosophila* circadian oscillation in constant light that otherwise induces behavioural arrhythmicity. *Eur. J. Neurosci.* 2, 1176–1184. doi: 10.1111/j.1460-9568.2005.04295.x

Yoshii, T., Todo, T., Wülbeck, C., Stanewsky, R., and Helfrich-Förster, C. (2008). Cryptochrome is present in the compound eyes and a subset of *Drosophila*'s clock neurons. *J. Compar. Neurol.* 508, 952–966. doi: 10.1002/cne.21702

Yu, E. A., and Weaver, D. R. (2011). Disrupting the circadian clock: gene-specific effects on aging, cancer, and other phenotypes. *Aging(Albany N. Y.)* 3, 479–493. doi: 10.18632/aging.100323

Yuan, Q., Metterville, D., Briscoe, A. D., and Reppert, S. M. (2007). Insect cryptochromes: gene duplication and loss define diverse ways to construct insect circadian clocks. *Mol. Biol. Evol.* 24, 948–955. doi: 10.1093/molbev/msm011

Zhang, E. E., Liu, Y., Dentin, R., Pongsawakul, P. Y., Liu, A. C., and Hirota, T. (2010). Cryptochrome mediates circadian regulation of cAMP signaling and hepatic gluconeogenesis. *Nat. Med.* 16, 1152–1156. doi: 10.1038/nm.2214

Zhang, Y., Liu, Y., Bilodeau-Wentworth, D., Hardin, P. E., and Emery, P. (2010). Light and temperature control the contribution of specific DN1 neurons to *Drosophila* circadian behavior. *Curr. Biol.* 20, 600–605. doi: 10.1016/j.cub.2010.02.044

Zoltowski, B. D., Vaidya, A. T., Top, D., Widom, J., Young, M. W., and Crane, B. R. (2011). Structure of full-length *Drosophila* cryptochrome. *Nature* 480, 396–399. doi: 10.1038/nature10618

Conflict of Interest: The authors declare that the research was conducted in the absence of any commercial or financial relationships that could be construed as a potential conflict of interest.

frontiers in Physiology

CORRECTION
published: 28 July 2020
doi: 10.3389/fphys.2020.00841

Corrigendum: One Actor, Multiple Roles: The Performances of Cryptochrome in *Drosophila*

Milena Damulewicz[1] *and Gabriella M. Mazzotta*[2]*

[1] Department of Cell Biology and Imaging, Jagiellonian University, Kraków, Poland, [2] Department of Biology, University of Padua, Padua, Italy

OPEN ACCESS

Approved by:
Frontiers Editorial Office, Frontiers Media SA, Switzerland

***Correspondence:**
Gabriella M. Mazzotta
gabriella.mazzotta@unipd.it

Specialty section:
This article was submitted to Invertebrate Physiology, a section of the journal Frontiers in Physiology

Received: *10 June 2020*
Accepted: *23 June 2020*
Published: *28 July 2020*

Citation:
Damulewicz M and Mazzotta GM (2020) Corrigendum: One Actor, Multiple Roles: The Performances of Cryptochrome in Drosophila. Front. Physiol. 11:841. doi: 10.3389/fphys.2020.00841

Keywords: cryptochrome, *Drosophila*, circadian clock, phototransduction, circadian plasticity, light-independent activity

A Corrigendum on

One Actor, Multiple Roles: The Performances of Cryptochrome in *Drosophila*
by Damulewicz, M., and Mazzotta, G. M. (2020). Front. Physiol. 11:99. doi: 10.3389/fphys.2020.00099

There is an error in the Funding statement. In the original article, we included by mistake the following funders: **CINCHRON: Comparative INsect CHRONobiology_European Union's Horizon 2020 under the Marie Skłodowska-Curie grant agreement no. 765937; National Research Council of Italy (EPIGEN Progetto Bandiera Epigenomica – Subproject 4) to GM**. These funders should be removed from the Funding Statement.

The authors apologize for these errors and state that they do not change the scientific conclusions of the article in any way. The original article has been updated.

frontiers in Physiology

REVIEW
published: 28 May 2020
doi: 10.3389/fphys.2020.00533

Drosophila as a Model to Study the Relationship Between Sleep, Plasticity, and Memory

*Stephane Dissel**

Department of Molecular Biology and Biochemistry, School of Biological and Chemical Sciences, University of Missouri-Kansas City, Kansas City, MO, United States

Humans spend nearly a third of their life sleeping, yet, despite decades of research the function of sleep still remains a mystery. Sleep has been linked with various biological systems and functions, including metabolism, immunity, the cardiovascular system, and cognitive functions. Importantly, sleep appears to be present throughout the animal kingdom suggesting that it must provide an evolutionary advantage. Among the many possible functions of sleep, the relationship between sleep, and cognition has received a lot of support. We have all experienced the negative cognitive effects associated with a night of sleep deprivation. These can include increased emotional reactivity, poor judgment, deficit in attention, impairment in learning and memory, and obviously increase in daytime sleepiness. Furthermore, many neurological diseases like Alzheimer's disease often have a sleep disorder component. In some cases, the sleep disorder can exacerbate the progression of the neurological disease. Thus, it is clear that sleep plays an important role for many brain functions. In particular, sleep has been shown to play a positive role in the consolidation of long-term memory while sleep deprivation negatively impacts learning and memory. Importantly, sleep is a behavior that is adapted to an individual's need and influenced by many external and internal stimuli. In addition to being an adaptive behavior, sleep can also modulate plasticity in the brain at the level of synaptic connections between neurons and neuronal plasticity influences sleep. Understanding how sleep is modulated by internal and external stimuli and how sleep can modulate memory and plasticity is a key question in neuroscience. In order to address this question, several animal models have been developed. Among them, the fruit fly *Drosophila melanogaster* with its unparalleled genetics has proved to be extremely valuable. In addition to sleep, *Drosophila* has been shown to be an excellent model to study many complex behaviors, including learning, and memory. This review describes our current knowledge of the relationship between sleep, plasticity, and memory using the fly model.

Keywords: *Drosophila*, sleep, memory, plasticity, neurobiology

OPEN ACCESS

Edited by:
Gabriella Mazzotta, University of Padova, Italy

Reviewed by:
Maria de la Paz Fernandez, Barnard College, Columbia University, United States
Ismael Santa-Maria Perez, Columbia University, United States

***Correspondence:**
Stephane Dissel
dissels@umkc.edu

Specialty section:
This article was submitted to Invertebrate Physiology, a section of the journal Frontiers in Physiology

Received: *06 November 2019*
Accepted: *30 April 2020*
Published: *28 May 2020*

Citation:
Dissel S (2020) Drosophila as a Model to Study the Relationship Between Sleep, Plasticity, and Memory. Front. Physiol. 11:533. doi: 10.3389/fphys.2020.00533

INTRODUCTION

Sleep is an universal phenomenon that has been described in a variety of species ranging from worms to humans (Keene and Duboue, 2018). In addition to animals with complex and organized nervous systems, recent studies have also described sleep in models with simpler nervous systems, such as jellyfish (Nath et al., 2017). At first look, sleep could appear to be a detrimental behavior. This is because when animals are sleeping they are not gathering food or attending to their progeny, they also are not performing vital evolutionary functions like reproduction and perhaps more importantly they are subject to predation. However, despite all the negative outcomes attached to it, sleep has been maintained throughout evolution, emphasizing its essential value (Miyazaki et al., 2017). This nearly ubiquitous presence of sleep in the animal kingdom strongly supports the view that sleep must provide an evolutionary advantage and perform a vital function for the organism. While this has been widely accepted by the scientific community, it is worth mentioning that a recent study challenged the notion that sleep performs a vital function (Geissmann et al., 2019).

Over the last 100 years, the fruit fly, *Drosophila melanogaster* has been used as a model to study many biological questions. The unparalleled genetic tools, cost effectiveness, short developmental time and relevance to human physiology of the fly has positioned it as a prominent model organism. One particular aspect of biology where *Drosophila* contributed extensively is neurobiology. Starting with the discovery of the *period* gene in 1971 by Konopka and Benzer (1971), *Drosophila* has been a workhorse in the study of complex behaviors, such as courtship (Yamamoto and Koganezawa, 2013), aggression (Kravitz and Fernandez, 2015), feeding (Bhumika and Singh, 2018), drug addiction (Kaun et al., 2012), learning and memory (Kahsai and Zars, 2011), circadian rhythms (Franco et al., 2018), and sleep (Ly et al., 2018).

While *Drosophila* has been the pioneer model used to elucidate the molecular mechanisms underlying circadian rhythms, leading to the 2017 Nobel Prize in Physiology and Medicine awarded to Hall, Rosbash and Young, whether flies displayed a behavioral state similar to mammalian sleep was unclear for many years. It is only in 2000, that two independent groups clearly demonstrated that fruit flies were indeed sleeping (Hendricks et al., 2000; Shaw et al., 2000).

Sleep is highly sensitive to internal and external factors and can be modulated accordingly to satisfy an individual's need. For example, in great frigatebirds, sleep manifests itself in a very different manner whether the birds are flying or on land (Rattenborg et al., 2016). Furthermore, some animals can function without sleep for various time durations, such as in neonates killer-whales and their mother during the first postpartum month (Lyamin et al., 2005) or in elephants if falling asleep puts them at risk of being killed (Gravett et al., 2017). In humans, sleep is not as efficient when sleeping in unfamiliar surroundings (Agnew et al., 1966). This so-called first-night effect appears to be caused by the fact that one hemisphere of our brain is more vigilant than the other when we sleep in a novel environment, probably reflecting a protective mechanism (Tamaki et al., 2016).

Beyond environmental and external stimuli, internal stimuli can also modulate sleep. For example, sleep deprivation leads to a homeostatic sleep rebound, illustrated by an increase in sleep quantity and depth following deprivation (Borbely, 1982). This increase in sleep is especially due to an increase in slow-wave sleep (Dijk et al., 1987). Finally, sleep interacts with many biological functions. For instance, there are bidirectional links between sleep and immunity, with immune system activation capable of modulating sleep (Besedovsky et al., 2019) and between diet/metabolism and sleep (Huang et al., 2011; Frank et al., 2017).

In this review, I will describe sleep in the *Drosophila* model and introduce the many brain regions involved in sleep regulation. I will then address the relationships between sleep and plasticity and between sleep and memory.

SLEEP IN *Drosophila*

Daily rhythms of rest/activity in flies have been extensively studied starting in the 1970's (Konopka and Benzer, 1971). Under laboratory conditions, flies are crepuscular animals displaying two peaks of activity centered on the dark to light and light to dark transitions. However, it remained unclear until the year 2000 whether the rest observed in flies could be considered as sleep or whether it was simply inactivity. From a behavioral point of view, human sleep is a period of reduced activity; it is associated with a typical posture, such as lying down; it leads to a reduction in responsiveness to mild external stimuli but it can be easily reversed if the stimuli is strong enough; that is sleep is different from other states of reduced responsiveness like coma. Mammalian sleep is also characterized by a change in brain electrical activity that can be measured by electroencephalography (EEG). Importantly, sleep is regulated by two processes, a circadian process that dictates when sleep can occur and a homeostatic process that controls how much sleep an individual needs (Borbely, 1982).

In *Drosophila*, assessing sleep using an electrophysiological criteria is a challenging task. Thus, in order to unequivocally characterize sleep in the fly model, two independent groups relied on a behavioral definition of sleep (Hendricks et al., 2000; Shaw et al., 2000). These groundbreaking studies demonstrated that locomotor inactivity lasting at least 5 min was associated with an increased arousal threshold, as assessed using mild mechanical stimulation. However, if the stimulus was strong enough, flies that had been inactive for 5 min or more would respond (Hendricks et al., 2000; Shaw et al., 2000). Importantly, both studies also found that the rest observed in flies was homeostatically regulated. Following rest deprivation, flies showed an increase in rest (Hendricks et al., 2000; Shaw et al., 2000). Video analysis of *Drosophila* rest/activity behavior revealed that flies adopt a specific posture to engage in rest periods. Moreover, they do so in a specific location within the tubes where they are housed (Hendricks et al., 2000). Additionally, rest is abundant in young flies and reduced in older flies; an observation that parallels

what we see in human sleep (Shaw et al., 2000). Rest is also modulated by stimulants and hypnotics (Hendricks et al., 2000; Shaw et al., 2000). The observations made in these two studies demonstrated that periods of rest lasting 5 min or more satisfy all the behavioral hallmark of sleep in humans, a typical posture, and withdrawal from the environment, higher arousal threshold and homeostatic regulation (Hendricks et al., 2000; Shaw et al., 2000). In addition, in *Drosophila* like in mammals, sleep is sexually dimorphic; male flies sleep more than female, especially during the day (Isaac et al., 2010; Khericha et al., 2016; Wu et al., 2018). Interestingly, sleep is also present in larvae, and is important for neurogenesis (Szuperak et al., 2018). Because of the strength of the *Drosophila* model, these seminal studies gave rise to new avenues of research that could help understand our knowledge of sleep regulation and function.

Although the definition of sleep in flies is a behavioral one, local field potential recordings demonstrated that sleep is a state of reduced neuronal activity (Nitz et al., 2002). Later studies, using the calcium indicator GCaMP, confirmed this electrophysiological observation and also reinforced the notion that sleep is a state of reduced behavioral responsiveness (Bushey et al., 2015).

Not surprisingly, in the years following the characterization of sleep in *Drosophila*, many progresses have been made regarding the genes that regulate sleep. Importantly, these studies demonstrated that the signaling mechanisms that regulate sleep are conserved between the fly and mammalian models (Sehgal and Mignot, 2011). For example, the role of monoamines in sleep regulation is similar in *Drosophila* and mammals (for instance, dopamine promotes wakefulness while serotonin promotes sleep in both models; Nall and Sehgal, 2014).

BRAIN REGIONS MODULATING SLEEP IN *Drosophila*

There are many brain regions involved in sleep regulation in the mammalian brain (Saper and Fuller, 2017). Similarly, the fly brain contains many sleep regulating centers. Chronologically, the Mushroom Bodies (MBs) was the first identified by two independent groups in 2006 (Joiner et al., 2006; Pitman et al., 2006). MBs are essential bilateral structures in the fly brain involved in learning and memory (**Figure 1**, blue; Hige, 2018). The Kenyon Cells (KCs), neurons intrinsic to the MBs synapse on to 21 different types of Mushroom Body Output Neurons (MBONs, **Figure 1**, yellow) to modulate attraction or avoidance (Aso et al., 2014a,b). These KCs-MBONs connections are modulated by dopaminergic neurons (DANs, **Figure 1**, red). In addition to learning and memory, the MBs and its associated MBONs and DANs regulate sleep; some KCs-MBONs connections promote sleep while other promote wake (Aso et al., 2014b; Sitaraman et al., 2015a,b).

Sleep is regulated by both a circadian process and a homeostatic process (Borbely, 1982), so perhaps it is not surprising that neurons regulating circadian rhythms are also capable of modulating sleep. Among the roughly 150 clock cells in the fly brain (Franco et al., 2018), Pigment-Dispersing factor

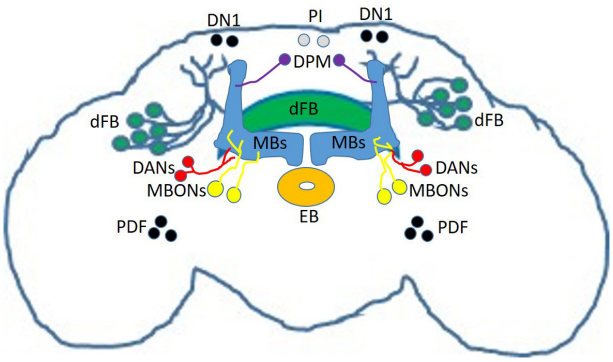

FIGURE 1 | Sleep-regulating circuits in the fly brain. Schematic representation of neurons and circuits involved in sleep regulation including Mushroom Bodies (MBs, blue); Mushroom Body Output Neurons (MBONs, yellow); dopaminergic neurons (DANs, red); circadian clock neurons (black) including Pigment-Dispersing Factor (PDF) neurons and Dorsal Neurons 1 (DN1); Ellipsoid Body neurons (EB, orange); dorsal Fan-Shaped Body neurons (dFB, green); Pars Intercerebralis neurons (PI, gray) and Dorsal-Paired Medial Neurons (DPM, purple).

(PDF) lateral neurons (Renn et al., 1999) play an essential role in controlling rhythmic locomotor activity (Grima et al., 2004; Stoleru et al., 2004). In addition to their central role in controlling the clock, studies demonstrated that PDF cells (**Figure 1**, black) are promoting wake (Parisky et al., 2008; Shang et al., 2008; Sheeba et al., 2008). Interestingly, PDF neurons are important for memory induced by courtship conditioning (Donlea et al., 2009). Furthermore, more recent studies demonstrated that another group of clock neurons, the Dorsal Neurons 1 (DN1s, **Figure 1**, black) can modulate sleep (Kunst et al., 2014; Guo et al., 2016, 2017; Lamaze et al., 2017), by making synaptic connections with tubercular-bulbar (TuBu) neurons (Guo et al., 2018; Lamaze et al., 2018). These TuBu neurons, are forming synaptic connections with R-neurons innervating the ellipsoid body (EB, **Figure 1**, orange) (Guo et al., 2018; Lamaze et al., 2018), a region involved in the control of homeostatic sleep drive (Liu et al., 2016). These data provide an anatomical and functional link between clock controlling neurons and sleep regulating centers.

The Fan-Shaped Body (FB) is part of the central complex (CX) in the *Drosophila* brain. It is a region organized into multiple layers that plays a role in many functions, including locomotion control (Strauss, 2002), courtship behavior (Sakai and Kitamoto, 2006) and memory (Joiner and Griffith, 1999; Sakai et al., 2012), nociception (Hu et al., 2018), visual feature recognition (Liu et al., 2006) and processing (Weir and Dickinson, 2015), and social behaviors (Kacsoh et al., 2019). Neurons that project to the dorsal Fan-Shaped Body (dFB, **Figure 1**, green) are sleep promoting (Donlea et al., 2011), and acute activation of these neurons can help convert short-term memory (STM) into long-term memory (LTM) (Donlea et al., 2011). However, a recent study questions whether this memory benefit is actually caused by dFB or by ventral Fan-Shaped Body (vFB) neurons activation (Dag et al., 2019). Nevertheless, vFB neurons can also promote sleep when activated, confirming that the FB is an important

sleep-regulating hub in the fly brain (Dag et al., 2019). The dFB is particularly important for the homeostatic regulation of sleep (Donlea et al., 2014). The electrical activity of dFB is modulated by sleep pressure, a point illustrated by the fact that sleep deprivation increases the excitability of dFB neurons (Donlea et al., 2014). dFB neurons are modulated by dopaminergic inputs (Liu et al., 2012; Ueno et al., 2012; Pimentel et al., 2016; Ni et al., 2019) with dopamine capable of switching dFB neurons from an electrically active ON state to an electrically silent OFF state (Pimentel et al., 2016). Importantly, this switching mechanism is reminiscent of the FLIP-FLOP switching model between sleep and wake in mammalian brains (Saper et al., 2010). Further work demonstrated that dFB neurons form inhibitory synaptic connections with helicon cells (Donlea et al., 2018). Interestingly, helicon cells themselves provide excitation to R2 neurons of the EB (Donlea et al., 2018), which as mentioned previously control homeostatic sleep drive (Liu et al., 2016).

Other regions regulating sleep include the Pars intercerebralis (PI, **Figure 1**, gray), a neuroendocrine structure in the fly brain (Foltenyi et al., 2007; Crocker et al., 2010). Interestingly, the PI is connected to the clock network and is an important component of the circadian output pathway for rest/activity rhythms (Cavanaugh et al., 2014). In addition, the dorsal paired medial (DPM, **Figure 1**, purple) neurons, which innervate the MBs and are involved in memory consolidation (Waddell et al., 2000; Keene et al., 2004), are sleep promoting cells (Haynes et al., 2015). Finally, and confirming data obtained from mammalian models (Halassa et al., 2009), glia is involved in sleep regulation in *Drosophila* (Seugnet et al., 2011b; Chen et al., 2015; Dissel et al., 2015c; Farca Luna et al., 2017; Gerstner et al., 2017b; Vanderheyden et al., 2018).

These data illustrate that similarly to the mammalian brain, the fly brain contains many regions that regulate sleep. Interestingly, many of these are also involved in learning and memory positioning them perfectly to modulate the interaction between these two processes.

SLEEP AND PLASTICITY

As mentioned previously, sleep is a plastic behavior, it is modulated by both internal, and external/environmental stimuli. Examples include the bidirectional relationship between sleep and the immune system (Williams et al., 2007; Dissel et al., 2015c; Toda et al., 2019). Interestingly, both neurons and glia are implicated in this process (Dissel et al., 2015c) with different outcomes in learning and memory. Another example is the strong bidirectional link between metabolism/diet and sleep (Catterson et al., 2010; Keene et al., 2010; Thimgan et al., 2010; Murphy et al., 2016; Yurgel et al., 2019). Because the focus of this review is on sleep and plasticity/memory, these relationships won't be described further but are nevertheless very important.

During wakefulness, when animals are performing their daily behavioral tasks, for instance exploring their surroundings, reacting to sensory stimuli, interacting with other individuals, making decisions, forming memories, they learn about their environment. These waking experiences are the behavioral basis of learning and memory. Within the brain, learning and memory can be seen as long-lasting changes in the strength or number of synaptic connections between neurons (Tononi and Cirelli, 2014). Importantly, sleep is influenced by neural activity and plasticity (Tononi and Cirelli, 2014). One of the prominent theories to explain the function of sleep is the synaptic homeostasis hypothesis (SHY) (Tononi and Cirelli, 2003). In the SHY model, the function of sleep is the downscaling of synaptic connections that have been strengthened during previous waking experiences (Tononi and Cirelli, 2003). Importantly, the SHY model has received experimental support in the mammalian brain (Huber et al., 2013; de Vivo et al., 2017; Diering et al., 2017; Li et al., 2017; Norimoto et al., 2018). However, it is important to note that synaptic potentiation has also been observed during sleep (Frank et al., 2001; Aton et al., 2013, 2014; Seibt and Frank, 2019). Nevertheless these data reinforce the strong relationship between synaptic plasticity and sleep.

Waking experiences modulate sleep and sleep and neuronal plasticity have a bidirectional relationship (Tononi and Cirelli, 2014). This is also true in flies. Obviously, the most important internal factor than can modulate sleep is sleep pressure. Following sleep deprivation, animals are subject to a strong drive to increase the duration and depth of sleep. The same observation was made in flies, where sleep deprivation triggers a homeostatic sleep rebound (Hendricks et al., 2000; Shaw et al., 2000; Huber et al., 2004). Studies have demonstrated that the dFB and the EB are important circuits regulating sleep homeostasis in *Drosophila* (Donlea et al., 2014, 2018; Liu et al., 2016). Importantly, dFB and EB interact to regulate sleep homeostasis (Liu et al., 2016; Donlea et al., 2018).

Extended waking periods not only increase sleep pressure, they also increase the strength of synaptic connections (Tononi and Cirelli, 2014). This potentiation of synaptic connections constitutes the mechanism that underlies learning and memory. In *Drosophila*, waking, whether spontaneous or imposed by sleep deprivation, led to an increase in several key synaptic proteins in the brain (Gilestro et al., 2009; Dissel et al., 2015a). Importantly, the level of these synaptic markers was reduced following sleep (Gilestro et al., 2009; Dissel et al., 2015a). Reinforcing this notion is the finding that the number and size of synapses in three different circuits, including MBs and PDF neurons, increases following wake and decreases following sleep (Donlea et al., 2009; Bushey et al., 2011). While these data support the hypothesis that sleep plays a role in downscaling synaptic connections that have been strengthened during previous waking experiences (the SHY model) (Tononi and Cirelli, 2003) in *Drosophila*, it is important to note that sleep has been found to potentiate some synaptic connections. This is especially important in the developing brain (Frank et al., 2001). Newborn babies spend a lot of time sleeping and this sleep is very important for their development (Bathory and Tomopoulos, 2017). Similarly, and as previously mentioned, newly hatched flies sleep a lot in the first days of their life (Shaw et al., 2000). This early-life sleep plays an essential role in brain development. Studies have demonstrated that early-life sleep deprivation caused long lasting behavioral defects that are linked to impaired development in key brain areas (Seugnet et al., 2011a; Kayser et al., 2014). Taken together, these data

clearly demonstrate that sleep and neuronal plasticity are tightly interconnected. However, they also suggest that this relationship is not unidirectional, sleep could both downscale and potentiate specific types of synaptic connections. Supporting this view are data collected in a classical memory mutant, where induction of sleep could restore learning and memory as well as increase levels of a key synaptic protein (Dissel et al., 2015a). It is thus very likely that sleep can modulate plasticity in both directions, in a manner adapted to specific needs or circuits.

While awake, *Drosophila* engage in a variety of behaviors, ranging from simple motor actions to very complex social interactions. One such waking experience is social enrichment, which consists of housing many flies within a single vial, increasing the likelihood of social interactions. Flies that are kept in a socially enriched environment display an increase in synapse numbers in the PDF expressing large Lateral Neurons (Donlea et al., 2009) and sleep more than flies that are socially isolated (Ganguly-Fitzgerald et al., 2006). Importantly, PDF cells are essential for the sleep increase triggered by social enrichment (Donlea et al., 2009).

Other waking experiences include different types of memory training. In *Drosophila*, such a memory training is courtship conditioning. In courtship conditioning, naïve males learn to suppress their drive to court by pairing them with non-receptive females (Griffith and Ejima, 2009). This training protocol can create long lasting memories that are dependent on the MBs (McBride et al., 1999). Importantly, courtship conditioning protocols that create LTM increase post-training sleep (Ganguly-Fitzgerald et al., 2006; Dag et al., 2019), and this post-training sleep is essential for the manifestation of LTM (Ganguly-Fitzgerald et al., 2006; Dag et al., 2019). Interestingly, during post-training sleep, the neurons that were engaged in memory acquisition are reactivated and this reactivation is essential for LTM formation (Dag et al., 2019). This finding parallels the memory consolidation processes observed in mammals (Stickgold, 2005; Born, 2010).

Altogether, these data clearly support the notion that sleep is plastic, and that sleep and neuronal plasticity mutually influence each other. Uncovering the molecular mechanisms underlying this relationship is an essential aspect of neurobiology that will help us understand how the brain can optimize its functions in oscillating behavioral states.

SLEEP AND MEMORY

We spend nearly a third of our life asleep, but despite years of research in humans and animal models, we still do not know why we sleep. The function, or probably the functions of sleep remain one of neuroscience biggest mystery (Krueger et al., 2016). Such an enigma has obviously attracted the curiosity of countless number of scientists and many theories to explain the function of sleep have been proposed over the years (Krueger et al., 2016). While some have more merits than others, one of the most attractive one is the one pertaining to the influence of sleep on learning and memory (Chen and Wilson, 2017). That is, on one hand, sleep plays a positive role in memory consolidation (Pavlides and Winson, 1989; Wilson and McNaughton, 1994; Walker and Stickgold, 2004; Stickgold, 2005; Born, 2010) while sleep deprivation and sleep disruption impairs learning and memory (Killgore, 2010; Havekes et al., 2015; Krause et al., 2017). In the brain, learning and memory can be observed at the level of synaptic connections between neurons. Importantly, sleep has been demonstrated to strongly modulate synaptic plasticity (Diekelmann and Born, 2010).

The relationship between sleep and memory can be investigated in flies that have spontaneously reduced levels of sleep or in wild-type flies that are sleep deprived (Dissel et al., 2015b). Flies with spontaneously fragmented sleep are STM impaired as assessed with Aversive Phototaxic Suppression assay (APS) (Le Bourg and Buecher, 2002; Seugnet et al., 2008, 2009a). In the APS, an individual fly is inserted in a T-maze and has a choice between two paths leading to two independent vials. One of them is illuminated while the other is in dark. The lighted portion of the maze contains an aversive stimulus, quinine. Once the fly has made a choice (light or dark), it is removed from the maze and reinserted at the entry point. Each individual fly goes through the maze 16 consecutive trials. At first, wild-type flies will go to the lighted vial where they will encounter the aversive stimulus. As the training progresses, flies will start to visit the dark vial more often. Performance in the APS is calculated as the percentage of dark choices in the last 4 trials of a training session. Typically, wild-type flies never make more than one visit to the dark vial in the last 4 trials if no quinine is present on the lighted vial. Thus, a performance index close to or superior to 50% (at least 2 dark visits in the last 4 trials) indicate learning (Seugnet et al., 2009a). Interestingly, performance in the APS requires the expression of the dopamine D1 receptor in the MBs (Seugnet et al., 2008).

Some studies have looked at memory impairments in mutant flies that display reduced sleep. Loss of function mutations in the ß modulatory subunit of the Shaker potassium channel, encoded by the *Hyperkinetic* (*Hk*) gene reduce sleep (Bushey et al., 2007). Interestingly, when tested for STM using the heat-box paradigm, *Hk* mutants were impaired (Bushey et al., 2007). The heat-box is an operant conditioning paradigm where flies learn and remember to avoid one-half of a dark chamber associated with a temperature that is aversive (Wustmann et al., 1996; Diegelmann et al., 2006). Another study demonstrated that mutations in the Rho-GTPase-activating protein encoded by the *crossveinless-c* (*cv-c*) gene lead to decreased sleep time and STM deficits as assessed with aversive olfactory conditioning (Donlea et al., 2014). In aversive olfactory classical conditioning, the fly learns to associate an odor and a mild electric shock (Krashes and Waddell, 2011).

In an effort to develop a fly model of insomnia, an insomnia-like strain was created by crossing short sleeping flies together for 60 generations (Seugnet et al., 2009b). These flies only slept 60 min a day and were memory impaired as assessed with the APS (Seugnet et al., 2009b).

These data indicate that a reduction in sleep quantity and quality can lead to learning and memory impairments, however, it is important to note that this is not always the case. For example, when looking at individual flies within a wild-type

stock, one can find individuals with fragmented sleep that have normal performance using the APS (Dissel et al., 2015c). Thus, these individuals have developed resilience to the negative effects of sleep degradation (Dissel et al., 2015c).

The remarkable capacity of sleep to benefit learning and memory was further demonstrated when sleep was increased in the classical memory mutants *rutabaga* (*rut*) and *dunce* (*dnc*) (Dissel et al., 2015a). Sleep was increased using three independent strategies (feeding the flies the GABA-A agonist THIP, genetic activation of the dFB and increasing the expression of Fatty acid binding protein) prior to APS training in both mutants. Surprisingly, both memory mutants could form STM following sleep induction (Dissel et al., 2015a). Furthermore, the capacity to form LTM as assessed with courtship conditioning was also restored by sleep induction before and after memory training (Dissel et al., 2015a). Importantly, THIP has been validated as a potent sleep-promoting drug in several subsequent studies (Berry et al., 2015; Dissel et al., 2017; Stahl et al., 2017; Yap et al., 2017; Artiushin et al., 2018; Hill et al., 2018; Ki and Lim, 2019; Liu et al., 2019). In particular, inducing sleep with THIP was shown to block dopamine neuron mediated forgetting of olfactory memories (Berry et al., 2015).

Neurodegenerative diseases like Alzheimer's disease (AD) are often accompanied with sleep deficits (Wang and Holtzman, 2019). In order to study this destructive disease, several fly models of AD have been developed over the years (Finelli et al., 2004; Greeve et al., 2004; Iijima et al., 2004; McBride et al., 2010; Chakraborty et al., 2011; Mhatre et al., 2013; Mhatre et al., 2014), and it was demonstrated that sleep is disrupted in some of these models (Dissel et al., 2015a; Tabuchi et al., 2015; Farca Luna et al., 2017; Gerstner et al., 2017a; Song et al., 2017; Buhl et al., 2019). Importantly, inducing sleep with THIP can restore memory in several fly models of Alzheimer's disease (Dissel et al., 2015a, 2017). Thus, inducing sleep can help the brain overcome memory deficits created by critical genetic lesions or neurodegenerative processes.

In addition to looking at flies with naturally occurring low levels of sleep, the relationship between sleep and learning/memory in *Drosophila* can be studied by looking at the effect of sleep deprivation (SD) on subsequent performance. Following SD, performance, measured as an escape response to an aversive stimulus made of a combination of noise and vibration was reduced (Huber et al., 2004). Furthermore, using the APS or aversive olfactory classical conditioning, it was demonstrated that following SD, wild-type flies are impaired (Seugnet et al., 2008; Li et al., 2009).

In addition to SD, it is possible to reduce sleep by increasing the activity of wake-promoting neurons. Activation of wake-promoting neurons results in subsequent STM impairments as assessed with an aversive-taste memory paradigm (Seidner et al., 2015). In aversive-taste memory, flies learn to suppress their proboscis extension reflex in response to the simultaneous pairing of appetitive fructose to the tarsi and aversive quinine at their proboscis (Keene and Masek, 2012). Importantly, the formation of aversive taste memory is dependent on the MBs.

Sleep is also important for the consolidation of recently acquired memories in long lasting LTM (Walker and Stickgold, 2004; Stickgold, 2005). For instance, a few hours of SD immediately following a courtship conditioning protocol that induces LTM blocked the formation of LTM (Ganguly-Fitzgerald et al., 2006; Dag et al., 2019). Furthermore, increasing sleep following a courtship protocol that normally only creates STM can create LTM (Donlea et al., 2011; Dissel et al., 2015a; Dag et al., 2019). These data suggest that sleep can help the brain recruit mechanisms that are beneficial for the formation of LTM, further illustrating the positive role that sleep plays in memory processing.

CONCLUSION

The nearly ubiquitous presence of sleep in the animal kingdom, despite the obvious detrimental consequences of being in this behavioral state, suggests that sleep must serve an absolutely vital function for the organism. However, despite many efforts, the function of sleep remains elusive. Among the many possible function of sleep, the bidirectional relationship between sleep and plasticity/memory has been extensively documented. Sleep is important for optimal cognitive performance, and sleep disruptions lead to defects in learning and memory. Conversely, many experiences that change plasticity and memory modulate sleep. In addition, neurodegenerative diseases like Alzheimer's disease often disrupts sleep. Thus, it is clear that understanding the sleep-plasticity-memory relationship could have major therapeutic impacts.

In that respect, *Drosophila* seems to be the perfect model. With its considerable strength as a genetic model, coupled with low cost and fast generation time, and almost constant technological advances, progress can be made in *Drosophila* in unparalleled ways. Importantly, the relationship between sleep and memory has been mostly characterized using a "what goes wrong in the brain when sleep is disrupted?" strategy using sleep deprivation, or mutations that disrupt sleep. This approach has proved to be extremely valuable but maybe it only gave us partial answers. With the ability to induce sleep on demand, one can now ask the following question "what good does sleep do to the brain?" While these two questions may look similar, the answers to them may be complementary and could help us get a better understanding of the function of sleep. In conclusion, the strength of the *Drosophila* model will be invaluable to help us understand how sleep can benefit cognitive processes in the context of health and diseases. This could prove especially important in the case of neurodegenerative diseases like Alzheimer's disease.

AUTHOR CONTRIBUTIONS

The author confirms being the sole contributor of this work and has approved it for publication.

FUNDING

This work was supported by the UMKC startup fund.

REFERENCES

Agnew, H. W. Jr., Webb, W. B., and Williams, R. L. (1966). The first night effect: an EEG study of sleep. *Psychophysiology* 2, 263–266. doi: 10.1111/j.1469-8986.1966.tb02650.x

Artiushin, G., Zhang, S. L., Tricoire, H., and Sehgal, A. (2018). Endocytosis at the *Drosophila* blood-brain barrier as a function for sleep. *eLife* 7:e43326. doi: 10.7554/eLife.43326

Aso, Y., Hattori, D., Yu, Y., Johnston, R. M., Iyer, N. A., Ngo, T. T., et al. (2014a). The neuronal architecture of the mushroom body provides a logic for associative learning. *eLife* 3:e04577. doi: 10.7554/eLife.04577

Aso, Y., Sitaraman, D., Ichinose, T., Kaun, K. R., Vogt, K., Belliart-Guerin, G., et al. (2014b). Mushroom body output neurons encode valence and guide memory-based action selection in *Drosophila*. *eLife* 3:e04580. doi: 10.7554/eLife.04580

Aton, S. J., Broussard, C., Dumoulin, M., Seibt, J., Watson, A., Coleman, T., et al. (2013). Visual experience and subsequent sleep induce sequential plastic changes in putative inhibitory and excitatory cortical neurons. *Proc. Natl. Acad. Sci. U.S.A.* 110, 3101–3106. doi: 10.1073/pnas.1208093110

Aton, S. J., Suresh, A., Broussard, C., and Frank, M. G. (2014). Sleep promotes cortical response potentiation following visual experience. *Sleep* 37, 1163–1170. doi: 10.5665/sleep.3830

Bathory, E., and Tomopoulos, S. (2017). Sleep regulation, physiology and development, sleep duration and patterns, and sleep hygiene in infants, toddlers, and preschool-age children. *Curr. Probl. Pediatr. Adolesc. Health Care* 47, 29–42. doi: 10.1016/j.cppeds.2017.01.001

Berry, J. A., Cervantes-Sandoval, I., Chakraborty, M., and Davis, R. L. (2015). Sleep facilitates memory by blocking dopamine neuron-mediated forgetting. *Cell* 161, 1656–1667. doi: 10.1016/j.cell.2015.05.027

Besedovsky, L., Lange, T., and Haack, M. (2019). The sleep-immune crosstalk in health and disease. *Physiol. Rev.* 99, 1325–1380. doi: 10.1152/physrev.00010.2018

Bhumika, and Singh, A. K. (2018). Regulation of feeding behavior in *Drosophila* through the interplay of gustation, physiology and neuromodulation. *Front. Biosci. (Landmark Ed.)* 23, 2016–2027.

Borbely, A. A. (1982). A two process model of sleep regulation. *Hum. Neurobiol.* 1, 195–204.

Born, J. (2010). Slow-wave sleep and the consolidation of long-term memory. *World J. Biol. Psychiatry* 11(Suppl. 1), 16–21. doi: 10.3109/15622971003637637

Buhl, E., Higham, J. P., and Hodge, J. J. L. (2019). Alzheimer's disease-associated tau alters *Drosophila* circadian activity, sleep and clock neuron electrophysiology. *Neurobiol. Dis.* 130:104507. doi: 10.1016/j.nbd.2019.104507

Bushey, D., Huber, R., Tononi, G., and Cirelli, C. (2007). *Drosophila* hyperkinetic mutants have reduced sleep and impaired memory. *J. Neurosci.* 27, 5384–5393. doi: 10.1523/JNEUROSCI.0108-07.2007

Bushey, D., Tononi, G., and Cirelli, C. (2011). Sleep and synaptic homeostasis: structural evidence in *Drosophila*. *Science* 332, 1576–1581. doi: 10.1126/science.1202839

Bushey, D., Tononi, G., and Cirelli, C. (2015). Sleep- and wake-dependent changes in neuronal activity and reactivity demonstrated in fly neurons using in vivo calcium imaging. *Proc. Natl. Acad. Sci. U.S.A.* 112, 4785–4790. doi: 10.1073/pnas.1419603112

Catterson, J. H., Knowles-Barley, S., James, K., Heck, M. M., Harmar, A. J., and Hartley, P. S. (2010). Dietary modulation of *Drosophila* sleep-wake behaviour. *PLoS One* 5:e12062. doi: 10.1371/journal.pone.0012062

Cavanaugh, D. J., Geratowski, J. D., Wooltorton, J. R., Spaethling, J. M., Hector, C. E., Zheng, X., et al. (2014). Identification of a circadian output circuit for rest:activity rhythms in *Drosophila*. *Cell* 157, 689–701. doi: 10.1016/j.cell.2014.02.024

Chakraborty, R., Vepuri, V., Mhatre, S. D., Paddock, B. E., Miller, S., Michelson, S. J., et al. (2011). Characterization of a *Drosophila* Alzheimer's disease model: pharmacological rescue of cognitive defects. *PLoS One* 6:e20799. doi: 10.1371/journal.pone.0020799

Chen, W. F., Maguire, S., Sowcik, M., Luo, W., Koh, K., and Sehgal, A. (2015). A neuron-glia interaction involving GABA transaminase contributes to sleep loss in sleepless mutants. *Mol. Psychiatry* 20, 240–251. doi: 10.1038/mp.2014.11

Chen, Z., and Wilson, M. A. (2017). Deciphering neural codes of memory during sleep. *Trends Neurosci.* 40, 260–275. doi: 10.1016/j.tins.2017.03.005

Crocker, A., Shahidullah, M., Levitan, I. B., and Sehgal, A. (2010). Identification of a neural circuit that underlies the effects of octopamine on sleep:wake behavior. *Neuron* 65, 670–681. doi: 10.1016/j.neuron.2010.01.032

Dag, U., Lei, Z., Le, J. Q., Wong, A., Bushey, D., and Keleman, K. (2019). Neuronal reactivation during post-learning sleep consolidates long-term memory in *Drosophila*. *eLife* 8:e42786. doi: 10.7554/eLife.42786

de Vivo, L., Bellesi, M., Marshall, W., Bushong, E. A., Ellisman, M. H., Tononi, G., et al. (2017). Ultrastructural evidence for synaptic scaling across the wake/sleep cycle. *Science* 355, 507–510. doi: 10.1126/science.aah5982

Diegelmann, S., Zars, M., and Zars, T. (2006). Genetic dissociation of acquisition and memory strength in the heat-box spatial learning paradigm in *Drosophila*. *Learn. Mem.* 13, 72–83. doi: 10.1101/lm.45506

Diekelmann, S., and Born, J. (2010). The memory function of sleep. *Nat. Rev. Neurosci.* 11, 114–126.

Diering, G. H., Nirujogi, R. S., Roth, R. H., Worley, P. F., Pandey, A., and Huganir, R. L. (2017). Homer1a drives homeostatic scaling-down of excitatory synapses during sleep. *Science* 355, 511–515. doi: 10.1126/science.aai8355

Dijk, D. J., Beersma, D. G., and Daan, S. (1987). EEG power density during nap sleep: reflection of an hourglass measuring the duration of prior wakefulness. *J. Biol. Rhythms* 2, 207–219. doi: 10.1177/074873048700200304

Dissel, S., Angadi, V., Kirszenblat, L., Suzuki, Y., Donlea, J., Klose, M., et al. (2015a). Sleep restores behavioral plasticity to *Drosophila* mutants. *Curr. Biol.* 25, 1270–1281. doi: 10.1016/j.cub.2015.03.027

Dissel, S., Klose, M., Donlea, J., Cao, L., English, D., Winsky-Sommerer, R., et al. (2017). Enhanced sleep reverses memory deficits and underlying pathology in *Drosophila* models of Alzheimer's disease. *Neurobiol. Sleep Circadian Rhythms* 2, 15–26. doi: 10.1016/j.nbscr.2016.09.001

Dissel, S., Melnattur, K., and Shaw, P. J. (2015b). Sleep, performance, and memory in flies. *Curr. Sleep Med. Rep.* 1, 47–54.

Dissel, S., Seugnet, L., Thimgan, M. S., Silverman, N., Angadi, V., Thacher, P. V., et al. (2015c). Differential activation of immune factors in neurons and glia contribute to individual differences in resilience/vulnerability to sleep disruption. *Brain Behav. Immun.* 47, 75–85. doi: 10.1016/j.bbi.2014.09.019

Donlea, J. M., Pimentel, D., and Miesenbock, G. (2014). Neuronal machinery of sleep homeostasis in *Drosophila*. *Neuron* 81, 860–872. doi: 10.1016/j.neuron.2014.03.008

Donlea, J. M., Pimentel, D., Talbot, C. B., Kempf, A., Omoto, J. J., Hartenstein, V., et al. (2018). Recurrent circuitry for balancing sleep need and sleep. *Neuron* 97, 378–389.e4. doi: 10.1016/j.neuron.2017.12.016

Donlea, J. M., Ramanan, N., and Shaw, P. J. (2009). Use-dependent plasticity in clock neurons regulates sleep need in *Drosophila*. *Science* 324, 105–108. doi: 10.1126/science.1166657

Donlea, J. M., Thimgan, M. S., Suzuki, Y., Gottschalk, L., and Shaw, P. J. (2011). Inducing sleep by remote control facilitates memory consolidation in *Drosophila*. *Science* 332, 1571–1576. doi: 10.1126/science.1202249

Farca Luna, A. J., Perier, M., and Seugnet, L. (2017). Amyloid precursor protein in *Drosophila* glia regulates sleep and genes involved in glutamate recycling. *J. Neurosci.* 37, 4289–4300. doi: 10.1523/JNEUROSCI.2826-16.2017

Finelli, A., Kelkar, A., Song, H. J., Yang, H., and Konsolaki, M. (2004). A model for studying Alzheimer's Abeta42-induced toxicity in *Drosophila melanogaster*. *Mol. Cell. Neurosci.* 26, 365–375. doi: 10.1016/j.mcn.2004.03.001

Foltenyi, K., Greenspan, R. J., and Newport, J. W. (2007). Activation of EGFR and ERK by rhomboid signaling regulates the consolidation and maintenance of sleep in *Drosophila*. *Nat. Neurosci.* 10, 1160–1167. doi: 10.1038/nn1957

Franco, D. L., Frenkel, L., and Ceriani, M. F. (2018). The underlying genetics of *Drosophila* circadian behaviors. *Physiology (Bethesda)* 33, 50–62.

Frank, M. G., Issa, N. P., and Stryker, M. P. (2001). Sleep enhances plasticity in the developing visual cortex. *Neuron* 30, 275–287. doi: 10.1016/s0896-6273(01)00279-3

Frank, S., Gonzalez, K., Lee-Ang, L., Young, M. C., Tamez, M., and Mattei, J. (2017). Diet and sleep physiology: public health and clinical implications. *Front. Neurol.* 8:393. doi: 10.3389/fneur.2017.00393

Ganguly-Fitzgerald, I., Donlea, J., and Shaw, P. J. (2006). Waking experience affects sleep need in *Drosophila*. *Science* 313, 1775–1781. doi: 10.1126/science.1130408

Geissmann, Q., Beckwith, E. J., and Gilestro, G. F. (2019). Most sleep does not serve a vital function: evidence from *Drosophila melanogaster*. *Sci. Adv.* 5:eaau9253. doi: 10.1126/sciadv.aau9253

Gerstner, J. R., Lenz, O., Vanderheyden, W. M., Chan, M. T., Pfeiffenberger, C., and Pack, A. I. (2017a). Amyloid-beta induces sleep fragmentation that is rescued by fatty acid binding proteins in *Drosophila*. *J. Neurosci. Res.* 95, 1548–1564. doi: 10.1002/jnr.23778

Gerstner, J. R., Perron, I. J., Riedy, S. M., Yoshikawa, T., Kadotani, H., Owada, Y., et al. (2017b). Normal sleep requires the astrocyte brain-type fatty acid binding protein FABP7. *Sci. Adv.* 3:e1602663. doi: 10.1126/sciadv.1602663

Gilestro, G. F., Tononi, G., and Cirelli, C. (2009). Widespread changes in synaptic markers as a function of sleep and wakefulness in *Drosophila*. *Science* 324, 109–112. doi: 10.1126/science.1166673

Gravett, N., Bhagwandin, A., Sutcliffe, R., Landen, K., Chase, M. J., Lyamin, O. I., et al. (2017). Inactivity/sleep in two wild free-roaming African elephant matriarchs – does large body size make elephants the shortest mammalian sleepers? *PLoS One* 12:e0171903. doi: 10.1371/journal.pone.0171903

Greeve, I., Kretzschmar, D., Tschape, J. A., Beyn, A., Brellinger, C., Schweizer, M., et al. (2004). Age-dependent neurodegeneration and Alzheimer-amyloid plaque formation in transgenic *Drosophila*. *J. Neurosci.* 24, 3899–3906. doi: 10.1523/JNEUROSCI.0283-04.2004

Griffith, L. C., and Ejima, A. (2009). Courtship learning in *Drosophila melanogaster*: diverse plasticity of a reproductive behavior. *Learn. Mem.* 16, 743–750. doi: 10.1101/lm.956309

Grima, B., Chelot, E., Xia, R., and Rouyer, F. (2004). Morning and evening peaks of activity rely on different clock neurons of the *Drosophila* brain. *Nature* 431, 869–873. doi: 10.1038/nature02935

Guo, F., Chen, X., and Rosbash, M. (2017). Temporal calcium profiling of specific circadian neurons in freely moving flies. *Proc. Natl. Acad. Sci. U.S.A.* 114, E8780–E8787. doi: 10.1073/pnas.1706608114

Guo, F., Holla, M., Diaz, M. M., and Rosbash, M. (2018). A circadian output circuit controls sleep-wake arousal in *Drosophila*. *Neuron* 100, 624–635.e4. doi: 10.1016/j.neuron.2018.09.002

Guo, F., Yu, J., Jung, H. J., Abruzzi, K. C., Luo, W., Griffith, L. C., et al. (2016). Circadian neuron feedback controls the *Drosophila* sleep–activity profile. *Nature* 536, 292–297. doi: 10.1038/nature19097

Halassa, M. M., Florian, C., Fellin, T., Munoz, J. R., Lee, S. Y., Abel, T., et al. (2009). Astrocytic modulation of sleep homeostasis and cognitive consequences of sleep loss. *Neuron* 61, 213–219. doi: 10.1016/j.neuron.2008.11.024

Havekes, R., Meerlo, P., and Abel, T. (2015). Animal studies on the role of sleep in memory: from behavioral performance to molecular mechanisms. *Curr. Top. Behav. Neurosci.* 25, 183–206. doi: 10.1007/7854_2015_369

Haynes, P. R., Christmann, B. L., and Griffith, L. C. (2015). A single pair of neurons links sleep to memory consolidation in *Drosophila melanogaster*. *eLife* 4:e03868. doi: 10.7554/eLife.03868

Hendricks, J. C., Finn, S. M., Panckeri, K. A., Chavkin, J., Williams, J. A., Sehgal, A., et al. (2000). Rest in *Drosophila* is a sleep-like state. *Neuron* 25, 129–138.

Hige, T. (2018). What can tiny mushrooms in fruit flies tell us about learning and memory? *Neurosci. Res.* 129, 8–16. doi: 10.1016/j.neures.2017.05.002

Hill, V. M., O'connor, R. M., Sissoko, G. B., Irobunda, I. S., Leong, S., Canman, J. C., et al. (2018). A bidirectional relationship between sleep and oxidative stress in *Drosophila*. *PLoS Biol.* 16:e2005206. doi: 10.1371/journal.pbio.2005206

Hu, W., Peng, Y., Sun, J., Zhang, F., Zhang, X., Wang, L., et al. (2018). Fan-shaped body neurons in the *Drosophila* brain regulate both innate and conditioned nociceptive avoidance. *Cell Rep.* 24, 1573–1584. doi: 10.1016/j.celrep.2018.07.028

Huang, W., Ramsey, K. M., Marcheva, B., and Bass, J. (2011). Circadian rhythms, sleep, and metabolism. *J. Clin. Invest.* 121, 2133–2141.

Huber, R., Hill, S. L., Holladay, C., Biesiadecki, M., Tononi, G., and Cirelli, C. (2004). Sleep homeostasis in *Drosophila melanogaster*. *Sleep* 27, 628–639.

Huber, R., Maki, H., Rosanova, M., Casarotto, S., Canali, P., Casali, A. G., et al. (2013). Human cortical excitability increases with time awake. *Cereb. Cortex* 23, 332–338. doi: 10.1093/cercor/bhs014

Iijima, K., Liu, H. P., Chiang, A. S., Hearn, S. A., Konsolaki, M., and Zhong, Y. (2004). Dissecting the pathological effects of human Abeta40 and Abeta42 in *Drosophila*: a potential model for Alzheimer's disease. *Proc. Natl. Acad. Sci. U.S.A.* 101, 6623–6628. doi: 10.1073/pnas.0400895101

Isaac, R. E., Li, C., Leedale, A. E., and Shirras, A. D. (2010). *Drosophila* male sex peptide inhibits siesta sleep and promotes locomotor activity in the post-mated female. *Proc. Biol. Sci.* 277, 65–70. doi: 10.1098/rspb.2009.1236

Joiner, M. A., and Griffith, L. C. (1999). Mapping of the anatomical circuit of CaM kinase-dependent courtship conditioning in *Drosophila*. *Learn. Mem.* 6, 177–192.

Joiner, W. J., Crocker, A., White, B. H., and Sehgal, A. (2006). Sleep in *Drosophila* is regulated by adult mushroom bodies. *Nature* 441, 757–760. doi: 10.1038/nature04811

Kacsoh, B. Z., Bozler, J., Hodge, S., and Bosco, G. (2019). Neural circuitry of social learning in *Drosophila* requires multiple inputs to facilitate inter-species communication. *Commun. Biol.* 2:309. doi: 10.1038/s42003-019-0557-5

Kahsai, L., and Zars, T. (2011). Learning and memory in *Drosophila*: behavior, genetics, and neural systems. *Int. Rev. Neurobiol.* 99, 139–167. doi: 10.1016/B978-0-12-387003-2.00006-9

Kaun, K. R., Devineni, A. V., and Heberlein, U. (2012). *Drosophila melanogaster* as a model to study drug addiction. *Hum. Genet.* 131, 959–975. doi: 10.1007/s00439-012-1146-6

Kayser, M. S., Yue, Z., and Sehgal, A. (2014). A critical period of sleep for development of courtship circuitry and behavior in *Drosophila*. *Science* 344, 269–274. doi: 10.1126/science.1250553

Keene, A. C., and Duboue, E. R. (2018). The origins and evolution of sleep. *J. Exp. Biol.* 221, jeb159533.

Keene, A. C., Duboue, E. R., Mcdonald, D. M., Dus, M., Suh, G. S., Waddell, S., et al. (2010). Clock and cycle limit starvation-induced sleep loss in *Drosophila*. *Curr. Biol.* 20, 1209–1215. doi: 10.1016/j.cub.2010.05.029

Keene, A. C., and Masek, P. (2012). Optogenetic induction of aversive taste memory. *Neuroscience* 222, 173–180. doi: 10.1016/j.neuroscience.2012.07.028

Keene, A. C., Stratmann, M., Keller, A., Perrat, P. N., Vosshall, L. B., and Waddell, S. (2004). Diverse odor-conditioned memories require uniquely timed dorsal paired medial neuron output. *Neuron* 44, 521–533. doi: 10.1016/j.neuron.2004.10.006

Khericha, M., Kolenchery, J. B., and Tauber, E. (2016). Neural and non-neural contributions to sexual dimorphism of mid-day sleep in *Drosophila melanogaster*: a pilot study. *Physiol. Entomol.* 41, 327–334. doi: 10.1111/phen.12134

Ki, Y., and Lim, C. (2019). Sleep-promoting effects of threonine link amino acid metabolism in *Drosophila* neuron to GABAergic control of sleep drive. *eLife* 8:e40593. doi: 10.7554/eLife.40593

Killgore, W. D. (2010). Effects of sleep deprivation on cognition. *Prog. Brain Res.* 185, 105–129.

Konopka, R. J., and Benzer, S. (1971). Clock mutants of *Drosophila melanogaster*. *Proc. Natl. Acad. Sci. U.S.A.* 68, 2112–2116.

Krashes, M. J., and Waddell, S. (2011). *Drosophila* aversive olfactory conditioning. *Cold Spring Harb. Protoc.* 2011:dbrot5608.

Krause, A. J., Simon, E. B., Mander, B. A., Greer, S. M., Saletin, J. M., Goldstein-Piekarski, A. N., et al. (2017). The sleep-deprived human brain. *Nat. Rev. Neurosci.* 18, 404–418. doi: 10.1038/nrn.2017.55

Kravitz, E. A., and Fernandez, M. P. (2015). Aggression in *Drosophila*. *Behav. Neurosci.* 129, 549–563.

Krueger, J. M., Frank, M. G., Wisor, J. P., and Roy, S. (2016). Sleep function: toward elucidating an enigma. *Sleep Med. Rev.* 28, 46–54. doi: 10.1016/j.smrv.2015.08.005

Kunst, M., Hughes, M. E., Raccuglia, D., Felix, M., Li, M., Barnett, G., et al. (2014). Calcitonin gene-related peptide neurons mediate sleep-specific circadian output in *Drosophila*. *Curr. Biol.* 24, 2652–2664. doi: 10.1016/j.cub.2014.09.077

Lamaze, A., Kratschmer, P., Chen, K. F., Lowe, S., and Jepson, J. E. C. (2018). A wake-promoting circadian output circuit in *Drosophila*. *Curr. Biol.* 28, 3098–3105.e3. doi: 10.1016/j.cub.2018.07.024

Lamaze, A., Ozturk-Colak, A., Fischer, R., Peschel, N., Koh, K., and Jepson, J. E. (2017). Regulation of sleep plasticity by a thermo-sensitive circuit in *Drosophila*. *Sci. Rep.* 7:40304. doi: 10.1038/srep40304

Le Bourg, E., and Buecher, C. (2002). Learned suppression of photopositive tendencies in *Drosophila melanogaster*. *Anim. Learn. Behav.* 30, 330–341. doi: 10.1016/j.neurobiolaging.2003.12.004

Li, W., Ma, L., Yang, G., and Gan, W. B. (2017). REM sleep selectively prunes and maintains new synapses in development and learning. *Nat. Neurosci.* 20, 427–437. doi: 10.1038/nn.4479

Li, X., Yu, F., and Guo, A. (2009). Sleep deprivation specifically impairs short-term olfactory memory in *Drosophila*. *Sleep* 32, 1417–1424. doi: 10.1093/sleep/32.11.1417

Liu, C., Meng, Z., Wiggin, T. D., Yu, J., Reed, M. L., Guo, F., et al. (2019). A serotonin-modulated circuit controls sleep architecture to regulate cognitive function independent of total sleep in *Drosophila*. *Curr. Biol.* 29, 3635–3646.e5. doi: 10.1016/j.cub.2019.08.079

Liu, G., Seiler, H., Wen, A., Zars, T., Ito, K., Wolf, R., et al. (2006). Distinct memory traces for two visual features in the *Drosophila* brain. *Nature* 439, 551–556. doi: 10.1038/nature04381

Liu, Q., Liu, S., Kodama, L., Driscoll, M. R., and Wu, M. N. (2012). Two dopaminergic neurons signal to the dorsal fan-shaped body to promote wakefulness in *Drosophila*. *Curr. Biol.* 22, 2114–2123. doi: 10.1016/j.cub.2012.09.008

Liu, S., Liu, Q., Tabuchi, M., and Wu, M. N. (2016). Sleep drive is encoded by neural plastic changes in a dedicated circuit. *Cell* 165, 1347–1360. doi: 10.1016/j.cell.2016.04.013

Ly, S., Pack, A. I., and Naidoo, N. (2018). The neurobiological basis of sleep: insights from *Drosophila*. *Neurosci. Biobehav. Rev.* 87, 67–86.

Lyamin, O., Pryaslova, J., Lance, V., and Siegel, J. (2005). Animal behaviour: continuous activity in cetaceans after birth. *Nature* 435:1177. doi: 10.1038/4351177a

McBride, S. M., Choi, C. H., Schoenfeld, B. P., Bell, A. J., Liebelt, D. A., Ferreiro, D., et al. (2010). Pharmacological and genetic reversal of age-dependent cognitive deficits attributable to decreased presenilin function. *J. Neurosci.* 30, 9510–9522. doi: 10.1523/JNEUROSCI.1017-10.2010

McBride, S. M., Giuliani, G., Choi, C., Krause, P., Correale, D., Watson, K., et al. (1999). Mushroom body ablation impairs short-term memory and long-term memory of courtship conditioning in *Drosophila melanogaster*. *Neuron* 24, 967–977.

Mhatre, S. D., Paddock, B. E., Saunders, A. J., and Marenda, D. R. (2013). Invertebrate models of Alzheimer's disease. *J. Alzheimers Dis.* 33, 3–16.

Mhatre, S. D., Satyasi, V., Killen, M., Paddock, B. E., Moir, R. D., Saunders, A. J., et al. (2014). Synaptic abnormalities in a *Drosophila* model of Alzheimer's disease. *Dis. Model. Mech.* 7, 373–385.

Miyazaki, S., Liu, C. Y., and Hayashi, Y. (2017). Sleep in vertebrate and invertebrate animals, and insights into the function and evolution of sleep. *Neurosci. Res.* 118, 3–12. doi: 10.1016/j.neures.2017.04.017

Murphy, K. R., Deshpande, S. A., Yurgel, M. E., Quinn, J. P., Weissbach, J. L., Keene, A. C., et al. (2016). Postprandial sleep mechanics in *Drosophila*. *eLife* 5:e19334.

Nall, A., and Sehgal, A. (2014). Monoamines and sleep in *Drosophila*. *Behav. Neurosci.* 128, 264–272.

Nath, R. D., Bedbrook, C. N., Abrams, M. J., Basinger, T., Bois, J. S., Prober, D. A., et al. (2017). The jellyfish *Cassiopea* exhibits a sleep-like state. *Curr. Biol.* 27, 2984–2990.e3. doi: 10.1016/j.cub.2017.08.014

Ni, J. D., Gurav, A. S., Liu, W., Ogunmowo, T. H., Hackbart, H., Elsheikh, A., et al. (2019). Differential regulation of the *Drosophila* sleep homeostat by circadian and arousal inputs. *eLife* 8:e40487. doi: 10.7554/eLife.40487

Nitz, D. A., Van Swinderen, B., Tononi, G., and Greenspan, R. J. (2002). Electrophysiological correlates of rest and activity in *Drosophila melanogaster*. *Curr. Biol.* 12, 1934–1940. doi: 10.1016/s0960-9822(02)01300-3

Norimoto, H., Makino, K., Gao, M., Shikano, Y., Okamoto, K., Ishikawa, T., et al. (2018). Hippocampal ripples down-regulate synapses. *Science* 359, 1524–1527. doi: 10.1126/science.aao0702

Parisky, K. M., Agosto, J., Pulver, S. R., Shang, Y., Kuklin, E., Hodge, J. J., et al. (2008). PDF cells are a GABA-responsive wake-promoting component of the *Drosophila* sleep circuit. *Neuron* 60, 672–682. doi: 10.1016/j.neuron.2008.10.042

Pavlides, C., and Winson, J. (1989). Influences of hippocampal place cell firing in the awake state on the activity of these cells during subsequent sleep episodes. *J. Neurosci.* 9, 2907–2918. doi: 10.1523/JNEUROSCI.09-08-02907.1989

Pimentel, D., Donlea, J. M., Talbot, C. B., Song, S. M., Thurston, A. J. F., and Miesenbock, G. (2016). Operation of a homeostatic sleep switch. *Nature* 536, 333–337. doi: 10.1038/nature19055

Pitman, J. L., Mcgill, J. J., Keegan, K. P., and Allada, R. (2006). A dynamic role for the mushroom bodies in promoting sleep in *Drosophila*. *Nature* 441, 753–756. doi: 10.1038/nature04739

Rattenborg, N. C., Voirin, B., Cruz, S. M., Tisdale, R., Dell'omo, G., Lipp, H. P., et al. (2016). Evidence that birds sleep in mid-flight. *Nat. Commun.* 7:12468.

Renn, S. C., Park, J. H., Rosbash, M., Hall, J. C., and Taghert, P. H. (1999). A pdf neuropeptide gene mutation and ablation of PDF neurons each cause severe abnormalities of behavioral circadian rhythms in *Drosophila*. *Cell* 99, 791–802. doi: 10.1016/s0092-8674(00)81676-1

Sakai, T., Inami, S., Sato, S., and Kitamoto, T. (2012). Fan-shaped body neurons are involved in period-dependent regulation of long-term courtship memory in *Drosophila*. *Learn. Mem.* 19, 571–574. doi: 10.1101/lm.028092.112

Sakai, T., and Kitamoto, T. (2006). Differential roles of two major brain structures, mushroom bodies and central complex, for *Drosophila* male courtship behavior. *J. Neurobiol.* 66, 821–834. doi: 10.1002/neu.20262

Saper, C. B., and Fuller, P. M. (2017). Wake-sleep circuitry: an overview. *Curr. Opin. Neurobiol.* 44, 186–192. doi: 10.1016/j.conb.2017.03.021

Saper, C. B., Fuller, P. M., Pedersen, N. P., Lu, J., and Scammell, T. E. (2010). Sleep state switching. *Neuron* 68, 1023–1042.

Sehgal, A., and Mignot, E. (2011). Genetics of sleep and sleep disorders. *Cell* 146, 194–207.

Seibt, J., and Frank, M. G. (2019). Primed to sleep: the dynamics of synaptic plasticity across brain states. *Front. Syst. Neurosci.* 13:2. doi: 10.3389/fnsys.2019.00002

Seidner, G., Robinson, J. E., Wu, M., Worden, K., Masek, P., Roberts, S. W., et al. (2015). Identification of neurons with a privileged role in sleep homeostasis in *Drosophila melanogaster*. *Curr. Biol.* 25, 2928–2938. doi: 10.1016/j.cub.2015.10.006

Seugnet, L., Suzuki, Y., Donlea, J. M., Gottschalk, L., and Shaw, P. J. (2011a). Sleep deprivation during early-adult development results in long-lasting learning deficits in adult *Drosophila*. *Sleep* 34, 137–146. doi: 10.1093/sleep/34.2.137

Seugnet, L., Suzuki, Y., Merlin, G., Gottschalk, L., Duntley, S. P., and Shaw, P. J. (2011b). Notch signaling modulates sleep homeostasis and learning after sleep deprivation in *Drosophila*. *Curr. Biol.* 21, 835–840. doi: 10.1016/j.cub.2011.04.001

Seugnet, L., Suzuki, Y., Stidd, R., and Shaw, P. J. (2009a). Aversive phototaxic suppression: evaluation of a short-term memory assay in *Drosophila melanogaster*. *Genes Brain Behav.* 8, 377–389. doi: 10.1111/j.1601-183X.2009.00483.x

Seugnet, L., Suzuki, Y., Thimgan, M., Donlea, J., Gimbel, S. I., Gottschalk, L., et al. (2009b). Identifying sleep regulatory genes using a *Drosophila* model of insomnia. *J. Neurosci.* 29, 7148–7157. doi: 10.1523/JNEUROSCI.5629-08.2009

Seugnet, L., Suzuki, Y., Vine, L., Gottschalk, L., and Shaw, P. J. (2008). D1 receptor activation in the mushroom bodies rescues sleep-loss-induced learning impairments in *Drosophila*. *Curr. Biol.* 18, 1110–1117. doi: 10.1016/j.cub.2008.07.028

Shang, Y., Griffith, L. C., and Rosbash, M. (2008). Light-arousal and circadian photoreception circuits intersect at the large PDF cells of the *Drosophila* brain. *Proc. Natl. Acad. Sci. U.S.A.* 105, 19587–19594. doi: 10.1073/pnas.0809577105

Shaw, P. J., Cirelli, C., Greenspan, R. J., and Tononi, G. (2000). Correlates of sleep and waking in *Drosophila melanogaster*. *Science* 287, 1834–1837.

Sheeba, V., Fogle, K. J., Kaneko, M., Rashid, S., Chou, Y. T., Sharma, V. K., et al. (2008). Large ventral lateral neurons modulate arousal and sleep in *Drosophila*. *Curr. Biol.* 18, 1537–1545. doi: 10.1016/j.cub.2008.08.033

Sitaraman, D., Aso, Y., Jin, X., Chen, N., Felix, M., Rubin, G. M., et al. (2015a). Propagation of homeostatic sleep signals by segregated synaptic microcircuits of the *Drosophila* mushroom body. *Curr. Biol.* 25, 2915–2927. doi: 10.1016/j.cub.2015.09.017

Sitaraman, D., Aso, Y., Rubin, G. M., and Nitabach, M. N. (2015b). Control of sleep by dopaminergic inputs to the *Drosophila* mushroom body. *Front. Neural Circuits* 9:73. doi: 10.3389/fncir.2015.00073

Song, Q., Feng, G., Huang, Z., Chen, X., Chen, Z., and Ping, Y. (2017). Aberrant axonal arborization of PDF neurons induced by Abeta42-mediated JNK activation underlies sleep disturbance in an Alzheimer's model. *Mol. Neurobiol.* 54, 6317–6328. doi: 10.1007/s12035-016-0165-z

Stahl, B. A., Slocumb, M. E., Chaitin, H., Diangelo, J. R., and Keene, A. C. (2017). Sleep-Dependent modulation of metabolic rate in *Drosophila*. *Sleep* 40:zsx084.

Stickgold, R. (2005). Sleep-dependent memory consolidation. *Nature* 437, 1272–1278.

Stoleru, D., Peng, Y., Agosto, J., and Rosbash, M. (2004). Coupled oscillators control morning and evening locomotor behaviour of *Drosophila*. *Nature* 431, 862–868. doi: 10.1038/nature02926

Strauss, R. (2002). The central complex and the genetic dissection of locomotor behaviour. *Curr. Opin. Neurobiol.* 12, 633–638. doi: 10.1016/s0959-4388(02)00385-9

Szuperak, M., Churgin, M. A., Borja, A. J., Raizen, D. M., Fang-Yen, C., and Kayser, M. S. (2018). A sleep state in *Drosophila* larvae required for neural stem cell proliferation. *eLife* 7:e33220. doi: 10.7554/eLife.33220

Tabuchi, M., Lone, S. R., Liu, S., Liu, Q., Zhang, J., Spira, A. P., et al. (2015). Sleep interacts with abeta to modulate intrinsic neuronal excitability. *Curr. Biol.* 25, 702–712. doi: 10.1016/j.cub.2015.01.016

Tamaki, M., Bang, J. W., Watanabe, T., and Sasaki, Y. (2016). Night watch in one brain hemisphere during sleep associated with the first-night effect in humans. *Curr. Biol.* 26, 1190–1194. doi: 10.1016/j.cub.2016.02.063

Thimgan, M. S., Suzuki, Y., Seugnet, L., Gottschalk, L., and Shaw, P. J. (2010). The perilipin homologue, lipid storage droplet 2, regulates sleep homeostasis and prevents learning impairments following sleep loss. *PLoS Biol.* 8:e1000466. doi: 10.1371/journal.pbio.1000466

Toda, H., Williams, J. A., Gulledge, M., and Sehgal, A. (2019). A sleep-inducing gene, nemuri, links sleep and immune function in *Drosophila*. *Science* 363, 509–515. doi: 10.1126/science.aat1650

Tononi, G., and Cirelli, C. (2003). Sleep and synaptic homeostasis: a hypothesis. *Brain Res. Bull.* 62, 143–150. doi: 10.1016/j.brainresbull.2003.09.004

Tononi, G., and Cirelli, C. (2014). Sleep and the price of plasticity: from synaptic and cellular homeostasis to memory consolidation and integration. *Neuron* 81, 12–34. doi: 10.1016/j.neuron.2013.12.025

Ueno, T., Tomita, J., Tanimoto, H., Endo, K., Ito, K., Kume, S., et al. (2012). Identification of a dopamine pathway that regulates sleep and arousal in *Drosophila*. *Nat. Neurosci.* 15, 1516–1523. doi: 10.1038/nn.3238

Vanderheyden, W. M., Goodman, A. G., Taylor, R. H., Frank, M. G., Van Dongen, H. P. A., and Gerstner, J. R. (2018). Astrocyte expression of the *Drosophila* TNF-alpha homologue, eiger, regulates sleep in flies. *PLoS Genet.* 14:e1007724. doi: 10.1371/journal.pgen.1007724

Waddell, S., Armstrong, J. D., Kitamoto, T., Kaiser, K., and Quinn, W. G. (2000). The amnesiac gene product is expressed in two neurons in the *Drosophila* brain that are critical for memory. *Cell* 103, 805–813. doi: 10.1016/s0092-8674(00)00183-5

Walker, M. P., and Stickgold, R. (2004). Sleep-dependent learning and memory consolidation. *Neuron* 44, 121–133.

Wang, C., and Holtzman, D. M. (2019). Bidirectional relationship between sleep and Alzheimer's disease: role of amyloid, tau, and other factors. *Neuropsychopharmacology* 45, 104–120. doi: 10.1038/s41386-019-0478-5

Weir, P. T., and Dickinson, M. H. (2015). Functional divisions for visual processing in the central brain of flying *Drosophila*. *Proc. Natl. Acad. Sci. U.S.A.* 112, E5523–E5532. doi: 10.1073/pnas.1514415112

Williams, J. A., Sathyanarayanan, S., Hendricks, J. C., and Sehgal, A. (2007). Interaction between sleep and the immune response in *Drosophila*: a role for the NFkappaB relish. *Sleep* 30, 389–400. doi: 10.1093/sleep/30.4.389

Wilson, M. A., and McNaughton, B. L. (1994). Reactivation of hippocampal ensemble memories during sleep. *Science* 265, 676–679. doi: 10.1126/science.8036517

Wu, B., Ma, L., Zhang, E., Du, J., Liu, S., Price, J., et al. (2018). Sexual dimorphism of sleep regulated by juvenile hormone signaling in *Drosophila*. *PLoS Genet.* 14:e1007318. doi: 10.1371/journal.pgen.1007318

Wustmann, G., Rein, K., Wolf, R., and Heisenberg, M. (1996). A new paradigm for operant conditioning of *Drosophila melanogaster*. *J. Comp. Physiol. A* 179, 429–436. doi: 10.1007/BF00194996

Yamamoto, D., and Koganezawa, M. (2013). Genes and circuits of courtship behaviour in *Drosophila* males. *Nat. Rev. Neurosci.* 14, 681–692. doi: 10.1038/nrn3567

Yap, M. H. W., Grabowska, M. J., Rohrscheib, C., Jeans, R., Troup, M., Paulk, A. C., et al. (2017). Oscillatory brain activity in spontaneous and induced sleep stages in flies. *Nat. Commun.* 8:1815. doi: 10.1038/s41467-017-02024-y

Yurgel, M. E., Kakad, P., Zandawala, M., Nassel, D. R., Godenschwege, T. A., and Keene, A. C. (2019). A single pair of leucokinin neurons are modulated by feeding state and regulate sleep-metabolism interactions. *PLoS Biol.* 17:e2006409. doi: 10.1371/journal.pbio.2006409

Conflict of Interest: The author declares that the research was conducted in the absence of any commercial or financial relationships that could be construed as a potential conflict of interest.

Advantages of publishing in Frontiers

OPEN ACCESS
Articles are free to read for greatest visibility and readership

FAST PUBLICATION
Around 90 days from submission to decision

HIGH QUALITY PEER-REVIEW
Rigorous, collaborative, and constructive peer-review

TRANSPARENT PEER-REVIEW
Editors and reviewers acknowledged by name on published articles

Frontiers
Avenue du Tribunal-Fédéral 34
1005 Lausanne | Switzerland

Visit us: www.frontiersin.org
Contact us: frontiersin.org/about/contact

REPRODUCIBILITY OF RESEARCH
Support open data and methods to enhance research reproducibility

DIGITAL PUBLISHING
Articles designed for optimal readership across devices

FOLLOW US
@frontiersin

IMPACT METRICS
Advanced article metrics track visibility across digital media

EXTENSIVE PROMOTION
Marketing and promotion of impactful research

LOOP RESEARCH NETWORK
Our network increases your article's readership